Development of Synthetic Strategies to Address Bottlenecks in Glycan Synthesis

Inaugural-Dissertation
to obtain the academic degree
Doctor rerum naturalium (Dr. rer. nat.)

Submitted to the Department of Biology, Chemistry and Pharmacy
of Freie Universität Berlin

by
Mónica L. Guberman
from Ciudad de Buenos Aires, Argentina

December 2019

This work was performed between December 2015 and September 2019 under the direction of Prof. Dr. Seeberger in the Department of Biomolecular Systems, at Max Planck Institute of Colloids and Interfaces.

1st reviewer: Prof. Dr. Peter H. Seeberger
2nd reviewer: Prof. Dr. Kevin Pagel

Date of oral defense: February 28, 2020

Acknowledgements

First and foremost, I would like to thank Prof. Dr. Seeberger for giving me the opportunity to perform research at the Max Planck Institute of Colloids and Interfaces, and his supervision, encouragement and support throughout my PhD studies. I thank Prof. Dr. Pagel for kindly agreeing to review my thesis.

I am very grateful to Dr. Maria Bräutigam for the excellent collaborative work, Dr. Martina Delbianco for training and advice in automation, and Dr. Bartholomäus Pieber for his guidance in flow chemistry. I am thankful to Dr. Anna Nickel for the initial training in the continuous flow lab. I would like to thank Dr. Oren Moscovitz, Felix Goerdeler and Katrin Sellrie, for continuining with this work into cancer research, and for always being willing to have a conversation about their work with me. I am grateful to Dr. Daniel Varon Silva, Dr. Fabian Pfrengle, and Dr. Cristoph Rademacher for their valuable input. A special mention to Dr. Maria Spassova for their advice regarding deprotection of final compounds. I deeply appreciate the work and help of Dorothee Böhme, Eva Settels and Olaf Niemeyer throughout these years, from which my research and my time at the Institute greatly benefited.

I thank all my friends and colleagues in the department of Biomolecular Systems for providing a friendly and supporting work atmosphere. To all present and former members of vaccine and automation groups for the fruitful scientific discussions, in particular to my labmates Adam, Fei-fei, Marilda, Dacheng, Maria, Mauro, Shuo, Somesh, Madhu, Petra, Sabrina, Jamal, Harin for the shared teas, coffees, sandwiches, and chemistry. To Ankita, Alonso, Mauro, Eric, Mara, Martina, Bart, Matt, Silvia, Pietro, Jamal and Vittorio for their friendship and support inside and outside the lab.

I dedicate my special thanks to my family and friends. To Clara, Yair and Ceci for bringing home to Berlin. To Dani and Quique for bringing home close, but somewhere warmer, sunnier, and with delicious food. To my friends and family in Argentina, for keeping home there in every visit, call and message. To my parents for their constant love, company and support. To el Abu, for a lifetime of loving memories.

List of Publications

Guberman, M.; Pieber, B.; Seeberger, P. H.; Safe and Scalable Continuous Flow Azidophenylselenylation of Galactal to Pepare Galactosamine Building Blocks, *Org. Process Res. Dev.* **2019,** *23*, 2764-2770.

Guberman, M;* Bräutigam, M.;* Seeberger, P.H.; Automated Glycan Assembly of Lewis Type I and Type II Chain Oligosaccharide Antigens, *Chem. Sci.* **2019,** *10*, 5634-5640.

Guberman, M; Seeberger, P.H.; Automated Glycan Assembly: A Perspective, *J. Am. Chem. Soc.* **2019,** *141*, 5581-5592.

* Equal authorship

Table of Contents

Abbreviation List

AGA	Automated glycan assembly
APS	Azidophenylselenylation
Araf	Arabinofuranose
Azmb	2-(Azidomethyl)benzoyl
BAIB	Bisacetoxy iodobenzene
BB	Building block
Bn	Benzyl
BPR	Back pressure regulator
Bz	Benzoyl
Cbz	Benzyloxycarbonyl
CFMS	Compartmented flow microrreactor system
CPS	Capsular polsaccharide
DDQ	2,3-Dichloro-5,6-dicyano-1,4-benzoquinone
FC	Fluorescein
Fmoc	9-Fluorenylmethyloxycarbonyl
FSPE	Fluorous solid-phase extraction
Fuc	Fucose
GAG	Glycosaminoglycan
Gal	Galactose
GalN	Galactosamine
GalNAc	*N*-Acetylgalactosamine
Glc	Glucose
GlcA	Glucuronic acid
GlcN	Glucosamine
GlcNAc	*N*-Acetylglucosamine
HPLC	High performance liquid chromatography
IdoA	Iduronic acid
IM-MS	Ion mobility spectrometry – mass spectrometry
LacNAc	*N*-Acetyllactosamine
Lc_4	Lactotetraosyl
Le	Lewis (antigen)

Lev	Levulinoyl
LG	Leaving group
mAbs	Monoclonal antibodies
MALDI	Matrix-assisted laser desorption-ionization
Man	Mannose
ManA	Mannuronic acid
MEB	Magnetic enzyme bead
Nap	2-Naphthylmethyl
Nbs	Nanobodies
Neu5Ac	*N*-Acetylneuramic acid
NHS	*N*-Hydrosuccinimide
NIS	*N*-Iodosuccinimide
nLc_4	Neolactotetraosyl
NP-HPLC	Normal-phase HPLC
PG	Protecting group
PivCN	Cyanopivaloyl
PMB	*p*-Methoxybenzyl
PNAG	β-1,6-Poly-*N*-acetylglucosamine
PNP	*p*-Nitrophenyl
Rha	Rhamnose
RP-HPLC	Reverse-phase HPLC
RRV	Relative reactivity value
SLe	Sialyl Lewis (antigen)
SNFG	Symbol nomenclature for glycans
TACA	Tumor associated carbohydrate antigen
TBS	*tert*-Butyldimethylsilyl
TCA	Trichloroacetyl
TEA	Triethylamine
TFA	Trifluoroacetic acid
TMS	Trimethylsilyl
tPG	Temporary protecting group
Xylp	Xylopyranose

Symbol Nomenclature for Glycans (SNFG)

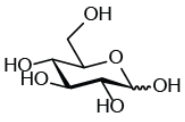

D-Glucose
(D-Glc)

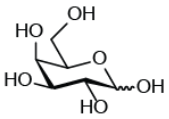

D-Galactose
(D-Gal)

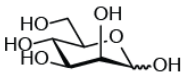

D-Mannose
(D-Man)

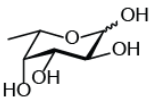

L-Fucose
(L-Fuc)

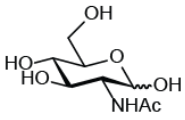

N-Acetyl-D-glucosamine
(D-GlcNAc)

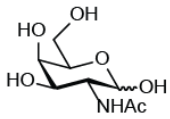

N-Acetyl-D-galactosamine
(D-GalNAc)

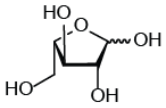

D-Arabinofuranose
(D-Ara*f*)

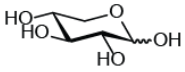

D-Xylopyranose
(D-Xyl*p*)

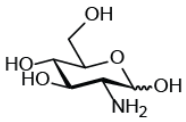

D-Glucosamine
(D-GlcN)

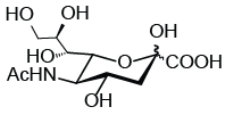

N-Acetylneuramic acid
(Neu5Ac)

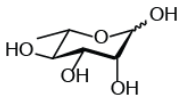

L-Rhamnose
(L-Rha)

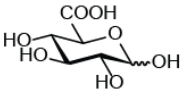

D-Glucuronic acid
(D-GlcA)

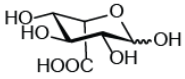

D-Iduronic acid
(D-IdoA)

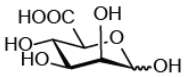

D-Mannuronic acid
(D-ManA)

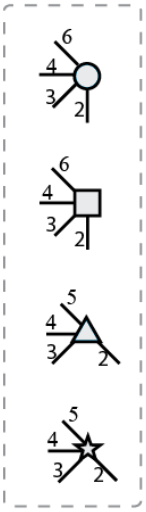

Summary

Carbohydrates are found in all kinds of living organisms, fulfilling structural functions or playing a role in diverse biological processes. Distinct carbohydrate chains are fundamental for events such as cell adhesion, pathogen-host interaction and numerous cell-signaling processes. Synthetic oligosaccharides are essential in the study of glycan function, and the development of tools for disease prevention, diagnostics and treatment.

Difficulties in glycan synthesis arise from the intrinsic complexity of oligosaccharide structures. Oligosaccharide synthesis is a streamlined process, and each step of this process represents a bottleneck that needs to be addressed. Automated Glycan Assembly (AGA) has facilitated access to a wide variety of mammalian, plant, and microorganism glycans. The approach is based on the establishment of an automated platform and compatible orthogonally protected monosaccharide building blocks (BBs, Chapter 1). The aim of this thesis was to develop methods to further expedite carbohydrate synthesis, and to provide access to synthetic glycans for their use in biology and chemistry research. Two projects were conducted to address distinct bottlenecks in glycan synthesis.

The first part of this thesis concentrated on expediting the oligosaccharide assembly of Lewis antigens, a family of complex glycans in high demand for biological studies. The focus was set on developing a method that, with a minimum set of orthogonally-protected monosaccharide BBs and by means of AGA, would provide access to an entire family of structurally-related glycans (Chapter 2). Conjugation-ready glycans were produced for ready use in diverse biological investigations. Of special interest within the Lewis family was tumor-associated carbohydrate antigen KH-1, a branched nonasaccharide containing three α-linkages, which was synthesized for its application in the research of cancer therapy.

While an increasing number of BBs of common use are commercially available, for some glycans the bottleneck still remains in BBs synthesis. A solution to a persistent limitation in galactosamine (GalN) building block synthesis was developed (Chapter 3). GalN BBs are required for the synthesis of mammalian, fungal and bacterial oligosaccharides. A key step during BB synthesis is the azidophenylselenylation (APS) of 3,4,6-tri-*O*-acetyl-D-galactal to prepare the corresponding 2-deoxy-2-*N*-glycoside. Poor reproducibility and the use of azido reagents, that lead to the production of potentially explosive and toxic species, limits this reaction on larger scales in batch. A continuous flow procedure for the safe and scalable APS of galactal was established. Engaging in basic research to establish safe and scalable reactions at the BB synthesis stage will facilitate expanding the AGA scope to other structural families.

Zusammenfassung

Kohlenhydrate kommen in allen Arten von lebenden Organismen vor, erfüllen strukturelle Funktionen oder spielen eine Rolle in diversen biologischen Prozessen. Bestimmte Kohlenhydratketten sind entscheidend für Ereignisse wie Zelladhäsion, Pathogen-Wirt-Interaktion und zahlreiche Zellsignalisierungsvorgänge. Synthetische Oligosaccharide sind unerlässlich für die Erforschung der Funktion von Glykanen und die Entwicklung von Methoden zur Prävention, Diagnose und Behandlung von Krankheiten.

Die Synthese von Glykanen wird vor allem durch die strukturelle Komplexität von Oligosacchariden erschwert. Die Synthese von Oligosacchariden ist ein rationalisierter Prozess, in dem jeder Schritt eine anzugehende Herausforderung darstellt. Die automatisierte Festphasensynthese von Glykanen (*Automated Glycan Assembly*, AGA) hat den Zugang zu vielen Glykanen von Säugetieren, Pflanzen und Mikroorganismen erleichtert. Der Ansatz basiert auf der Etablierung einer automatisierten Plattform und dazu kompatiblen orthogonal geschützten Monosaccharid-Bausteinen (*building blocks*, BBs, Kapitel 1). Das Ziel dieser Arbeit war die Entwicklung von Methoden, um die Kohlenhydratsynthese weiter zu beschleunigen und den Zugang zu synthetischen Glykanen für ihren Einsatz in der Forschung im Bereich der Biologie und Chemie zu ermöglichen. Es wurden zwei Projekte durchgeführt, um signifikante Schwierigkeiten in der Glykansynthese anzugehen.

Der erste Teil dieser Arbeit konzentrierte sich auf die Beschleunigung der Herstellung von Oligosacchariden der Lewis-Antigene, einer Familie von komplexen Glykanen, die für biologische Untersuchungen von großem Interesse sind. Im Mittelpunkt stand die Entwicklung eines Verfahrens, das mit einem Minimum an orthogonal geschützten Monosaccharid-BBs und mittels AGA den Zugang zu einer ganzen Familie von strukturell verwandten Glykanen ermöglicht (Kapitel 2). Mittels dieses Verfahrens wurden Glykane hergestellt, die bereit zur Konjugation für den Einsatz in biologischen Untersuchungen sind. Von besonderem Interesse innerhalb der Lewis-Familie war das tumorassoziierte Kohlenhydrat-Antigen KH-1 - ein verzweigtes Nonasaccharid mit drei α-Verknüpfungen, das für die Anwendung in der Krebstherapie-Forschung synthetisiert wurde.

Auch wenn zunehmend BBs mit gängiger Verwendung kommerziell erhältlich sind, ist für einige Glykane die BBs-Synthese immer noch eine Herausforderung. Hier wurde ein Lösungsansatz für die bisher eingeschränkte BBs-Synthese von Galaktosamin (GalN) entwickelt (Kapitel 3). GalN-BBs werden für die Synthese von Säugetier-, Pilz- und Bakterienoligosacchariden benötigt. Ein wichtiger Schritt ihrer Synthese ist die Azidophenyl-Selenylierung (APS) von 3,4,6-Tri-*O*-acetyl-D-galaktal zur Herstellung des entsprechenden 2-

desoxy-2-*N*-Glykosids. Allerdings erlaubt die schlechte Reproduzierbarkeit und der Einsatz von Azidoreagenzien, die zur Produktion von potenziell explosiven und toxischen Spezies führen, keine Vergrößerung des Ansatzes unter Bedingungen der klassischen Kolben-Chemie. Aus diesem Grund wurde ein kontinuierliches Durchflussverfahren für die sichere und skalierbare APS des Galaktals etabliert. Die Grundlagenforschung zur Etablierung sicherer und skalierbarer Reaktionen in der BBs-Synthese wird es zukünftig erleichtern die Möglichkeiten von AGA auf andere Strukturfamilien zu erweitern.

1 Introduction

This chapter has been partly modified from: Guberman, M.; Seeberger, P. H. Automated Glycan Assembly: A Perspective. *J. Am. Chem. Soc.* **2019,** *141*, 5581–5592.[1] https://doi.org/10.1021/jacs.9b00638. https://pubs.acs.org/doi/10.1021/jacs.9b00638. *Further permissions related to the material excerpted should be directed to the ACS.*

1.1 General Aspects of Carbohydrate Synthesis

Carbohydrates are ubiquitous in nature. They are found in all kinds of living organisms, fulfilling structural functions or playing a role in diverse biological processes. Distinct carbohydrate chains -or glycans- are fundamental for events such as cell adhesion, pathogen-host interaction and numerous cell-signaling processes.[2] Together with nucleic acids and proteins, they constitute the major biopolymers in nature. Glycans stand out for the complexity and diversity of their sequences, which arises from their monomer constituent units: the monosaccharides. Unlike polypeptides or polynucleotides, information is not only contained in the identity of the monomers in the sequence, but also in the way they are linked to one another.[3] While polynucleotides and polypeptides are linear polymers, polysaccharides can be, and often are, branched, as each monosaccharide unit contains multiple hydroxyl groups that can serve as attachment points for further chain growth. Furthermore, in contrast to the phosphate diester that connects nucleotides or the peptide bond for aminoacids, the connection of two monomers by a glycosidic linkage generates a stereocenter (Figure 1.1).

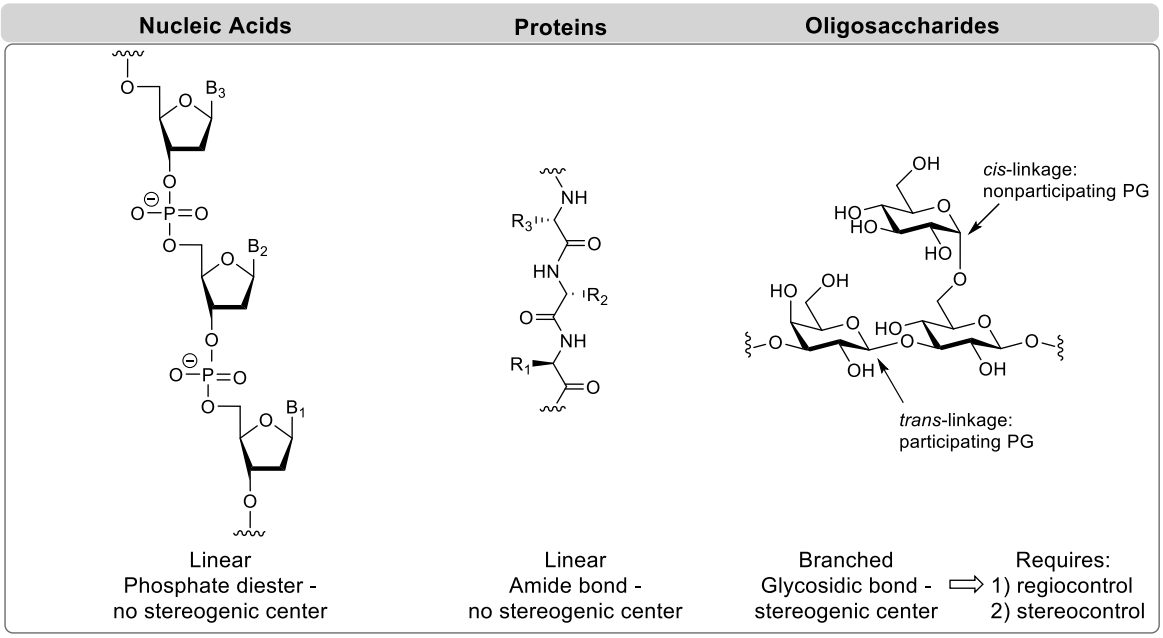

Figure 1.1. Complexity in biopolymer primary structures.

The complexity of carbohydrates greatly accounts for the rather belated progress in glycosciences when compared to the fields of nucleic acids and proteins.[4] Access to pure glycans has been a bottleneck for the research of glycan function. Isolation from natural sources is somewhat unsuitable as carbohydrates are normally present in small amounts and in a microheterogeneous fashion.[5] Thereby this method renders a distribution of different sequences rather than defined structures. Moreover, isolated glycans may carry cellular contaminants.[6] Synthetic glycans are essential tools to study glycan function.

The synthesis of glycans for their application as molecular tools depends on a series of sequential steps: Starting from free monosaccharides, protecting group manipulations are performed to afford protected building blocks (BBs) that will allow for achieving regio- and stereoselective reactions in the subsequent oligosaccharide assembly step (Figure 1.2). Protecting groups (PGs) are next removed to afford an unprotected oligosaccharide. A linker is often pre-installed at the oligosaccharide reducing end to attend requirements of the specific application.

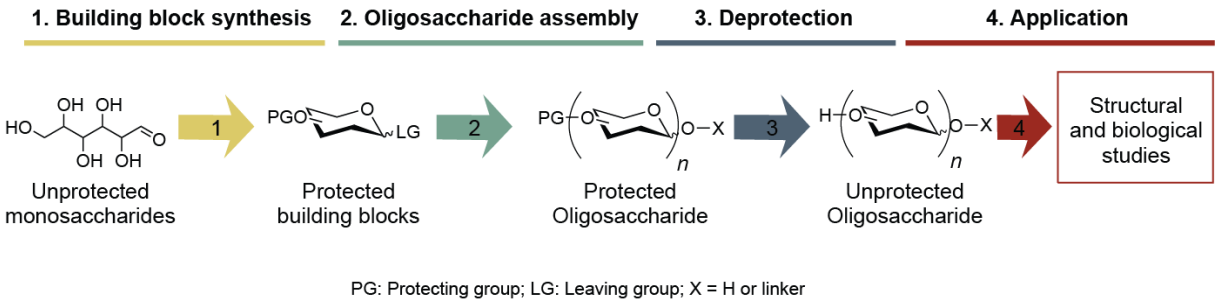

Figure 1.2. Workflow for the synthesis of glycans for their use as molecular tools: step 1, building block synthesis; step 2, oligosaccharide assembly; step 3, deprotection; step 4, application.

1.1.1 Glycosidic Bond Formation

A chemical glycosylation generally involves a fully protected monosaccharide bearing the anomeric carbon for the glycosidic linkage (glycosyl donor), and another monosaccharide bearing only one unprotected hydroxyl group, at the position where installation of glycosidic linkage is desired (glycosyl acceptor, Scheme 1.1). Typically used glycosyl donors such as glycosyl halides, thioglycosides, phosphates or imidates provide good leaving groups at the anomeric position.[7] Regioselectivity is achieved by using protecting groups to mask hydroxyl groups, remaining unprotected only a specific hydroxyl group. Ether, ester, acetal, carbonate or silyl ether protecting groups are usually used to mask hydroxyls.[8] Alternatively, difference in reactivity between unprotected hydroxyl groups can be used to achieve regioselective glycosylation.[9]

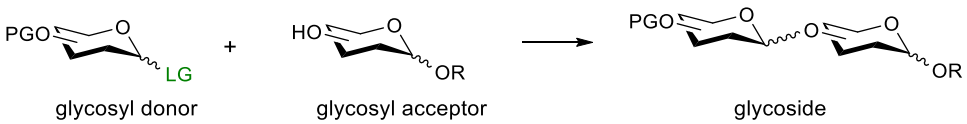

Scheme 1.1. Glycosidic bond formation.

Stereoselectivity is often the most challenging aspect of chemical glycosylation. Glycosylation reactions usually proceed by nucleophilic substitution at the anomeric center. The formation of an oxacarbenium ion intermediate is stabilized by the lone pair of O5. An activator may aid the leaving group departure for the formation of the glycosyl cation. Nucleophilic attack can occur from the top or the bottom face, leading to a mixture of 1,2-*trans* and 1,2-*cis* products (Scheme 1.2, A). If a group capable of performing neighboring group participation (typically an acyl moiety) is present at C2, the formation of an acyloxonium ion will be favoured (anchimeric assistance), and the nucleophilic attack can only proceed from the face opposite to the acyloxocycle, leading to the 1,2-*trans* product (Scheme 1.2, B).

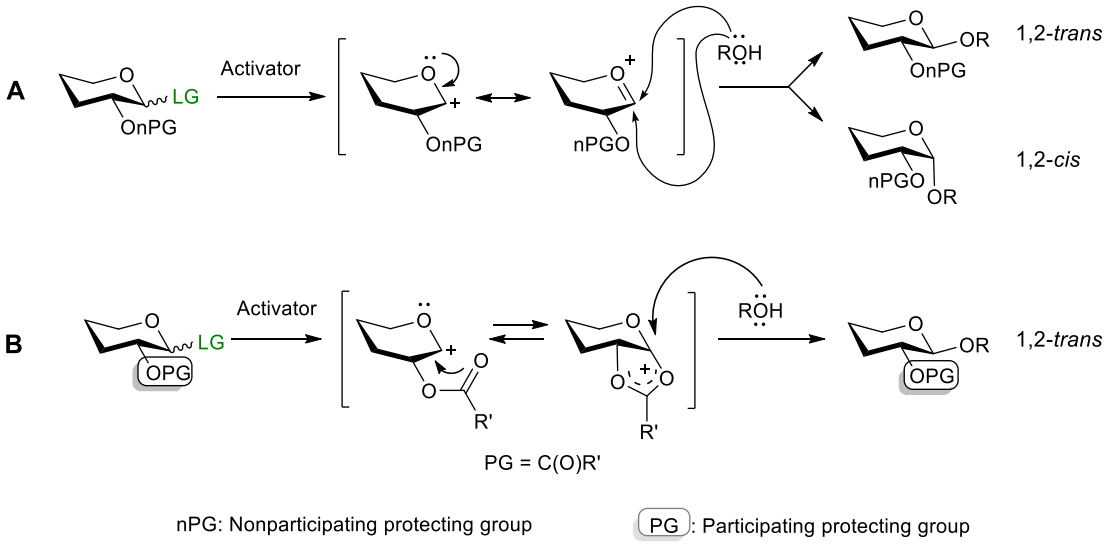

Scheme 1.2. General mechanism of chemical glycosylation (A) via an oxacarbenium pathway, and (B) with anchimeric assistance of a participating group at C2.

While 1,2-*trans* glycosides can be efficiently obtained by anchimeric assistance of a C2 participating group, it is not possible to describe a general strategy to obtain exclusively 1,2-*cis* glycosides. Instead, strategies that allow for the selective formation of 1,2-*cis* or 1,2-*trans* glycosides should be considered. Solvent effects play a key role in those cases. Solvents as diethyl ether or acetonitrile can participate in glycosylation reactions and therefore influence the reaction stereoselectivity. In the *gluco* and *galacto* series, preferred equatorial coordination for diethyl ether and axial coordination for nitrile afford selectively 1,2-*cis* (Scheme 1.3, A) and

1,2-*trans* glycosides (Scheme 1.3, B) respectively.[10] The remote anchimeric effect,[11] or steric hindrance[12] are as well common methods for obtaining 1,2-*cis* glycosides.

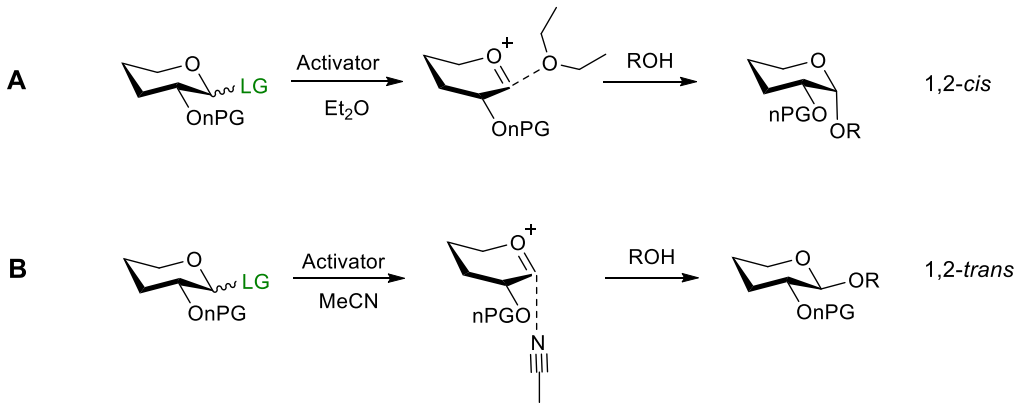

nPG: Nonparticipating protecting group; LG: Leaving group

Scheme 1.3. Effect of solvent participation on glycosylation stereoselectivity. A) Effect of ethereal solvents. B) Nitrile effect.

1.1.2 Approaches to Carbohydrate Synthesis

For the syntheses of glycans, multiple steps and protecting group manipulations are required to ensure the desired regio- and stereochemistry of the products. For traditional solution-phase approaches this often means several months of work.[7] In order to accelerate oligosaccharide syntheses several strategies have been developed, including convergent, one-pot, solid-supported and tag-assisted syntheses[13] in combination with chemical, enzymatic or chemoenzymatic glycosylations.

1.1.2.1 Enzymatic Synthesis

Enzymatic approaches offer the advantage of using unprotected sugars as substrates. This circumvents the need of protecting group manipulation and deprotection steps (Figure 1.2). The variety of structures accessible through enzymatic synthesis is constrained by the available enzymes and their substrate specificities. With the current advances in molecular biology, the portfolio of available enzymes for the synthesis of diverse complex oligosaccharides keeps expanding.[14]

Different enzymatic methods have been explored in an attempt to reduce the number of manipulations and purification steps.[15–18] Approaches where the growing oligosaccharide is bound to a tag or solid support can be potentially combined with an automated process for expeditious glycan synthesis. However, tag methods are of very limited application, as oligosaccharides that are large when compared to their tag suffer from purification difficulties, while on the other hand large tags have a negative influence on synthesis efficiency.[16,19,20]

Incompatibilities between solid supports and efficient enzymatic reactions have hampered the advance of solid-phase enzymatic synthesis.[16] In 2010, an automated method for enzymatic glycan synthesis was first presented. The HPLC-based glycan synthesizer (Golgi) was used for the synthesis of sialyl Lewis^x (SLe^x) antigen.[21] A dendrimer used as solid support provided enhanced synthesis efficiency, but yields were affected by significant material loss during the process. Recently, a commercial CEM Liberty Blue peptide synthesizer was used for the fully-automated enzymatic synthesis of a series of representative glycan antigens.[22] Efficient enzymatic glycosylation and minimized product loss were achieved by using a thermoresponsive polymer as support.

Enzymatic glycan synthesis was tested as well using a compartmented flow microreactor system (CFMS).[23] The combination of parallel and in-line immobilized enzyme modules aimed to produce enzyme cascade reactions, and was exemplified on a trisaccharide synthesis. Enzymes were immobilized using magnetic beads for diligent purification. The use of histidine tags for enzyme immobilization intended to prevent loss of enzymatic activity by conferring a specific enzyme orientation.[23,24] These recent results present automated enzymatic synthesis as a promising avenue for obtaining synthetic glycans, but with only a reduced number of available examples, the scope of this method is not yet determined.

1.1.2.2 Streamlined Chemical Synthesis

In one-pot strategies, glycosylation steps are performed sequentially without intermediate protecting group manipulation or product isolation. Diverse glycans have been synthesized using one-pot glycosylation,[25] but the approach has not been fully automated and, in general, procedures remain target-oriented and time-consuming. One-pot iterative glycosylation afforded the largest well-defined synthetic oligosaccharide chain published to date. The arabinogalactan 92mer was obtained by coupling shorter oligosaccharide segments, each of them assembled using iterative glycosylation protocols.[26] This convergent strategy is limited to the synthesis of highly repetitive glycans.

A widespread one-pot methodology is to exploit anomeric reactivity differences between glycosyl donors for their sequential glycosylation. A systematic approach was attempted with the introduction of ‘programmable one-pot synthesis’. This strategy is based on the quantification of relative reactivity values (RRVs) for several glycosyl donors. The software ‘Optimer’ was developed as database and guide tool for the selection of glycosyl donor building blocks based or their RRVs.[27] An extended library of RRVs for building blocks, including virtual values predicted through machine learning, was recently incorporated into an updated software. The ‘Auto-CHO’ software can also assist hierarchical one-pot synthesis by guiding the selection of building blocks, including fragments generated through one-pot

synthesis.[28] The application of RRVs is limited as it neglects the influence of parameters such as acceptor or solvent influence.[25] Reactivity-based protocols are hardly generalizable as small changes in protecting groups can greatly influence reactivity, and are further limited – like are other solution-phase one-pot methodologies – by the difficulty to remove reagents and reaction side products.

1.1.2.3 Continuous Flow Chemical Synthesis

Continuous flow technology was first applied to address issues in carbohydrate synthesis fifteen years ago.[29,30] Precise control of reaction parameters, and efficient mixing and heat transfer processes in flow could help tackling two issues in glycosylations: coupling efficiencies and reproducibility in stereoselectivity. Minute sample amounts sufficed for screening and optimization of glycosylation conditions in flow microreactors in the context of disaccharide syntheses.[29,31] Chip-based flow reactors allowed screening the influence of different reaction parameters, providing tools for an empirical understanding of glycosylations.[32]

On a preparative scale, syntheses were attempted in combination with purification via solid-phase extraction with the aid of an affinity tag installed at the oligosaccharide reducing end.[30,33] This method allowed for producing glycans as long as tetrasaccharides via iterative couplings. Oligosaccharide assembly in continuous flow can alternatively be performed by multistep continuous flow synthesis using interconnected microreactors. This approach was exemplified with a trisaccharide synthesis,[34] but a wider scope of the method has not yet been demonstrated. Solid-phase continuous flow synthesis assisted by an HPLC system has been implemented in an automated fashion (see section 1.1.2.4).[13]

A barely explored area of continuous flow in carbohydrate synthesis is its application on building block synthesis and protecting group manipulations. Continuous flow has been applied to the Fischer glycosylation of monosaccharides, to afford pyranosides and furanosides under controlled conditions.[35,36] Synthetic procedures could be expedited using continuous multistep reactions, as illustrated in a glycosylation followed by deprotection in flow applied to nucleoside synthesis.[35] Additionally, a two-step flow synthesis was used to expedite access to a glucose BB. However, this protocol would require further development for a practical application, as it consisted in two consecutive flow steps instead of one multistep synthesis.[37] A glimpse to the potential of applying flow technology in challenging synthetic steps was exhibited with the microreactor synthesis of deoxysugars via radical-mediated deoxygenation and dehalogenation reactions.[38] The use of continuous flow in building block synthesis to attend to safety and reproducible concerns on a preparative scale is a promising approach to be investigated.

1.1.2.4 Automated Chemical Synthesis

Different platforms have been explored for the automation of oligosaccharide chemical synthesis, which can be distinguished in three categories: electrochemical assembly, "assisted" synthesis, and solid-phase synthesis. Electrochemical assembly is essentially an automated iterative sequential one-pot methodology, and as such counts with the disadvantages above mentioned (see Section 1.1.2.2).[39,40] Both "assisted" and solid-phase methodologies rely on a handle to which the growing oligosaccharide chain is attached, to allow for excess reagent removal and thereby facilitate purification. Fluorous-assisted solution-phase[41] and HPLC-assisted synthesis[42] have been limited to few examples not exceeding hexasaccharides.[13] Access to synthetic glycans has been expedited with the introduction of Automated Glycan Assembly (AGA).[43] From the proof-of-concept using a modified peptide synthesizer in 2001 to the first commercial Glyconeer 2.1™ synthesizer,[44] AGA has been developed with the syntheses of glycans of mammalian, bacterial, and plant origin, including structures up to 50mer[i] length.[4,45]

1.2 The AGA Approach

In solid-phase synthesis, a solid support equipped with a linker is used to successively couple building blocks and assemble a growing oligomer chain. Monomers carry a temporary protecting group (tPG) that is removed from the resin-bound oligomer to allow for subsequent chain growth in the next coupling cycle. While this suffices for the solid-phase synthesis of nucleic acids and proteins, the complexity of carbohydrates is reflected in the solid-phase synthetic strategy. For oligosaccharide assembly, regio- and stereocontrol of the coupling is ensured by the appropriate selection of orthogonally-protected monosaccharide building blocks that carry a combination of temporary and permanent protecting groups (Figure 1.3).

[i] Recently, after the completion of the experimental work conducted for this thesis, structures up to 100mer length were assembled in the Seeberger group using AGA (unpublished results).

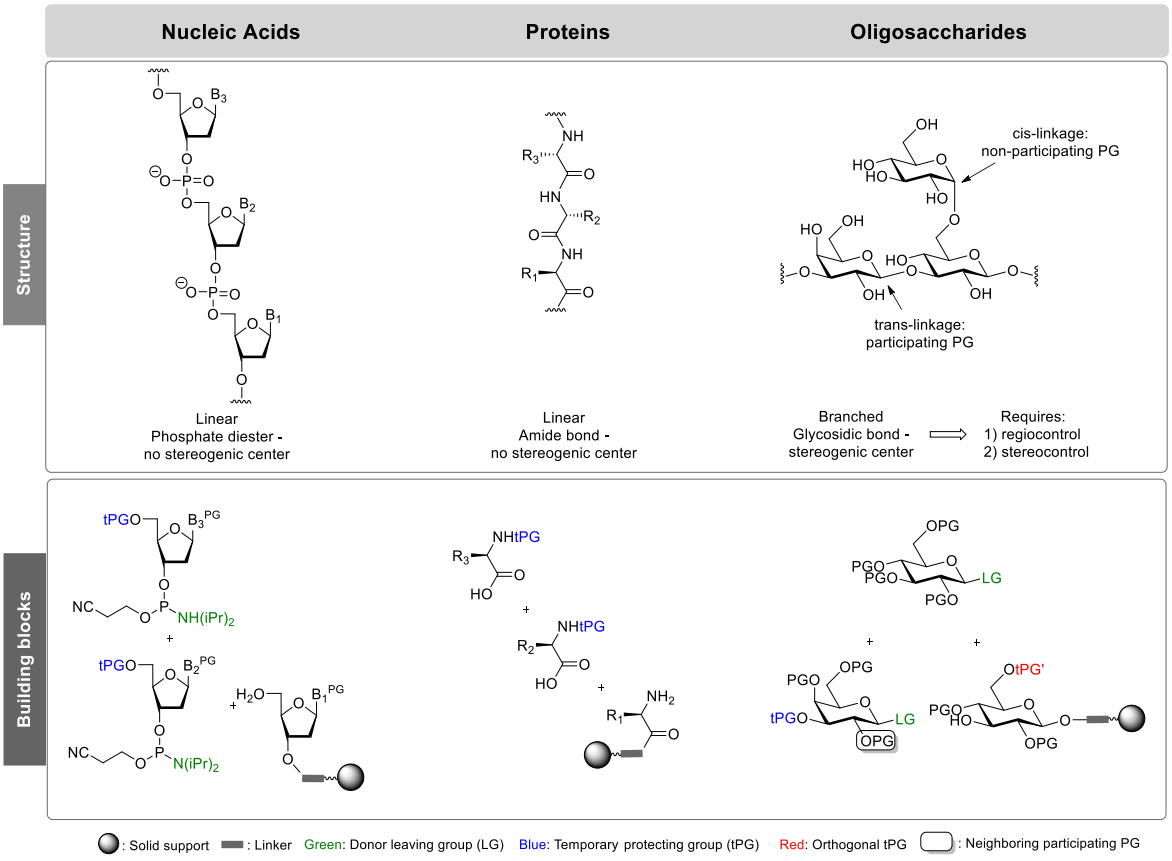

Figure 1.3. Solid-phase synthetic strategy depends on biopolymer structure.

The AGA oligosaccharide synthesis workflow is designed to minimize the number of purification steps and manipulations (Figure 1.4). Inside the synthesizer's reaction vessel, a resin-bound linker serves as an anchor to successively attach monosaccharide building blocks. In this way, excess reagents can be washed away and time-consuming intermediate purification steps can be avoided. After completion of the synthesis, the resin-bound oligosaccharide is removed from the synthesizer and the oligosaccharide is cleaved from the solid support. Analytical normal-phase high performance liquid chromatography (NP-HPLC) and MALDI analysis of the crude product after cleavage are used to qualitatively assess the synthesis success ('Control point 1', Figure 1.4). The protected glycan is purified using preparative NP-HPLC. Global deprotection removes all permanent protecting groups (PGs) and after reverse-phase HPLC (RP-HPLC) the unprotected glycan is obtained. The final product is characterized typically by ^{1}H, ^{13}C, 2D NMR, and HRMS ('Control point 2', Figure 1.4).

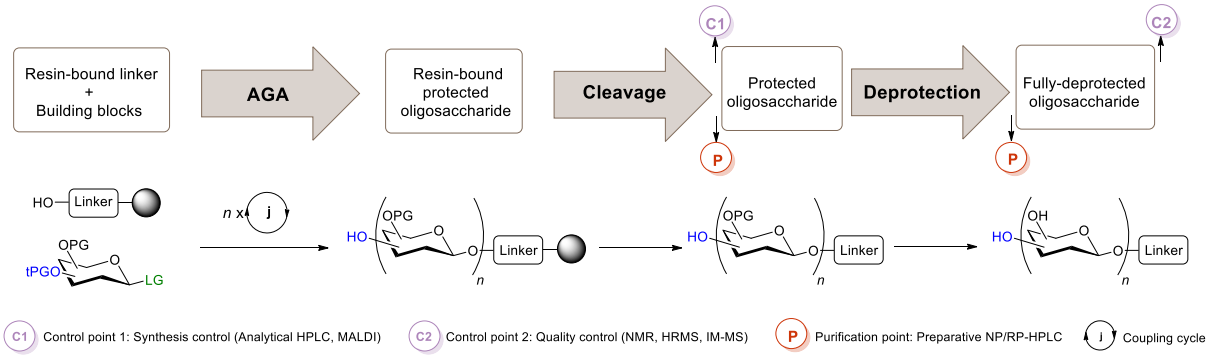

Figure 1.4. AGA oligosaccharide synthesis workflow.

AGA syntheses require careful selection of a compatible set of linker-functionalized solid support and building blocks (Figure 1.5). Merrifield polystyrene resin, a common solid support for peptide and oligonucleotide assembly, is used for its swelling and mechanical properties and chemical stability.[46,47] The linker has to be readily and effectively cleaved at the end of the synthesis, but has to withstand all reaction conditions including acidic glycosylation and basic deprotection conditions. Additionally, cleavage from solid support and global deprotection should render a convenient moiety at the glycan reducing end. 'Approved building blocks' for AGA are those that can be easily produced on large scale, are stable over long periods of time but upon activation react with high yield and stereoselectivity, and bear protecting groups that can be selectively and effectively removed.

1.2.1 Building Blocks

Building block selection is critical for AGA. The anomeric leaving group and protecting groups influence reactivity, stereoselectivity and regioselectivity of the building block as glycosyl donor and subsequently as nucleophile (glycosyl acceptor). Thioglycosides,[44,48] glycosyl phosphates[49,50] and glycosyl imidates[51,52] are commonly used in AGA (Figure 1.5). Stock solutions for the activation of these glycosyl donors (NIS/TfOH for thioglycosides, or TMSOTf for glycosyl phosphates and imidates) remain stable for several days when kept under argon on the synthesizer. Thioglycosides are particularly attractive for commercial use as they are bench stable over long periods of time.[53] In addition, thioglycosides generally react with reduced formation of hydrolized donor side product at temperatures around 0 °C. Building blocks that require very low glycosylation temperatures are inconvenient as they pose challenges to instrumentation and prolonged cycle times are required for cooling and warming.

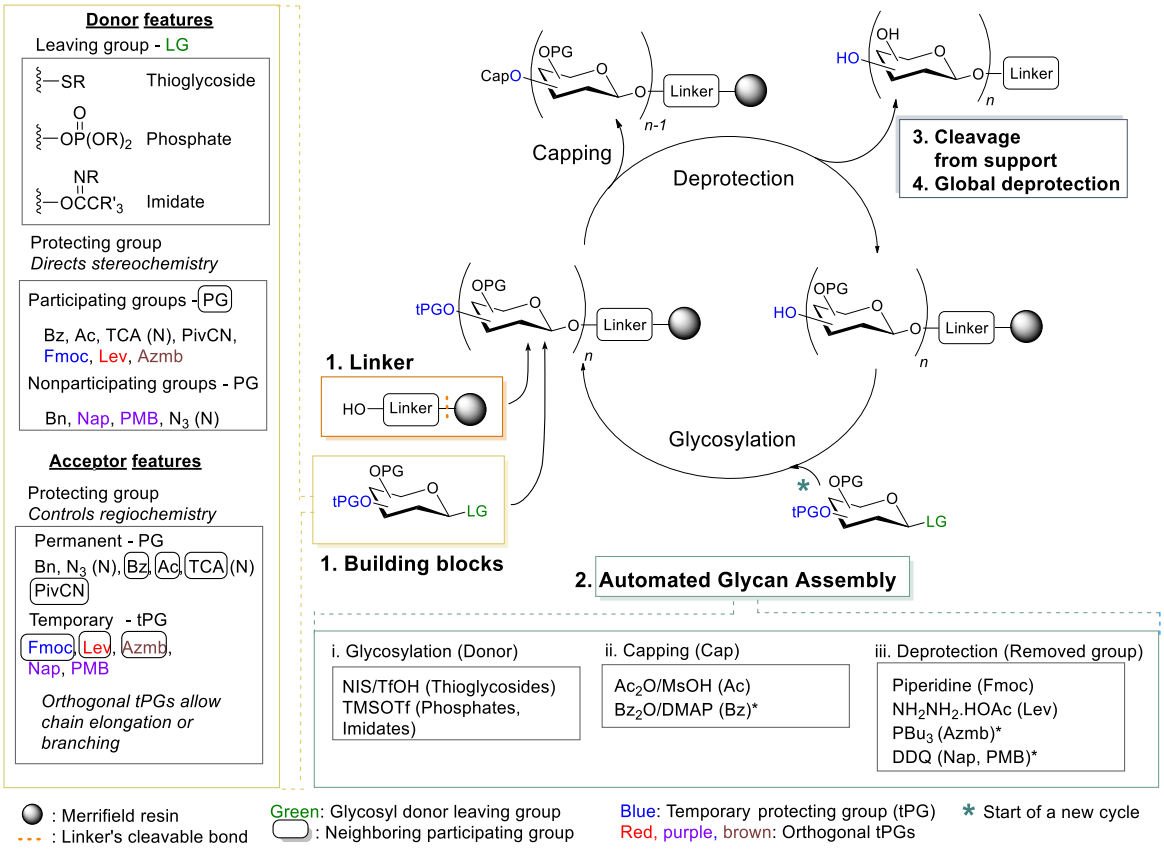

Figure 1.5. Summary of reactions and conditions commonly used for oligosaccharide synthesis. Commonly used leaving groups: R = Et, Tol, Ph (thioglycosides); R = Bu (phosphates); R = Ph, R' = F (imidates). Transformations indicated with "*" either of limited utility or have been tested only for a small number of glycans such that the scope remains to be fully determined.

In AGA, glycosylation stereoselectivity is directed by the selection of protecting groups in the glycosyl donor. Anchimeric assistance of participating groups at C2 hydroxyl is efficiently used to obtain 1,2-*trans* anomers. Nonparticipating groups at C2 are used to preferentially install *cis* glycosidic linkages, but do not allow for complete stereocontrol. Syntheses of 1,2-*cis* glycosides are achieved with aid of remote participating groups, and/or the influence of solvent and glycosylation temperature.[7,32,54]

The regioselectivity of the glycosylation reaction is controlled by protecting group selection in the acceptor. Permanent protecting groups are installed on hydroxyl groups that are present as free hydroxyls in the target molecule, and are removed by a global deprotection strategy after automated assembly. Temporary protecting groups (tPGs) are installed in hydroxyl groups that are involved in glycosidic linkages in the target molecule. Orthogonal tPGs are used for branching. Positions where modifications (*eg.* sulfatation) are present in the target molecule are protected with orthogonal tPGs as well.

Under the concept of 'approved building blocks', a minimum number of PGs are used in AGA (Figure 1.5). Benzyl (Bn) ether groups are used as permanent nonparticipating PG

and benzoyl (Bz) esters are used as permanent participating PG. Acetyl (Ac) esters are occasionally used for remote participation or to tune building block reactivity.[48] Recently, cyanopivaloyl (PivCN) was introduced as a participating group for the AGA of oligorhamnans.[51] Azido and trichloroacetyl (TCA) protecting groups are used as nitrogen nonparticipating and participating PGs, respectively. Permanent PGs are removed after AGA by methanolysis or hydrogenolysis.

2-Naphthylmethyl (Nap) ether, levulinoyl (Lev) ester, and 9-fluorenylmethyloxycarbonyl (Fmoc) carbonate groups serve as tPGs. They can be orthogonally deprotected using 2,3-dichloro-5,6-dicyano-1,4-benzoquinone (DDQ), hydrazine, and piperidine, respectively. The Fmoc protecting group is preferentially installed at positions meant for chain elongation, due to its fast deprotection (5 min) and the possibility of cleavage UV-monitoring. Levulinoyl ester is the orthogonal tPG of most extended use for branching. Syntheses including Nap tPG should be carefully designed, since occasional cleavage of primary benzyl groups was observed under Nap deprotection conditions.[55] To overcome this limitation, a *p*-methoxybenzyl (PMB) ether group was used instead of Nap as a nonparticipating tPG for the synthesis of galactosylated xyloglucans.[55] Its milder DDQ deprotection conditions were found compatible with the presence of primary benzyl ether groups. A 2-(azidomethyl)benzoyl (Azmb) ester was used as participating tPG for the AGA of arabinoxylans.[49] Azmb is chemoselectively removed with tributylphosphine and therefore adds an extra orthogonality degree to preexisting AGA tPGs.

1.2.2 Linker

Different linkers have been developed to enable diverse combinations of anomeric and protecting group schemes for AGA. Linkers should be regarded as support-bound protecting groups. Upon cleavage, linkers should render a suitable form of the glycan reducing end. Metathesis-labile linker **1.1** is cleaved under conditions that are chemo-orthogonal to the deprotection of temporary and permanent protecting groups, and furnishes an *n*-pentenyl glycoside that can serve as glycosylating agent (Figure 1.6). Use of **1.1** became infrequent as it is not compatible with electrophilic reagents required for thioglycoside activation.[56,57] Base-labile linker **1.2** affords a C5-aminolinker after treatment with sodium methoxide in methanol. In this way, conjugation-ready glycans for use in glycan arrays or glycoconjugates are readily obtained. Photolabile linker **1.3**, now commonly used in AGA, is fast, easily and chemoselectively removed by photocleavage in a commercial flow photoreactor, and affords conjugation-ready glycans after global deprotection.[58,59] Traceless linker **1.4**, a modified version of linker **1.3**, was developed to obtain glycans with a free reducing end.[60] The use of

chemo-orthogonal methods for cleavage from the solid support produces fully-protected oligosaccharides that are easier to purify using NP-HPLC conditions than the partially-protected glycans obtained after cleavage of a base-labile linker. Semi-deprotected glycans greatly vary in terms of solubility and polarity such that finding appropriate conditions for chromatographic separation is time-consuming and difficult to generalize. Photocleavable linkers offer strategical and practical advantages, but cleavage efficiency is affected by photochemical side-reactions.[61] The development of modified linkers with higher cleavage efficiency is key to furhter improve AGA.

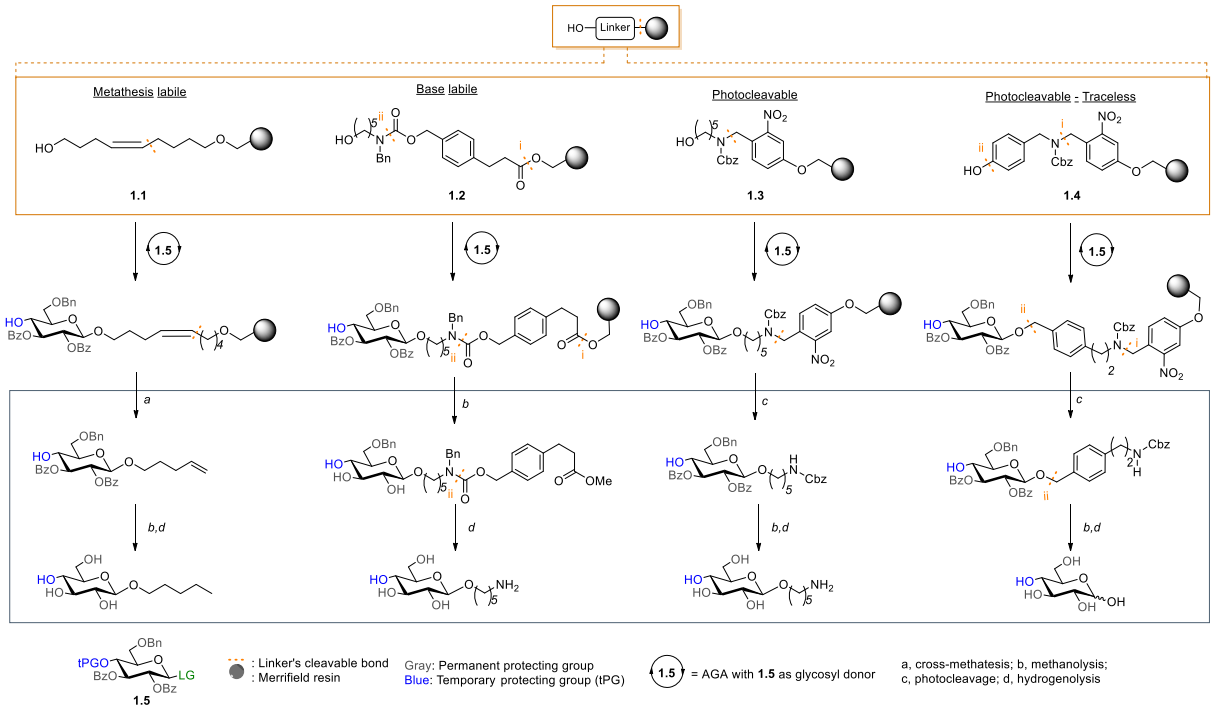

Figure 1.6. Linkers used for AGA. LG: -OP(O)(OR)$_2$, -OC(NR)CR'$_3$ for **1.1** or -SR, -OP(O)(OR)$_2$, -OC(NR)CR'$_3$ for **1.2**-**1.4**. Cleavage and deprotection conditions: a. Grubbs's catalyst, DCM; b. NaOMe/MeOH; c. flow photoreactor (UV 305 nm); d. H_2, Pd/C.

1.2.3 Automated Synthesis

The retrosynthetic analysis that precedes AGA is straightforward as it dissects the target glycan to identify building blocks based on monosaccharide identity (glucose, mannose, etc.), connectivity (1→4, 1→6, branching, etc.), and glycosidic linkage stereochemistry (α or β). An increasing number of 'approved building blocks' and linker-functionalized resins are commercially available.[62] The operator adds the linker-functionalized resin to the reaction vessel and attaches the bottles that contain the dissolved building blocks to the instrument. Building block solutions are freshly prepared with anhydrous solvent, but all other reagents and solvents can be used for several automated syntheses. After the operator selects a

program for coupling the building blocks according to the target sequence, a fully-automated assembly process is executed.

AGA is performed using the Glyconeer 2.1™ or home-built synthesizers. These instruments are similar to peptide synthesizers, but the temperature in the reactor can be controlled from -50 °C to +50 °C. Syntheses are currently performed at 12.5-45 μmol scales.[51,58,63] The addition of each monomer relies on a coupling cycle that consists of glycosylation, capping and cleavage of a tPG (Figure 1.5), as well as intermediate washing steps to remove excess reagents. Inside the reaction vessel, the first monosaccharide is attached via its reducing end to the resin-bound linker. Then, a temporary protecting group is removed, to unmask a hydroxyl group on the resin-bound oligosaccharide that will act as a nucleophile in the subsequent glycosylation step. A capping step between the glycosylation and deprotection steps minimizes the formation of side-products by preventing further reaction of deletion sequences that are the product of incomplete glycosylations. For each step, the automated synthesizer controls reagent delivery, temperature and time. The output line from the reaction vessel can be directed to a fraction collector, to recover the excess building block used to drive glycosylation reactions to completion. This set-up is particularly useful in homopolymer syntheses. Glyconeer 2.1™ tracks coupling efficiencies by UV-monitoring of dibenzofulvene, the product of Fmoc release.[44]

Until recently, capping was used rarely, to avoid further prolongation of already long synthesis times.[45] A fast, mild, and quantitative capping protocol based on Ac_2O/MsOH now [ii] allows for capping to be performed in every coupling cycle and can be incorporated in most AGA syntheses.[64] A more time-consuming capping method that incorporates benzoate esters offers an alternative when acetyl caps are not suitable due to acetyl cleavage or migration in subsequent steps.[65,66]

1.2.4 Postautomation Operations

After AGA, cleavage from the solid support is performed according to the linker used (see Section 1.2.2), and the protected oligosaccharide is purified using NP-HPLC. If no further modifications are required, the protected oligosaccharide is globally deprotected to remove all permanent PGs. A combination of methanolysis followed by hydrogenolysis is suitable for the removal of all permanent PGs of common use in AGA. After hydrogenolysis RP-HPLC purification renders the final oligosaccharide. As larger or more complex oligosaccharides are synthesized through AGA, difficulties in deprotection arise due to solubility issues.[67]

[ii] The protocol was developed simultaneously to the experimental work in AGA conducted for this thesis.

1.3 Scope of AGA

Constant improvement in methods and synthesis protocols enabled access to a large number of fully-deprotected glycans was possible through AGA (Figure 1.7). Major classes of mammalian carbohydrates have been synthesized. The synthesis of poly *N*-acetyllactosamine required efficient glycosylation methods to incorporate GlcNAc,[68] which is a challenging monosaccharide both as glycosyl donor and acceptor.[69] Adequate AGA-sulfatation strategies and glycosylations involving uronic acids were implemented for the syntheses of glycosaminoglycans (GAGs) such as keratan sulfates,[68] dermatan sulfates[70] and hyaluronan.[71] The identification of appropriate glycosylation conditions for the installation of multiple *cis*-glycosidic linkages was key to the synthesis of globoside oligosaccharides and α-galactosyl epitopes, and for the initial work in lactoside oligosaccharides.[48,54] A wide variety of microorganism-related glycans also were obtained through AGA. This includes polyglucosides such as α-, β-glucans and dextran;[54,67] GlcNAc oligomers like chitin and β-1,6-poly-*N*-acetylglucosamine (PNAG);[67] mycobacterial arabinofuranosides;[72] α-oligorhamnans;[73] and α-mannans.[45,67] Moreover, AGA was used to synthesize defined frameshift sequences from the capsular polysaccharides of *Streptococcus pneumoniae* serotypes 3 and 8.[6,74] β-mannosidic linkages were implemented in the syntheses of mannuronic acid alginates,[75] but to date there are no examples of highly stereoselective β-mannosylations by AGA.[76] This type of linkage remains challenging as neither neighbouring group participation nor anomeric effect can be used to obtain the desired anomer.

Plant carbohydrates such as polyglucosides amylose, cellulose, and mixed-linkage glucans are also part of the AGA catalogue.[50,54,67] AGA helped to generate plant glycan libraries of type-I and type-II arabinogalactans and arabinoxylans.[49,63,65,66] Arabinogalactans feature multiple challenging β-(1,4)-Gal linkages and arabinoxylans have diverse branching patterns, including disubstituted xylose residues. This illustrates the versatility of AGA to generate linkages involving hydroxyl groups that are poorly nucleophilic or hindered with high yield and stereoselectivity. AGA of a 50mer polymannoside is the longest published synthetic glycan assembled from monosaccharides.[45] Recent improvements in AGA methods, like optimization of coupling cycles to reduce the amount of time and solvent required,[67] and a capping procedure based on Ac_2O/MsOH were tested on the polymannoside 50mer synthesis,[iii] resulting on an increased yield with reduced synthesis time.[64]

[iii] Developed simultaneously to the experimental work in AGA conducted for this thesis.

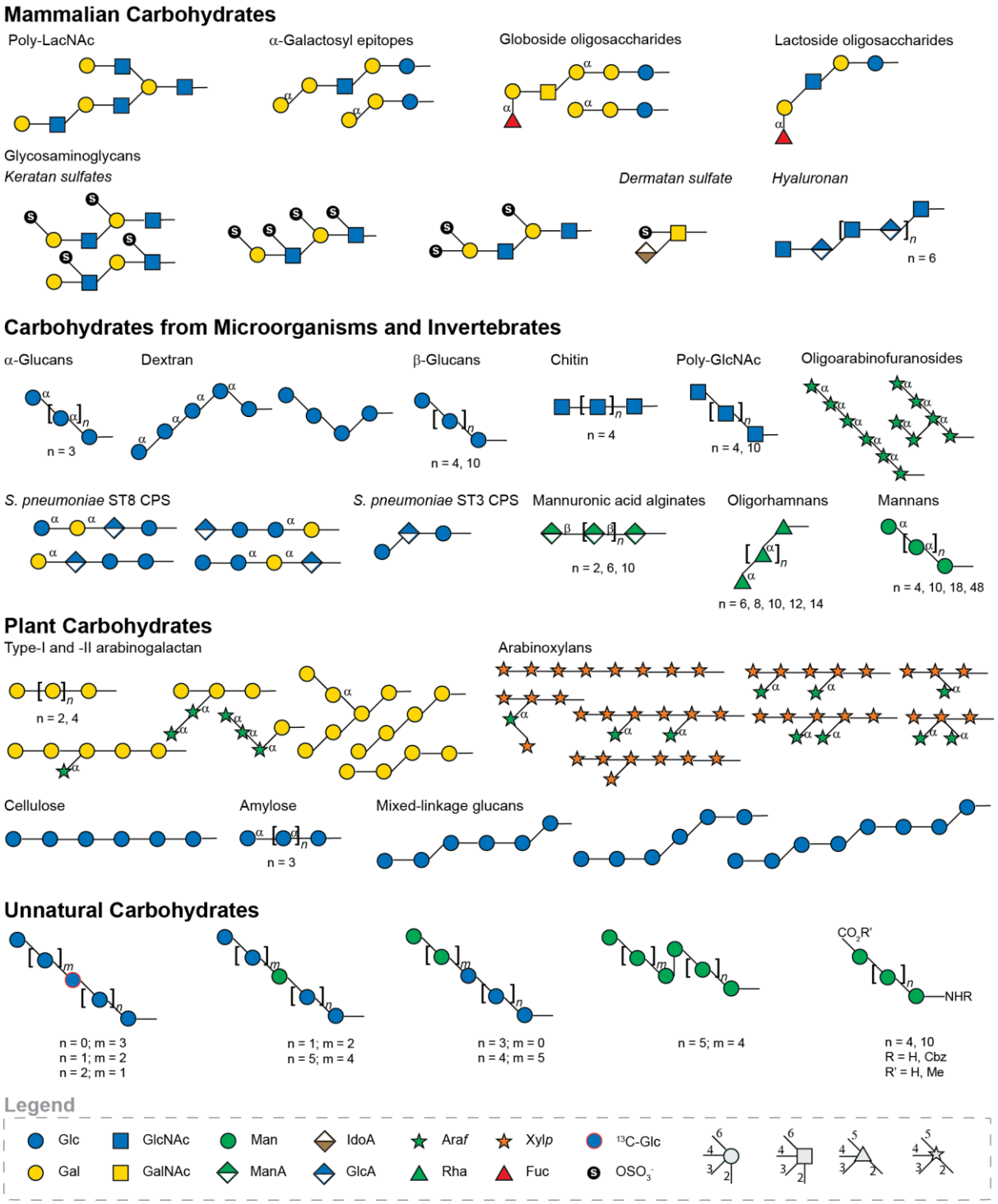

Figure 1.7. Representative structures of oligosaccharides synthesized using AGA. The stereochemistry of the glycosidic linkage is β for pyranoses with *gluco* configuration and α for pyranoses with *manno* configuration at C2, unless indicated otherwise. Glc, glucose; GlcNAc, *N*-acetylglucosamine; Gal, galactose; GalNAc, *N*-acetylgalactosamine; Man, mannose; IdoA, iduronic acid; ManA, mannuronic acid; GlcA, glucuronic acid; Ara*f*, arabinofuranose; Xyl*p*, xylopyranose; Rha, rhamnose; Fuc, fucose; ^{13}C-Glc, ^{13}C-labelled glucose. Structures are represented following the Symbol Nomenclature for Glycans (SNFG),[77] see page 7.

High yields and stereoselectivities for glycosylations are key to the success of an AGA synthesis. The construction of certain linkages remains challenging. In those cases, synthetic strategies that combine AGA to accelerate construction of a glycan backbone or a glycan segment, together with other techniques to install the challenging glycosidic linkage can be employed (Figure 1.8). The difficulties derived from poor stereoselectivity in the AGA of α-xylosidic linkages were bypassed by using a disaccharide BB for the AGA of xyloglucans and galactosylated xyloglucans (Figure 1.8, A).[55,59] Solution-phase xylosylation followed by purification of the anomeric mixture was used to obtain a disaccharide glycosyl donor containing exclusively the desired α-xylose.

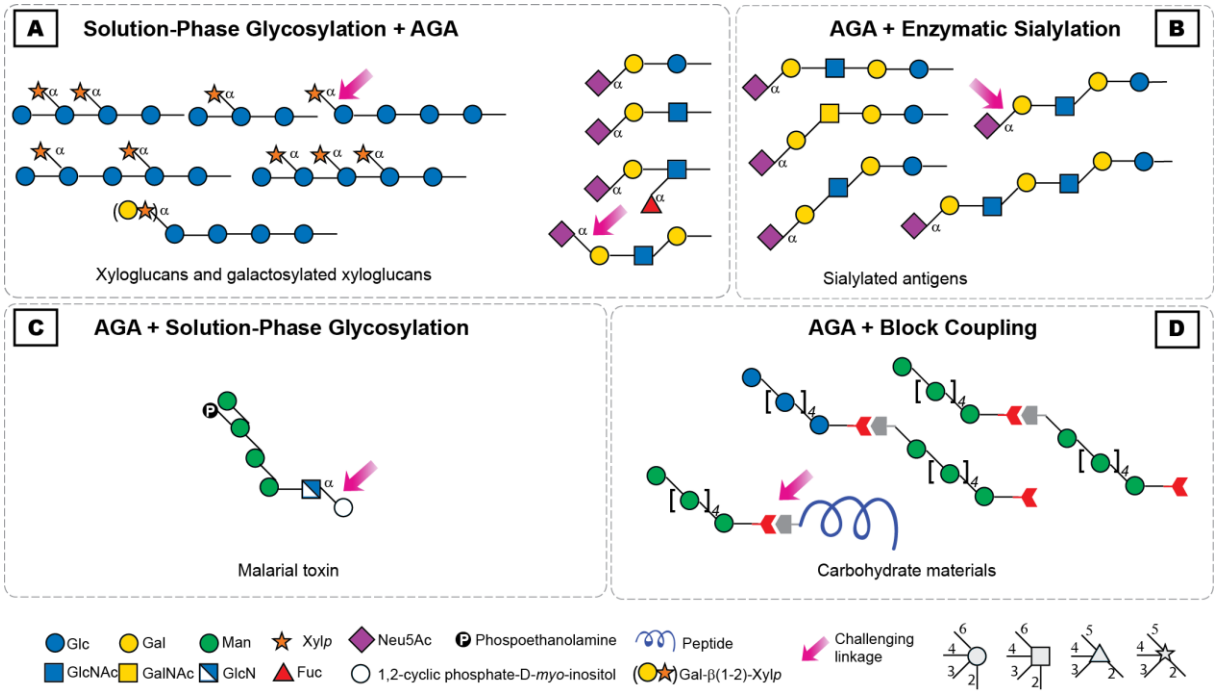

Figure 1.8. Selected oligosaccharides assembled using AGA in combination with other techniques. Structures are represented following the SNFG nomenclature,[77] see page 7. The stereochemistry of the glycosidic linkage is β for pyranoses with *gluco* configuration and α for pyranoses with *manno* configuration at C2, unless indicated otherwise. Neu5Ac, *N*-acetylneuramic acid. Challenging linkages for AGA are indicated by a pink arrow. A) Solution phase glycosylation is used to install a challenging linkage in a disaccharide that will serve as a building block for AGA. B) AGA is used to generate a variety of structures that serve as substrates for enzymatic sialylation. C) AGA provides rapid access to a tetrasaccharide donor, which is then coupled in solution phase to a myo-inositol-containing acceptor. D) Fragments obtained as AGA are used as scaffolds for the syntheses of carbohydrate materials using block coupling.

Sialosides are important mammalian glycans that mediate pathogen host-interactions, cell-signaling processes, and the immune response.[2] Sialic acids are nine-carbon monosaccharides bearing a carboxylic acid at C1. High-yielding, stereoselective chemical sialylation is troublesome since the anomeric center is an unreactive quaternary carbon

adjacent to the C1 carboxyl electron-withdrawing group. Moreover, no participating group can be placed at C3 to favor the desired α-stereoselectivity. Different AGA methods were tested for the syntheses of sialosides. Sialyl α-(2,3) and α-(2,6) galactosyl imidates were employed as disaccharide building blocks for the AGA of sialosides including tetrasaccharide sialyl Lewis^x (Figure 1.8, A).[52] Protected sialyl α-(2,3) and α-(2,6) di- and trisaccharides were obtained through an AGA-only glycosylation strategy using 4*O*,5*N*-oxazolidinone *N*-acetylneuramic acid (Neu5Ac) derivatives as sialyl donors.[78] Satisfactory results were achieved for the AGA of some α-(2,6) sialosides, but for α-(2,6) sialosides with GlcNAc in the backbone and for α-(2,3) linkages the glycosylation efficiencies remain significantly lower than those obtained for other couplings. Those target structures are among the less reactive acceptors, as the TCA protecting group in GlcNAc is electron-withdrawing and the C3 hydroxyl in galactose (in α-(2,3) sialosides) is less reactive than the primary C6 hydroxyl. An alternative approach combines AGA with enzymatic sialylation (Figure 1.8, B). Linear oligosaccharides obtained by AGA, bearing a C5-aminolinker at the reducing end, served as substrates for enzymatic sialylation with α-(2,3)-sialyltransferase and cytodine monophosphate (CMP)-Neu5Ac.[79]

Fast access to parasite glycosylphosphatidylinositol (GPI) glycans is pivotal for the research for a malaria vaccine candidate.[80] A method for generating the required α-linkage between inositol and glucosamine in AGA is not yet available. Thus, a tetra-mannosyl fragment was rapidly prepared using AGA and then converted into a glycosyl donor for solution-phase coupling to an inositol-containing disaccharide (Figure 1.8, C).[81]

Oligosaccharides obtained via AGA can be combined through block-coupling for the reaearch of tailor-made carbohydrate materials (Figure 1.8, D).[67] The covalent link between oligomer blocks was achieved in solution phase by coupling of amino and carboxylic acid groups placed at the termini of each block. The same strategy was used to produce glycan-peptide hybrid materials. This glycan-peptide hybrid differs from the glycopeptide previously synthesized in the AGA-dedicated synthesizer.[82] Coupling through amide bonds in AGA was so far only applied to link amino acids, as a proof-of-concept and in a reduced number of examples. Further development is required for future fully-automated assembly of hybrid materials.

1.4 Synthetic Glycans as Molecular Tools

Defined oligosaccharide structures find a wide range of applications, from addressing fundamental questions of glycan biological function, to the development of instrumental techniques and the production of novel materials. Glycans synthesized via AGA have been employed in diverse experimental setups, including the study oligosaccharide structure-

property relationships, enzyme characterization, and the research of disease diagnostics and therapeutics.

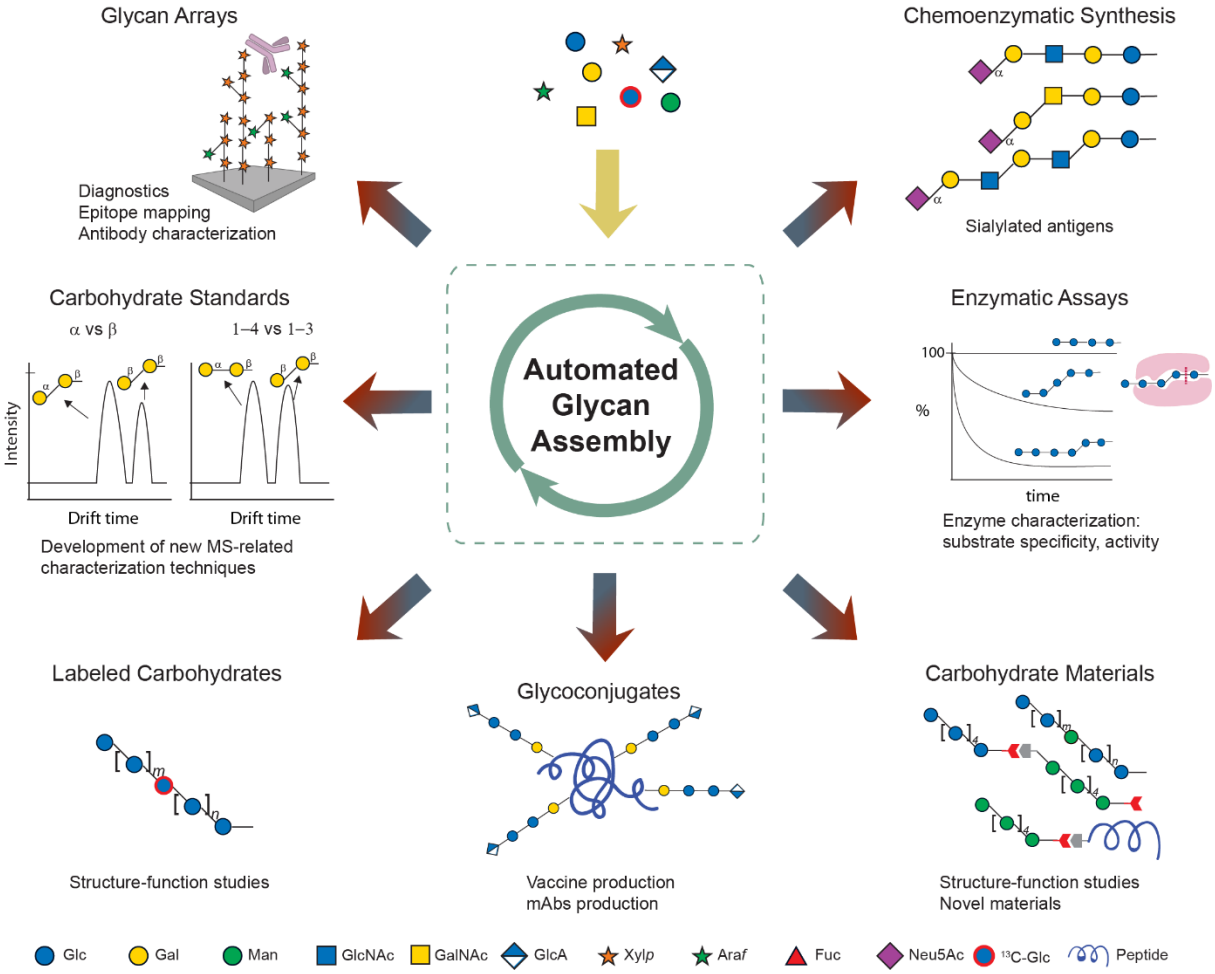

Figure 1.9. Applications of oligosaccharides synthesized by AGA. Structures are represented following SNFG nomenclature,[77] see page 7.

1.4.1 Glycan Arrays

In a glycan array, oligosaccharides are immobilized on a slide that serves as solid support. This results on a spatially-defined arrangement of diverse carbohydrate sequences that allow high-throughput screening of carbohydrate-binding macromolecules.[83] Binding of soluble proteins, whole viruses, bacteria, yeast or mammalian cells can be screened.[84] AGA is an ideal technology for generating glycan libraries for arrays, since a whole family of carbohydrates with different lengths and substitution patterns can be produced using a set of monosaccharide building blocks and by only introducing changes in the glycosylation program (Figure 1.9). AGA-produced glycans bearing a C5-aminolinker are ready for covalent immobilization on commercially available slides that are functionalized with *N*-hydroxysuccinimide (NHS) esters or epoxides.[84,85] A glycan array containing keratan sulfate

GAGs served to identify keratan sulfate as a receptor candidate for a viral gene-therapy vector.[68] Synthetic arabinoxylans, xyloglucans and galactosylated xyloglucans with custom-made substitution patterns helped determining the binding specificities of several monoclonal antibodies (mAbs) commonly used for immunolabelling studies of plant cell walls.[55,63] Different frameshifts of native *S. pneumoniae* ST8 CPS synthesized by AGA were placed on glycan arrays for mAb epitope mapping, a key step for the identification of protective glycotopes.[6]

1.4.2 Glycoconjugates

Oligosaccharides obtained by AGA using linkers **1.2** or **1.3** are readily conjugated to functionalized surfaces (see above, section 1.4.1), small molecules such as fluorescent probes (see below, section 1.4.3), and carrier proteins (Figure 1.9). Semisynthetic vaccine candidates may confer protective immune responses against infectious diseases. Based on microarray glycotope screening, a *S. pneumoniae* ST8 CPS sequence was selected for conjugation to CRM_{197} carrier protein, immunization studies, and mAb production for the identification of protective glycotopes.[6] Combination of the glycoconjugate with the pneumococcal vaccine Prevnar 13™ resulted in a 14-valent coformulation that generated a robust antibacterial immune response against ST8 without undermining the immunogenicity of Prevnar 13™. AGA was used to synthesize fragments of *S. pneumoniae* ST3 CPS that are tested as vaccine candidates.[74]

1.4.3 Enzymatic Assays

Synthetic glycans are useful tools for active site mapping and to determine the substrate specificity of enzymes such as hydrolases and transglycosylases. Arabinoxylans, arabinogalactans and mixed-linkage glucans obtained through AGA were applied for determining substrate specificity of xylan-deconstructing enzymes,[49] endogalactanases[66] and lichenase.[50] To this end, tailor-made carbohydrates with specific substitution patterns were used as enzyme substrates and time-course experiments and HPLC analysis of digestion products were performed.

HPLC analysis of the products of the enzymatic reaction of xyloglucan sequences were used to probe the acceptor-substrate specificity of a xylosyltransferase. In addition, the synthetic, conjugation-ready xyloglucans were coupled to fluorescein (FC) to evaluate the activity of plant xyloglucan endo-transglycosylases on glycan arrays.[86] Furthermore, *in muro* experiments showed that synthetic FC-labelled xyloglucans were incorporated into plant sections.

1.4.4 Chemoenzymatic Synthesis

Sialylated glycans were obtained using AGA-synthesized oligosaccharides combined with enzymatic synthesis (see above). It was shown that linear oligosaccharides bearing a C5-aminolinker are suitable substrates for α-(2,3) enzymatic sialylation.[79] The extension of this methodology to branched fucosylated oligosaccharides and α-(2,6) sialosides is under study.

1.4.5 Labeled Carbohydrates

Linear β-(1,6) glucose hexasaccharides were prepared using a standard building block and its ^{13}C-labelled analogue by placing the ^{13}C-labelled monosaccharide at different positions in the sequence.[67] Thereby, chemical shifts corresponding to specific monosaccharides could be identified and structural information from the coupling constants $^{1}J_{H1C1}$ and $^{3}J_{H1H2}$ was obtained. Rapid access to labeled glycans by AGA offers new tools to gain conformational and geometric information from synthetic glycans.

1.4.6 Carbohydrate Standards

Synthetic glycans served as standards for developing ion mobility spectrometry - mass spectrometry (IM-MS) as a glycan characterization technique.[87] In IM-MS, molecules are separated according to their mass, charge, size and shape. The analysis of synthetic trisaccharide standards showed that IM-MS can differentiate carbohydrate connectivity and anomeric stereoisomers, a feat that cannot be achieved by simple MS techniques (Figure 1.9). IM-MS detects as little as 0.1% of a minor isomer in a mixture quickly, while requiring minute amounts of sample without prior derivatization. Therefore, IM-MS has the potential to replace time-consuming and sample-demanding NMR experiments for the full characterization of oligosaccharides.

1.4.7 Carbohydrate Materials

Oligosaccharides were combined through block-coupling to create tailor-made carbohydrate materials and glycan-peptide hybrids (Figure 1.9).[67] Structural studies revealed that single-site substitutions on homooligomer chains can dramatically impact their conformation. The production of novel carbohydrate materials based on changes in monomer substitution and the combination of different blocks is currently being investigated.

1.5 Aim of this Thesis

The aim of this thesis was to develop methods to further expedite carbohydrate synthesis, and to provide access to synthetic glycans for their use as molecular tools. Within this frame, two projects were executed to address distinct bottlenecks in glycan synthesis.

The first project concentrated on expediting the oligosaccharide assembly (Figure 1.2, step 2) of Lewis antigens, a family of complex glycans highly demanded for diverse biological studies. The focus was set on developing a method that, with a minimum set of orthogonally-protected monosaccharide BBs and by means of AGA, would provide access to a whole family of structurally-related glycans (Chapter 2). Conjugation-ready glycans were produced for their use as molecular tools. Of special interest within the Lewis family was tumor-associated carbohydrate antigen (TACA) KH-1, a branched nonasaccharide containing three α-linkages, which was synthesized for its application in the research of cancer therapy.

While under the concept of 'approved' building blocks an increasing number of BBs are commercially available, for some glycans the bottleneck still remains in BBs synthesis (Figure 1.2, step 1). A solution to a persistent limitation in galactosamine (GalN) building block synthesis was developed (Chapter 3). GalN BBs are required for the synthesis of mammalian and bacterial oligosaccharides. A key step during BB synthesis is the azidophenylselenylation (APS) of 3,4,6-tri-*O*-acetyl-D-galactal to prepare the corresponding 2-nitrogenated glycoside. Poor reproducibility and the use of azido reagents, that lead to the production of potentially explosive and toxic species, limits this reaction on larger scales in batch. A continuous flow procedure for the safe and scalable APS of galactal was established.

2 Automated Glycan Assembly of Lewis Type-I and Type-II Chain Oligosaccharides

Part of this chapter has been modified from: Guberman, M.;[i] Bräutigam, M.;[i] Seeberger, P. H. Automated glycan assembly of Lewis type I and II oligosaccharide antigens. *Chem. Sci.* **2019**, *10*, 5634–5640.[88] https://doi.org/10.1039/C9SC00768G. Reproduced in part from Ref. 88 with permission from the Royal Society of Chemistry.

[i] These authors contributed equally.

2.1 Introduction

Lewis antigens are a family of fucosylated glycans which are commonly found as glycoproteins or glycolipids on the cell surface of many eukaryotic cells.[2] They are related to the ABO blood-group system, associated to developmental processes, reproductive physiology, oncogenic transformations, cell-cell communication and pathogen-host interactions.[89–94] Structurally, Lewis type-I chain antigens **2.1**-**2.3** are fucosylated versions of a lactotetraosyl core (Lc_4, **2.4**). In the same way, type-II chain Lewis antigens **2.5**-**2.7** are the fucosylation products of a neolactotetraosyl (nLc_4, **2.8**) core (Figure 2.1). They only differ from their type-I chain analogues on the regiochemistry of the glycosidic linkage in the *N*-acetyllactosamine (LacNAc) subunit (β(1-3) vs β(1-4)).

Despite their structural similarity, Lewis antigens can be implicated in diverse physiological and pathological processes. While the importance of blood group antigens for blood transfusions and transplantation is established,[95] their involvement in infectious diseases and cancer development are active research areas. Lewis^b (Le^b) **2.3** is key to the initial adhesion to gastric epithelium of *Helicobacter pylori*, the main etiological agent for chronic gastritis and gastroduodenal ulcers.[89,96] On the other hand, its type-II chain analogue Lewis^y (Le^y) **2.7** is a tumor-associated carbohydrate antigen (TACA), known to be overexpressed in the cell surface several types of cancer.[97–99] Extended chain versions of Lewis antigens (Figure 2.1) such as Le^x-dimer (Le^x-Le^x, **2.9**) and KH-1 (Le^x-Le^y, **2.10**) are TACAs associated with colorectal cancer and are especially appealing in the tumor immunotherapy research area.[100,101]

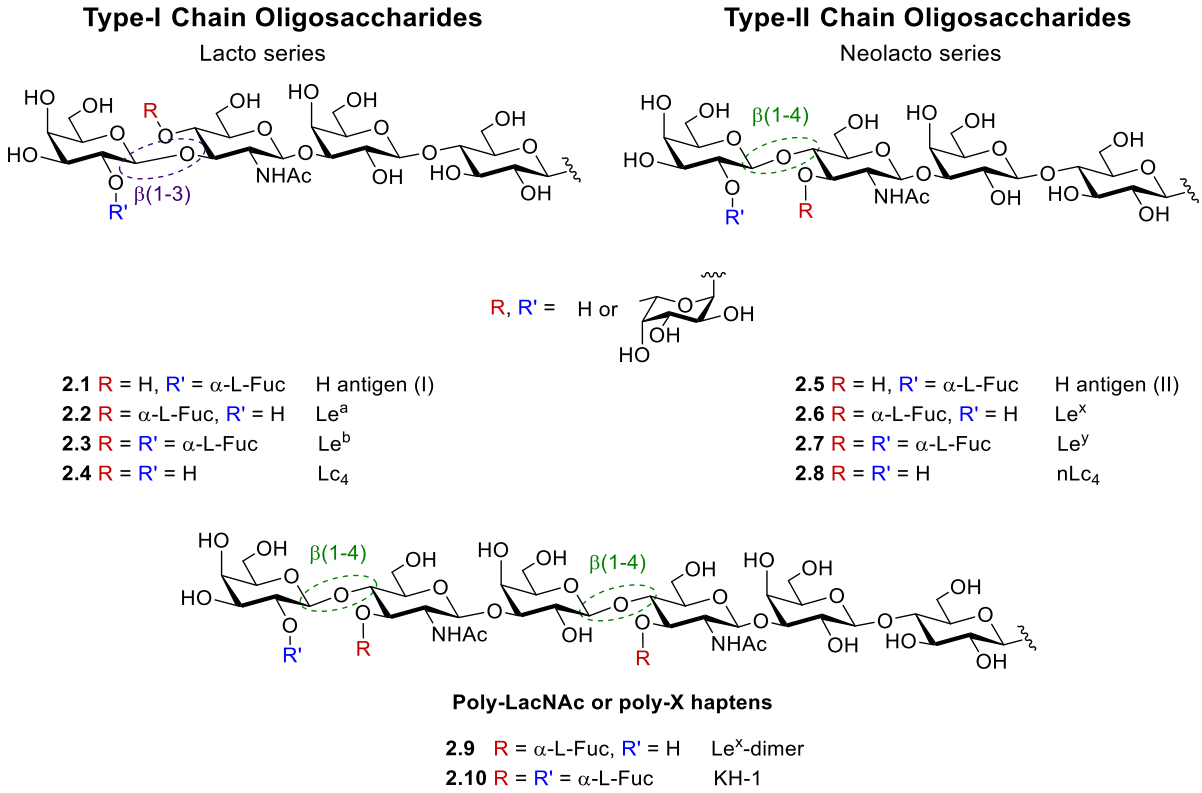

Figure 2.1. Lewis type-I and type-II chain oligosaccharides.

2.1.1 Tumor Associated Carbohydrate Antigens and Cancer Immunotherapy

Cancer is a leading cause of morbidity and mortality worldwide. By 2025, the number of new cancer cases per year is estimated to be over 20 million.[102] Currently available cancer treatments such as chemotherapy and radiation therapy have major limitations, due to a lack of selectivity and resistance.[103] Emerging immunotherapeutic approaches are characterized by the unique specificity, potency and memory of the immune system.[104]

The human immune system can identify and eradicate tumor cells by recognizing tumor antigens.[105,106] Carbohydrate antigen-based immunotherapies capitalize on the fact that tumor cells express modifications in cell-surface carbohydrate profiles when compared to healthy progenitor cells. These aberrant oligosaccharide structures are known as TACAs.[107–109] The TACA KH-1 (**2.10**) is of special interest for glycan-targeted therapies for colorectal cancer. Preliminary results indicate that this TACA is an attractive alternative to overcome the low immunogenicity observed in human trials when using shorter antigens like Le^y.[100,110–112] Access to antibodies against KH-1 (**2.10**) is of interest for the development of diagnostics and therapeutics tools for colorectal cancer. Besides the application of monoclonal antibodies (mAbs) for passive immunization approaches,[113] an emerging research area is the development of nanobodies (Nbs). Nbs are are the smallest intact functional antigen-binding

fragment of heavy-chain only antibodies, a type of immunoglobulins found in camelids.[114] They are about half the size of the smallest functional antigen-binding fragment of conventional antibodies. These small, soluble antibodies are nonimmunogenic, offer high tissue penetration, can present different binding specificities than traditional antibodies, and have a short half life, which makes them suitable for a wide variety of applications including use as cargo for therapeutics, and *in vivo* imaging.[115]

2.1.2 Project Aim

Synthetic access to oligosaccharide antigens is essential as isolation of useful amounts of pure glycans from biological sources is difficult.[116] Numerous publications aimed to provide access to different synthetic Lewis antigens for diverse applications, including the study of cell-protein interaction, diagnostic tools or immunotherapeutic treatments.[112,117,118] Synthetic approaches include solution-phase, solid-phase and automated synthesis.[48,119–122] Despite their wide range of potential applications and their structural similarity, Lewis antigen syntheses have been so far mainly limited to total synthesis of single structures.[123–125]

I wanted to develop a general method for the syntheses of a collection of Lewis antigens (Figure 2.2). The lacto- and neolacto-series target molecules differ in three structural aspects: the presence or absence of fucose on the terminal galactose; the presence or absence of fucose on GlcNAc, and the β(1–3) or β(1–4) linkage in the LacNAc subunit. The logic of automated glycan assembly (AGA) is based on the selection of a minimum set of monosaccharide building blocks to assemble all targeted glycans via a linear glycosylation and deprotection sequence. AGA reduces the synthesis time considerably (see section 1.2) and should facilitate the assembly of large, complex antigens such as **2.9** or **2.10**. Access to lacto- and neolacto-series variants that carry a linker for conjugation allows them to be used as tools for diverse biological applications. In particular, KH-1 **2.10** was used as a glycoconjugate for alpaca immunization, *en route* to the development anti-KH-1 nanobodies.

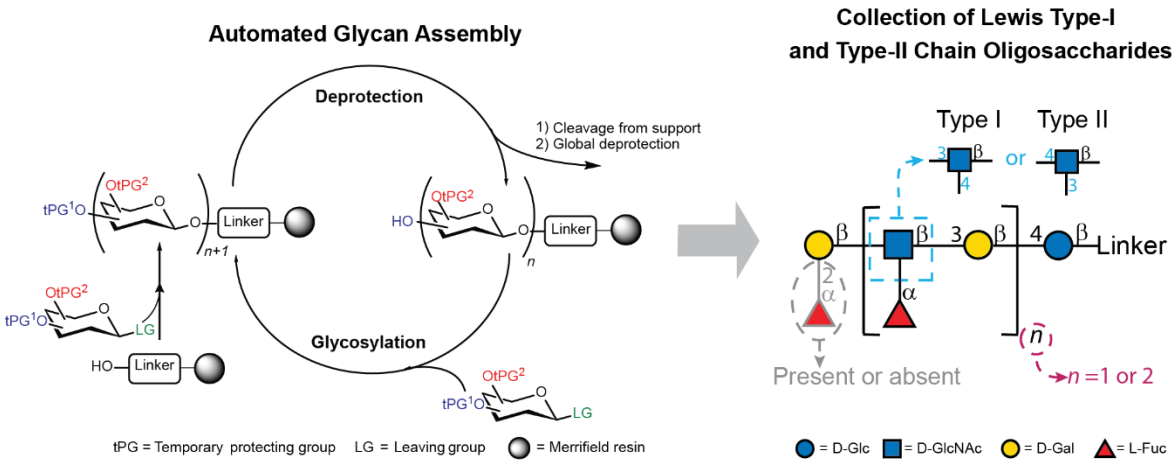

Figure 2.2. Overview on the research aims described in this chapter.

2.2 Results and Discussion

2.2.1 Building Block Design and Synthesis

For the design of building blocks, a retrosynthetic analysis was performed on conjugation-ready KH-1 (**2.11**, Figure 2.3), the target oligosaccharide of highest complexity. The use of Merrifield resin equipped with photocleavable linker **2.12**[i] enables access to conjugation-ready glycans, after cleavage from the solid support and global deprotection. Building blocks **2.13**-**2.17** were selected based on the concept of 'approved' building blocks for AGA (section 1.2).

[i] Provided by Dr. Kim Lemaihoang.

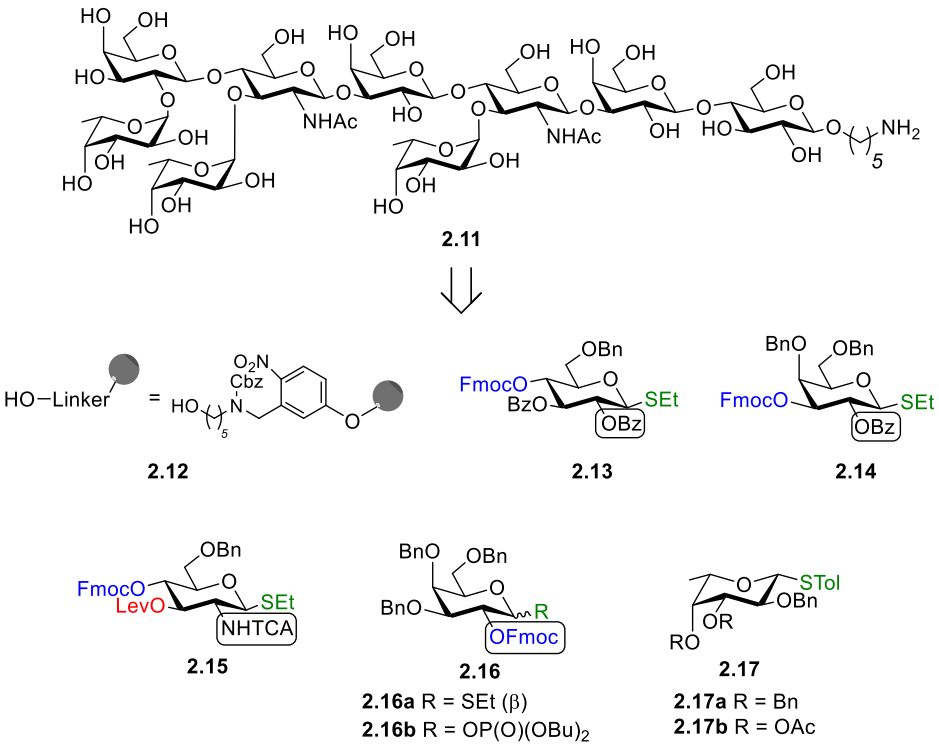

Figure 2.3. Building blocks for the AGA of Lewis antigens.

Thioglycosides were chosen as glycosyl donors as they can be easily synthesized on large scale and are stable over long periods of time. β-Thioglycosides are desired due to their higher reactivity.[126] Hydroxyl groups of building blocks **2.13**-**2.17** that engage in chain elongation were temporarily protected as Fmoc carbonates. A levulinoyl (Lev) ester masked the C3 hydroxyl in GlcNAc **2.15** as orthogonal tPG. Benzyl (Bn) ether and benzoyl (Bz) esters, were used as permanent nonparticipating and participating PGs, respectively. The amine of GlcNAc **2.15** was protected as an *N*-trichloroacetyl (TCA) group to ensure β-selectivity. After AGA and cleavage from the solid support, the permanent PGs could be removed by methanolysis (Bz) and hydrogenolysis (TCA, Bn and Cbz). Two different fucose building blocks **2.17a** and **2.17b** were chosen for preliminary glycosylation studies in AGA. According to the principles of building block design for AGA, perbenzylated building block **2.17a** should be adequate for the assembly of all fucose units present in the target oligosaccharide. However, previous work on linear Lewis oligosaccharides indicated that, for a given fucosyl donor, the stereoselectivity achieved dependended strongly on the structure of the acceptor chain.[48] As the influence of penultimate fucosyl residue on glycosylation of terminal fucose unit within the proposed oligosaccharide synthesis was unknown, AGA using both **2.17a** and **2.17b** was tested.

2.2.1.1 Synthesis of a Galactose (1-3) Building Block

Building block **2.14**[87] requires the regioselective protection at the C2 hydroxyl with a group capable of engaging in neighboring group participation during glycosylation reaction, and regioselective protection at the C3 hydroxyl for chain elongation. The synthetic route chosen for this purpose relies on the regioselective protection at C3 of a benzylidene-protected monosaccharide. The main difficulty in the synthesis of building block **2.14** was finding a convenient synthetic route for the selective introduction of a Fmoc group in C3 hydroxyl, as due to Fmoc relative lability under basic conditions, it cannot be installed at an early step in the synthetic route. This means that an additional temporary protecting group must be selectively introduced at C3 first.

For the regioselective protection at C3, two major routes involving benzylidene acetal **2.18** were considered. Regioselectivity can be achieved via a stannylene ketal intermediate that enhances the nucleophilicity of O3 ('route a', Scheme 2.1). Alternatively, a bulky protecting group as *tert*-butyldimethylsilyl (TBS) can be selectively placed at C3 hydroxyl due to steric hindrance ('route b', Scheme 2.1). Route *a* via a stannylene acetal derivative includes a relatively low-yielding step for the synthesis, counts with practical difficulties for monitoring stannylene acetal formation, and uses a toxic reagent. On the other hand, the drawbacks of route *b* reside in that the use of bulky TBS drastically elongates reaction times, and that TBS at a secondary hydroxyl is prone to migration. As AGA coupling cycles require excess of glycosyl donor, both strategies were attempted to determine which one was more suitable for the large scale synthesis of **2.14**.

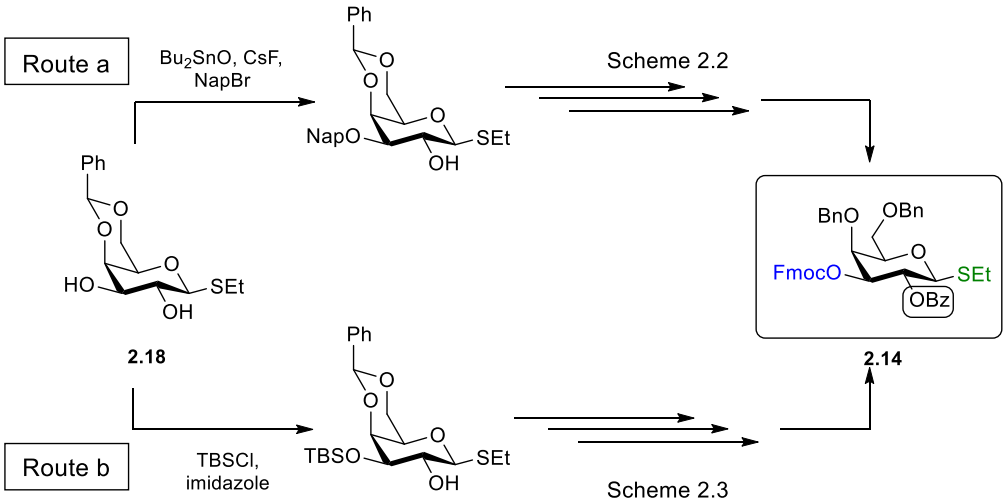

Scheme 2.1. Evaluated synthetic routes to building block **2.14**: stannylene-mediated route ('route *a*'), and TBS-mediated route ('route *b*').

Benzylidene acetal **2.18** was synthesized in three steps starting from peracetylated galactose (Scheme 2.2).[127] Regioselective protection of **2.18** to afford **2.19** was first attempted following a procedure described in the literature for the glucose analogue, in which the stannylene ketal is prepared using toluene as solvent.[128] This led to low conversion of starting material after 24 h. Performing the ketal formation reaction in methanol allowed obtaining **2.19** in 52% yield (compared to 60% reported for the glucose analogue[128]). Derivative **2.20** was obtained through benzoylation of **2.19** using benzoyl chloride (BzCl) and a 10% pyridine solution in DCM (93%). Benzylidene cleavage with ethanethiol and catalytic amounts of camphorsulfonic acid (CSA) afforded diol **2.21** (94%). Treatment with DDQ on benzylation product **2.22** and subsequent Fmoc protection afforded target building block **2.14** (80%, two steps).

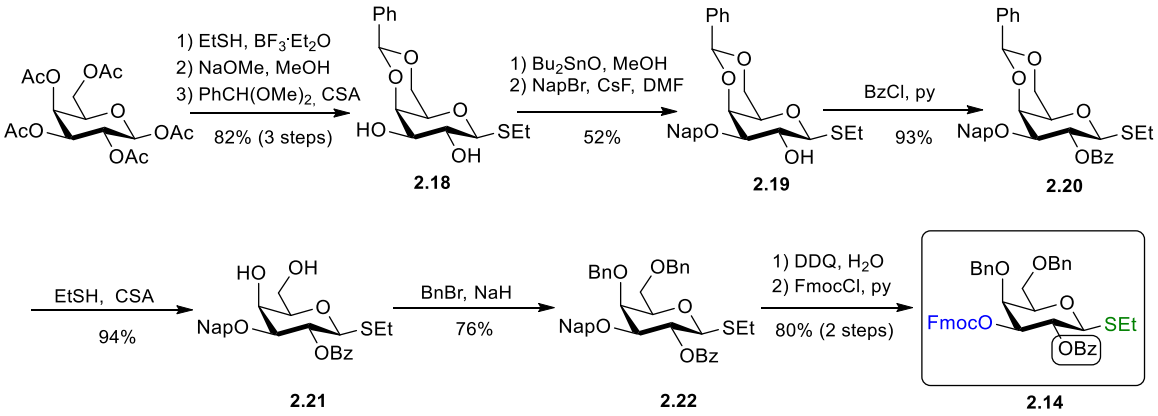

Scheme 2.2. Synthetic route *a* to **2.14**.

Route *b* involving **2.23**-**2.26** was based on previously described work.[87] Treatment of **2.18** with TBSCl and imidazole for 60 h at room temperature afforded **2.23** (88%) without detectable amounts of a 2-*O*-TBS protected undesired product (Scheme 2.3). Benzoylation of the 3-*O*-TBS protected derivative **2.23** required 48 h (**2.24**, 77%). Regioselective ring opening of **2.24** was achieved with BH_3·THF complex and TMSOTf (**2.25**, 94%). Benzylation of **2.25** was followed by TBS deprotection with BF_3·Et_2O and treatment with FmocCl to obtain the target building block **2.14** (90% yield, two steps). The reproducibility of the regioselective ring opening to afford **2.25** from **2.24** was found dependent on the quality of the BH_3·THF reagent used. Alternative synthetic routes starting from **2.24** were evaluated. Procedures to afford the 4-OH or the 4,6-diol derivatives of **2.24** were reproducible and high-yielding (97% and 84%, respectively, as evaluated by ^{1}H NMR, HSQC and LC-MS analysis). However, the 4-OH and the 4,6-diol compounds were not suitable for benzylation under neutral, basic or slightly acidic conditions, due to low conversion of the starting material or formation of inseparable mixtures of migration products. Route *b* (Scheme 2.3), albeit prolonged reaction times required in

presence of TBS, resulted in an approved procedure for the large-scale synthesis of **2.14**, as it represents a synthetic route with no low-yielding reaction steps when compared to route *a*.

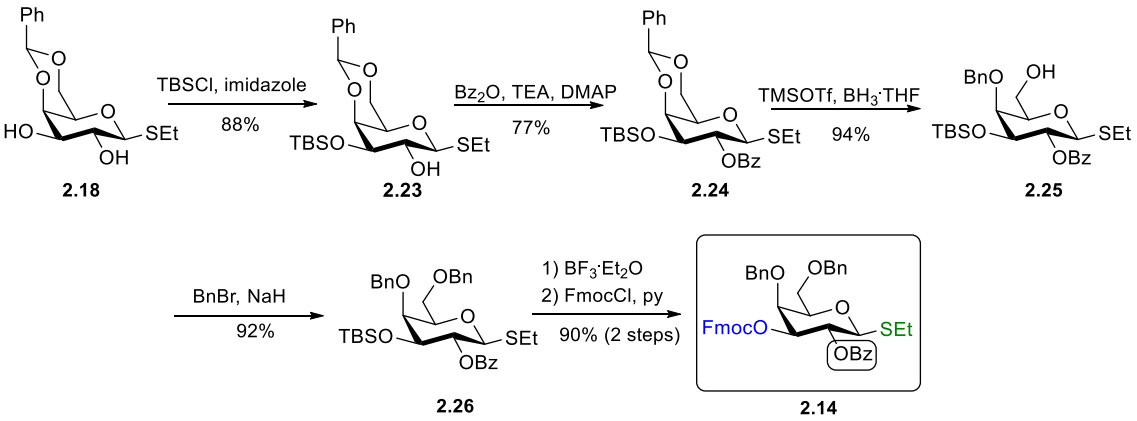

Scheme 2.3. Synthetic route *b* to **2.14**.

2.2.1.2 Synthesis of Fucose Building Blocks

Building block **2.17a** was obtained in five steps starting from L-fucose (Scheme 2.4). Common procedures for acetylation and bromination were used. β-Thioglycoside **2.29** was obtained by reaction of *p*-methylthiophenolate with the corresponding glycosyl bromide, based on adapted conditions reported for β-rhamnosylation.[129] The procedure was modified to reduce the amount of thiocresol and sodium hydride from two and three to 1.2 and 1.3 equivalents respectively, which avoided formation of acetate deprotection products, as assessed by ^{1}H NMR on the reaction mixture, and resulted in a 20% increase in yield (90% over two steps). Methanolysis of **2.29** resulted in triol **2.30** (quantitative) followed by benzylation afforded target building block **2.17a** (88%).

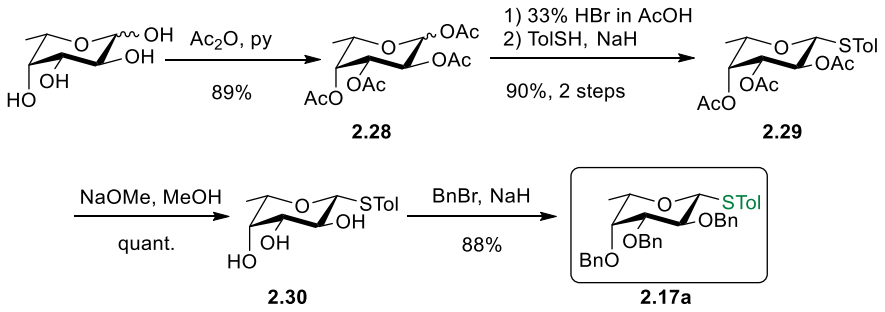

Scheme 2.4. Synthetic route to **2.17a**.

Building block **2.17b** was synthesized starting from isopropylidene acetal **2.31**[ii] (Scheme 2.5). 3-*O*-Bn derivative **2.32** was obtained via treatment of **2.31** with benzyl bromide and sodium hydride. Subsequent acetal cleavage in the presence of trifluoroacetic acid (TFA)

[ii] Provided by Dr. Marilda Lisboa.

and water afforded 3,4-diol derivative **2.33** (72%, 2 steps). After acetylation of **2.33**, target building block **2.17b** was obtained (89%).

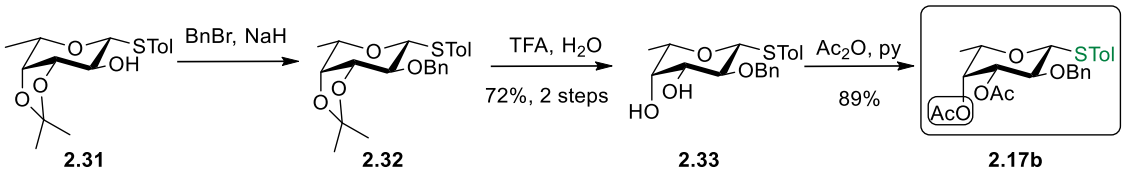

Scheme 2.5. Synthetic route to **2.17b**.

2.2.2 AGA

2.2.2.1 Optimization of Glycosylation Conditions

With building blocks **2.13**-**2.17**[iii] in hand, optimization of the reaction conditions, in order to find the appropriate conditions for the assembly of large structures, was first persued. Optimization was tested on the context of disaccharide and trisaccharide fragments, aiming to achieve full conversion and maximum stereoselectivity in each glycosylation cycle (Table 2.1). Analytical HPLC chromatograms (complemented with MALDI data) were used as main tools for a qualitative optimization of the reaction conditions in AGA.

Glycosylation reagents are added dropwise to the reaction vessel at a controlled incubation temperature (T_1). T_1 is typically 20 °C below the glycosylation temperature (T_2), to minimize reactivity before the reagent delivery process is completed. Afterwards, the reaction vessel is warmed up to T_2 to perform the coupling. Full conversion and excellent stereoselectivity were achieved for thioglycosides **2.13** and **2.14** when eight equivalents of building block and a glycosylation time of 20 min at 0 °C, after a short incubation (incubation time, t_1) at lower temperatures were employed (Table 2.1, entries 1-2). Deletion sequences were observed when less equivalents of building block were used. Longer glycosylation times did not produce an improvement of the reaction outcome. It is noteworthy that **2.13** was successfully used in combination with **2.14** for the formation of Gal-β(1,4)-Glc linkages, but failed to produce Glc-β(1,4)-Glc disaccharides. Glucosamine **2.15** proved less reactive than the other building blocks and required 40 min glycosylation time to achieve full conversion (Table 2.1, entry 3).

[iii] **2.13**,[48] **2.15**[76] and **2.16**[48] were originally provided by Dr. Maria Bräutigam. After AGA optimization, commercial building blocks **2.14**, **2.15**, **2.16a** and **2.17a** were used.

Table 2.1. Optimized glycosylation conditions for AGA with building blocks **2.13**-**2.17**.

Entry	BB	# Equiv.	T_1 (ºC)	t_1 (min)	T_2 (ºC)	t_2 (min)
1	**2.13**	8	-20	5	0	20
2	**2.14**	8	-20	5	0	20
3	**2.15**	8	-20	5	0	40
4	**2.16b**	5	-35	5	-15	30
5	**2.17a**	8	-40	5	-20	20

T_1: Incubation temperature; t_1: incubation time; T_2: glycosylation temperature; t_2: glycosylation time.

For the installation of the terminal galactose moiety, the originally selected thioglycoside donor **2.16a** had to be replaced with the phosphate analogue **2.16b**[iv] to achieve the desired β-stereoselectivity (Table 2.1, entry 4). Indeed, for the synthesis of the nonreducing end Gal-GlcNAc disaccharide, **2.16a** resulted in low stereoselectivity from the β-thioglycoside (Scheme 2.6, Figure 2.4), as identified from HSQC experiments and $^{1}J_{C\text{-}H}$ coupling constants. The stereoselectivity could not be improved by performing the glycosylation at lower temperature. The dibutyl phosphate building block **2.16b** ensured excellent stereoselectivity. The selectivity differences may be a result of a change in solvent used during the glycosylation, since dioxane is added to ensure solubility of NIS/TfOH required for thioglycoside activation. Dioxane coordinates the β-face of the oxocarbenium ion that forms during glycosylation and favors the formation of the α-glycosylation product (see section 1.1.1).[130] Dibutyl phosphates can be activated by TMSOTf in DCM, hence solvent coordination does not influence the reaction. Glycosylation using the thioglycoside donor **2.16c** (Figure 2.4, C) led to an intermediate stereoselectivity between those observed for **2.16a** and **2.16b**. The difference in β-stereoselectivity observed between thioglycosides **2.16c** and **2.16a** suggests that a Fmoc carbamate protecting group in C2 is not as effective as an ester participating group in providing anchimeric assistance. Thus, the oxacarbenium pathway with solvent participation, leading to increased α-stereoselectivity, is more relevant for donor **2.16a** than for donor **2.16c**.

[iv] **2.16a-c** were provided by Dr. Maria Bräutigam.

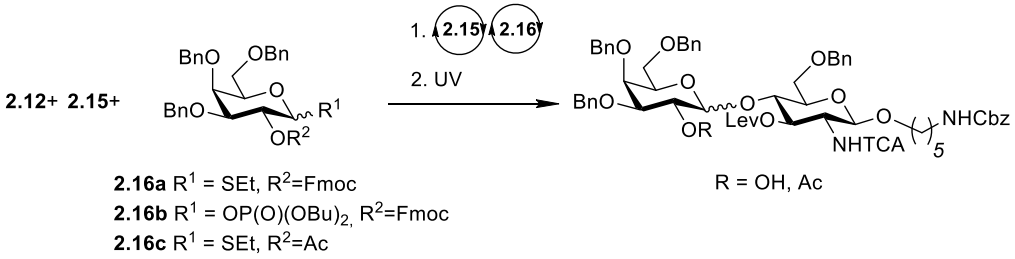

Scheme 2.6. Glycosyl donors tested for the AGA of the nonreducing end Gal-GlcNAc linkage.

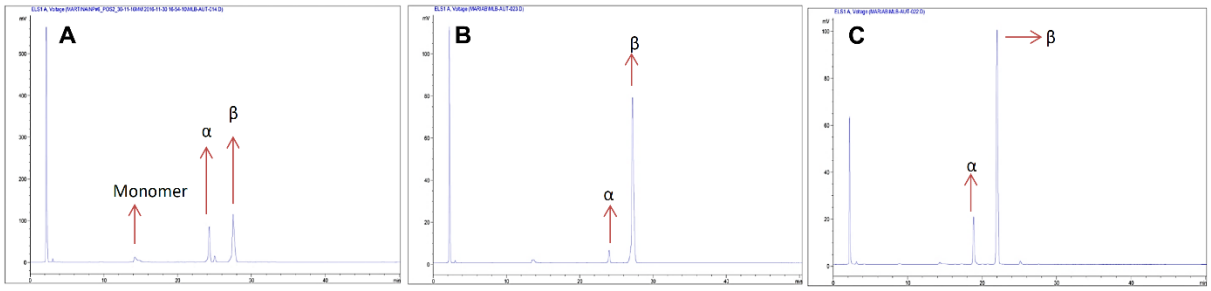

Figure 2.4. Analytical NP-HPLC chromatograms of crude reaction mixture after photocleavage for the AGA of the nonreducing end Gal-GlcNAc linkage (crude reaction mixture after photocleavage). A) Using **2.16a** as glycosyl donor, B) using **2.16b** as glycosyl donor and C) using **2.16c** as glycosyl donor. Detection: ELSD.

Highly reactive perbenzylated fucose **2.17a** was activated at -20 °C to avoid hydrolysis (Table 2.1, entry 5). For the assembly of trisaccharide **2.34** (Scheme 2.7), excellent α-stereoselectivities were obtained for fucosylations at 0 °C and -20 °C when **2.17a** was used as fucosyl donor. When performing the fucosylation at 0 °C, a disaccharide lacking fucose was also obtained (Figure 2.5, A). By lowering the fucosylation temperature, the formation of disaccharide product was avoided and a higher yield for the reaction was obtained (Table 2.2; Figure 2.5, B). This finding indicates that for fucosylations involving the armed glycosyl donor **2.17a**, lower reaction temperatures have a relevant effect on minimizing the amount of donor hydrolysis.

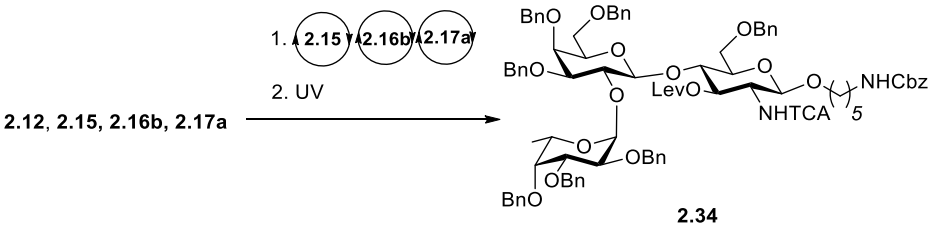

Scheme 2.7. AGA of trisaccharide **2.34**. Conditions for AGA: (1) For each coupling step: i) acidic wash: TMSOTf in DCM; ii) glycosylation: eight equiv. of **2.15** or **2.17a** and NIS, TfOH in DCM/dioxane, -20 °C (5 min) → 0 °C (40 min) for **2.15**, or -40 or -20 °C (5 min) → -20 or 0 °C (20 min) for **2.17a** or five equiv of **2.16b**, TMSOTf, DCM, -35 °C (5 min) → -15 °C (30 min),; iii) Deprotection: 20% piperidine in DMF, 25 °C. (2) UV cleavage. Isolated yields are based on resin loading.

Table 2.2. Reaction conditions and yield for the AGA of **2.34**.

Entry	BB	# Equiv.	T_1 (ºC)	t_1 (min)	T_2 (ºC)	t_2 (min)	Yield (%)
1	**2.17a**	8	-20	5	0	20	47 (α)
2	**2.17a**	8	-40	5	-20	20	57 (α)

T_1: Incubation temperature; t_1: incubation time; T_2: glycosylation temperature; t_2: glycosylation time.

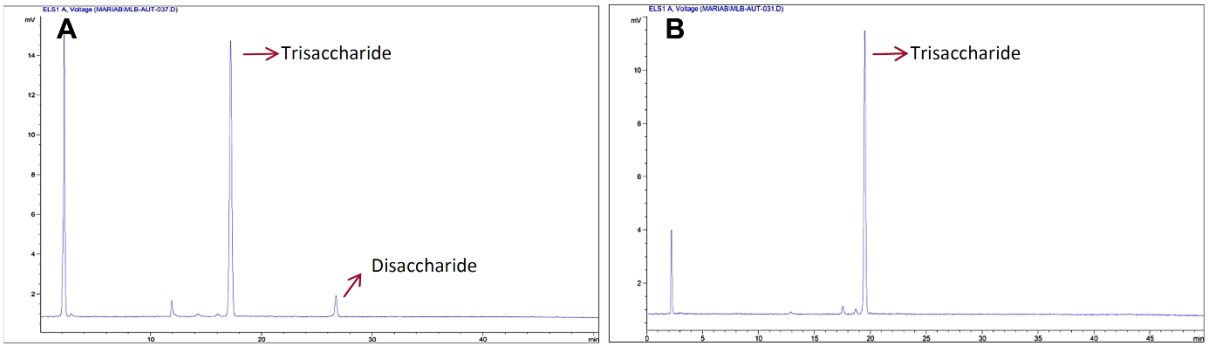

Figure 2.5. Analytical NP-HPLC chromatograms for the AGA of **2.34** (crude reaction mixture after photocleavage). A) Fucosylation with eight equiv. of **2.17a**, -20 ºC (5 min) → 0 ºC (20 min). B) Fucosylation with eight equiv. of **2.17a**, -40 ºC (5 min) → -20 ºC (20 min). Detection: ELSD.

Considering the excellent α-stereoselectivity results obtained with **2.17a**, fucosylation with a different fucosyl donor would only be advantageous if a) it could be performed at 0 °C instead of -20 °C and b) it required less equivalents of building block. To this end, less reactive fucosyl donor **2.17b** was used in the attempt to synthesize a trisaccharide analogue of **2.34**. While no disaccharide product was detected under these conditions, a mixture of fucosylated trisaccharides was obtained. Therefore, glycosylation with **2.17a** at -20 °C (Table 2.1, entry 5) was identified as the best method to achieve α-fucosylation.

2.2.2.2 Effect of Capping

Introducing a capping step after glycosylation and before the subsequent Fmoc/Lev deprotection step aims to minimize the amount of deletion sequences, thereby providing facile purification of the target product. A capping procedure using Ac_2O/TMSOTf[64] was tested during AGA optimization of disaccharide fragments. This lead to partial cleavage and capping of benzyl ether groups, as detected by MALDI and HSQC experiments. Although these capping conditions previously showed to be adequate for the assembly of structures containing 1→6 linkages, they resulted incompatible with the presence of primary benzyl ether groups. Capping was therefore excluded from AGA coupling cycles in this project. Upon this finding, milder capping procedures have since been developed in the Seeberger group.[64]

2.2.2.3 Assembly of Type-II Chain Structures

The glycosylation conditions optimized for dimers and trimers (Table 2.1) were then tested in the AGA of longer structures. Linear hexasaccharide nLc_6 (**2.35**, 55% yield, Scheme

2.8), was successfully assembled under those conditions. For the syntheses of branched structures, AGA of pentasaccharide **2.36** was evaluated by two different assembly strategies (Scheme 2.9). These strategies differ in the order in which fucose and galactose are attached to the GlcNAc moiety. After introduction of building block **2.15** to the resin-bound oligosaccharide, the Fmoc group can be removed and a galactose can be attached at the C4 hydroxyl of GlcNAc before the Lev at the C3 hydroxyl is cleaved and a fucose is attached; subsequently chain elongation continues ('strategy 1', Scheme 2.9). Alternatively, this process can be inversed ('strategy 2', Scheme 2.9). Both assembly strategies resulted in excellent stereoselecitvity towards the α-difucosylated glycan (Figure 2.6). It is noteworthy that strategy 2 afforded comparable stereoselectivity to strategy 1, indicating that **2.16b** is appropriate for the installation of the Gal-β(1,4)-GlcNAc linkage also when a fucose is attached to the C3 of GlcNAc. Based on the isolated yields of **2.36** (39 and 51% for strategies 1 and 2, respectively), strategy 2 was selected for the assembly of type-II chain structures.

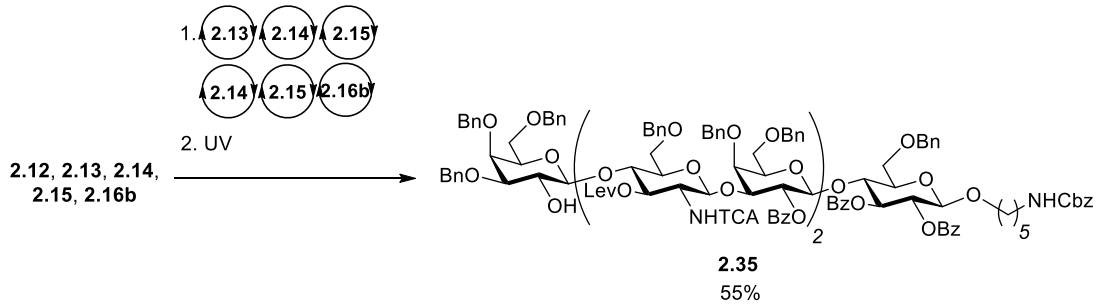

Scheme 2.8. AGA of linear hexamer **2.35**. Conditions for AGA: (1) For each coupling step: i) acidic wash: TMSOTf in DCM; ii) glycosylation: eight equiv. of **2.13**, **2.14** or **2.15** and NIS, TfOH, DCM/dioxane, -20 °C (5 min) → 0 °C (20 min or 40 min), and five equiv of **2.16b**, TMSOTf, DCM, -35 °C (5 min) → -15 °C (30 min); iii) Deprotection: 20% piperidine in DMF, 25 °C. (2) UV cleavage. Isolated yields are based on resin loading.

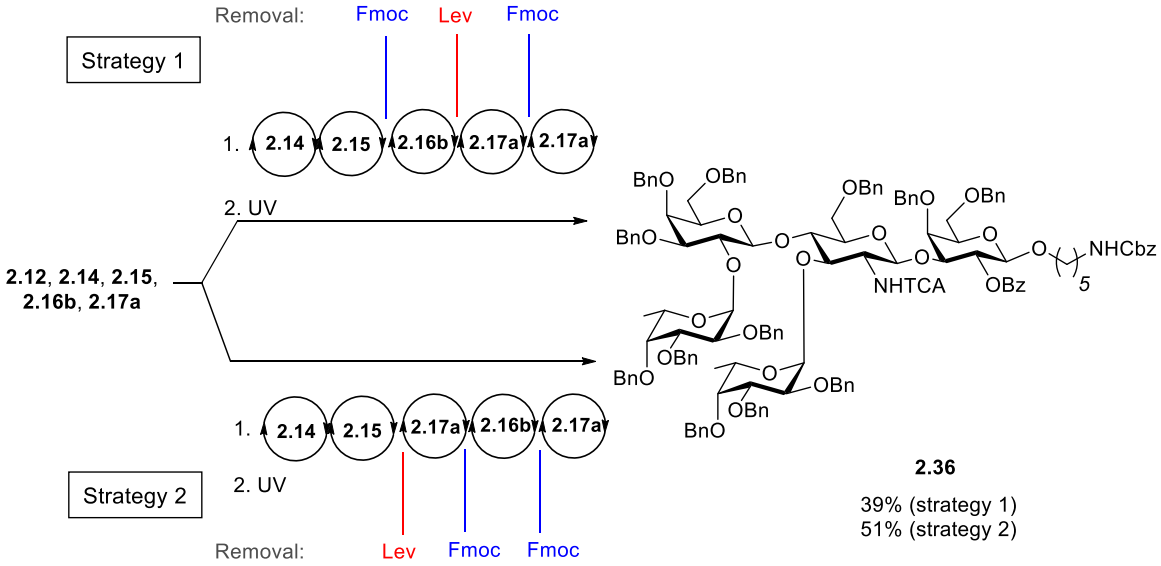

Scheme 2.9. Braching strategies tested for the AGA of **2.36**. Conditions for AGA: (1) For each coupling step: i) acidic wash: TMSOTf in DCM; ii) glycosylation: eight equiv. of **2.14**, **2.15** or **2.17a** and NIS, TfOH, DCM/dioxane, -20 °C (5 min) → 0 °C (20 min or 40 min), or -40 °C (5 min) → -20 °C (20 min or 40 min) and five equiv of **2.16b**, TMSOTf, DCM, -35 °C (5 min) → -15 °C (30 min); iii) Deprotection: Fmoc removal 20% piperidine in DMF, 25 °C; Lev removal 0.15 M $NH_2NH_2{\cdot}HOAc$ in py/AcOH/H_2O for 2 x 30 min. (2) UV cleavage. Isolated yields are based on resin loading.

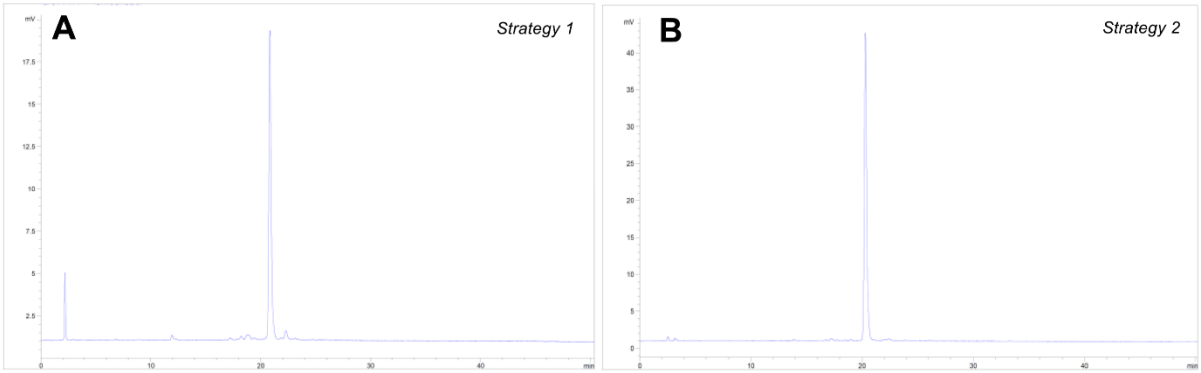

Figure 2.6. Analytical NP-HPLC of the crude reaction mixture after photocleavage for the AGA of **2.36** A) Using assembly strategy 1. B) Using assembly strategy 2 (Scheme 2.9). Detection: ELSD.

Lewis type-II chain structures **2.37**-**2.44** (28-65% yield, Scheme 2.10) were assembled with excellent stereoselectivity using the optimized glycosylation conditions (Table 2.1) and assembly strategy 2 (Scheme 2.9), in addition to **2.34**-**2.36**. No signifigant amounts of deletion sequences were detected by analytical HPLC on the crude reaction mixture of **2.34**-**2.42** (Figure 2.7, Experimental Section). H-antigen and Le^x were assembled with the initial lactose unit (**2.38** and **2.39**) or without (**2.34** and **2.37**) to provide access to all variants of these structures for biological studies. Lewis glycosphingolipids on the surface of human cells carry the initial lactose unit,[131] while many biological studies only consider the terminal fucosylated epitope, lacking the lactosylceramide core.[132,133]

For the AGA of extended chain Lewis antigens Le^x-dimer **2.43** and KH-1 **2.44**, a double glycosylation with GlcNAc donor **2.15** had to be implemented for the attachment of the second GlcNAc unit to ensure full conversion in each glycosylation cycle. When using only one glycosylation cycle for the attachment of both GlcNAc units, a significant amount of a deletion sequence was observed. For the AGA of Le^x-dimer **2.43**, the side product was identified as an hexasaccharide lacking a GlcNAc and a galactose unit when compared to the target octasaccharide, based on HRMS analysis and diagnostic NMR signals (Figure 2.8, A). Furthermore, when attempting the AGA using strategy 1, a deletion sequence lacking a GlcNAc and a fucose unit was identified (Figure 2.8, B). These results could be explained by an incomplete coupling of the second GlcNAc unit to the resin-bound oligosaccharide, likely due to the combination of the low reactivity of the GlcNAc donor and a sterically-hindered branched acceptor. The introduction of a double glycosylation cycle for the attachment of the second GlcNAc allowed overcoming this difficulty (Figure 2.8, C). Streamlined coupling cycles rendered the assembly of KH-1 nonasaccharide **2.44** (15 h, 28% yield, Scheme 2.10) significantly faster than an earlier AGA version that required 23 h.[120]

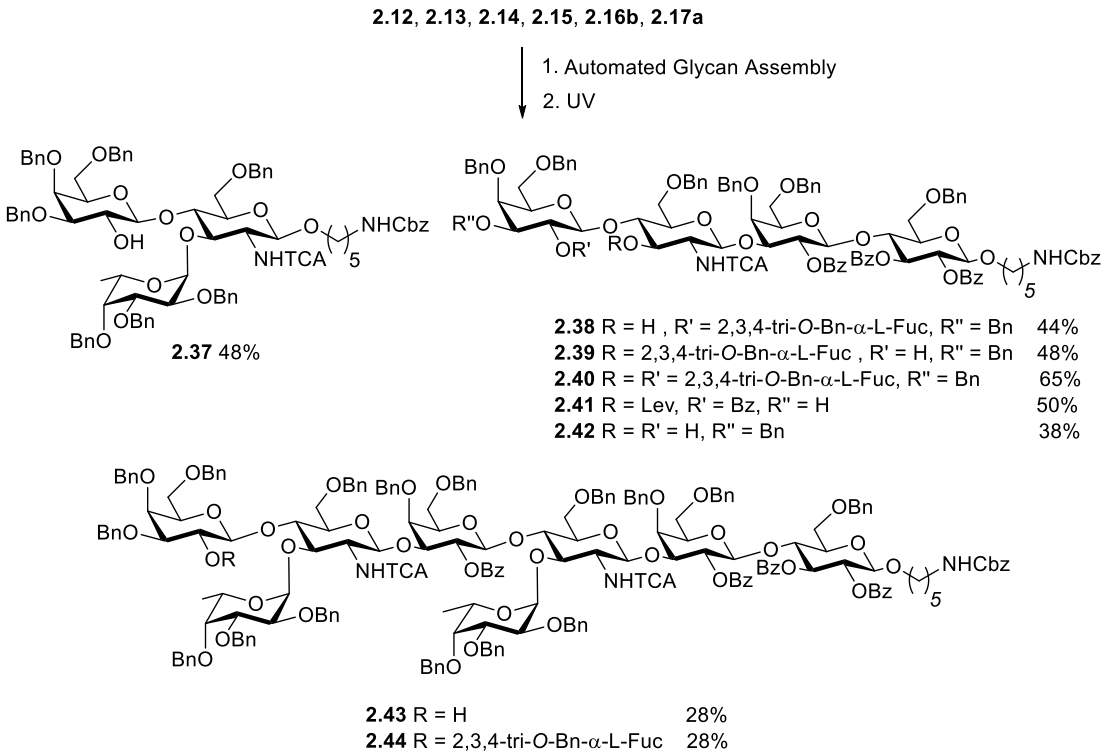

Scheme 2.10. AGA of Lewis type-II chain glycans **2.37**-**2.44**. Conditions for AGA: (1) For each coupling step: i) acidic wash: TMSOTf in DCM; ii) glycosylation: eight equiv. of **2.13**, **2.14**, **2.15** or **2.17a** and NIS, TfOH, DCM/dioxane, -20 °C (5 min) → 0 °C (20 min or 40 min), or -40 °C (5 min) → -20 °C (20 min or 40 min) and five equiv of **2.16b**, TMSOTf, DCM, -35 °C (5 min) → -15 °C (30 min); iii) Deprotection: Fmoc removal 20% piperidine in DMF, 25 °C; Lev removal 0.15 M $NH_2NH_2{\cdot}HOAc$ in py/AcOH/H_2O for 2 x 30 min. (2) UV cleavage. Isolated yields are based on resin loading.

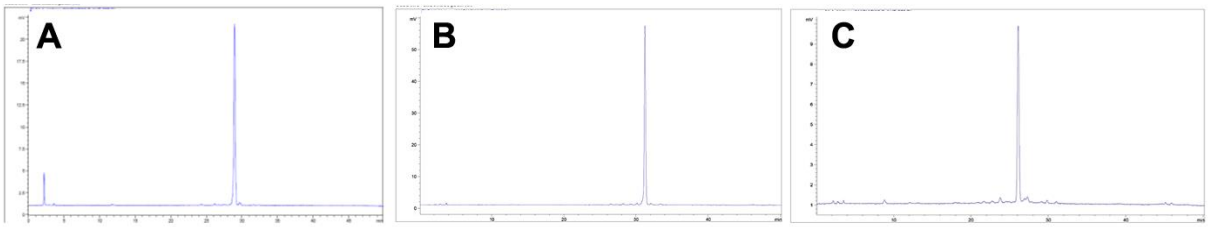

Figure 2.7. Analytical NP-HPLC for the AGA of protected type-II chain structures (A) H-antigen **2.38** (B) Le^x **2.39** and (C) Le^y **2.40**. Crude reaction mixtures after photocleavage. Detection: ELSD.

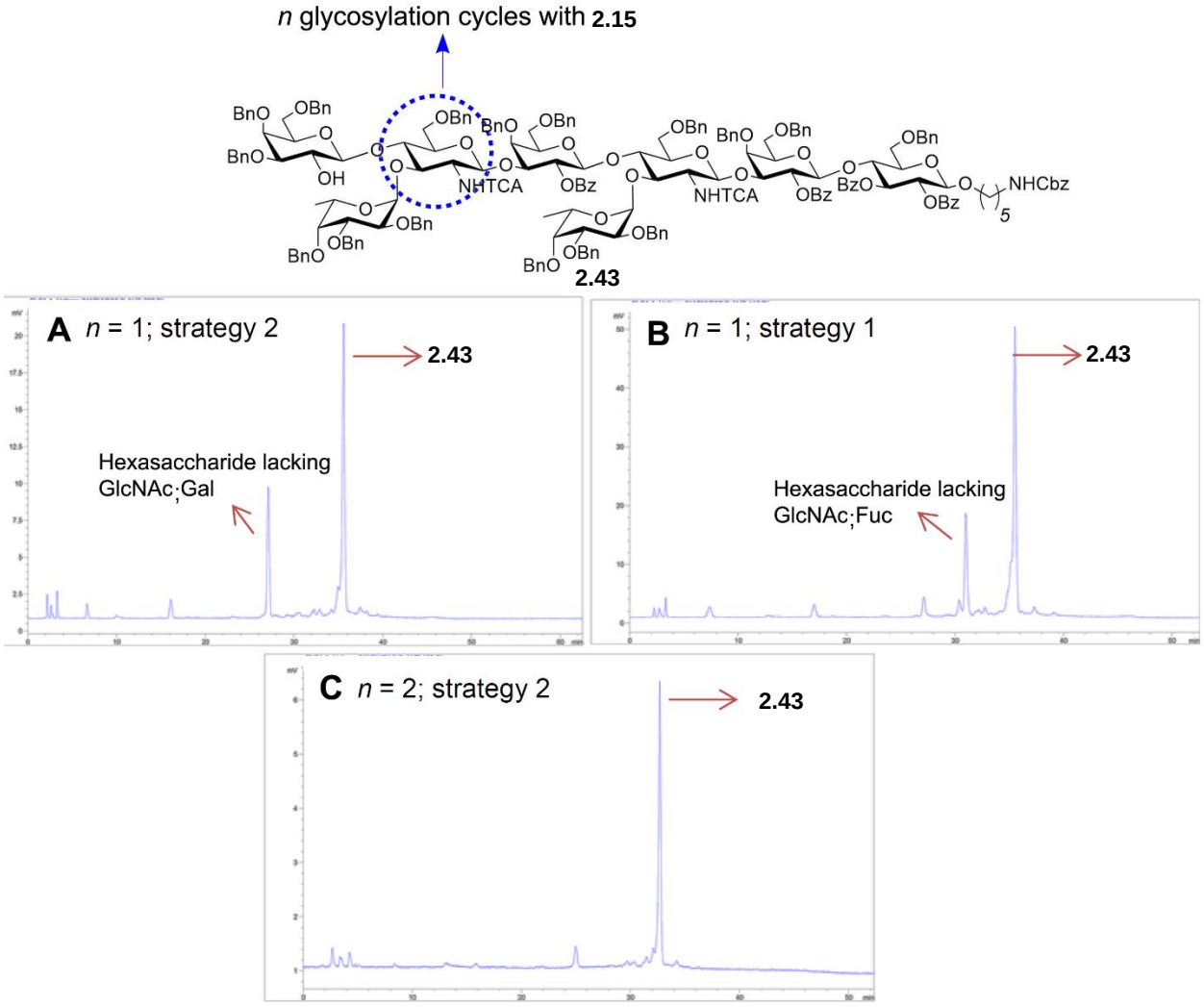

Figure 2.8. Analytical NP-HPLC of crude reaction mixtures after photocleavage for the AGA of Le^x-dimer **2.43**. A) Using branching strategy 2 and one glycosylation cycle for the attachment of each GlcNAc unit. B) Using branching strategy 1 and one glycosylation cycle for the attachment of each GlcNAc unit. C) Using branching strategy 2 and two glycosylation cycles for the attachment of the second GlcNAc.

In the same way, assembly of Le^x-trimer **2.45** (Figure 2.9) was pursued with double glycosylation cycles for the attachment of the second and third GlcNAc units. The AGA of **2.45** rendered a considerable amount of deletion sequences, judged by analytical HPLC of the crude reaction mixture after photocleavage (Figure 2.9, A). Although target oligosaccharide

2.45 was identified as the main product and was isolated (4.29 mg, 7% yield, Figure 2.9, B) as supported by HSQC (Figure 2.10) and MALDI analysis, further optimization on AGA will be required for the full characterization and subsequent deprotection.

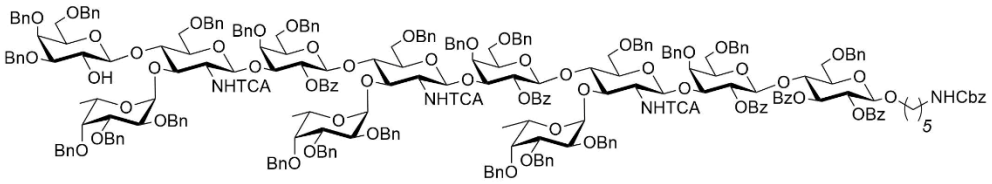

2.45

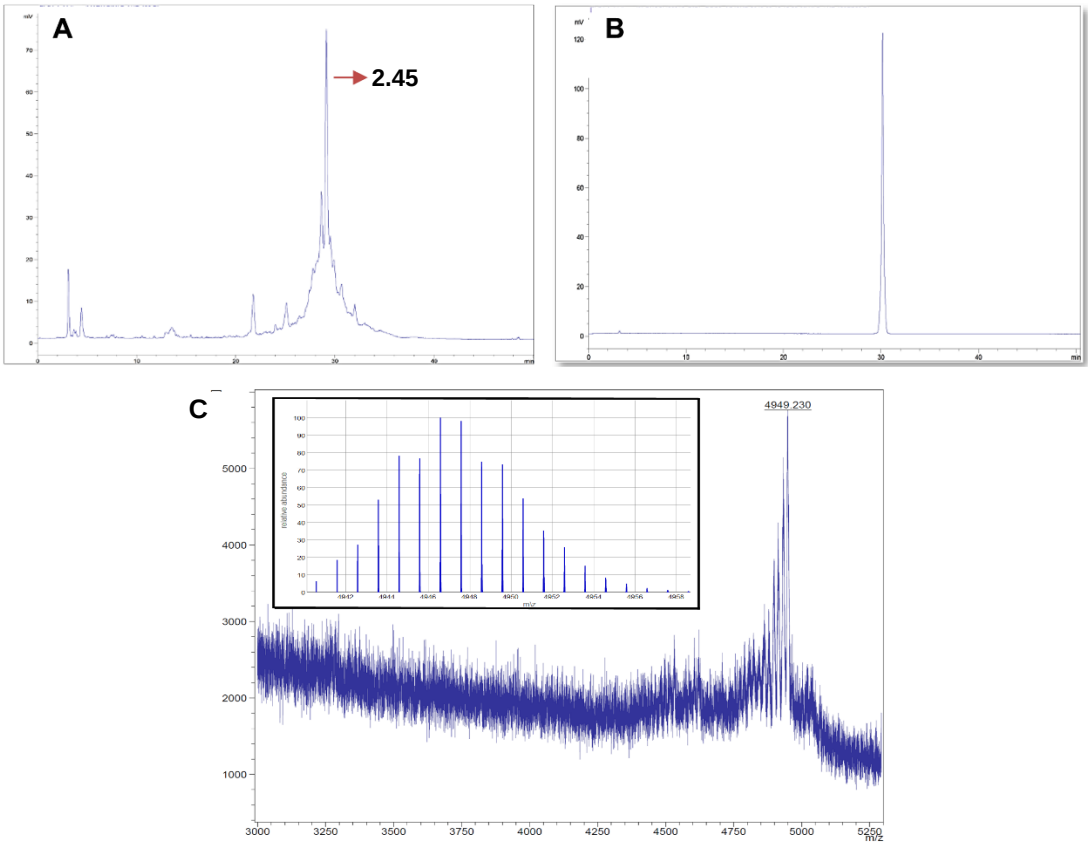

Figure 2.9. AGA of Le^x-trimer **2.45**. A) Analytical NP-HPLC of crude reaction mixture after photocleavage. B) purified product for the AGA of **2.45** (Detection: ELSD). C) MALDI of purified product (top left: calculated spectrum).

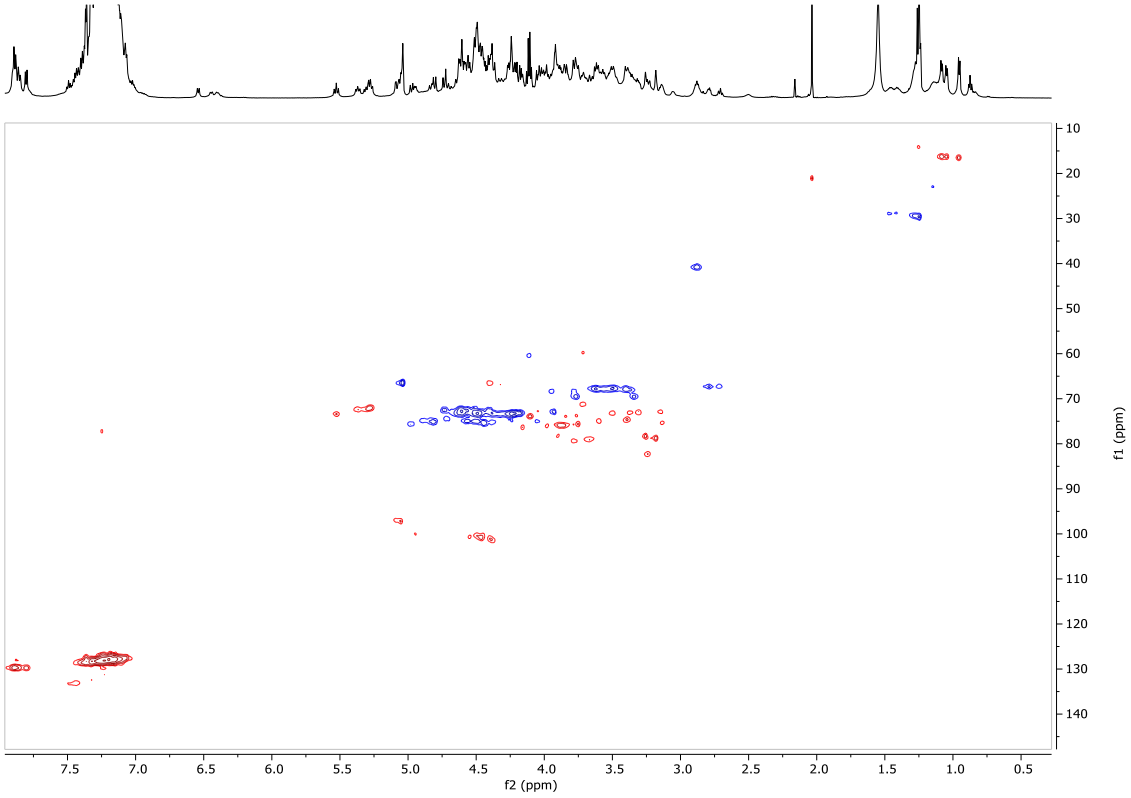

Figure 2.10. HSQC ($CDCl_3$, 600 MHz) of isolated **2.45**.

2.2.2.4 Assembly of Type-I Chain Structures

Since type-I and type-II chain antigens differ only in the substituents attached at the nonreducing end of the GlcNAc unit, an AGA strategy for type-I chain structures relying on the sequential cycles developed for their type-II chain analogues was first envisioned. In this way, the glycosylation conditions and assembly strategies developed earlier (Section 2.2.2.3) could be employed, and only the order of deprotection of Fmoc and Lev after glycosylation with GlcNAc **2.15** needed to be exchanged. This approach was successful for the AGA of protected tetrasaccharide Lc_4 **2.46** (Scheme 2.11, 47% yield). However, it failed for the AGA of branched oligosaccharides. Under these conditions, after fucosylation of the C4 hydroxyl on GlcNAc, the levulinate ester was not properly cleaved from C3. Alternative Lev deprotection conditions were tested (three cycles of hydrazine acetate 0.15 M in pyridine/AcOH/H_2O 16:4:1, hydrazine acetate 0.56 M in pyridine/AcOH 2:1, and 10% hydrazine monohydrate in DMF), but also failed to remove Lev after fucosylation. Thus, assembly strategies where galactosylation of GlcNAc precedes Fmoc deprotection and fucosylation were used for the AGA of protected Le^b **2.47** and Le^a **2.48** (Scheme 2.11).

AGA of protected Le^b **2.47** was achieved via a double deprotection-difucosylation strategy: A single Fmoc deprotection cycle was used to unmask the hydroxyl groups at C2 of galactose and at C4 of GlcNAc in the LacNAc subunit of the resin-bound oligosaccharide.

Subsequently, a double glycosylation cycle with donor **2.17a** was used to introduce simultaneously both fucosyl moieties (**2.51**, 34% yield). For the AGA of **2.48**, galactosyl donor **2.16b** was replaced with **2.49**,[v] which can be synthesized in two steps from a commercially-available intermediate common to **2.16b**. Building block **2.49** bears a permanent benzoyl ester protecting group at C2. Therefore, after glycosylation with **2.49**, a deprotection cycle with 20% piperidine in DMF allowed to selectively free C4 hydroxyl of the GlcNAc subunit in the resin-bound oligosaccharide. Finally, a fucosylation cycle with donor **2.17a** followed by photocleavage and HPLC purification afforded protected Le^a **2.48** (47% yield).

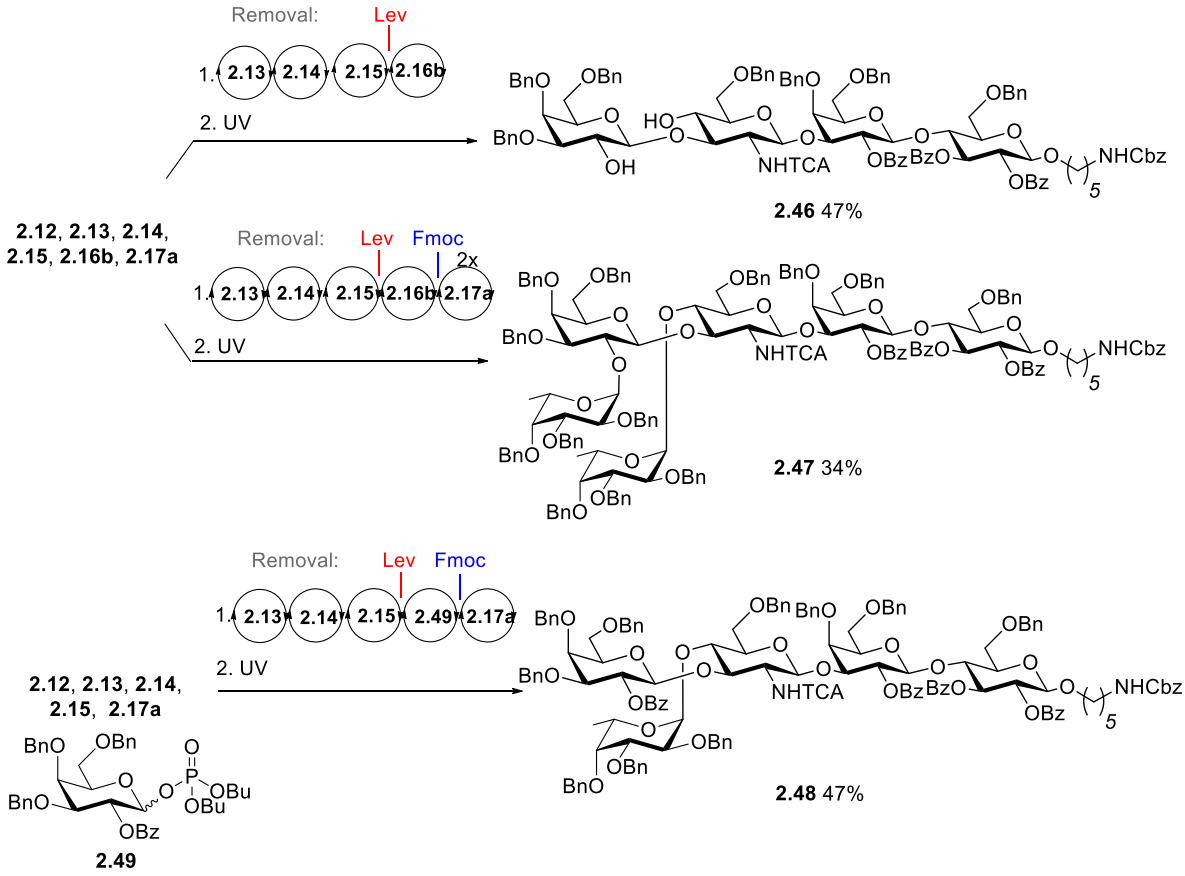

Scheme 2.11. AGA of type-I chain structures **2.46**-**2.48**. Conditions for AGA: (1) For each coupling step: i) acidic wash: TMSOTf in DCM; ii) glycosylation: eight equiv. of **2.13**, **2.14**, **2.15** or **2.17a** and NIS, TfOH, DCM/dioxane, -20 °C (5 min) → 0 °C (20 min or 40 min), or -40 °C (5 min) → -20 °C (20 min or 40 min) and five equiv of **2.16b** or **2.49**, TMSOTf, DCM, -35 °C (5 min) → -15 °C (30 min); iii) Deprotection: Fmoc removal 20% piperidine in DMF, 25 °C; Lev removal 0.15 M $NH_2NH_2{\cdot}HOAc$ in py/AcOH/H_2O for 2 x 30 min. (2) UV cleavage. Isolated yields are based on resin loading.

[v] Provided by Dr. Maria Bräutigam.

Notes on Levulinic Ester Cleavage in Type-I Chain Structures

The cleavage of levulinic esters from C3 hydroxyl of GlcNAc in the resin-bound oligosaccharide was further investigated. For the AGA of type-II chain oligosaccharides, it was possible to remove the levulinoyl protecting group in GlcNAc after O4-galactosylation (strategy 1, Scheme 2.9). Moreover, linear hexamer **2.35** (Scheme 2.8) and its analogue in which Lev is cleaved during AGA were obtained without detectable traces of side products. Therefore, the difficulties observed in the AGA of type-I structures cannot be due to Lev migration after C4-OFmoc deprotection.

Replacing **2.17a** for **2.17b** did not allow for levulinate ester cleavage after O4-fucosylation in the resin-bound oligosaccharide. The analysis of the reaction outcome under this circumstances proved elusive, as the difficulties in Lev cleavage were accompanied by low yields after photocleavage, thus preventing the full characterization of reaction products. Low yields after photocleavage may be a result of a reaction involving the linker that prevents its cleavage or of linker cleavage during AGA.

2.2.3 Global Deprotection

In order to gain access to fully-deprotected antigens, permanent protecting groups had to be removed from the assembled oligosaccharides. A methanolysis-hydrogenolysis sequence was used as a global deprotection approach (Scheme 2.12). After photocleavage and HPLC purification, oligosaccharides obtained by AGA were treated with sodium methoxide in MeOH/DCM for 24-96 h for the removal of ester protecting groups (Bz and/or Lev), until complete conversion was detected by MALDI analysis. Partial cleavage of TCA group during methanolysis was occasionally observed, as identified by MALDI. MALDI analysis proved to be more sensitive to compounds lacking TCA, therefore it was not possible to identify at this stage the extent of TCA cleavage. No TCA cleavage was observed for compound bearing fucose attached to the GlcNAc. It is possible that the fucosyl residue shields the TCA group at the glucosamine, thus preventing its cleavage.

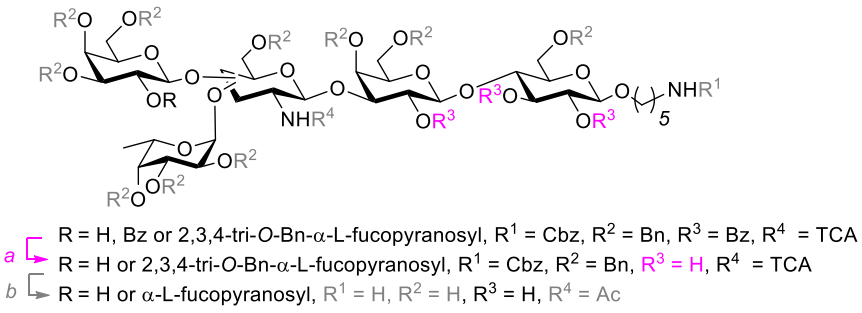

Scheme 2.12. Global deprotection by methanolysis/hydrogenolysis sequence. a) Sodium methoxide in MeOH/DCM; b) Pd/C, H_2 in DCM/tBuOH/H_2O or AcOEt/tBuOH/H_2O 2:1:1

Hydrogenolysis was performed on the crude reaction mixture after methanolysis, using palladium on carbon as catalyst. A DCM/*t*-BuOH/H_2O 2:1:1 mixture was first selected as reaction solvent. Under those conditions, partial cleavage of fucose was observed. This was attributed to acidification of the reaction medium due to HCl production during hydrogenolysis. Fucose cleavage could be avoided by replacement of DCM by EtOAc in the solvent mixture, and quenching the reaction with triethylamine. The crude reaction mixture was then purified by RP-HPLC. In this way, conjugation-ready antigens **2.50**-**2.58** (Figure 2.11, 17-54% yield) were obtained. Deprotection yields may be affected by loss of material during purification, in particular during RP-HPLC purification with a Hypercarb column. A method to avoid using a Hypercarb column, by implementing the HPLC purification after the methanolysis step, was unsuccessful. Despite the purity of the starting material used for the hydrogenolysis step, the crude reaction mixture after removing all permanent protecting groups still required HPLC purification. Attempts to replace the Hypercarb column by other columns were unsuccessful. Use of a Synergi column allowed for the recovery of more material, but purification was unsatisfactory as assesed by ^{1}H NMR analysis. Additionally, HILIC HPLC-column was evaluated for the purification of **2.50**, but it was not possible to achieve experimental conditions that helped to obtain well-resolved analytical HPLC traces.

The global deprotection strategy described above was found unsuitable for the deprotection of poly-LacNAc oligosaccharides **2.59**, **2.60** and **2.11**. Solubility issues were observed for the partially-deprotected compounds, and hydrogenolysis reactions were not completed after prolonged reaction times. Attempts to complete hydrogenolyses by minimal addition of acetic acid or the use of a hydrogen bomb resulted in compound degradation. A one-pot Birch deprotection-peracetylation protocol[125] may have been advantageous to facilitate purification and avoid solubility issues in partially-deprotected compounds, but could not be successfully implemented due to irreversible *N*-acetylation of the linker. Birch reduction followed by methanolysis was used for the deprotection of **2.35**, **2.43** and **2.44** to afford poly-LacNac glycans **2.11**, **2.59**-**2.60** (9-19%, Figure 2.11). Due to their relatively high molecular weight (>1400), size exclusion using a Sephadex-G25 column, and subsequent reverse-phase chromatography using C-18 cartridges, was preferred for the final purification of **2.60** (13%) and **2.11** (19%, Figure 2.12).

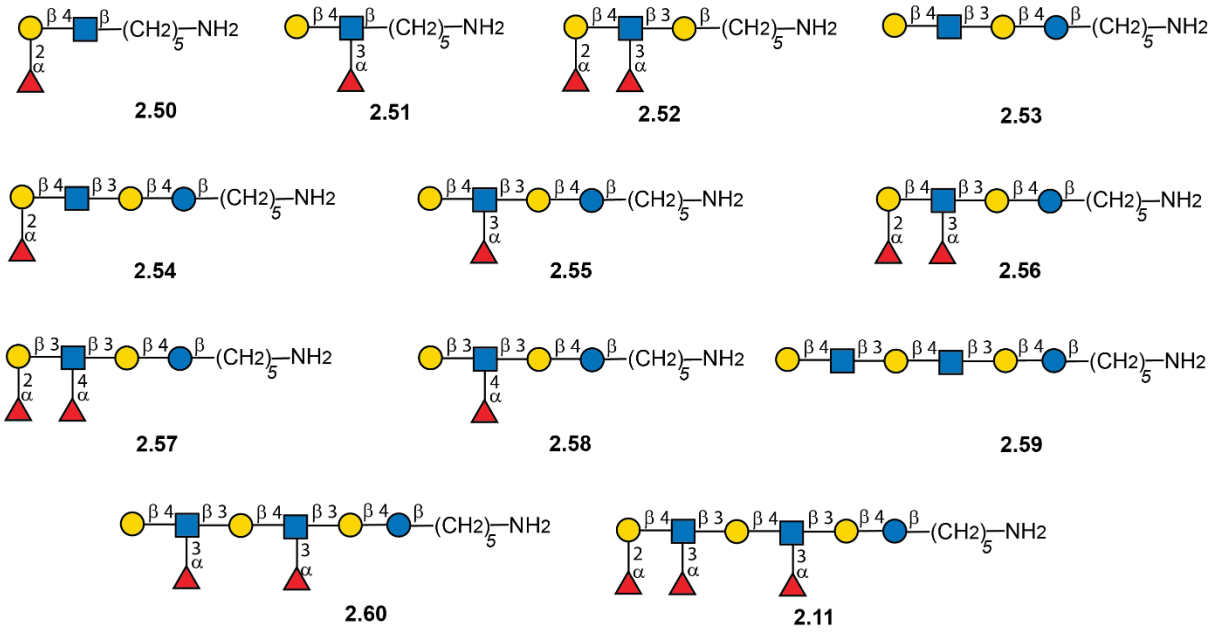

Figure 2.11. Synthetic Lewis type-I and type-II chain antigens **2.11**, **2.50**-**2.60**. Structures represented according to SNFG,[77] see page 7.

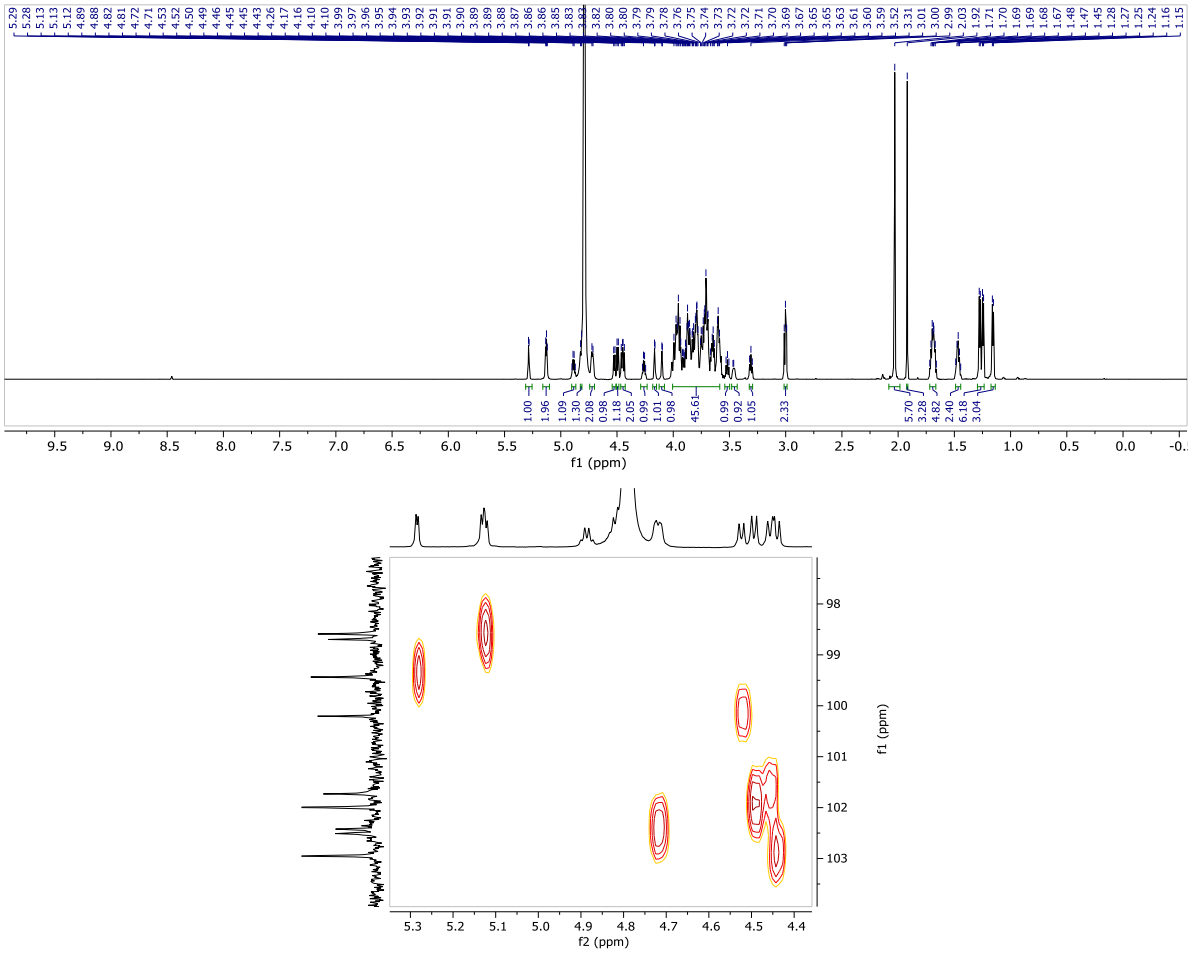

Figure 2.12. ^{1}H NMR (600 MHz, D_2O) of C5 aminopentyl nonasaccharide KH-1 (**2.11**) and HSQC 2D-NMR of the anomeric region.

2.2.4 Application of the Synthetic Oligosaccharides in Cancer Diagnostics and Therapeutics Research by the Moscovitz Group

Glycans **2.11** and **2.60** were transferred for their application in cancer immunology.[vi] These results are only briefly mentioned. C5-Aminopentyl KH-1 **2.11** was conjugated to carrier protein CRM_{197} using an homobifunctional adipic acid *p*-nitrophenyl diester. A male alpaca was immunized with the glycoconjugate over a period of eight weeks. The presence of anti-KH-1 antibodies in the serum was verified by glycan array (Figure 2.13). Glycan array results indicated the presence of antibodies that bind to nLc_6-core fucosylated antigens Le^x-dimer **2.60** and KH-1 **2.11**, but no binding to shorter glycans. The extracted samples will be further use for the production of anti-KH-1 nanobodies.

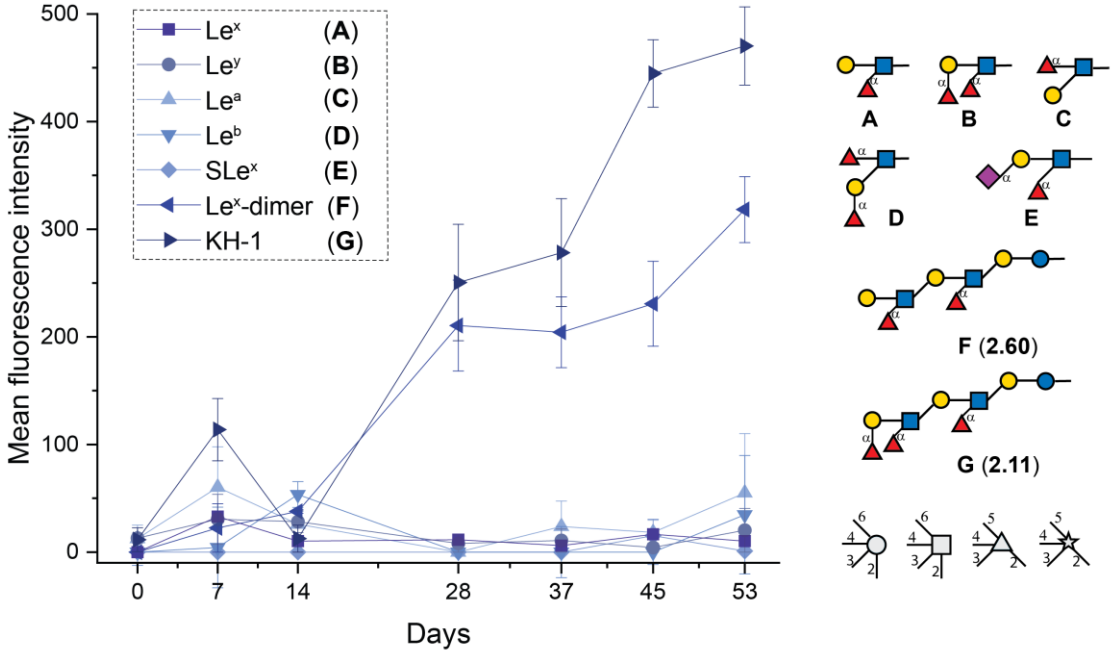

Figure 2.13. Glycan array of sera extracted from a male alpaca immunized with KH-1 glycoconjugate on days 0, 7 ,14 , 28, 37, 45 and 53. Glycans are represented according to SNFG,[77] see page 7. Glycosidic linkages are β, unless indicated otherwise.

2.3 Conclusion

A general method for the AGA of a whole set of Lewis type-I and type-II chain antigens was established. With the exception of Le^a, all synthesized antigens were assembled using five monosaccharide building blocks and the same glycosylation conditions for each glycosyl donor. From the original building block design based on the AGA approach, only two

[vi] Conjugation was performed by Felix Goerdeler and Dr. Maria Bräutigam. Immunization was performed by Felix Goerdeler under the supervision of Dr. Oren Moscovitz. Glycan array slides were printed by Katrin Sellrie.

modifications were required: the replacement of thioglycoside **2.16a** for phosphate **2.16b** in the terminal galactose unit and its replacement for **2.49** bearing a permantent protecting group at C2 for the assembly of Le^a. Use of phosphate donor **2.16b** was necessary to achieve β-stereoselectivity, presumably to avoid dioxane coordination influence. In the case of Le^a, donor **2.49** had to be used instead of **2.16b**, as the effectiveness of Lev deprotection showed to be sensitive to the glycosylation order in the assembly of type-I chain structures.

By means of AGA and a selection of a minimum set of orthogonally protected building blocks, a combinatorial approach allowed for the assembly of all intended glycans, by simply modifying the glycosylation sequence and deprotection cycles. Complex and large structures like trifucosylated nonasaccharide KH-1 **2.44** were assembled by this methodology in overnight reactions. Optimized glycosylation cycles led to full conversion and excellent stereoselectivity during AGA and minimized the formation of side products. However, for the assembly of larger, branched glycans such as protected Le^x-trimer **2.45** further optimization is required in order to afford sufficient amounts of glycan for full characterization and subsequent deprotection.

A global deprotection strategy based on a methanolysis-hydrogenolysis sequence yielded conjugation-ready oligosaccharides **2.50**-**2.58**. A Birch-methanolysis deprotection had to be implemented for the deprotection of poly-LacNAc glycans **2.11**, **2.59**-**2.60**. The bottleneck of chemical glycan synthesis proved to be the removal of protective groups from the final molecules, which is common to AGA and other approaches to obtain synthetic glycans (see chapter 1, Figure 1.2). Conjugation-ready Lewis antigens for their further application in diverse studies were obtained. First results from Alpaca immunizations indicate that the obtained samples are suitable for the production of anti-KH-1 nanobodies.

2.4 Outlook

The synthetic glycans I prepared are now used in diverse projects, including the development of tools for cancer diagnostics and therapeutics, in liposome formulations for binding studies on cell-based assays, for glycan arrays, and NMR studies on carbohydrate-protein interactions. Additionally, the solubility issues and difficulties in the deprotection observed for poly-LacNAc glycans inspired further analysis of the structure of these oligosaccharides, and raised questions on whether chain length and fucose presence have an effect on aggregation. Indeed, structures containing the fragment Gal-β(1,4)-[Fuc-α(1,3)]GlcNAc correspond to the group of the [3,4]Fuc-branch motif, presenting a nonconventional H-bond between H5 of fucose and O5 of galactose, to which a secondary structure is attributed.[134] Further investigation into the influence of these three factors (chain

length, presence of fucose, and presence of nonconventional H-bond) in the conformation of these molecules could be valuable both for the development of improved deprotection methods and to get insights into their collective behavior in solution, or in other contexts such as the cell-surface microenvironment.

The AGA method established in this work sets the basis for further modification to establish tailor-made modifications into Lewis antigens. In this context, two different research lines were envisioned, in collaboration with the Carbohydrate Materials group of Dr. Martina Delbianco. On one hand, the installment of a fluorine in the initial glucose unit at the glycan reducing end is envisioned to produce useful probes for ^{19}F-NMR studies on protein-carbohydrate interactions.[135,136] These analogues could be produced by AGA by replacing glucose BB **2.13**, by its 3-deoxy-3-fluoro analogue **2.61** (Figure 2.14), already successfully introduced in the AGA syntheses of unnatural polyglucosides.[137] In contrast, the introduction of a 2-deoxy-2-fluoro analogue of **2.16b** (**2.62**, Figure 2.14) in fragments Gal-β(1,4)-[Fuc-α(1,3)]GlcNAc is expected to disrupt the nonconventional H-bond involving H5 of fucose and the galactose unit. The influence of chain length, fucosylation patterns, and the presence or absence of the nonconventional H-bond in the conformation and solubility will be investigated through the construction and characterization of unnatural synthetic glycans.

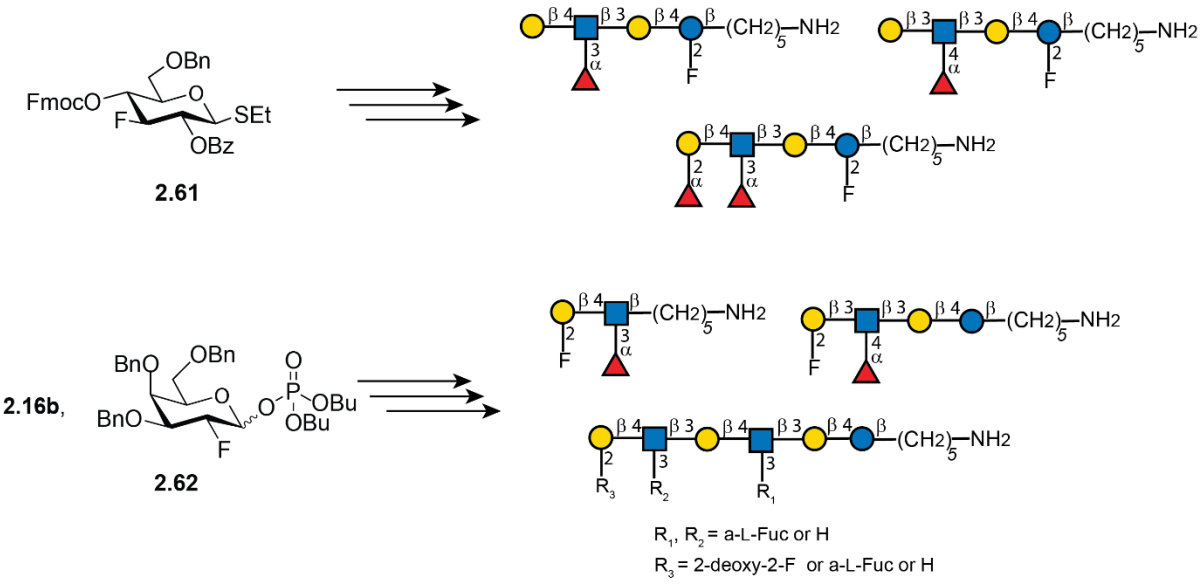

Figure 2.14. Unnatural analogues of Lewis antigens. Structures represented according to SNFG,[77] see page 7.

2.5 Experimental Section

2.5.1 General Methods

All reagents and solvents were acquired from commercial sources, unless stated otherwise. Commercial monosaccharide building blocks were purchased from GlycoUniverse. Anhydrous solvents were obtained from a Solvent Dispensing System (J.C. Meyer). TLC was performed on 0.25 mm Kieselgel 60 F_{254} glass-supported plates (Macherey-Nagel), with detection via UV light (254 nm) and sugar stain (3.70 mL of *p*-anisaldehyde in 140 mL of a solution 3.5% H_2SO_4 in ethanol). For flash chromatography purifications, a Reveleris X2 Flash Chromatography System (GRACE Discovery Sciences) and Reveleris Silica Gel columns were used. Amberlite IR-120 (Across Organics) protonic exchange resin was rinsed with THF, water, methanol and dichloromethane before use. Palladium on carbon was removed from reaction mixtures by filtration with Rotilabo syringe filters (Roth), PTFE filters (pore size: 0.45 µm). Sephadex G25 resin was used for size-exclusion chromatography. NMR spectra were obtained using Ascend 400 (Bruker) and Agilent 400 MHz NMR Magnet (Agilent Technologies) spectrometers at 400 MHz (^{1}H) and 100 MHz (^{13}C) or a Varian 600 (Agilent) at 600 MHz (^{1}H) and 150 MHz (^{13}C), or a Ascend 700 (Bruker) at 700 MHz (^{1}H) and 176 MHz (^{13}C). $CDCl_3$, CD_3OD or D_2O were used as solvents and chemical shifts (δ) referenced to internal standards ($CDCl_3$: 7.26 ppm ^{1}H, 77.16 ppm ^{13}C; CD_3OD: 4.87 or 3.31 ppm ^{1}H, 49.0 ppm ^{13}C; D_2O: 4.79 ppm ^{1}H) unless stated otherwise. Assignments were supported by COSY and HSQC experiments. IR spectra were measured with a Spectrum 100 FT-IR Spectrometer (Perkin Elmer). Only diagnostic signals are listed. Optical rotations were measured using a UniPol L 1000 polarimeter (Schmidt + Haensch), at 25 °C and λ = 589 nm. The solvent and concentrarion (*c*, expressed in g/100 mL) are noted in parentheses. For monitoring reactions by mass spectrometry, an Agilent 1100 Series LC/MSD mass spectrometer was used. MALDI spectra were obtained with a Daltonics Autoflex Speed spectrometer (Bruker). ESI-HRMS were performed with a Xevo G2-XS Q-Tof (Waters). HPLCs were performed on Agilent 1200 Series systems.

2.5.2 Building Block Syntheses

Ethyl 2-*O*-benzoyl-4,6-di-*O*-benzyl-3-*O*-(9-fluorenylmethoxycarbonyl)-1-thio-β-D-galactopyranoside (2.14)[48]

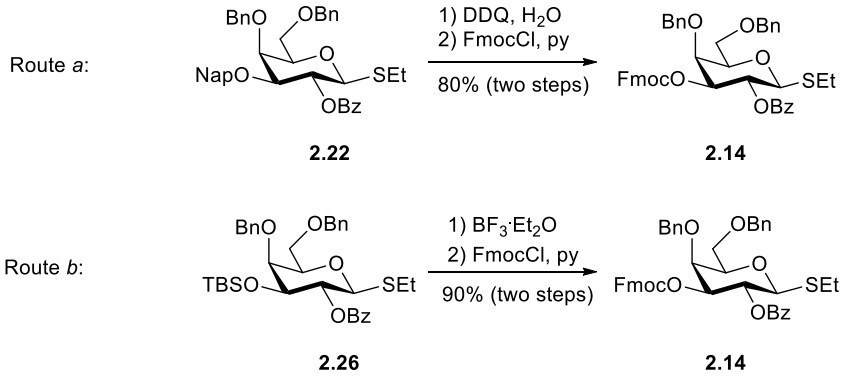

Route a: Starting material **2.22** (655 mg, 1.01 mmol) was dissolved in DCM (15 mL), and water (7.0 mL) was added. The solution was cooled to 0 °C (ice bath) and DDQ (1.00 g, 4.40 mmol) was added. The mixture was allowed to warm up slowly to room temperature and stirred for 2 h, until no starting material was detected by LC-MS analysis. The mixture was quenched with sat aq $NaHCO_3$ (30 mL), and transferred to a separatory funnel. Water (30 mL) was added and the mixture was extracted with DCM (3 x 50 mL). The organic layer was dried over Na_2SO_4, filtrated and concentrated *in vacuo*. The 3-OH product was crystallized from DCM/hexanes and without further purification was dissolved in anhydrous DCM (4.85 mL). Pyridine (0.267 mL, 3.30 mmol) and FmocCl (0.426 g, 1.65 mmol) were added and the mixture was stirred for 3.5 h, until no traces of starting material were detected by TLC. The reaction was diluted with DCM (20 mL), extracted with 1M HCl (10 mL), sat. aq. $NaHCO_3$ (10 mL) and water (10 mL). The organic layer was dried over Na_2SO_4, filtered and concentrated. Purification by column chromatography (EtOAc in hexanes 0 to 20%) afforded **2.14** (583 mg, 0.80 mmol, 80% over two steps) as a colorless syrup. *Route b:* Compound **2.26** (4.05 g, 6.50 mmol) was dissolved in anhydrous ACN (81 mL), cooled to 0 ºC and $BF_3{\cdot}Et_2O$ (0.989 mL, 7.80 mmol) was added. The reaction mixture was stirred for 20 min, until no starting material was detected by TLC. The reaction was quenched with sat. aq. $NaHCO_3$ (60 mL), diluted with DCM (100 mL), and extracted with $NaHCO_3$ (60 mL) and water (60 mL). The organic layer was dried over Na_2SO_4, filtered and concentrated. Without further purification, the 3-OH derivative of **2.26** was dissolved in anhydrous DCM (37.1 mL). Pyridine (2.00 mL, 24.7 mmol) and FmocCl (3.76 g, 14.5 mmol) were added and the mixture was stirred for 3.5 h, until no traces of starting material were detected. The reaction was diluted with DCM (50 mL), extracted with 1M HCl (60 mL), sat. aq. $NaHCO_3$ (60 mL) and water (60 mL). The organic layer was dried over Na_2SO_4, filtered and concentrated. Purification by column chromatography (EtOAc in hexanes

0 to 20%) afforded **2.14** (4.35 g, 5.95 mmol, 90% over two steps) as a colorless syrup. Product **2.14**: ^{1}H NMR (400 MHz, $CDCl_3$) δ 8.05 (dd, *J* = 8.3, 1.3 Hz, 2H), 7.73 – 7.65 (m, 2H), 7.56 – 7.51 (m, 1H), 7.48 – 7.28 (m, 16H), 7.17 – 7.08 (m, 2H), 5.76 (t, *J* = 9.9 Hz, 1H, H-2), 5.08 (dd, *J* = 10.0, 3.0 Hz, 1H, H-3), 4.80 (d, *J* = 11.4 Hz, 1H), 4.61 (d, *J* = 9.9 Hz, 1H, **H-1**), 4.58 – 4.43 (m, 3H), 4.31 (dd, *J* = 10.4, 7.2 Hz, 1H, H-6), 4.22 (dd, *J* = 10.4, 7.8 Hz, 1H, H-6'), 4.15 (d, J = 2.5 Hz, 1H, H-4), 4.07 (t, *J* = 7.4 Hz, 1H, H-5), 3.83 (t, *J* = 6.6 Hz, 1H, CH Fmoc), 3.70 – 3.66 (m, 2H, CH_2 fluorenyl), 2.86 – 2.66 (m, 2H, S-C*H*$_2$CH$_3$), 1.24 (t, *J* = 7.5 Hz, 3H, S-CH$_2$C*H*$_3$). ^{13}C NMR (101 MHz, CDCl3) δ 165.3 (C=O Bz), 154.6 (C=O Fmoc), 143.3, 142.8, 141.2, 141.1, 137.9, 137.7, 133.3, 130.0, 129.6, 128.5, 128.4, 128.3, 128.2, 127.93, 127.90, 127.83, 127.75, 127.13, 127.10, 125.2, 124.98, 120.0, 83.7 (**C-1**), 79.0 (C-3), 77.28, 77.24, 75.10, 73.98, 73.6, 70.1 (C-6), 68.6 (C-2), 68.1 (CH_2 Fmoc), 46.5 (C-5), 23.9 (S-*C*H$_2$CH$_3$), 14.8 (S-CH$_2$*C*H$_3$).

p-Tolyl 2,3,4-tri-*O*-benzyl-1-thio-β-L-fucopyranoside (2.17a)[138]

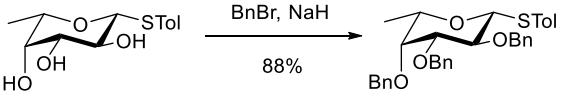

2.30 **2.17a**

To a solution of triol **2.30** (1.30 g, 4.81 mmol) in anhydrous DMF (16 mL), a 60% NaH dispersion in mineral oil (1.35 g, 33.7 mmol) at 0 °C was added. The mixture was stirred for 20 min and then benzyl bromide (4.00 mL, 33.7 mmol) was added dropwise. The reaction was allowed to warm up to room temperature and stirred overnight. Reaction was quenched by adding MeOH (5 mL) at 0 °C. DMF was evaporated *in vacuo*, the crude reaction mixture was dissolved in DCM (150 mL) and extracted with water (2 x 40 mL). The organic layer was dried over Na_2SO_4, filtrated and solvent was removed *in vacuo*. Purification by flash chromatography (hexanes:AcOEt 0 to 30%) afforded product **2.17a** (2.30 g, 4.25 mmol, 88% yield). ^{1}H NMR (400 MHz,$CDCl_3$) δ 7.50 (d, *J* = 7.8 Hz, 2H), 7.44 – 7.28 (m, 15H), 7.02 (d, *J* = 7.8 Hz, 2H), 5.01 (d, *J* = 11.6 Hz, 1H), 4.81 (d, *J* = 10.2 Hz, 1H), 4.73 (m, 3H), 4.68 (d, *J* = 11.6 Hz, 1H), 4.56 (d, *J* = 9.6 Hz, 1H, **H-1**), 3.90 (t, *J* = 9.4 Hz, 1H, H-2), 3.63 (s, 1H, H-4), 3.59 (dd, *J* = 9.2, 2.9 Hz, 1H, H-3), 3.51 (q, *J* = 6.3 Hz, 1H, H-5), 2.31 (s, 3H, S-Ph-C*H*$_3$), 1.27 (d, *J* = 6.3 Hz, 3H, CH_3 Fuc). ^{13}C NMR (101 MHz, $CDCl_3$) δ 138.7, 138.4, 138.6, 137.1, 132.2, 130.4, 129.5, 128.4, 128.33, 128.30, 128.1, 127.9, 127.66, 127.65, 127.55, 127.4, 87.8 (**C-1**), 84.6 (C-3), 77.1 (C-2), 76.6 (C-4), 75.5, 74.53, 74.52 (C-5), 72.8, 21.1 (S-Ph-*C*H$_3$), 17.3 (C-6).

_p_-Tolyl 3,4-di-_O_-acetyl-_2_-_O_-benzyl-1-thio-β-L-fucopyranoside (2.17b)[139]

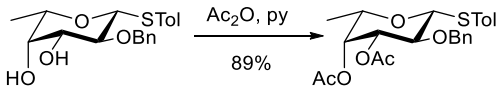

2.33 **2.17b**

A solution of **2.33** (1.65 g, 4.58 mmol) in anhydrous pyridine (2.22 mL, 27.5 mmol) was cooled to 0 °C and then acetic anhydride (1.73 mL, 18.3 mmol) was added dropwise. The reaction was allowed to warm up to room temperature and then stirred overnight. After complete conversion of the starting material, the reaction was quenched with MeOH (3 mL) at 0 °C. Solvent was removed *in vacuo* and the remaining oil was dissolved in EtOAc (100 mL) and extracted with 1 M HCl (50 mL), aq. sat $NaHCO_3$ (50 mL) and brine (50 mL). The organic layer was dried over Na_2SO_4, filtrated and solvent was removed *in vacuo* to give a colorless syrup. Purification using flash chromatography (hexanes:AcOEt 0 to 12%) afforded compound **2.17b** (1.81 g, 4.07 mmol, 89% yield). ^{1}H NMR (400 MHz, $CDCl_3$) δ 7.50 (d, *J* = 8.2 Hz, 2H), 7.37 – 7.26 (m, 5H), 7.13 (d, *J* = 7.9 Hz, 2H), 5.24 (dd, *J* = 3.3, 1.0 Hz, 1H, H-4), 5.01 (dd, *J* = 9.7, 3.3 Hz, 1H, H-3), 4.86 (d, *J* = 10.9 Hz, 1H, C*H*H'-Ph), 4.65 (d, *J* = 9.7 Hz, 1H, **H-1**), 4.57 (d, *J* = 10.9 Hz, 1H, CH*H'*-Ph), 3.77 (qd, *J* = 6.4, 1.1 Hz, 1H, H-5), 3.70 (t, *J* = 9.7 Hz, 1H, H-2), 2.35 (s, 3H, -C*H*$_3$ STol), 2.15 (s, 3H, C(O)C*H*$_3$), 1.93 (s, 3H, C(O)C*H*$_3$), 1.22 (d, *J* = 6.4 Hz, 3H, C*H*$_3$ Fuc). ^{13}C NMR (101 MHz, $CDCl_3$) δ 170.7 (*C*(O)CH_3), 170.1 (*C*(O)CH_3), 138.2, 138.0, 132.7, 129.9, 129.8, 128.5, 128.01, 127.95, 88.2 (**C-1**), 75.6 (*C*H_2-Ph), 75.3 (C-2), 74.8 (C-3), 73.0 (C-5), 71.1 (C-4), 21.3, 20.9 (2 x C(O)C*H*$_3$, S-Ph-*C*H_3), 16.7 (C-6).

Ethyl 4,6-_O_-benzylidene-1-thio-β-D-galactopyranoside (2.18)[127]

2.18

Benzylidene acetal **2.18** was synthesized in three steps starting from peracetylated galactose following previously described procedures.[127] ^{1}H NMR (400 MHz, $CDCl_3$) δ 7.51 – 7.46 (m, 2H), 7.39 – 7.35 (m, 3H), 5.54 (s, 1H), 4.36 (s, 1H), 4.33 (s, 1H), 4.26 (d, *J* = 3.3 Hz, 1H), 4.03 (dd, *J* = 12.5, 1.6 Hz, 1H), 3.81 (t, *J* = 9.3 Hz, 1H), 3.69 (td, *J* = 8.9, 3.6 Hz, 1H), 3.52 (s, 1H), 2.89 – 2.70 (m, 2H), 2.63 (d, *J* = 8.9 Hz, 1H), 2.60 (s, 1H), 1.35 (t, *J* = 7.5 Hz, 3H). ^{13}C NMR (101 MHz, $CDCl_3$) δ 137.7, 129.4, 128.4, 126.5, 101.6, 85.4, 75.7, 74.0, 70.2, 69.8, 69.4, 23.6, 15.4.

Ethyl 4,6-*O*-benzylidene-3-*O*-(2-naphthylmethyl)-1-thio-β-D-galactopyranoside (2.19)

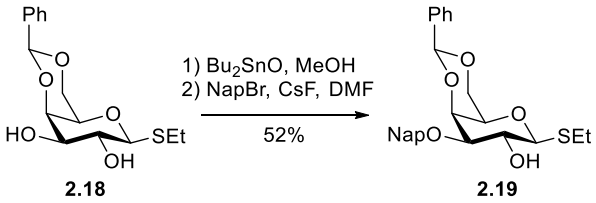

2.18 **2.19**

In a round-bottom flask equipped with a reflux condenser, compound **2.18** (3.75 g, 12.0 mmol) was dissolved in anhydrous methanol (40 mL) and dibutyltin oxide (3.59 g, 14.4 mmol) was added. The mixture was stirred at 80 °C overnight, and then the solvent was evaporated using a rotatory evaporator. The crude stannylene ketal was coevaporated with toluene twice, and subsequently dissolved in anhydrous DMF (40 mL). Cesium fluoride (2.74 g, 18.0 mmol), 2-(bromomethyl)naphthalene (2.92 g, 13.2 mmol) and sodium sulfate (2.04 g, 14.4 mmol) were added, and the reaction was stirred under reflux at 60 °C for 4 h. The mixture was diluted with ethyl acetate (150 mL) and washed with water (2 x 50 mL). The organic layer was dried over Na_2SO_4, filtered and concentrated. Compound **2.19** (2.82 g, 6.23 mmol, 52% yield) was obtained as a white solid after purification using flash chromatography (hexanes:AcOEt 20 to 100 %). $[\alpha]_D^{25}$ (*c* 1, $CHCl_3$) + 21.4. IR (film): 3386 cm^{-1} (b, OH), 3062 cm^{-1}, 2977 cm^{-1}, 2881 cm^{-1} (w, C-H Ar), 1075 cm^{-1}, 1047 cm^{-1}, 1002 cm^{-1} (s, C-O ether), 819 cm^{-1} (s), 732 cm^{-1} (s). 697 cm^{-1} (w).^{1}H NMR (400 MHz, $CDCl_3$) δ 7.89 – 7.75 (m, 4H), 7.60 – 7.45 (m, 5H), 7.41 – 7.35 (m, 3H), 5.42 (s, 1H, C*H*Ph), 4.93 (s, 2H, C*H*$_2$ Nap) 4.34 (d, *J* = 9.6 Hz, 1H, **H-1**), 4.27 (d, *J* = 12.4 Hz, 1H, H-6), 4.15 (d, *J* = 3.5 Hz, 1H, H-5), 4.11 (t, *J* = 9.3 Hz, 1H, H-2), 3.88 (d, *J* = 12.3 Hz, 1H, H-6'), 3.53 (dd, *J* = 9.2, 3.4 Hz, 1H, H-3), 3.29 (s, 1H, H-4), 2.93 – 2.66 (m, 3H, SC*H*$_2$CH$_3$ and HO-2), 1.34 (t, *J* = 7.4 Hz, 3H, SCH$_2$C*H*$_3$). ^{13}C NMR (101 MHz, $CDCl_3$) δ 137.9, 135.7, 133.2, 133.0, 129.0, 128.3, 128.2, 127.9, 127.7, 126.6, 126.4, 126.2, 126.0, 125.8, 101.2 (*C*HPh), 85.3 (**C-1**), 80.3 (C-3), 73.5 (C-5), 71.6 (*C*H$_2$ Nap), 70.0 (C-4), 69.3 (C-6), 68.1 (C-2), 23.0 (S*C*H$_2$CH$_3$), 15.3 (SCH$_2$*C*H$_3$). HRMS (ESI) calc. for $C_{26}H_{28}O_5SNa$, $[M+Na]^+$ 475.1550; found: 475.1562.

Ethyl 2-*O*-benzoyl-4,6-*O*-benzylidene-3-*O*-(2-naphthylmethyl)-1-thio-β-D-galactopyranoside (2.20)

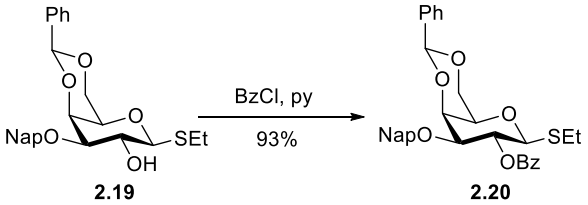

2.19 **2.20**

To a solution of compound **2.19** (3.50 g, 7.73 mmol) in anhydrous DCM/pyridine 10:1 (48 mL), benzoyl chloride (3.14 mL, 27.1 mmol) was added and the reaction mixture was stirred at room temperature for 4 h. The reaction was quenched by adding methanol (2 mL) at 0 °C, diluted with DCM (60 mL) and washed with sat. aq. $NaHCO_3$ (40 mL) and water (40 mL). The organic layer was dried over Na_2SO_4, filtered and the solvent was removed *in vacuo*. Purification using column chromatography (DCM/acetone 0 to 3%) afforded **33** (4.00 g, 7.19 mmol, 93% yield). $[\alpha]_D^{25}$ (*c* 0.82, $CHCl_3$) + 0.9. IR (film): 2869 cm^{-1} (w, C-H Ar), 1723 cm^{-1} (s, C=O), 1268 cm^{-1} (s, C-O ester), 1101 cm^{-1} (s, C-O ether), 996 cm^{-1} (s), 818 cm^{-1} (w), 710 cm^{-1} (s). ^{1}H NMR (400 MHz, $CDCl_3$) δ 8.04 – 8.00 (m, 2H), 7.80 – 7.75 (m, 1H), 7.69 – 7.53 (m, 6H), 7.49 – 7.31 (m, 8H), 5.76 (t, *J* = 9.7 Hz, 1H, H-2), 5.52 (s, 1H, C*H*Ph), 4.84 (d, *J* = 13.0 Hz, 1H, C*H*H' Nap), 4.77 (d, *J* = 13.0 Hz, 1H, CH*H'* Nap), 4.52 (d, *J* = 9.8 Hz, 1H, **H-1**), 4.35 (dd, *J* = 12.3, 1.6 Hz, 1H, H-6), 4.31 (d, *J* = 3.3 Hz, 1H, H-4), 4.01 (dd, *J* = 12.4, 1.7 Hz, 1H, H-6'), 3.79 (dd, *J* = 9.6, 3.4 Hz, 1H, H-3), 3.45 (d, *J* = 1.4 Hz, 1H, H-5), 2.92 (dq, *J* = 12.2, 7.5 Hz, 1H, SC*H*H'CH_3), 2.77 (dq, *J* = 12.3, 7.5 Hz, 1H, SCH*H'*CH_3), 1.27 (t, *J* = 7.5 Hz, 3H, SCH_2CH_3). ^{13}C NMR (101 MHz, $CDCl_3$) δ 165.4 (C=O Bz), 137.8, 135.4, 133.2, 133.2, 133.1, 130.3, 130.0, 129.25, 128.5, 128.40, 128.35, 127.9, 127.8, 126.65, 126.64, 126.3, 126.1, 125.9, 101.6 (*C*HPh), 83.0 (**C-1**), 78.2 (C-3), 73.6 (C-4) , 71.3 (CH_2 Nap), 70.3 (C-5), 69.5 (C-6), 68.8 (C-2), 22.9 (SCH_2CH_3), 15.0 (SCH_2CH_3). HRMS (ESI) calc. for $C_{33}H_{32}O_6SNa$, $[M+Na]^+$ 579.1812; found: 579.1807.

Ethyl 2-*O*-benzoyl-3-*O*-(2-naphthylmethyl)-1-thio-β-D-galactopyranoside (2.21)

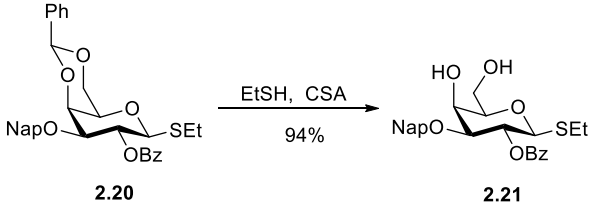

2.20 **2.21**

To a solution of **2.20** (4.00 g, 7.19 mmol) in DCM/MeOH 99:1 (24 mL), ethanethiol (2.66 mL, 35.9 mmol) was added, followed by CSA (0.334 g, 1.44 mmol). The reaction was stirred overnight at room temperature, and then quenched by TEA addition (0.300 mL, 2.16 mmol).

Solvent was removed using a rotatory evaporator and the remaining crude was purified by column chromatography (DCM/acetone 0 to 10 %), to afford diol **2.21** (3.16 g, 6.74 mmol, 94% yield). $[\alpha]_D^{25}$ (*c* 1, $CHCl_3$) -10.6. IR (film): 3434 cm^{-1} (b, OH), 2873 cm^{-1} (w, C-H Ar), 1722 cm^{-1} (s, C=O), 1270 cm^{-1} (s, C-O ester), 1094 cm^{-1}, 1071 cm^{-1} (s, C-O ether), 710 cm^{-1} (s). ^{1}H NMR (400 MHz, $CDCl_3$) δ 7.98 (dd, *J* = 8.3, 1.4 Hz, 2H), 7.80 – 7.68 (m, 1H), 7.66 – 7.53 (m, 4H), 7.49 – 7.37 (m, 4H), 7.26 (dd, *J* = 8.4, 1.7 Hz, 1H), 5.56 (t, *J* = 9.7 Hz, 1H, H-2), 4.84 (d, *J* = 12.5 Hz, 1H, C*H*H' Nap), 4.68 (d, *J* = 12.5 Hz, 1H, CH*H'* Nap), 4.48 (d, *J* = 10.0 Hz, 1H, **H-1**), 4.21 (dd, *J* = 3.4, 1.3 Hz, 1H, H-4), 4.01 (dd, *J* = 11.7, 6.7 Hz, 1H, H-6), 3.85 (dd, *J* = 11.7, 4.7 Hz, 1H, H-6'), 3.71 (dd, *J* = 9.3, 3.3 Hz, 1H, H-3), 3.59 (m, 1H, H-5), 2.85 – 2.62 (m, 2H, S*CH*$_2$CH$_3$), 2.46 (bs, 2H, HO), 1.21 (t, *J* = 7.5 Hz, 3H, SCH$_2$*CH*$_3$). ^{13}C NMR (101 MHz, $CDCl_3$) δ 165.6 (C=O Bz), 134.5, 133.3, 133.2, 133.1, 130.00, 129.97, 128.6, 128.5, 128.0, 127.8, 127.0, 126.4, 126.2, 125.8, 83.6 (**C-1**), 79.1 (C-3), 78.5 (C-5), 71.5 (*C*H$_2$ Nap), 69.5 (C-2), 67.0 (C-4), 62.7 (C-6), 23.8 (S*C*H$_2$CH$_3$), 15.0 (SCH$_2$*C*H$_3$). HRMS (ESI) calc. for $C_{26}H_{28}O_6SNa$, $[M+Na]^+$ 491.1499; found: 491.1513.

Ethyl *2-O*-benzoyl-4,6-di-*O*-benzyl-3-*O*-(2-naphthylmethyl)-1-thio-β-D-galactopyranoside (2.22)

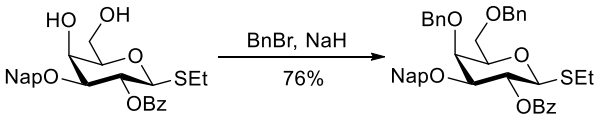

2.21 **2.22**

Diol **2.21** (3.16 g, 6.74 mmol) was dissolved in anhydrous THF/DMF 10:1 (31mL). The solution was cooled to 0 °C and sodium hydride (60% dispersion in mineral oil) (0.620 g, 15.5 mmol) was added. After stirring for 20 min, benzyl bromide (2.40 mL, 20.2 mmol) was added dropwise. The solution was kept at 0 °C for 2 h, and then quenched by adding acetic acid (0.964 mL, 16.8 mmol) dropwise. The reaction mixture was diluted with DCM (70 mL), and extracted with aq. sat. $NaHCO_3$ (40 mL) and water (40 mL). The organic layer was dried over Na_2SO_4, filtered and solvent was removed *in vacuo*. Product **2.22** was purified by flash chromatography hexanes:AcOEt 0 to 20% (3.35 g, 5.16 mmol, 77% yield). $[\alpha]_D^{25}$ (*c* 1, $CHCl_3$) + 17.4. IR (film): 3063 cm^{-1} (w, C-H Ar), 2870 cm^{-1} (w, C-H Ar), 1726 cm^{-1} (s, C=O), 1268 cm^{-1} (s, C-O ester), 1098 cm^{-1}, 1071 (s, C-O ether), 710 cm^{-1} (s). ^{1}H NMR (400 MHz, $CDCl_3$) δ 8.03 – 7.95 (m, 2H), 7.78 – 7.68 (m, 1H), 7.62 (s, 1H), 7.60 – 7.52 (m, 4H), 7.47 – 7.23 (m, 14H), 5.73 (t, *J* = 9.7 Hz, 1H, H-2), 5.04 (d, *J* = 11.7 Hz, 1H), 4.81 (d, *J* = 12.5 Hz, 1H), 4.66 (m, 2H), 4.52 – 4.40 (m, 3H, including **H-1**), 4.11 (d, *J* = 2.8 Hz, 1H, H-4), 3.72 (dd, *J* = 9.6, 2.7 Hz, 1H, H-3), 3.66 (m, 3H), 2.83 – 2.57 (m, 2H, S*CH*$_2$CH$_3$), 1.21 (t, *J* = 7.4 Hz, 3H,

SCH_2CH_3). ^{13}C NMR (101 MHz, $CDCl_3$) δ 165.4 (C=O Bz), 138.6 , 137.8, 135.1, 133.0, 132.94, 132.90, 130.1, 129.9, 128.4, 128.3, 128.2, 128.2, 128.04, 127.97, 127.84, 127.80, 127.6, 127.5, 126.8, 126.0, 125.9, 125.7, 83.7 (**C-1**), 80.9 (C-3), 77.5 (C-5), 74.5, 73.6 (CH_2), 72.7 (C-4), 71.7, 70.2 (C-2), 68.5 (CH_2), 23.7 (SCH_2CH_3), 14.8 (SCH_2CH_3). HRMS (ESI) calc. for $C_{40}H_{40}O_6SNa$, $[M+Na]^+$ 671.2438; found: 671.2438.

Ethyl 4,6-*O*-benzylidene-3-*O*-*tert*-butyldimethylsilyl-1-thio-β-D-galactopyranoside (2.23)[140]

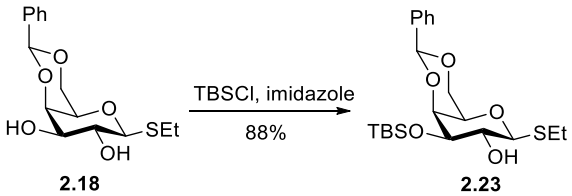

2.18 **2.23**

To a solution of benzylidene acetal **2.18** (5.00 g, 16.0 mmol) in anhydrous DCM (160 mL) TBSCl (3.14 g, 20.8 mmol) and imidazole (1.53 g, 22.4 mmol) were added at 0 °C. The reaction mixture was stirred at room temperature for 48 h and quenched with addition of sat. aq. $NaHCO_3$ (50 mL). The organic layer was washed with sat. aq. $NaHCO_3$ (2 x 50 mL). The aqueous layers were combined and back extracted with DCM. The organic layer was dried over Na_2SO_4, filtered and concentrated. The crude product was crystallized from hexanes to obtain the product as a white solid (5.22 g, 76%). Mother liquors were purified by column chromatography (20% AcOEt in hexanes), affording **2.23** (6.01 g, 14.0 mmol, 88% yield). ^1H NMR (400 MHz, $CDCl_3$) δ 7.54 – 7.48 (m, 2H), 7.41 – 7.31 (m, 3H), 5.50 (s, 1H), 4.37 – 4.33 (m, 2H), 4.08 (dd, *J* = 3.6, 1.1 Hz, 1H), 4.02 (dd, *J* = 12.5, 1.9 Hz, 1H), 3.88 (t, *J* = 9.3 Hz, 1H), 3.72 (dd, *J* = 9.0, 3.6 Hz, 1H), 3.48 (d, *J* = 1.4 Hz, 1H), 2.88 – 2.68 (m, 2H), 1.32 (t, *J* = 7.4 Hz, 3H), 0.91 (s, 9H), 0.13 (s, 3H), 0.12 (s, 3H). ^{13}C NMR (101 MHz, $CDCl_3$) δ 138.1, 128.9, 128.2, 126.3, 101.1, 85.3, 76.9, 75.6, 70.4, 69.58, 68.9, 25.9, 23.2, 18.4, 15.4, -4.2, -4.5.

Ethyl 2-*O*-benzoyl-4,6-*O*-benzylidene-3-*O*-tert-butyldimethylsilyl-1-thio-β-D-galactopyranoside (2.24)[87]

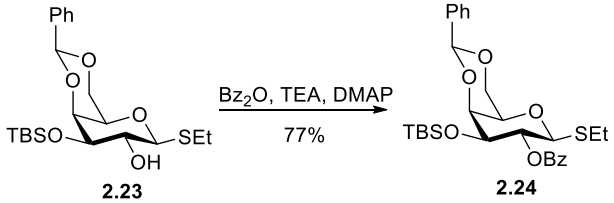

2.23 **2.24**

To a solution of **2.23** (9.44 g, 22.1 mmol) in DCM (111 mL), TEA (15.4 mL, 111 mmol), Bz_2O (15.0 g, 66.4 mmol) and dimethylaminopyridine (DMAP) (1.08 g, 8.85 mmol) were added. The

reaction mixture was stirred at room temperature for 36 h. The reaction was quenched by adding methanol at 0 °C, and the solvents were removed solvents *in vacuo*. The concentrated was disolved in DCM (200 mL), extracted with $NaHCO_3$ (100 mL) and H_2O (2 x 80 mL). The organic layer was dried with Na_2SO_4, filtered and evaporated. Crystallization from hexanes afforded **2.24** (9.01 g, 17.0 mmol, 77%) as a white solid. ^{1}H NMR (400 MHz, $CDCl_3$) δ 8.05 – 8.02 (m, 2H), 7.59 – 7.33 (m, 8H), 5.60 (t, *J* = 9.6 Hz, 1H), 5.53 (s, 1H), 4.56 (d, *J* = 9.9 Hz, 1H), 4.39 (dd, *J* = 12.4, 1.6 Hz, 1H), 4.14 (dd, *J* = 3.7, 1.0 Hz, 1H), 4.06 (dd, *J* = 12.4, 1.7 Hz, 1H), 4.01 (dd, *J* = 9.3, 3.6 Hz, 1H), 3.55 (d, *J* = 1.3 Hz, 1H), 2.98 – 2.65 (m, 2H), 1.25 (t, *J* = 7.5 Hz, 3H), 0.74 (s, 9H), 0.04 (s, 3H), -0.12 (s, 3H). ^{13}C NMR (101 MHz, $CDCl_3$) δ 165.4, 138.0, 133.0, 130.4, 129.9, 129.0, 128.4, 128.3, 126.4, 101.2, 82.9, 76.9, 73.6, 70.3, 69.5, 25.6, 22.8, 18.0, 15.0, -4.5, -4.6.

Ethyl 2-*O*-benzoyl-4-*O*-benzyl-3-*O*-tert-butyldimethylsilyl-1-thio-β-D-galactopyranoside (2.25)[87]

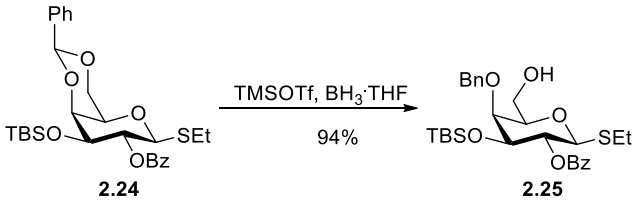

A 1 M solution of BH_3·THF (14.8 mL, 14.8 mmol) and TMSOTf (0.267 mL, 1.48 mmol) were added to a solution of **2.24** (3.50 g, 5.90 mmol) in anhydrous DCM (34.7 mL) at 0 °C under Ar. The reaction was stirred for 2 h, until no starting material was detected by TLC (hexanes:AcOEt 6:4). A TEA/MeOH (1:10) solution (10 mL) was added portionwise to quench the reaction. The reaction mixture was concentrated *in vacuo*, and the concentrated was dissolved in DCM (150 mL), washed with aq. sat. $NaHCO_3$ (60 mL) and brine (60 mL). The organic layer was dried over Na_2SO_4, filtered and concentrated. Purification by column chromatography (hexanes/EtOAc 8:2) afforded **2.25** (3.29 g, 5.53 mmol, 94%) as colorless syrup. ^{1}H NMR (400 MHz, $CDCl_3$) δ 8.08 – 8.02 (m, 2H), 7.60 – 7.54 (m, 1H), 7.48 – 7.43 (m, 2H), 7.41 – 7.28 (m, 5H), 5.65 (t, *J* = 9.3 Hz, 1H), 5.10 (d, *J* = 11.7 Hz, 1H), 4.60 (d, *J* = 11.7 Hz, 1H), 4.51 (d, *J* = 9.6 Hz, 1H), 3.97 (d, *J* = 8.2 Hz, 1H), 3.84 (dd, *J* = 10.9, 6.4 Hz, 1H), 3.77 (d, *J* = 2.3 Hz, 1H), 3.63 – 3.59 (m, 1H), 3.55 (dd, *J* = 10.8, 5.0 Hz, 1H), 2.82 – 2.64 (m, 2H), 1.21 (t, *J* = 7.5 Hz, 3H), 0.79 (s, 9H), 0.12 (s, 3H), -0.08 (s, 3H). ^{13}C NMR (101 MHz, $CDCl_3$) δ 165.5, 138.6, 133.1, 130.4, 130.0, 128.6, 128.4, 128.2, 128.0, 83.9, 79.1, 77.2, 75.9, 74.9, 71.0, 62.4, 25.7, 23.8, 17.9, 15.0, -3.8, -4.9.

Ethyl 2-*O*-benzoyl-4,6-di-*O*-benzyl-3-*O*-tert-butyldimethylsilyl-1-thio-β-D-galactopyranoside (2.26)[87]

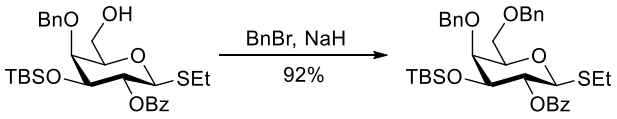

2.25 **2.26**

Compound **2.25** (3.77 g, 7.08 mmol) was dissolved in a THF/DMF 10:1 mixture (39.3 mL). The solution was cooled to 0°C and a 60% dispersion of NaH in mineral oil (0.651 g, 16.3 mmol) was added. After 15 min, BnBr (2.95 mL, 24.8 mmol) was added and the reaction was allowed to proceed at room temperature for 2 h. The reaction was quenched at 0 ºC by HAc (1.22 mL, 21.2 mmol) addition, then diluted with DCM (100 mL), and washed with $NaHCO_3$ (60 mL) and H_2O (60 mL). The organic layer was dried over Na_2SO_4, filtered and concentrated. Purification by column chromatography (EtOAc in hexanes 0 to 20%) afforded **2.26** (4.07 g, 6.53 mmol, 92%) as colorless syrup. ^{1}H NMR (400 MHz, $CDCl_3$) δ 8.08 – 8.02 (m, 2H), 7.60 – 7.52 (m, 1H), 7.47 – 7.40 (m, 2H), 7.37 – 7.26 (m, 10H), 5.63 (t, *J* = 9.5 Hz, 1H), 5.09 (d, *J* = 11.4 Hz, 1H), 4.59 – 4.38 (m, 3H), 3.96 (d, *J* = 8.7 Hz, 1H), 3.85 (d, *J* = 2.2 Hz, 2H), 3.73 (m, 1H), 3.63 (m, 2H), 2.84 – 2.59 (m, 2H), 1.19 (t, *J* = 7.5 Hz, 3H), 0.77 (s, 9H), 0.11 (s, 3H), -0.09 (s, 3H). ^{13}C NMR (101 MHz, $CDCl_3$) δ 165.5, 139.0, 138.0, 133.0, 130.5, 130.0, 128.6, 128.4, 128.3, 128.1, 127.9, 127.8, 127.5, 83.8, 77.7, 77.4 75.8, 75.3, 73.7, 71.1, 68.8, 25.7, 23.7, 17.9, 15.0, -3.9, -4.9.

1,2,3,4-Tetra-*O*-acetyl-α,β-L-fucopyranoside (2.28)[141]

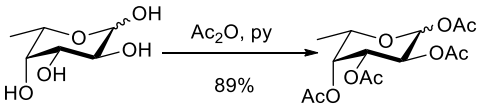

2.27 **2.28**

Pyridine (59 mL) was added to fucose **2.27** (10.0 g, 60.9 mmol) and the mixture was cooled to 0 °C. Acetic anhydride (46.0 mL, 487 mmol) was added dropwise over 10 min. The reaction was stirred overnight at room temperature, and was quenched by adding MeOH at 0 °C. The solvent was removed *in vacuo* and the evaporated was dissolved in DCM (300 mL) and extracted with 1 M HCl (60 mL), $NaHCO_3$ (60 mL), and water (60 mL). The organic layer was dried over Na_2SO_4 and filtered. The solvent was removed *in vacuo* to afford **2.28** as a colorless syrup (18.0 g, 54.2 mmol, α/β 2.6:1, 89% yield). ^{1}H NMR (400 MHz, $CDCl_3$) δ 6.34 (d, *J* = 2.6 Hz, 0.72H, **H-1α**), 5.68 (d, *J* = 8.3 Hz, 0.28H, **H-1β**), 5.40 – 5.24 (m, 2.72H, 3 x Hα and 1 x Hβ), 5.07 (dd, *J* = 10.4, 3.4 Hz, 0.28H, Hβ), 4.32 – 4.22 (m, 0.72 H, H-5α), 4.03 – 3.90 (m, 0.28H, H-5β), 2.19 (s, 0.84H, *CH$_3$* Ac-β), 2.18 (s, 2.16H, *CH$_3$* Ac-α), 2.15 (s, 2.16H, *CH$_3$* Ac-

α), 2.12 (s, 0.84H, *CH₃* Ac-β), 2.04 (s, 0.84H, *CH₃* Ac-β), 2.02 (s, 2.16H, *CH₃* Ac-α), 2.00 (s, 2.16H, *CH₃* Ac-α), 1.99 (s, 0.84H, *CH₃* Ac-β), 1.23 (d, *J* = 6.4 Hz, 0.84H, H-6β), 1.16 (d, *J* = 6.5 Hz, 2.16H, H-6α). ^{13}C NMR (101 MHz, $CDCl_3$) δ 170.67, 170.65, 170.3, 170.2, 170.1, 169.6, 169.30, 169.28, 92.3 (**C-1β**), 90.1 (**C-1α**), 71.4, 70.7, 70.4, 70.1, 68.04, 67.95, 67.4, 66.6, 21.1 (C(O)C*H₃*), 21.0 (C(O)C*H₃*), 20.82 (2 x C(O)C*H₃*), 20.78 (C(O)C*H₃*), 20.75 (C(O)C*H₃*), 20.71 (2 x C(O)C*H₃*), 16.07, 16.05 (C-6α,β).

_p_-Tolyl 2,3,4-tri-_O_-acetyl-β-1-thio-L-fucopyranoside (2.29)[141]

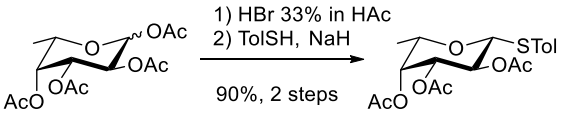

2.28 **2.29**

To a cooled solution of peracetylated fucose **2.28** (7.20 g, 21.7 mmol) in anhydrous DCM (87 mL) was added acetic anhydride (1.02 mL, 10.8 mmol) under nitrogen. HBr (33% in acetic acid, 17.8 mL, 108 mmol) was then added dropwise using an addition funnel. The mixture was allowed to warm up to room temperature and stirred for 3 h. The reaction was cooled to 0 °C, diluted with DCM (50 mL), and sat. aq. $NaHCO_3$ (40 mL) was added portionwise with stirring. The organic layer was separated and washed with sat. aq. $NaHCO_3$ (40 mL), brine (40 mL), dried over Na_2SO_4, filtered and concentrated to obtain the corresponding glycosyl bromide[142] as an oil. To a solution of *p*-thiocresol (3.23 g, 26.0 mmol) in anhydrous DMF (27 mL), sodium hydride (1.13 g, 28.2 mmol) was added slowly at 0 °C. After stirring for 15 min, a 1.6 M solution of the glycosyl bromide in DMF (13.5 mL, 21.7 mmol) was added slowly, using an addition funnel. After TLC showed complete conversion of the starting material (1 h) the reaction mixture was diluted with DCM (150 mL) and extracted with aq. sat. AcONa (50 mL) and water (50 mL). The organic layer was dried with Na_2SO_4, filtered and the solvent was removed *in vacuo*. Crystallization from hexanes afforded **2.29** (7.70 g, 19.4 mmol, 90% yield) as a white solid. ^{1}H NMR (400 MHz, $CDCl_3$) δ 7.45 – 7.37 (m, 2H), 7.13 (d, *J* = 7.9 Hz, 2H), 5.25 (dd, *J* = 3.4, 1.1 Hz, 1H), 5.20 (t, *J* = 9.9 Hz, 1H), 5.04 (dd, *J* = 9.9, 3.4 Hz, 1H), 4.63 (d, *J* = 9.9 Hz, 1H), 3.80 (qd, *J* = 6.5, 1.1 Hz, 1H), 2.34 (s, 3H), 2.14 (s, 3H), 2.09 (s, 3H), 1.97 (s, 3H), 1.23 (d, *J* = 6.4 Hz, 3H). ^{13}C NMR (101 MHz, $CDCl_3$) δ 170.8, 170.3, 169.7, 138.4, 133.1, 129.8, 129.2, 87.0, 73.5, 72.6, 70.5, 67.5, 21.3, 21.1, 20.84, 20.81, 16.6.

***p*-Tolyl 1-thio-β-L-fucopyranoside (2.30)**[143]

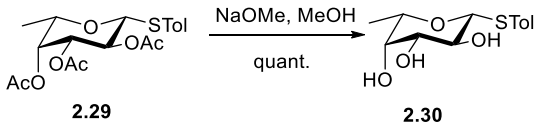

To a solution of **2.29** (2.00 g, 5.04 mmol) in MeOH (25mL), was added NaOMe (0.273 g, 5.04 mmol). The reaction mixture was stirred at room temperature for 4 h. Amberlite resin was added to quench. When the pH decreased from 7 to 5 the reaction was filtered. After solvent evaporation, compound **2.30** (1.35 g, 4.99 mmol, quantitative) was obtained as a white solid. ^{1}H NMR (400 MHz, CD_3OD) δ 7.42 (d, *J* = 8.1 Hz, 2H), 7.12 (d, *J* = 8.0 Hz, 2H), 4.49 (d, *J* = 9.4 Hz, 1H), 3.65 – 3.60 (m, 2H), 3.54 (t_a, *J* = 9.3 Hz, 1H), 3.48 (dd, *J* = 9.2, 3.2 Hz, 1H), 2.32 (s, 3H), 1.26 (d, *J* = 6.4 Hz, 3H). ^{13}C NMR (101 MHz, CD_3OD) δ 138.5, 133.0, 132.1, 130.5, 90.4, 76.5, 76.0, 73.1, 70.8, 21.1, 17.0.

***p*-Tolyl 2-*O*-benzyl-1-thio-β-L-fucopyranoside (2.33)**

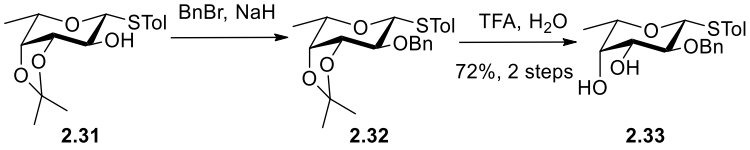

To a solution of tolyl 3,4-*O*-isopropylidene-β-L-fucopyranoside **2.31** (2.00 g, 6.44 mmol) in anhydrous DMF (22 mL) kept at 0 °C, a 60% NaH dispersion in mineral oil (0.335 g, 8.38 mmol) was added. The mixture was stirred for 15 min and then benzyl bromide (0.990 mL, 8.38 mmol) was added dropwise. The solution was allowed to warm to room temperature. After 1 h, conversion of the starting material was complete (observed by TLC), and the reaction was quenched by adding MeOH at 0 °C. DMF was evaporated *in vacuo*, the crude reaction mixture was dissolved in DCM (150 mL) and extracted with water (2 x 40 mL). The organic layer was dried over Na_2SO_4, filtrated and solvent was removed *in vacuo*. Without further purification, **2.32**[139] was dissolved in a mixture of DCM/water 99.5:0.5 (33 mL). At 0 °C and with magnetic stirring, TFA (3.92 mL, 50.9 mmol) was added. The reaction was then stirred at room temperature until complete conversion of the starting material. The product was purified by flash chromatography (Hex:AcOEt 0 to 60%) to obtain diol **2.33** as a colorless solid (1.65 g, 6.37 mmol, 72% over two steps). ^{1}H NMR of **2.32** (400 MHz, $CDCl_3$) δ 7.48 – 7.39 (m, 4H), 7.37 – 7.27 (m, 3H), 7.10 (d, *J* = 9.0 Hz, 2H), 4.82 (d, *J* = 11.3 Hz, 1H), 4.68 (d, *J* = 11.3 Hz, 1H), 4.52 (d, *J* = 9.7 Hz, 1H), 4.24 – 4.18 (m, 1H), 4.04 (d, *J* = 7.7 Hz, 1H), 3.79 (qd, *J* = 6.5, 2.1 Hz, 1H), 3.48 (dd, *J* = 9.7, 6.5 Hz, 1H), 2.33 (s, 3H), 1.41 (s, 3H), 1.39 (d, *J* = 6.6 Hz, 3H), 1.36 (s, 3H). ^{13}C NMR (101 MHz, $CDCl_3$) δ 138.2, 137.7, 132.9, 130.1, 129.7, 128.41, 128.37,

127.8, 109.8, 86.7, 80.0, 78.4, 76.6, 73.6, 72.5, 28.1, 26.6, 21.3, 17.0. Analytical data for **2.33**: $[\alpha]_D^{25}$ (*c* 1, $CHCl_3$) – 9.6. IR (film): 3433 cm^{-1} (b, OH), 2922 cm^{-1} (w, C-H Ar), 1494 cm^{-1} (s), 1075 cm^{-1} (s, C-O ether) 1050 cm^{-1} (s), 864 cm^{-1} (w), 811 cm^{-1} (w), 738 cm^{-1} (s), 699 cm^{-1} (w). ^{1}H NMR of 24 (400 MHz, $CDCl_3$) δ 7.50 – 7.45 (m, 2H), 7.43 – 7.28 (m, 5H), 7.13 (d, *J* = 7.9 Hz, 2H), 4.96 (d, *J* = 11.0 Hz, 1H, C*H*H'-Ph), 4.70 (d, *J* = 11.0 Hz, 1H, CH*H'*-Ph), 4.54 (d, *J* = 9.7 Hz, 1H, **H-1**), 3.70 (d, *J* = 2.9 Hz, 1H, H-4), 3.64 (dd, *J* = 8.9, 3.3 Hz, 1H, H-3), 3.58 (q, *J* = 6.0 Hz, 1H, H-5), 3.51 (t, *J* = 9.3 Hz, 1H, H-2), 2.34 (s, 3H, S-Ph-C*H*$_3$), 1.34 (d, *J* = 6.4 Hz, 3H, C*H*$_3$ Fuc). ^{13}C NMR (101 MHz, $CDCl_3$) δ 138.3, 137.8, 132.53, 132.51, 129.8, 128.71, 128.71, 128.4, 87.9 (**C-1**), 78.3 (C-2), 75.45 (C-3), 75.41(*C*H_2-Ph), 74.6 (C-5), 71.9 (C-4), 21.3 (S-Ph-*C*H_3), 16.8 (C-6). HRMS (ESI) calc. for $C_{20}H_{24}O_4SNa$, $[M+Na]^+$ 383.1288; found: 383.1312.

2.5.3 Synthesis of Protected Oligosaccharides

General Procedure for Automated Glycan Assembly

The automated synthesizers of the Seeberger group were used.[58] All solutions were freshly-prepared and kept under argon during the automation run. Oven-heated, argon-flushed flasks were used to prepare all moisture-sensitive solutions.

Solution A (acidic wash / phosphate activation): TMSOTf (450 µL, 2.49 mmol) was dissolved in anhydrous DCM (40 mL). **Solution B (thioglycoside activation)**: NIS (1.35 g, 6.00 mmol) was dissolved in anhydrous DCM/dioxane (40 mL, v/v, 2:1), and TfOH (55.0 µL, 0.63 mmol) was added. The solution was kept at 0 °C by using an ice bath. **Solution C (Fmoc deprotection)**: A solution of 20% piperidine in DMF (v/v) was prepared (80 mL). **Solution D (Lev deprotection)**: Hydrazine acetate (550 mg, 5.97 mmol) was dissolved in pyridine/AcOH/H_2O (40 mL, v/v, 32:8:2), unless stated otherwise. **Solutions E$_j$ (building blocks)**: 5.0, 6.5 or 8.0 equiv. of building block ***j*** were coevaporeted with toluene twice, kept under vacuum overnight and dissolved in 1.00 mL of anhydrous DCM.

Automated Synthesis

Photocleavable linker-functionalized resin **2.12**[58] (37.8 mg, 12.5 µmol) was added into the reaction vessel, and swollen in 2 mL DCM for 20 min. All reagent lines needed for the synthesis were washed and primed. The resin was washed with DMF, THF, and DCM (3 x 2 mL, 25 s each).

To couple each building block ***j***, a cycle consistent in the sequential use of **Modules 1-3** was used:

1. **Module 1 – acidic wash:** DCM (2 mL) was added to the reaction vessel and the mixture was cooled to -20 °C. **Solution A** (1.00 mL) was delivered dropwise into the reaction vessel, and kept under Ar bubbling for 3 min. The reaction vessel was emptied and the resin was washed with DCM (2 mL, 25 s).
2. **Module 2 – glycosylation with building block *j*: Module 2.a** (for activation of thioglycoside donors) or **module 2.b** (for activation of phosphate donors) was used.
    a. **Module 2.a – thioglycoside donors: Solution E_j** (1.00 mL, *n* equiv.) was delivered into the reaction vessel and the mixture was cooled to an incubation temperature (T_1). Then **solution B** (1.00 mL) was added into the reaction vessel dropwise. After the incubation time (t_1) was completed, the temperature was increased to a glycosylation temperature (T_2) and kept for a glycosylation time (t_2) (*see* Table 2.1). The solution was drained and the resin was washed with dioxane (2 mL, 20 s) for 20 s and DCM (2 x 2 mL, 25 s). The temperature of the reaction vessel was increased to 25 °C.
    b. **Module 2.b – phosphate donors: Solution E_j** (1.00 mL, *n* equiv.) was delivered into the reaction vessel and the mixture was cooled to an incubation temperature (T_1). Then **solution A** (1.00 mL) was added into the reaction vessel dropwise. After the incubation time (t_1) was completed, the temperature was increased to a glycosylation temperature (T_2) and kept for a glycosylation time (t_2) (see Table 2.1). The solution was drained and the resin was washed with DCM (6 x 2 mL, 15 s).
3. **Module 3 – deprotection: Module 3.a** (for Fmoc deprotection) or **module 3.b** (for Lev deprotection) was used.
    a. **Module 3.a:** After washing the resin with DCM (3 x 2 mL, 25 s), **solution C** (2 mL) was delivered into the reaction vessel, and kept under Ar bubbling for 5 min at 25 ºC. The solution was drained and the resin was washed with DMF (3 x 3 mL, 25 s) and DCM (5 x 2 mL, 25 s).
    b. **Module 3.b:** After washing the resin with DCM (6 x 2 mL, 25 s), DCM (1.3 mL) was delivered to the reaction vessel. **Solution D** (0.8 mL) was added and kept under Ar bubbling (pulsed bubbling, 2 x 30 min) at 25 ºC. The solution was drained and the resin was washed with DMF (3 x 3 mL, 25 s) and DCM (5 x 2 mL, 25 s).

Note on the AGA of oligosaccharides that require the use of five building blocks. The automated oligosaccharide synthesizer has four lines for building block solutions. For the

AGA of compounds **2.38**-**2.40**, and **2.43**-**2.49** five different building blocks were used, and the following procedure was implemented:

I. Preparation of building block **solutions $\mathbf{E}_j$** (j = **2.13**-**2.16**) and attachment of each solution to building block lines 1 to 4 (respectively).
II. One coupling cycle (**Modules 1-3**) was performed for building block **2.13**.
III. **Solution $\mathbf{E}_{2.13}$** was removed from building block line 1 and the line was washed. **Solution $\mathbf{E}_{2.17}$** was prepared and connected to building block line 1.
IV. AGA continued with the subsequent coupling cycles of building blocks **2.14**-**2.17** as above described.

Photocleavage and Purification

After the automated synthesis was completed, the resin was removed from the reaction vessel, suspended in DCM (20 mL), and photocleaved in a flow reactor. A Vapourtec E-Series easy-MedChem, equipped with a UV-150 Photochemical reactor was used. A UV-150 Medium-Pressure Mercury Lamp (arc length 27.9 cm, 450 W) surrounded by a long-pass UV filter (Pyrex, 50% transmittance at 305 nm). A Pump 11 Elite Series (Harvard Apparatus) syringe pump at a flow rate of 0.8 mL/min was used to pump the mixture through a FEP tubing (i.d. 3.0 inch, volume: 12 mL), at 20 °C. The reactor was washed with 20 mL DCM at a flow rate of 2.0 mL/min. The output solution was filtered to remove the resin, and the solvent was evaporated *in vacuo*. The crude material was analyzed by MALDI and analytical NP-HPLC. Purification was performed by NP-HPLC. HPLCs were performed on Agilent 1200 Series systems. A YMC-Diol-300-NP column (150 mm x 4.60 mm I.D.) was used for analytical NP-HPLC, with a flow rate of 1.00 mL/min and hexanes/EtOAc as eluent. A YMC-Pack Diol-300-NP column (150 mm x 20.0 mm I.D.) was used for preparative NP-HPLC, with a flow rate of 15.0 mL/min and hexanes/EtOAc as eluent. Unless stated otherwise, the gradient program detailed hereafter was used:

1. Isocratic 20% EtOAc in hexanes (5 min).
2. Linear gradient 20 to 55% EtOAc in hexanes (35 min).
3. Linear gradient to 100% EtOAc (10 min).

Experimental Data for Protected Oligosaccharides 2.34-2.48

β-Stereoselectivity for the nonreducing end Gal-GlcNAc linkage

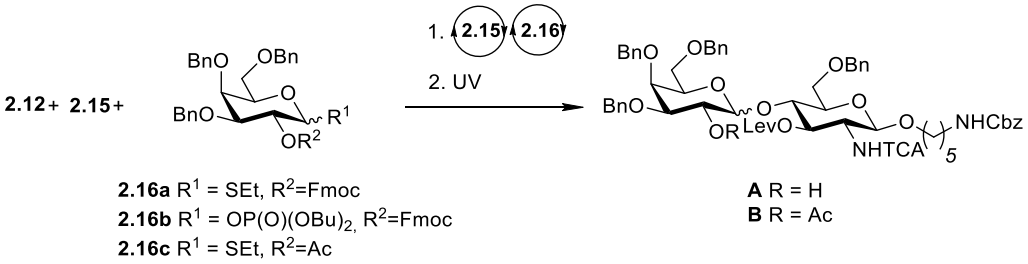

2.16a R^1 = SEt, R^2=Fmoc
2.16b R^1 = OP(O)$(OBu)_2$, R^2=Fmoc
2.16c R^1 = SEt, R^2=Ac

A R = H
B R = Ac

AGA of the 2'-OH (**A**) and 2'-OAc (**B**) Gal-GlcNAc disaccharides (section 2.2.2.1) was attempted as a test for optimization purposes only, and were identified based on diagnostic ^{1}H and HSQC NMR analysis, complemented with HRMS.

Table 2.3. Anomeric coupling constants for the nonreducing end Gal-β(1-4)-GlcNAc fragment.

Product	**H-1'**			**H-1**			**m/z**
	δ (ppm)	$^3J_{H-H}$ (Hz)	$^1J_{C-H}$ (Hz)	**δ** (ppm)	$^3J_{H-H}$ (Hz)	$^1J_{C-H}$ (Hz)	
A 2'-OH α	5.20	4.10	173	4.62	8.30	166	1185.3662[1]
A 2'-OH β	4.53	-	162	4.21	7.60	165	1185.3650[1]
B 2'-OAc α	5.38	4.30	177	4.75	8.30	166	1227.3749[2]
B 2'-OAc β	4.45	-	165	4.33	7.90	164	1227.3766[2]

[1]Calc. for $C_{60}H_{69}Cl_3N_2O_{15}Na$, 1185.3656. [2]Calc. for $C_{62}H_{71}Cl_3N_2O_{16}Na$, 1127.3761.

A 2'-OH β: ^{1}H NMR (600 MHz, $CDCl_3$) δ 7.37 – 7.22 (m, 25H), 7.13 (d, *J* = 8.5 Hz, 1H, NHTCA), 5.28 (t, *J* = 10.0 Hz, 1H), 5.08 (s, 2H), 4.82 (d, *J* = 11.5 Hz, 1H), 4.71 – 4.59 (m, 4H), 4.55 – 4.42 (m, 4H, **H-1**, 3 x CHH'), 4.21 (d, *J* = 7.6 Hz, 1H, **H-1**), 3.94 (q, *J* = 9.1 Hz, 1H), 3.89 – 3.80 (m, 5H), 3.75 – 3.67 (m, 2H), 3.57 (t, *J* = 8.4 Hz, 1H), 3.55 – 3.51 (m, 1H), 3.45 – 3.37 (m, 2H), 3.28 (dd, *J* = 9.7, 2.8 Hz, 1H), 3.11 (m, 2H, CH_2-NHCbz), 2.55 – 2.35 (m, 4H, *C*H_2 Lev), 1.95 (s, 3H, CH_3 Lev), 1.52 – 1.27 (m, 6H, CH_2 pentane). HRMS (ESI) calc. for $C_{60}H_{69}Cl_3N_2O_{15}Na$, 1185.3656; found: 1185.3662. **B** 2'-OAc β: ^{1}H NMR (600 MHz, $CDCl_3$) δ 7.39 – 7.21 (m, 25H), 6.81 (d, *J* = 8.8 Hz, 1H, NHTCA), 5.16 (dd, *J* = 10.0, 8.0 Hz, 1H), 5.12 – 5.06 (m, 3H), 4.87 (d, *J* = 11.4 Hz, 1H), 4.68 (d, *J* = 12.1 Hz, 1H), 4.64 (d, *J* = 12.2 Hz, 1H), 4.52 – 4.42 (m, 6H, including **H-1**), 4.33 (d, *J* = 7.9 Hz, 1H, **H-1**), 3.96 – 3.83 (m, 4H), 3.70 (d, *J* = 2.7 Hz, 2H), 3.61 (t, *J* = 8.5 Hz, 1H), 3.55 (dd, *J* = 8.8, 5.1 Hz, 1H), 3.46 (dt, *J* = 9.1, 2.9 Hz, 1H), 3.42 (dd, *J* = 7.9, 5.3 Hz, 2H), 3.35 (dd, *J* = 10.1, 2.7 Hz, 1H), 3.19 – 3.11 (m, 2H, CH_2-NHCbz), 2.59 – 2.34 (m, 4H, *C*H_2 Lev), 1.96 (s, 3H, CH_3 Lev), 1.93 (s, 3H, CH_3 Ac), 1.58

– 1.53 (m, 2H, CH_2 pentane), 1.51 – 1.45 (m, 2H, CH_2 pentane), 1.40 – 1.30 (m, 2H, CH_2 pentane). HRMS (ESI) calc. for $C_{62}H_{71}Cl_3N_2O_{16}Na$, $[M+Na]^+$ 1127.3761; found 1227.3766.

***N*-Benzyloxycarbonyl-5-amino-pentyl 2,3,4-tri-*O*-benzyl-α-L-fucopyranosyl-(1→2)-3,4,6-tri-*O*-benzyl-β-D-galactopyranosyl-(1→4)-6-*O*-benzyl-2-deoxy-2-*N*-trichloroacetyl-3-*O*-levunoyl-β-D-glucopyranoside (2.34)**

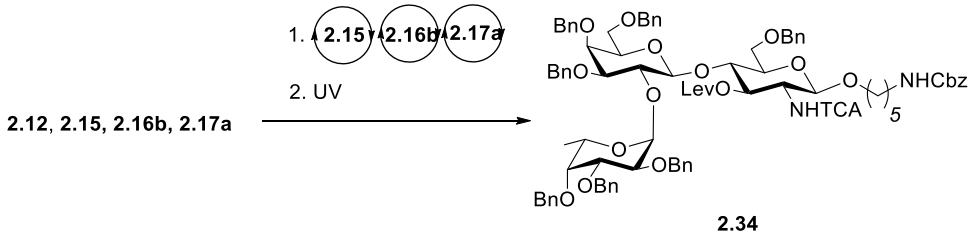

2.34

Yield: 57%, 11.3 mg

^{1}H NMR (600 MHz, $CDCl_3$) δ 7.41 – 7.11 (m, 38H), 7.07 (d, *J* = 7.0 Hz, 2H), 6.78 (d, *J* = 8.7 Hz, 1H, N-H TCA), 5.66 (d, *J* = 3.8 Hz, 1H, **H-1α**), 5.11 – 5.05 (m, 3H), 4.92 (d, *J* = 11.6 Hz, 1H), 4.77 – 4.68 (m, 3H), 4.66 – 4.61 (m, 3H), 4.55 – 4.46 (m, 7H, including **H-1β**), 4.39 – 4.32 (m, 2H, including **H-1β**), 4.17 (q, *J* = 6.5 Hz, 1H, H-5 Fuc), 4.03 – 3.98 (m, 2H), 3.93 – 3.83 (m, 4H), 3.80 (dd, *J* = 10.2, 2.6 Hz, 1H), 3.71 (d, *J* = 3.0 Hz, 2H), 3.66 (s, 1H), 3.63 – 3.52 (m, 3H), 3.48 – 3.43 (m, 1H), 3.43 – 3.38 (m, 1H), 3.34 (dt, *J* = 9.2, 3.1 Hz, 1H), 3.19 – 3.13 (m, 2H, C*H*$_2$-NHCbz), 2.47 – 2.33 (m, 3H, 3H, CH_2 Lev), 2.16 – 2.08 (m, 1H, CH_2 Lev), 1.88 (s, 3H, CH_3 Lev), 1.62 – 1.56 (m, 2H, CH_2 pentane), 1.52 – 1.47 (m, 2H, CH_2 pentane), 1.43 – 1.34 (m, 2H, CH_2 pentane), 1.19 (d, *J* = 6.5 Hz, 3H, CH_3 Fuc). ^{13}C NMR (151 MHz, $CDCl_3$) δ 206.7 (*C*(O)CH_3), 172.8 (OC(O)CH_2), 162.1, 156.6 (C=O Cbz, TCA), 139.02, 138.91, 138.73, 138.64, 138.13, 138.06, 137.9, 136.8, 130.0, 128.7, 128.64, 128.60, 128.5, 128.43, 128.38, 128.36, 128.3, 128.24, 128.19, 128.15, 128.12, 128.08, 127.9, 127.72, 127.68, 127.62, 127.50, 127.47, 127.34, 127.30, 126.4, 122.2 (Ar), 101.06 (**C-1**, $J_{C\text{-}H}$ = 176 Hz), 100.94 (**C-1**, $J_{C\text{-}H}$ = 160 Hz), 97.3 (**C-1**, $J_{C\text{-}H}$ = 166 Hz), 92.5 (*C*Cl_3 TCA), 84.2, 79.4, 78.0, 76.0, 75.9, 74.85, 74.83, 73.7, 73.6, 73.4, 73.2, 72.8, 72.7, 72.53, 72.47, 71.4, 71.3, 69.7, 68.2, 66.7, 66.6 (C-5 Fuc), 55.6, 41.0 (*C*H_2-NHCbz), 37.6 (*C*H_2 Lev), 29.8 (*C*H_2 pentane), 29.7 (*C*H_3 Lev), 29.1(*C*H_2 pentane), 28.0 (*C*H_2 Lev), 23.4 (*C*H_2 pentane), 16.7 (*C*H_3 Fuc). HRMS (ESI) calc. for $C_{87}H_{97}Cl_3N_2O_{19}Na$, $[M+Na]^+$ 1601.5643; found: 1601.5697.

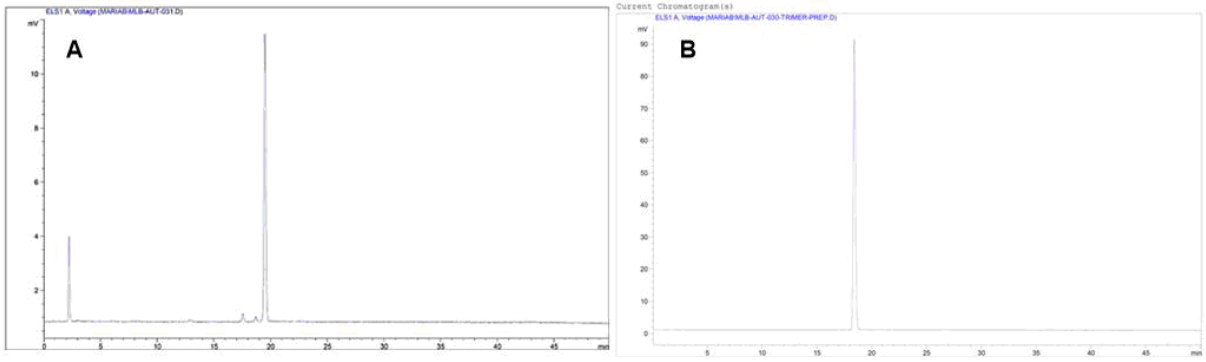

Analytical NP-HPLC of (**A**) crude reaction mixture after photocleavage and (**B**) the purified product. Detection: ELSD.

***N*-Benzyloxycarbonyl-5-amino-pentyl 3,4,6-tri-*O*-benzyl-β-D-galactopyranosyl-(1→4)-6-*O*-benzyl-2-deoxy-2-*N*-trichloroacetyl-3-*O*-levulinoyl-β-D-glucopyranosyl-(1→3)-2-*O*-benzoyl-4,6-di-*O*-benzyl-β-D-galactopyranosyl-(1→4)-6-*O*-benzyl-2-deoxy-2-*N*-trichloroacetyl-3-*O*-levulinoyl-β-D-glucopyranosyl-(1→3)-2-*O*-benzoyl-4,6-di-*O*-benzyl-β-D-galactopyranosyl-(1→4)-2,3-di-*O*-benzoyl-6-*O*-benzyl-β-D-glucopyranoside (2.35)**

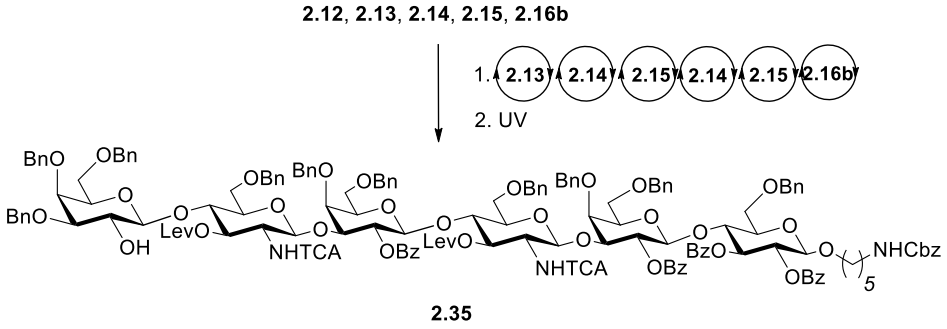

2.35

Yield: 55%, 16.1 mg

^{1}H NMR (600 MHz, $CDCl_3$) δ 7.91 – 7.80 (m, 8H), 7.60 – 7.52 (m, 2H), 7.48 – 7.07 (m, 65H), 6.36 (d, *J* = 9.2 Hz, 1H, NHTCA), 6.30 (d, *J* = 9.1 Hz, 1H, NHTCA), 5.52 (t, *J* = 9.3 Hz, 1H), 5.34 – 5.25 (m, 3H), 5.05 (s, 2H), 4.98 – 4.91 (m, 2H), 4.87 (d, *J* = 11.7 Hz, 1H), 4.82 (d, *J* = 11.3 Hz, 1H), 4.76 (dd, *J* = 10.4, 8.7 Hz, 1H), 4.70 (d, *J* = 11.9 Hz, 1H), 4.61 – 4.35 (m, 18H, including 5 x **H-1**), 4.31 (d, *J* = 11.7 Hz, 1H), 4.26 – 4.20 (m, 2H, including **H-1**), 4.13 (d, *J* = 12.0 Hz, 1H), 4.03 – 3.97 (m, 4H), 3.93 – 3.77 (m, 10H), 3.73 (dd, *J* = 9.8, 7.6 Hz, 1H), 3.68 (dd, *J* = 10.2, 3.0 Hz, 1H), 3.59 – 3.38 (m, 11H), 3.35 (dd, *J* = 11.0, 2.3 Hz, 2H), 3.19 – 3.13 (m, 1H), 2.93 – 2.82 (m, 3H, including C*H*$_2$-NHCbz), 2.78 (t, *J* = 8.8 Hz, 1H), 2.47 – 2.34 (m, 6H, C*H*$_2$ Lev), 2.32 – 2.24 (m, 2H, C*H*$_2$ Lev), 1.91 (s, 3H, C*H*$_3$ Lev), 1.89 (s, 3H, C*H*$_3$ Lev), 1.47 – 1.14 (m, 6H, C*H*$_2$ pentane). ^{13}C NMR (151 MHz, $CDCl_3$) δ 206.6 (*C*(O)CH_3), 206.4 (*C*(O)CH_3), 172.7 (O*C*(O)CH_2), 172.5 (O*C*(O)CH_2), 165.34 (C=O Bz), 165.28 (C=O Bz), 164.5 (C=O Bz), 164.4 (C=O Bz), 162.07, 162.03, 156.35 (C=O Cbz, 2 x TCA), 139.1, 138.8, 138.7,

138.3, 138.12, 138.04, 137.94, 137.83, 137.79, 136.81, 133.76, 133.6, 133.2, 132.5, 130.6, 130.0, 129.8, 129.7, 129.5, 129.4, 128.91, 128.85, 128.67, 128.62, 128.61, 128.59, 128.58, 128.58, 128.4, 128.34, 128.31, 128.25, 128.22, 128.17, 128.10, 128.08, 128.04, 128.01, 127.94, 127.90, 127.74, 127.71, 127.69, 127.61, 127.2, 102.9 (**C-1**, J_{C-H} = 163 Hz), 101.13 (**C-1**, J_{C-H} = 165 Hz), 101.09 (**C-1**, J_{C-H} = 163 Hz), 101.04 (**C-1**, J_{C-H} = 161 Hz), 100.9 (**C-1**, J_{C-H} = 163 Hz), 100.6 (**C-1**, J_{C-H} = 163 Hz), 92.03 (CCl_3), 91.95 (CCl_3), 82.0, 79.0, 78.7, 76.0, 75.8, 75.27, 75.20, 75.1, 74.86, 74.84, 74.73, 74.65, 73.9, 73.65, 73.63, 73.59, 73.53, 73.49, 73.38, 73.1, 73.0, 72.8, 72.63, 72.61, 72.59, 72.4, 72.3, 72.2, 72.1, 71.5, 69.76, 68.3, 68.11, 68.05, 67.7, 67.5, 67.3, 66.6, 56.1, 55.8, 40.9 (CH_2-NHCbz), 37.8 (CH_2 Lev), 37.7 (CH_2 Lev), 29.78 (CH_3 Lev), 29.76 (CH_3 Lev), 29.5 (CH_2 pentane), 29.0 (CH_2 pentane), 27.99 (CH_2 Lev), 27.95 (CH_2 Lev), 23.2 (CH_2 pentane). HRMS (ESI) calc. for $C_{161}H_{167}Cl_{16}N_3O_{41}Na_2$, $[M+2Na]^{2+}$ 1526.9495; found: 1526.9541.

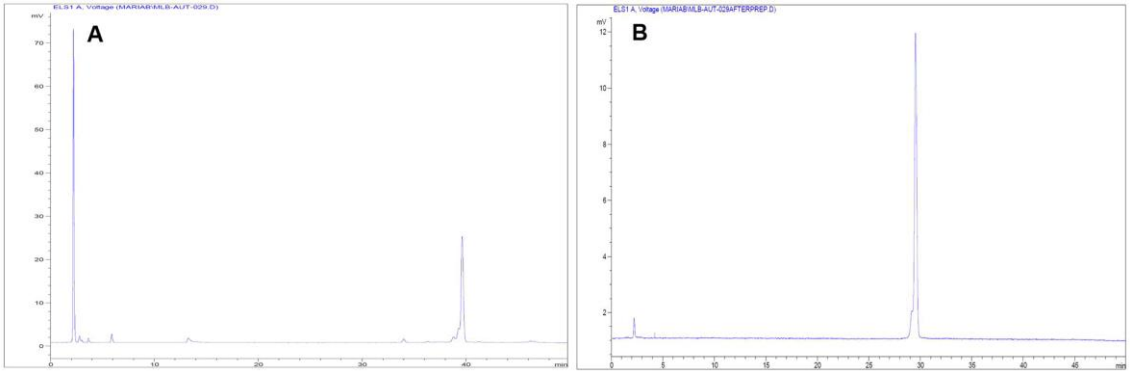

Analytical NP-HPLC of (**A**) crude reaction mixture after photocleavage and (**B**) the purified product. Detection: ELSD.

***N*-Benzyloxycarbonyl-5-amino-pentyl 2,3,4-tri-*O*-benzyl-α-L-fucopyranosyl-(1→2)-3,4,6-tri-*O*-benzyl-β-D-galactopyranosyl-(1→4)-6-*O*-benzyl-3-*O*-(2,3,4-tri-*O*-benzyl-α-L-fucopyranosyl)-2-deoxy-2-*N*-trichloroacetyl-β-D-glucopyranosyl-(1→3)-2-*O*-benzoyl-4,6-di-*O*-benzyl-β-D-galactopyranoside (2.36)**

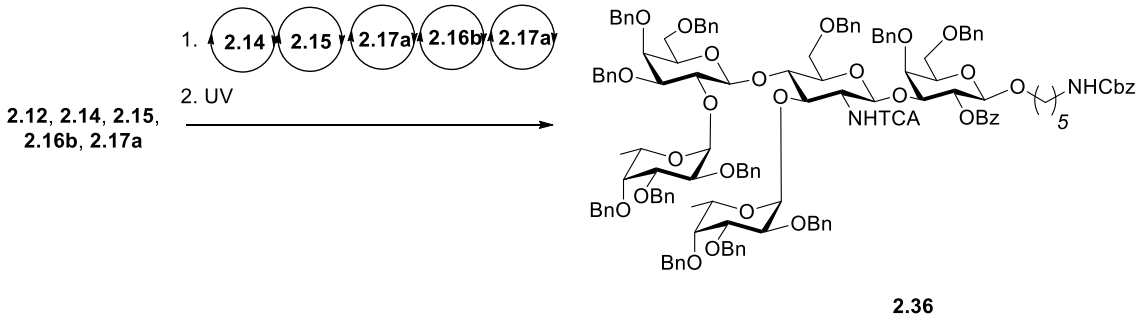

2.36

Yield: 51%, 14.9 mg

^{1}H NMR (600 MHz, $CDCl_3$) δ 7.99 – 7.93 (m, 2H), 7.37 – 7.13 (m, 66H), 7.09 – 7.03 (m, 2H), 6.69 (d, *J* = 7.4 Hz, 1H, N-H TCA), 5.68 (d, *J* = 3.8 Hz, 1H, **H-1α**), 5.51 (dd, *J* = 10.1, 7.8 Hz, 1H), 5.10 – 5.05 (m, 3H, including **H-1**), 5.03 – 4.94 (m, 3H, including **H-1**), 4.78 – 4.68 (m, 5H), 4.65 – 4.31 (m, 19H, including 2 x **H-1**), 4.21 – 4.12 (m, 3H), 4.09 – 3.99 (m, 4H), 3.95 (d, *J* = 3.2 Hz, 1H), 3.91 – 3.87 (m, 2H), 3.84 – 3.80 (m, 3H), 3.78 (dd, *J* = 10.2, 2.7 Hz, 1H), 3.70 – 3.51 (m, 9H), 3.35 – 3.27 (m, 3H), 3.18 (s, 1H), 2.83 (q, *J* = 6.9 Hz, 2H, NH-C*H*$_2$ linker), 1.47 – 0.99 (m, 6H, CH_2 pentane), 1.17 (d, *J* = 6.5 Hz, 3H, CH_3 Fuc), 1.06 (d, *J* = 6.4 Hz, 3H, CH_3 Fuc). ^{13}C NMR (151 MHz, $CDCl_3$) δ 165.5 (C=O Bz), 161.5, 156.4 (C=O TCA, Cbz), 139.3, 139.02, 138.97, 138.92, 138.70, 138.66, 138.13, 138.11, 138.05, 137.8, 136.9, 133.3, 130.4, 130.1, 128.8, 128.68, 128.66, 128.64, 128.58, 128.55, 128.52, 128.48, 128.44, 128.41, 128.33, 128.31, 128.25, 128.23, 128.19, 128.15, 128.12, 128.10, 128.07, 128.05, 128.04, 127.94, 127.93, 127.85, 127.8, 127.62, 127.59, 127.55, 127.50, 127.48, 127.37, 127.34, 127.24, 127.21, 127.19, 127.17, 126.29, 102.0 (**C-1**, J_{C-H}= 161 Hz), 100.5 (**C-1**, J_{C-H}= 165 Hz), 99.7 (**C-1**, J_{C-H}= 171 Hz), 98.1 (**C-1**, J_{C-H}= 172 Hz), 98.0 (**C-1**, J_{C-H}= 176 Hz), 91.9 (*C*Cl_3 TCA), 84.2, 80.0, 79.46, 79.41, 78.56, 78.50, 76.5, 76.0, 75.7, 75.6, 75.19, 75.11, 75.05, 75.04, 73.9, 73.77, 73.71, 73.69, 73.57, 73.4, 73.1, 72.76, 72.71, 72.69, 72.5, 72.2, 71.2, 69.5, 68.9, 68.4, 67.9, 67.0, 66.7, 66.6, 61.1, 40.9 (*C*H_2-NHCbz), 29.5 (*C*H_2 pentane), 29.1 (*C*H_2 pentane), 23.2 (*C*H_2 pentane), 16.6 (*C*H_3 Fuc), 16.4 (*C*H_3 Fuc). HRMS (ESI) calc. for $C_{136}H_{145}Cl_3N_2O_{27}Na$, $[M+Na]^+$ 2365.8993; found: 2365.9055.

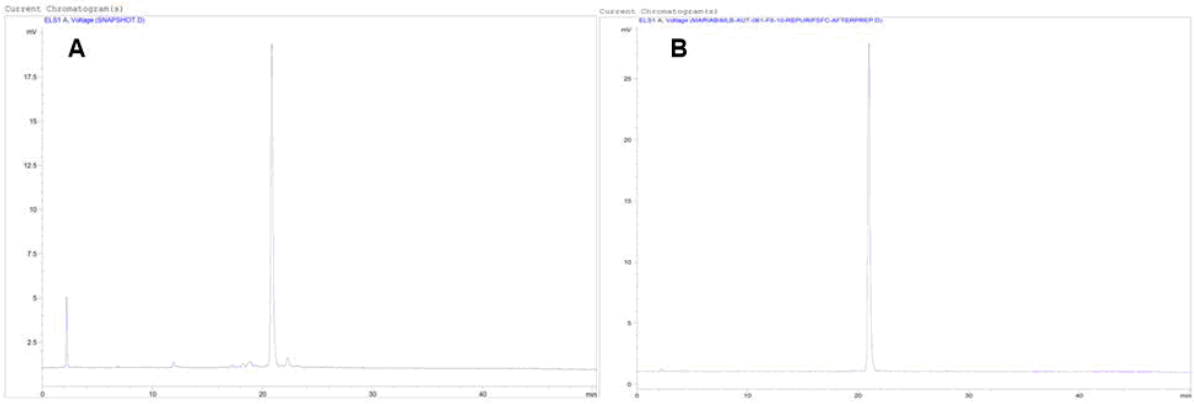

Analytical NP-HPLC of (**A**) crude reaction mixture after photocleavage and (**B**) the purified product. Detection: ELSD.

_N_-Benzyloxycarbonyl-5-amino-pentyl 3,4,6-tri-_O_-benzyl-β-D-galactopyranosyl-(1→4)-6-_O_-benzyl-3-_O_-(2,3,4-tri-_O_-benzyl-α-L-fucopyranosyl)-2-deoxy-2-_N_-trichloroacetyl-3-_O_-levulinoyl-β-D-glucopyranoside (2.37)

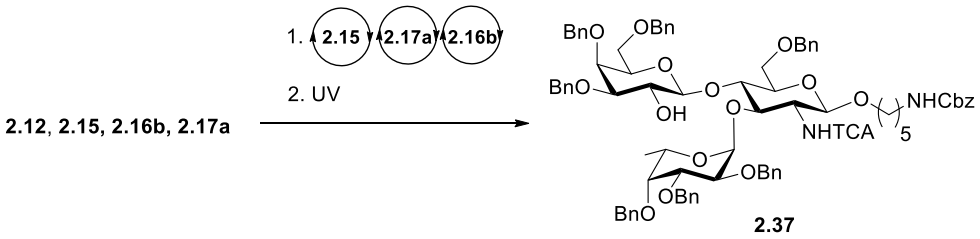

Yield: 48%, 8.90 mg

^{1}H NMR (600 MHz, $CDCl_3$) δ 7.43 – 7.17 (m, 40H), 6.92 (d, *J* = 7.7 Hz, 1H, N*H*TCA), 5.14 (d, *J* = 3.7 Hz, 1H, **H-1α**), 5.08 (s, 2H), 4.86 (d, *J* = 10.8 Hz, 1H), 4.81 (d, *J* = 7.8 Hz, 1H, **H-1**), 4.78-4.74 (m, 2H), 4.70 – 4.59 (m, 6H), 4.50 – 4.46 (m, 3H), 4.44 (d, *J* = 7.7 Hz, 1H, **H-1**), 4.38 – 4.32 (m, 2H), 4.28 (t, *J* = 8.9 Hz, 1H), 4.11 (d, *J* = 11.3 Hz, 1H), 4.06 (t, *J* = 8.8 Hz, 1H), 3.99 – 3.92 (m, 3H), 3.89 (dd, *J* = 10.2, 2.7 Hz, 1H), 3.84 – 3.77 (m, 3H), 3.68 (t, *J* = 8.6 Hz, 1H), 3.64 – 3.59 (m, 2H), 3.57 (dt, *J* = 9.3, 3.0 Hz, 1H), 3.43 – 3.38 (m, 1H), 3.35 (dd, *J* = 8.7, 5.1 Hz, 1H), 3.33 (s, 1H), 3.28 (dd, *J* = 9.7, 2.9 Hz, 1H), 3.13 (q, *J* = 6.8 Hz, 2H, C*H*$_2$-NHCbz), 1.56 – 1.50 (m, 2H, C*H*$_2$ pentane), 1.49 – 1.42 (m, 2H, C*H*$_2$ pentane), 1.34 – 1.28 (m, 2H, C*H*$_2$ pentane), 1.02 (d, *J* = 6.5 Hz, 3H, CH_3 Fuc). ^{13}C NMR (151 MHz, $CDCl_3$) δ 161.6, 156.5 (C=O Cbz, TCA), 139.2, 139.0, 138.86, 138.84, 138.3, 138.2, 138.0, 136.8, 128.73, 128.70, 128.63, 128.63, 128.51, 128.49, 128.47, 128.40, 128.22, 128.18, 128.09, 128.05, 128.03, 127.99, 127.8, 127.77, 127.74, 127.72, 127.53, 127.51, 127.45, 127.3, 101.8 (**C-1**, $J_{C\text{-}H}$ = 164 Hz), 99.5 (**C-1**, $J_{C\text{-}H}$ = 165 Hz), 97.4 (**C-1**, $J_{C\text{-}H}$ = 171 Hz), 92.5 (*C*Cl_3 TCA), 82.4, 79.7, 78.5, 76.3, 75.4, 75.2, 75.0, 74.2, 73.8, 73.48, 73.46, 73.3, 73.1, 72.6, 72.5, 71.6, 69.7, 68.6, 68.1, 66.74, 66.69, 59.3, 41.1 (*C*H_2-NHCbz), 29.8 (*C*H_2 pentane), 29.2 (*C*H_2 pentane), 23.4 (*C*H_2 pentane), 16.7 (*C*H_3 Fuc). HRMS (ESI) calc. for $C_{82}H_{91}Cl_3N_2O_{17}Na$, $[M+Na]^+$ 1503.5276; found: 1503.5294.

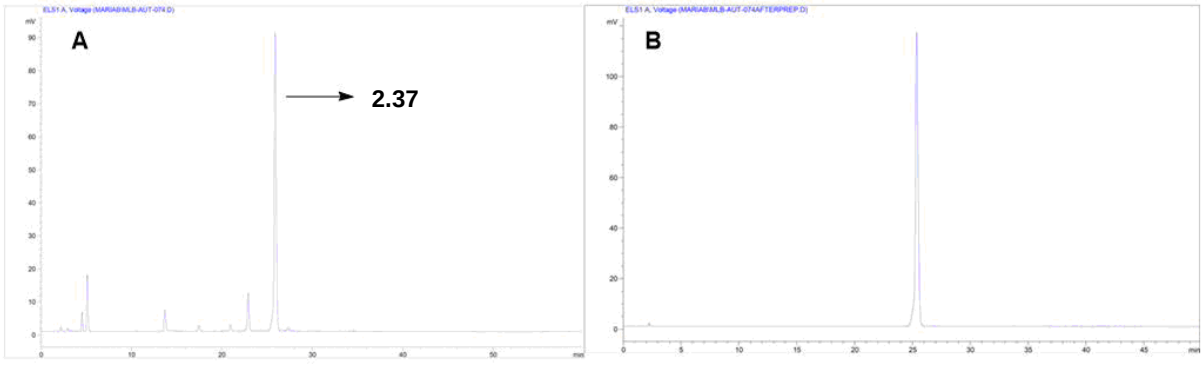

Analytical NP-HPLC of (**A**) crude reaction mixture after photocleavage and (**B**) the purified product. Detection: ELSD.

***N*-Benzyloxycarbonyl-5-amino-pentyl 2,3,4-tri-*O*-benzyl-α-L-fucopyranosyl-(1→2)-3,4,6-tri-*O*-benzyl-β-D-galactopyranosyl-(1→4)-6-*O*-benzyl-2-deoxy-2-*N*-trichloroacetyl-β-D-glucopyranosyl-(1→3)-2-*O*-benzoyl-4,6-di-*O*-benzyl-β-D-galactopyranosyl-(1→4)-2,3-di-*O*-benzoyl-6-*O*-benzyl-β-D-glucopyranoside (2.38)**

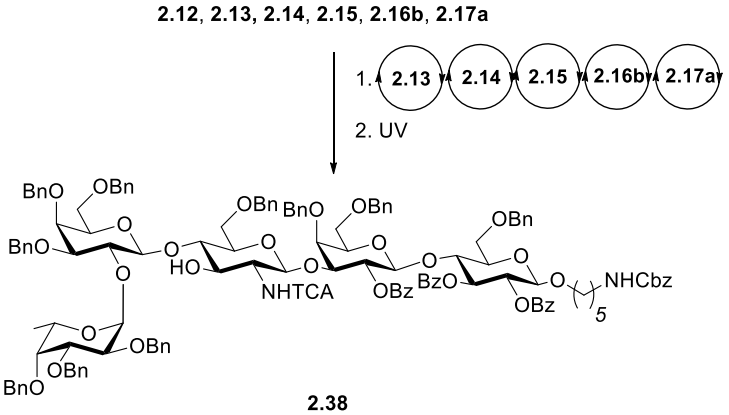

2.38

Yield: 44%, 13.0 mg

^{1}H NMR (600 MHz, $CDCl_3$) δ 7.94 (d, *J* = 7.8 Hz, 2H), 7.90 (d, *J* = 8.0 Hz, 2H), 7.82 (d, *J* = 7.8 Hz, 2H), 7.54 (t, *J* = 7.4 Hz, 1H), 7.48 – 7.06 (m, 61H), 7.01 (d, *J* = 7.5 Hz, 2H), 6.41 (d, *J* = 8.1 Hz, 1H, N*H*TCA), 5.69 (d, *J* = 3.9 Hz, 1H, **H-1**), 5.56 (t, *J* = 9.3 Hz, 1H), 5.42 (dd, *J* = 10.1, 7.8 Hz, 1H), 5.32 – 5.26 (m, 1H), 5.05 (s, 2H), 4.91 (d, *J* = 11.8 Hz, 1H), 4.84 (d, *J* = 11.6 Hz, 1H), 4.78 – 4.66 (m, 4H, including **H-1**), 4.56 – 4.47 (m, 8H, including 2 x **H-1**), 4.43 (s, 2H), 4.41-4.38 (m, 2H), 4.35 – 4.32 (m, 2H, including **H-1**), 4.27 (d, *J* = 12.3 Hz, 1H), 4.19 – 4.15 (m, 1H), 4.12 (q, *J* = 6.9, 6.3 Hz, 1H), 4.07 – 3.99 (m, 5H), 3.93 (s, 1H), 3.89 – 3.78 (m, 5H), 3.69 – 3.64 (m, 2H), 3.62 – 3.58 (m, 2H), 3.55 – 3.41 (m, 9H), 3.36 (m, 1H), 3.24 (dd, *J* = 8.7, 5.0 Hz, 1H), 2.94 – 2.79 (m, 4H), 1.50 – 1.15 (m, 6H, CH_2 pentane), 1.13 (d, *J* = 6.4 Hz, 3H, CH_3 Fuc). ^{13}C NMR (151 MHz, $CDCl_3$) δ 165.36 (C=O Bz), 165.30 (C=O Bz), 164.7 (C=O Bz), 161.9, 156.4 (C=O TCA, Cbz), 139.1, 138.89, 138.84, 138.4, 138.10, 138.08, 137.98, 137.8, 137.5, 136.8, 133.5, 133.2, 132.6, 130.5, 129.98, 129.92, 129.84, 129.78, 129.69, 128.74, 128.63, 128.60, 128.56, 128.50, 128.45, 128.45, 128.43, 128.39, 128.30, 128.28, 128.25, 128.22, 128.20, 128.17, 128.14, 128.11, 128.11, 127.99, 127.94, 127.87, 127.81, 127.80, 127.72, 127.64, 127.61, 127.55, 127.50, 127.39, 127.32, 127.30, 126.4, 102.0 (**C-1**, $J_{C\text{-}H}$ = 167 Hz), 101.1 (**C-1**, $J_{C\text{-}H}$ = 163 Hz), 100.9 (**C-1**, $J_{C\text{-}H}$ = 163 Hz), 100.2 (**C-1**, $J_{C\text{-}H}$ = 165 Hz), 97.8 (**C-1**, $J_{C\text{-}H}$ = 176 Hz), 92.4 (*C*Cl_3), 84.0, 80.2, 79.6, 79.2, 77.9, 75.81, 75.77, 75.67, 75.3, 75.0, 74.82, 74.80, 74.78, 73.95, 73.91, 73.86, 73.6, 73.4, 73.2, 73.1, 73.0, 72.8, 72.7, 72.5, 72.2, 72.1, 71.5, 71.0, 69.8, 69.5, 68.49, 67.8, 67.2, 66.6, 66.5, 58.5, 40.9 (*C*H_2-NHCbz), 29.8 (*C*H_2 pentane), 29.0 (*C*H_2 pentane), 23.2 (*C*H_2 pentane), 16.8 (CH_3 Fuc). HRMS (ESI) calc. for $C_{136}H_{141}Cl_3N_2O_{30}Na$, $[M+Na]^+$ 2409.8527; found: 2409.8503.

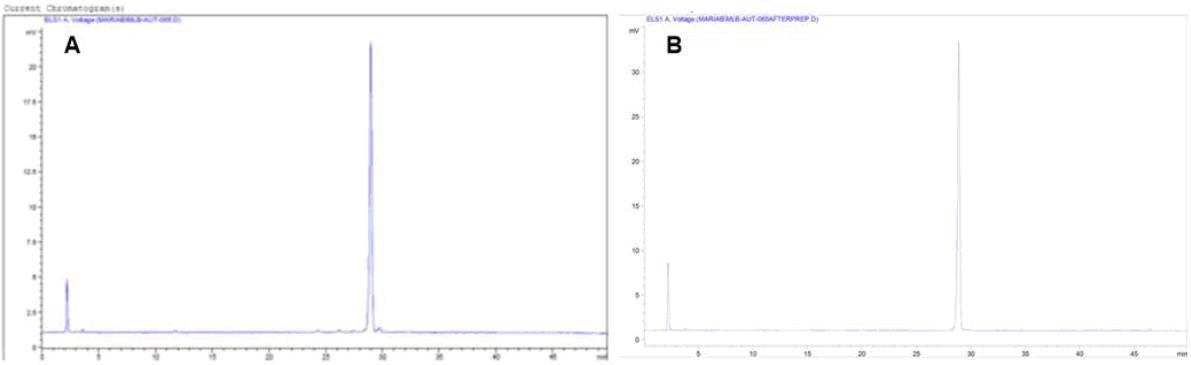

Analytical NP-HPLC of (**A**) crude reaction mixture after photocleavage and (**B**) the purified product. Detection: ELSD.

***N*-Benzyloxycarbonyl-5-amino-pentyl 3,4,6-tri-*O*-benzyl-β-D-galactopyranosyl- (1→4)-6-*O*-benzyl-3-*O*-(2,3,4-tri-O-benzyl-α-L-fucopyranosyl)-2-deoxy-2-*N*-trichloroacetyl-β-D-glucopyranosyl-(1→3)-2-*O*-benzoyl-4,6-di-*O*-benzyl-β-D-galactopyranosyl-(1→4)-2,3-di-*O*-benzoyl-6-*O*-benzyl-β-D-glucopyranoside (2.39)**

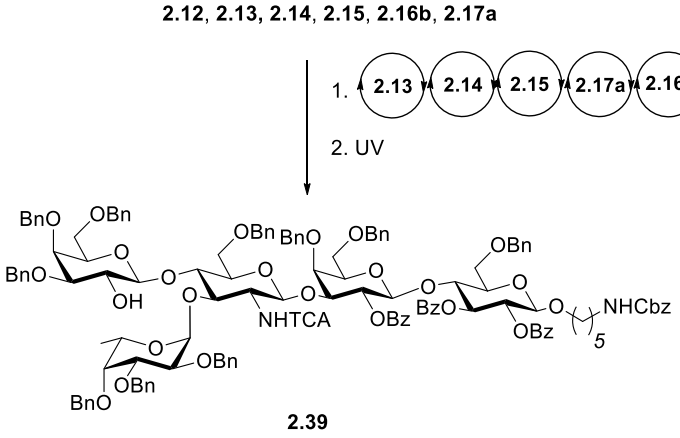

2.39

Yield: 48%, 14.5 mg

^{1}H NMR (600 MHz, $CDCl_3$) δ 7.91 – 7.85 (m, 4H), 7.80 (d, *J* = 8.2 Hz, 2H), 7.49 (t, *J* = 7.4 Hz, 1H), 7.44 (t, *J* = 7.4 Hz, 1H), 7.37 – 7.15 (m, 58H), 7.13 – 7.08 (m, 4H), 6.57 (d, *J* = 7.9 Hz, 1H, N-H TCA), 5.53 (t, *J* = 9.4 Hz, 1H), 5.36 (dd, *J* = 10.2, 7.8 Hz, 1H), 5.28 (dd, *J* = 9.7, 7.9 Hz, 1H), 5.08 – 5.01 (m, 3H, including **H-1**), 4.91 – 4.87 (m, 2H, including **H-1**), 4.80 (d, *J* = 10.9 Hz, 1H), 4.72 (d, *J* = 11.7 Hz, 1H), 4.65 – 4.61 (m, 3H), 4.59 – 4.55 (m, 2H), 4.53 – 4.41 (m, 7H, including 2 x **H-1**), 4.39 – 4.31 (m, 4H, including **H-1**), 4.28 – 4.22 (m, 3H), 4.12 – 3.97 (m, 6H), 3.94 (d, *J* = 2.9 Hz, 1H), 3.92 – 3.83 (m, 4H), 3.80 – 3.68 (m, 4H), 3.64 – 3.58 (m, 2H), 3.54 – 3.49 (m, 2H), 3.46 (dd, *J* = 11.1, 4.0 Hz, 1H), 3.41 – 3.33 (m, 3H), 3.32 – 3.28 (m, 1H), 3.26 – 3.22 (m, 2H), 2.92 – 2.84 (m, 3H, including C*H*$_2$-NH linker), 2.77 (t, *J* = 8.7 Hz, 1H), 1.49 – 1.08 (m, 6H, CH_2 pentane), 0.94 (d, *J* = 6.5 Hz, 3H, CH_3 Fuc). ^{13}C NMR (151 MHz, $CDCl_3$) δ 165.39 (C=O Bz), 165.36 (C=O Bz), 164.8 (C=O Bz), 161.29, 156.4 (C=O TCA, Cbz),

139.3, 139.17, 139.12, 138.8, 138.7, 138.3, 138.22, 138.15, 138.09, 137.90, 136.9, 133.3, 133.2, 132.5, 130.6, 130.1, 129.95, 129.93, 129.84, 129.72, 128.71, 128.67, 128.64, 128.63, 128.59, 128.53, 128.49, 128.46, 128.45, 128.42, 128.39, 128.29, 128.23, 128.18, 128.10, 128.08, 128.05, 128.02, 127.98, 127.96, 127.87, 127.82, 127.74, 127.68, 127.62, 127.45, 127.40, 127.24, 127.20, 101.6 (**C-1**, $J_{C\text{-}H}$ = 163 Hz), 101.06 (**C-1**, $J_{C\text{-}H}$ = 162 Hz), 100.94 (**C-1**, $J_{C\text{-}H}$ = 165 Hz), 99.8 (**C-1**, $J_{C\text{-}H}$ = 167 Hz), 97.3 (**C-1**, $J_{C\text{-}H}$ = 171 Hz), 92.0 (CCl_3), 82.4, 79.58, 78.53, 78.4, 76.17, 76.03, 75.4, 75.1, 75.01, 74.96, 74.92, 74.8, 74.0, 73.6, 73.45, 73.43, 73.41, 73.2, 73.14, 73.07, 72.9, 72.60, 72.56, 72.2, 71.4, 69.8, 68.6, 67.9, 67.8, 67.5, 66.62, 66.58, 60.0, 40.9 (CH_2-NHCbz), 29.5 (CH_2 pentane), 29.0 (CH_2 pentane), 23.2 (CH_2 pentane), 16.6 (CH_3 Fuc). HRMS (ESI) calc. for $C_{136}H_{141}Cl_3N_2O_{30}Na$, $[M+Na]^+$ 2409.8527; found: 2409.8574.

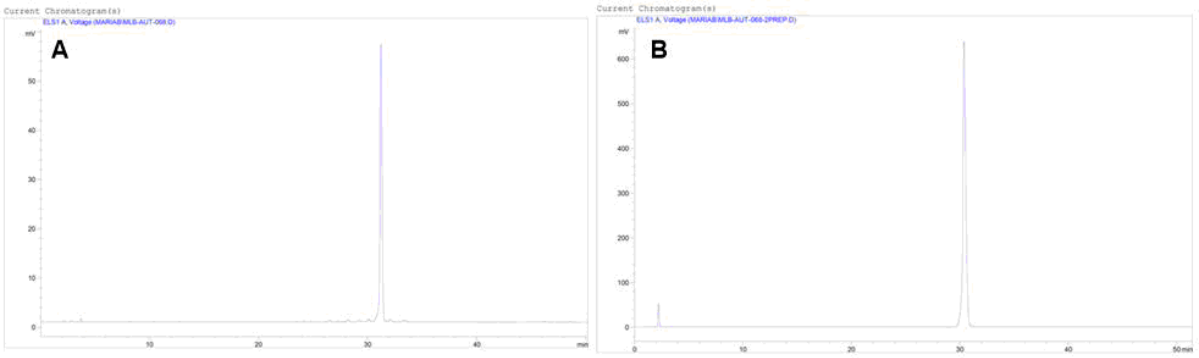

Analytical NP-HPLC of (**A**) crude reaction mixture after photocleavage and (**B**) the purified product. Detection: ELSD.

***N*-Benzyloxycarbonyl-5-amino-pentyl 2,3,4-tri-*O*-benzyl-α-L-fucopyranosyl-(1→2)-3,4,6-tri-*O*-benzyl-β-D-galactopyranosyl-(1→4)-6-*O*-benzyl-3-*O*-(2,3,4-tri-*O*-benzyl-α-L-fucopyranosyl)-2-deoxy-2-*N*-trichloroacetyl-β-D-glucopyranosyl-(1→3)-2-*O*-benzoyl-4,6-di-*O*-benzyl-β-D-galactopyranosyl-(1→4)-2,3-di-*O*-benzoyl-6-*O*-benzyl-β-D-glucopryanoside (2.40)**

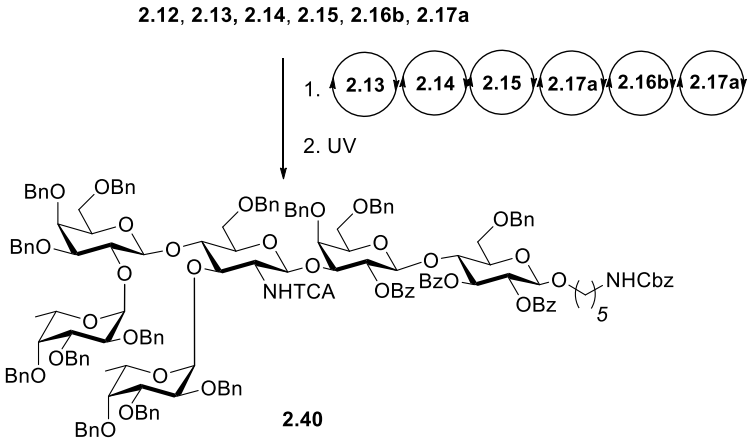

Yield: 65%, 23.1 mg

^{1}H NMR (600 MHz, $CDCl_3$) δ 7.91 (td, *J* = 8.4, 1.4 Hz, 4H), 7.82 – 7.79 (m, 2H), 7.48 – 7.44 (m, 2H), 7.36 – 7.08 (m, 75H), 7.06 – 7.03 (m, 2H), 6.66 (d, *J* = 7.2 Hz, 1H, N*H*TCA), 5.65 (d, *J* = 3.9 Hz, 1H, H-1), 5.55 (t, *J* = 9.4 Hz, 1H), 5.40 (dd, *J* = 10.1, 7.8 Hz, 1H), 5.28 (dd, *J* = 9.8, 7.9 Hz, 1H), 5.04 (d, *J* = 14.9 Hz, 3H), 4.98 – 4.90 (m, 3H), 4.76-4.69 (m, 3H), 4.70 – 4.60 (m, 3H), 4.57 – 4.45 (m, 13H), 4.42 (d, *J* = 11.3 Hz, 1H), 4.36 – 4.26 (m, 6H), 4.18 (q, *J* = 6.3 Hz, 1H), 4.10 (t, *J* = 8.9 Hz, 1H), 4.07 – 3.98 (m, 6H), 3.92 (d, *J* = 2.9 Hz, 1H), 3.89 – 3.82 (m, 3H), 3.77 (m, 4H), 3.67 – 3.63 (m, 2H), 3.54 (td, *J* = 7.4, 6.4, 3.3 Hz, 2H), 3.50 – 3.46 (m, 2H), 3.44 (s, 1H), 3.42 – 3.23 (m, 6H), 3.16 (s, 1H), 2.93 – 2.86 (m, 3H, including C*H*$_2$-NHCbz), 2.80 (t, *J* = 8.7 Hz, 1H), 1.49 – 1.39 (m, 4H, C*H*$_2$ pentane), 1.17 (d, *J* = 6.5 Hz, 3H, C*H*$_3$ Fuc), 1.23 – 1.06 (m, 2H, C*H*$_2$ pentane), 1.04 (d, *J* = 6.5 Hz, 3H C*H*$_3$ Fuc). ^{13}C NMR (151 MHz, $CDCl_3$) δ 165.36 (C=O Bz), 165.34 (C=O Bz), 164.9 (C=O Bz), 161.3, 156.4 (C=O TCA, Cbz), 139.35, 139.33, 139.02, 138.93, 138.91, 138.71, 138.68, 138.4, 138.13, 138.08, 137.8, 136.9, 133.3, 133.2, 132.5, 130.5, 130.2, 129.98, 129.93, 129.8, 129.7, 128.8, 128.63, 128.61, 128.57, 128.53, 128.50, 128.46, 128.44, 128.43, 128.3, 128.22, 128.20, 128.18, 128.16, 128.14, 128.11, 128.09, 128.03, 127.86, 127.84, 127.83, 127.78, 127.76, 127.72, 127.63, 127.60, 127.58, 127.57, 127.47, 127.35, 127.32, 127.30, 127.23, 127.20, 126.3, 101.0 (**C-1**, $J_{C\text{-}H}$ = 167 Hz), 100.9 (**C-1**, $J_{C\text{-}H}$ = 160 Hz), 100.4 (**C-1**, $J_{C\text{-}H}$ = 168 Hz), 99.4 (**C-1**, $J_{C\text{-}H}$ = 169 Hz), 98.02 (**C-1**, $J_{C\text{-}H}$ = 171 Hz), 97.96 (**C-1**, $J_{C\text{-}H}$ = 175 Hz), 91.8 (*C*Cl_3 TCA), 84.1, 80.1, 79.3, 79.2, 78.6, 78.5, 76.3, 76.0, 75.8, 75.6, 75.05, 75.02, 74.96, 74.8, 73.8, 73.7, 73.59, 73.55, 73.52, 73.37, 73.32, 73.26, 73.06, 72.89, 72.77, 72.72, 72.6, 72.5, 72.2, 71.2, 69.8, 68.3,

67.90, 67.88, 67.4, 67.0, 66.68, 66.62, 61.2, 40.9 (*C*H_2-NHCbz), 29.5 (*C*H_2 pentane), 29.0 (*C*H_2 pentane), 23.2 (*C*H_2 pentane), 16.6 (*C*H_3 Fuc), 16.3 (*C*H_3 Fuc). HRMS (ESI) calc. for $C_{163}H_{169}Cl_3N_2O_{34}Na$, $[M+Na]^+$ 2826.0515; found: 2826.0513.

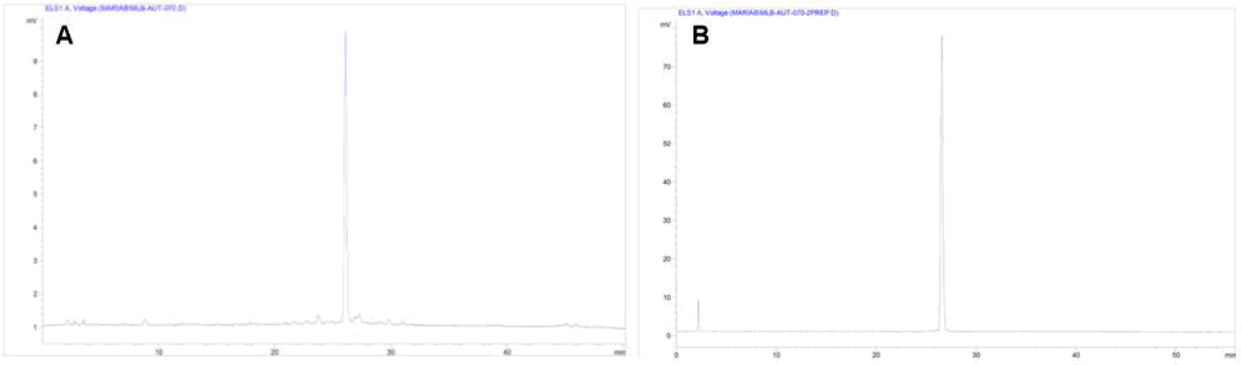

Analytical NP-HPLC of (**A**) crude reaction mixture after photocleavage and (**B**) the purified product. Detection: ELSD.

***N*-Benzyloxycarbonyl-5-amino-pentyl 2-*O*-benzoyl-4,6-di-*O*-benzyl-β-D-galactopyranosyl-(1→4)-6-*O*-benzyl-2-deoxy-2-*N*-trichloroacetyl-3-*O*-levulinoyl-β-D-glucopyranosyl-(1→3)-2-*O*-benzoyl-4,6-di-*O*-benzyl-β-D-galactopyranosyl-(1→4)-2,3-di-*O*-benzoyl-6-*O*-benzyl-β-D-glucopyranoside (2.41)**

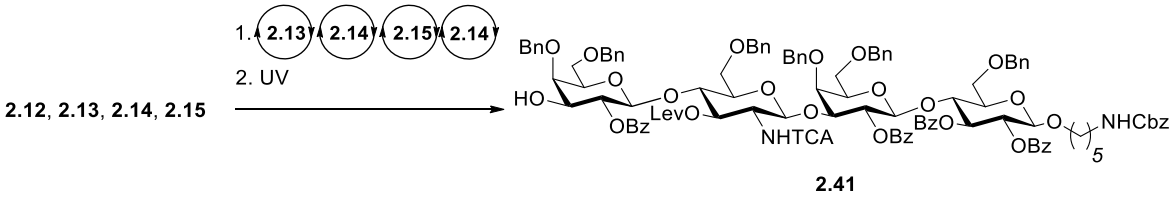

2.41

Yield: 50%, 13.0 mg

^{1}H NMR (600 MHz, $CDCl_3$) δ 7.94 – 7.88 (m, 4H), 7.85 – 7.81 (m, 4H), 7.58 – 7.52 (m, 2H), 7.47 – 7.10 (m, 45H), 6.36 (d, *J* = 9.2 Hz, 1H, NHTCA), 5.53 (t, *J* = 9.4 Hz, 1H), 5.34 (dd, *J* = 10.2, 7.8 Hz, 1H), 5.29 (dd, *J* = 9.8, 7.9 Hz, 1H), 5.09 – 5.02 (m, 3H), 4.89 (d, *J* = 11.7 Hz, 1H), 4.83 (dd, *J* = 10.7, 8.8 Hz, 1H), 4.65 (s, 2H), 4.56 – 4.45 (m, 6H), 4.43-4.37 (m, , 2H), 4.34 (d, *J* = 11.7 Hz, 1H), 4.23 (dd, *J* = 12.1, 2.0 Hz, 2H), 4.06 – 3.98 (m, 3H), 3.91 – 3.83 (m, 4H), 3.80 – 3.73 (m, 2H), 3.66 (t, *J* = 8.2 Hz, 1H), 3.63 – 3.58 (m, 4H), 3.54 – 3.46 (m, 2H), 3.42 – 3.38 (m, 2H), 3.37 – 3.32 (m, 1H), 3.29 – 3.25 (m, 2H), 2.92 – 2.84 (m, 3H, including C*H*$_2$-NHCbz), 2.79 (t, *J* = 8.8 Hz, 1H), 2.59 – 2.50 (m, 1H, CH*H*' Lev), 2.47 – 2.40 (m, 3H, CH_2 Lev), 1.98 (s, 3H, CH_3 Lev), 1.51 – 1.38 (m, 2H), 1.30 – 1.26 (m, 2H), 1.19 – 1.10 (m, 2H). ^{13}C NMR (151 MHz, $CDCl_3$) δ 206.3 (*C*(O)CH_3), 172.5 (OC(O)CH_2), 166.3 (C=O Bz), 165.35 (C=O Bz), 165.32 (C=O Bz), 164.5 (C=O Bz), 162.1, 156.4 (C=O TCA, Cbz), 139.1, 138.3, 138.12, 138.09, 137.8, 137.6, 136.8, 133.7, 133.5, 133.2, 132.5, 130.5, 130.0, 129.86, 129.82, 129.68,

129.64, 129.5, 128.9, 128.73, 128.68, 128.68, 128.65, 128.62, 128.59, 128.47, 128.45, 128.24, 128.22, 128.18, 128.12, 128.02, 127.95, 127.88, 127.79, 127.74, 127.3, 101.1 (**C-1**, $J_{C\text{-}H}$ = 161 Hz) 100.88 (**C-1**, $J_{C\text{-}H}$ = 164 Hz), 100.85 (**C-1**, $J_{C\text{-}H}$ = 164 Hz), 100.4 (**C-1**, $J_{C\text{-}H}$ = 161 Hz), 92.0 (*C*Cl_3 TCA), 78.8, 76.4, 75.8, 75.6, 75.2, 75.0, 74.9, 74.7, 74.39, 74.37, 73.7, 73.6, 73.5, 73.4, 73.3, 73.2, 73.05, 73.01, 72.8, 72.3, 72.1, 69.8, 67.67, 67.66, 67.2, 66.6, 56.0, 40.9 (*C*H_2-NHCbz), 37.9 (*C*H_2 Lev), 29.8 (*C*H_3 Lev), 29.5 (*C*H_2 pentane), 29.0 (*C*H_2 pentane), 28.0 (*C*H_2 Lev), 23.2 (*C*H_2 pentane). HRMS (ESI) calc. for $C_{114}H_{117}Cl_3N_2O_{29}Na_2$, $[M+2Na]^{2+}$ 1064.3296; found: 1064.3237.

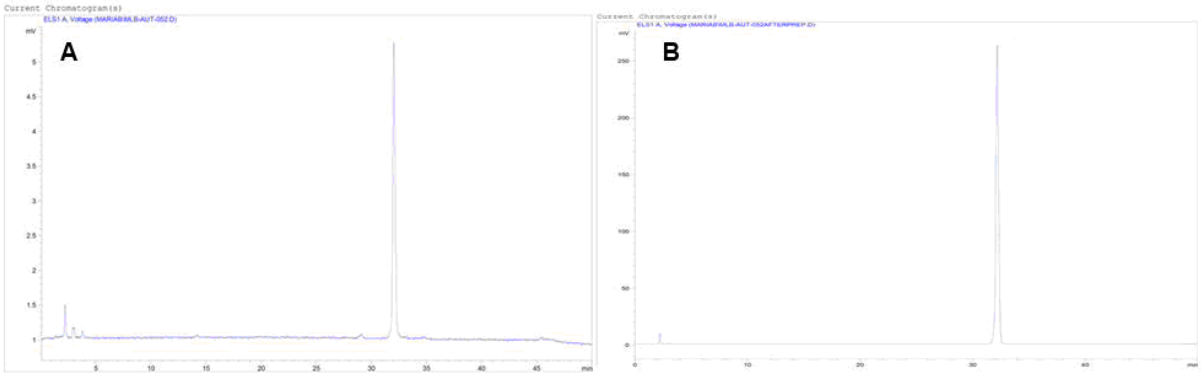

Analytical NP-HPLC of (**A**) crude reaction mixture after photocleavage and (**B**) the purified product. Detection: ELSD.

_N_-Benzyloxycarbonyl-5-amino-pentyl 3,4,6-tri-_O_-benzyl-β-D-galactopyranosyl-(1→4)-6-_O_-benzyl-2-deoxy-2-_N_-trichloroacetyl-β-D-glucopyranosyl-(1→3)-2-_O_-benzoyl-4,6-di-_O_-benzyl-β-D-galactopyranosyl-(1→4)-2,3-di-_O_-benzoyl-6-_O_-benzyl-β-D-glucopyranoside (2.42)

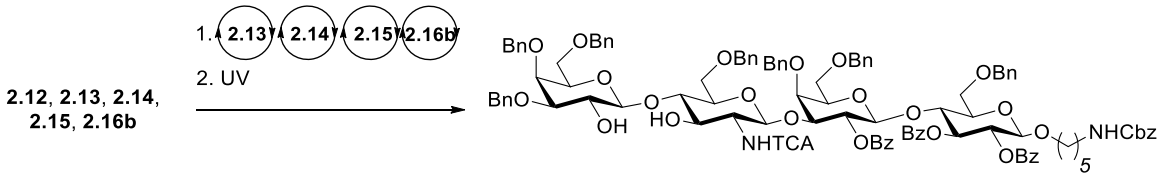

2.42

Yield: 38%, 9.40 mg

^{1}H NMR (600 MHz, $CDCl_3$) δ 7.90 (d, *J* = 8.0 Hz, 4H), 7.84 (d, *J* = 7.2 Hz, 2H), 7.56 (t, *J* = 7.4 Hz, 1H), 7.47 – 7.39 (m, 3H), 7.39 – 7.19 (m, 41H), 7.18 – 7.13 (m, 4H), 6.37 (d, *J* = 8.1 Hz, 1H, N*H*TCA), 5.55 (t, *J* = 9.3 Hz, 1H), 5.41 (dd, *J* = 10.2, 7.8 Hz, 1H), 5.30 (dd, *J* = 9.8, 7.9 Hz, 1H), 5.05 (s, 2H), 4.88 (d, *J* = 11.9 Hz, 1H), 4.82 (d, *J* = 11.6 Hz, 1H), 4.74 – 4.68 (m, 2H, including **H-1**), 4.62 (d, *J* = 11.9 Hz, 1H), 4.54 – 4.47 (m, 5H, including **H-1**), 4.45 (d, *J* = 8.0 Hz, 1H, **H-1**), 4.41 – 4.36 (m, 2H), 4.33 (d, *J* = 11.7 Hz, 1H), 4.26 (d, *J* = 12.3 Hz, 1H),

4.21 (d, *J* = 7.7 Hz, 1H, **H-1**), 4.08 – 4.01 (m, 3H), 3.90 (d, *J* = 2.3 Hz, 1H), 3.87 – 3.73 (m, 6H), 3.68 (dd, *J* = 10.3, 7.5 Hz, 1H), 3.57 – 3.40 (m, 8H), 3.39 – 3.34 (m, 2H), 3.33 – 3.29 (m, 2H), 2.92 – 2.82 (m, 4H), 1.52 – 1.39 (m, 2H, CH_2 pentane), 1.33 – 1.24 (m, 2H, CH_2 pentane), 1.21 – 1.10 (m, 2H, CH_2 pentane). ^{13}C NMR (151 MHz, $CDCl_3$) δ 165.36 (C=O Bz), 165.33 (C=O Bz), 164.7 (C=O Bz), 162.0, 156.4 (C=O Cbz, C=O TCA), 139.2, 138.3, 138.21, 138.16, 138.0, 137.9, 137.5, 136.9, 133.5, 133.2, 132.6, 130.6, 130.0, 129.9, 129.8, 129.7, 128.8, 128.7, 128.63, 128.61, 128.54, 128.50, 128.45, 128.42, 128.35, 128.23, 128.18, 128.11, 128.09, 128.06, 127.9, 127.83, 127.80, 127.75, 104.3 (**C-1**, $J_{C\text{-}H}$ = 164 Hz), 101.1 (**C-1**, $J_{C\text{-}H}$ = 164 Hz), 100.9 (**C-1**, $J_{C\text{-}H}$ = 161 Hz), 100.3 (**C-1**, $J_{C\text{-}H}$ = 163 Hz), 92.4 (CCl_3 TCA), 82.9, 82.1, 78.8, 75.8, 75.2, 74.82, 74.75, 74.7, 74.2, 73.9, 73.8, 73.62, 73.58, 73.5, 73.2, 73.1, 72.9, 72.7, 72.6, 72.2, 71.5, 71.1, 69.8, 69.5, 68.6, 67.7, 67.4, 66.6, 58.2, 40.9 (CH_2-NHCbz), 29.5 (CH_2 pentane), 29.0 (CH_2 pentane), 23.2 (CH_2 pentane). HRMS (ESI) calc. for $C_{109}H_{113}Cl_3N_2O_{26}Na$, $[M+Na]^+$ 1993.6539; found: 1993.6580.

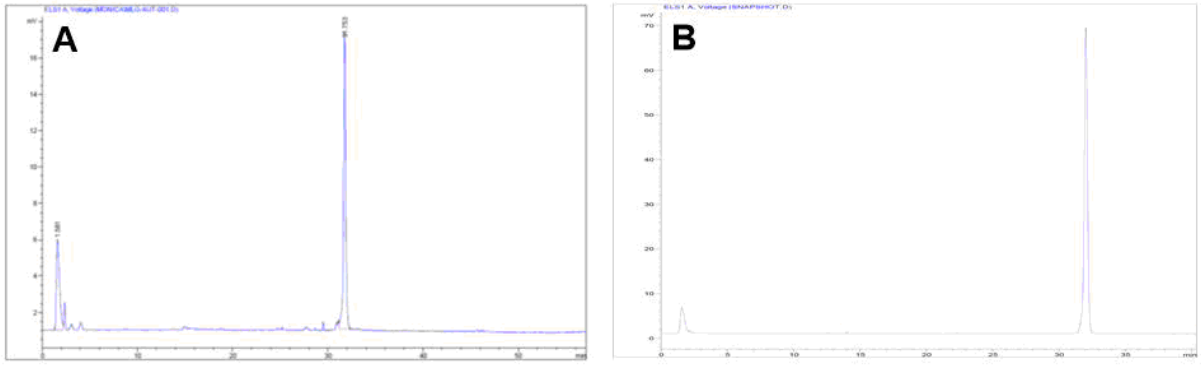

Analytical NP-HPLC of (**A**) crude reaction mixture after photocleavage and (**B**) the purified product. Detection: ELSD.

***N*-Benzyloxycarbonyl-5-amino-pentyl 3,4,6-tri-*O*-benzyl-β-D-galactopyranosyl-(1→4)-6-*O*-benzyl-3-*O*-(2,3,4-tri-*O*-benzyl-α-L-fucopyranosyl)-2-deoxy-2-*N*-trichloroacetyl-β-D-glucopyranosyl-(1→3)-2-*O*-benzoyl-4,6-di-*O*-benzyl-β-D-galactopyranosyl-(1→4)-6-*O*-benzyl-3-*O*-(2,3,4-tri-*O*-benzyl-α-L-fucopyranosyl)-2-deoxy-2-*N*-trichloroacetyl-β-D-glucopyranosyl-(1→3)-2-*O*-benzoyl-4,6-di-*O*-benzyl-β-D-galactopyranosyl-(1→4)-2,3-di-*O*-benzoyl-6-*O*-benzyl-β-D-glucopyranoside (2.43)**

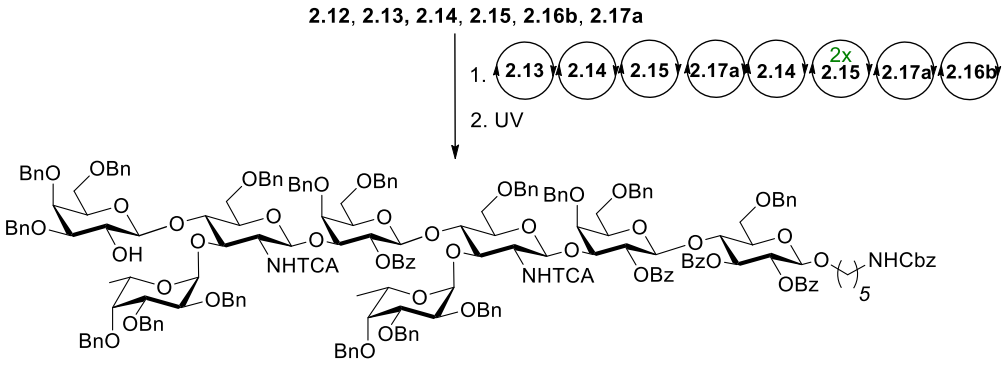

2.43

Yield: 28%, 12.9 mg

^{1}H NMR (600 MHz, $CDCl_3$) δ 7.90 (d, *J* = 8.0 Hz, 4H), 7.85 (d, *J* = 7.4 Hz, 2H), 7.83 – 7.80 (m, 2H), 7.53 – 7.06 (m, 97H), 6.59 (d, *J* = 8.1 Hz, 1H, NHTCA), 6.44 (d, *J* = 7.9 Hz, 1H, NHTCA), 5.54 (t, *J* = 9.3 Hz, 1H), 5.39 – 5.26 (m, 3H), 5.09 – 5.03 (m, 4H), 4.98 (d, *J* = 10.9 Hz, 1H), 4.94 (d, *J* = 7.4 Hz, 1H), 4.82 (d, *J* = 10.8 Hz, 1H), 4.78 – 4.72 (m, 2H), 4.65 – 4.56 (m, 7H), 4.54 – 4.43 (m, 12H), 4.39 (td, *J* = 10.5, 8.6, 6.0 Hz, 4H), 4.35 – 4.31 (m, 1H), 4.29 – 4.20 (m, 7H), 4.17 – 4.15 (m, 1H), 4.13 – 4.09 (m, 2H), 4.07 – 3.99 (m, 4H), 3.97 – 3.88 (m, 6H), 3.86 (dd, *J* = 10.1, 3.7 Hz, 1H), 3.82 – 3.75 (m, 6H), 3.75 – 3.68 (m, 3H), 3.67 – 3.55 (m, 6H), 3.53 – 3.45 (m, 3H), 3.42 – 3.34 (m, 4H), 3.32 (dd, *J* = 8.9, 5.0 Hz, 1H), 3.28 – 3.23 (m, 2H), 3.20 (s, 1H), 3.17 (dd, *J* = 8.3, 5.1 Hz, 1H), 3.07 – 3.02 (m, 1H), 2.93 – 2.85 (m, 2H, CH_2-NHCbz), 2.83 – 2.79 (m, 1H), 2.72 (t, *J* = 8.7 Hz, 1H), 1.50 – 1.37 (m, 2H, CH_2 pentane), 1.33 – 1.23 (m, 2H, CH_2 pentane), 1.15 (m, 2H, CH_2 pentane), 1.09 (d, *J* = 6.5 Hz, 3H, CH_3 Fuc), 0.96 (d, *J* = 6.4 Hz, 3H, CH_3 Fuc). ^{13}C NMR (151 MHz, $CDCl_3$) δ 165.37 (C=O Bz), 165.32 (C=O Bz), 164.7 (C=O Bz), 164.5 (C=O Bz), 161.2, 156.4 (C=O Cbz, 2 x C=O TCA), 139.37, 139.37, 139.34, 139.14, 139.11, 139.05, 138.8, 138.7, 138.6, 138.4, 138.3, 138.1, 138.02, 137.95, 137.94, 137.87, 136.86, 133.5, 133.4, 133.2, 132.4, 130.6, 130.0, 129.9, 129.8, 129.7, 129.1, 128.8, 128.7, 128.63, 128.60, 128.55, 128.52, 128.49, 128.48, 128.44, 128.41, 128.38, 128.33, 128.32, 128.26, 128.20, 128.17, 128.15, 128.12, 128.11, 128.09, 128.02, 128.01, 127.99, 127.90, 127.88, 127.86, 127.84, 127.71, 127.68, 127.65, 127.61, 127.48, 127.47, 127.44, 127.3, 127.18, 127.17, 101.7 (**C-1**, $J_{C\text{-}H}$ = 162 Hz), 101.06 (**C-1**, $J_{C\text{-}H}$ = 162 Hz), 101.04

(**C-1**, $J_{C\text{-}H}$ = 162 Hz), 100.4 (**C-1**, $J_{C\text{-}H}$ = 166 Hz), 100.24 (**C-1**, $J_{C\text{-}H}$ = 162 Hz), 100.17 (**C-1**, $J_{C\text{-}H}$ = 167 Hz), 97.4 (**C-1**, $J_{C\text{-}H}$ = 171 Hz), 97.1 (**C-1**, $J_{C\text{-}H}$ = 171 Hz), 92.08 (CCl$_3$), 92.06 (CCl$_3$), 82.5, 79.6, 79.3, 78.9, 78.8, 78.48, 78.45, 76.1, 75.83, 75.80, 75.4, 75.17, 75.14, 75.10, 74.8, 74.7, 74.2, 74.0, 73.7, 73.6, 73.5, 73.44, 73.42, 73.41, 73.3, 73.13, 73.10, 73.08, 73.06, 73.02, 73.02, 72.97, 72.68, 72.64, 72.56, 72.48, 72.2, 71.4, 69.7, 68.6, 67.89, 67.87, 67.86, 67.78, 67.5, 66.8, 66.6, 59.9, 59.0, 40.9 (CH$_2$-NHCbz), 29.5 (CH$_2$ pentane), 29.0 (CH$_2$ pentane), 23.2 (CH$_2$ pentane), 16.6 (CH$_3$ Fuc), 16.4 (CH$_3$ Fuc). HRMS (ESI) calc. for $C_{205}H_{211}Cl_6N_3O_{45}Na_2$, $[M+2Na]^{2+}$ 1845.1115; found: 1845.1084.

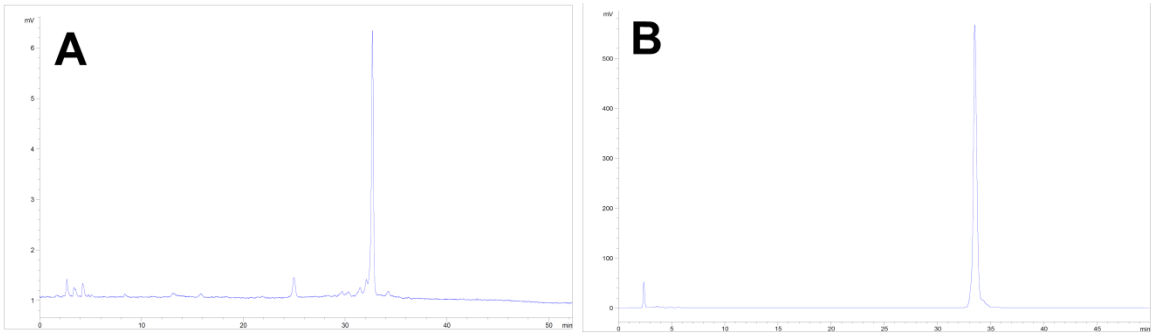

Analytical NP-HPLC of (**A**) crude reaction mixture after photocleavage and (**B**) the purified product. Detection: ELSD.

***N*-Benzyloxycarbonyl-5-amino-pentyl 2,3,4-tri-*O*-benzyl-α-L-fucopyranosyl-(1→2)-3,4,6-tri-*O*-benzyl-β-D-galactopyranosyl-(1→4)-6-*O*-benzyl-3-*O*-(2,3,4-tri-*O*-benzyl-α-L-fucopyranosyl)-2-deoxy-2-*N*-trichloroacetyl-β-D-glucopyranosyl-(1→3)-2-*O*-benzoyl-4,6-di-*O*-benzyl-β-D-galactopyranosyl-(1→4)-6-*O*-benzyl-3-*O*-(2,3,4-tri-*O*-benzyl-α-L-fucopyranosyl)-2-deoxy-2-*N*-trichloroacetyl-β-D-glucopyranosyl-(1→3)-2-*O*-benzoyl-4,6-di-*O*-benzyl-β-D-galactopyranosyl-(1→4)-2,3-di-*O*-benzoyl-6-*O*-benzyl-β-D-glucopyranoside (2.44)**

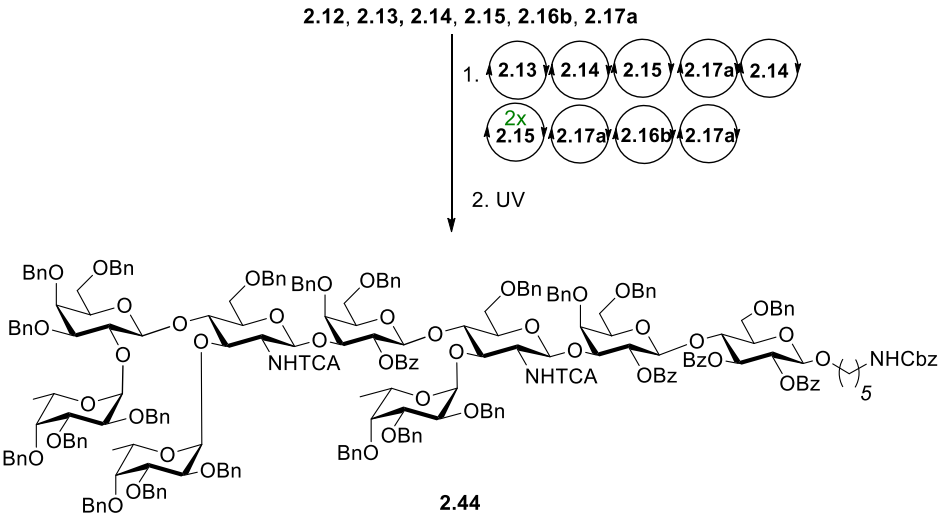

2.44

Yield: 28%, 14.6 mg

^{1}H NMR (600 MHz, $CDCl_3$) δ 7.95 – 7.78 (m, 8H), 7.49 (tt, *J* = 7.3, 1.3 Hz, 1H), 7.45 – 7.41 (m, 2H), 7.39 – 7.03 (m, 109H), 6.66 (d, *J* = 7.3 Hz, 1H, NHTCA), 6.44 (d, *J* = 8.2 Hz, 1H, NHTCA), 5.66 (d, *J* = 3.9 Hz, 1H, **H-1**), 5.52 (t, *J* = 9.3 Hz, 1H), 5.40 (dd, *J* = 10.2, 8.0 Hz, 1H), 5.33 – 5.25 (m, 2H), 5.11 (d, *J* = 7.5 Hz, 1H), 5.06 (d, *J* = 3.8 Hz, 1H), 5.04 (s, 2H), 4.99 (d, *J* = 10.9 Hz, 1H), 4.97 – 4.93 (m, 2H), 4.78 – 4.70 (m, 4H), 4.69 – 4.62 (m, 3H), 4.58 – 4.20 (m, 33H), 4.14 – 4.09 (m, 1H), 4.09 – 4.05 (m, 2H), 4.04 – 3.99 (m, 4H), 3.92 (d, *J* = 4.6 Hz, 2H), 3.89 – 3.75 (m, 12H), 3.70 – 3.55 (m, 9H), 3.54 – 3.44 (m, 5H), 3.43 – 3.36 (m, 3H), 3.35 – 3.31 (m, 2H), 3.28 (dd, *J* = 8.9, 5.0 Hz, 1H), 3.19 – 3.14 (m, 3H), 3.05 (d, *J* = 7.7 Hz, 1H), 2.91 – 2.85 (m, 2H, C*H*$_2$-NHCbz), 2.79 (dd, *J* = 8.9, 4.7 Hz, 1H), 2.69 (t, *J* = 8.7 Hz, 1H), 1.49 – 1.34 (m, 4H, CH_2 pentane), 1.21 (d, *J* = 6.5 Hz, 3H, CH_3 Fuc), 1.17 – 1.12 (m, 2H, CH_2 pentane), 1.09 (d, *J* = 6.4 Hz, 3H, CH_3 Fuc), 1.04 (d, *J* = 6.4 Hz, 3H, CH_3 Fuc). ^{13}C NMR (151 MHz, $CDCl_3$) δ 165.37 (C=O Bz), 165.34 (C=O Bz), 164.68 (C=O Bz), 164.67 (C=O Bz), 161.27, 161.22, 156.4 (C=O Cbz, 2x C=O TCA), 139.36, 139.33, 139.31, 139.14, 139.03, 138.95, 138.93, 138.87, 138.69, 138.65, 138.5, 138.3, 138.2, 138.1, 138.0, 137.83, 137.81, 136.9, 133.5, 133.4, 133.2, 132.4, 130.6, 130.1, 129.95, 129.92, 129.8, 129.7, 129.0, 128.77, 128.71, 128.68, 128.65, 128.63, 128.58, 128.55, 128.52, 128.45, 128.43, 128.41, 128.3,

128.27, 128.24, 128.22, 128.18, 128.16, 128.12, 128.07, 128.03, 128.00, 127.98, 127.93, 127.83, 127.81, 127.76, 127.71, 127.66, 127.64, 127.57, 127.50, 127.4, 127.3, 127.2, 126.3, 101.07 (**C-1**, $J_{C\text{-}H}$ = 165 Hz), 101.01 (**C-1**, $J_{C\text{-}H}$ = 163 Hz), 100.5 (**C-1**, $J_{C\text{-}H}$ = 167 Hz), 100.4 (**C-1**, $J_{C\text{-}H}$ = 165 Hz), 100.3 (**C-1**, $J_{C\text{-}H}$ = 163 Hz), 99.7 (**C-1**, $J_{C\text{-}H}$ = 169 Hz), 98.0 (**2 x C-1**, $J_{C\text{-}H}$ = 176 Hz, $J_{C\text{-}H}$ = 171 Hz), 97.2 (**C-1**, $J_{C\text{-}H}$ = 171 Hz), 92.1 (CCl_3), 91.8 (CCl_3), 84.0, 80.1, 79.43, 79.41, 79.3, 79.0, 78.9, 78.46, 78.43, 76.7, 76.04, 76.02, 75.86, 75.82, 75.6, 75.2, 75.08, 75.05, 75.02, 74.9, 74.7, 73.86, 73.81, 73.7, 73.58, 73.55, 73.49, 73.43, 73.3, 73.18, 73.11, 73.07, 73.05, 72.8, 72.70, 72.66, 72.61, 72.2, 72.1, 71.3, 69.8, 68.4, 68.2, 67.86, 67.82, 67.75, 67.5, 67.0, 66.78, 66.7, 66.6, 61.2, 59.0, 40.9 (CH_2-NHCbz), 29.5 (CH_2 pentane), 29.0 (CH_2 pentane), 23.2 (CH_2 pentane), 16.7 (CH_3 Fuc), 16.44 (CH_3 Fuc), 16.37 (CH_3 Fuc). HRMS (ESI) calc. for $C_{232}H_{239}Cl_6N_3O_{49}Na_2$, $[M+2Na]^{2+}$ 2053.2109; found: 2053.2148.

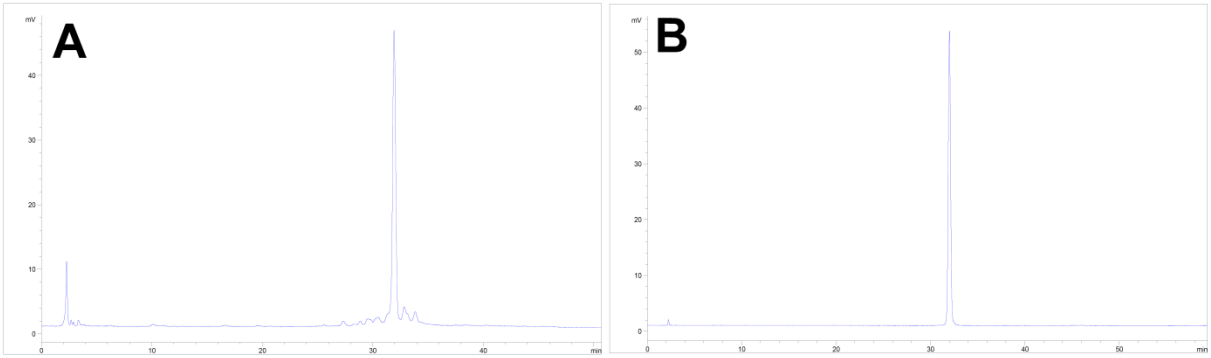

Analytical NP-HPLC of (**A**) crude reaction mixture after photocleavage and (**B**) the purified product. Detection: ELSD.

_N_-Benzyloxycarbonyl-5-amino-pentyl 2,4,6-tri-_O_-benzyl-β-D-galactopyranosyl-(1→3)-6-_O_-benzyl-2-deoxy-2-_N_-trichloroacetyl-β-D-glucopyranosyl-(1→3)-2-_O_-benzoyl-4,6-di-_O_-benzyl-β-D-galactopyranosyl-(1→4)-2,3-di-_O_-benzoyl-6-_O_-benzyl-β-D-glucopyranoside (2.46)

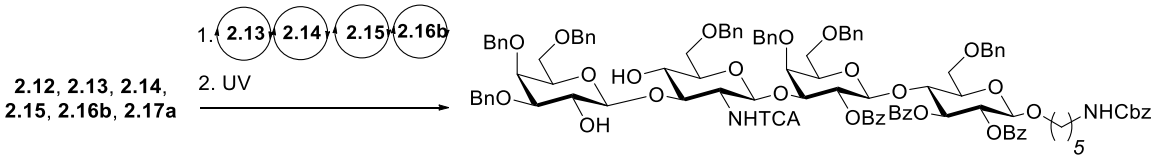

2.46

Yield: 47%, 11.5 mg

^{1}H NMR (600 MHz, $CDCl_3$) δ 7.93 – 7.87 (m, 4H), 7.84 (d, J = 8.1 Hz, 2H), 7.55 (t, J = 7.4 Hz, 1H), 7.45 (t, J = 7.4 Hz, 1H), 7.41 (t, J = 7.6 Hz, 2H), 7.37 – 7.23 (m, 39H), 7.20 – 7.12 (m, 6H), 6.60 (d, J = 7.6 Hz, 1H, NHTCA), 5.54 (t, J = 9.4 Hz, 1H), 5.39 – 5.35 (m, 1H), 5.33 – 5.28 (m, 1H), 5.06 (s, 2H), 4.86 (d, J = 11.7 Hz, 1H), 4.81 (d, J = 11.9 Hz, 1H), 4.70 – 4.63 (m, 3H), 4.55 – 4.48 (m, 5H), 4.43 – 4.35 (m, 5H), 4.24 (d, J = 12.3 Hz, 1H), 4.11 – 4.03 (m, 4H),

3.93 – 3.83 (m, 4H), 3.79 (dt, *J* = 10.6, 5.8 Hz, 1H), 3.73 (d, *J* = 2.5 Hz, 1H), 3.62 – 3.57 (m, 2H), 3.56 – 3.32 (m, 11H), 3.28 (dd, *J* = 9.7, 2.5 Hz, 1H), 2.94 – 2.80 (m, 4H, including C*H*$_2$-NHCbz), 1.45 (m, 2H, CH_2 pentane), 1.30 – 1.28 (m, 2H, CH_2 pentane), 1.20 – 1.13 (m, 2H, CH_2 pentane). ^{13}C NMR (151 MHz, $CDCl_3$) δ 165.3 (2x C=O Bz), 164.9 (C=O Bz), 162.7 (C=O Cbz), 156.4 (C=O TCA), 139.2, 138.3, 138.24, 138.23, 138.15, 138.13, 137.56, 133.52, 133.2, 132.6, 130.6, 129.99, 129.97, 129.84, 129.75, 129.73, 128.8, 128.63, 128.59, 128.55, 128.51, 128.49, 128.46, 128.42, 128.20, 128.18, 128.16, 128.13, 128.11, 128.04, 128.01, 127.94, 127.92, 127.91, 127.84, 127.79, 127.77, 127.72, 127.70, 127.3, 104.3 (**C-1**, J_{C-H} = 165 Hz), 101.1 (**C-1**, J_{C-H} = 163 Hz), 100.8 (**C-1**, J_{C-H} = 162 Hz), 99.4 (**C-1**, J_{C-H} = 165 Hz), 92.3 (*C*Cl_3), 84.9, 81.2, 78.0, 76.1, 75.7, 75.06, 74.95, 74.75, 74.72, 74.3, 73.8, 73.7, 73.57, 73.52, 73.2, 73.1, 72.8, 72.2, 71.3, 69.9, 69.80, 69.75, 68.9, 67.6, 67.3, 66.6, 57.7, 40.9 (*C*H_2-NHCbz), 29.5 (*C*H_2 pentane), 29.0 (*C*H_2 pentane), 23.2 (*C*H_2 pentane). HRMS (ESI) calc. for $C_{109}H_{113}Cl_3N_2O_{26}Na$, $[M+Na]^+$ 1993.6539; found: 1993.6573.

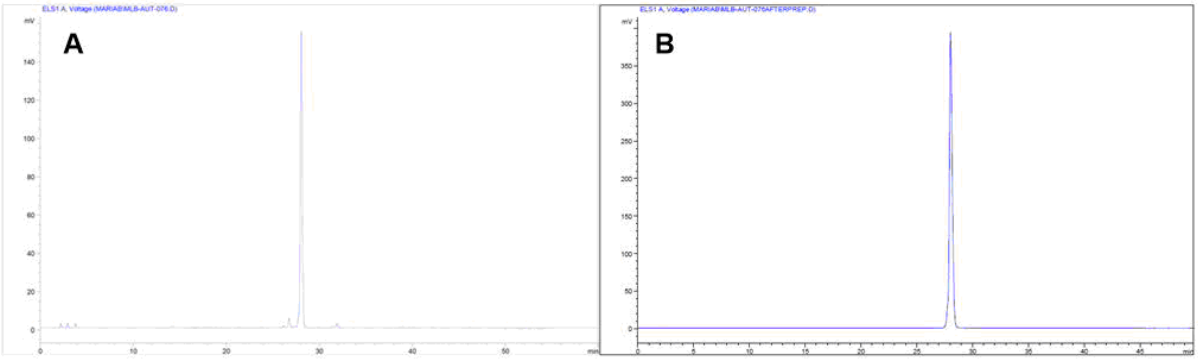

Analytical NP-HPLC of (**A**) crude reaction mixture after photocleavage and (**B**) the purified product. Detection: ELSD.

***N*-Benzyloxycarbonyl-5-amino-pentyl 2,3,4-tri-*O*-benzyl-α-L-fucopyranosyl-(1→2)-3,4,6-tri-*O*-benzyl-β-D-galactopyranosyl-(1→3)-6-*O*-benzyl-4-*O*-(2,3,4-tri-*O*-benzyl-α-L-fucopyranosyl)-2-deoxy-2-*N*-trichloroacetyl-β-D-glucopyranosyl-(1→3)-2-*O*-benzoyl-4,6-di-*O*-benzyl-β-D-galactopyranosyl-(1→4)-2,3-di-*O*-benzoyl-6-*O*-benzyl-β-D-glucopyranoside (2.47)**

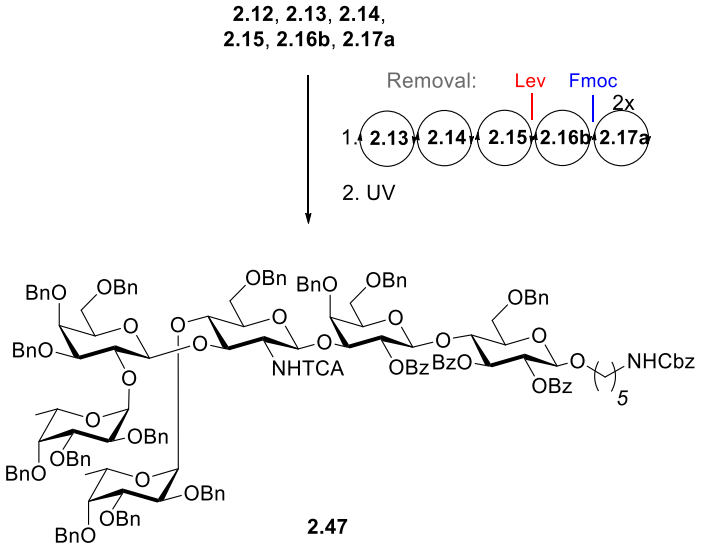

Yield: 34%, 12.1 mg

^{1}H NMR (600 MHz, $CDCl_3$) δ 7.92 – 7.86 (m, 4H), 7.80 (d, *J* = 8.2 Hz, 2H), 7.51 (t, *J* = 7.4 Hz, 1H), 7.45 (t, *J* = 7.4 Hz, 1H), 7.40 – 7.07 (m, 75H), 7.01 (dd, *J* = 6.4, 2.8 Hz, 2H), 6.53 (d, *J* = 9.4 Hz, 1H, NHTCA), 5.54 – 5.49 (m, 2H, including **H-1**), 5.35 (dd, *J* = 10.1, 7.8 Hz, 1H), 5.30 (dd, *J* = 9.8, 7.9 Hz, 1H), 5.06 (s, 2H), 4.99 – 4.94 (m, 2H, including **H-1**), 4.82 – 4.74 (m, 4H), 4.72 (d, *J* = 10.9 Hz, 1H), 4.65 (d, *J* = 11.9 Hz, 1H), 4.58 – 4.52 (m, 4H, including **H-1**), 4.50 – 4.29 (m, 18H, including 3 x **H-1**), 4.24 (d, *J* = 12.3 Hz, 2H), 4.07 – 4.02 (m, 3H), 4.01 – 3.89 (m, 6H), 3.87 – 3.83 (m, 3H), 3.81 – 3.76 (m, 4H), 3.69 – 3.59 (m, 3H), 3.54 (dd, *J* = 8.7, 5.5 Hz, 1H), 3.49 (dd, *J* = 11.2, 3.9 Hz, 1H), 3.41 – 3.32 (m, 6H), 3.15 (s, 1H), 2.93 – 2.88 (m, 3H), 2.83 (t, *J* = 8.6 Hz, 1H), 1.50 – 1.40 (m, 2H, CH_2 pentane), 1.33 – 1.29 (m, 2H, CH_2 pentane), 1.20 – 1.13 (m, 8H, CH_2 pentane, 2x CH_3 Fuc). ^{13}C NMR (151 MHz, $CDCl_3$) δ 165.4 (C=O Bz), 165.3 (C=O Bz), 164.3 (C=O Bz), 161.2, 156.4 (C=O Cbz, TCA), 139.6, 139.5, 139.4, 139.3, 139.2, 138.87, 138.82, 138.6, 138.33, 138.27, 138.15, 138.12, 137.9, 136.9, 133.3, 133.2, 132.5, 130.6, 129.97, 129.96, 129.93, 129.8, 129.7, 128.84, 128.75, 128.73, 128.6, 128.54, 128.51, 128.48, 128.46, 128.45, 128.31, 128.29, 128.24, 128.18, 128.14, 128.12, 128.10, 128.07, 128.04, 127.91, 127.87, 127.83, 127.75, 127.72, 127.70, 127.66, 127.60, 127.54, 127.51, 127.32, 127.28, 127.24, 127.23, 127.12, 127.06, 101.3 (**C-1**, $J_{C\text{-}H}$ = 162 Hz), 101.1 (**C-1**, $J_{C\text{-}H}$ = 161 Hz), 100.8 (**C-1**, $J_{C\text{-}H}$ = 163 Hz), 100.5 (**C-1**, $J_{C\text{-}H}$ = 164 Hz), 99.0 (**C-1**, $J_{C\text{-}H}$ = 175 Hz), 98.0 (**C-1**, $J_{C\text{-}H}$ = 172 Hz), 92.5 (CCl_3), 83.4, 80.4, 79.6, 78.4, 78.2, 78.0, 76.1, 76.0, 75.67,

75.65, 75.57, 75.00, 74.98, 74.94, 74.86, 74.79, 74.6, 74.5, 74.0, 73.6, 73.47, 73.44, 73.24, 73.22, 73.16, 73.0, 72.8, 72.4, 72.1, 71.9, 71.7, 69.8, 68.7, 67.7, 67.43, 67.40, 67.2, 66.7, 66.6, 58.9, 40.9 (*C*H_2-NHCbz), 29.5 (*C*H_2 pentane), 29.0 (*C*H_2 pentane), 23.2 (*C*H_2 pentane), 16.4 (2x *C*H_3 Fuc). HRMS (ESI) calc. for $C_{163}H_{169}Cl_3N_2O_{34}Na_2$, $[M+2Na]^{2+}$ 1424.5203; found: 1424.5269.

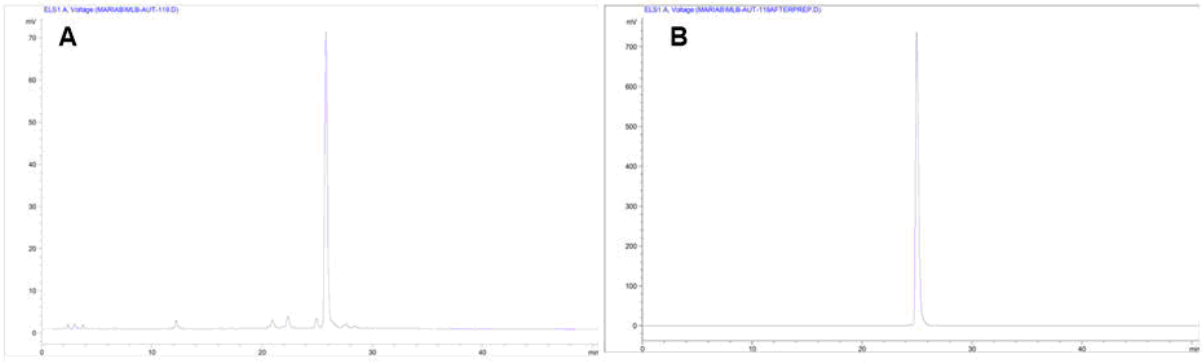

Analytical NP-HPLC of (**A**) crude reaction mixture after photocleavage and (**B**) the purified product. Detection: ELSD.

***N*-Benzyloxycarbonyl-5-amino-pentyl 2-*O*-benzoyl-*3*,4,6-tri-*O*-benzyl-β-D-galactopyranosyl-(1→3)-4-*O*-(2,3,4-tri-*O*-benzyl-α-L-fucopyranosyl)-6-*O*-benzyl-*N*-trichloroacetyl-2-deoxy-β-D-glucopyranosyl-(1→3)-2-*O*-benzoyl-4,6-di-*O*-benzyl-β-D-galactopyranosyl-(1→4)-2,3-di-*O*-benzyl-β-D-glucopyranoside (2.48)**

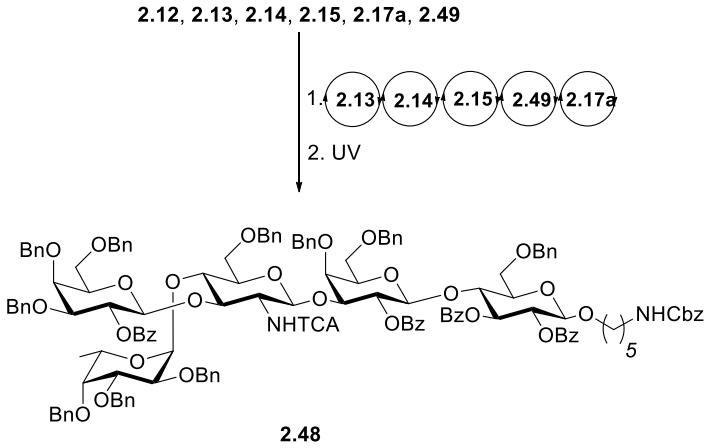

Yield: 47%, 14.5 mg

^{1}H NMR (600 MHz, $CDCl_3$) δ 7.99 (d, *J* = 7.2 Hz, 2H), 7.92 – 7.88 (m, 2H), 7.85 – 7.79 (m, 4H), 7.55 – 7.50 (m, 2H), 7.45 (t, *J* = 7.4 Hz, 1H), 7.41 – 7.07 (m, 59H), 7.05 – 6.99 (m, 5H), 6.31 (d, *J* = 6.8 Hz, 1H), 5.54 – 5.48 (m, 2H), 5.29 (dd, *J* = 9.8, 8.0 Hz, 1H), 5.22 (dd, *J* = 10.2, 7.9 Hz, 1H), 5.06 (s, 2H), 4.96 (d, *J* = 10.6 Hz, 1H), 4.88 (d, *J* = 3.8 Hz, 1H, **H-1**), 4.79 – 4.73 (m, 2H, including **H-1**), 4.65 – 4.50 (m, 7H), 4.49 – 4.45 (m, 4H, including **2 x H-1**), 4.44 – 4.38

(m, 4H), 4.26 – 4.14 (m, 5H, including **H-1**), 4.08 – 3.96 (m, 6H), 3.83 (d, *J* = 2.8 Hz, 1H), 3.82 – 3.75 (m, 3H), 3.70 – 3.56 (m, 5H), 3.44 – 3.24 (m, 9H), 2.94 – 2.87 (m, 3H), 2.72 (t, *J* = 8.7 Hz, 1H), 2.49 – 2.40 (m, 1H), 1.51 – 1.39 (m, 4H, 2x CH_2 pentane), 1.30 (d, *J* = 6.4 Hz, 3H, CH_3 Fuc), 1.19 – 1.10 (m, 2H, CH_2 pentane). ^{13}C NMR (151 MHz, $CDCl_3$) δ 165.4 (C=O Bz), 165.3 (C=O Bz), 165.2 (C=O Bz), 164.6 (C=O Bz), 161.0, 156.4 (C=O Cbz, TCA), 139.5, 139.3, 138.91, 138.87, 138.5, 138.16, 138.07, 138.01, 137.8, 137.3, 136.9, 133.5, 133.16, 133.13, 132.4, 130.7, 130.2, 130.03, 129.96, 129.91, 129.8, 129.7, 129.1, 128.9, 128.64, 128.62, 128.54, 128.50, 128.45, 128.44, 128.43, 128.27, 128.22, 128.17, 128.16, 128.12, 128.0, 127.89, 127.87, 127.84, 127.76, 127.73, 127.69, 127.65, 127.4, 127.31, 127.26, 101.1 (**C-1**, J_{C-H} = 165 Hz), 100.9 (**C-1**, J_{C-H} = 162 Hz), 100.5 (**C-1**, J_{C-H} = 164 Hz), 98.2 (**C-1**, J_{C-H} = 169 Hz), 97.7 (**C-1**, J_{C-H} = 173 Hz), 92.2 (CCl_3), 80.4, 79.2, 78.4, 77.5, 75.7, 75.4, 75.2, 74.9, 74.8, 74.73, 74.67, 74.59, 73.8, 73.48, 73.43, 73.26, 73.20, 73.1, 72.9, 72.3, 72.09, 72.08, 71.9, 71.6, 71.5, 69.7, 67.72, 67.68, 67.4, 67.3, 66.9, 66.6, 61.0, 40.9 (CH_2-NHCbz), 29.0 (2x CH_2 pentane), 23.2 (CH_2 pentane), 16.6 (CH_3 Fuc). HRMS (ESI) calc. for $C_{143}H_{145}Cl_3N_2O_{31}Na$, $[M+Na]^+$ 2513.8789; found: 2513.8787.

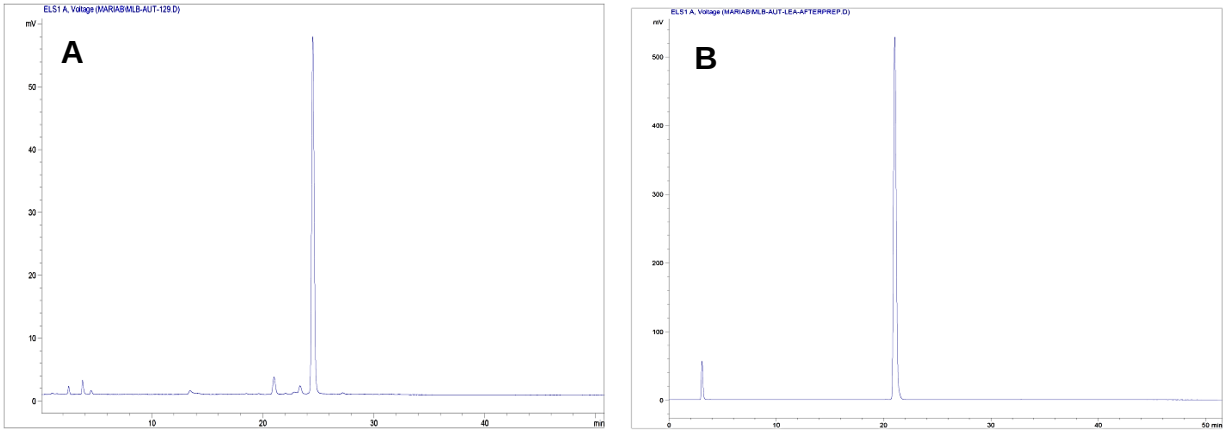

Analytical NP-HPLC of (**A**) crude reaction mixture after photocleavage and (**B**) the purified product. Detection: ELSD.

2.5.4 Deprotection of Oligosaccharides

Global Deptrotection: Methanolysis – Hydrogenolysis

AGA-synthesized, photocleaved, NP-HPLC purified product was sequentially subjected to methanolysis (when containing ester protecting groups) and hydrogenolysis. Hydrogenolysis product was purified by RP-HPLC to afford the final deprotected compound.

1) Methanolysis

The protected oligosaccharide was coevaporated twice with toluene and kept under vacuum. Subsequently, it was dissolved in DCM (0.50 mL) under N_2 atmosphere and MeOH (0.50 mL)

was added. NaOMe in MeOH 0.5 M (0.735 mL) was added and the solution was stirred until reaction completion (~48h, monitored by MALDI). Amberlite resin was added and when the pH of the solution was neutral it was filtered. Solvents were removed *in vacuo* to obtain the partially deprotected oligosaccharide.

2) Hydrogenolysis

The methanolysis crude reaction mixture was dissolved in AcOEt/t-BuOH/H_2O 2:1:1 (2 mL) and Pd/C was added. The mixture was degassed using N_2, purged with H_2 and kept under H_2 atmosphere until all TCA, Cbz and Bn protecting groups were removed (monitored by ^{1}H NMR, MALDI and/or LC-MS). TEA (5.00 µL) was added, the reaction mixture was filtrated through a PTFE syringe filter, and washed with MeOH (0.50 mL) and H_2O (0.5 mL). Solvents were removed *in vacuo*. The concentrated was lyophilized.

3) Purification

The lyophilized crude reaction mixture was dissolved in water and purified by RP-HPLC. A Thermo-Scientific Hypercarb column (150 mm x 4.60 mm I.D.) was used for analytical RP-HPLC with a flow rate of 0.70 mL/min and 0.1 % HCO_2H in H_2O/ACN as eluents. A Thermo-Scientific Hypercarb column (150 mm x 10.0 mm I.D.) was used for preparative RP-HPLC, with a flow rate of 3.50 mL/min and 0.1 % HCO_2H in H_2O/ACN as eluents. Unless stated otherwise, the gradient program detailed hereafter was used:

1. Isocratic 0.1 % HCO_2H in H_2O (5 min).
2. Linear gradient 0 to 30% ACN in 0.1 % HCO_2H in H_2O (30 min).
3. Linear gradient to 100% ACN (5 min).

The product was lyophilized and isolated as its formate salt.

Experimental Data for Deprotected Oligosaccharides 2.50-2.58

5-Amino-pentyl α-L-fucopyranosyl-(1→2)-β-D-galactopyranosyl-(1→4)-2-*N*-acetyl-2-deoxy-β-D-glucopyranoside (2.50)

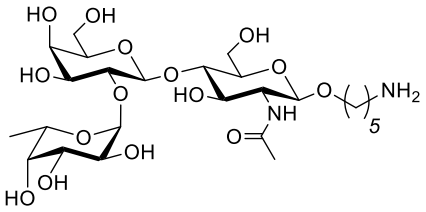

2.50

Compound **2.34** (8.33 mg, 5.62 µmol) was subjected to hydrogenolysis (see above *global deprotection* method). After RP-HPLC purification, conjugation-ready compound **2.50** was isolated as its formate salt (38%, 1.42 mg). ^{1}H NMR (600 MHz, D_2O) δ 8.47 (s, 1H, *H*COO^-),

5.32 (d, *J* = 3.2 Hz, 1H, **H-1**), 4.55 (d, *J* = 7.7 Hz, 1H, **H-1**), 4.51 (d, *J* = 8.4 Hz, 1H, **H-1**), 4.24 (q, *J* = 6.6 Hz, 1H, H-5 Fuc), 4.00 (dd, *J* = 12.0, 2.0 Hz, 1H), 3.96 – 3.87 (m, 3H), 3.84 – 3.78 (m, 6H), 3.77 – 3.66 (m, 5H), 3.61 (dt, *J* = 10.2, 6.3 Hz, 1H), 3.49 – 3.45 (m, 1H), 3.03 – 2.98 (m, 2H, C*H*$_2$-NH$_3^+$), 2.05 (s, 3H, C*H*$_3$ NHAc), 1.69 (p, *J* = 7.7 Hz, 2H, CH$_2$ pentane), 1.62 (p, *J* = 6.5 Hz, 2H, CH$_2$ pentane), 1.46 – 1.38 (m, 2H, CH$_2$ pentane), 1.25 (d, *J* = 6.6 Hz, 3H, CH$_3$ Fuc). ^{13}C NMR (151 MHz, D$_2$O) δ 174.4 (H*C*OO$^-$), 171.0 (C=O NHAc), 101.1 (**C-1**, $J_{C\text{-}H}$ = 166 Hz), 100.2 (**C-1**, $J_{C\text{-}H}$ = 165 Hz), 99.4 (**C-1**, $J_{C\text{-}H}$ = 175 Hz), 76.4, 76.1, 75.24, 75.19, 73.5, 72.3, 71.6, 70.1, 69.6, 69.0, 68.1, 66.8 (C-5 Fuc), 61.0, 60.1, 55.2, 39.3 (*C*H$_2$-NH$_3^+$), 28.0 (*C*H$_2$ pentane), 26.3 (*C*H$_2$ pentane), 22.10 (*C*H$_3$ NHAc), 22.06 (*C*H$_2$ pentane), 15.2 (*C*H$_3$ Fuc). HRMS (ESI) calc. for $C_{25}H_{47}N_2O_{15}$, $[M+H]^+$ 615.2971; found: 615.2976.

5-Amino-pentyl β-D-galactopyranosyl-(1→4)-2-*N*-acetyl-2-deoxy-3-*O*-(α-L-fucopyranosyl)-β-D-glucopyranoside (2.51)

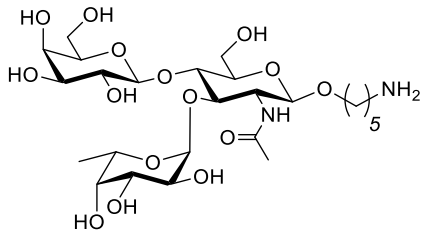

2.51

Compound **2.37** (8.89 mg, 6.00 μmol) was subjected to hydrogenolysis (see above *global deprotection* method). After RP-HPLC purification, conjugation-ready compound **2.51** was isolated as its formate salt (54%, 2.12 mg). ^{1}H NMR (600 MHz, D$_2$O) δ 8.50 (s, 1H, *H*COO$^-$), 5.12 (d, *J* = 4.1 Hz, 1H, **H-1** Fuc), 4.87 – 4.82 (m, 1H, H-5 Fuc), 4.54 (d, *J* = 8.1 Hz, 1H, **H-1**), 4.47 (d, *J* = 7.8 Hz, 1H, **H-1**), 4.02 (dd, *J* = 12.3, 2.3 Hz, 1H), 3.97 – 3.84 (m, 7H), 3.81 (d, *J* = 3.3 Hz, 1H), 3.78 – 3.65 (m, 4H), 3.63 – 3.58 (m, 3H), 3.51 (dd, *J* = 9.9, 7.8 Hz, 1H), 3.03 – 2.98 (m, 2H, C*H*$_2$-NH$_3^+$), 2.04 (s, 3H, C*H*$_3$ NHAc), 1.69 (p, *J* = 7.7 Hz, 2H, C*H*$_2$ pentane), 1.61 (p, *J* = 6.6 Hz, 2H, CH$_2$ pentane), 1.45 – 1.37 (m, 2H, CH$_2$ pentane), 1.19 (d, *J* = 6.6 Hz, 3H, CH$_3$ Fuc). ^{13}C NMR (151 MHz, D$_2$O) δ 174.1 (C=O NHAc), 170.9 (H*C*OO$^-$), 101.8 (**C-1**, $J_{C\text{-}H}$ = 165 Hz), 100.9 (**C-1**, $J_{C\text{-}H}$ = 166 Hz), 98.6 (**C-1**, $J_{C\text{-}H}$ = 174 Hz), 75.3, 74.9, 73.3, 72.4, 71.8, 71.0, 70.1, 69.1, 68.3, 67.6, 66.7 (C-5 Fuc), 61.4, 59.7, 55.8, 39.3 (*C*H$_2$-NH$_3^+$), 28.0 (*C*H$_2$ pentane), 26.3 (*C*H$_2$ pentane), 22.15 (*C*H$_3$ NHAc), 22.06 (*C*H$_2$ pentane), 15.2 (*C*H$_3$ Fuc). HRMS (ESI) calc. for $C_{25}H_{47}N_2O_{15}$, $[M+H]^+$ 615.2971; found: 615.2974.

5-Amino-pentyl α-L-fucopyranosyl-(1→2)-β-D-galactopyranosyl-(1→4)-2-*N*-acetyl-2-deoxy-3-*O*-(α-L-fucopyranosyl)-β-D-glucopyranosyl-(1→3)-β-D-galactopyranoside (2.52)

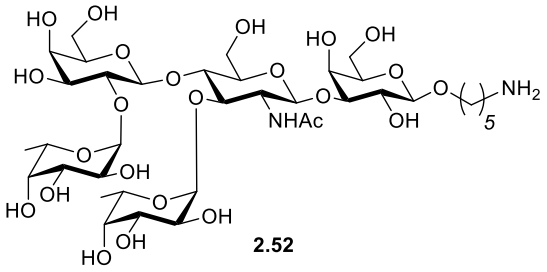

2.52

Compound **2.36** (14.4 mg, 6.10 µmol) was subjected to hydrogenolysis (see above *global deprotection* method). After RP-HPLC purification, conjugation-ready compound **2.52** was isolated as its formate salt (35%, 2.0 mg). ^{1}H NMR (700 MHz, D_2O) δ 8.46 (s, 1H, *H*COO$^-$), 5.29 (d, *J* = 3.8 Hz, 1H, **H-1** Fuc), 5.12 (d, *J* = 4.0 Hz, 1H, **H-1** Fuc), 4.88 (q, *J* = 7.1 Hz, 1H, H-5 Fuc), 4.73 (d, *J* = 9.0 Hz, 1H, **H-1**), 4.52 (d, *J* = 7.8 Hz, 1H, **H-1**), 4.39 (d, *J* = 8.0 Hz, 1H, **H-1**), 4.26 (q, *J* = 6.6 Hz, 1H, H-5 Fuc), 4.17 – 4.13 (m, 1H), 4.01 (d, *J* = 10.3 Hz, 1H), 3.96 – 3.91 (m, 4H), 3.88 – 3.65 (m, 17H), 3.63 – 3.58 (m, 1H), 3.57 – 3.53 (m, 1H), 3.46 (dd, *J* = 9.7, 5.0 Hz, 1H), 3.01 (t, *J* = 7.5 Hz, 2H, C*H*$_2$-NH_3^+), 2.03 (s, 3H, CH_3 NHAc), 1.74 – 1.64 (m, 4H, 2 x CH_2 pentane), 1.47 (p, *J* = 7.7 Hz, 2H, CH_2 pentane), 1.27 (d, *J* = 6.6 Hz, 3H, CH_3 Fuc), 1.24 (d, *J* = 6.6 Hz, 3H, CH_3 Fuc). ^{13}C NMR (176 MHz, D_2O) δ 174.8 (C=O NHAc), 171.0 (H*C*OO$^-$), 102.8 (**C-1**, $J_{C\text{-}H}$ = 161 Hz), 102.4 (**C-1**, $J_{C\text{-}H}$ = 163 Hz), 100.2 (**C-1**, $J_{C\text{-}H}$ = 166 Hz), 99.5 (**C-1**, $J_{C\text{-}H}$ = 178 Hz), 98.6 (**C-1**, $J_{C\text{-}H}$ = 176 Hz), 82.5, 76.4, 75.4, 74.9, 74.7, 74.6, 73.6, 73.1, 71.9, 71.7, 70.0, 69.8, 69.2, 68.8, 68.29, 68.26, 67.7, 66.9, 66.8, 62.5, 61.5, 60.9, 59.8, 56.2, 39.4 (*C*H_2-NH_3^+), 28.2 (CH_2 pentane), 26.4 (CH_2 pentane), 22.3 (CH_3 NHAc), 22.1 (CH_2 pentane), 15.46 (CH_3 Fuc), 15.45 (CH_3 Fuc). HRMS (ESI) calc. for $C_{37}H_{67}N_2O_{24}$, $[M+H]^+$ 923.4078; found: 923.4081.

5-Amino-pentyl β-D-galactopyranosyl-(1→4)-2-*N*-acetyl-2-deoxy-β-D-glucopyranosyl-(1→3)-β-D-galactopyranosyl-(1→4)-β-D-glucopyranoside (2.53)[48]

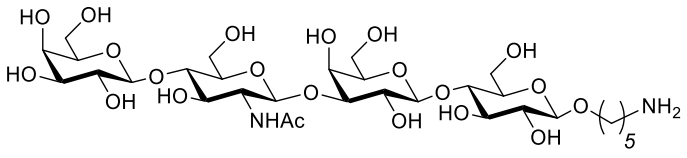

2.53

Compound **2.42** (9.40 mg, 4.76 µmol) was subjected to hydrogenolysis (see above *global deprotection* method). After RP-HPLC purification, conjugation-ready compound **2.53** was

isolated as its formate salt (32%, 1.3 mg). ^{1}H NMR (400 MHz, D_2O) δ 8.40 (s, 1H, *H*COO$^-$), 4.65 (d, *J* = 8.2 Hz, 1H), 4.46 – 4.40 (m, 2H), 4.39 (d, *J* = 7.8 Hz, 1H), 4.11 (d, *J* = 3.2 Hz, 1H), 3.99 – 3.86 (m, 4H), 3.83 – 3.45 (m, 20H), 3.25 (t, *J* = 8.4 Hz, 1H), 2.96 (t, *J* = 7.5 Hz, 2H), 1.99 (s, 3H), 1.71 – 1.57 (m, 4H), 1.41 (p, *J* = 7.8, 7.3 Hz, 2H). ^{13}C NMR (151 MHz, D_2O) δ 174.8, 171.0 (C=O NHAc, H*C*OO$^-$), 102.9, 102.8, 102.7, 101.9 (4 x **C-1**), 82.0, 78.4, 78.1, 75.3, 74.8, 74.7, 74.5, 74.4, 72.7, 72.4, 72.1, 70.9, 70.1, 61.0, 60.9, 55.1, 39.3, 28.1, 26.3, 22.1, 22.0. HRMS (ESI) calc. for $C_{31}H_{57}N_2O_{21}$, $[M+H]^+$ 793.3448; found: 793.3460.

5-Amino-pentyl α-L-fucopyranosyl-(1→2)-β-D-galactopyranosyl-(1→4)-2-*N*-acetyl-2-deoxy-β-D-glucopyranosyl-(1→3)-β-D-galactopyranosyl-(1→4)-β-D-glucopyranoside (2.54)

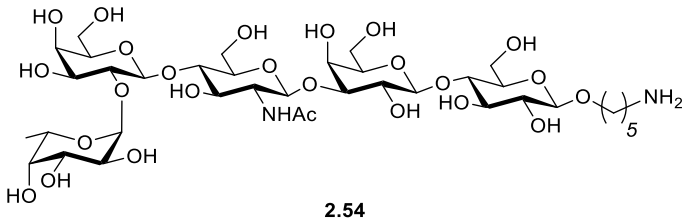

2.54

Compound **2.38** (13.0 mg, 5.40 µmol) was subjected to hydrogenolysis (see above *global deprotection* method). After RP-HPLC purification, conjugation-ready compound **2.54** was isolated as its formate salt (22%, 1.2 mg). ^{1}H NMR (700 MHz, D_2O) δ 8.46 (s, 1H, *H*COO$^-$), 5.33 – 5.31 (d, *J* = 1.4 Hz, 1H, **H-1** Fuc), 4.71 (d, *J* = 8.3 Hz, 1H, **H-1**), 4.56 (d, *J* = 7.7 Hz, 1H, **H-1**), 4.49 (d, *J* = 8.0 Hz, 1H, **H-1**), 4.45 (d, *J* = 7.8 Hz, 1H, **H-1**), 4.23 (q, *J* = 6.5 Hz, 1H), 4.15 (s, 1H), 4.00 – 3.93 (m, 4H), 3.91 – 3.86 (m, 2H), 3.85 – 3.57 (m, 20H), 3.50 – 3.45 (m, 1H), 3.31 (t, *J* = 8.2 Hz, 1H), 3.02 (t, *J* = 7.5 Hz, 2H, C*H*$_2$-NH_3^+), 2.05 (s, 3H, C*H*$_3$ NHAc), 1.74 – 1.65 (m, 4H, 2 x CH_2 pentane), 1.47 (p, *J* = 7.7 Hz, 2H, CH_2 pentane), 1.24 (d, *J* = 6.5 Hz, 3H, CH_3 Fuc). ^{13}C NMR (176 MHz, D_2O) δ 174.9 (C=O NHAc), 171.0 (H*C*OO$^-$), 102.9 (**C-1**, $J_{C\text{-}H}$ = 160 Hz), 102.8 (**C-1**, $J_{C\text{-}H}$ = 162 Hz), 102.0 (**C-1**, $J_{C\text{-}H}$ = 159 Hz), 100.3 (**C-1**, $J_{C\text{-}H}$ = 167 Hz), 99.4 (**C-1**, $J_{C\text{-}H}$ = 177 Hz), 82.0, 78.4, 76.5, 75.9, 75.3, 75.1, 74.9, 74.8, 74.5, 73.5, 72.8, 72.1, 71.7, 70.1, 70.0, 69.6, 69.1, 68.3, 68.2, 67.0, 61.1, 60.9, 60.1, 60.0, 55.4, 39.4 (*C*H_2-NH_3^+), 28.2 (*C*H_2 pentane), 26.4 (*C*H_2 pentane), 22.2 (*C*H_3 NHAc), 22.1 (*C*H_2 pentane), 15.3 (*C*H_3 Fuc). HRMS (ESI) calc. for $C_{37}H_{67}N_2O_{25}$, 939.4027; found: 939.4030.

5-Amino-pentyl β-D-galactopyranosyl-(1→4)-2-*N*-acetyl-2-deoxy-3-*O*-(α-L-fucopyranosyl)-β-D-glucopyranosyl-(1→3)-β-D-galactopyranosyl-(1→4)-β-D-glucopyranoside (2.55)

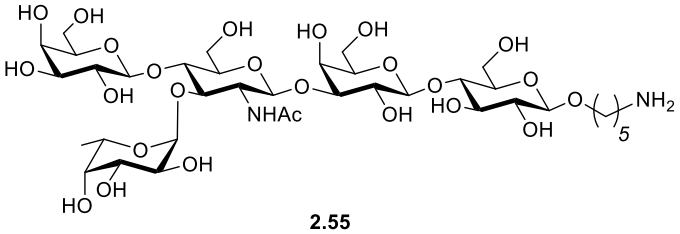

2.55

Compound **2.39** (28.3 mg, 11.8 µmol) was subjected to methanolysis followed by hydrogenolysis (see above *global deprotection* method). After RP-HPLC purification, conjugation-ready compound **2.55** was isolated as its formate salt (35%, 4.21 mg). ^{1}H NMR (600 MHz, D_2O) δ 8.47 (s, 1H, *H*COO$^-$), 5.14 (d, *J* = 4.1 Hz, 1H, **H-1**), 4.85 (dd, *J* = 6.8 Hz, 1H, H-5 Fuc), 4.73 (d, *J* = 8.6 Hz, 1H, **H-1**), 4.52 – 4.43 (m, 3H, 3x **H-1**), 4.17 (d, *J* = 3.3 Hz, 1H), 4.01 – 3.86 (m, 9H), 3.82 – 3.69 (m, 10H), 3.69 – 3.58 (m, 7H), 3.51 (dd, *J* = 9.8, 7.9 Hz, 1H), 3.32 (t, *J* = 8.6 Hz, 1H), 3.05 – 3.01 (m, 2H, C*H*$_2$-NH_3^+), 2.04 (s, 3H, C*H*$_3$ NHAc), 1.75 – 1.66 (m, 4H, 2x CH_2 pentane), 1.47 (p, *J* = 7.7 Hz, 2H, CH_2 pentane), 1.19 (d, J = 6.6 Hz, 3H, CH_3 Fuc). ^{13}C NMR (151 MHz, D_2O) δ 174.6 (C=O NHAc), 171.0 (H*C*OO$^-$), 102.9 (**C-1**, $J_{C\text{-}H}$ = 167 Hz), 102.5 (**C-1**, $J_{C\text{-}H}$ = 165 Hz), 101.9 (**C-1**, $J_{C\text{-}H}$ = 164 Hz), 101.7 (**C-1**, $J_{C\text{-}H}$ = 164 Hz), 98.5 (**C-1**, $J_{C\text{-}H}$ = 173 Hz), 82.0, 78.3, 75.1, 74.9, 74.8, 74.71, 74.67, 74.4, 73.0, 72.7, 72.4, 71.8, 71.0, 70.0, 69.9, 69.1, 68.3, 68.2, 67.6, 66.6 (C-5 Fuc), 61.4, 60.9, 60.0, 59.6, 55.9, 39.3 (*C*H_2-NH_3^+), 28.1 (*C*H_2 pentane), 26.3 (*C*H_2 pentane), 22.2 (*C*H_3 NHAc), 22.0 (*C*H_2 pentane), 15.2 (*C*H_3 Fuc). HRMS (ESI) calc. for $C_{37}H_{67}N_2O_{25}$, 939.4027; found: 939.4024.

5-Amino-pentyl α-L-fucopyranosyl-(1→2)-β-D-galactopyranosyl-(1→4)-2-*N*-acetyl-2-deoxy-3-*O*-(α-L-fucopyranosyl)-β-D-glucopyranosyl-(1→3)-β-D-galactopyranosyl-(1→4)-β-D-glucopyranoside (2.56)

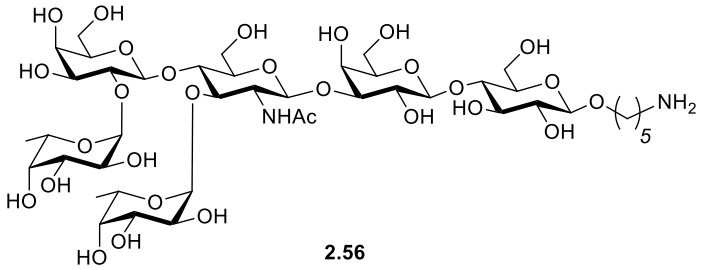

2.56

Compound **2.40** (31.7 mg, 11.3 µmol) was subjected to methanolysis followed by hydrogenolysis (see above *global deprotection* method). After RP-HPLC purification,

conjugation-ready compound **2.55** was isolated as its formate salt (17%, 2.2 mg). ^{1}H NMR (600 MHz, D_2O) δ 8.48 (s, 1H, *H*COO$^-$), 5.29 (d, *J* = 3.4 Hz, 1H, **H-1** Fuc), 5.13 (d, *J* = 4.1 Hz, 1H, **H-1** Fuc), 4.89 (q, *J* = 6.8 Hz, 1H, H-5 Fuc), 4.73 (d, *J* = 8.4 Hz, 1H, **H-1**), 4.53 (d, *J* = 7.8 Hz, 1H, **H-1**), 4.50 (d, *J* = 8.0 Hz, 1H, **H-1**), 4.45 (d, *J* = 7.9 Hz, 1H, **H-1**), 4.27 (q, *J* = 6.7 Hz, 1H, H-5 Fuc), 4.16 (d, *J* = 3.2 Hz, 1H), 4.03 – 3.57 (m, 29H), 3.47 (dd, *J* = 9.2, 4.2 Hz, 1H), 3.32 (t, *J* = 8.5 Hz, 1H), 3.02 (t, *J* = 7.5 Hz, 2H, C*H*$_2$-NH$_3^+$), 2.04 (s, 3H, C*H*$_3$ NHAc), 1.75 – 1.65 (m, 4H, 2 x C*H*$_2$ pentane), 1.47 (p, *J* = 7.7 Hz, 2H, C*H*$_2$ pentane), 1.28 (d, *J* = 6.6 Hz, 3H, CH_3 Fuc), 1.25 (d, *J* = 6.6 Hz, 3H, CH_3 Fuc). ^{13}C NMR (151 MHz, D_2O) δ 174.6 (C=O NHAc), 170.9 (H*C*OO$^-$), 102.9 (**C-1**, $J_{C\text{-}H}$ = 166 Hz), 102.4 (**C-1**, $J_{C\text{-}H}$ = 168 Hz), 101.9 (**C-1**, $J_{C\text{-}H}$ = 163 Hz), 100.1 (**C-1**, $J_{C\text{-}H}$ = 166 Hz), 99.4 (**C-1**, $J_{C\text{-}H}$ = 175 Hz), 98.5 (**C-1**, $J_{C\text{-}H}$ = 173 Hz), 82.0, 78.3, 76.3, 75.3, 74.79, 74.71, 74.68, 74.4, 73.5, 73.0, 72.7, 71.9, 71.6, 70.01, 69.91, 69.7, 69.1, 68.7, 68.2, 67.6, 66.9 (C-5 Fuc), 66.7 (C-5 Fuc), 61.4, 60.9, 60.0, 59.7, 56.1, 39.3 (*C*H_2-NH$_3^+$), 28.1 (*C*H_2 pentane), 26.3 (*C*H_2 pentane), 22.2 (*C*H_3 NHAc), 22.0 (*C*H_2 pentane), 15.39 (*C*H_3 Fuc), 15.37 (*C*H_3 Fuc). HRMS (ESI) calc. for $C_{43}H_{77}N_2O_{29}$, $[M+H]^+$ 1085.4607; found: 1085.4613.

5-Amino-pentyl α-L-fucopyranosyl-(1→2)-β-D-galactopyranosyl-(1→3)-*N*-acetyl-2-deoxy-4-*O*-(α-L-fucopyranosyl)-β-D-glucosaminopyranosyl-(1→3)-β-D-galactopyranosyl-(1→4)-β-D-glucopryanoside (2.57)

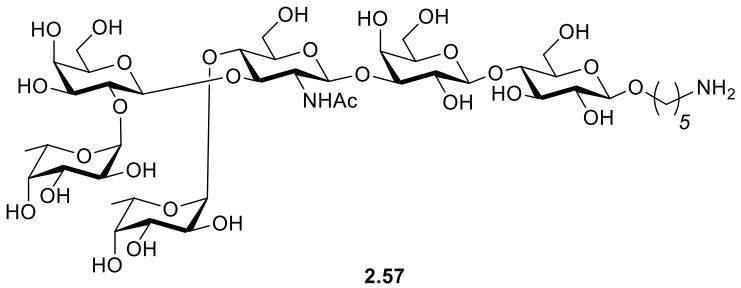

2.57

Compound **2.47** (13.7 mg, 4.87 μmol) was subjected to methanolysis followed by hydrogenolysis (see above *global deprotection* method). After RP-HPLC purification, conjugation-ready compound **2.57** was isolated as its formate salt (28%, 1.5 mg). ^{1}H NMR (600 MHz, D_2O) δ 8.47 (s, 1H, *H*COO$^-$), 5.17 (d, *J* = 4.0 Hz, 1H, **H-1**), 5.04 (d, *J* = 3.9 Hz, 1H, **H-1**), 4.88 (q, *J* = 6.7 Hz, 1H, H-5 Fuc), 4.67 (d, *J* = 7.7 Hz, 1H, **H-1**), 4.62 (d, *J* = 8.4 Hz, 1H, **H-1**), 4.50 (d, *J* = 8.0 Hz, 1H, **H-1**), 4.43 (d, *J* = 7.9 Hz, 1H, **H-1**), 4.36 (q, *J* = 6.7 Hz, 1H, H-5 Fuc), 4.17 – 4.12 (m, 2H), 4.01 – 3.52 (m, 29H), 3.32 (t, *J* = 8.4 Hz, 1H), 3.03 – 2.98 (m, 2H, C*H*$_2$-NH$_3^+$), 2.08 (s, 3H, C*H*$_3$ NHAc), 1.75 – 1.65 (m, 4H, 2x C*H*$_2$ pentane), 1.47 (p, *J* = 7.7 Hz, 2H, C*H*$_2$ pentane), 1.31 – 1.26 (m, 6H, 2x CH_3 Fuc). ^{13}C NMR (151 MHz, D_2O) δ 174.1, 170.9

(H*C*OO$^-$, C=O NHAc), 103.2 (**C-1**, $J_{C\text{-}H}$ = 167 Hz), 102.9 (**C-1**, $J_{C\text{-}H}$ = 164 Hz), 101.9 (**C-1**, $J_{C\text{-}H}$ = 161 Hz), 100.6 (**C-1**, $J_{C\text{-}H}$ = 167 Hz), 99.5 (**C-1**, $J_{C\text{-}H}$ = 175 Hz), 97.7 (**C-1**, $J_{C\text{-}H}$ = 172 Hz), 81.5, 78.2, 76.4, 75.1, 74.8, 74.7, 74.41, 74.35, 73.6, 72.7, 71.9, 71.7, 70.1, 70.0, 69.4, 69.0, 68.7, 68.5, 68.2, 67.7, 67.0 (C-5 Fuc), 66.2 (C-5 Fuc), 61.5, 60.9, 60.0, 59.4, 55.7, 39.3 (*C*H$_2$-NH$_3^+$), 28.1 (*C*H$_2$ pentane), 26.4 (*C*H$_2$ pentane), 22.1 (*C*H$_3$ NHAc), 22.0 (*C*H$_2$ pentane), 15.29 (*C*H$_3$ Fuc), 15.24 (*C*H$_3$ Fuc). HRMS (ESI) calc. for $C_{43}H_{77}N_2O_{29}$, $[M+H]^+$ 1085.4607; found: 1085.4615.

5-Amino-pentyl β-D-galactopyranosyl-(1→3)-*N*-acetyl-2-deoxy-4-*O*-(α-L-fucopyranosyl)-β-D-glucosaminopyranosyl-(1→3)-β-D-galactopyranosyl-(1→4)-β-D-glucopryanoside (2.58)

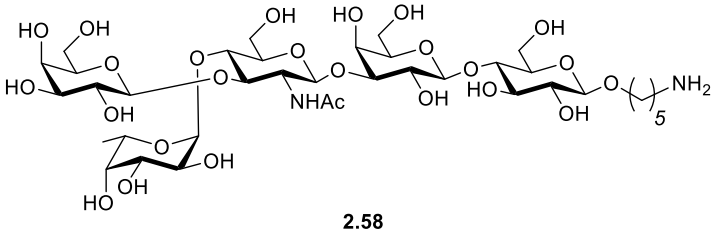

2.58

Compound **2.48** (22.7 mg, 9.50 µmol) was subjected to methanolysis followed by hydrogenolysis (see above *global deprotection* method). After RP-HPLC purification, conjugation-ready compound **2.58** was isolated as its formate salt (23%, 2.2 mg). ^{1}H NMR (600 MHz, D$_2$O) δ 8.47 (s, 1H, *H*COO$^-$), 5.05 (d, *J* = 3.9 Hz, 1H, **H-1**), 4.90 (q, *J* = 7.4 Hz, 1H, H-5 Fuc), 4.72 (d, *J* = 8.7 Hz, 1H, **H-1**), 4.55 – 4.49 (m, 2H, 2x **H-1**), 4.46 (d, *J* = 7.8 Hz, 1H, **H-1**), 4.18 (d, *J* = 2.8 Hz, 1H), 4.10 (t, *J* = 9.7 Hz, 1H), 4.02 – 3.93 (m, 4H), 3.93 – 3.86 (m, 3H), 3.85 – 3.70 (m, 11H), 3.68 – 3.54 (m, 7H), 3.54 – 3.49 (m, 1H), 3.33 (t, *J* = 8.5 Hz, 1H), 3.03 (t, *J* = 7.5 Hz, 2H, C*H*$_2$-NH$_3^+$), 2.06 (s, 3H, C*H*$_3$ NHAc), 1.78 – 1.64 (m, 4H, 2 x C*H*$_2$ pentane), 1.48 (p, *J* = 7.8 Hz, 2H, C*H*$_2$ pentane), 1.20 (d, *J* = 6.6 Hz, 3H, CH$_3$ Fuc). ^{13}C NMR (151 MHz, D$_2$O) δ 174.7, 171.0 (H*C*OO$^-$, C=O NHAc), 102.9 (**C-1**, $J_{C\text{-}H}$ = 163 Hz), 102.8 (**C-1**, $J_{C\text{-}H}$ = 163 Hz), 102.5 (**C-1**, $J_{C\text{-}H}$ = 163 Hz), 101.9 (**C-1**, $J_{C\text{-}H}$ = 165 Hz), 98.0 (**C-1**, $J_{C\text{-}H}$ = 172 Hz), 82.0, 78.4, 75.8, 75.2, 74.82, 74.76, 74.71, 74.4, 72.7, 72.3, 72.1, 71.9, 70.4, 70.0, 69.9, 69.1, 68.28, 68.21, 67.7, 66.8, 61.6, 60.9, 60.0, 59.6, 55.8, 39.3 (*C*H$_2$-NH$_3^+$), 28.1 (*C*H$_2$ pentane), 26.4 (*C*H$_2$ pentane), 22.2 (*C*H$_3$ NHAc), 22.0 (*C*H$_2$ pentane), 15.3 (*C*H$_3$ Fuc). HRMS (ESI) calc. for $C_{37}H_{67}N_2O_{25}$, $[M+H]^+$ 939.4027; found: 939.4044.

Global Deprotection: Birch Deprotection - Methanolysis

AGA-synthesized, protected oligosaccharide was dissolved in anhydrous THF (0.55 mL) and *t*-BuOH (0.1 mL). The solution was added to a three-necked flask containing a dark-blue

solution of sodium (30.0 mg, 1.30 mmol) in liquid ammonia (20.0 mL), under argon at -78 °C. The dark-blue mixture was stirred at -78 °C for 50 min. Then MeOH (4.00 mL) was added dropwise until the solution became colorless. The mixture was concentrated with a stream of argon, allowed to warm up to room temperature and stirred overnight. Then AcOH was added dropwise to neutralize the solution. The solvent was evaporated and the crude reaction mixture was purified through a Sephadex G-25 size-exclusion column using water as eluent. Subsequent reverse phase chromatography using a Chromabond® SPE catridge (MeOH in water 1 to 10%) afforded deprotected, conjugation-ready oligosaccharide as its acetate salt.

Experimental Data for Deprotected Oligosaccharides 2.11, 2.59, 2.60

5-Amino-pentyl β-D-galactopyranosyl-(1→4)-β-D-glucosaminopyranosyl-(1→3)-β-D-galactopyranosyl-(1→4)-β-D-glucosaminopyranosyl-(1→3)-β-D-galactopyranosyl-(1→4)- β-D-glucopyranoside (2.59)[79]

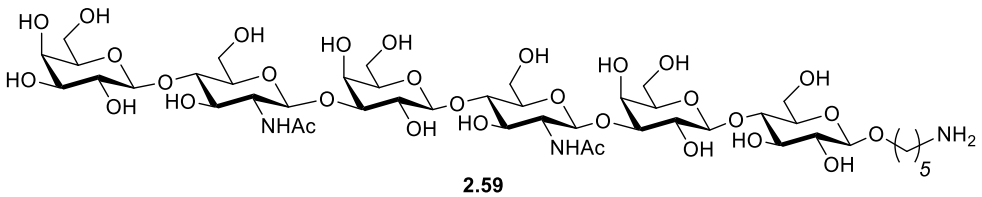

2.59

Protected nLc$_6$ **2.35** (17.5 mg, 6.2 µmol) was deprotected following the experimental procedure for *Birch reduction and methanolysis* (see above). After RP-HPLC purification, conjugation-ready compound **2.59** was isolated as its formate salt (0.7 mg, 9%). ^{1}H NMR (600 MHz, D_2O) δ 8.47 (s, 1H, *H*COO$^-$), 4.74 – 4.70 (m, 2H, 2 x **H-1**), 4.52 – 4.43 (m, 4H, 4 x **H-1**), 4.17 (m, 2H), 4.02 – 3.92 (m, 5H), 3.89 – 3.53 (m, 30H), 3.35 – 3.28 (m, 1H), 3.02 (t, *J* = 7.5 Hz, 2H) 2.05 (s, 6H), 1.75-1.64 (m, 4H), 1.47 (p, *J* = 7.7 Hz, 2H). ^{13}C NMR (151 MHz, D_2O) δ 174.8, 171.0 (H*C*OO$^-$, 2 x C=O NHAc), 102.9, 102.83, 102.80, 102.68, 102.66, 101.9 (6 x **C-1**), 82.02, 82.00, 78.4, 78.1, 75.3, 74.8, 74.7, 74.5, 74.4, 72.7, 72.5, 72.1, 70.9, 70.0, 69.9, 68.5, 68.2, 61.0, 60.88, 60.85, 59.8, 55.13, 55.09, 39.3, 28.1, 26.3, 22.1, 22.0. HRMS (ESI) calc. for $C_{45}H_{80}N_3O_{31}$, $[M+H]^+$ 1158.4770; found: 1158.4767.

5-Amino-pentyl β-D-galactopyranosyl-(1→4)-3-*O*-(α-L-fucopyranosyl)-β-D-glucosaminopyranosyl-(1→3)-β-D-galactopyranosyl-(1→4)-3-*O*-(α-L-fucopyranosyl)-β-D-glucosaminopyranosyl-(1→3)-β-D-galactopyranosyl-(1→4)- β-D-glucopyranoside (2.60)

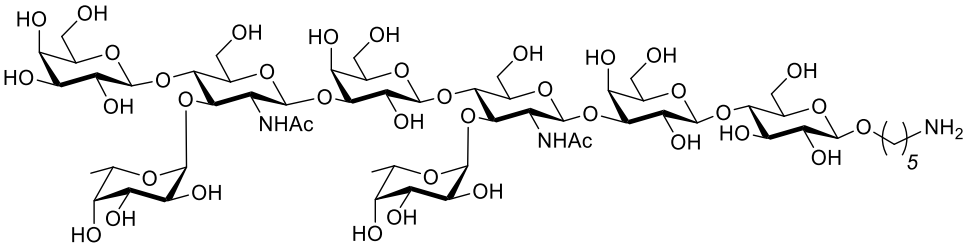

2.60

Protected Le^x-dimer **2.43** (35.1 mg, 9.6 µmol) was deprotected following the experimental procedure for *Birch deprotection and methanolysis* (see above). Purification using size-exclusion followed by reverse-phase chromatography afforded the acetate salt of Le^x-dimer **2.60** (1.83 mg, 13%). ^{1}H NMR (700 MHz, D_2O) δ 5.14 (d, *J* = 4.0 Hz, 1H, **H-1** Fuc), 5.12 (d, *J* = 4.0 Hz, 1H, **H-1** Fuc), 4.87 – 4.81 (m, 2H, 2 x H-5 Fuc), 4.74 – 4.69 (m, 1H, **H-1**), 4.50 – 4.42 (m, 5H, 5 x **H-1**), 4.16 (d, *J* = 3.1 Hz, 1H), 4.11 (d, *J* = 3.0 Hz, 1H), 4.00 – 3.94 (m, 7H), 3.93 – 3.86 (m, 7H), 3.81 – 3.77 (m, 4H), 3.76 – 3.68 (m, 10H), 3.67 – 3.63 (m, 3H), 3.62 – 3.57 (m, 6H), 3.54 – 3.48 (m, 2H), 3.31 (t, *J* = 8.5 Hz, 1H), 3.02 (d, *J* = 7.7 Hz, 2H, C*H*$_2$NH$_3^+$), 2.03 (m, 6H, 2 x CH_3 NHAc), 1.92 (s, 3H, CH_3 AcO^-), 1.73 – 1.65 (m, 4H, 2 x CH_2 pentane), 1.47 (p, *J* = 7.7 Hz, 2H, CH_2 pentane), 1.18 (d, *J* = 6.6 Hz, 3H, CH_3 Fuc), 1.16 (d, *J* = 6.6 Hz, 3H, CH_3 Fuc). ^{13}C NMR (176 MHz, D_2O) δ 181.5 (C=O AcO^-), 174.71 (C=O NHAc), 174.65 (C=O NHAc), 103.0 (2 x **C-1**, J_{C-H} = 164 Hz), 102.5 (**C-1**, J_{C-H} = 164 Hz), 102.0 (2 x **C-1**, J_{C-H} = 163 Hz), 101.8 (**C-1**, J_{C-H} = 162 Hz), 98.7 (**C-1**, J_{C-H} = 174 Hz), 98.6 (**C-1**, J_{C-H} = 174 Hz), 82.1, 81.7, 78.4, 75.13, 75.09, 74.92, 74.88, 74.8, 74.5, 73.1, 72.8, 72.5, 71.92, 71.86, 71.1, 70.5, 70.08, 69.95, 69.20, 69.19, 68.4, 68.28, 68.23, 67.72, 67.66, 66.7, 61.51, 61.46, 61.0, 60.1, 59.6, 55.99, 55.97, 39.4 (*C*H_2-NH_3^+), 28.2 (CH_2 pentane), 26.4 (CH_2 pentane), 23.3 (CH_3 AcO^-), 22.3 (CH_3 NHAc), 22.1 (2C, CH_3 NHAc, CH_2 pentane), 15.3 (2 x CH_3 Fuc). HRMS (ESI) calc. for $C_{57}H_{100}N_3O_{39}$, $[M+H]^+$ 1450.5928; found: 1450.5925.

5-Amino-pentyl α-L-fucopyranosyl-(1→2)-β-D-galactopyranosyl-(1→4)-3-*O*-(α-L-fucopyranosyl)-β-D-glucosaminopyranosyl-(1→3)-β-D-galactopyranosyl-(1→4)-3-*O*-(α-L-fucopyranosyl)-β-D-glucosaminopyranosyl-(1→3)-β-D-galactopyranosyl-(1→4)-β-D-glucopyranoside (2.11)

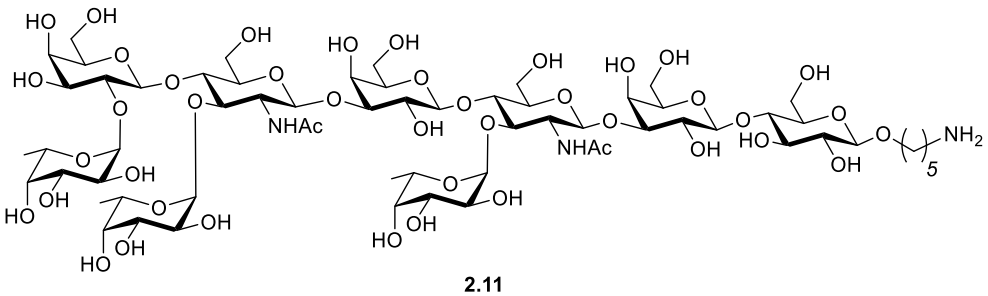

2.11

Protected KH-1 **2.44** (56.0 mg, 13.7 µmol) was deprotected following the experimental procedure for *Birch deprotection and methanolysis* (see above). Purification using size-exclusion followed by reverse-phase chromatography afforded the acetate salt of KH-1 antigen **2.11** (4.33 mg, 19%). ^{1}H NMR (700 MHz, D_2O) δ 5.28 (d, *J* = 2.9 Hz, 1H, **H-1α**), 5.15 – 5.11 (m, 2H, 2 x **H-1α**), 4.89 (q, *J* = 7.3, 6.9 Hz, 1H, H-5 Fuc), 4.84 – 4.81 (m, 1H, H-5 Fuc), 4.73 – 4.70 (m, 2H, 2 x **H-1**), 4.54 – 4.51 (d, *J* = 7.6 Hz,1H, **H-1**), 4.49 (d, *J* = 8.0 Hz, 1H, **H-1**), 4.47 – 4.42 (m, 2H, 2 x **H-1**), 4.26 (q, *J* = 6.4 Hz, 1H, H-5 Fuc), 4.16 (d, *J* = 2.9 Hz, 1H), 4.10 (d, *J* = 2.9 Hz, 1H), 4.01 – 3.57 (m, 42H), 3.52 (d, *J* = 8.8 Hz, 1H), 3.47 – 3.44 (m, 1H), 3.31 (t, *J* = 8.3 Hz, 1H), 3.00 (d, *J* = 7.5 Hz, 2H, C*H*$_2$NH$_3^+$), 2.03 (s, 6H, 2 x NHC(O)OC*H*$_3$), 1.92 (s, 3H, C*H*$_3$C(O)O$^-$), 1.73 – 1.65 (m, 4H, 2 x CH_2 pentane), 1.47 (p, *J* = 7.7 Hz, 2H, CH_2 pentane), 1.27 (d, *J* = 6.5 Hz, 3H, CH_3 Fuc), 1.25 (d, *J* = 6.5 Hz, 3H, CH_3 Fuc), 1.16 (d, *J* = 6.5 Hz, 3H, CH_3 Fuc). ^{13}C NMR (176 MHz, D_2O) δ 181.5 (C=O AcO$^-$), 174.71 (C=O NHAc), 174.66 (C=O NHAc), 103.0 (**C-1**, $J_{C\text{-}H}$ = 164 Hz), 102.5 (**C-1**, $J_{C\text{-}H}$ = 166 Hz), 102.4 (**C-1**, $J_{C\text{-}H}$ = 166 Hz), 102.0 (**C-1**, $J_{C\text{-}H}$ = 166 Hz), 101.7 (**C-1**, $J_{C\text{-}H}$ = 165 Hz), 100.2 (**C-1**, $J_{C\text{-}H}$ = 166 Hz), 99.4 (**C-1** Fuc, $J_{C\text{-}H}$ = 174 Hz), 98.7 (**C-1** Fuc, $J_{C\text{-}H}$ = 173 Hz), 98.6 (**C-1** Fuc, $J_{C\text{-}H}$ = 173 Hz), 82.1, 81.6, 78.4, 76.4, 75.3, 75.1, 74.9, 74.78, 74.74, 74.46, 74.43, 73.6, 73.0, 72.8, 72.0, 71.9, 71.7, 70.6, 70.1, 70.0, 69.7, 69.2, 68.8, 68.28, 68.21, 67.71, 67.65, 67.0, 66.8, 66.7, 61.5, 61.4, 61.0, 60.1, 59.8, 59.7, 56.1, 56.0, 48.9, 39.4 (*C*H_2-NH_3^+), 28.2 (CH_2 pentane), 26.7 (CH_2 pentane), 23.3 (CH_3 AcO$^-$), 22.3 (2 x CH_3 NHAc), 22.1 (CH_2 pentane), 15.5 (CH_3 Fuc), 15.4 (CH_3 Fuc), 15.3 (CH_3 Fuc). HRMS (ESI) calc. for $C_{63}H_{110}N_3O_{43}$, $[M+H]^+$ 1596.6508; found: 1596.6504.

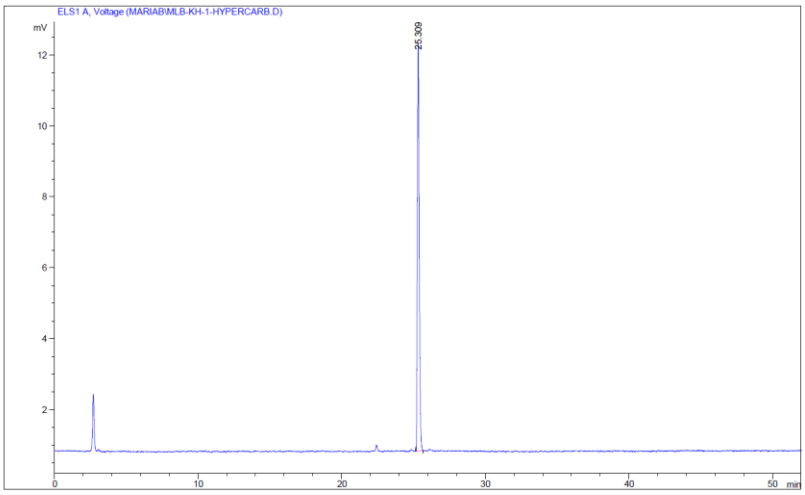

RP-HPLC of final product **2.11** (detection: ELSD).

2.5.5 Conjugation

In a vial, oligosaccharide **2.11** (0.94 mg, 0.57 µmol) was dissolved in DMSO (200 µL), and pyridine (25 µL) and TEA (10 µL) TEA were added. A solution of adipate p-nitrophenyl (PNP) diester in DMSO (2.2 mg, 100 µL) was added. After mixing for 3 h with magnetic stirring, the stirring bar was removed and the reaction mixture was freeze-dried and kept overnight in a lyophilizer. The concentrate was washed with $CHCl_3$ (5 x 1 mL) and DCM (3 x 1 mL). TLC analysis was used to confirm absence of excess linker (60:40 Hex:EtOAc).

Protein CRM_{197} (90 µL, 0.5 mg) was washed using a centrifugal filter (Amicon 10kDa filter, Merck Milipore, prewashed with water). The Eppedorf tube containing the protein solution was washed with water (300 µL) and transferred to the filter, and then centrifuged (10000 rpm, 8 min). The washing was repeated with water (350 µL) and 0.1 M phosphate buffer pH 8 (350 µL), and the sample was concentrated. The filtrate (~70 µL) was transferred to the vial containing the oligosaccharide PNP ester, stirred slowly for 24 h, transferred to a centrifugal filter, washed with the phosphate buffer (300 µL) and water (3 x 400 µL). A sample (10 µL) was taken for MALDI analysis. The remaining mixture was washed with phosphate-buffered saline (PBS, 400 µL), the filtrate was centrifuged, and the filtrate was diluted with PBS (150 µL). Carbohydrate loading as determined by MALDI (DHAP Matrix): 12.0 glycans per protein (m/z observed for glycoconjugate: 78549; for protein: 58016; for **2.11**-PNP ester: 1708).

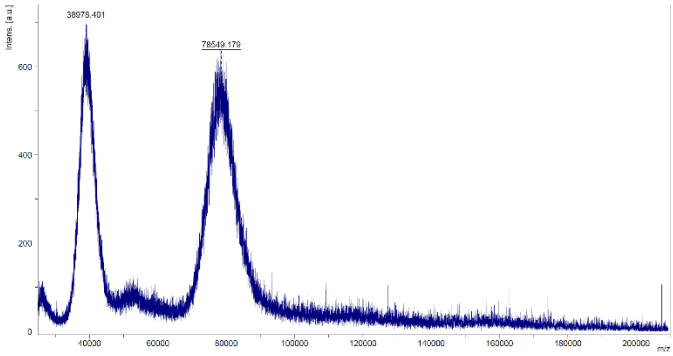

MALDI analysis of the glycoconjugate.

2.5.6 Immunization

Animal experiments were approved by governmental authorities (Landesamt für Arbeitsschutz, Verbraucherschutz und Gesundheit, Abteilung Verbraucherschutz, Land Brandenburg, approval ID 2347-A-30-1-2018 Ä1). Equal volumes of the KH-1-CRM_{197} glycoconjugate solution described above (Section 2.5.5) containing 16 µg of KH-1 and Alhydrogel® 2% (Brenntag) adjuvant were mixed overnight at 4°C. A male alpaca was immunized (subcutaneous injection) seven times (on days 0, 7, 14, 28, 37, 45, 53) over a period of eight weeks. Blood was extracted through the neck vein for isolation of serum and peripheral blood mononuclear cells. The presence of anti-KH-1 antibodies in the serum was verified by glycan array.

2.5.7 Glycan Arrays

Briefly, synthetic oligosaccharides were dissolved in 50 mM sodium phosphate buffer, pH 8.5 (glycan concentration in printing buffer: 0.1 mM) and spotted to epoxy coated glass slides (Epoxy slides; PolyAn) using an S3 robotic non-contact microarray printer. Slides were incubated overnight in a humidified chamber at room temperature, and quenched by treatment with 100 mM ethanolamine and 50 mM sodium phosphate (pH 9.0) for 1 h at room temperature. Slides were washed three times with water, and dried by centrifugation.

Slides were blocked by incubation with 1% bovine serum albumin (BSA) in phosphate buffered saline (PBS) (1% BSA-PBS) for at least 1 h at room temperature. Slides were washed twice with PBS and dried by centrifugation. A 64-well incubation grid (Grace Biolabs) was applied to the slide. Dilutions (1:10 and 1:50) of alpaca sera of each week in 1% BSA-PBS were applied to the wells and incubated for 1 h at room temperature in a humid and dark chamber. Wells were washed three times with PBS containing 0.1% Tween-20 (PBS-T). Rabbit anti-llama IgG FITC (1:100, Novus Biotech) was added to the wells and incubated for 1 h at room temperature in a humid and dark chamber. Wells were washed twice with PBS-T and once

with PBS. The incubation grid was removed and the slideswere rinsed with water and dried by centrifugation. Slides were scanned at 488 nm using a GenePix 4300A microarray scanner (Molecular Devices, Sunnyvale, CA, USA) and evaluated using GenePix Pro 7.2 (Molecular Devices). The photomultiplier tube (PMT) voltage was adjusted such that scans were free of saturation signals.

3 Accessing Galactosamine Building Blocks through Continuos Flow Azidophenyselenylation of Galactal

This chapter has been partly modified from: Guberman, M.; Pieber, P.; Seeberger, P. H. Safe and Scalable Continuous Flow Azidophenylselenylation of Galactal to Prepare Galactosamine Building Blocks, *Org. Process Res. Dev.* **2019,** *23*, 2764-2770.[144] https://doi.org/10.1021/acs.oprd.9b00456. https://pubs.acs.org/doi/10.1021/acs.oprd.9b00456 *Further permissions related to the excerpted material should be directed to the ACS.*

3.1 Introduction

Galactosamine (GalN) is ubiquitous in living organisms. Its *N*-acetyl version, *N*-acetylgalactosamine (GalNAc) is found on the cell surface or extracellular matrix of mammalian glycans that are fundamental for tissue lubrication, protection from mechanical damage and pathogen infections,[2,145,146] or are implicated in inflammatory and immune responses.[147] Increased levels on the mammalian cell surface of certain GalNAc-containing glycans is associated with cancer.[97,148] Additionally, GalNAc is present in the cell-surface glycans of many pathogenic bacteria,[149] *e.g.* in the Vi antigen of *Salmonella typhi*, the etiological agent of typhoid fever, or in the extracellular matrix of fungi such as *Aspergillus fumigatus*, responsible for fatal systemic infections in immunocompromised individuals (Figure 3.1). These structures are associated with pathogen survival, virulence, and host-microorganism interactions.[149–152]

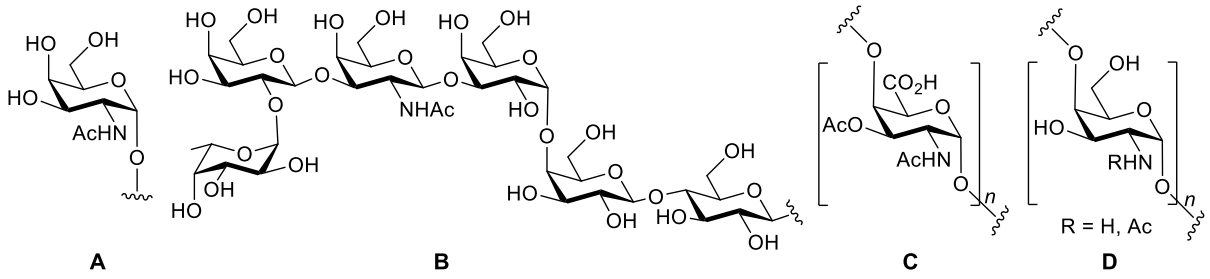

Figure 3.1. Representative structures of GalNAc-containing glycans. a) TACA and mucin core Tn antigen; b) TACA Globo-H; c) repeating unit of the Vi antigen in *Salmonella typhi* capsular polysaccharide; d) poly-GalN/GalNAc rich sequence of galactosaminogalactan in the *Aspergillus fumigatus*.

Synthetic oligosaccharides are required for further investigation of the biological functions of these glycans, as well as the development of new tools for diagnostics, prevention and treatment of related diseases (see Chapter 1). In order to assemble the desired oligosaccharides, suitably protected monosaccharide building blocks are needed. While commercially available glucosamine (GlcN) can be used as starting material for *N*-acetyl glucosamine (GlcNAc) building blocks, the high price of galactosamine limits large scale synthetic applications. Therefore, several strategies to prepare 2-nitrogenated analogues from inexpensive starting materials have been developed.[153–158] Azidophenylselenylation (APS)[159–161] is broadly used as nitrogen transfer reaction during building block synthesis. The APS reaction offers the advantage of introducing two functional groups in one reaction step, affording a selenoglycoside that is stable under a wide range of protecting group manipulations, and can be activated to prepare 1,2-*cis* and 1,2-*trans* glycosides (Scheme 3.1). For the installation of 1,2-*cis* glycosidic linkages, as in the case of glycans containing α-GalNAc, 2-azidoglycosides are used as glycosyl donors;[162] azido reduction is then performed at a late step in the synthetic route. When 1,2-*trans* glycosides are targeted, azido reduction and subsequent protection with a suitable participating group, typically TCA, precede glycosylation.[58]

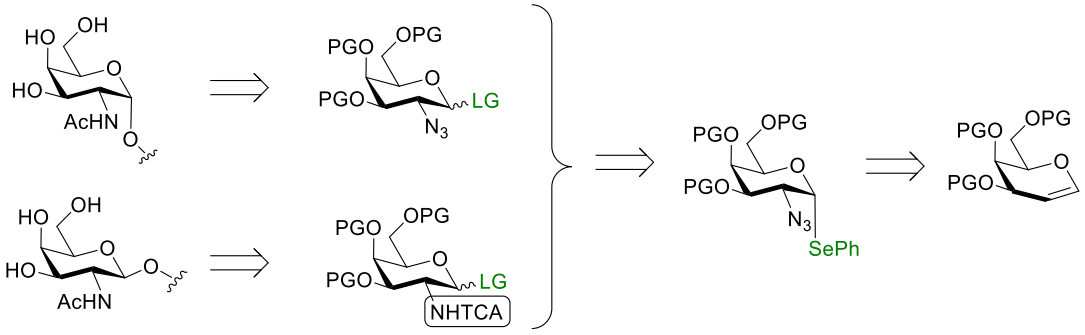

Scheme 3.1. Galactosamine building blocks are obtained via nitrogen transfer to glycals. PG: protecting group; LG: leaving group.

Homogeneous APS reaction uses trimethylsilyl azide ($TMSN_3$) as an azido source and was first introduced by Mironov and coworkers.[159] Lower explosion hazard as well as higher solubility in organic solvents offer advantages in terms of safety and reaction time compared to previous NaN_3 procedures.[158,161,163] While relatively good yields are reported,[159] it is difficult to reproduce this transformation reliably. Yields of 23 homogeneous APS reactions carried out in our department over the past ten years range from 10-65% with an average yield of 35% (Figure 3.2). Additionally, the use of azido compounds, leading to the production of potentially toxic and explosive species (in particular hydrazoic acid), limits reaction scale-up.[164]

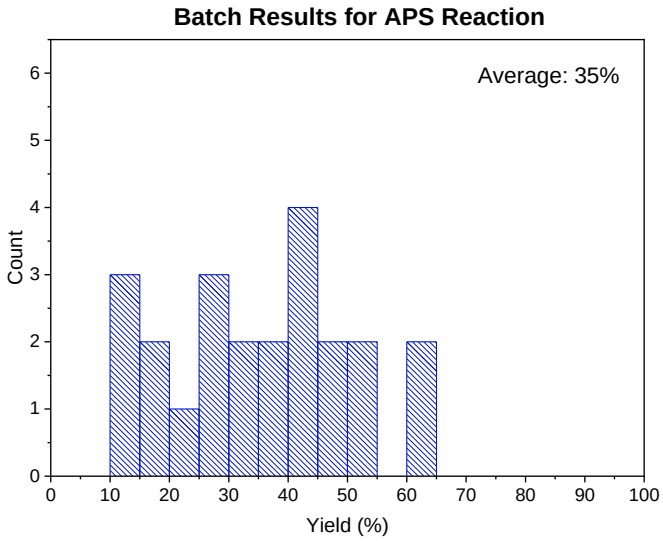

Figure 3.2. Yields obtained for homogeneous APS reaction in batch by PhD students and postdocs at the Max Planck Institute of Colloids and Interfaces.

3.1.1 Project Aim

Poor reactivity and low selectivity are in many occasions the consequence of deficiencies in mixing and temperature control in batch reactions. It was envisioned that these difficulties could be overcome by performing the reaction in continuous flow, due to the reproducible and efficient mixing and heat transfer offered by this technology. In addition, by performing the reaction in flow, the concentration of potentially hazardous side products generated at a given time is kept at minimum levels, facilitating the reaction scale-up.[165–167]

The aim of the project described in this chapter was to develop a safe and reliable APS method to facilitate access to galactosamine building blocks, by establishing a continuous flow procedure for the APS of 3,4,6-tri-*O*-acetyl-D-galactal. The focus was set on the optimization of the reaction in order to maximize yield and selectivity towards the desired product. Improved access to galactosamine is important for the development of AGA methods for effective installation of GalN 1,2-*cis* linkages, which to this date have not been implemented in AGA (Section 1.3).

3.2 Results and Discussion

3.2.1 Experimental Design and Initial Screening

In the common protocol for APS in batch,[159] $TMSN_3$ is added to a solution of 3,4,6-tri-*O*-acetyl-D-galactal **3.1** and Ph_2Se_2 in anhydrous DCM at -30 °C. After the addition of bisacetoxy iodobenzene (BAIB), the reaction mixture is warmed to -10 °C. Reaction times are

variable and typically range from 4 h to 16 h.[58,159] Low temperatures during mixing minimize explosion hazards and avoid high concentrations of azido radicals due to the fast reaction between $TMSN_3$ and BAIB[168] that would lead to unproductive formation of N_2 and undesired bisazido side products.

Initial experiments showed that mixing galactal **3.1**, Ph_2Se_2 and $TMSN_3$ at -30 °C did not result in any reaction over a 2 h period as analyzed by ^1H NMR (Figure 3.3), and the reaction only started after BAIB addition. The procedure was repeated at room temperature, and results varied from observing no reaction at all after BAIB addition, to reaction starting only after BAIB addition, as observed in the -30 °C case. Variability may be attributed to differences in mixing, as dissolution of BAIB in the reaction mixture is not immediate at any temperature tested. Alternative solvents for the flow APS reaction were considered, but the solvent choice was constrained by the incompatibility of $TMSN_3$ with protic solvents, and solubility requirements for flow reactions.

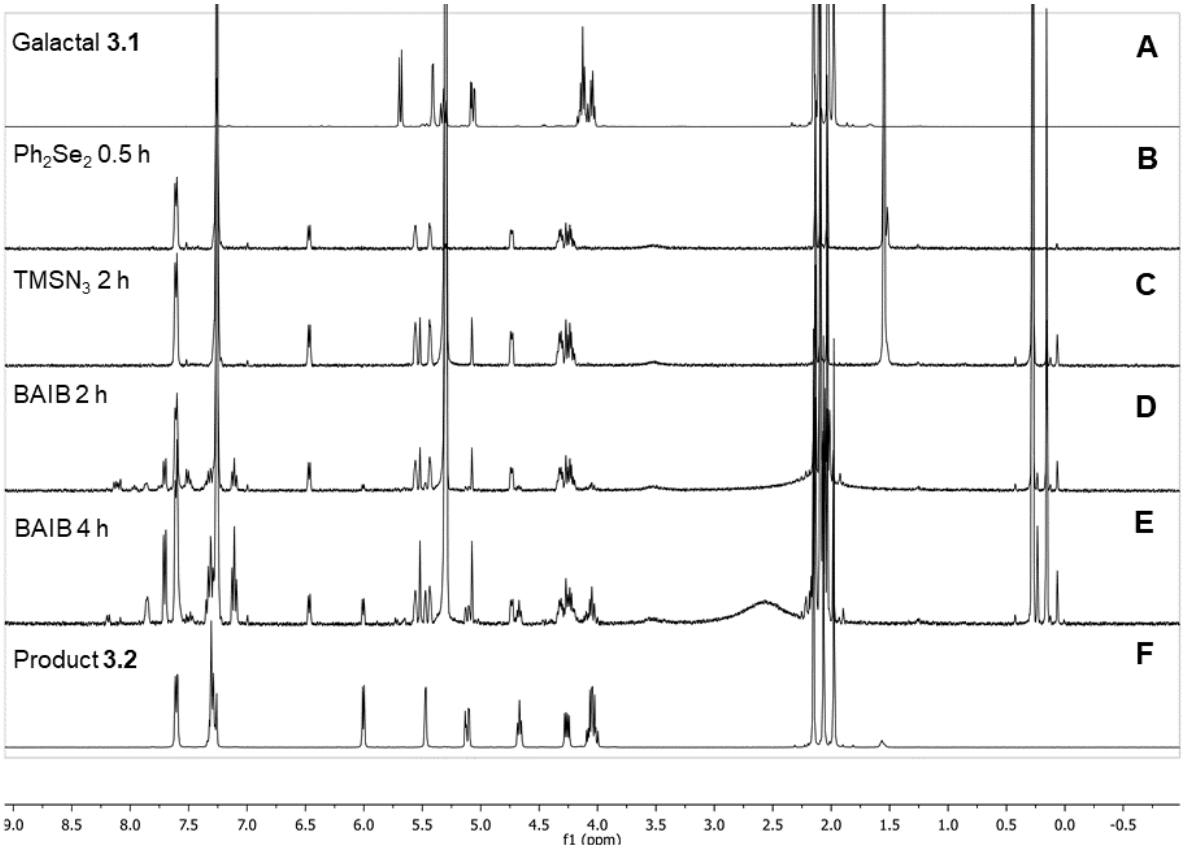

Figure 3.3. Reactivity evaluation of substrate-reagent combinations in batch. ^1H NMR (400 MHz, $CDCl_3$) of (A) starting material **3.1**, (B) reaction mixture 0.5 h after Ph_2Se_2 addition, (C) reaction mixture 2 h after $TMSN_3$ addition, (D) reaction mixture 2 h after BAIB addition, (E) reaction mixture 4 h after BAIB addition, at -10 °C and (F) product **3.2**.

Based on the reactivity observations in batch, a compatible flow set-up was assembled. Two reagent feeds (Feed A: 3,4,6-tri-*O*-acetyl-D-galactal (**3.1**), Ph_2Se_2 and $TMSN_3$; Feed B: BAIB) were used (Figure 3.4). Reagent solutions were prepared with anhydrous DCM and loaded into sample loops. The liquid streams were pumped using HPLC pumps and chloroform was used as carrier solvent for improved pump performance. The two feeds were mixed in a T-piece before entering a residence time unit that was immersed in a thermostatic bath. Sample loops were connected to the liquid stream via six-way-valves to introduce the reagent solution to the flow stream. The reaction mixture finally passed a backpressure regulating unit (17 bar) and was quenched offline. Presurizing the system was essential to guarantee a reproducible flow process, as it prevented the formation of a biphasic gas/liquid flow pattern resulting from the formation of N_2. To ensure immediate quenching, the reaction mixture was collected in a vigorously stirred mixture of dichloromethane and an aqueous solution containing $Na_2S_2O_3$ (to reduce unreacted BAIB) and $NaHCO_3$ to prevent the formation of hydrazoic acid (for details see Experimental Section).

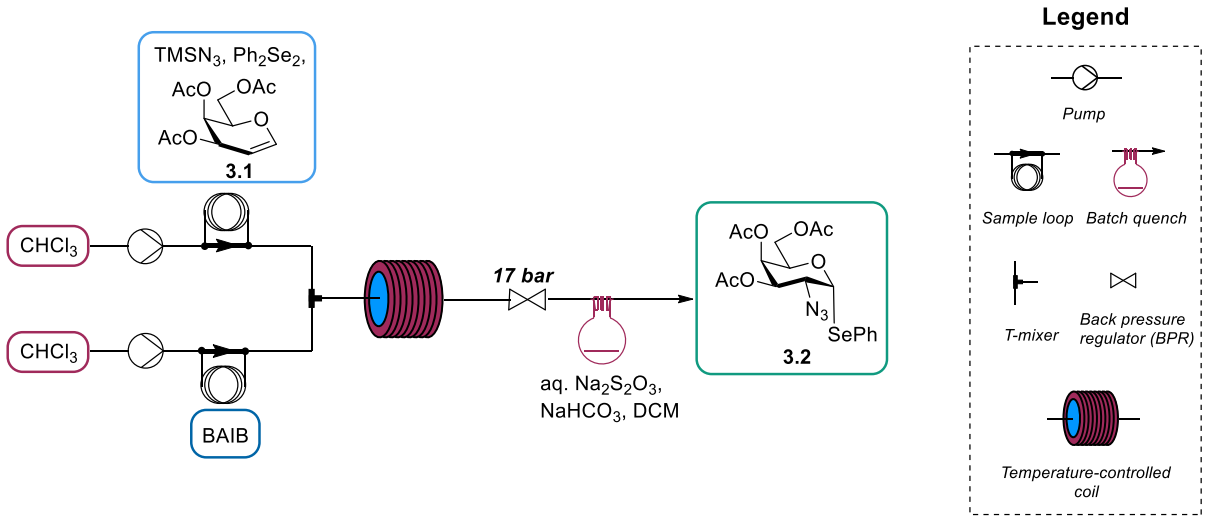

Figure 3.4. Continuous flow setup for the azidophenylselenylation of 3,4,6-tri-*O*-acetyl-D-galactal.

3.2.2 Analysis of the Reaction Outcome by ^{1}H NMR

In order to optimize the reaction conditions, the crude reaction mixtures were carefully analyzed by ^{1}H NMR. Preliminary experiments showed the presence in the mixture of the desired azidophenylselenylation product **3.2** and up to six different side products (**3.3**-**3.8**, Scheme 3.2): the *talo* stereoisomer **3.3**, the regioisomers **3.4** and **3.5**, the bisazido monosaccharides **3.6** and **3.7**, and 1-*O*-acetyl glycoside **3.8** (Scheme 3.2). A remarkable selectivity towards α-glycosides (**3.2**-**3.6**, **3.8**) was noted, with the β-bisazido species **3.7** only observed occasionally. A mechanism where an initial ligand exchange on the BAIB generates

the azido radicals was previously proposed.[168] Subsequent addition of the azido radical to the glycal double bond to form an anomeric (pyranos-1-yl) radical accounts for the regioselectivity towards 2-azido products (**3.2**, **3.3**, **3.6**-**3.8**). The preferred pseudoaxial disposition for the C4-substituent[169] hindering the *β*-face accounts for the stereoselectivity for equatorial (*galacto* products **3.2**, **3.5**-**3.8**) over axial (*talo* products **3.3**-**3.4**) substituents at C2 (Scheme 3.3). α-Selectivity is commonly observed in galactal reactions and it is attributed to the anomeric effect and hindrance of the *β*-face.[157] BAIB is the source for the acetoxy moiety in acetyl glycoside **3.8**. Side products bearing acetoxy groups were observed in the presence of BAIB in the azidophenylselenylation of olefins, where acetoxyphenylsenelyl compounds were identified.[170] Formation of both 2-phenylselenyl products (**3.4, 3.5**) is likely due to the production of electrophilic selenium species, but the observation of 1,2-*cis* glycoside **3.5** argues against the involvement of a cyclic selenium cation that was previously suggested.[168]

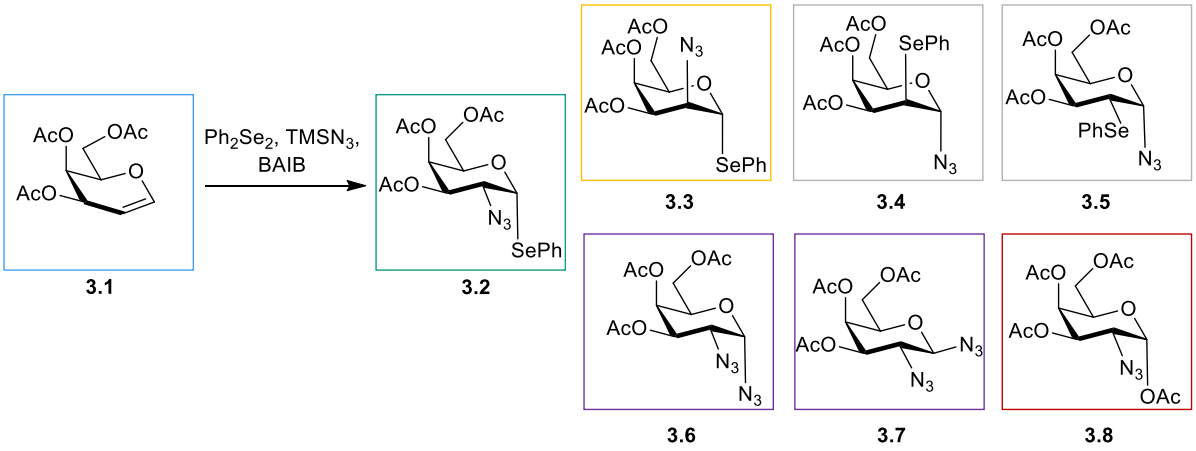

Scheme 3.2. Observed products for the APS reaction of **3.1**.

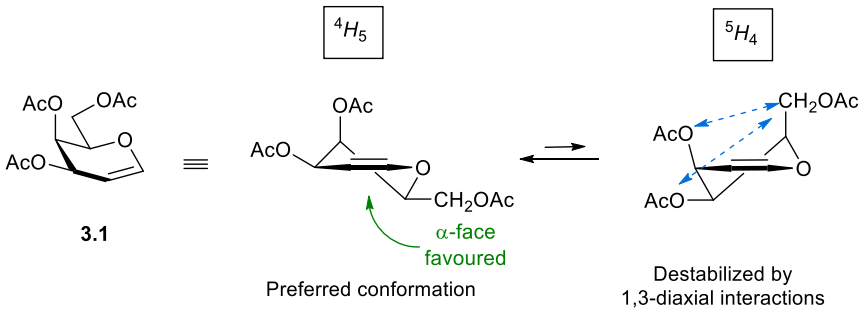

Scheme 3.3. Conformational equilibrium is shifted towards half chair $^{4}H_{5}$ for galactal **3.1**, in which the pseudoaxial disposition of C4-OAc hinders the β-face. The half chair $^{5}H_{4}$ conformation is destabilized by 1,3-diaxial interactions.[169]

Isolation and characterization of all compounds allowed for the identification of each monosaccharide (**3.1**-**3.8**) a distinct ^{1}H NMR signal *a*-*h* that enabled to assess the reaction selectivity using crude ^{1}H NMR analysis (Table 3.1, Figure 3.5). Identification of

monosaccharides **3.2**, **3.4**, **3.6** and **3.7** was corroborated with literature data, and individual signal assignments were supported by HSQC and COSY experiments. In addition to mass analysis and the IR signal characteristic for N_3 stretching around 2100 cm^{-1}, H1 and H2 chemical shifts and coupling constants were key for the identification of monosaccharides **3.5** and **3.8.** For monosaccharide **3.5**, the shift towards higher fields of H1 (δ 5.67 ppm) respect to phenylselenoglycoside **3.2** (δ 6.01) and comparable to **3.4** (δ 5.71 ppm, Table 3.1) was found consistent with a 1-azido-2-deoxy-2-phenylselenyl regiochemistry, and further supported by H2 chemical shift, compatible with a shielding effect from the phenylselenyl subsituent (δ 3.57 compared to δ 3.42 ppm observed for **3.4**, see Experimental Section). The one-bond heteronuclear coupling constant at the anomeric center ($^1J_{C1H1}$ = 170 Hz) allowed identifying **3.5** as the α-stereoisomer. The stereochemistry at C2 was established based on homonuclear vicinal coupling constants for H2 (dd, J = 11.8, 4.0 Hz, in agreement with a *trans*-diaxial and *cis*-axial-equatorial coupling pattern of α-galactosides). Analogously, the H1 lower-field chemical shift of **3.8** (δ 6.32), and the shift towards higher fields of H2 (δ 3.94) matched a 2-azido-2-deoxy-1-*O*-acetyl regiochemistry, while the $^1J_{CH}$ for H1 and the $^3J_{HH}$ values for H2 indicated α-galactoside stereochemistry (see Experimental Section).

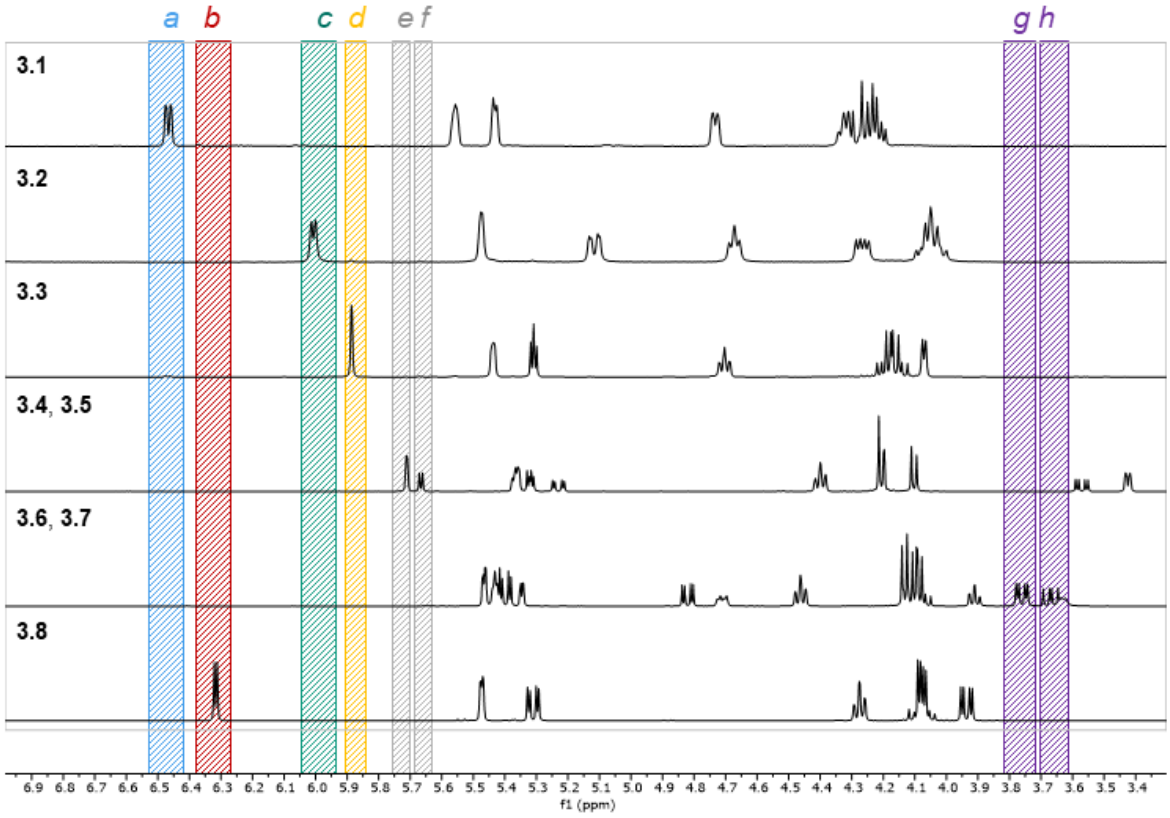

Figure 3.5. Stacked ^{1}H NMR ($CDCl_3$, 400 MHz) spectra of monosaccharides **3.1**-**3.8**. The spectral regions highlighted in color correspond to the signals (*a*-*h*,Table 3.1) selected to analyze APS crude reaction mixtures.

Table 3.1. ^{1}H NMR signals used to assess the reaction outcome from the ^{1}H NMR of the crude reaction mixture.

Signal	δ (ppm)	Compound (assignment)
a	6.47	**3.1** (H-1)
b	6.32	**3.8** (H-1)
c	6.01	**3.2** (H-1)
d	5.86	**3.3** (H-1)
e	5.71	**3.4** (H-1)
f	5.67	**3.5** (H-1)
g	3.76	**3.6** (H-2)
h	3.67	**3.7** (H-2)

3.2.3 Reproducibility and Quenching Protocol

Initial continuous flow reactions revealed a rather invariable selectivity between desired product **3.2** and its isomers **3.3**-**3.5** (ratios **3.2**/**3**/**4**/**5** greater than 10:1:1:1), as well as high fluctuations of the amounts of bisazido and 1-*O*-acetyl side products **3.6**-**3.8** (Figure 3.6, A-C). Occasionally, drastic changes in reaction outcome could be observed, and acetyl glycoside **3.8** was obtained as main product, accompanied by increased amounts of bisazido side products **3.6**-**3.7** and the absence of selenoglycosides **3.2**-**3.3** (Figure 3.6, D).

The magnitude of this variability in results was found to be related to some extent with the reaction stoichiometry. When using two or 1.3 equiv. of Ph_2Se_2, two equiv. of $TMSN_3$ and 1.3 equiv. of BAIB, the selectivity between **3.2** and **3.3**-**3.5** was maintained, but significant fluctuations in the amounts of **3.6**-**3.8** were observed (Figure 3.7, Table S1). When 1.3 equiv. of Ph_2Se_2, 1.3 equiv. of $TMSN_3$ and two equiv. of BAIB were used, the selectivity between **3.2** and **3.3**-**3.5** was not maintained, and the drastic changes in reaction outcomes described above (Figure 3.6, D), lacking products **3.2**-**3.3** were frequent (Figure 3.8).

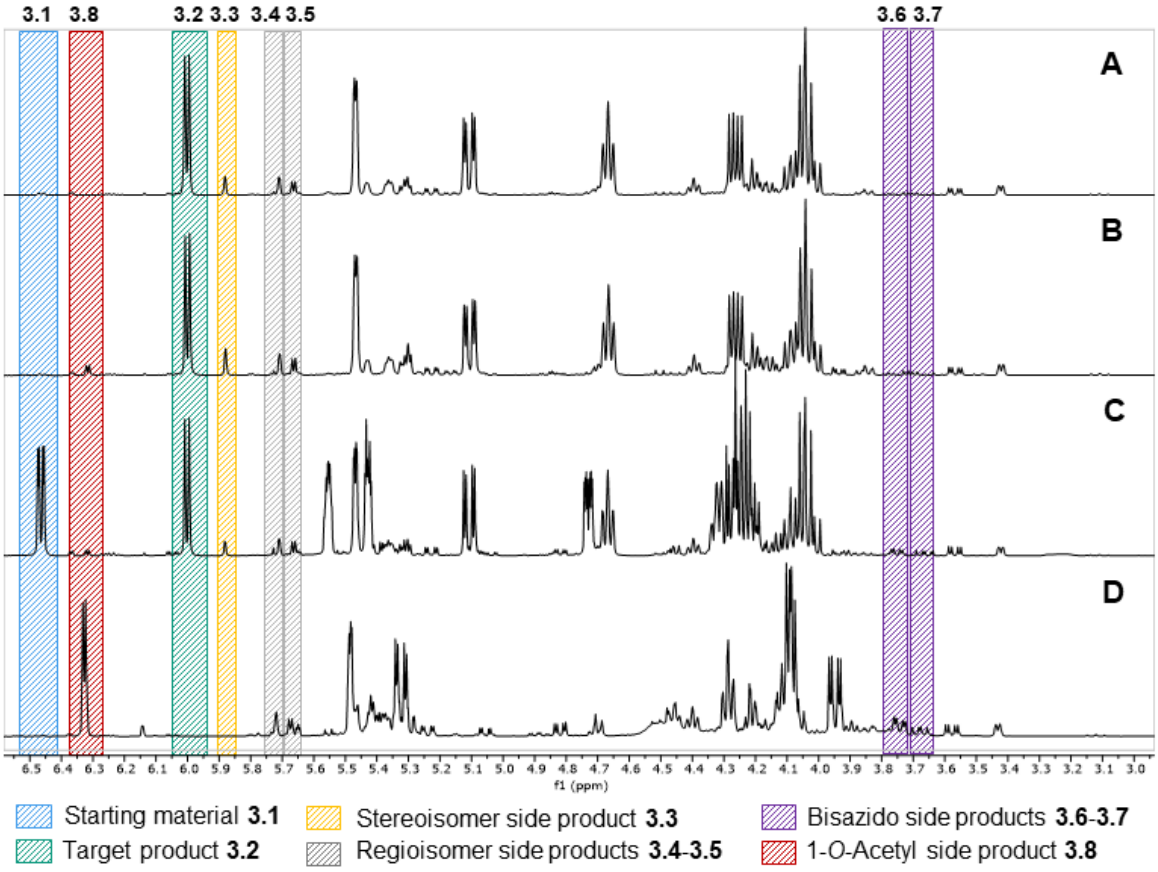

Figure 3.6. ^{1}H NMR ($CDCl_3$, 400 MHz) analysis of crude reaction mixtures for the APS reaction of galactal **3.1**. ^{1}H NMR spectra were recorded after solvent evaporation. Highlighted signals correspond to the ^{1}H chemical shifts used to assess the presence of **3.1**-**3.8** in the crude reaction mixture (Table 3.1). Representative examples: A) excellent outcome, only regio- and stereoisomers of **3.2** (**3.3**-**3.5**) observed as side products; B) acceptable outcome, where side products **3.3**-**3.5** and minimum amounts of **3.8** are observed; C) complex case, with incomplete conversion and products **3.2**-**3.7**; D) extreme case with **3.8** as main product, absence of glycosyl selenides **3.2** and **3.3**, and presence of side products **3.4**-**3.7**.

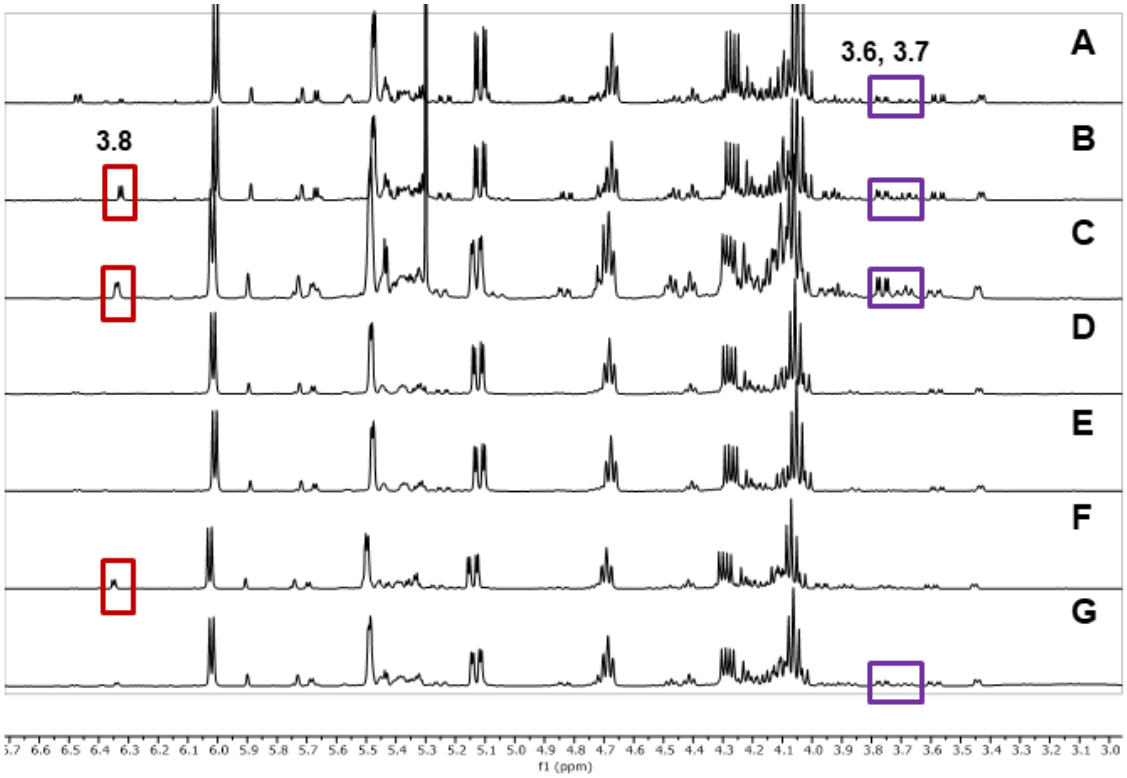

Figure 3.7. ^{1}H NMR (400 MHz, $CDCl_3$) showing the variability in flow APS reactions (A-G) without filtration through silica prior to evaporation. Conditions: Galactal **3.1** (0.49 mmol), Ph_2Se_2 (1.3 equiv.), $TMSN_3$ (2 equiv.), BAIB (1.3 equiv); total flow rate = 0.24 mL/min, 27 °C.

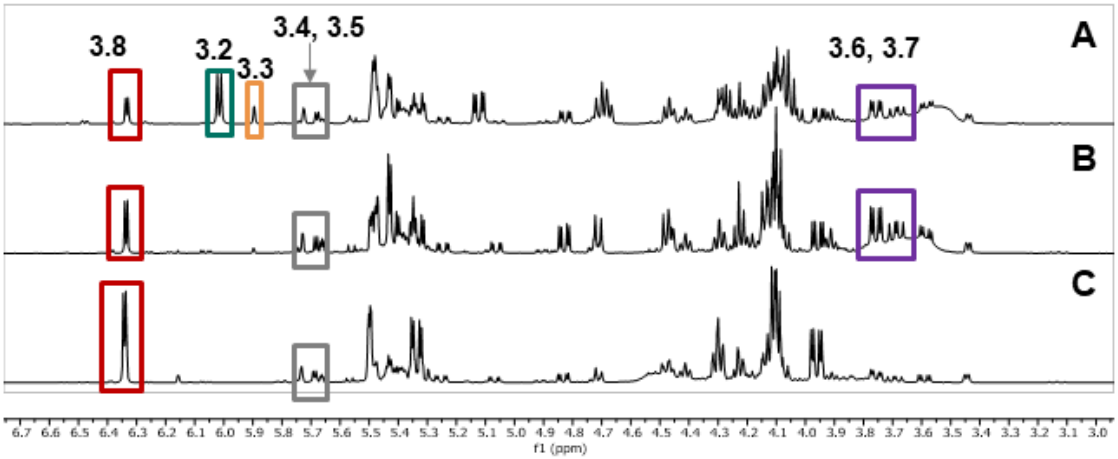

Figure 3.8. ^{1}H NMR (400 MHz, $CDCl_3$) showing the variability in three flow APS reactions without filtration through silica prior to evaporation. A) Target product **3.2** was obtained with significant amounts of 1-*O*-acetyl glycoside **3.8** and bisazido compounds **3.6**-**3.7**; B) main products are **3.6**-**3.8**, and no selenoglycosides **3.2**-**3.3** are observed; C) **3.8** is the main product, and no selenoglycosides **3.2**-**3.3** are present. Conditions: Galactal **3.1** (0.49 mmol), Ph_2Se_2 (1.3 equiv.), $TMSN_3$ (1.3 equiv.), BAIB (2 equiv); total flow rate = 0.24 mL/min, 27 °C.

Comparison of ^{1}H NMRs of the organic layer before and after solvent evaporation revealed that **3.6**-**3.8** were formed during solvent evaporation rather than during the

continuous flow process. Filtration of the crude reaction mixture through a silica plug (see Experimental Section) served to avoid high variability in the amount of side products **3.6**-**3.8**. When filtration through silica was introduced as part of the quenching protocol, no change in the monosaccharide composition of the crude reaction mixture was observed between the mixture prior to solvent evaporation, or after short (15 min) or long (1 h) times at reduced pressure and 40 °C (Figures 3.9-3.10). It should be noted that removal of selenide impurities through silica filtration is required for an adequate crystallization of **3.2**. The use of silica filtration prior to evaporation therefore does not introduce an extra step to the preparative protocol, but simply exchanges the order between silica filtration and solvent evaporation. Presumably, selenoglycosides **3.2**-**3.3** are converted into **3.6**-**3.8** *via* radical-mediated homolytic cleavage of the C-Se anomeric bond or β-elimination to afford galactal **3.1** as intermediate.[168,171,172] Alternatively, oxidation of the phenylselenyl group to the corresponding selenone would afford a good leaving group, rendering C1 susceptible to nucleophilic attack.[173] Involvement of BAIB on the formation of **3.6**-**3.8** under reduced pressure resulting from incomplete reduction in the aqueous quenching was ruled out, as no BAIB signals were observed during ^{1}H NMR analysis. Moreover, silica filtration was required to prevent formation of **3.6**-**3.7** even when one equiv. of BAIB was used (Figure 3.11).

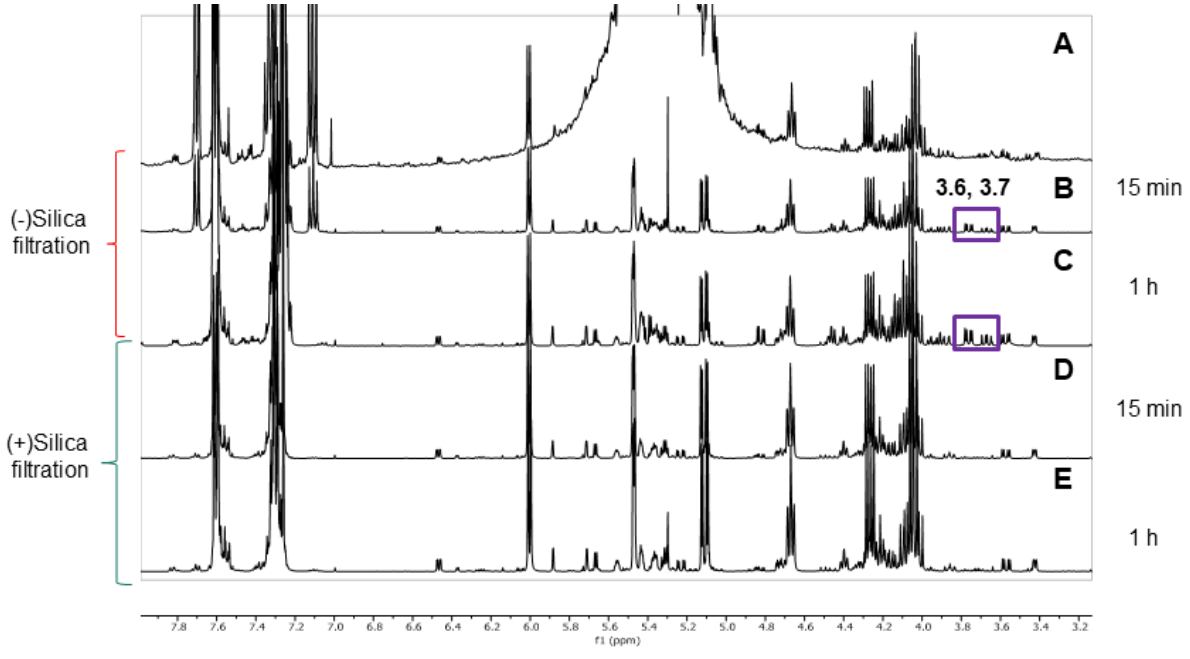

Figure 3.9. ^{1}H NMR (400 MHz, $CDCl_3$) of flow APS crude reaction mixture A) prior to solvent evaporation, no filtration through silica; B) after 15 min in rotatory evaporator at 40 °C; C) after 1 h in rotatory evaporator at 40 °C; D) after 15 min in rotatory evaporator at 40 °C with filtration through silica prior to solvent evaporation; E) after 1 h in rotatory evaporator at 40 °C with filtration through silica prior to solvent evaporation. Conditions: Galactal **3.1** (0.49 mmol), Ph_2Se_2 (1.3 equiv.), $TMSN_3$ (2 equiv.), BAIB (1.3 equiv.); total flow rate = 0.24 mL/min, 27 °C.

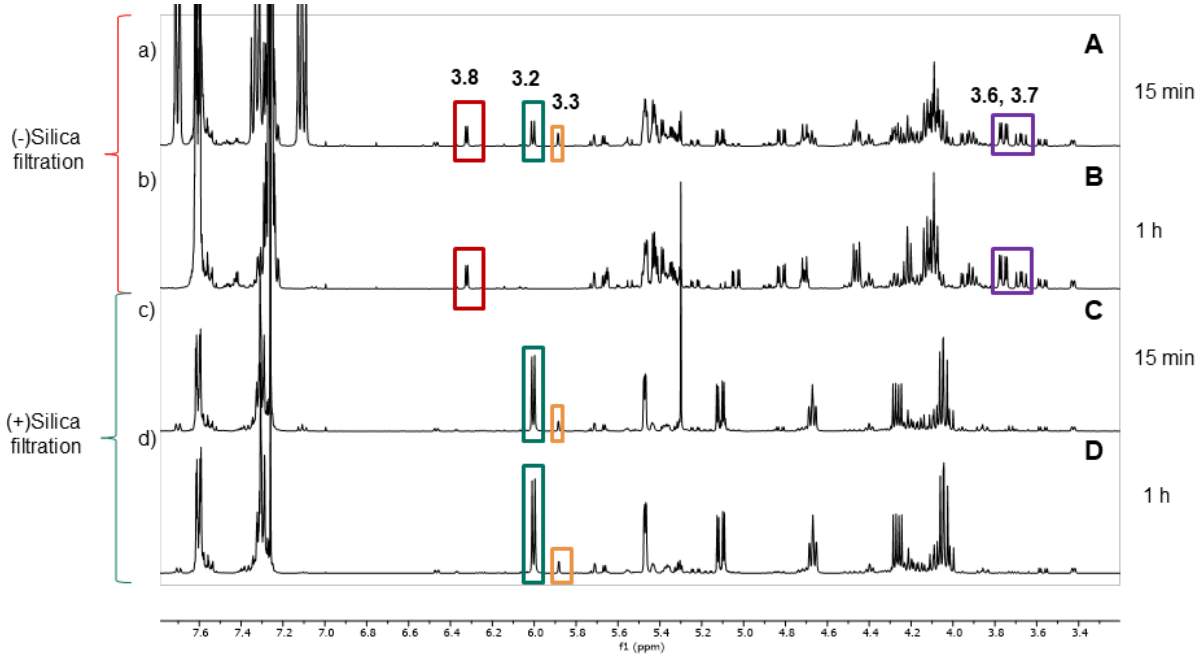

Figure 3.10. ^{1}H NMR (400 MHz, $CDCl_3$) of flow APS crude reaction mixture a) without filtration through silica, after 15 min in rotatory evaporator at 40 °C; b) after 1 h in rotatory evaporator at 40 °C; c) after 15 min in rotatory evaporator at 40 °C with filtration through silica prior to solvent evaporation; d) after 1 h in rotatory evaporator at 40 °C with filtration through silica prior to solvent evaporation. Conditions: Galactal **3.1** (0.49 mmol), Ph_2Se_2 (1.3 equiv.), $TMSN_3$ (1.3 equiv.), BAIB (2 equiv.); total flow rate = 0.24 mL/min, 27 °C.

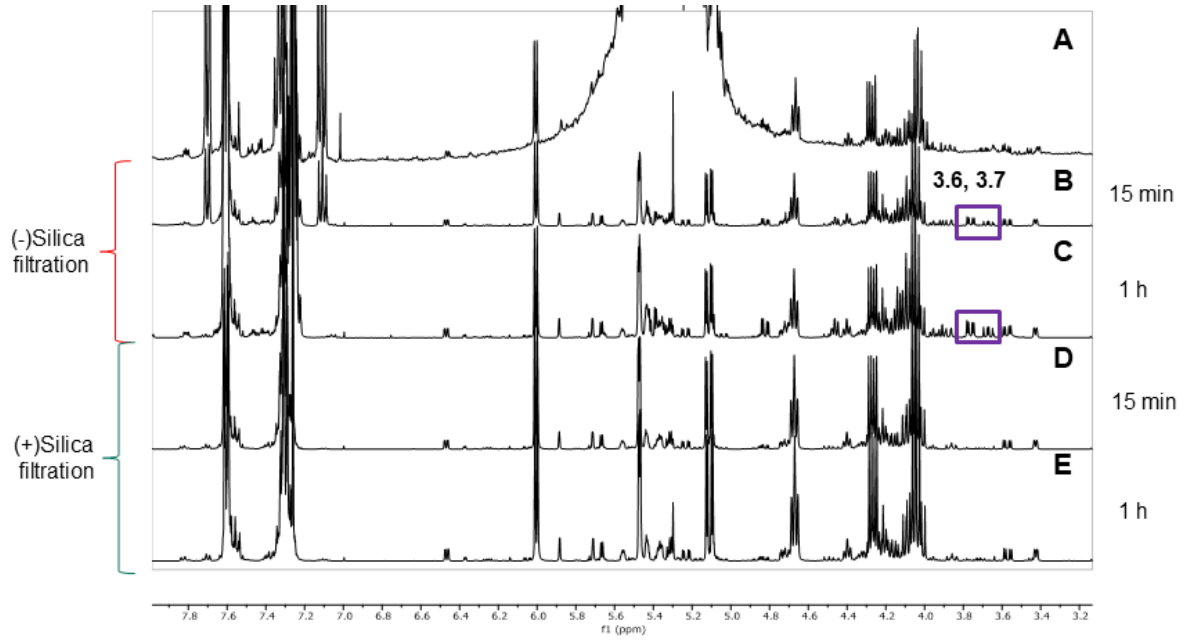

Figure 3.11. ^{1}H NMR (400 MHz, $CDCl_3$) of crude reaction mixture of flow APS reaction a) prior to solvent evaporation, no filtration through silica; b) after 15 min in rotatory evaporator at 40 °C; c) after 1 h in rotatory evaporator at 40 °C; d) after 15 min in rotatory evaporator at 40 °C with filtration through silica prior to solvent evaporation; e) after 1 h in rotatory evaporator at 40 °C with filtration through silica prior to solvent evaporation. Conditions: Galactal **3.1** (0.49 mmol), Ph_2Se_2 (1.3 equiv.), $TMSN_3$ (2 equiv.), BAIB (1 equiv.); total flow rate = 0.24 mL/min, 27 °C.

3.2.4 Optimization and Scale-up

Once the flow setup with a reliable quenching protocol and a suitable method to assess the reaction outcome was established, reaction conditions were screened aiming to maximize the yield of selenoglycoside **3.2** by achieving full conversion and minimizing side product formation (Table 3.2). Best results were obtained with 1.6 equivalents of Ph_2Se_2, two equivalents of $TMSN_3$ and 1.3 equivalents of BAIB at room temperature (Table 3.2, entry 5) to afford target product **3.2** in 79% yield within 25 min. Excess Ph_2Se_2 was crucial to minimize the formation of **3.6**-**3.8**, and was necessary for complete substrate consumption (entries 1, 2, 5). A two-fold excess of BAIB did not lead to a significant formation of 1-*O*-acetyl product **3.8**, but a low mass balance (full consumption of **3.1**, sum of the yields for **3.2**-**3.5** = 73%) was obtained (entry 3). Lowering the reaction temperature to 0 °C resulted in a significantly reduced conversion, without any improvement in selectivity towards **3.2** (entry 7). At higher temperatures (40 °C) a significantly lower selectivity was observed due to the formation of bisazido side products **3.6**-**3.7** (Table 3.2, entries 8-9). Longer residence times at 40 °C resulted in a slightly production of acetoxyglycoside **3.8**, (entry 9) though not as drastic as the observations at 40 °C during the solvent evaporation process (see above). The selectivity for product distribution of the for isomers **3.2**-**3.5** remained roughly unaltered by temperature changes (ratios **3.2**/**3**/**4**/**5** greater than 10:1:1:1) and did not differ from control experiments in batch (see Experimental Section).

Table 3.2. Screening of reaction conditions for the flow APS reaction of galactal **3.1**.

Entry	t_{res} / min	T /°C	Ph_2Se_2 /equiv	$TMSN_3$ /equiv	BAIB /equiv	Conv. /%[b]	Yield/%[c]						
							3.2	**3.3**	**3.4**	**3.5**	**3.6**	**3.7**	**3.8**
1	25	27	2	2	1.3	100	78	6	8	7	0	0	0
2	25	27	1.3	2	1.3	98	74	6	7	7	0	0	0
3	25	27	1.3	1.3	2	98	58	5	5	5	0	0	0
4	25	27	1.3	2	1	95	72	6	7	8	0	0	0
5	**25**	**27**	**1.6**	**2**	**1.3**	**100**	**79**	**6**	**7**	**7**	**0**	**0**	**0**
6	20	27	1.6	2	1.3	95	71	6	7	7	0	0	0
7	25	0	1.6	2	1.3	62	41	3	4	5	4	3	0
8	25	40	1.6	2	1.3	100	65	7	8	8	4	0	0
9	40	40	1.6	2	1.3	100	60	7	7	7	4	0	4

[a]Conversion of galactal (**3.1**) determined by ^{1}H NMR using 1,2,4,5-tetramethylbenzene as internal standard. [c]NMR yields determined by ^{1}H NMR using 1,2,4,5-tetramethylbenzene as internal standard.

For the large scale production of **3.2**, the residence time was extended to 35 minutes to guarantee full conversion, and the overall flow rate was increased from 0.24 to 0.34 mL/min for enhanced throughput. These conditions were tested at a 1 mmol scale and resulted in 72% NMR yield of **3.2**. Recrystallization yielded 281 mg (61% yield) of **3.2**. The success in purification by recrystallization most likely relies on the relative amounts of **3.2**-**3.5** rather than in differential solubility, as monosaccharides **3.2**-**3.5** present similar chromatographic behaviors, such that full peak resolution is not achievable using NP-HPLC. In that context, a 10% difference between NMR and isolated yields is expected, as it reflects the mixture composition. Only a seventh of the time originally reported in batch is required in flow for the full conversion of 1 mmol of starting material **3.1**. The isolated yield from the flow approach ranks together with the top yields observed in batch (65%), and well above the average yield of 35% (Figure 3.2). These results were subsequently reproduced on a gram scale APS reaction (5 mmol of **3.1**) that resulted in 63% (1.46 g) of analytically pure selenogalactoside **3.2**. Analysis of sequential aliquots of the crude reaction mixture showed that the reaction outcome observed in an analytical scale was consistenly reproduced during the process (Figure 3.12), demonstrating the ability of the continuous flow process to afford reproducible results when scaling-up.

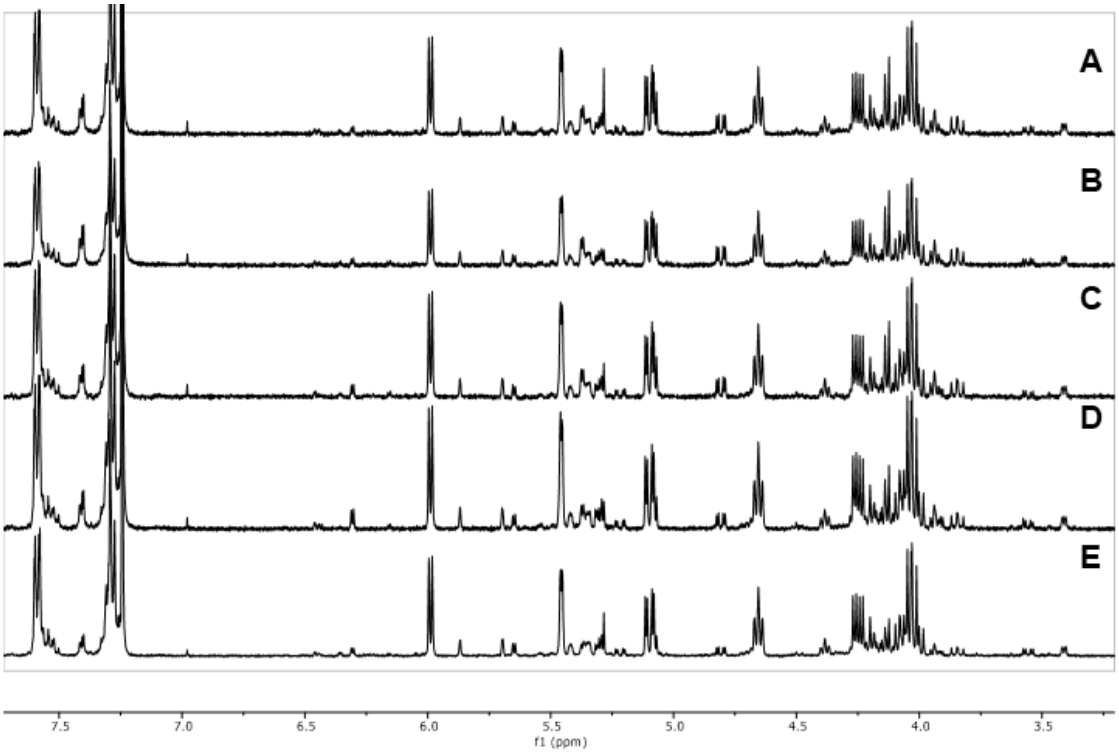

Figure 3.12. ^{1}H NMR (400 MHz, $CDCl_3$) of crude reaction mixture for flow APS reaction (A-D) of sequential aliquots and (E) of the total reaction output combined. Conditions: Galactal **3.1** (4.90 mmol), Ph_2Se_2 (1.6 equiv.), $TMSN_3$ (2 equiv.), BAIB (1.3 equiv.); total flow rate = 0.34 mL/min, 27 °C.

3.3 Conclusions

A thorough analysis revealed that the APS is a complex reaction, in which six different side products can be formed that significantly reduce the yield of the desired selenogalactoside **3.2**. An additional degree of complexity is added when considering that formation of the target product is reversible. Several factors account for low reproducibility of standard batch APS reactions. The lack of control in the mixing of $TMSN_3$ and BAIB and slow heat transfer processes produce variable results, since elevated local concentrations of azido species can lead either to an increase in bisazido side products (**3.6**-**3.7**), or to low conversions if azido species are consumed in N_2 formation.[174] Additionally, significant differences in the reaction outcome can result from insufficient quenching as the desired product is prone to form bisazido and 1-*O*-acetyl compounds. Performing the reaction in flow allowed for the safe reaction of $TMSN_3$ with BAIB at room temperature, enabling reaction conditions that narrowed the number of side products and reduced the reaction time significantly. Effective and reproducible quenching conditions were key to achieve reproducible, selective reactions. The flow setup allowed for a straightforward scale-up, as the results observed in an analytical scale were steadily reproduced throughout the entire process of a gram-scale synthesis.

3.4 Outlook

The flow setup is readily scalable to process 5 mmol of galactal in 3 h, producing 1.2 mmol/h of product. The method can be further extended to larger scales in an automated fashion by combination with an autosampler unit.[175] Additionally, this platform is promising to expand the substrate scope to access rare 2-deoxy-2-aminosugars gulosamine (core of streptothricin class antibiotics[176]) and fucosamine (present in the capsular polysaccharide of pathogens such as *Streptococcus pneumoniae* ST5[177]).

The developed flow APS method will be implemented in the Seeberger group for the production of GalN BBs. In particular, the AGA of the GalN-rich fraction of the galactosamino glycan present in the extracellular matrix of *Aspergillus fumigatus* (Figure 3.1, D) will be used for the study of this antigenic and immunosuppressive oligosaccharide. Facile production of diverse galactosamine BB is fundamental for the development of an AGA strategy for the installmation of (multiple) GalN α-linkages. Thorough screening for a suitable BB will be required, as tools such as remote participation, and effect of temperature and solvent for glycosylations (which will demand in some cases the use of diverse leaving groups) are needed for the stereoselective introduction of these challenging 1,2-*cis* linkages.

3.5 Experimental Section

3.5.1 General Methods

Reagents and solvents were obtained from commercial sources, unless stated otherwise. Anhydrous DCM was obtained from a Solvent Dispensing System (J.C. Meyer), and anhydrous chloroform was prepared by adding preactivated molecular sieves (4 Å, Roth) to HPLC grade chloroform (Merck). Analytical thin layer chromatography (TLC) was performed on glass pre-coated TLC-plates SIL G/UV_{254} sheets (Macherey-Nagel) and visualized with 254 nm light and sugar stain (3.70 mL of *p*-anisaldehyde in 140 mL of a solution 3.5% H_2SO_4 in ethanol). NMR spectra were obtained using an Ascend 400 (Bruker) and Agilent 400 MHz NMR Magnet (Agilent Technologies) spectrometers at 400 MHz (^{1}H) and 100 MHz (^{13}C). $CDCl_3$ was used as solvent and chemical shifts (δ) are reported in ppm relative to the residual solvent peaks ($CDCl_3$: 7.26 ppm ^{1}H, 77.16 ppm ^{13}C). Assignments were supported by COSY and HSQC experiments. IR spectra were measured with a Spectrum 100 FT-IR Spectrometer (Perkin Elmer). Only diagnostic signals are listed. Specific rotations were measured using a UniPol L 1000 polarimeter (Schmidt + Haensch), at 25 °C and λ = 589 nm. The solvent and concentrarion (*c*, expressed in g/100 mL) are noted in parentheses. ESI-HRMS were performed with a Xevo G2-XS Q-Tof (Waters). HPLCs were performed on Agilent 1200 Series systems.

Safety note: Even under continuous flow conditions, extreme caution in the handling of potentially hazardous starting materials and product mixtures is required. The possibility of formation of poisonous and explosive hydrazoic acid must be contemplated at all times.

3.5.2 General Procedure and Equipment for Azidophenylselenylation of Galactal Under Continuous Flow Conditions

For screening conditions (0.49 mmol of **3.1**): The flow setup was assembled using 1.6 mm O.D. x 0.8 mm I.D. FEP tubing (residence time unit volume: 6 mL) and connected by simple T-mixer (0.8 mm I.D.). The temperature of the residence time unit was regulated at 27 °C using a thermostatic bath unless stated otherwise. 3,4,6-Tri-*O*-acetyl-α-D-galactal **3.1** was coevaporated with anhydrous toluene twice and kept under high vacuum for at least 30 minutes prior to every reaction. Galactal **3.1** was defined as limiting reagent, and concentrations of other reagents and flow rates were calculated according to desired stoichiometry and residence time. Sample loops were made out of 1.6 mm O.D. x 0.8 mm I.D. FEP tubing (loop A: 3 mL; loop B: 5 mL) and were washed and filled with anhydrous DCM prior to reactions. The sample loops were loaded with the following solutions for continuous

flow experiments: *Solution A*: 0.163 M solution of galactal **3.1**, Ph_2Se_2 and $TMSN_3$ in anhydrous DCM. Solution A was loaded in loop A and injected using pump A set to a flow rate f_A, 1.5 min after injection of solution B had started. *Solution B*: BAIB in anhydrous DCM. Solution B was loaded in loop B, and then injected using pump B set to a flow rate $f_B = f_A$. Knauer BlueShadow 40P pumps were used for pumping. A Vapourtec R2 series was used for sample loop command and in-line pressure monitoring. An exchangeable cartridge back pressure regulator (BPR) loaded with a 17-bar cartridge (Upchurch Scientific) was placed downstream and the reaction mixture was collected and quenched by dropping it into a mixture of DCM (50 mL) and aq. sat. $NaHCO_3$ (25 mL), $Na_2S_2O_3$ (25 mL) that was stirred vigorously. After phase separation, the organic layer was passed through a 6 cm silica gel plug preloaded on a disposable sample syringe with filter, eluted with additional 50 mL of DCM (fraction 1, 'f1'), then eluted with 100 mL of DCM/Acetone 95:5 (fraction 2, 'f2') and 100 mL of DCM/Acetone 90:10 (fraction 3, 'f3'). The solvent of f2 was evaporated under reduced pressure and was analyzed by ^{1}H NMR to assess reaction outcome, and/or crystallized from isopropanol to obtain target product **3.2**. Fractions f1 and f3 were kept until the absence of carbohydrates (only required for screening and optimization purposes) was confirmed by thin layer chromatography and/or ^{1}H-NMR. Quantifications were performed by ^{1}H NMR of the crude reaction mixture, using 1,2,4,5-tetramethylbenzene as internal standard (**IS**). Peak areas of **IS** δ 6.91 (s, 2H), and of the diagnostic of compounds **3.1**-**3.8** (Table 3.1) were used for calculations.

Effective Quenching

Preliminary results in batch showed that quenching may be incomplete with low volumes of quenching solution or ineffective mixing. To ensure immediate quenching, the reaction mixture was collected in a vigorously stirred mixture of DCM and an aqueous solution containing $Na_2S_2O_3$ (to reduce unreacted BAIB) and $NaHCO_3$ to prevent the formation of hydrazoic acid (Figure 3.4). A flow APS reaction on a 0.49 mmol scale was performed as described above, using 1.6 equiv. of Ph_2Se_2, 2 equiv. of $TMSN_3$ and 1.3 equiv. of BAIB. The residence time was set to 10 min using total flow rate to 0.60 mL/min ($f_A = f_B = 0.30$ mL/min) to ensure incomplete conversion. The reaction output was collected in a quenching solution as described above. The total collected volume was split in two fractions. Fraction 1 was filtrated through a silica plug as described in the experimental section, and the mixture was analyzed by ^{1}H NMR after solvent evaporation (Figure 3.13, A-B). Fraction 2 was kept for 1.5 h before applying the same treatment as for fraction 1 (Figure 3.13, C-D). No change in the ratio between monosaccharides was detected.

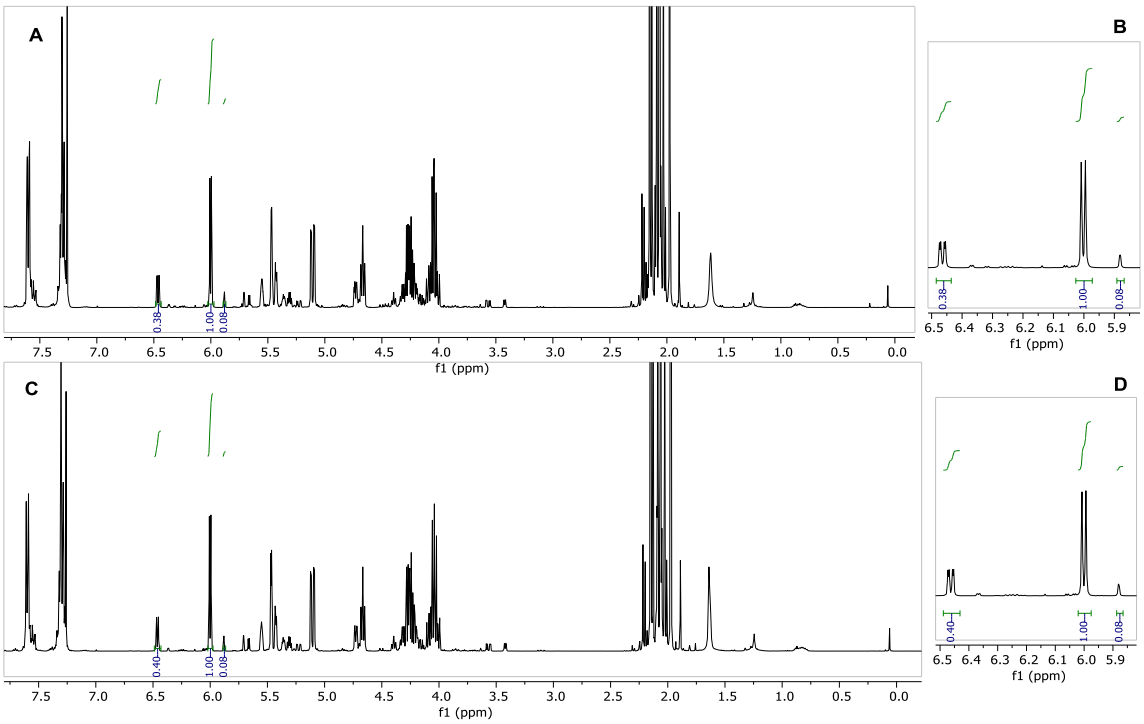

Figure 3.13. ^{1}H NMR (400 MHz, $CDCl_3$) of APS reaction by continuous flow (t_{res} = 10 min), with quenching protocol as described above A) performed immediately; B) performed after 1.5 h. C) Anomeric region of ^{1}H-NMR for figure 3.13, A and D) 3.13, B.

Reproducibility and Quenching Protocol. Variability in Results without Silica Filtration

Table 3.3. Relative amounts of compounds **3.1**-**3.8** for seven APS flow reactions without filtration through silica prior to evaporation (Figure 3.7). Relative amounts were calculated in relation to target product **3.2** based on peak areas of ^{1}H NMR signals (Table 3.1). Conditions: Galactal **3.1** (0.49 mmol), Ph_2Se_2 (1.3 equiv.), $TMSN_3$ (2 equiv.), BAIB (1.3 equiv); total flow rate = 0.24 mL/min, 27 °C.

Entry	Relative amount							
	3.1	**3.2**	**3.3**	**3.4**	**3.5**	**3.6**	**3.7**	**3.8**
1	0.09	1	0.09	0.11	0.11	0.09	0.03	0.02
2	0	1	0.12	0.13	0.13	0.19	0.13	0.13
3	0	1	0.10	0.14	0.13	0.24	0.11	0.10
4	0	1	0.08	0.09	0.09	0	0	0
5	0	1	0.09	0.10	0.10	0	0	0
6	0	1	0.10	0.11	0.11	0.11	0.02	0.14
7	0	1	0.10	0.13	0.12	0.15	0.07	0.05

Batch Control Experiments

Galactal **3.1** (50.0 mg, 0.18 mmol) was coevaporated with toluene twice and kept overnight under high vacuum, then subjected to batch homogeneous APS reaction.[159] After 2.5 h, an aliquote was quenched with $Na_2S_2O_3$/$NaHCO_3$ as described above, and the organic layer was analyzed via ^{1}H NMR. Compounds **3.1**-**3.8** were observed via ^{1}H NMR, with over 40% of starting material remaining (Figure 3.14).

Galactal **3.1** (272.2 mg, 1.00 mmol) was coevaporated with toluene twice and kept overnight under high vacuum, and subsequently used for batch homogeneous APS reaction, with stoichiometry used as in flow 0.98 mmol experiment (1.6 equiv. Ph_2Se_2, 2 equiv. $TMSN_3$, 1.3 equiv. BAIB). Reagents were added at -30 °C and then allowed to warm up to room temperature. After 3 h the reaction was complete, and it was quenched following the quenching protocol described for flow APS (see above). Analysis via ^{1}H NMR showed products **3.2**-**3.6** (Figure 3.15).

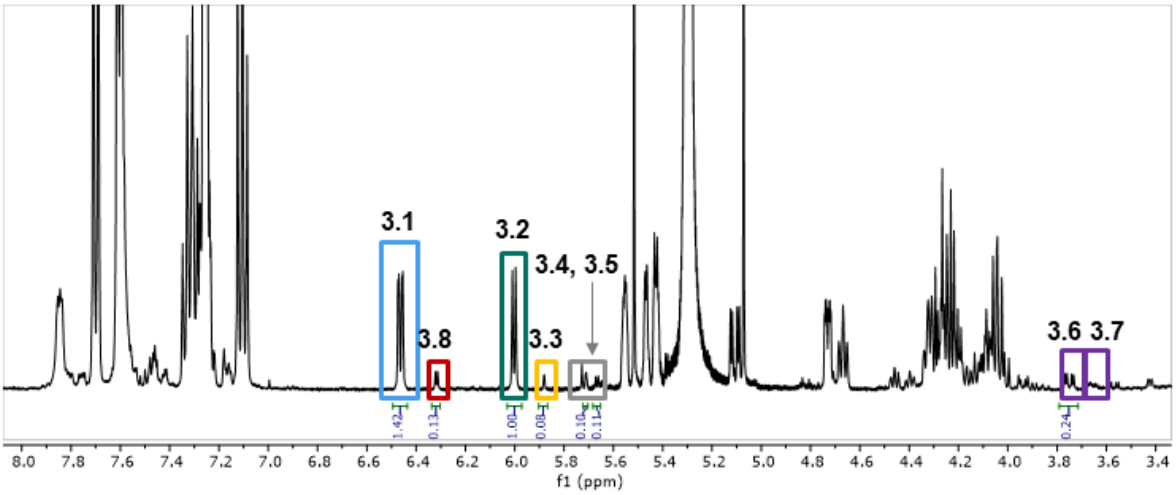

Figure 3.14. ^{1}H NMR (400 MHz, $CDCl_3$) of crude reaction mixture after 2.5 h reaction time using standard batch homogeneous APS conditions.

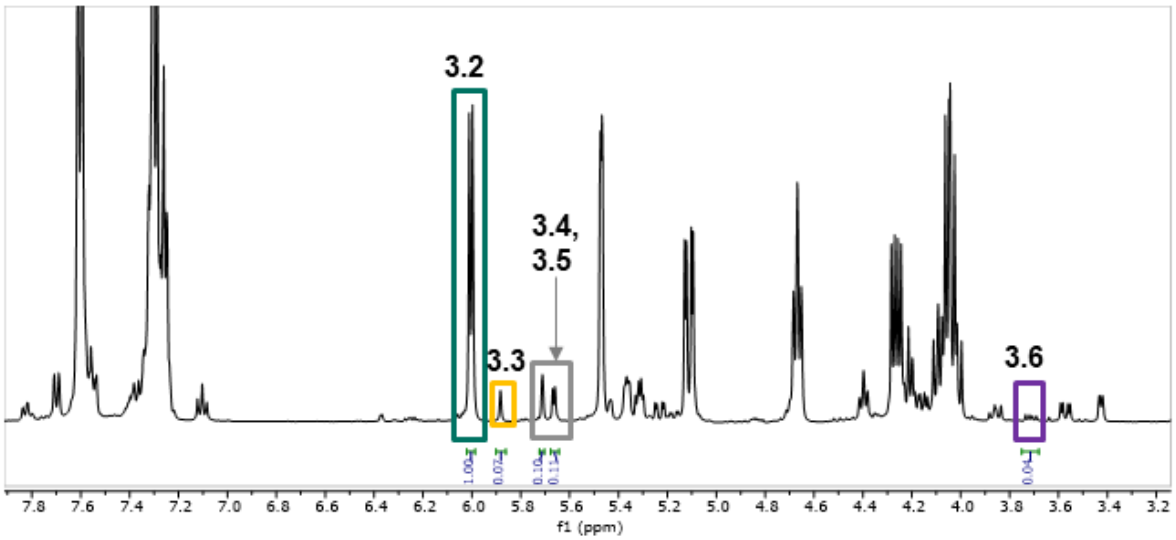

Figure 3.15. ^{1}H NMR (400 MHz, $CDCl_3$) of batch APS crude reaction mixture after evaporation (3 h reaction time). Conditions: galactal **3.1** (0.98 mmol), Ph_2Se_2 (1.6 equiv.), $TMSN_3$ (2 equiv.), BAIB (1.3 equiv.); 3 h reaction time, T = -30°C to r.t.

Experimental Data for Monosaccharides 3.1-3.8

Galactal **3.1** was synthesized following previously reported procedures.[58] Monosaccharides **3.2**-**3.8** were isolated from flow APS reactions. Selenoglycoside **3.2** was isolated through recrystallization (see below). Fractions enriched in monosaccharides **3.3**-**3.8** were isolated exclusively for characterization purposes. Monosaccharides **3.2**-**3.5** and **3.6**-**3.7** showed similar chromatographic behavior, such that it was not possible to achieve full peak resolution using preparative normal-phase HPLC. The isopropanol filtrate of a 0.49 mmol flow APS synthesis was purified using preparative HPLC purification, from which a fraction enriched in **3.3** was isolated and repurified through semi-preparative HPLC to afford pure selenoglycoside **3.3**. Monosaccharides **3.4**-**3.8** were isolated from flow APS syntheses on 0.49 mmol scale without filtration through silica prior to evaporation. Purification via silica gel chromatography (toluene/acetone 0 to 10% as eluent) and subsequent preparative normal-phase HPLC chromatography (hexanes/AcOEt 2-20% as eluent) allowed for the isolation of fractions enriched in **3.4**-**3.5**, **3.6**-**3.7**, and **3.8**. For NP-HPLC, YMC-Diol-300-NP columns were used (analytical: 150 mm x 4.60 mm I.D; semi-preparative: 150 mm x 10.0 mm I.D; preparative: 150 mm x 20.0 mm I.D.), with hexanes/EtOAc as eluent (flow rates: 1.0, 5.0 and 15.0 mL/min for analytical, semi-preparative and preparative chromatography, respectively). The following gradient was used: 1) isocratic 2% EtOAc in hexanes (5 min); 2) linear gradient 2 to 20% EtOAc in hexanes (30 min); 3) linear gradient to 100% EtOAc (10 min).

3,4,6-Tri-*O*-acetyl-α-D-galactal (3.1)[178]

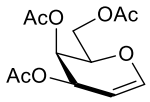

3.1

^{1}H NMR (400 MHz, $CDCl_3$) δ 6.47 (d, *J* = 6.1, 1H, **H-1**), 5.56 (s, 1H, H-3), 5.43 (s, 1H, H-4), 4.73 (d, *J* = 6.1, 1H, H-2), 4.38 – 4.28 (m, 1H), 4.28 – 4.16 (m, 2H), 2.13 (s, 3H), 2.09 (s, 3H), 2.03 (s, 3H). ^{13}C NMR (101 MHz, $CDCl_3$) δ 170.7, 170.4, 170.3 (O*C*(O)CH_3), 145.5 (**C-1**), 98.9 (C-2), 72.9 (C-5), 64.0 (C-3), 63.8 (C-4), 62.0 (C-6), 20.98, 20.93, 20.8 (OC(O)*C*H_3).

Phenyl 3,4,6-tri-*O*-acetyl-2-azido-2-deoxy-1-seleno-α-D-galactopyranoside (3.2)[158]

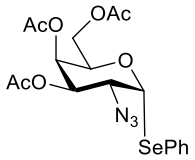

3.2

Flow APS syntheses were performed as described above, with stoichiometry and temperature as in Table 3.2, entry 5. The following modifications on the reaction setup were performed for the scale-up: The flow reactor was built using 1.6 mm O.D. x 0.8 mm I.D. FEP tubing (reactor volume: 12 mL). Sample loops were built with 3.2 mm O.D. x 1.6 mm I.D. FEP or PFA tubing (Loop A: 6 mL and Loop B: 10 mL for 0.98 mmol scale; Loop A: 30 mL and Loop B: 34 mL for 4.9 mmol scale). Flow rates were set at $f_A = f_B =$ 0.17 mL/min. Loop A was cooled to 0 °C for 4.9 mmol scale reaction. Recrystallization from isopropanol afforded the product **3.2** as a white solid (281 mg, 0.60 mmol, 61% for 0.98 mmol scale; 1.46 g, 3.09 mmol, 63% for 4.90 mmol scale). IR (film): 2958 cm^{-1} (w, C-H Ar) 2113 cm^{-1} (s, N_3), 1749 cm^{-1} (s, C=O), 1227 cm^{-1} (s, C-O ester). ^{1}H NMR (400 MHz, $CDCl_3$) δ 7.64 – 7.57 (m, 2H), 7.36 – 7.27 (m, 3H), 6.00 (d, *J* = 5.4 Hz, 1H, **H-1**), 5.47 (m, 1H, H-4), 5.11 (dd, *J* = 10.8, 3.2 Hz, 1H, H-3), 4.67 (t, *J* = 6.4 Hz, 1H, H-5), 4.26 (dd, *J* = 10.8, 5.4 Hz, 1H, H-2), 4.05 (m, 2H, H-6,6'), 2.15 (s, 3H, OC(O)C*H*$_3$), 2.07 (s, 3H, OC(O)C*H*$_3$), 1.98 (s, 3H, OC(O)C*H*$_3$). ^{13}C NMR (101 MHz, $CDCl_3$) δ 170.5, 170.1, 169.7 (3 x O*C*(O)CH_3), 134.9, 129.4, 128.4, 127.7, 84.3 (**C-1**), 71.3 (C-3), 69.1 (C-5), 67.3 (C-4), 61.7 (C-6), 58.9 (C-2), 20.79, 20.77, 20.76 (3 x OC(O)*C*H_3). HRMS (ESI) calc. for $C_{18}H_{21}N_3O_7SeNa$, $[M+Na]^+$ 494.0437; found: 494.0427.

Phenyl 3,4,6-tri-*O*-acetyl-2-azido-2-deoxy-1-seleno-α-D-talopyranoside (3.3)

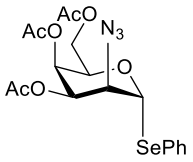

3.3

IR (film) 2950 cm^{-1} (w, C-H Ar)**,** 2109 cm^{-1} (s, N_3), 1750 cm^{-1} (s, C=O), 1260 cm^{-1} (s, C-O ester). ^{1}H NMR (400 MHz, $CDCl_3$) δ 7.59 (dd, *J* = 7.7, 1.8 Hz, 2H), 7.35 – 7.28 (m, 3H), 5.89 (s, 1H, **H-1**), 5.45 – 5.42 (m, 1H, H-4), 5.31 (t, *J* = 3.8 Hz, 1H, H-3), 4.70 (ddd, *J* = 7.3, 5.7, 1.7 Hz, 1H, H-5), 4.23 – 4.11 (m, 2H, H-6,6'), 4.08 – 4.06 (m, 1H, H-2), 2.20 (s, 3H, OC(O)C*H*$_3$), 2.10 (s, 3H, OC(O)C*H*$_3$), 2.02 (s, 3H, OC(O)C*H*$_3$). ^{13}C NMR (101 MHz, $CDCl_3$) δ 170.6 (O*C*(O)CH_3), 170.5 (O*C*(O)CH_3), 169.6 (O*C*(O)CH_3), 134.34, 129.57, 128.63, 128.03, 83.1 (**C-1**, $J_{C\text{-}H}$ = 174 Hz), 69.7 (C-5), 68.4 (C-3), 65.8 (C-4), 61.9 (C-6), 59.8 (C-2), 20.8 (2 x OC(O)*C*H_3), 20.7 (OC(O)*C*H_3). HRMS (ESI) calc. for $C_{18}H_{21}N_3O_7SeNa$, $[M+Na]^+$ 494.0437; found: 494.0439.

3,4,6-Tri-*O*-acetyl-2-deoxy-2-selenophenyl-1-azido-α-D-talopyranoside (3.4)[159] **and 3,4,6-tri-*O*-acetyl-2-deoxy-2-selenophenyl-1-azido-α-D-galactopyranoside (3.5)**

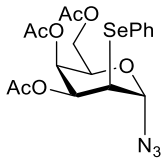

3.4

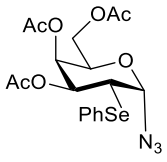

3.5

Mixture of glycosides **3.4** and **3.5** (1.7:1). IR (film) 2965 cm^{-1} (w, C-H Ar)**,** 2113 cm^{-1} (s, N_3), 1746 cm^{-1} (s, C=O), 1214 cm^{-1} (s, C-O ester). ^{1}H NMR (400 MHz, $CDCl_3$) δ 7.60 – 7.52 (m, 2H), 7.35 – 7.27 (m, 3H), 5.71 (d, *J* = 1.6 Hz, 0.6 H, **H-1 3.4**), 5.67 (d, *J* = 4.0 Hz, 0.4 H, **H-1 3.5**), 5.39 – 5.35 (m, 1H), 5.33 – 5.30 (m, 0.6 H, C-H **3.4**), 5.23 (dd, *J* = 11.8, 3.1 Hz, 0.4 H, C-H **3.5**), 4.40 (t_a, *J* = 6.5 Hz, 1H, H-5 **3.4** and **3.5**), 4.15 (m, 2H, H-6,6' **3.4** and **3.5**), 3.57 (dd, *J* = 11.8, 4.0 Hz, 0.4 H, H-2 **3.5**), 3.42 (ddd, *J* = 5.1, 1.4, 0.8 Hz, 0.6 H, H-2 **3.4**), 2.22 (s, 1.8 H, C(O)C*H*$_3$ **3.4**), 2.11 (s, 1.8 H, C(O)C*H*$_3$ **3.4**), 2.10 (s, 1.2 H, C(O)C*H*$_3$ **3.5**), 2.07 (s, 1.8 H, C(O)C*H*$_3$ **3.4**), 2.06 (s, 1.2H, C(O)C*H*$_3$ **3.5**), 1.89 (s, 1.2H, C(O)C*H*$_3$ **3.5**). ^{13}C NMR (101 MHz, $CDCl_3$) δ 170.70 (*C*(O)CH_3), 170.66 (*C*(O)CH_3), 170.1 (*C*(O)CH_3), 170.00 (*C*(O)CH_3), 169.98 (*C*(O)CH_3), 169.8 (*C*(O)CH_3), 134.5, 134.4, 130.3, 129.7, 129.4, 128.9, 128.5, 128.2, 91.6 (**C-1 3.4**, $J_{C\text{-}H}$ = 177 Hz), 90.9 (**C-1 3.5**, $J_{C\text{-}H}$ = 173 Hz), 69.8, 69.3, 69.0, 67.6, 66.7, 66.2, 62.0, 61.9, 46.0 (C-2 **3.4**), 43.4 (C-2 **3.5**), 21.07 (C(O)*C*H_3), 21.03 (C(O)*C*H_3), 20.86 (2 x C(O)*C*H_3), 20.81 (C(O)*C*H_3), 20.7 (C(O)*C*H_3). HRMS (ESI) calc. for $C_{18}H_{21}N_3O_7SeNa$, $[M+Na]^+$ 494.0437; found: 494.0438.

3,4,6-Tri-*O*-acetyl-2-azido-2-deoxy-1-azido-α,β-D-galactopyranoside (3.6, 3.7)[179]

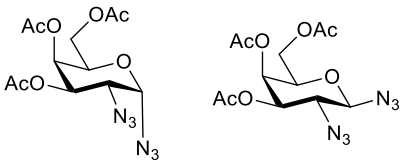

3.6 **3.7**

Mixture of glycosides **3.6** and **3.7** (7:1). IR (film) 2113 cm^{-1} (s, N_3), 1745 cm^{-1} (s, C=O), 1224 cm^{-1} (s, C-O ester). ^{1}H NMR (400 MHz, $CDCl_3$) δ 5.46 (dd, *J* = 3.3, 1.4 Hz, 0.87 H, H-4 **3.6**), 5.43 (d, *J* = 3.4 Hz, 0.87H, **H-1 3.6**), 5.40 (dd, *J* = 11.0, 3.2 Hz, 0.87H, H-3 **3.6**), 5.35 (d, *J* = 3.3 Hz, 0.13H, H-4 **3.7**), 4.82 (dd, *J* = 10.9, 3.3 Hz, 0.13H, H-3 **3.7**), 4.71 (d, *J* = 7.9 Hz, 0.13H, **H-1 3.7**), 4.46 (t, *J* = 7.0 Hz, 0.87H, H-5 **3.6**), 4.16 – 4.03 (m, 2H, H-6,6' **3.6**, **3.7**), 3.91 (td, *J* = 6.6, 1.2 Hz, 0.13H, H-5 **3.7**), 3.76 (dd, *J* = 11.0, 3.4 Hz, 0.87H, H-2 **3.6**), 3.67 (dd, *J* = 10.9, 8.0 Hz, 0.13H, H-2 **3.7**), 2.16 (s, 0.39H, OC(O)C*H*$_3$ **3.7**), 2.15 (s, 2.61H, OC(O)C*H*$_3$ **3.6**), 2.06 (m, 6H, 2 x OC(O)C*H*$_3$ **3.6**, **3.7**). ^{13}C NMR (101 MHz, $CDCl_3$) δ 170.72 (*C*(O)CH_3), 170.68 (*C*(O)CH_3), 170.3 (*C*(O)CH_3), 170.1 (*C*(O)CH_3), 96.6 (**C-1 3.7**, $J_{C\text{-}H}$ = 165 Hz), 92.5 (**C-1 3.6**, $J_{C\text{-}H}$ = 176 Hz), 71.3 (C-3 **3.7**), 71.1 (C-5 **3.7**), 68.5 (C-3 **3.6**), 67.8 (C-4 **3.6**), 66.8 (C-5 **3.6**), 66.5 (C-4 **3.7**), 62.1 (C-6 **3.7**), 61.9 (C-6 **3.6**), 61.7 (C-2 **3.7**), 58.1 (C-2 **3.6**), 20.89 (C(O)*C*H_3), 20.87 (C(O)*C*H_3), 20.84 (C(O)*C*H_3), 20.81 (C(O)*C*H_3), 20.79 (C(O)*C*H_3), 20.78 (C(O)*C*H_3).

1,3,4,6-Tetra-*O*-acetyl-2-azido-2-deoxy-α-D-galactopyranoside (3.8)

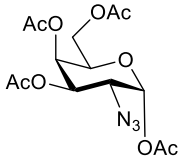

3.8

$[\alpha]_D^{25}$ (*c* 1.00, $CHCl_3$) +85.9. IR (film) 2116 cm^{-1} (s, N_3), 1751 cm^{-1} (s, C=O), 1215 cm^{-1} (s, C-O ester). ^{1}H NMR (400 MHz, $CDCl_3$) δ 6.32 (d, *J* = 3.6 Hz, 1H, **H-1**), 5.49 – 5.46 (m, 1H, H-4), 5.31 (dd, *J* = 11.0, 3.2 Hz, 1H, H-3), 4.27 (t, *J* = 6.8 Hz, 1H, H-5), 4.08 (dd, *J* = 6.7, 3.4 Hz, 2H, H-6,6'), 3.94 (dd, *J* = 11.0, 3.6 Hz, 1H, H-2), 2.17 (s, 3H, C(O)C*H*$_3$), 2.17 (s, 3H, C(O)C*H*$_3$), 2.07 (s, 3H, C(O)C*H*$_3$), 2.03 (s, 3H, C(O)C*H*$_3$). ^{13}C NMR (101 MHz, $CDCl_3$) δ 170.5 (*C*(O)CH_3), 170.2 (*C*(O)CH_3), 170.0 (*C*(O)CH_3), 168.9 (*C*(O)CH_3), 90.5 (**C-1**, $J_{C\text{-}H}$ = 180 Hz), 68.9 (C-3), 68.8 (C-5), 66.9 (C-4), 61.2 (C-6), 56.9 (C-2), 21.1 (C(O)*C*H_3), 20.81 (2 x C(O)*C*H_3), 20.78 (C(O)*C*H_3). HRMS (ESI) calc. for $C_{14}H_{19}N_3O_9Na$, $[M+Na]^+$ 396.1014; found: 396.1021.

4 Conclusions and Perspectives

A part of the perspectives presented in this chapter have been modified from: Guberman, M.; Seeberger, P. H. Automated Glycan Assembly: A perspective. *J. Am. Chem. Soc.* **2019,** *141*, 5581-5592. https://doi.org/10.1021/jacs.9b00638. https://pubs.acs.org/doi/10.1021/jacs.9b00638. *Further permissions related to the material excerpted should be directed to the ACS.*

Synthetic oligosaccharides play a key role in the study of glycan function, and the development of tools for disease prevention, diagnotics and treatment. Difficulties in glycan synthesis arise from the intrinsic complexity of oligosaccharide structures. Oligosaccharide synthesis is a streamlined process (Figure 2.1), and each step of this process represents a bottleneck that needs to be addressed.

The establishment of an automated platform and compatible “approved” BBs, following the definition of a reliable set of orthogonal protecting groups, provided access to diverse structures, including mammalian, plant, and microorganism glycans. This thesis addressed the bottleneck in oligosaccharide assembly of Lewis type-I and type-II chain antigens (Chapter 2). A minimum set of monosaccharide BBs produced a whole family of these structurally-related glycans, which are in high demand for diverse biological studies. Careful BB design and optimization of AGA conditions allowed me to assemble the desired oligosaccharides with excellent stereoselectivity, and complex, branched oligosaccharides like nonasaccharide KH-1 were assembled overnight. Many BBs and the linker-functionalized resin used are now commercially available. In this project, a new bottleneck was faced in the deprotection step, and evidenced the importance of the choice of deprotection and purification methods, especially in the case of large or complex structures. The synthesized glycans, bearing a C5-aminolinker at the reducing end, are readily used and the produced structures are currently being utilized in diverse applications, as illustrated by the production of a KH-1 glycoconjugate used in cancer immunotherapy research. The AGA methodology developed holds great potential for prompt expansion into the assembly of unnatural analogues, that could serve as tools for understanding structure-property relationships or as probes for NMR studies.

In the case of GalN-containing glycans, a bottleneck resided in the key APS step during building block synthesis. This was addressed by establishing a continuous flow procedure for the APS of 3,4,6-tri-*O*-acetyl-D-galactal, that yielded a reproducible and scalable method and at the same time addressed safety concerns in the handling of azido species (Chapter 3). This method will be used in the Seeberger group to facilitate the production of diverse GalN building blocks, which are required for the development of AGA methods for stereoselective poly α-

GalN linkages, an area of the glycospace that remains to be covered by this approach. Studies related to antigenic oligosaccharides of certain bacterial and fungal pathogens will benefit from expeditious access to glycans bearing multiple α-GalN units.

While the work performed in this thesis successfully attended to certain limitations in glycan synthesis, it also highlighted remaining challenges where the focus needs to be set next. Some of the obstacles detected during the AGA optimization conducted in this thesis started being investigated in the Seeberger group since then. A milder capping procedure, compatible with the presence of primary benzyl groups, was developed.[64] The introduction of this capping step in the AGA coupling cycle facilitates purification from deletion sequences and reduces overall building block consumption. The use of photocleavable linkers is of great practicity for the synthetic strategy. However, AGA yields are limited by photocleavage efficiency to realease the oligosaccharide from the solid support, as it is affected by photochemical side reactions.[61] Studies into modified photocleavable groups were conducted, but an alternative that would provide conjugation-ready glycans with improved cleavage efficiency was not met yet.[180]

As longer or more complex oligosaccharides are being synthesized, the bottleneck moved downstream in the overall process. Current challenges rest in the deprotection and purification of final structures, which may be difficulted by aggregation and solubility issues.[67,137] Recently developed protocols in which methanolysis is performed on the resin-bound oligosaccharide seem to be advantageous.[137] This may be due to a combined effect of oligosaccharide aggregation being prevented by the solid support, and the possibility of introducing a washing step prior to photocleavage that facilitates subsequent hydrogenolysis. Additionally, the field would benefit from a better understanding of the collective behavior of oligosaccharides in solution, and the development of new, efficient deprotection methods.

Due to the complexity of carbohydrate structures, NMR characterization of limited sample amounts is time-consuming. Moreover, on occasion more glycan is required for NMR characterization than for its intended application (*e.g.* glycan arrays). The combination of mass spectrometry with other spectroscopic techniques are attractive alternatives since the analysis is fast and requires minimum sample amounts without derivatization. IM-MS or infrared multiple photon dissociation (IRPMD)-MS are techniques that have shown the capability to resolve diverse carbohydrate isomerisms such as monosaccharide content, anomeric configuration, regiochemistry and stereochemistry of the glycosidic linkage. Furthermore, IM-MS proved fit for discerning between regiosiomeric Lewis epitopes.[133] Synthetic carbohydrate standards will help to further develop these technologies for carbohydrate sequencing.

Glycan production through AGA will continue providing molecular tools that are fundamental for glycobiology research. The supply of a variety of Lewis antigens with this platform will hopefully expedite its use in diverse research areas. The synthesis through AGA of poly-LacNAc TACAs KH-1 and Le^x-dimer is the starting point for the development of new therapeutic and diagnostic tools for cancer. Finally, engaging in basic research to establish safe and scalable reactions at the building block synthesis stage will facilitate expanding the AGA scope to other structural families.

5 References

(1) Guberman, M.; Seeberger, P. H. *J. Am. Chem. Soc.* **2019**, *141*, 5581–5592.

(2) *Essentials of Glycobiology*, 2nd ed.; Varki, A., Cummings, R. D., Esko, J. D., Freeze, H. H., Stanley, P., Bertozzi, C. R., Hart, G. W., Etzler, M. E., Eds.; Cold Spring Harbor Laboratory Press: Cold Spring Harbor, 2009.

(3) Werz, D. B.; Ranzinger, R.; Herget, S.; Adibekian, A.; Von der Lieth, C. W.; Seeberger, P. H. *ACS Chem. Biol.* **2007**, *2*, 685–691.

(4) Seeberger, P. H. *Acc. Chem. Res.* **2015**, *48*, 1450–1463.

(5) Nedra, D.; Castro, S. P. M.; Paulín, E. G. L.; Kwiatkowski, S.; Edgar, S.; Reyes, R. E.; González, C. R.; Jiménez, R. C.; Herrera, O.; Andrade, A. A.; et al. *The Complex World of Polysaccharides*; Karunaratne, D. N., Ed.; InTech, 2012.

(6) Schumann, B.; Hahm, H. S.; Parameswarappa, S. G.; Reppe, K.; Wahlbrink, A.; Govindan, S.; Kaplonek, P.; Pirofski, L.; Witzenrath, M.; Anish, C.; et al. *Sci. Transl. Med.* **2017**, *9*, eaaf5347.

(7) Zhu, X.; Schmidt, R. R. *Angew. Chem. Int. Ed.* **2009**, *48*, 1900–1934.

(8) Stick, R. V; Williams, S. J. Synthesis and Protecting Groups. In *Carbohydrates: the Essential Molecules of Life*; Elsevier Ltd: Amsterdam, 2009; pp 35–74.

(9) Lipták, a; Borbás, A.; Bajza, A. Protecting Group Manipulations in Carbohydrate Synthesis. In *Comprehensive Glycoscience*; Elsevier Ltd, 2007; pp 203–259.

(10) *Handbook of Chemical Glycosylation*; Demchenko, A. V., Ed.; Wiley-VCH: Weinheim, 2008.

(11) Komarova, B. S.; Tsvetkov, Y. E.; Nifantiev, N. E. Design of α-Selective Glycopyranosyl Donors Relying on Remote Anchimeric Assistance. *Chemical Record*. 2016, pp 488–506.

(12) Imamura, A.; Ando, H.; Korogi, S.; Tanabe, G.; Muraoka, O.; Ishida, H.; Kiso, M. *Tetrahedron Lett.* **2003**, *44*, 6725–6728.

(13) Panza, M.; Pistorio, S. G.; Stine, K. J.; Demchenko, A. V. *Chem. Rev.* **2018**, *118*, 8105–8150.

(14) Moremen, K. W.; Ramiah, A.; Stuart, M.; Steel, J.; Meng, L.; Forouhar, F.; Moniz, H. A.; Gahlay, G.; Gao, Z.; Chapla, D.; et al. *Nat. Chem. Biol.* **2018**, *14*, 156–162.

(15) Yu, H.; Chen, X. *Org. Biomol. Chem.* **2016**, *14*, 2809–2818.

(16) Wen, L.; Edmunds, G.; Gibbons, C.; Zhang, J.; Gadi, M. R.; Zhu, H.; Fang, J.; Liu, X.; Kong, Y.; Wang, P. G. *Chem. Rev.* **2018**, *118*, 8151–8187.

(17) Zhu, H.; Wu, Z.; Gadi, M. R.; Wang, S.; Guo, Y.; Edmunds, G.; Guan, W.; Fang, J.

Bioorganic Med. Chem. Lett. **2017**, *27*, 4285–4287.

(18) Prudden, A. R.; Liu, L.; Capicciotti, C. J.; Wolfert, M. A.; Wang, S.; Gao, Z.; Meng, L.; Moremen, K. W.; Boons, G.-J. *Proc. Natl. Acad. Sci.* **2017**, *114*, 6954–6959.

(19) Santra, A.; Li, Y.; Yu, H.; Slack, T. J.; Wang, P. G.; Chen, X. *Chem. Commun.* **2017**, *53*, 8280–8283.

(20) Hwang, J.; Yu, H.; Malekan, H.; Sugiarto, G.; Li, Y.; Qu, J.; Nguyen, V.; Wu, D.; Chen, X. *Chem. Commun.* **2014**, *50*, 3159–3162.

(21) Matsushita, T.; Nagashima, I.; Fumoto, M.; Ohta, T.; Yamada, K.; Shimizu, H.; Hinou, H.; Naruchi, K.; Ito, T.; Kondo, H.; et al. *J. Am. Chem. Soc.* **2010**, *132*, 16651–16656.

(22) Zhang, J.; Chen, C.; Gadi, M. R.; Gibbons, C.; Guo, Y.; Cao, X.; Edmunds, G.; Wang, S.; Liu, D.; Yu, J.; et al. *Angew. Chem. Int. Ed.* **2018**, *57*, 16638–16642.

(23) Heinzler, R.; Fischöder, T.; Elling, L.; Franzreb, M. *Adv. Synth. Catal.* **2019**, 4506–4516.

(24) Cha, T. W.; Quo, A.; Zhu, X. Y. *Proteomics* **2005**, *5*, 416–419.

(25) Kulkarni, S. S.; Wang, C. C.; Sabbavarapu, N. M.; Podilapu, A. R.; Liao, P. H.; Hung, S. C. *Chem. Rev.* **2018**, *118*, 8025–8104.

(26) Wu, Y.; Xiong, D.-C.; Chen, S.-C.; Wang, Y.-S.; Ye, X.-S. *Nat. Commun.* **2017**, *8*, 14851.

(27) Zhang, Z.; Ollmann, I. R.; Ye, X. S.; Wischnat, R.; Baasov, T.; Wong, C. H. *J. Am. Chem. Soc.* **1999**, *121*, 734–753.

(28) Cheng, C.-W.; Zhou, Y.; Pan, W.-H.; Dey, S.; Wu, C.-Y.; Hsu, W.-L.; Wong, C.-H. *Nat. Commun.* **2018**, *9*, 5202.

(29) Ratner, D. M.; Murphy, E. R.; Jhunjhunwala, M.; Snyder, D. A.; Jensen, K. F.; Seeberger, P. H. *Chem. Commun.* **2005**, No. 5, 578–580.

(30) Fukase, K.; Takashina, M.; Hori, Y.; Tanaka, D.; Tanaka, K.; Kusumoto, S. *Synlett* **2005**, No. 15, 2342–2346.

(31) Geyer, K.; Seeberger, P. H. *Helv. Chim. Acta* **2007**, *90*, 395–403.

(32) Chatterjee, S.; Moon, S.; Hentschel, F.; Gilmore, K.; Seeberger, P. H. *J. Am. Chem. Soc.* **2018**, *140*, 11942–11953.

(33) Carrel, F. R.; Geyer, K.; Codée, J. D. C.; Seeberger, P. H. *Org. Lett.* **2007**, *9*, 2285–2288.

(34) Cancogni, D.; Lay, L. *Synlett* **2014**, *25*, 2873–2878.

(35) Aronow, J.; Stanetty, C.; Baxendale, I. R.; Mihovilovic, M. D. *Monatsh. Chem.* **2019**, *150*, 11–19.

(36) Masui, S.; Manabe, Y.; Hirao, K.; Shimoyama, A.; Fukuyama, T.; Ryu, I.; Fukase, K. *Synlett* **2019**, *30*, 397–400.

(37) Marion, K. C.; Wooke, Z.; Pohl, N. L. B. *Carbohydr. Res.* **2018**, *468*, 23–29.

(38) Odedra, A.; Geyer, K.; Gustafsson, T.; Gilmour, R.; Seeberger, P. H. *Chem. Commun.* **2008**, No. 26, 3025–3027.

(39) Manmode, S.; Tanabe, S.; Yamamoto, T.; Sasaki, N.; Nokami, T.; Itoh, T. *ChemistryOpen* **2019**, *8*, 869–872.

(40) Nokami, T.; Hayashi, R.; Saigusa, Y.; Shimizu, A.; Liu, C.-Y.; Mong, K.-K. T.; Yoshida, J. *Org. Lett.* **2013**, *15*, 4520–4523.

(41) Tang, S. L.; Linz, L. B.; Bonning, B. C.; Pohl, N. L. B. *J. Org. Chem.* **2015**, *80*, 10482–10489.

(42) Ganesh, N. V.; Fujikawa, K.; Tan, Y. H.; Stine, K. J.; Demchenko, A. V. *Org. Lett.* **2012**, *14*, 3036–3039.

(43) Plante, O. J.; Palmacci, E. R.; Seeberger, P. H. *Science* **2001**, *291*, 1523–1527.

(44) Hahm, H. S.; Schlegel, M. K.; Hurevich, M.; Eller, S.; Schuhmacher, F.; Hofmann, J.; Pagel, K.; Seeberger, P. H. *Proc. Natl. Acad. Sci.* **2017**, *114*, E3385–E3389.

(45) Naresh, K.; Schumacher, F.; Hahm, H. S.; Seeberger, P. H. *Chem. Commun.* **2017**, *53*, 9085–9088.

(46) Merrifield, R. B. *J. Am. Chem. Soc.* **1963**, *85*, 2149–2154.

(47) Collot, M.; Eller, S.; Weishaupt, M.; Seeberger, P. H. *Beilstein J. Org. Chem.* **2013**, *9*, 97–105.

(48) Hahm, H. S.; Liang, C.-Fu; Lai, C.-H.; Fair, R. J.; Schuhmacher, F.; Seeberger, P. H. *J. Org. Chem.* **2016**, *81*, 5866–5877.

(49) Senf, D.; Ruprecht, C.; de Kruijff, G. H. M.; Simonetti, S. O.; Schuhmacher, F.; Seeberger, P. H.; Pfrengle, F. *Chem. Eur. J.* **2017**, *23*, 3197–3205.

(50) Dallabernardina, P.; Schuhmacher, F.; Seeberger, P. H.; Pfrengle, F. *Chem. Eur. J.* **2017**, *23*, 3191–3196.

(51) Geert Volbeda, A.; Van Mechelen, J.; Meeuwenoord, N.; Overkleeft, H. S.; Van Der Marel, G. A.; Codée, J. D. C. *J. Org. Chem.* **2017**, *82*, 12992–13002.

(52) Esposito, D.; Hurevich, M.; Castagner, B.; Wang, C. C.; Seeberger, P. H. *Beilstein J. Org. Chem.* **2012**, *8*, 1601–1609.

(53) Seeberger, P. H.; Haase, W. C. *Chem. Rev.* **2000**, *100*, 4349–4393.

(54) Hahm, H. S.; Hurevich, M.; Seeberger, P. H. *Nat. Commun.* **2016**, *7*, 12482.

(55) Dallabernardina, P.; Ruprecht, C.; Smith, P. J.; Hahn, M. G.; Urbanowicz, B. R.; Pfrengle, F. *Org. Biomol. Chem.* **2017**, *15*, 9996–10000.

(56) Andrade, R. B.; Plante, O. J.; Melean, L. G.; Seeberger, P. H. *Org. Lett.* **1999**, *1*, 1811–1814.

(57) Fraser-Reid, B.; Udodong, U. E.; Wu, Z.; Ottosson, H.; Merritt, J. R.; Rao, C. S.; Roberts, C.; Madsen, R. *Synlett* **1992**, *1992*, 927–942.

(58) Eller, S.; Collot, M.; Yin, J.; Hahm, H. S.; Seeberger, P. H. *Angew. Chem. Int. Ed.* **2013**, *52*, 5858–5861.

(59) Dallabernardina, P.; Schuhmacher, F.; Seeberger, P. H.; Pfrengle, F. *Org. Biomol. Chem.* **2016**, *14*, 309–313.

(60) Wilsdorf, M.; Schmidt, D.; Bartetzko, M. P.; Dallabernardina, P.; Schuhmacher, F.; Seeberger, P. H.; Pfrengle, F. *Chem. Commun.* **2016**, *52*, 10187–10189.

(61) Guillier, F.; Orain, D.; Bradley, M. *Chem. Rev.* **2000**, *100*, 2091–2158.

(62) GlycoUniverse www.glycouniverse.com (accessed December 4, 2019).

(63) Schmidt, D.; Schuhmacher, F.; Geissner, A.; Seeberger, P. H.; Pfrengle, F. *Chem. Eur. J.* **2015**, *21*, 5709–5713.

(64) Yu, Y.; Kononov, A.; Delbianco, M.; Seeberger, P. H. *Chem. Eur. J.* **2018**, *24*, 6075–6078.

(65) Bartetzko, M. P.; Schuhmacher, F.; Hahm, H. S.; Seeberger, P. H.; Pfrengle, F. *Org. Lett.* **2015**, *17*, 4344–4347.

(66) Bartetzko, M. P.; Schuhmacher, F.; Seeberger, P. H.; Pfrengle, F. *J. Org. Chem.* **2017**, *82*, 1842–1850.

(67) Delbianco, M.; Kononov, A.; Poveda, A.; Yu, Y.; Diercks, T.; Jiménez-Barbero, J.; Seeberger, P. H. *J. Am. Chem. Soc.* **2018**, *140*, 5421–5426.

(68) Hahm, H. S.; Broecker, F.; Kawasaki, F.; Mietzsch, M.; Heilbronn, R.; Fukuda, M.; Seeberger, P. H. *Chem* **2017**, *2*, 114–124.

(69) Crich, D.; Dudkin, V. *J. Am. Chem. Soc.* **2001**, *123*, 6819–6825.

(70) Kandasamy, J.; Schuhmacher, F.; Hahm, H. S.; Klein, J. C.; Seeberger, P. H. *Chem. Commun.* **2014**, *50*, 1875–1877.

(71) Walvoort, M. T. C.; Volbeda, A. G.; Reintjens, N. R. M.; Van Den Elst, H.; Plante, O. J.; Overkleeft, H. S.; Van Der Marel, G. A.; Codée, J. D. C. *Org. Lett.* **2012**, *14*, 3776–3779.

(72) Kandasamy, J.; Hurevich, M.; Seeberger, P. H. *Chem. Commun.* **2013**, *49*, 4453–4455.

(73) Geert Volbeda, A.; Reintjens, N. R. M.; Overkleeft, H. S.; van der Marel, G. A.; Codée, J. D. C. *European J. Org. Chem.* **2016**, *2016*, 5282–5293.

(74) Weishaupt, M. W.; Matthies, S.; Hurevich, M.; Pereira, C. L.; Hahm, H. S.; Seeberger, P. H. *Beilstein J. Org. Chem.* **2016**, *12*, 1440–1446.

(75) Walvoort, M. T. C.; van den Elst, H.; Plante, O. J.; Kröck, L.; Seeberger, P. H.; Overkleeft, H. S.; van der Marel, G. A.; Codée, J. D. C. *Angew. Chem. Int. Ed.* **2012**,

51, 4393–4396.

(76) Kröck, L.; Esposito, D.; Castagner, B.; Wang, C.-C.; Bindschädler, P.; Seeberger, P. H. *Chem. Sci.* **2012**, *3*, 1617.

(77) Stanley, P.; Hart, G.; Schnaar, R. L.; Darvill, A.; Prestegard, J. J.; Kinoshita, T.; Varki, A.; Cummings, R. D.; Aebi, M.; Packer, N. H.; et al. *Glycobiology* **2015**, *25*, 1323–1324.

(78) Lai, C.-H.; Hahm, H. S.; Liang, C.-F.; Seeberger, P. H. *Beilstein J. Org. Chem.* **2015**, *11*, 617–621.

(79) Fair, R. J.; Hahm, H.-S. S.; Seeberger, P. H. *Chem. Commun.* **2015**, *51*, 6183–6185.

(80) Kamena, F.; Tamborrini, M.; Liu, X.; Kwon, Y. U.; Thompson, F.; Pluschke, G.; Seeberger, P. H. *Nat. Chem. Biol.* **2008**, *4*, 238–240.

(81) Hewitt, M. C.; Snyder, D. A.; Seeberger, P. H. *J. Am. Chem. Soc.* **2002**, *124*, 13434–13436.

(82) Hurevich, M.; Seeberger, P. H. *Chem. Commun.* **2014**, *50*, 1851–1853.

(83) Oyelaran, O.; Gildersleeve, J. C. *Curr. Opin. Chem. Biol.* **2009**, *13*, 406–413.

(84) Geissner, A.; Seeberger, P. H. *Annu. Rev. Anal. Chem.* **2016**, *9*, 223–247.

(85) Geissner, A.; Anish, C.; Seeberger, P. H. *Curr. Opin. Chem. Biol.* **2014**, *18*, 38–45.

(86) Ruprecht, C.; Dallabernardina, P.; Smith, P. J.; Urbanowicz, B. R.; Pfrengle, F. *ChemBioChem* **2018**, *19*, 793–798.

(87) Hofmann, J.; Hahm, H. S.; Seeberger, P. H.; Pagel, K. *Nature* **2015**, *526*, 241–244.

(88) Guberman, M.; Bräutigam, M.; Seeberger, P. H. *Chem. Sci.* **2019**, *10*, 5634–5640.

(89) Cooling, L. *Clin. Microbiol. Rev.* **2015**, *28*, 801–870.

(90) Garcia-Vallejo, J. J.; van Kooyk, Y. *Trends Immunol.* **2013**, *34*, 482–486.

(91) Muramatsu, T.; Muramatsu, H. *Glycoconj. J.* **2004**, *21*, 41–45.

(92) Hakomori, S.-I. *Cancer Res.* **1985**, *45*, 2405–2414.

(93) Feizi, T. *Curr. Opin. Struct. Biol.* **1993**, *3*, 701–710.

(94) Clark, G. F. *Hum. Reprod.* **2013**, *28*, 566–577.

(95) Ramsey, G.; Wolford, J.; Boczkowski, D. J.; Cornell, F. W.; Larson, P.; Starzl, T. E. *Transplant. Proc.* **1987**, *19*, 4591–4594.

(96) Boren, T.; Falk, P.; Roth, K.; Larson, G.; Normark, S. *Science* **1993**, *262*, 1892–1895.

(97) Hakomori, S. -I. *Adv. Cancer Res.* **1989**, *52*, 257–331.

(98) Yan, L.; Lin, B.; Gao, L.; Gao, S.; Liu, C.; Wang, C.; Wang, Y.; Zhang, S.; Iwamori, M. *Int. J. Mol. Sci.* **2010**, *11*, 4441–4451.

(99) Heimburg-Molinaro, J.; Lum, M.; Vijay, G.; Jain, M.; Almogren, A.; Rittenhouse-Olson, K. *Vaccine* **2011**, *29*, 8802–8826.

(100) Hakomori, S. -I.; Nudelman, E.; Levery, S. B.; Kannagi, R. *J. Biol. Chem.* **1984**, *259*,

4672–4680.

(101) Fukushi, Y.; Hakomori, S. -I.; Nudelman, E.; Cochran, N. *J. Biol. Chem.* **1984**, *259*, 4681–4685.

(102) *World Cancer Report 2014*; Stewart, B. W., Wild, C. P., Eds.; International Agency for Research on Cancer: Lyon, 2014.

(103) Mihich, E.; Ehrke, M. J. Immunomodulation by Anticancer Drugs in Therapeutics. In *Cancer Therapy*; Springer-Verlag: Berlin Heidelberg, 1993; pp 121–133.

(104) Snook, A. E.; Waldman, S. A. *Discov. Med.* **2013**, *15*, 120–125.

(105) Swann, J. B.; Smyth, M. J. *J. Clin. Invest.* **2007**, *117*, 1137–1146.

(106) Sengupta, N.; MacFie, T. S.; MacDonald, T. T.; Pennington, D.; Silver, A. R. *Pathol. Res. Pract.* **2010**, *206*, 1–8.

(107) Hakomori, S. -I. *Cancer Res.* **1996**, *53*, 5309–5318.

(108) Hakomori, S. -I.; Zhang, Y. *Chem. Biol.* **1997**, *4*, 97–104.

(109) Hakomori, S.-I. *Annu. Rev. Immunol.* **1984**, *2*, 103–126.

(110) O'Cearbhaill, R. E.; Ragupathi, G.; Zhu, J.; Wan, Q.; Mironov, S.; Yang, G.; Spassova, M. K.; Iasonos, A.; Kravetz, S.; Ouerfelli, O.; et al. *Cancers.* **2016**, *8*, 46.

(111) Ragupathi, G.; Koide, F.; Livingstoi, P. O.; Cho, Y. S.; Endo, A.; Wan, Q.; Spassova, M. K.; Keding, S. J.; Allen, J.; Ouerfelli, O.; et al. *J. Am. Chem. Soc.* **2006**, *128*, 2715–2725.

(112) Ragupathi, G.; Deshpande, P. P.; Coltart, D. M.; Kim, H. M.; Williams, L. J.; Danishefsky, S. J.; Livingston, P. O. *Int. J. Cancer* **2002**, *99*, 207–212.

(113) Mellman, I.; Coukos, G.; Dranoff, G. *Nature* **2011**, *480*, 480–489.

(114) Muyldermans, S. *Annu. Rev. Biochem.* **2013**, *82*, 775–797.

(115) Schoonooghe, S.; Laoui, D.; Van Ginderachter, J. A.; Devoogdt, N.; Lahoutte, T.; De Baetselier, P.; Raes, G. *Immunobiology* **2012**, *217*, 1266–1272.

(116) Lloyd, K. O. *Glycoconj. J.* **2000**, *17*, 531–541.

(117) Ryzhov, I. M.; Korchagina, E. Y.; Tuzikov, A. B.; Popova, I. S.; Tyrtysh, T. V.; Pazynina, G. V.; Henry, S. M.; Bovin, N. V. *Carbohydr. Res.* **2016**, *435*, 83–96.

(118) Kamath, V.; Hindsgaul, O. *Synlett* **2003**, *2003*, 1327–1330.

(119) Spassova, M. K.; Bornmann, W. G.; Ragupathi, G.; Sukenick, G.; Livingston, P. O.; Danishefsky, S. J. *J. Org. Chem.* **2005**, *70*, 3383–3395.

(120) Routenberg Love, K.; Seeberger, P. H. *Angew. Chem. Int. Ed.* **2004**, *43*, 602–605.

(121) Mandal, P. K.; Turnbull, W. B. *Carbohydr. Res.* **2011**, *346*, 2113–2120.

(122) Blixt, O.; Norberg, T. *J. Org. Chem.* **1998**, *63*, 2705–2710.

(123) Bommer, R.; Kinzy, W.; Schmidt, R. R. *Liebigs Ann. Chem.* **1991**, 425–433.

(124) Li, Q.; Guo, Z. *Org. Lett.* **2017**, *19*, 6558–6561.
(125) Deshpande, P. P.; Danishefsky, S. J. *Nature* **1997**, *387*, 164–166.
(126) Smith, R.; Müller-Bunz, H.; Zhu, X. *Org. Lett.* **2016**, *18*, 3578–3581.
(127) Calosso, M.; Tambutet, G.; Charpentier, D.; St-Pierre, G.; Vaillancourt, M.; Bencheqroun, M.; Gratton, J. P.; Prévost, M.; Guindon, Y. *ACS Med. Chem. Lett.* **2014**, *5*, 1054–1059.
(128) De Jong, A. R.; Hagen, B.; Van Der Ark, V.; Overkleeft, H. S.; Codée, J. D. C.; Van Der Marel, G. A. *J. Org. Chem.* **2012**, *77*, 108–125.
(129) Crich, D.; Picione, J. *Org. Lett.* **2003**, *5*, 781–784.
(130) Satoh, H.; Hansen, H. S.; Manabe, S.; Van Gunsteren, W. F.; Hünenberger, P. H. *J. Chem. Theory Comput.* **2010**, *6*, 1783–1797.
(131) Hakomori, S. -I. *Biochim. Biophys. Acta, Gen. Subj.* **2008**, *1780*, 325–346.
(132) Blank, D.; Dotz, V.; Geyer, R.; Kunz, C. *Adv. Nutr.* **2012**, *3*, 440S-449S.
(133) Hofmann, J.; Stuckmann, A.; Crispin, M.; Harvey, D. J.; Pagel, K.; Struwe, W. B. *Anal. Chem.* **2017**, *89*, 2318–2325.
(134) Aeschbacher, T.; Zierke, M.; Smieško, M.; Collot, M.; Mallet, J. M.; Ernst, B.; Allain, F. H. T.; Schubert, M. *Chem. Eur. J.* **2017**, *23*, 11598–11610.
(135) Dalvit, C.; Vulpetti, A. *J. Med. Chem.* **2019**, *62*, 2218–2244.
(136) Martínez, J. D.; Valverde, P.; Delgado, S.; Romanò, C.; Linclau, B.; Reichardt, N. C.; Oscarson, S.; Ardá, A.; Jiménez-Barbero, J.; Cañada, F. J. *Molecules* **2019**, *24*, 2337.
(137) Yu, Y.; Tyrikos-Ergas, T.; Zhu, Y.; Fittolani, G.; Bordoni, V.; Singhal, A.; Fair, R. J.; Grafmüller, A.; Seeberger, P. H.; Delbianco, M. *Angew. Chem.* **2019**, *131*, 13261–13266.
(138) Lee, J.-C.; Greenberg, W. A.; Wong, C.-H. *Nat. Protoc.* **2007**, *1*, 3143–3152.
(139) Pal, K. B.; Mukhopadhyay, B. *Carbohydr. Res.* **2014**, *400*, 9–13.
(140) Shibata, T. K.; Matsumura, F.; Wang, P.; Yu, S.; Chou, C.-C.; Khoo, K.-H.; Kitayama, K.; Akama, T. O.; Sugihara, K.; Kanayama, N.; et al. *J. Biol. Chem.* **2012**, *287*, 6592–6602.
(141) Tai, C. A.; Kulkarni, S. S.; Hung, S. C. *J. Org. Chem.* **2003**, *68*, 8719–8722.
(142) Vankayalapati, H.; Singh, G. *J. Chem. Soc. Perkin Trans. 1* **2000**, No. 14, 2187–2193.
(143) Hou, D.; Lowary, T. L. *J. Org. Chem.* **2006**, *74*, 2278–2289.
(144) Guberman, M.; Pieber, B.; Seeberger, P. H. *Org. Process Res. Dev.* **2019,** *23*, 2764-2770.
(145) Hang, H. C.; Bertozzi, C. R. *Bioorg. Med. Chem.* **2005**, *13*, 5021–5034.

(146) Gill, D. J.; Clausen, H.; Bard, F. *Trends Cell Biol.* **2011**, *21*, 149–158.
(147) Linhardt, R. J.; Toida, T. *Acc. Chem. Res.* **2004**, *37*, 431–438.
(148) Wilson, R. M.; Danishefsky, S. J. *J. Am. Chem. Soc.* **2013**, *135*, 14462–14472.
(149) Knirel, Y. A. O-Specific Polysaccharides of Gram-Negative Bacteria. In *Microbial Glycobiology*; Moran, A. P., Ed.; Elsevier, 2010; pp 57–73.
(150) Roberts, I. S. *Annu. Rev. Microbiol.* **1996**, *50*, 285–315.
(151) Guzman, C. A.; Borsutzky, S.; Griot-Wenk, M.; Metcalfe, I. C.; Pearman, J.; Collioud, A.; Favre, D.; Dietrich, G. *Vaccine* **2006**, *24*, 3804–3811.
(152) Fontaine, T.; Delangle, A.; Simenel, C.; Coddeville, B.; van Vliet, S. J.; van Kooyk, Y.; Bozza, S.; Moretti, S.; Schwarz, F.; Trichot, C.; et al. *PLoS Pathog.* **2011**, *7*, e1002372.
(153) Winterfeld, G. a; Schmidt, R. R. *Angew. Chem. Int. Ed.* **2001**, *40*, 2654–2657.
(154) Leblanc, Y.; Fitzsimmons, B. J.; Springer, J. P.; Rokach, J. *J. Am. Chem. Soc.* **1989**, *111*, 2995–3000.
(155) Bois, J. Du; Tomooka, C. S.; Hong, J.; Carreira, E. M. *J. Am. Chem. Soc.* **1997**, *119*, 3179–3180.
(156) Danishefsky, S. J.; Koseki, K.; Griffith, D. A.; Gervay, J.; Peterson, J. M.; McDonald, F. E.; Oriyama, T. *J. Am. Chem. Soc.* **1992**, *114*, 8331–8333.
(157) Lemieux, R. U.; Ratcliffe, R. M. *Can. J. Chem.* **1979**, *57*, 1244–1251.
(158) Santoyo-Gonzalez, F.; Calvo-Flores, F. G.; Garcia-Mendoza, P.; Hernandez-Mateo, F.; Isac-Garcia, J.; Robles-Diaz, R. *J. Org. Chem.* **1993**, *58*, 6122–6125.
(159) Mironov, Y. V.; Sherman, A. A.; Nifantiev, N. E. *Tetrahedron Lett.* **2004**, *45*, 9107–9110.
(160) Mironov, Y. V.; Sherman, A. A.; Nifantiev, N. E. *Mendeleev Commun.* **2008**, *18*, 241–243.
(161) Czernecki, S.; Ayadi, E.; Randriamandimby, D. *J. Org. Chem.* **1994**, *59*, 8256–8260.
(162) Thompson, P.; Lakshminarayanan, V.; Supekar, N. T.; Bradley, J. M.; Cohen, P. A.; Wolfert, M. A.; Gendler, S. J.; Boons, G. J. *Chem. Commun.* **2015**, *51*, 10214–10217.
(163) Czernecki, S.; Randriamandimby, D. *Tetrahedron Lett.* **1993**, *34*, 7915–7916.
(164) Langerman, N. Chemical Safety: Explosion hazard in synthesis of azidotrimethylsilane http://cen.acs.org/articles/92/i43/Chemical-Safety-Explosion-hazard-synthesis.html (accessed October 10, 2019).
(165) Baxendale, I. R. *J. Chem. Technol. Biotechnol.* **2013**, *88*, 519–552.
(166) Gutmann, B.; Cantillo, D.; Kappe, C. O. *Angew. Chem. Int. Ed.* **2015**, *54*, 6688–6728.
(167) Plutschack, M. B.; Pieber, B.; Gilmore, K.; Seeberger, P. H. *Chem. Rev.* **2017**, *117*, 11796–11893.
(168) Mironov, Y. V.; Grachev, A. A.; Lalov, A. V.; Sherman, A. A.; Egorov, M. P.; Nifantiev,

N. E. *Russ. Chem. Bull.* **2009**, *58*, 284–290.

(169) Nowacki, A.; Liberek, B. *Carbohydr. Res.* **2018**, *462*, 13–27.

(170) Tingoli, M.; Tiecco, M.; Testaferri, L.; Temperini, A. *Synth. Commun.* **1998**, *28*, 1769–1778.

(171) Santoyo-González, F.; Calvo-Flores, F. G.; Hernández-Mateo, F.; García-Mendoza, P.; Isac-García, J.; Pérez-Alvarez, M. D. *Synlett* **1994**, *1994*, 454–456.

(172) SanMartin, R.; Tavassoli, B.; Walsh, K. E.; Walter, D. S.; Gallagher, T. *Org. Lett.* **2000**, *2*, 4051–4054.

(173) Tiecco, M.; Tingoli, M.; Testaferri, L. *Pure Appl. Chem.* **1993**, *65*, 715–722.

(174) Pedersen, C. M.; Marinescu, L. G.; Bols, M. *Org. Biomol. Chem.* **2005**, *3*, 816–822.

(175) Guetzoyan, L.; Nikbin, N.; Baxendale, I. R.; Ley, S. V. *Chem. Sci.* **2013**, *4*, 764–769.

(176) Hamano, Y.; Matsuura, N.; Kitamura, M.; Takagi, H. *J. Biol. Chem.* **2006**, *281*, 16842–16848.

(177) Lisboa, M. P.; Khan, N.; Martin, C.; Xu, F.-F.; Reppe, K.; Geissner, A.; Govindan, S.; Witzenrath, M.; Pereira, C. L.; Seeberger, P. H. *Proc. Natl. Acad. Sci.* **2017**, *114*, 11063–11068.

(178) Shiao, T. C.; Rodrigue, J.; Renaudet, O.; Roy, R. Synthesis of 3,4,6-Tri-*O*-Acetyl-D-Galactal. In *Carbohydrate Chemistry: Proven Synthetic Methods, Vol. 2*; van der Marel, G. A., Codée, J. D. C., Eds.; CRC Press: Boca Raton, 2014; pp 253–256.

(179) Snider, B. B.; Lin, H. *Synth. Commun.* **1998**, *28*, 1913–1922.

(180) Le Mai Hoang, K.; Pardo-Vargas, A.; Zhu, Y.; Yu, Y.; Loria, M.; Delbianco, M.; Seeberger, P. H. *J. Am. Chem. Soc.* **2019**, *141*, 9079–9086.

According to EU privacy protection prescription, the CV was removed for publication.

According to EU privacy protection prescription, the CV was removed for publication.

According to EU privacy protection prescription, the CV was removed for publication.

Declaration

My doctoral degree thesis entitled “Development of Synthetic Strategies to Address Bottlenecks in Glycan Synthesis” has been prepared by myself and is based on my own work; the work from others has been specifically acknowledged in the text. This thesis is submitted to the Department of Biology, Chemistry and Pharmacy of Freie Universität Berlin to obtain the academic degree Doctor rerum naturalium (Dr. rer. nat.) and has not been submitted for any other degree.

Berlin, March 2020

7 Appendix: NMR Spectra of New Compounds

^{1}H NMR: **2.19**

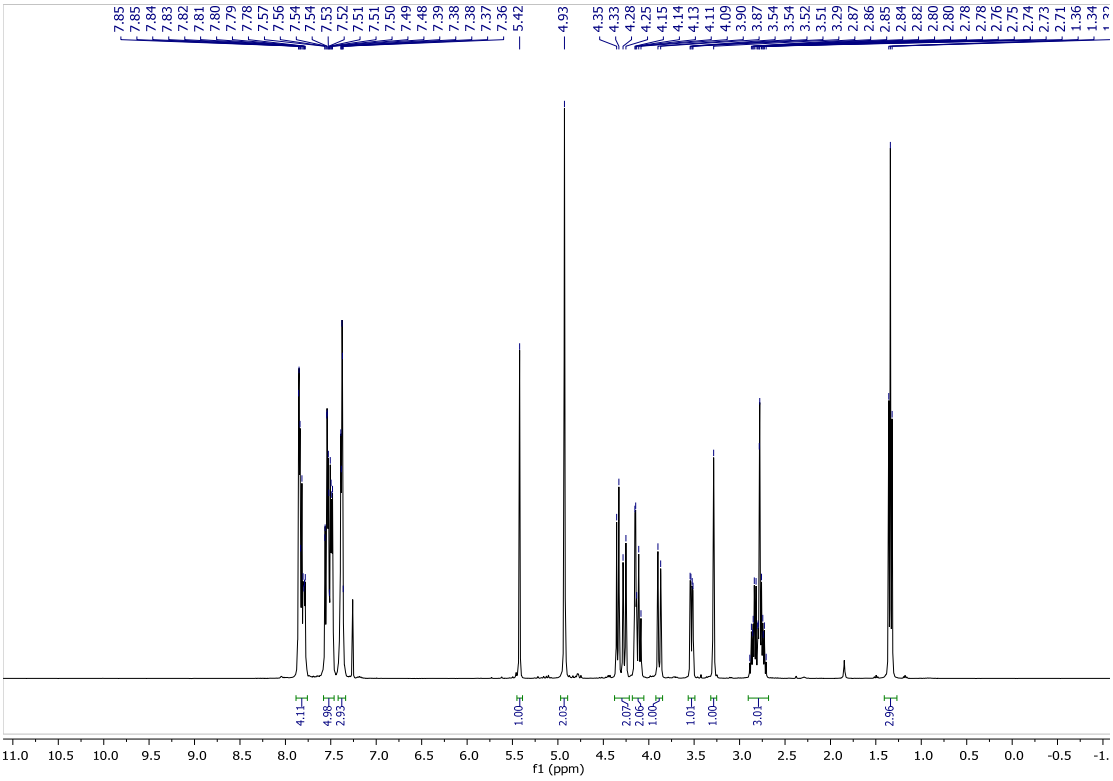

^{13}C NMR: **2.19**

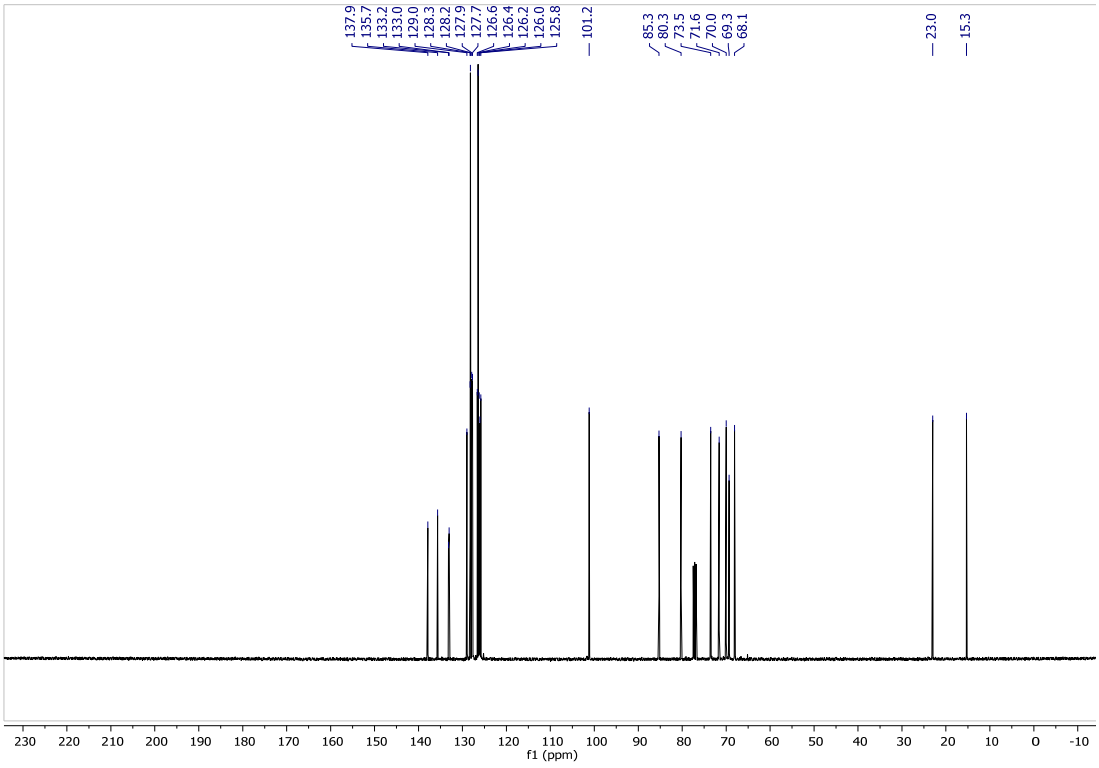

COSY: **2.19**

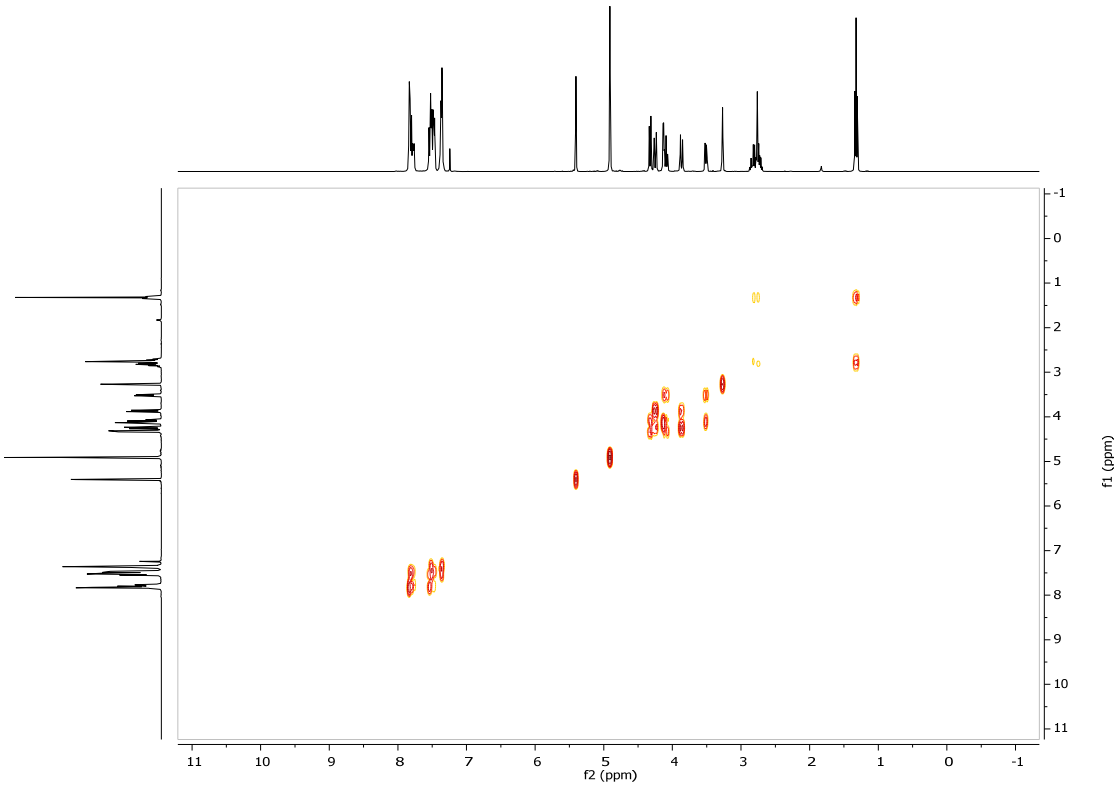

HSQC: **2.19**

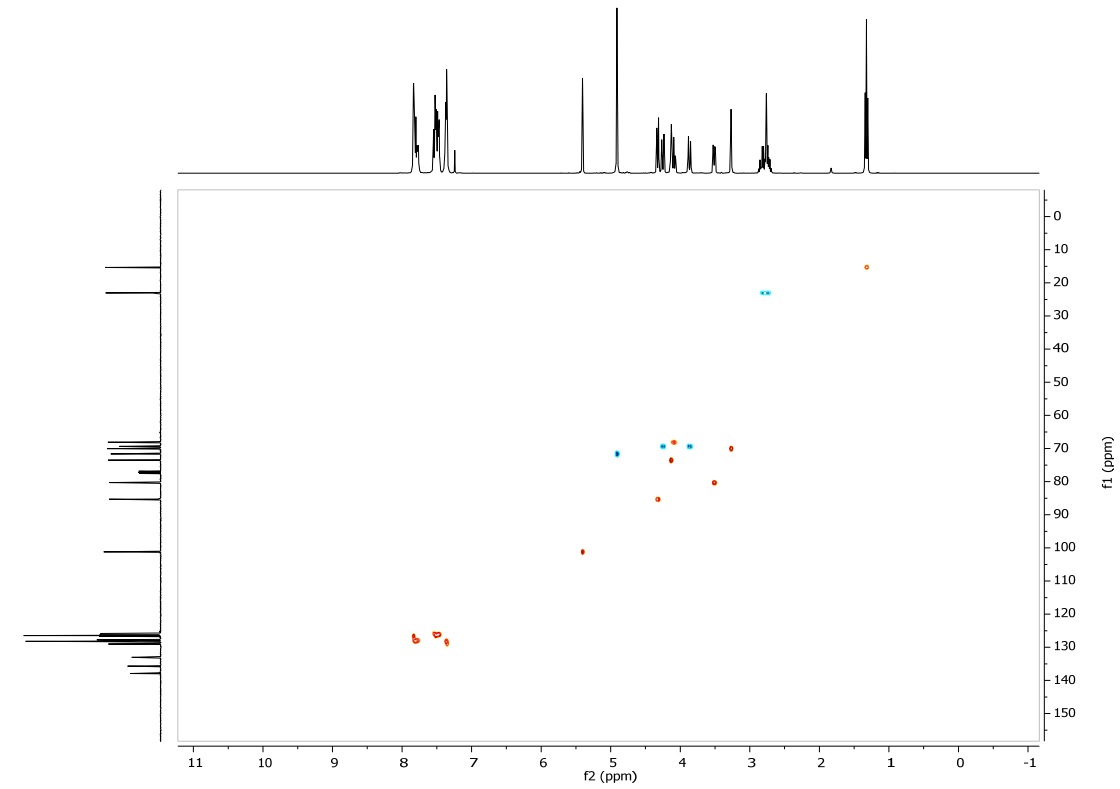

^{1}H NMR: **2.20**

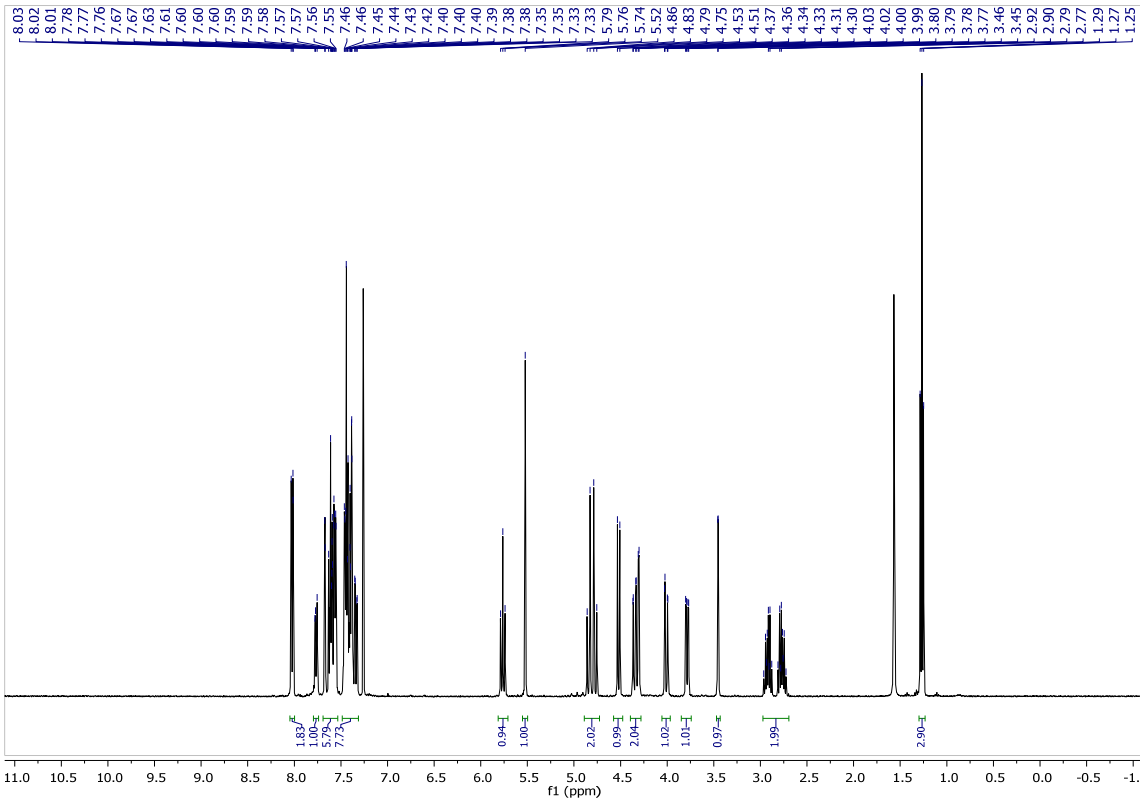

^{13}C NMR: **2.20**

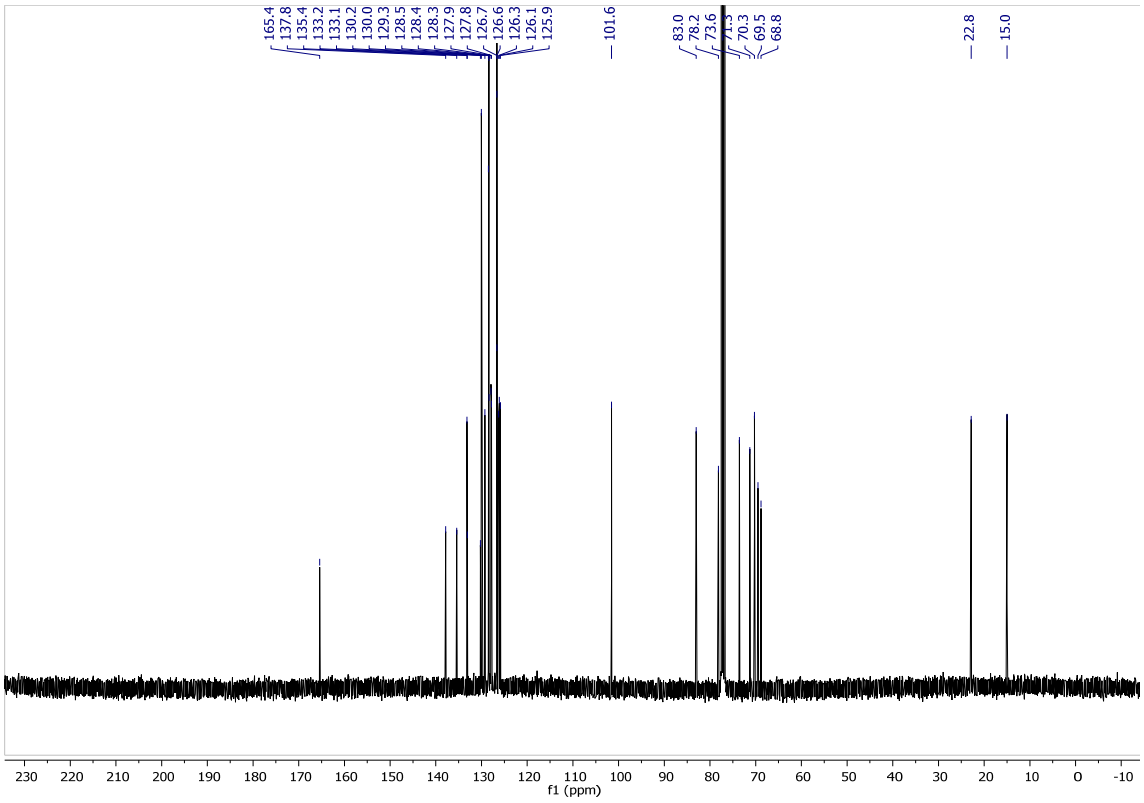

COSY: **2.20**

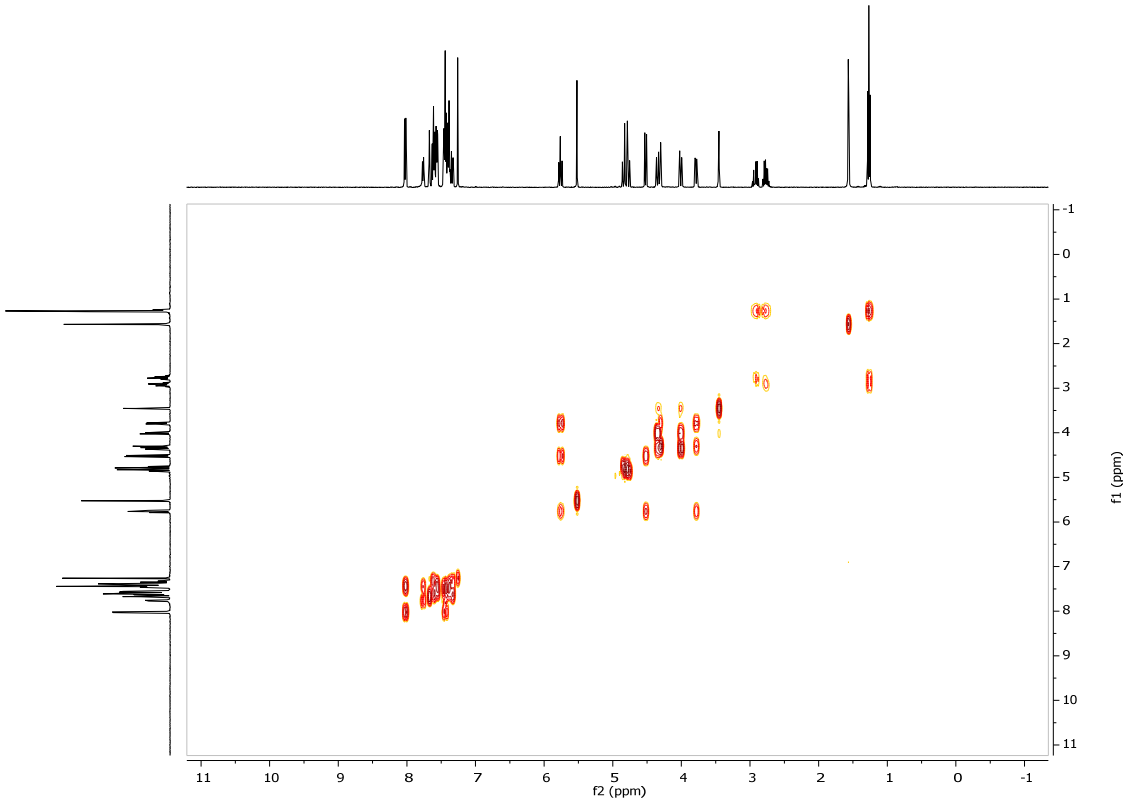

HSQC: **2.20**

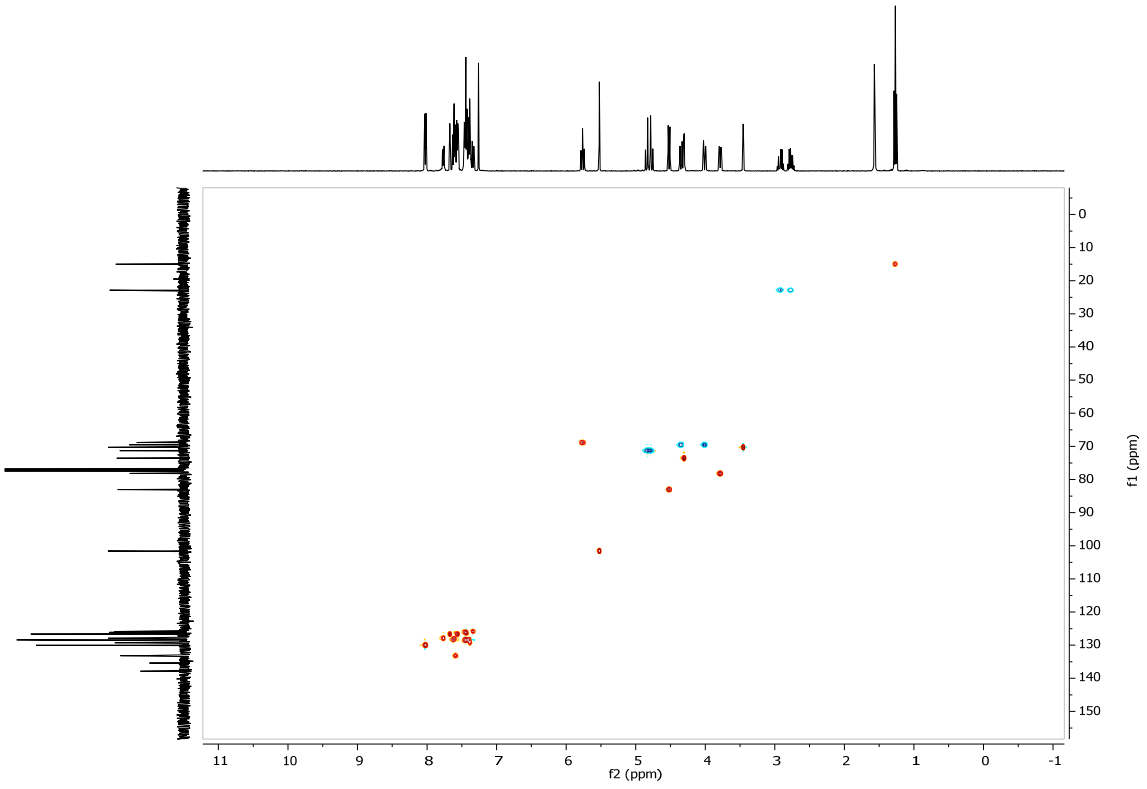

^{1}H NMR: **2.21**

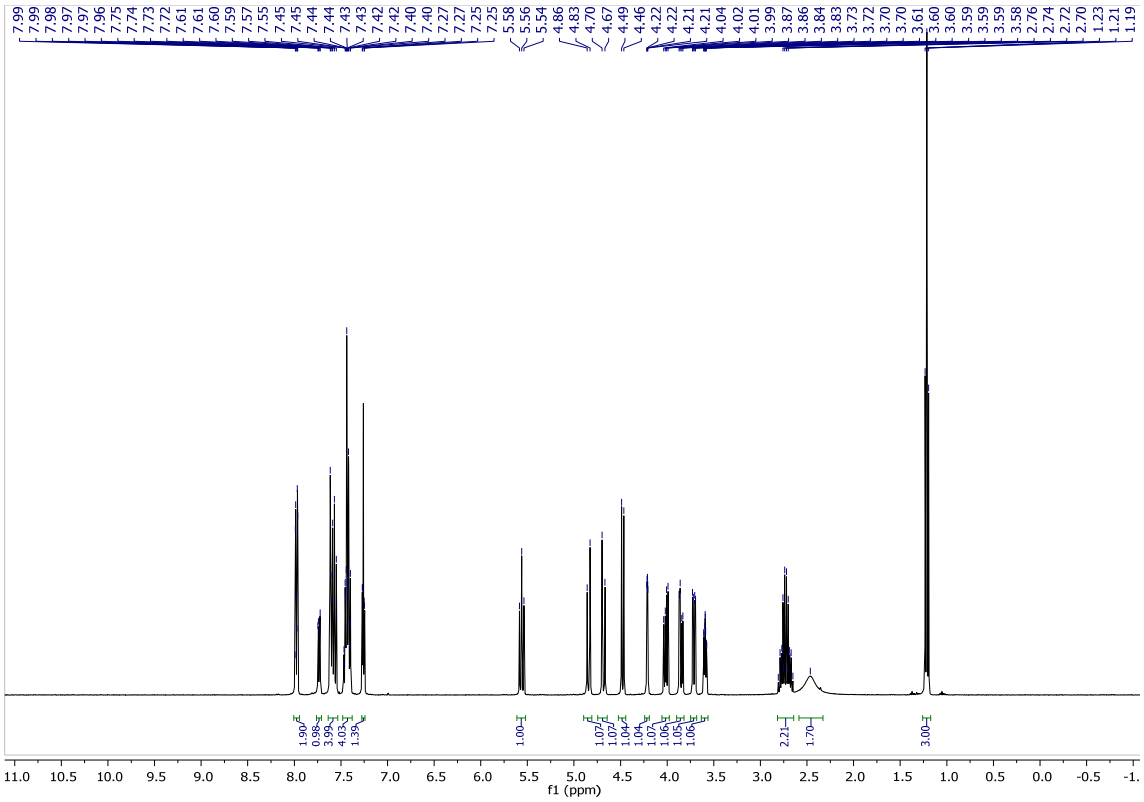

^{13}C NMR: **2.21**

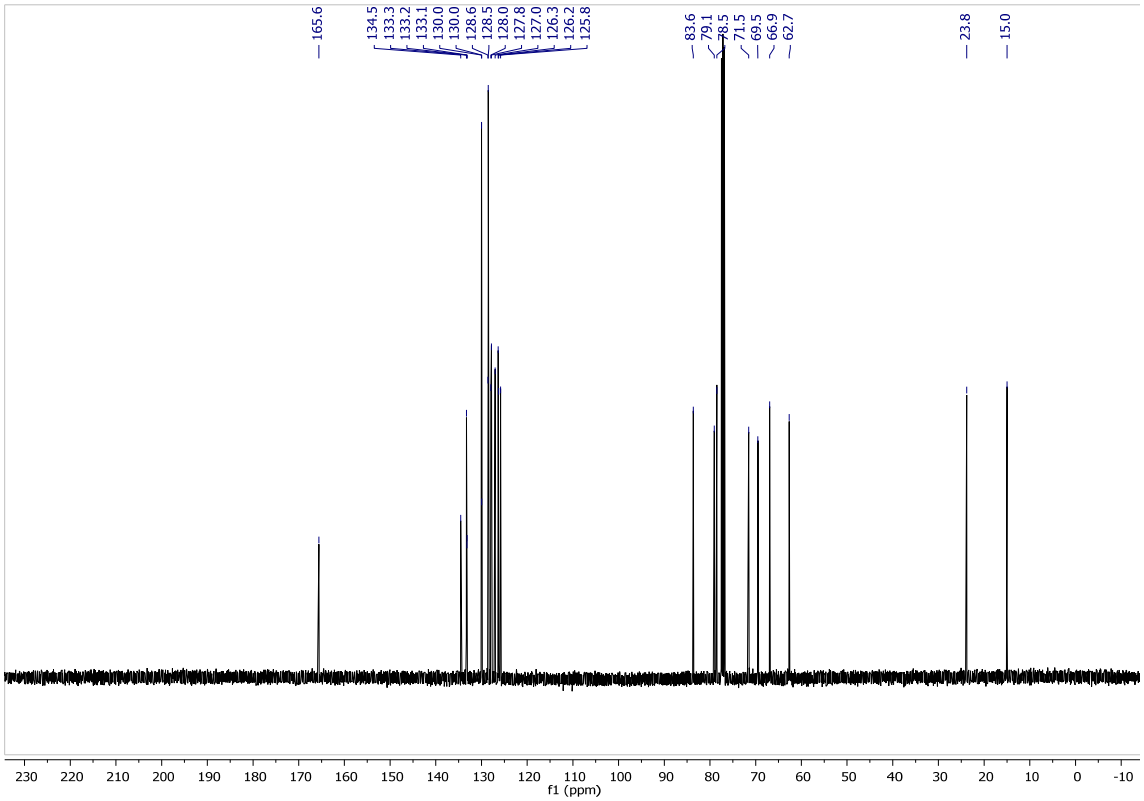

COSY: **2.21**

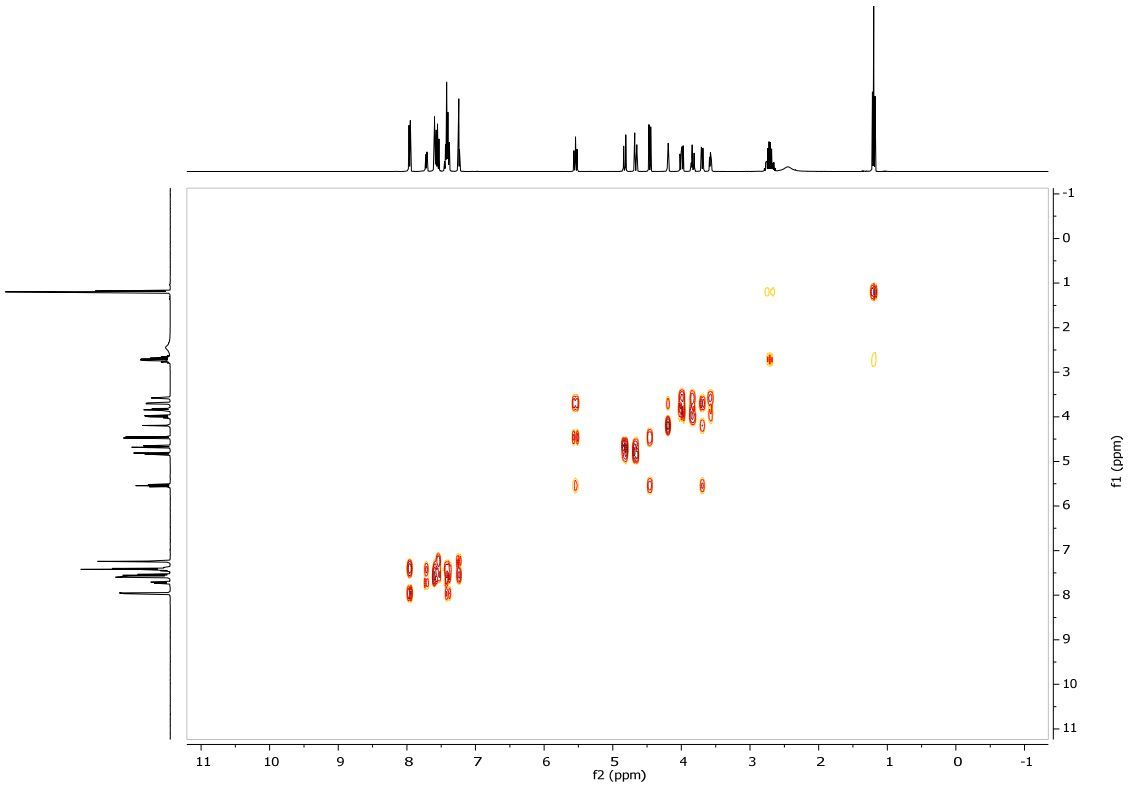

HSQC: **2.21**

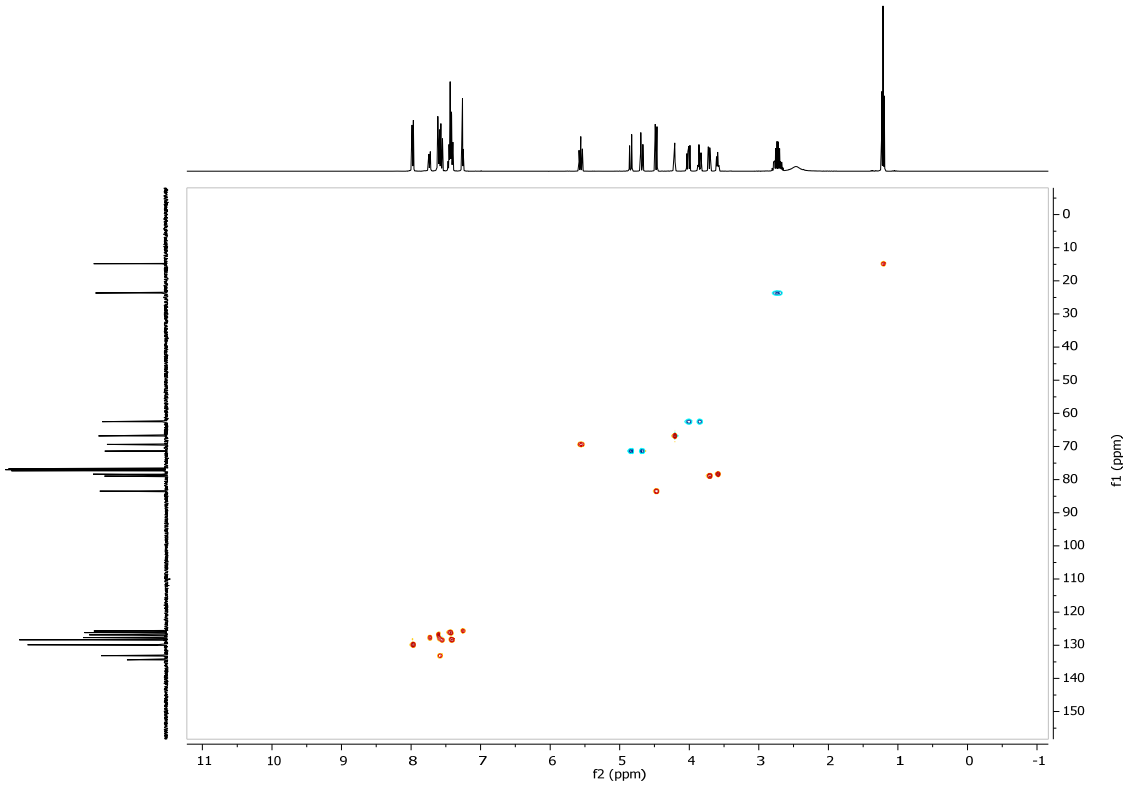

^{1}H NMR: **2.22**

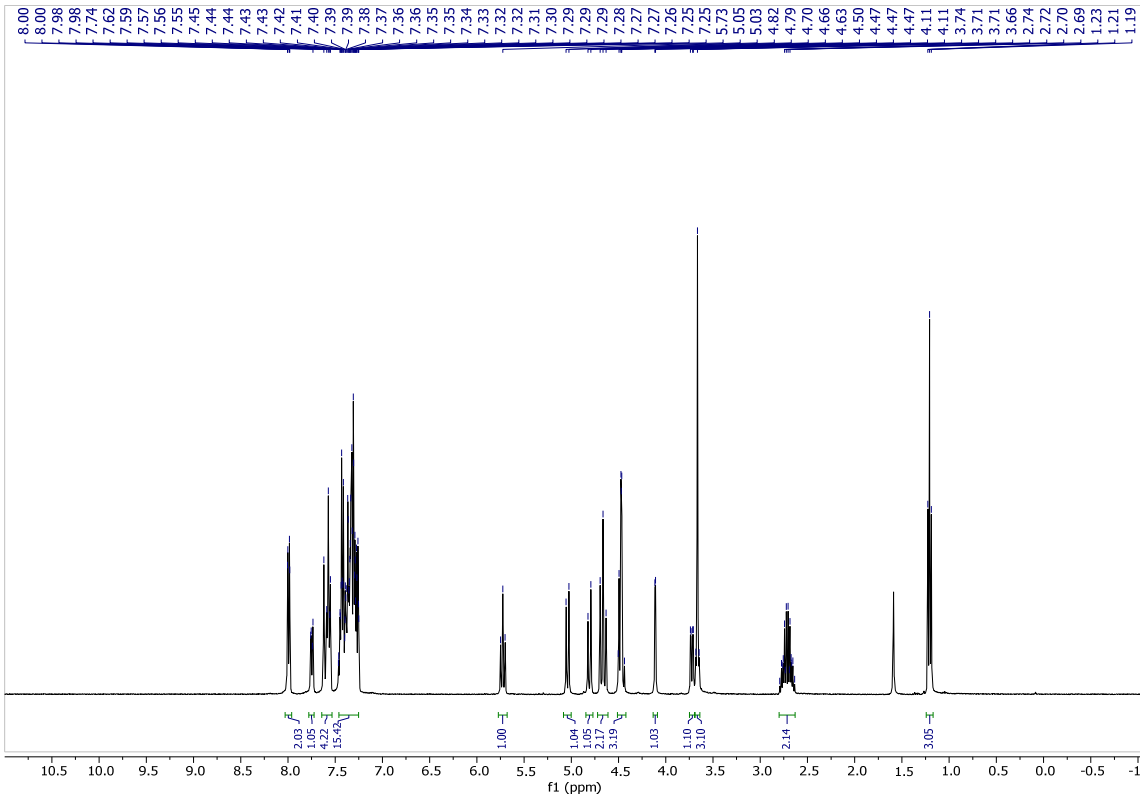

^{13}C NMR: **2.22**

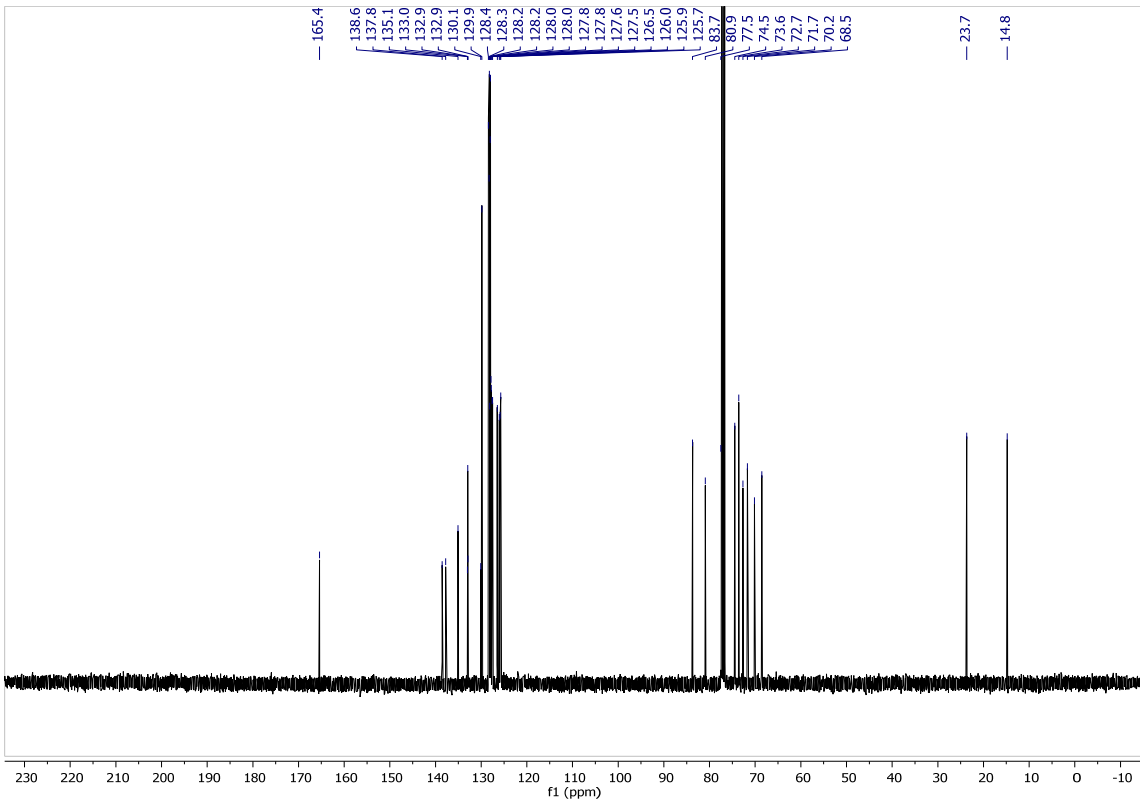

COSY: **2.22**

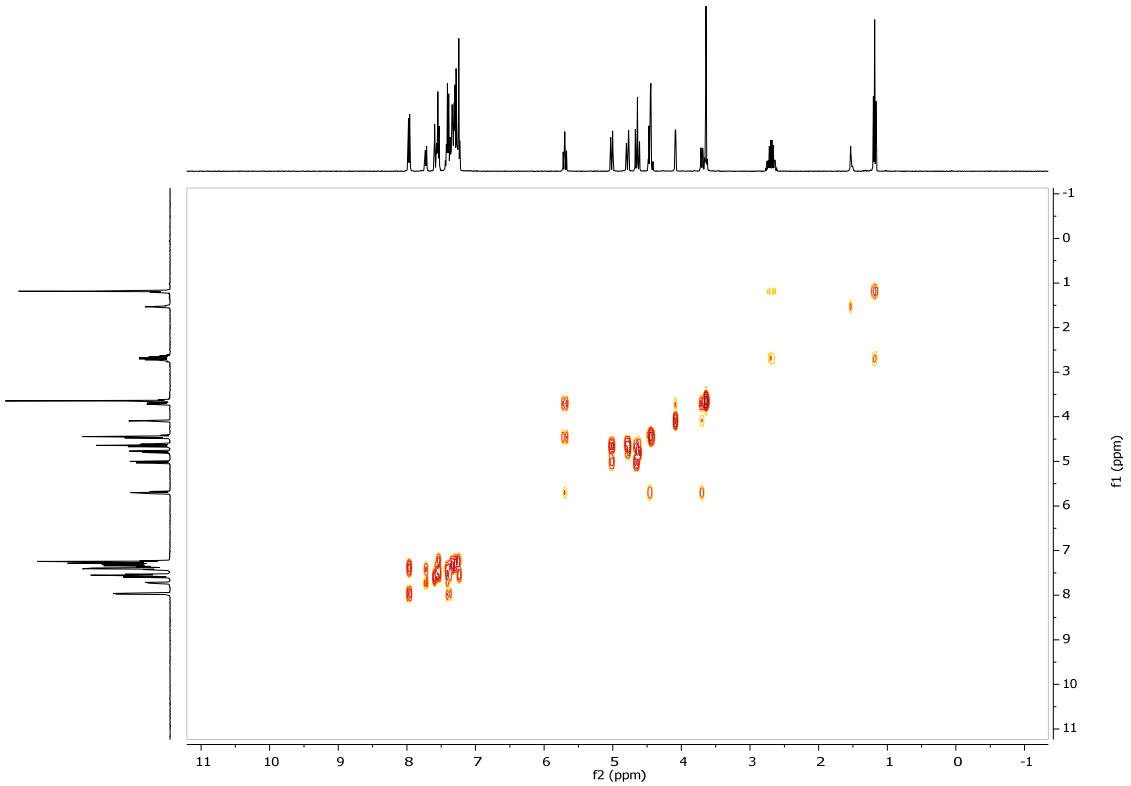

HSQC: **2.22**

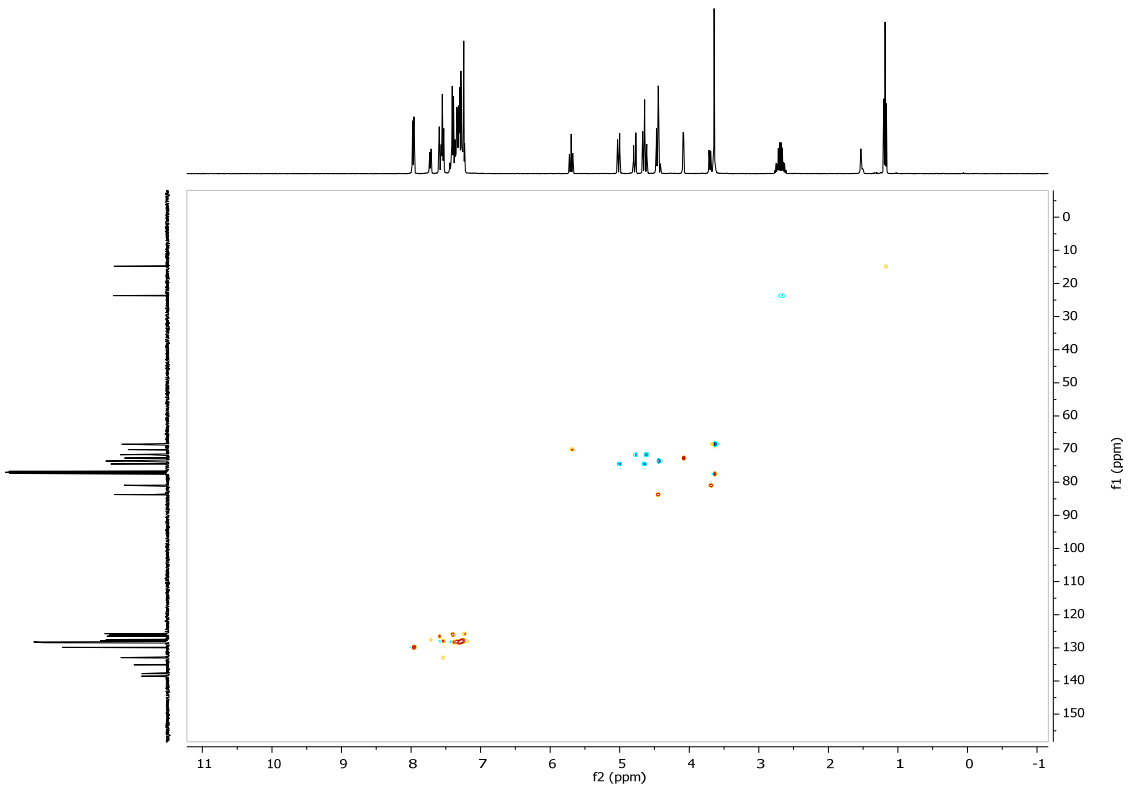

^{1}H NMR: **2.33**

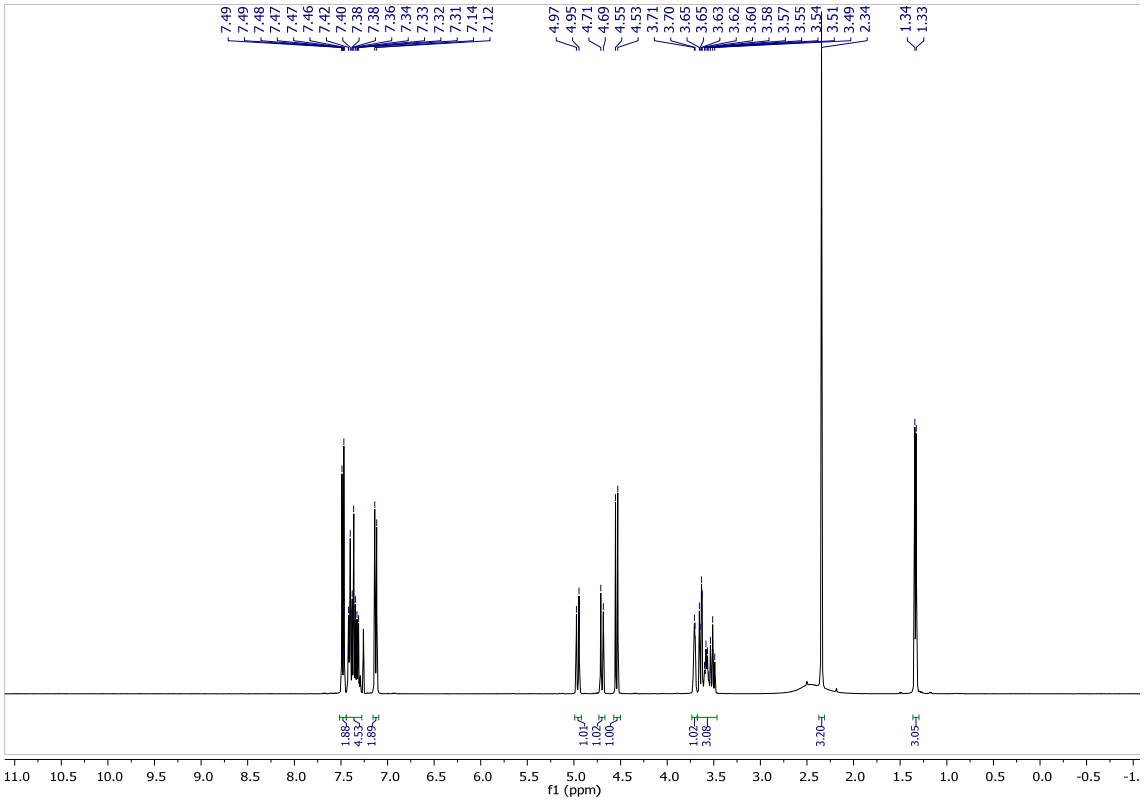

^{13}C NMR: **2.33**

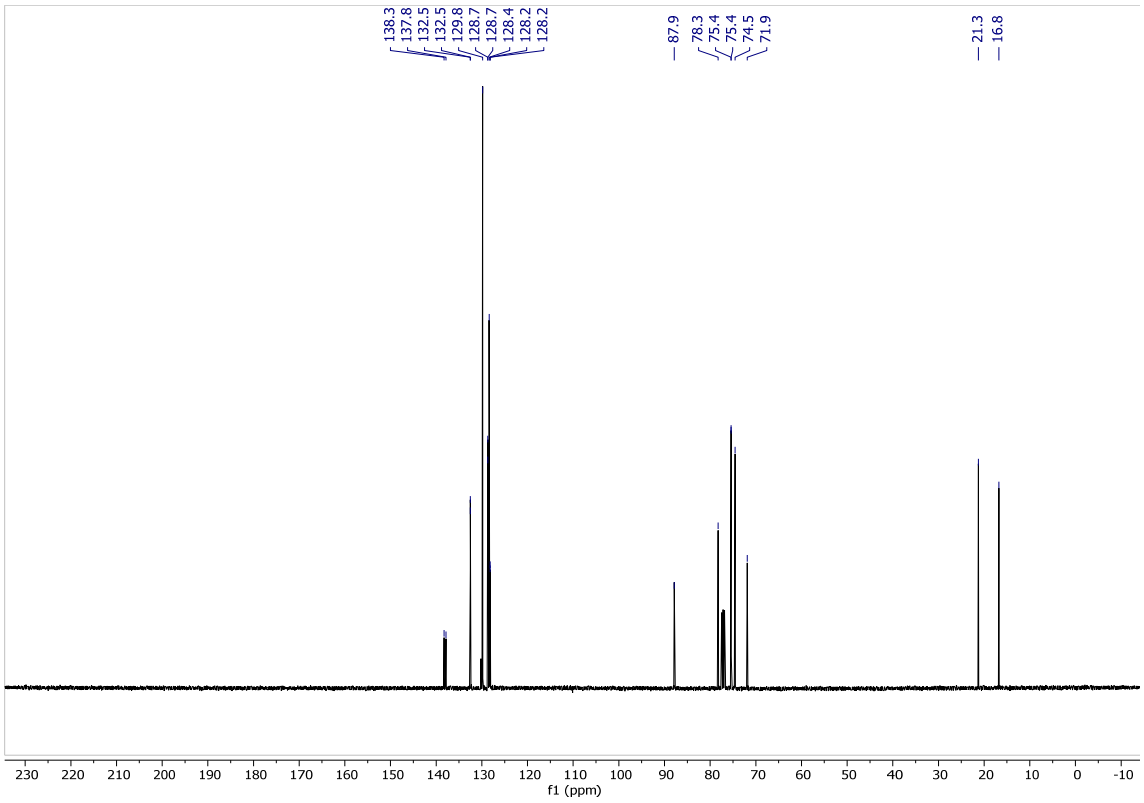

COSY: **2.33**

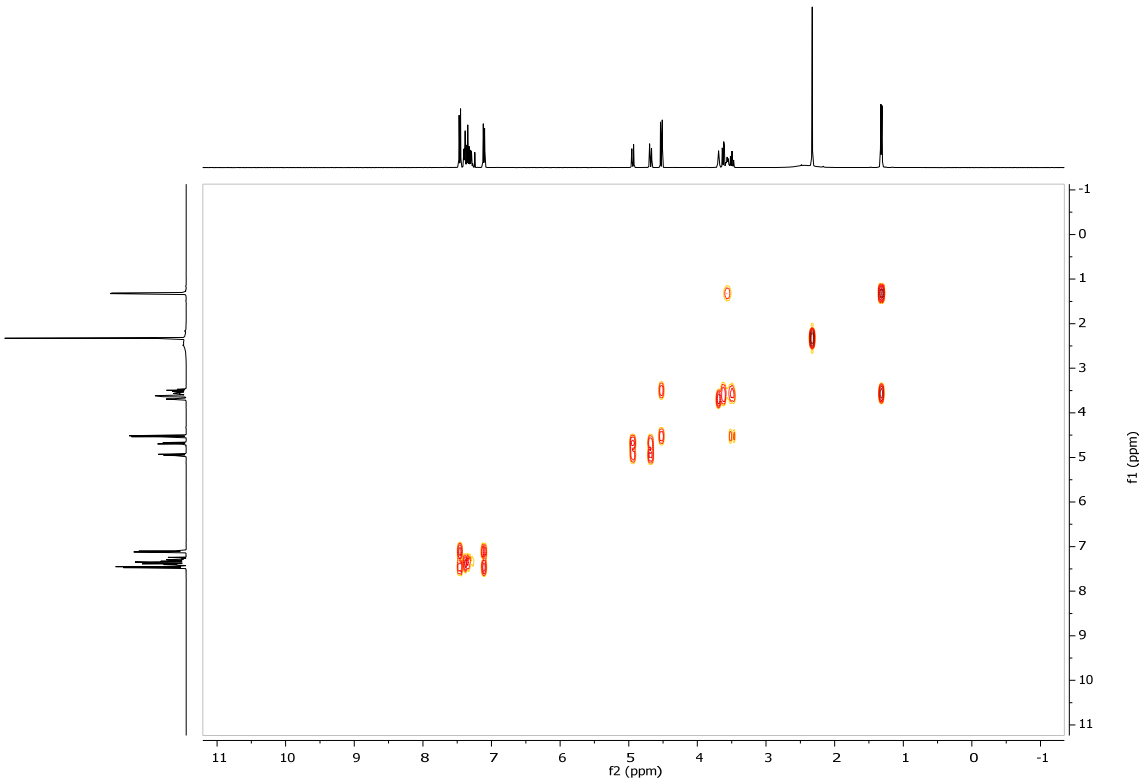

HSQC: **2.33**

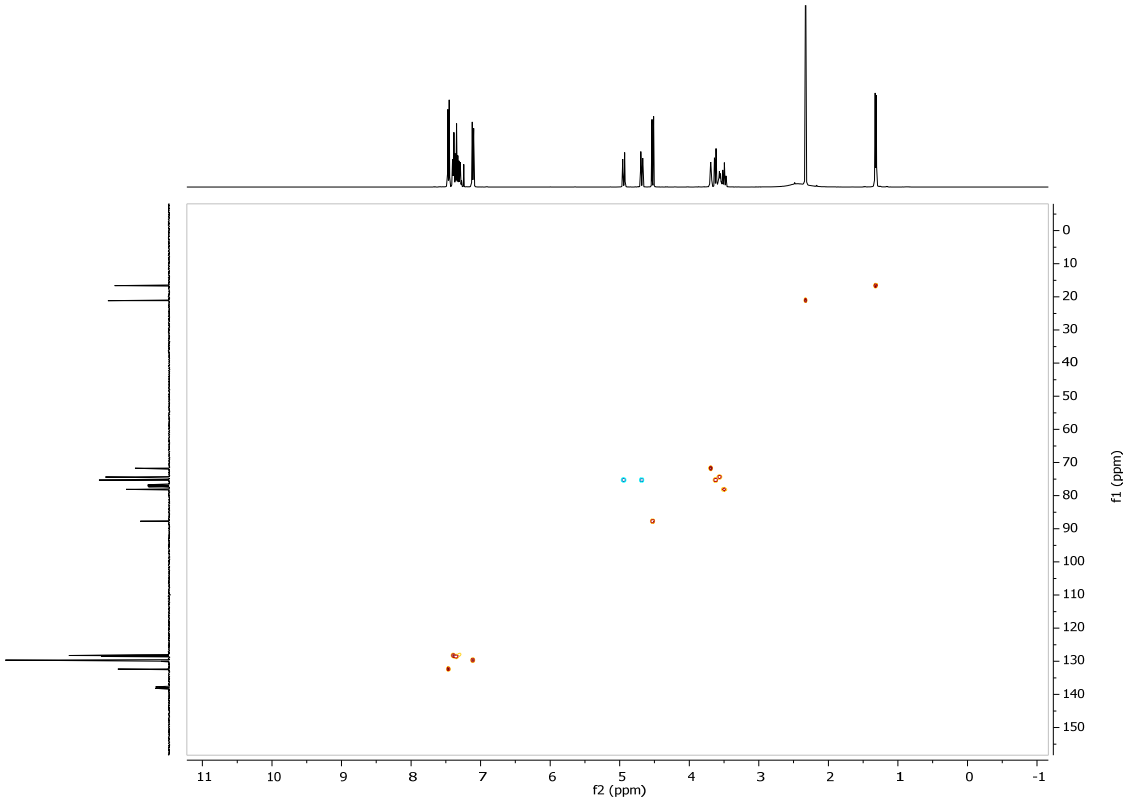

^{1}H NMR: **2.34**

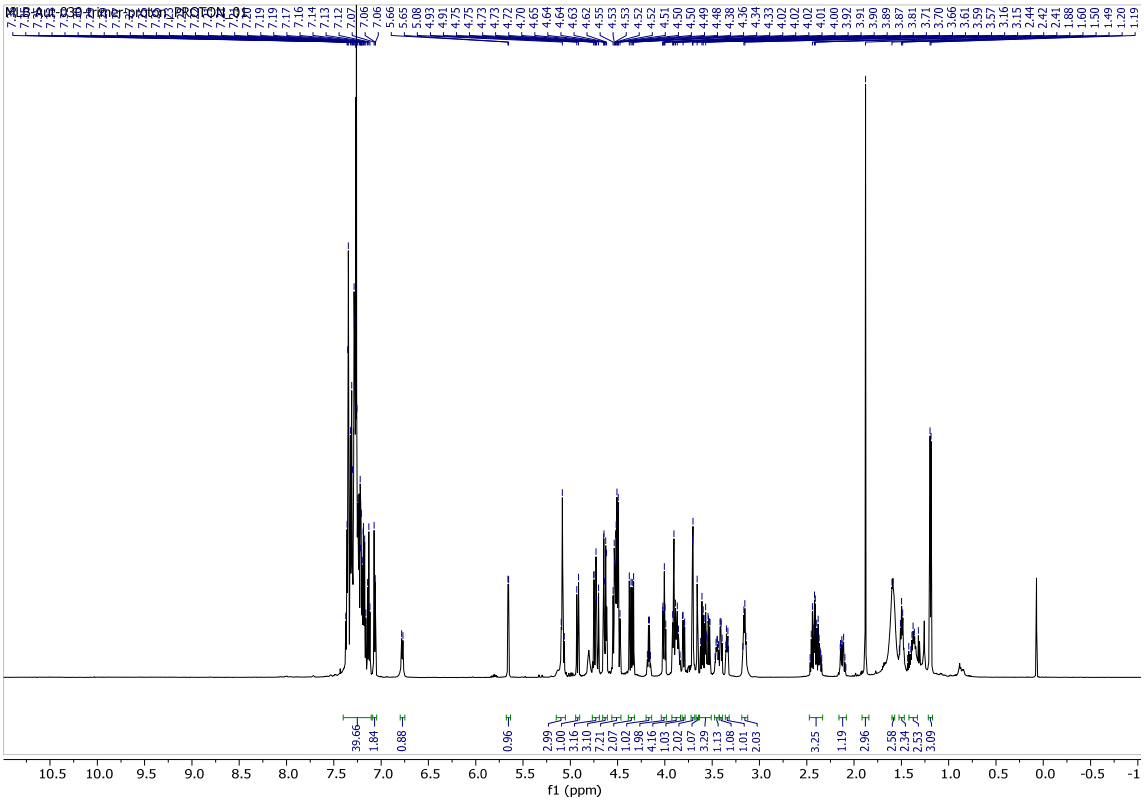

^{13}C NMR: **2.34**

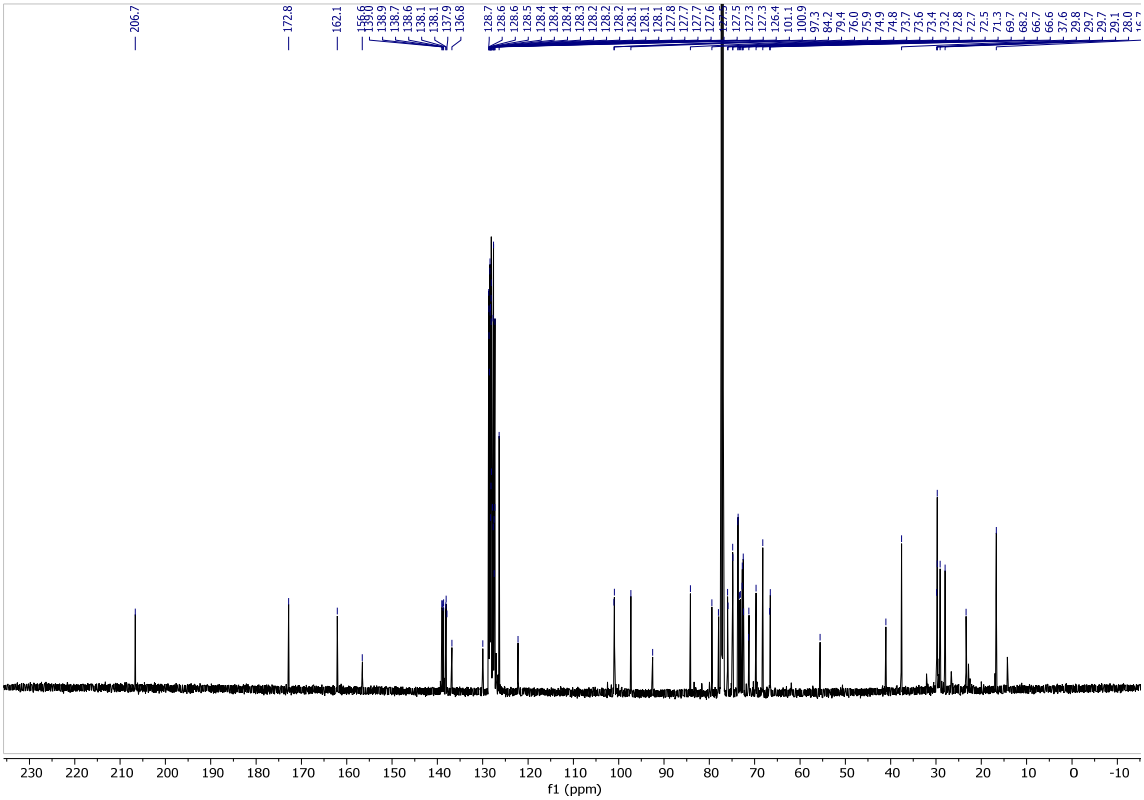

COSY: **2.34**

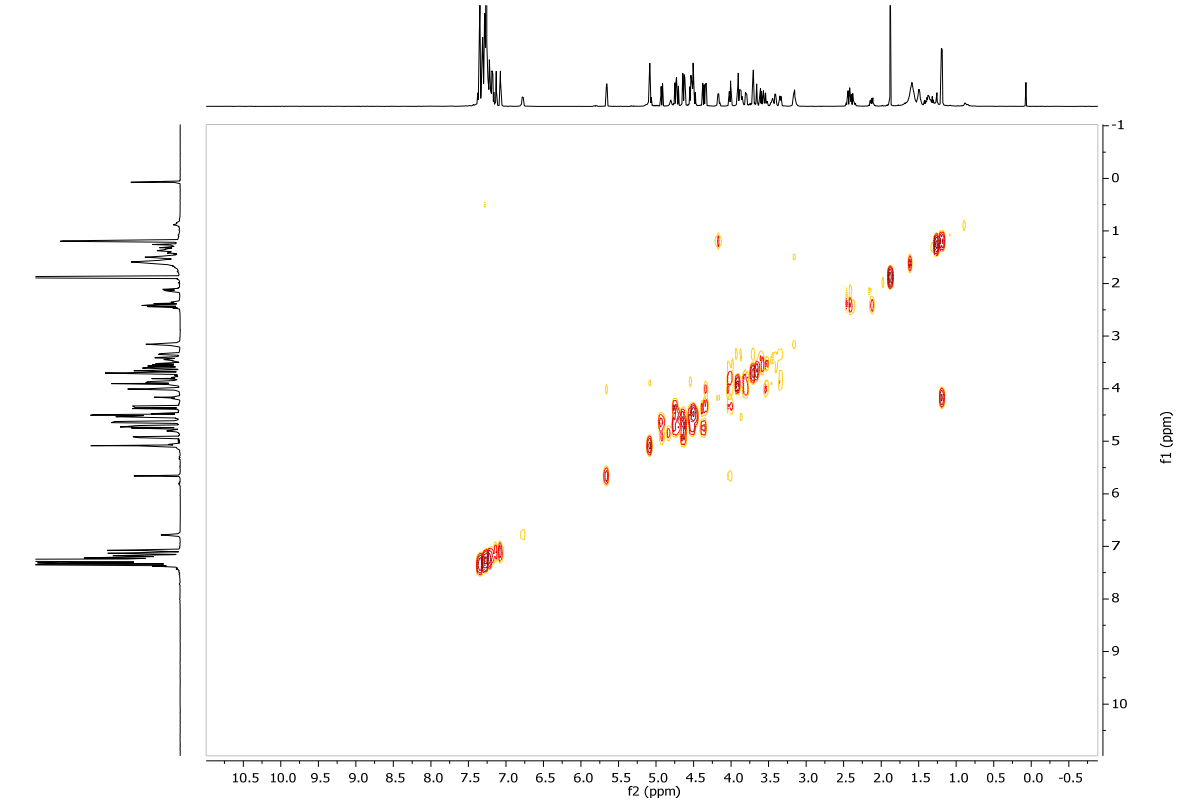

HSQC: **2.34**

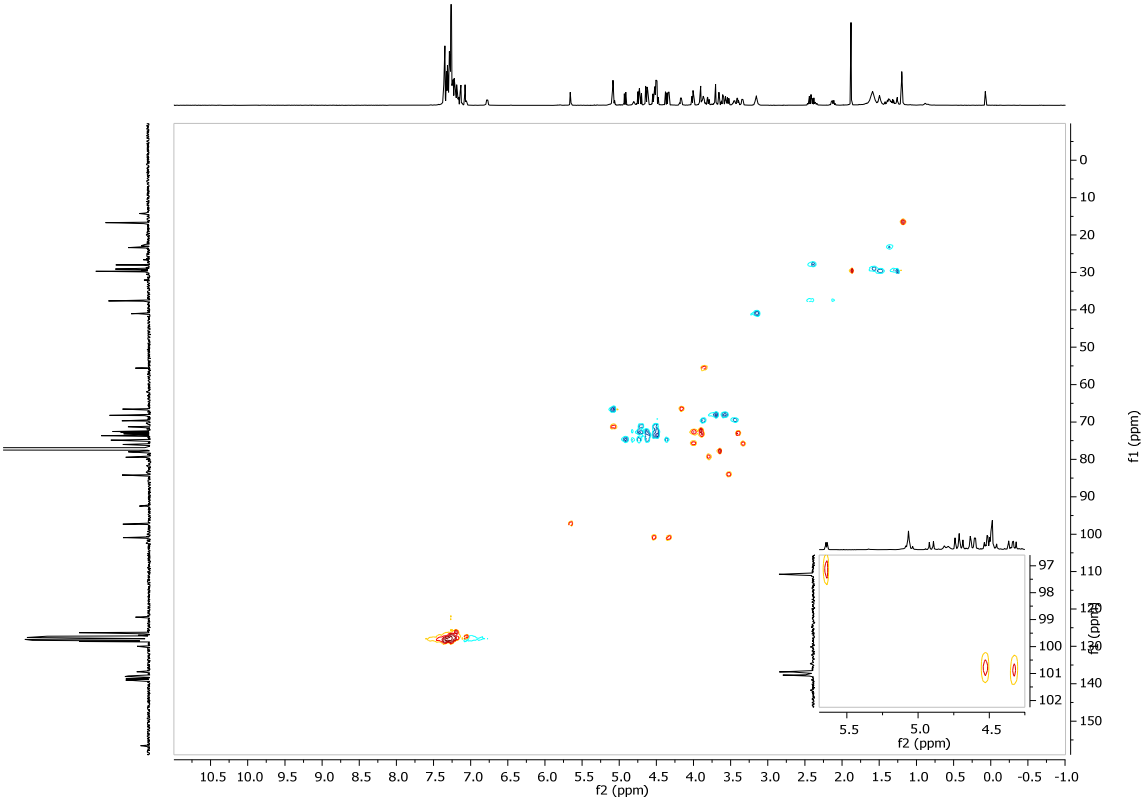

Coupled HSQC: **2.34**

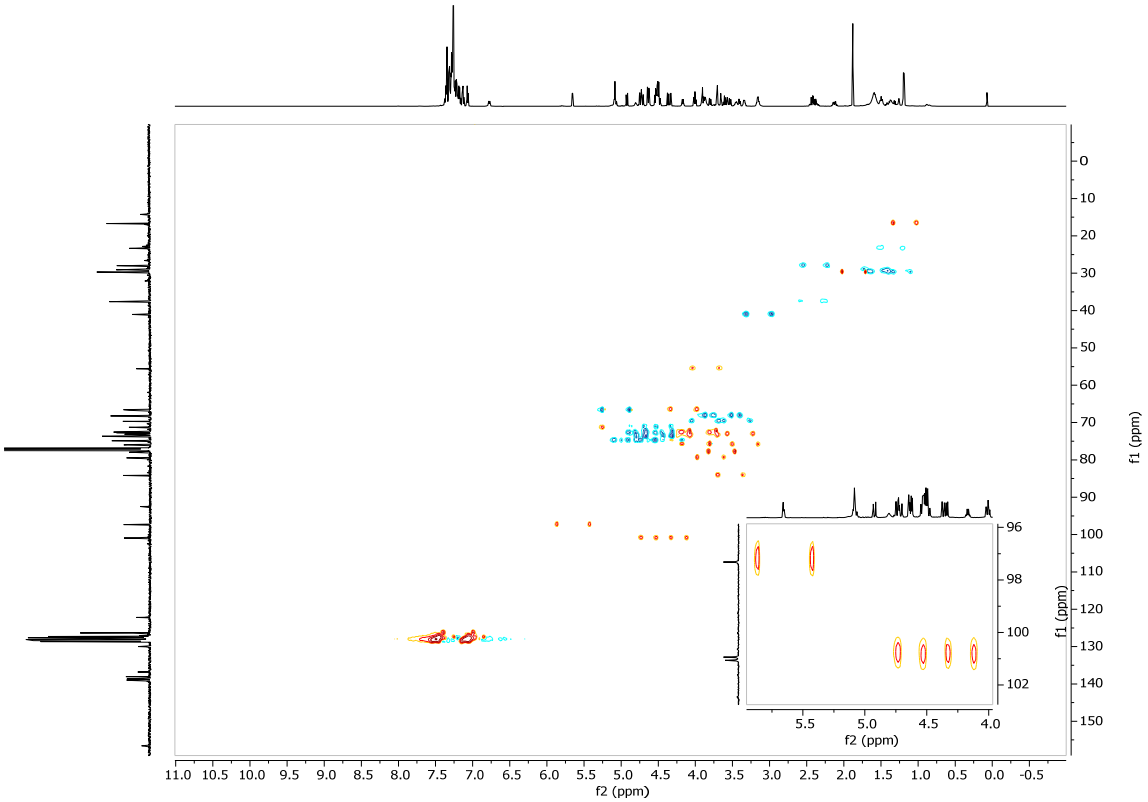

^{1}H NMR: **2.35**

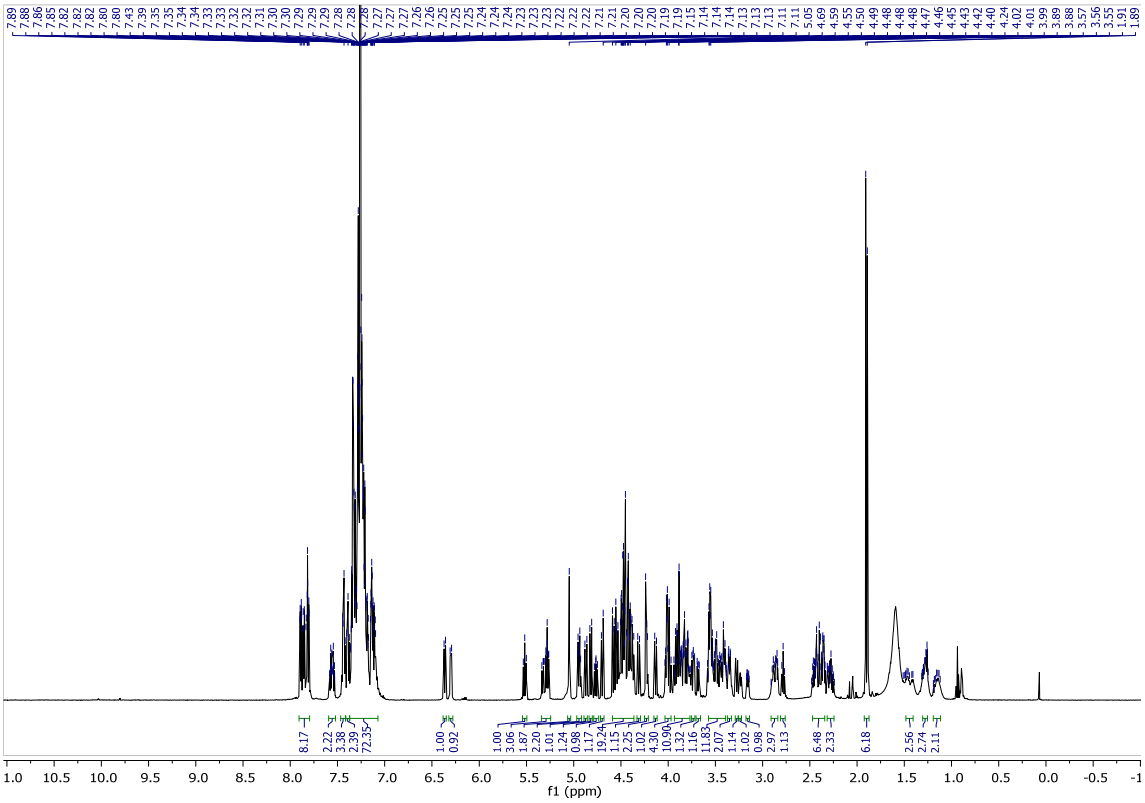

^{13}C NMR: **2.35**

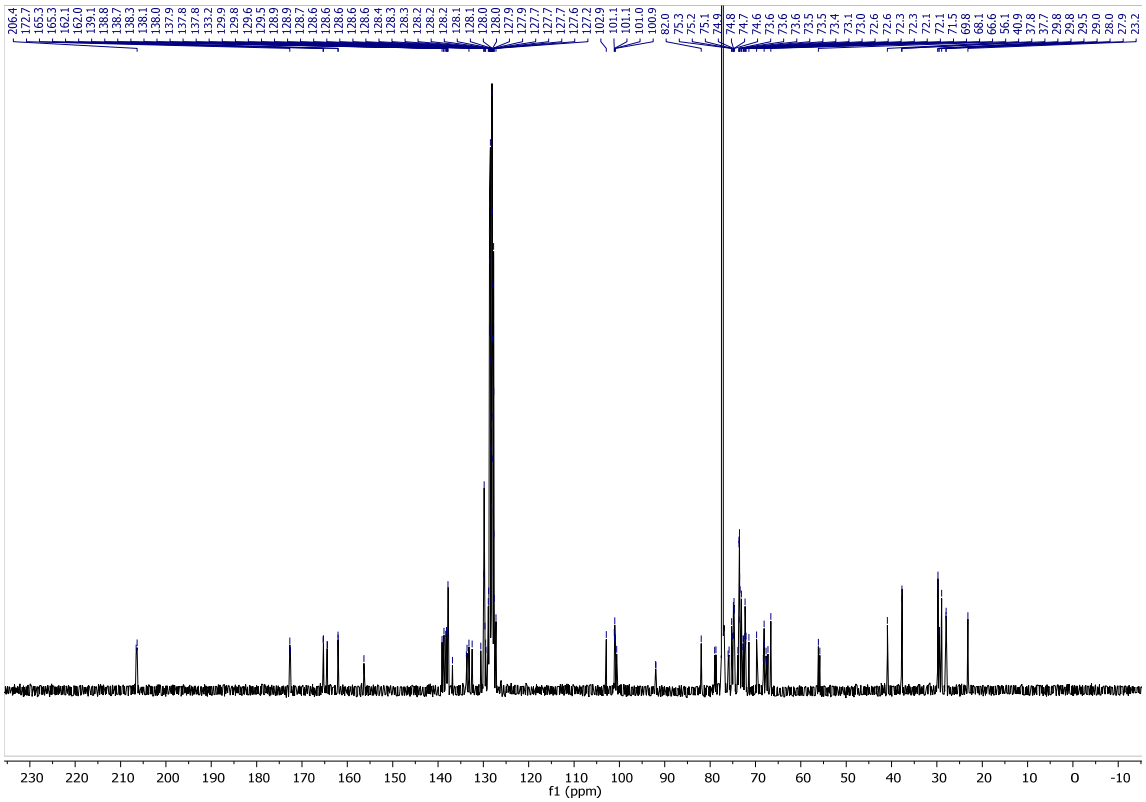

COSY: **2.35**

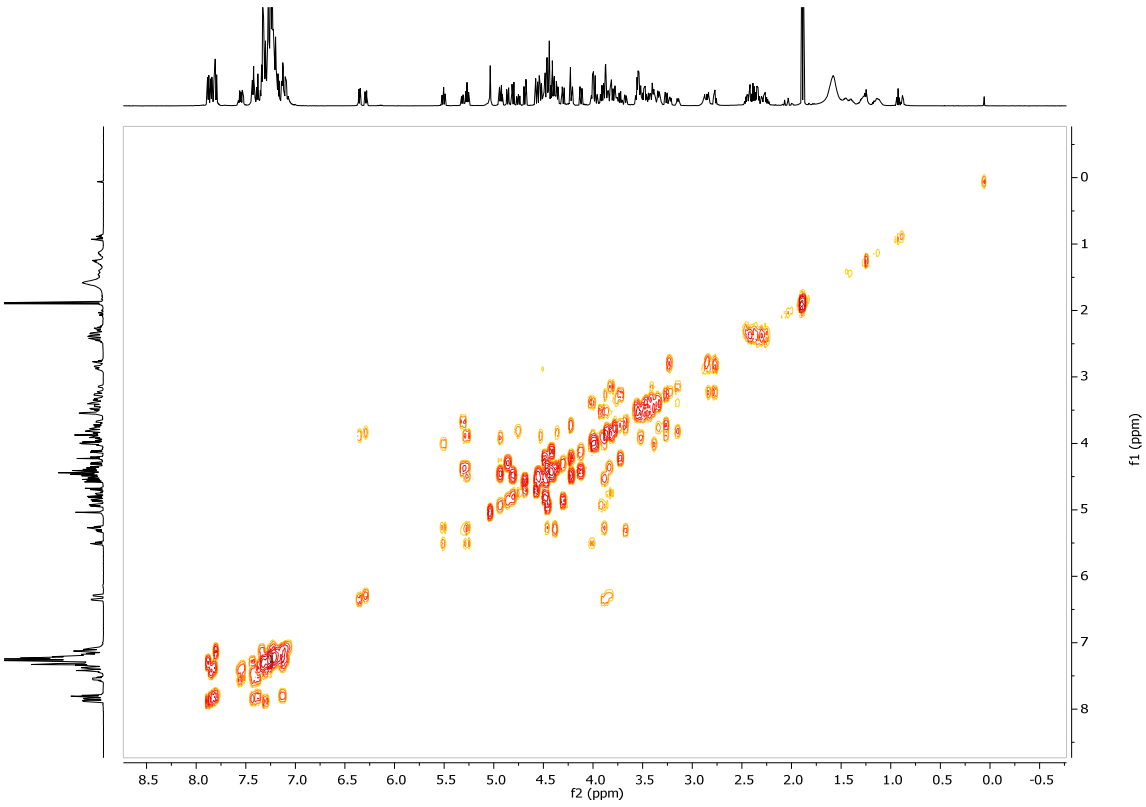

HSQC: **2.35**

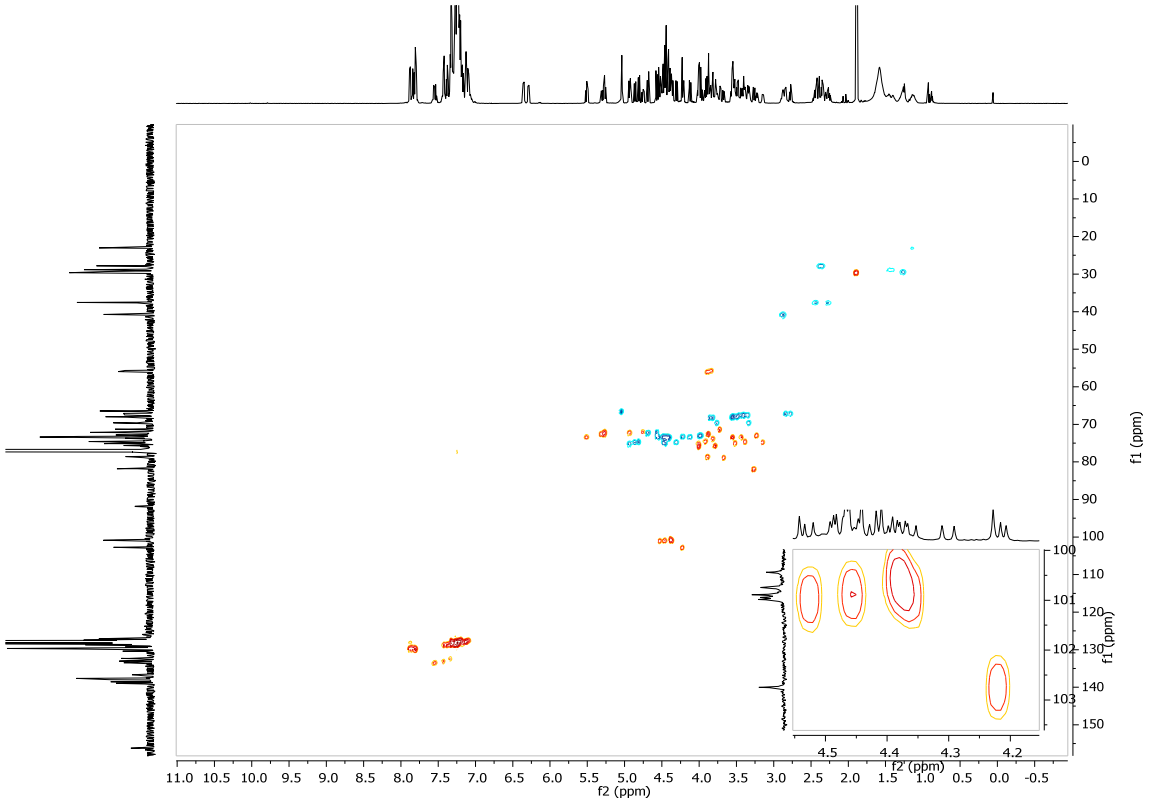

Coupled HSQC: **2.35**

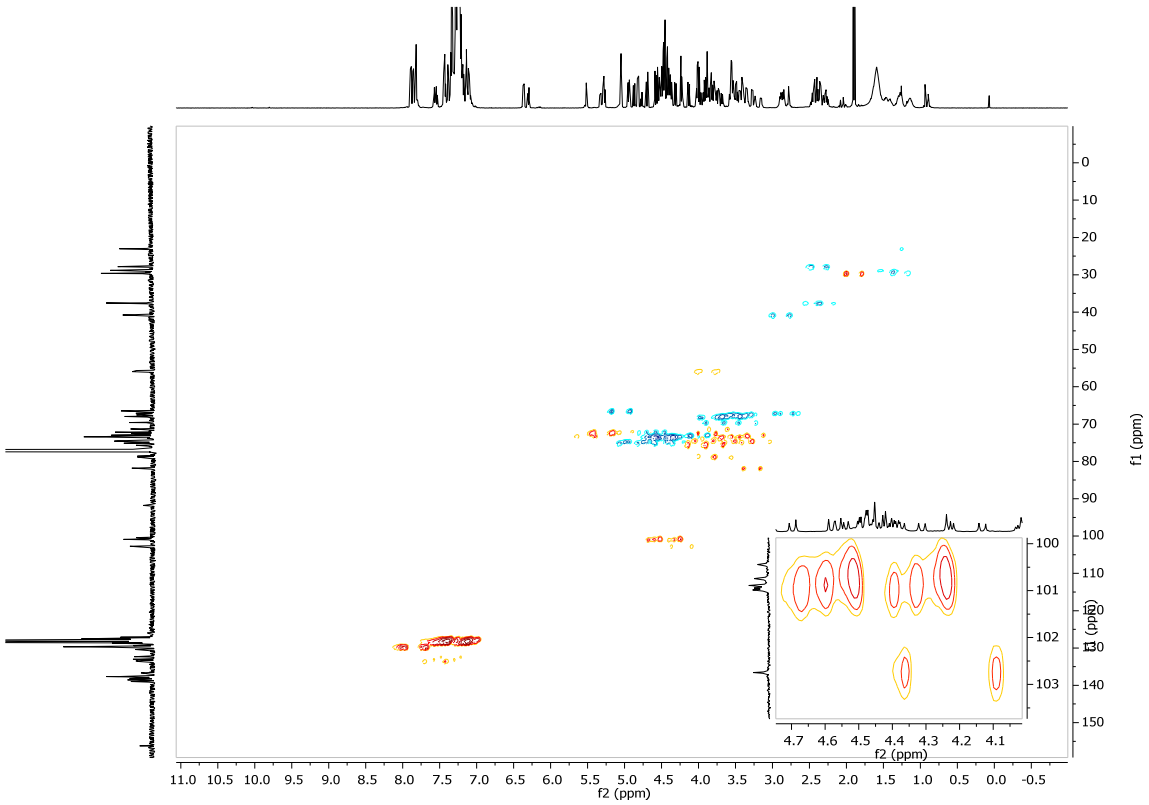

^{1}H NMR: **2.36**

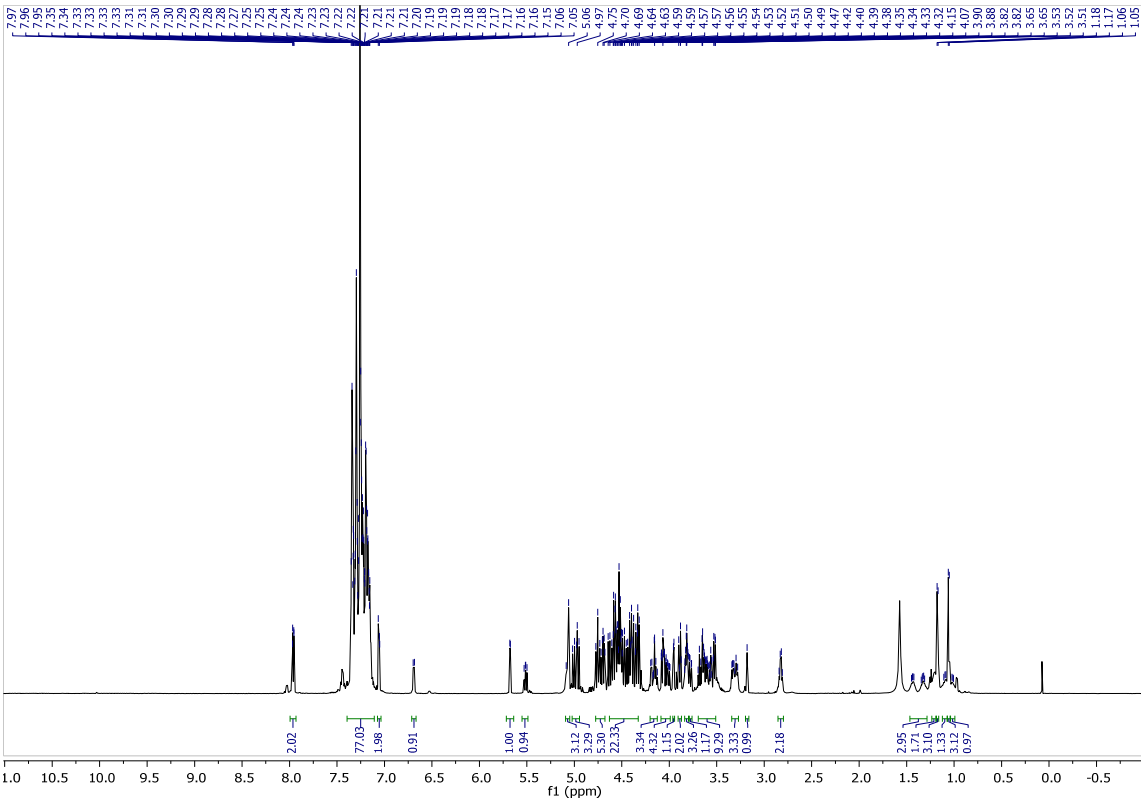

^{13}C NMR: **2.36**

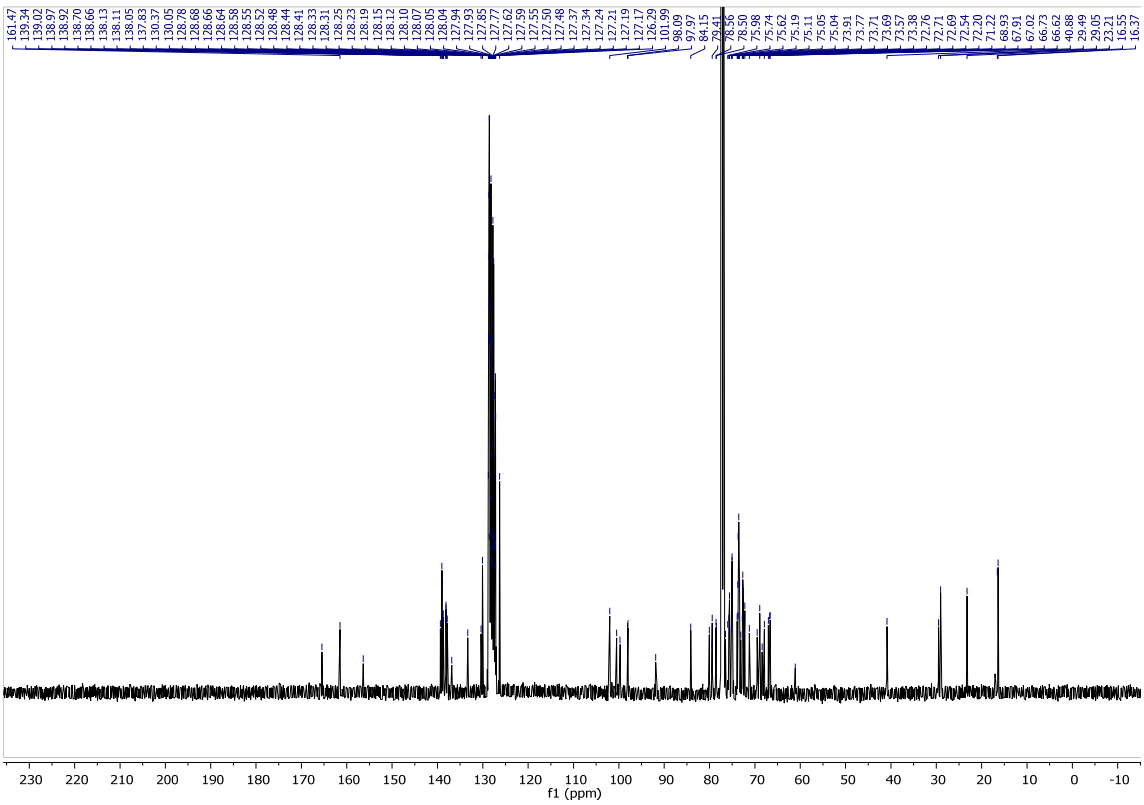

COSY: **2.36**

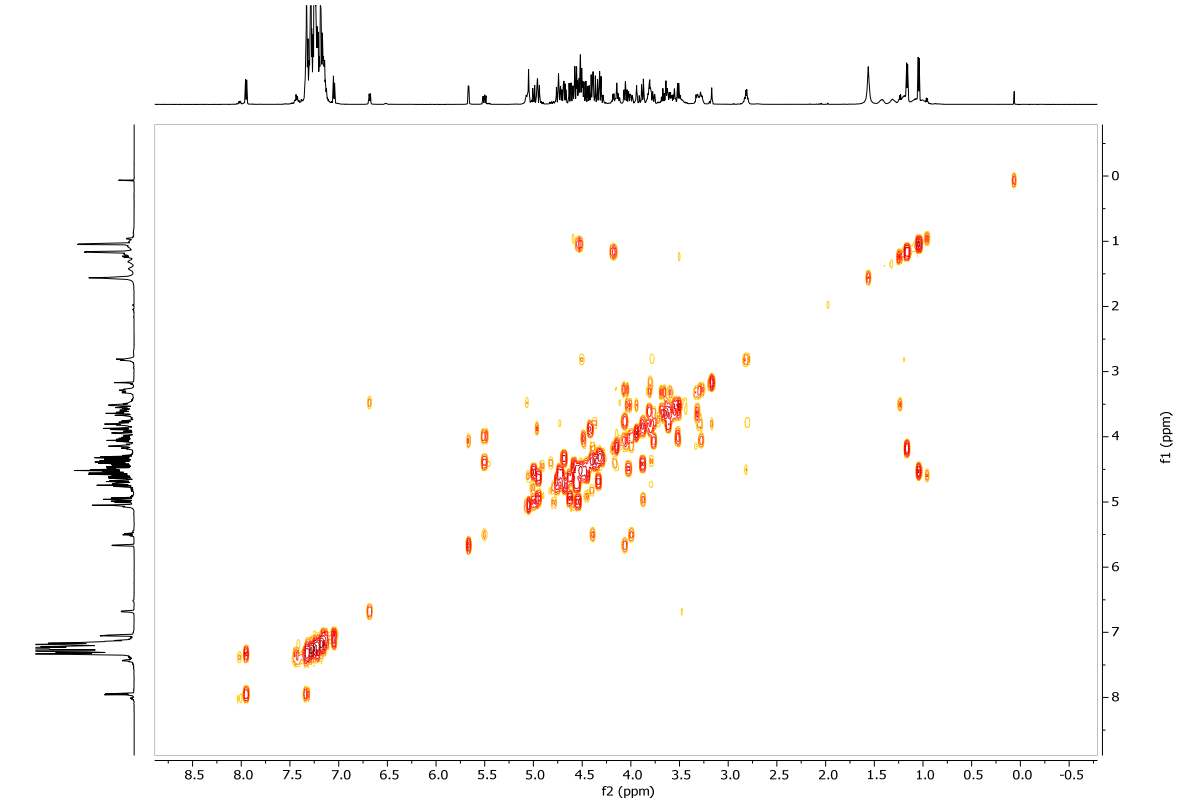

HSQC: **2.36**

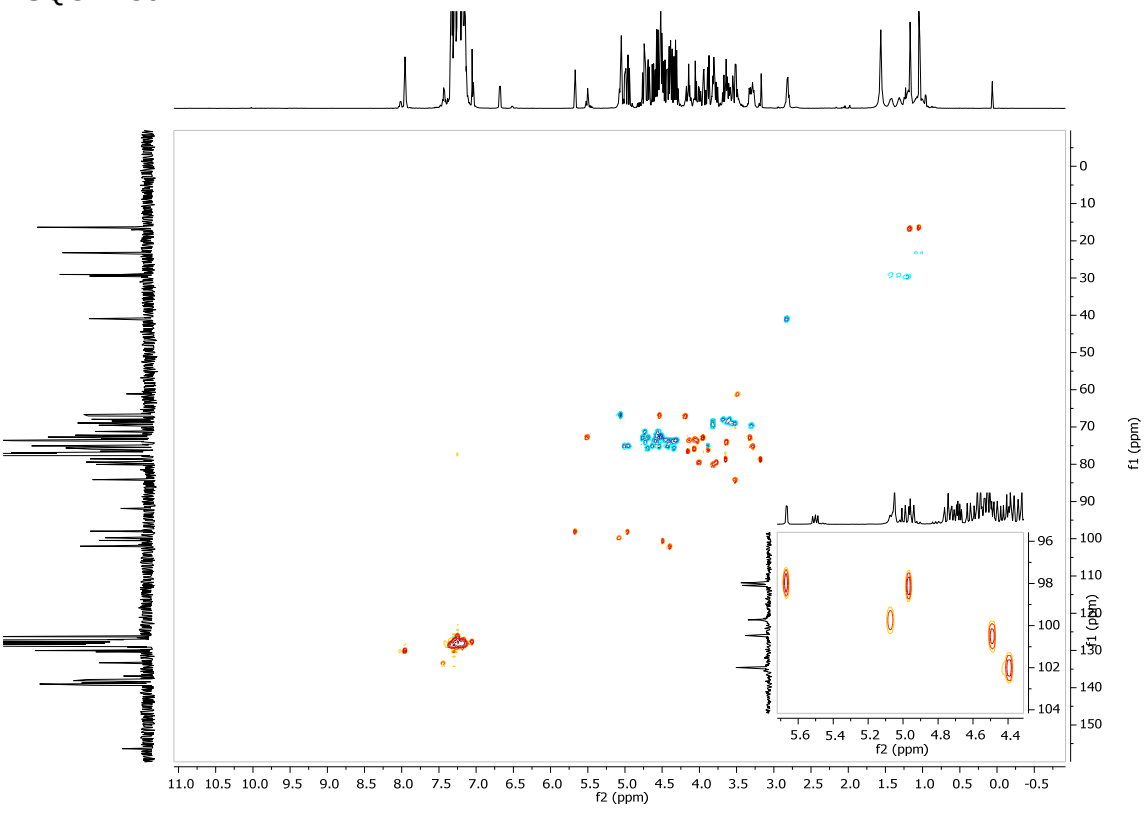

Coupled HSQC: **2.36**

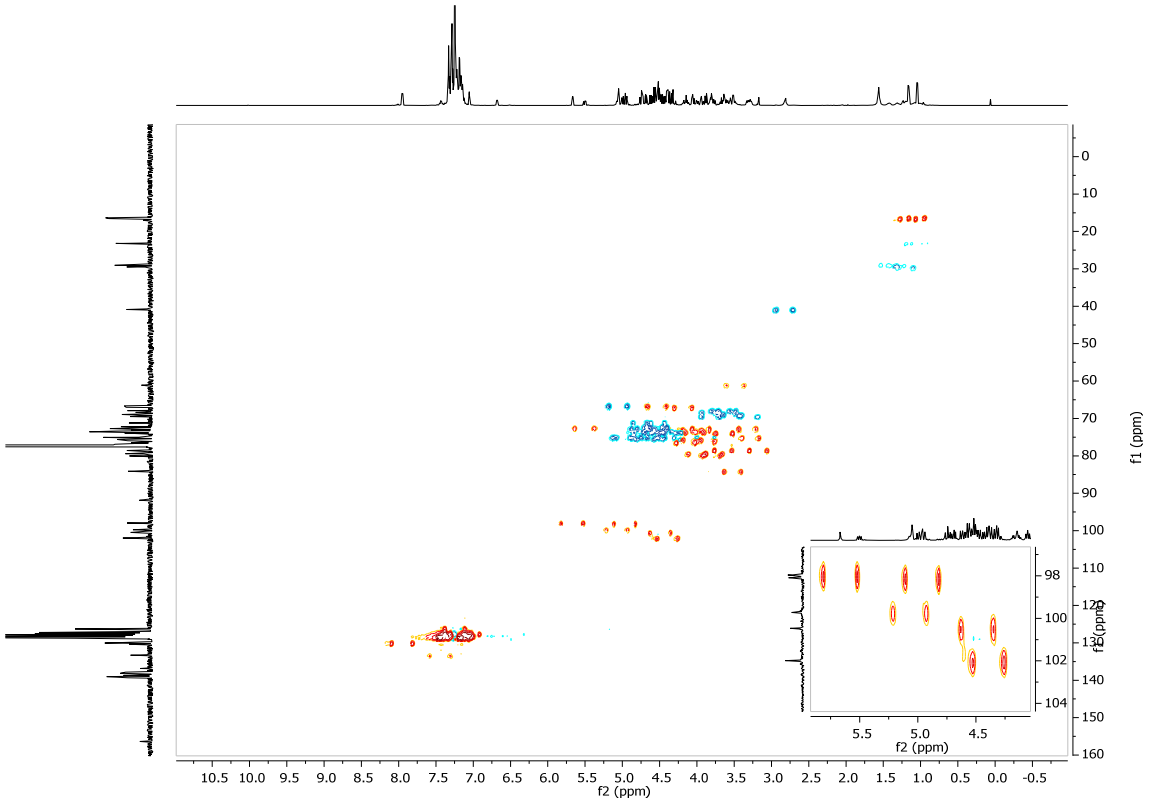

^{1}H NMR: **2.37**

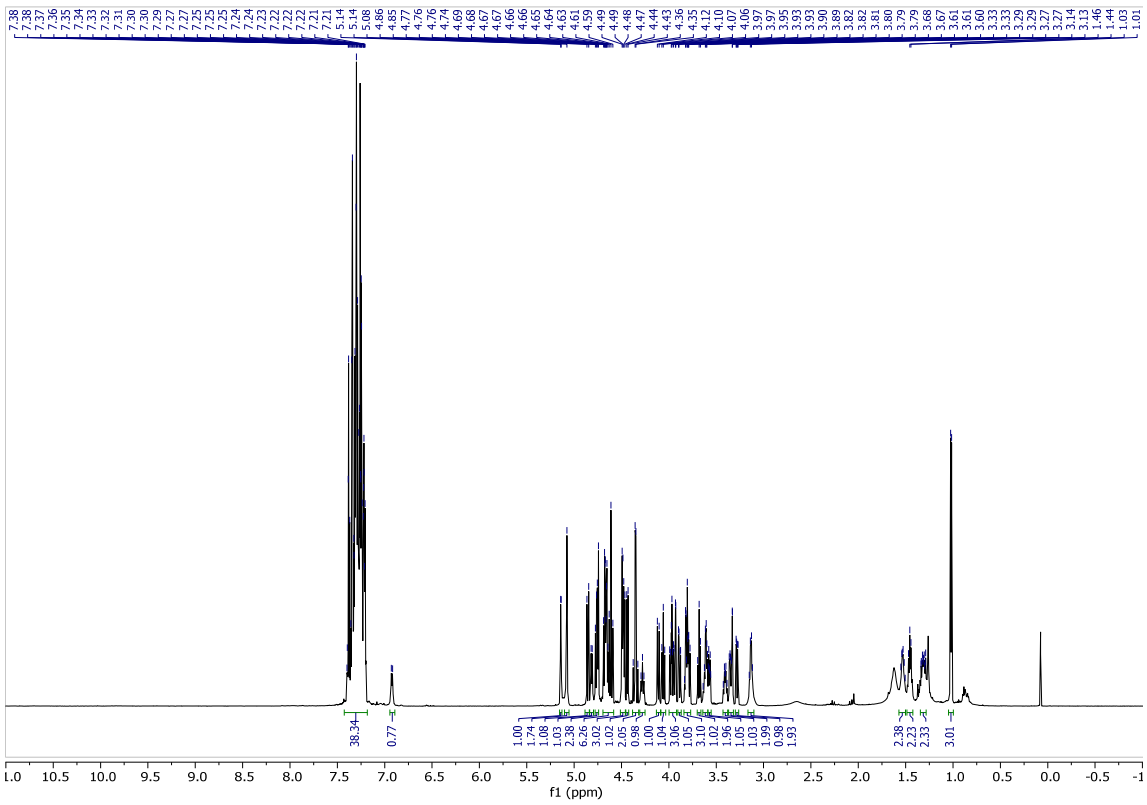

^{13}C NMR: **2.37**

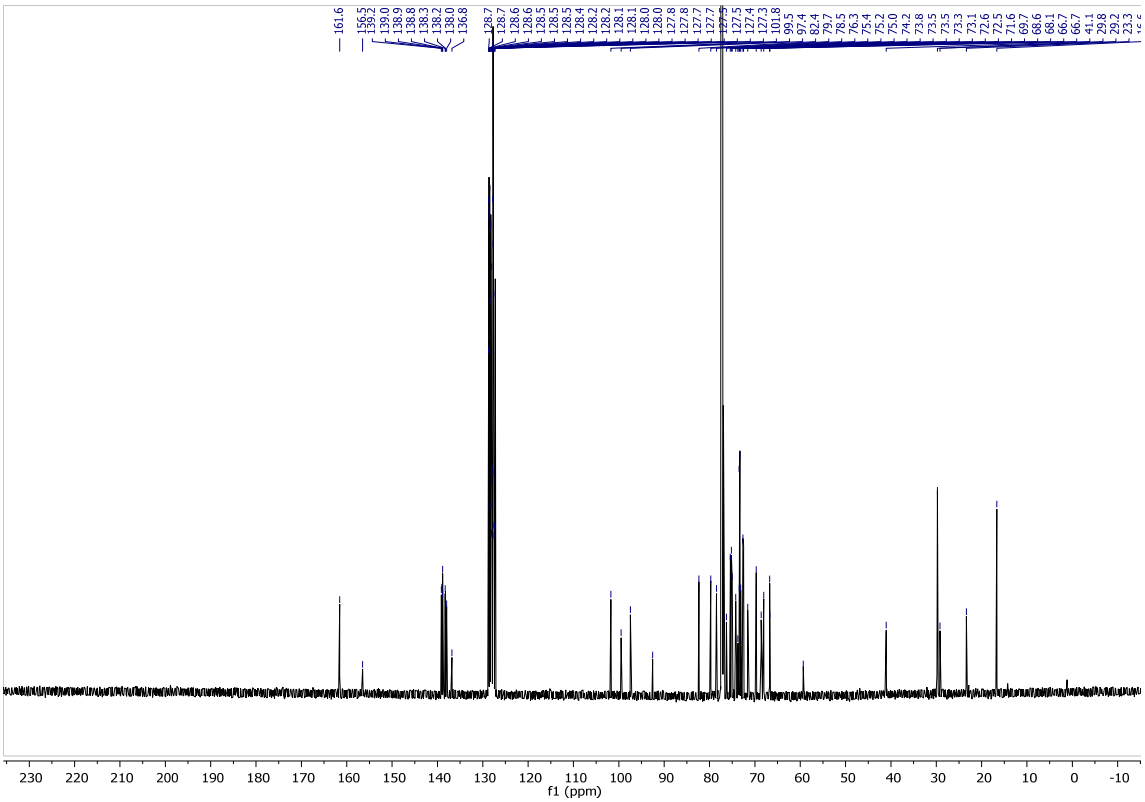

COSY: **2.37**

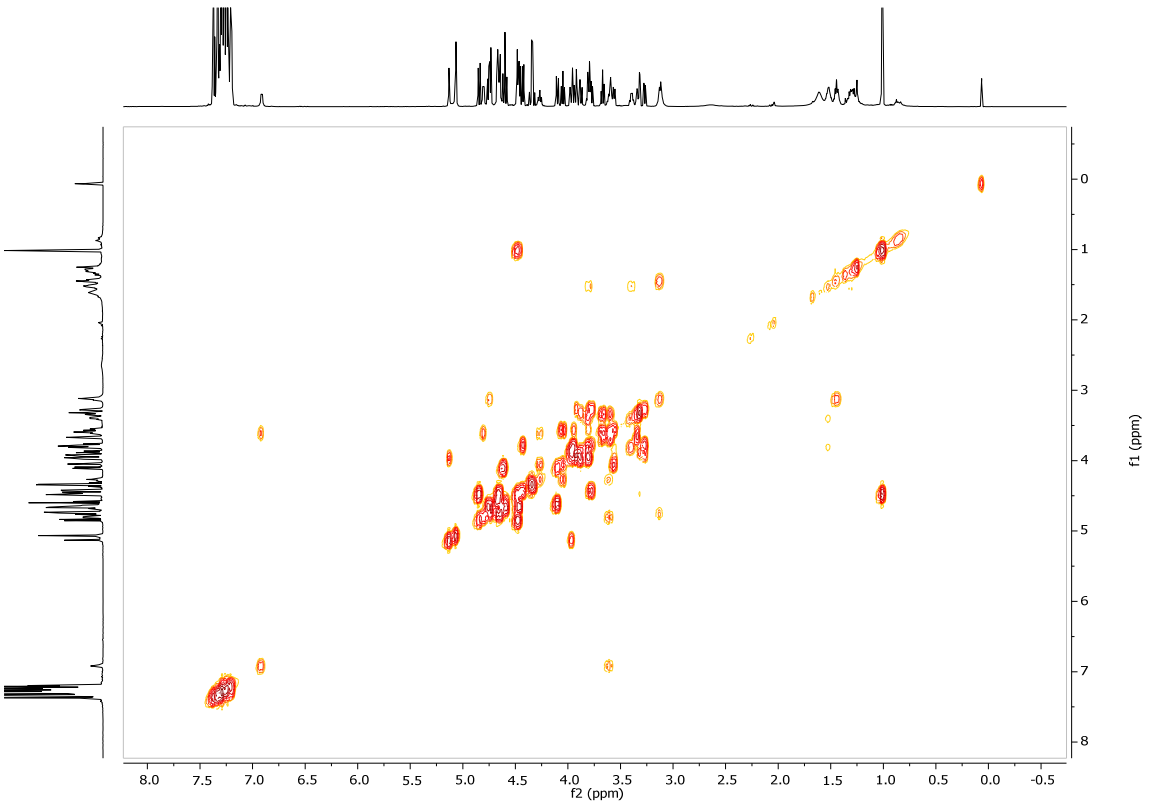

HSQC: **2.37**

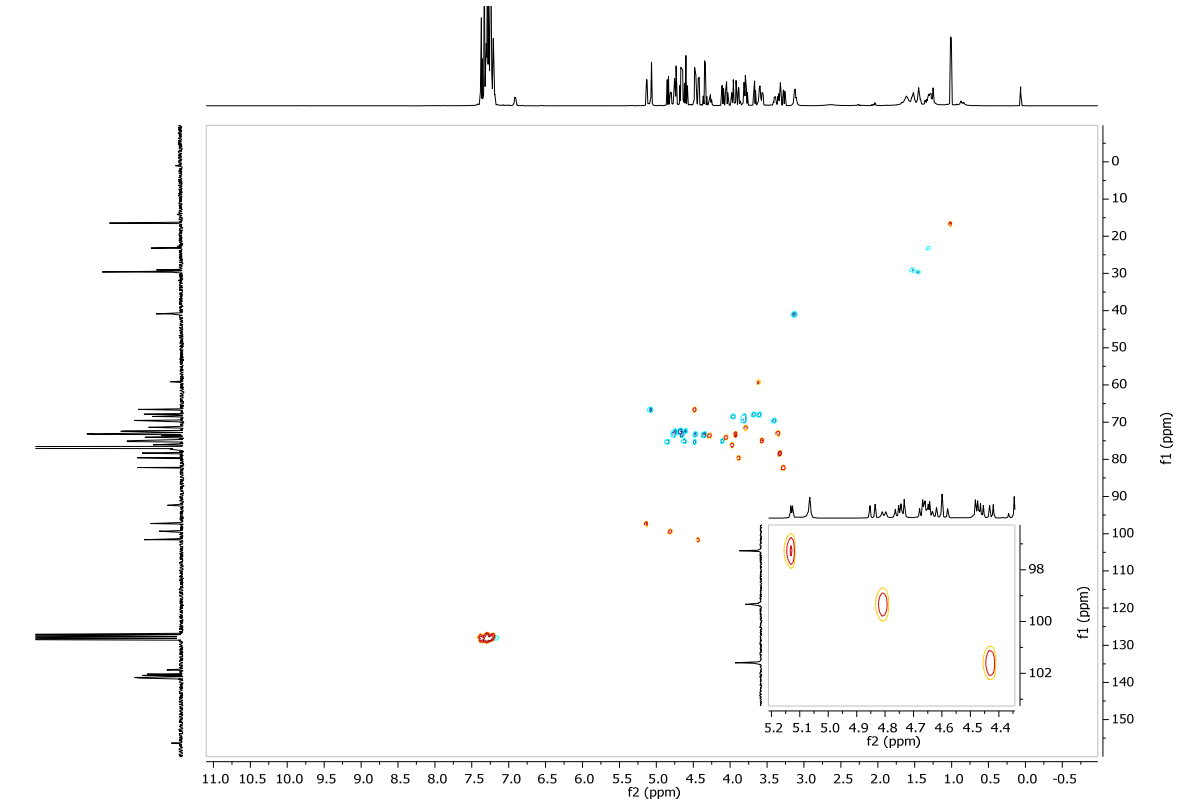

Coupled HSQC: **2.37**

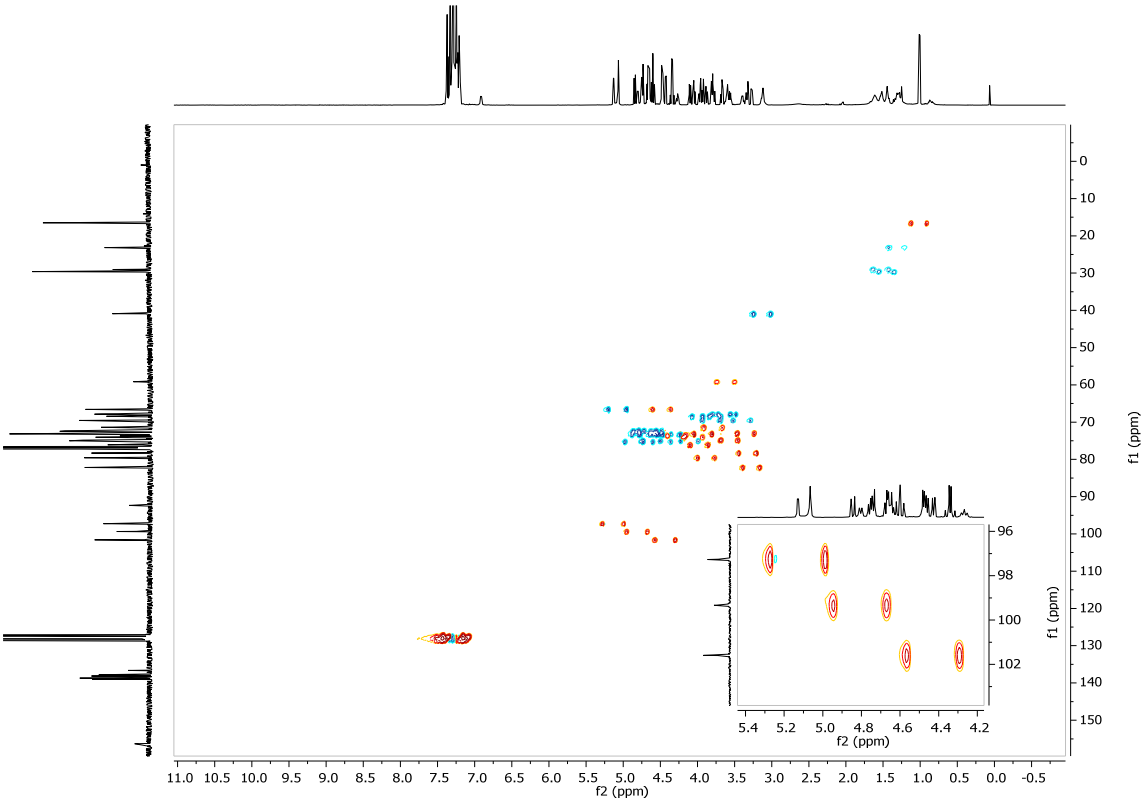

^{1}H NMR: **2.38**

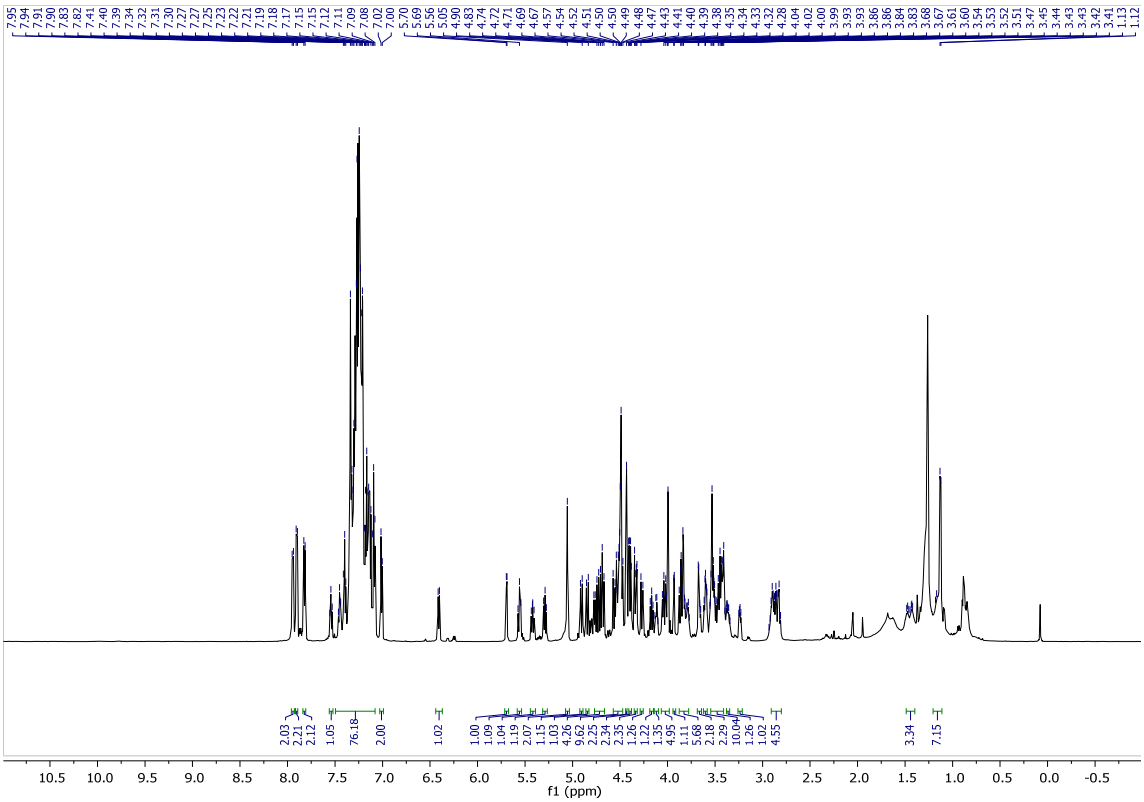

^{13}C NMR: **2.38**

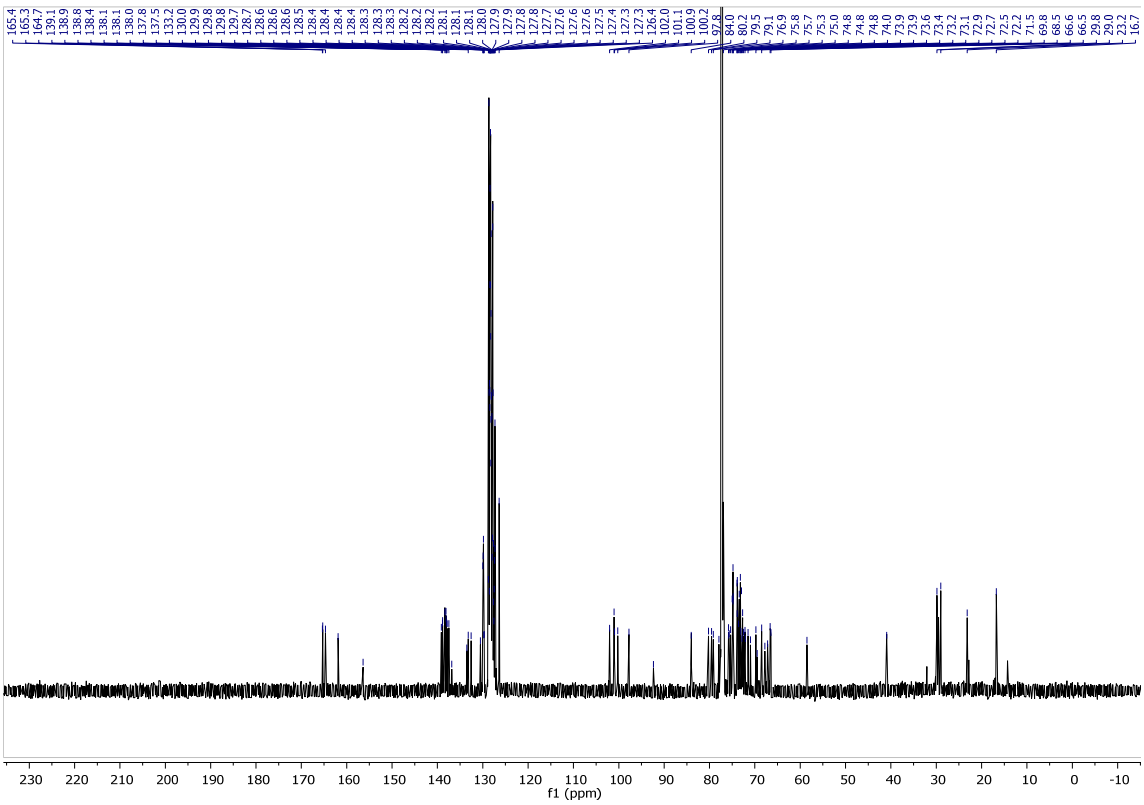

COSY: **2.38**

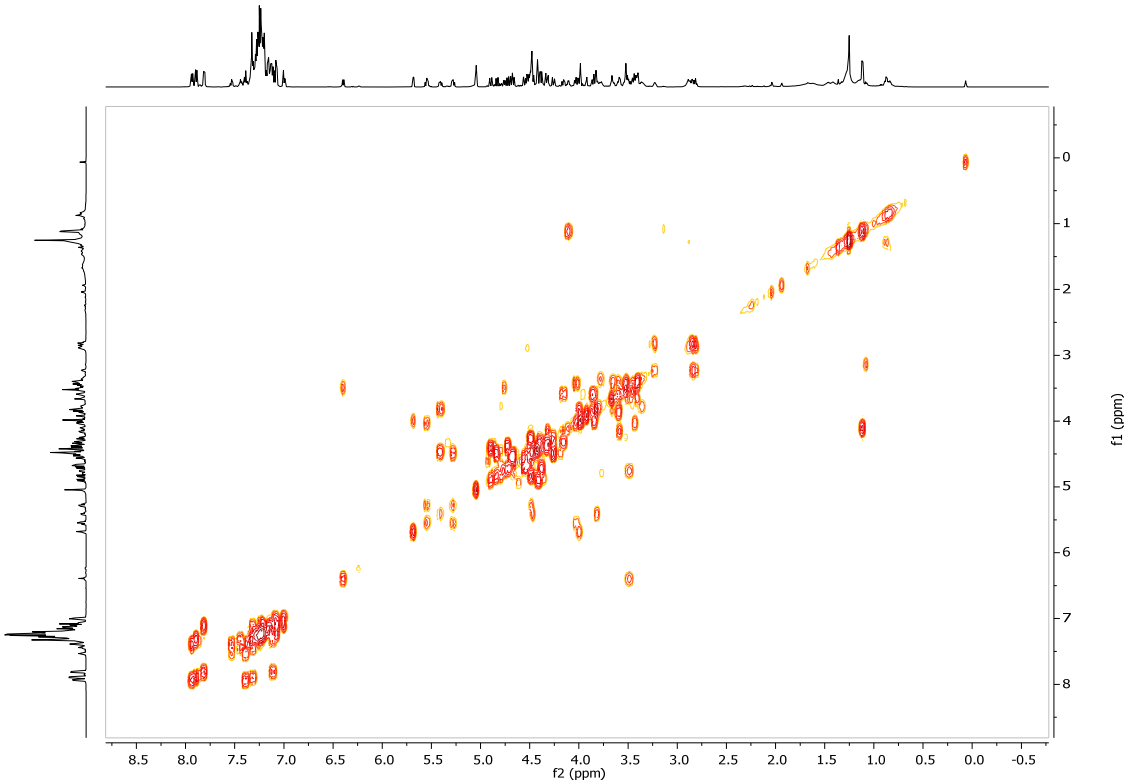

HSQC: **2.38**

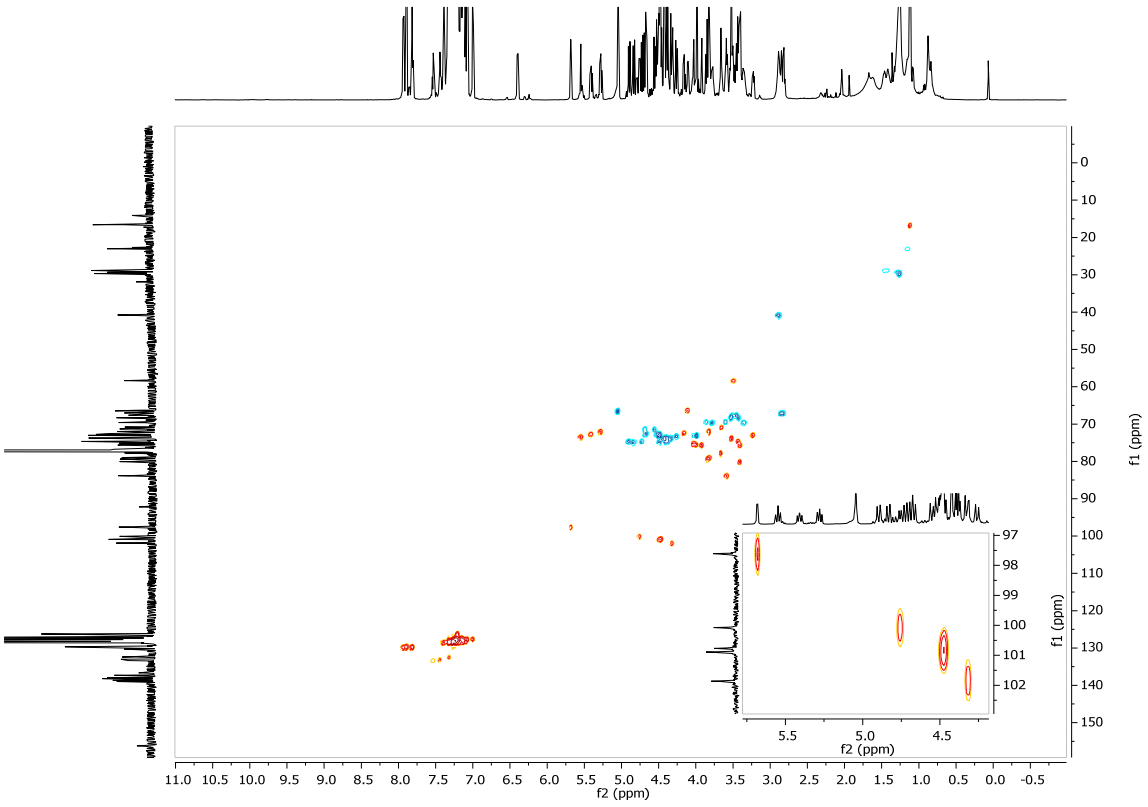

Coupled HSQC: **2.38**

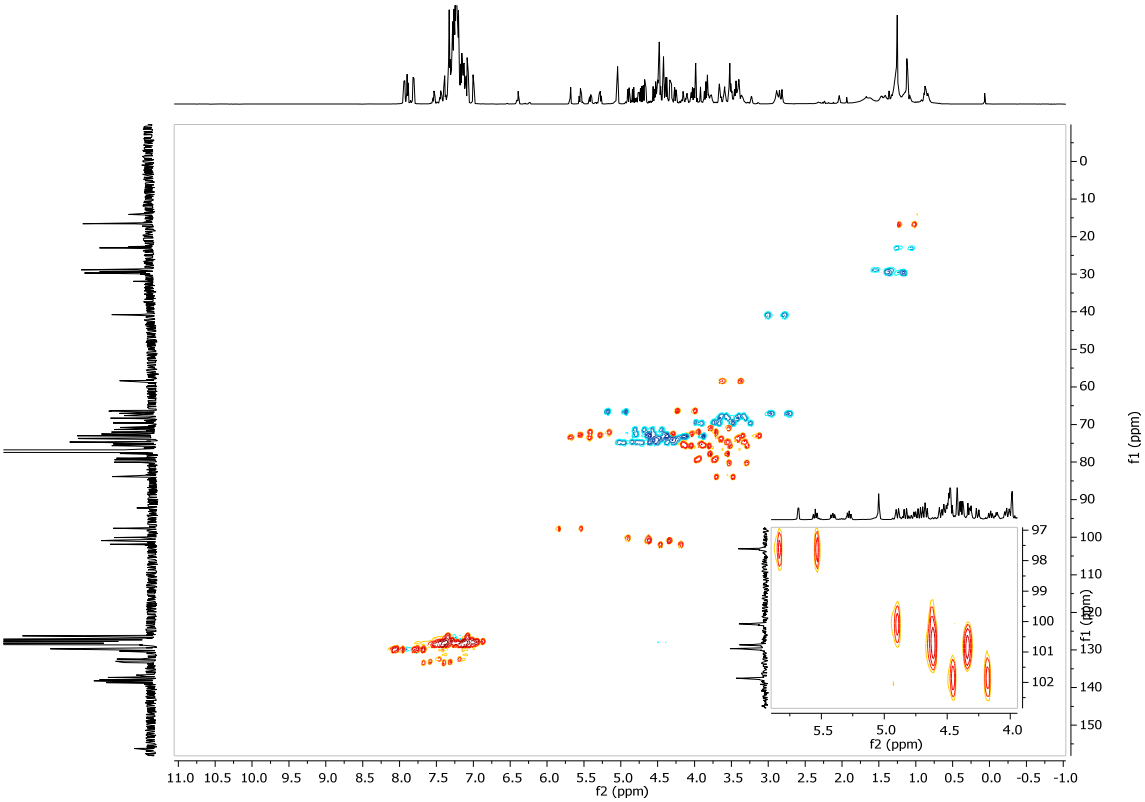

^{1}H NMR: **2.39**

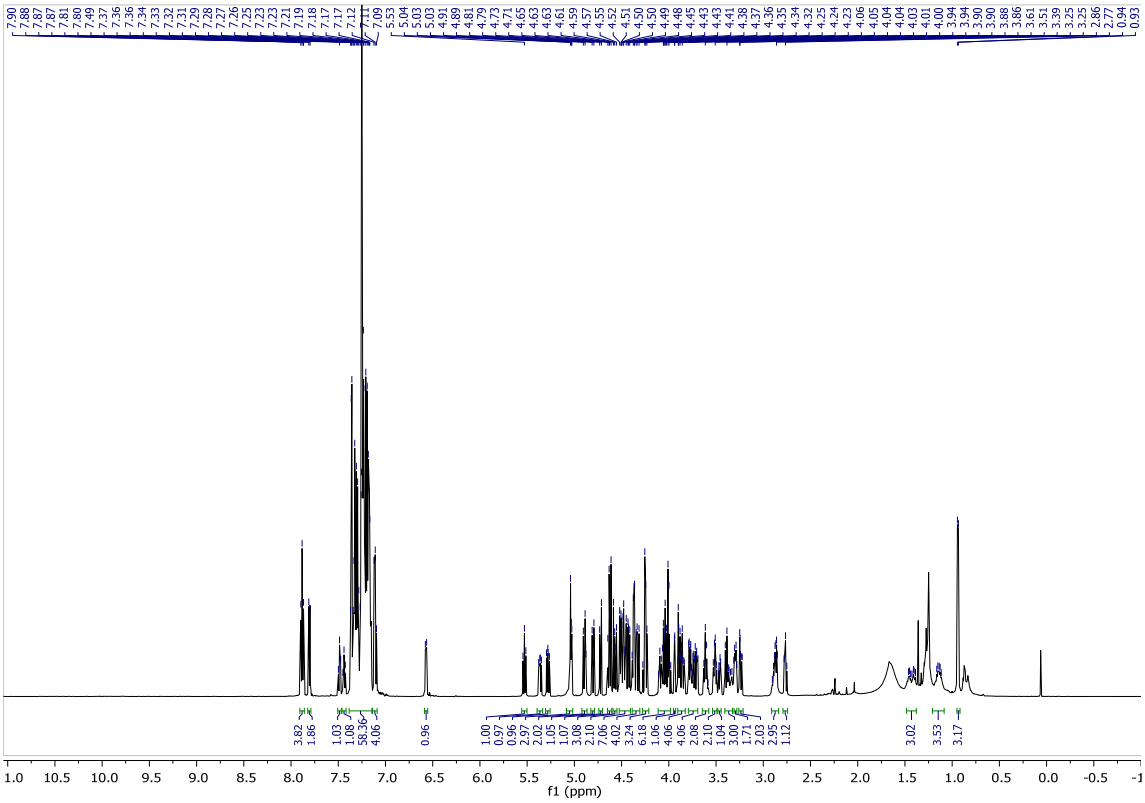

^{13}C NMR: **2.39**

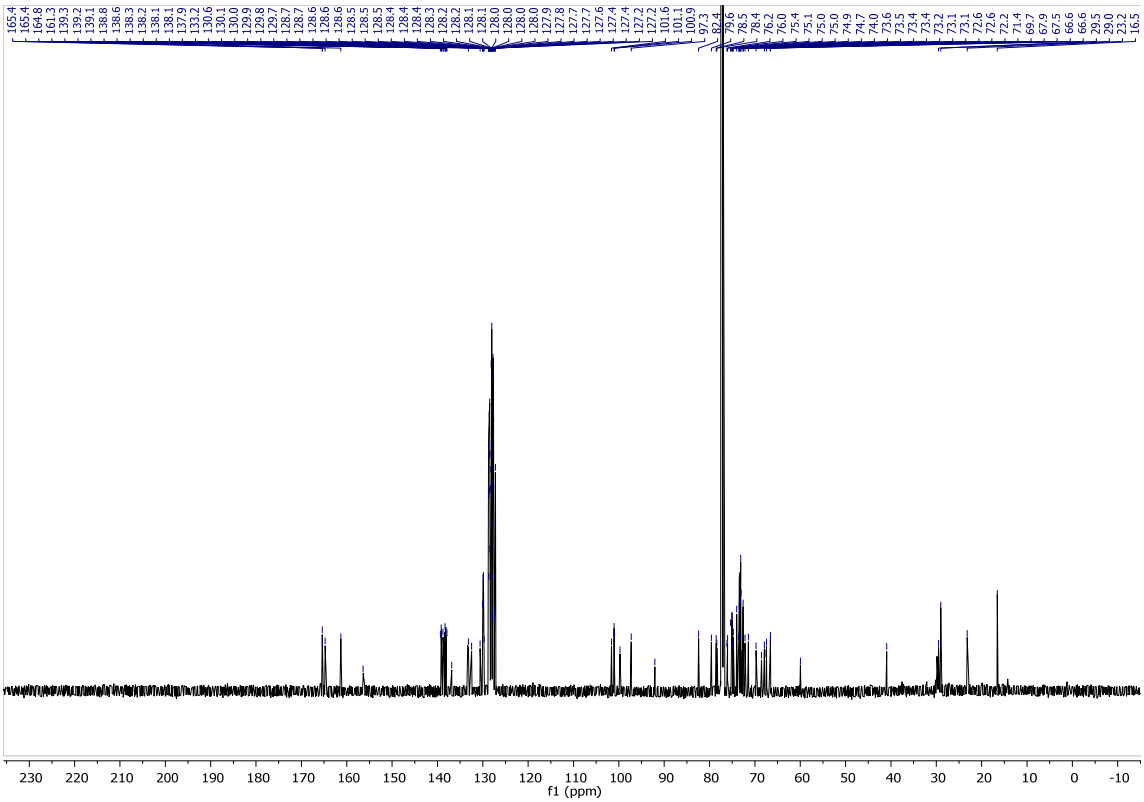

COSY: **2.39**

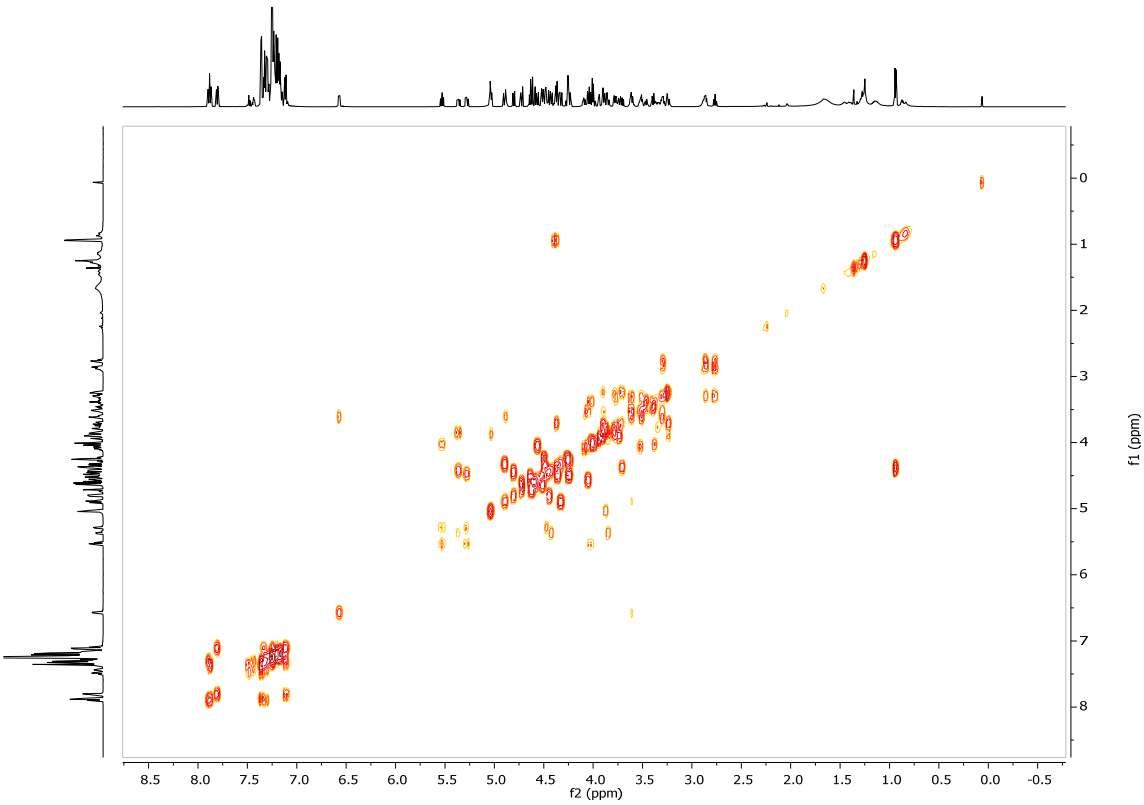

HSQC: **2.39**

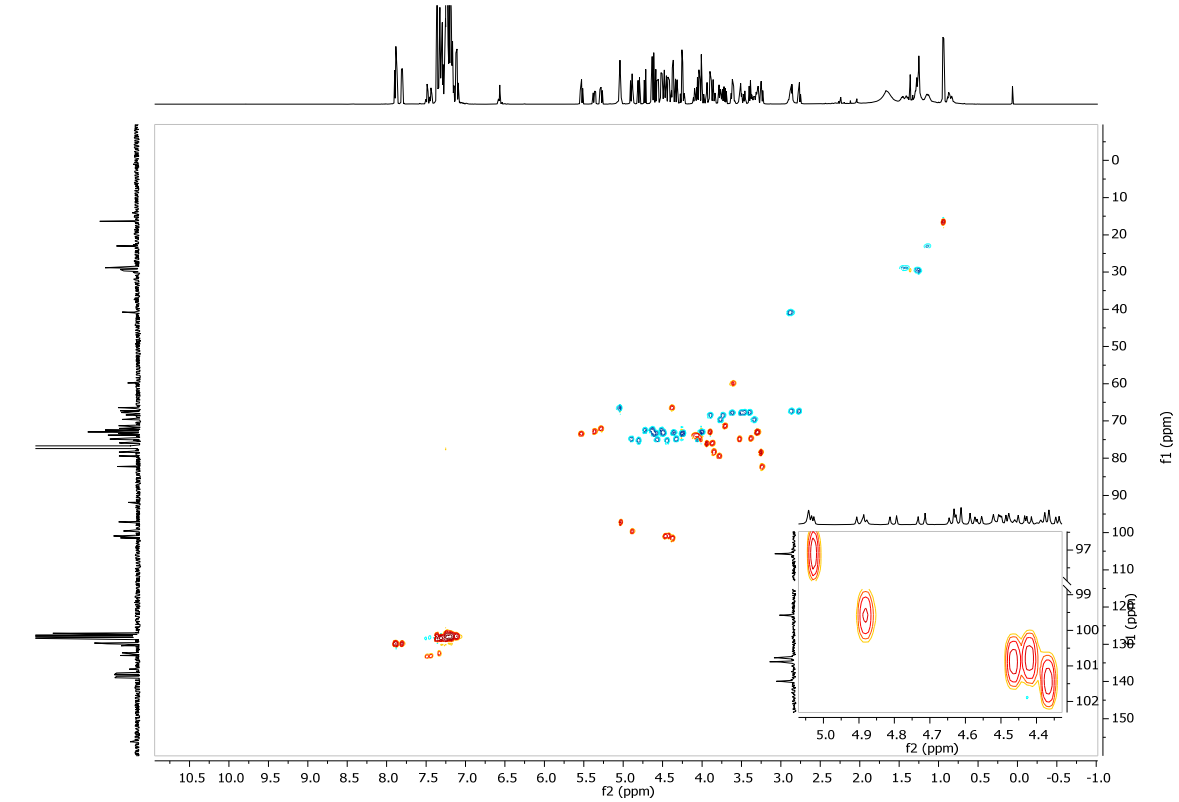

Coupled HSQC: **2.39**

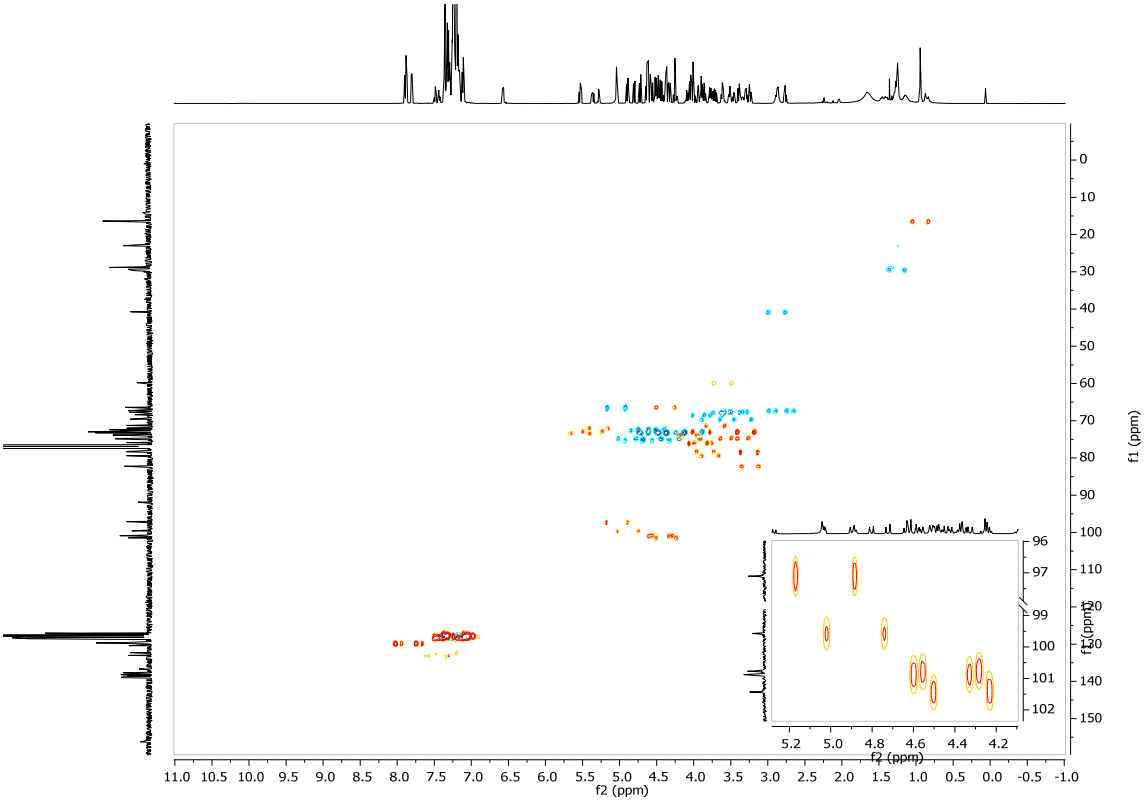

^{1}H NMR: **2.40**

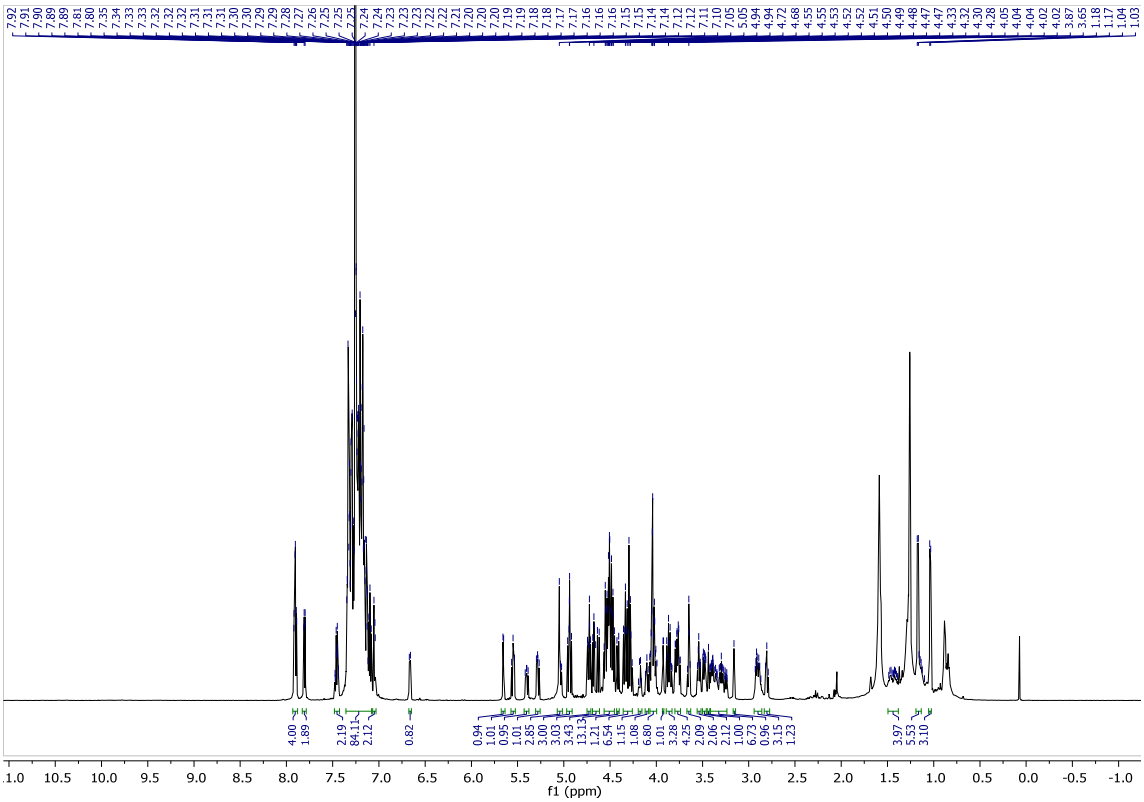

^{13}C NMR: **2.40**

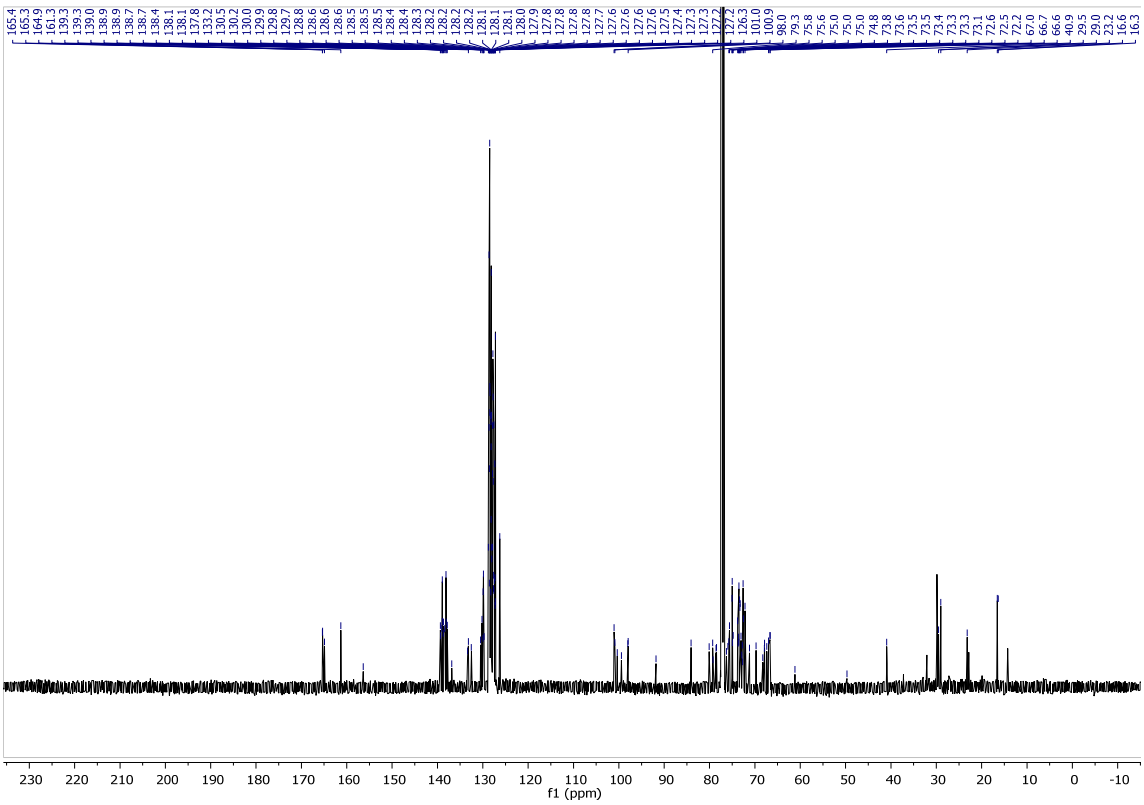

COSY: **2.40**

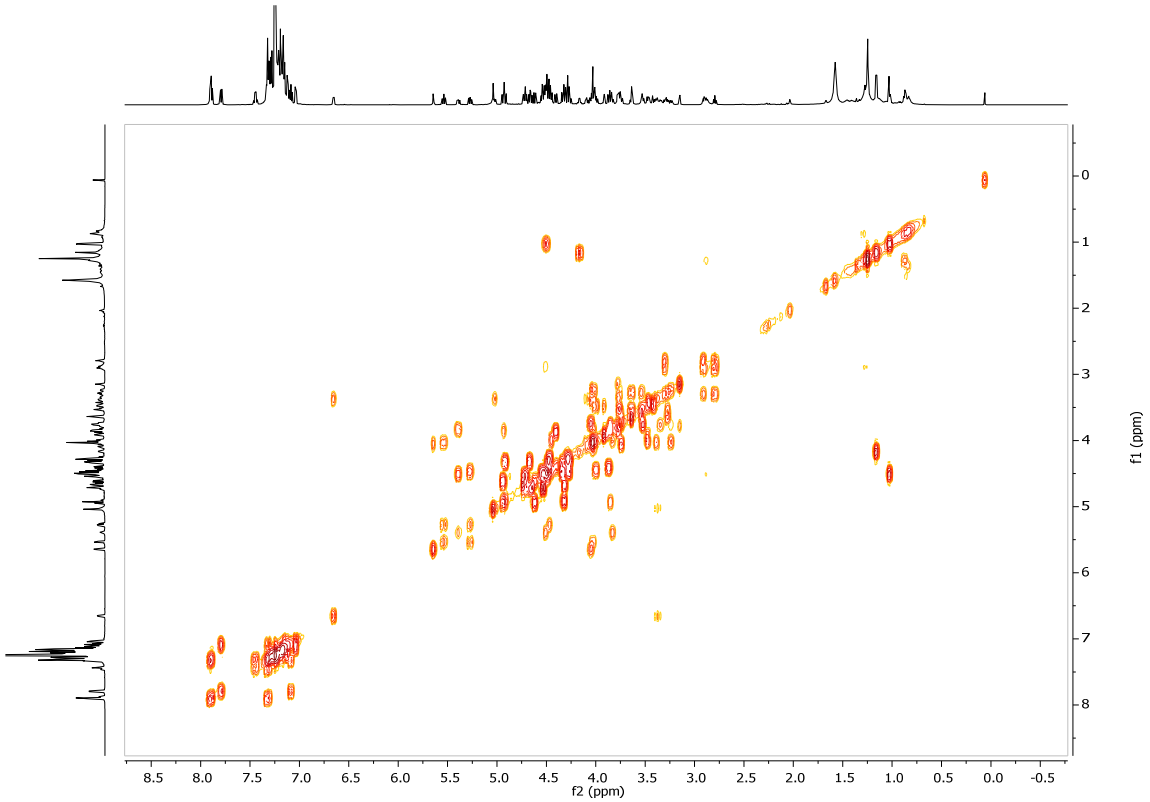

HSQC: **2.40**

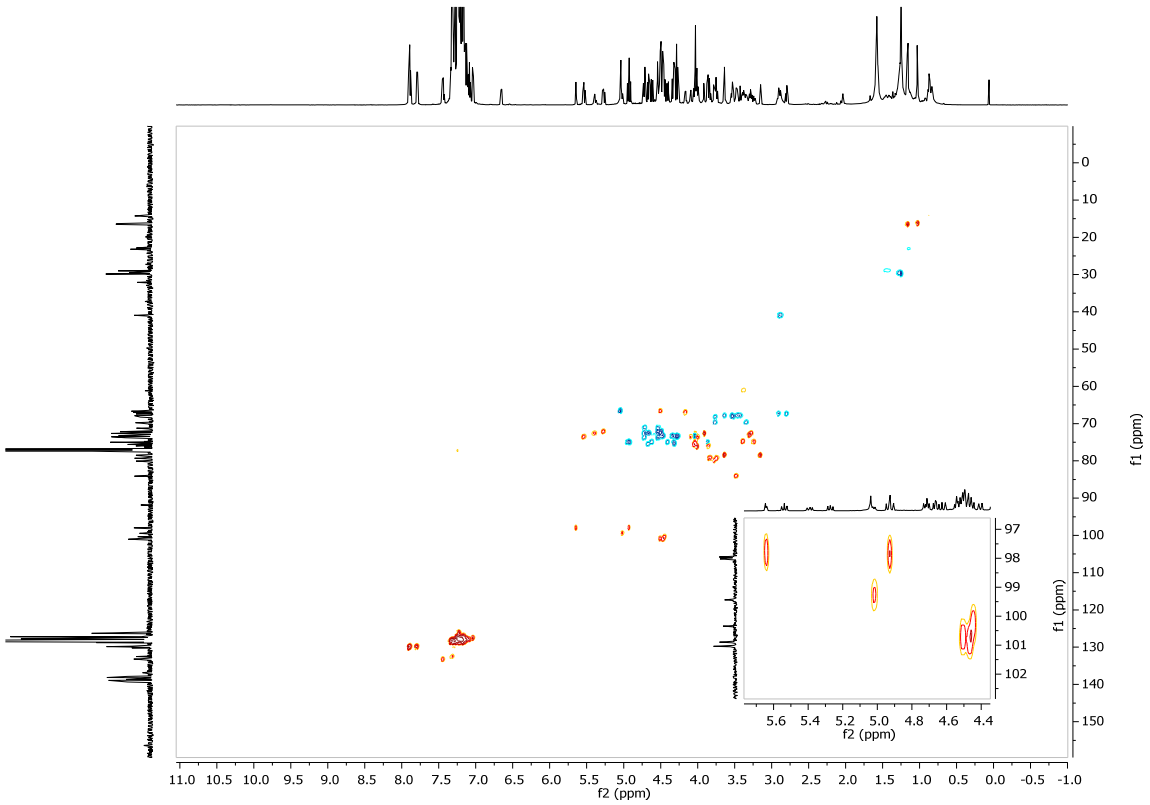

Coupled HSQC: **2.40**

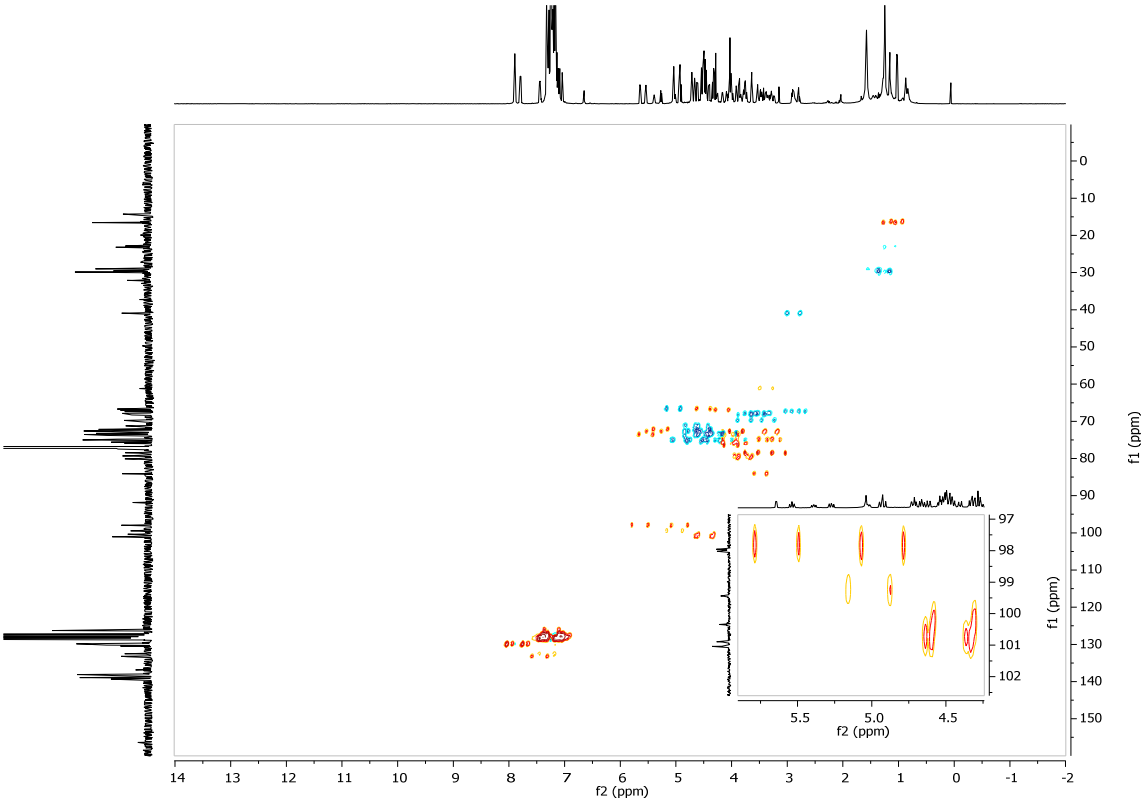

^{1}H NMR: **2.41**

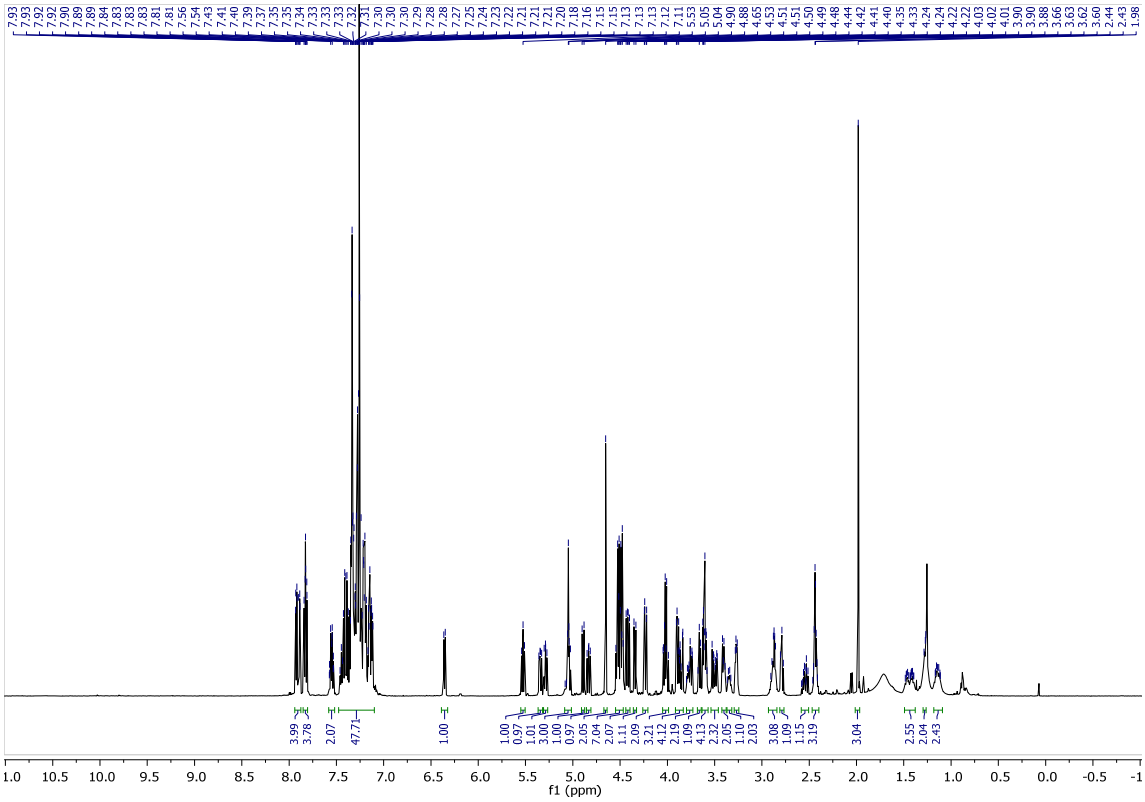

^{13}C NMR: **2.41**

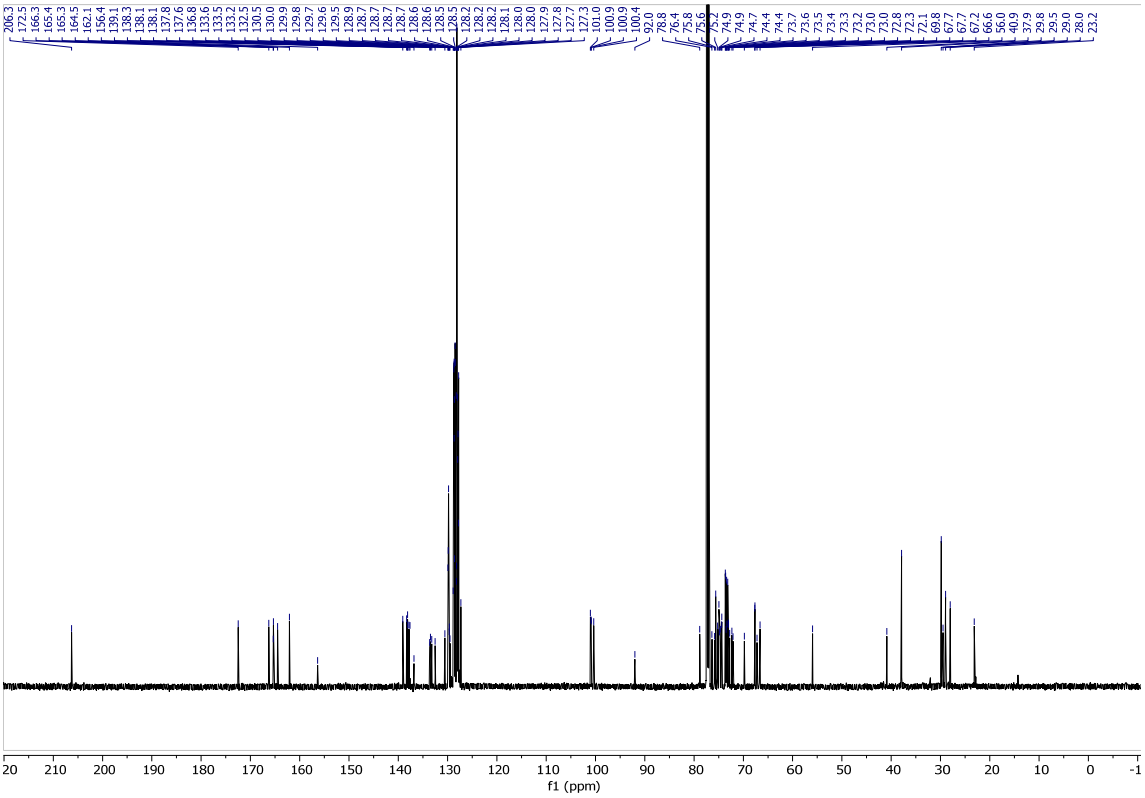

COSY: **2.41**

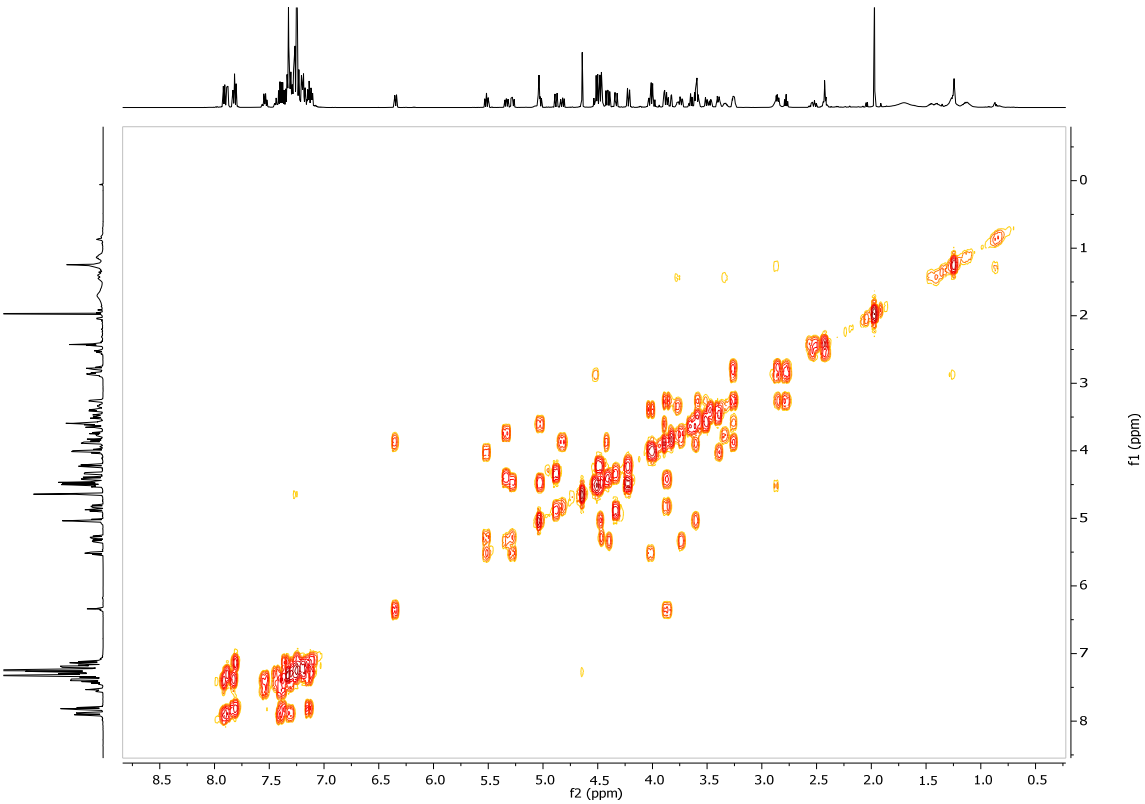

HSQC: **2.41**

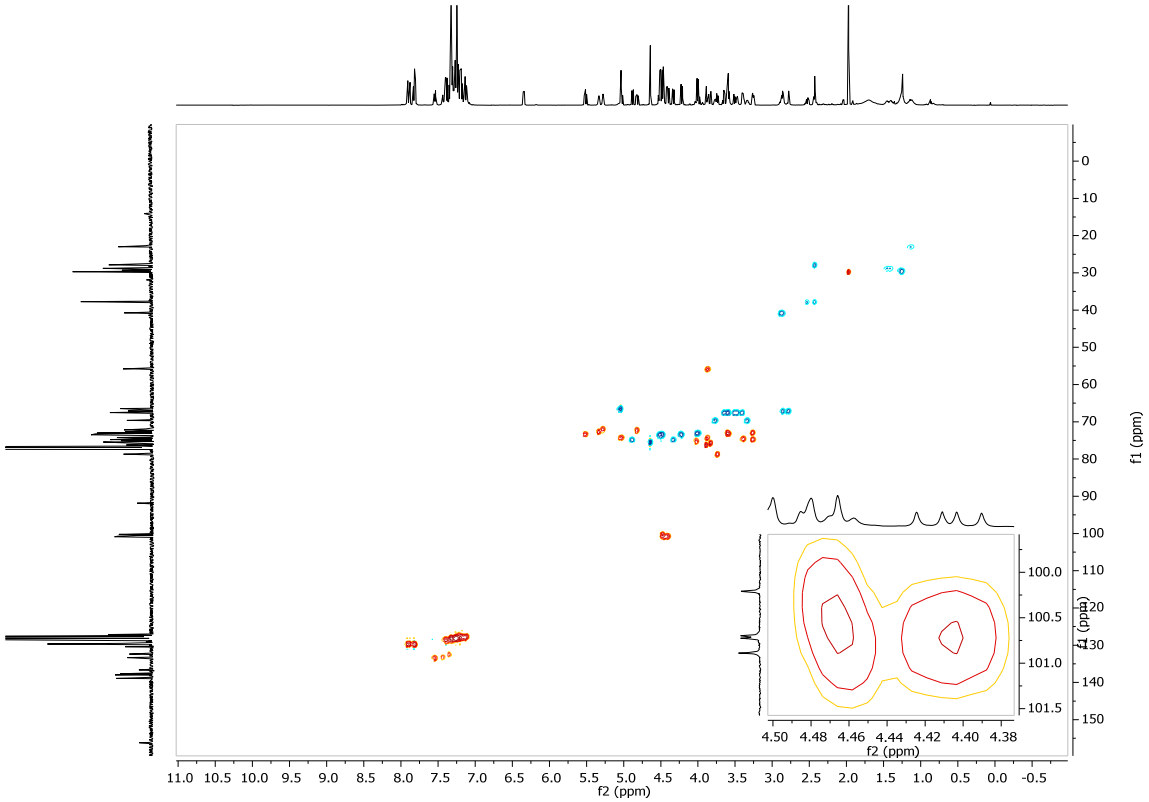

Coupled HSQC: **2.41**

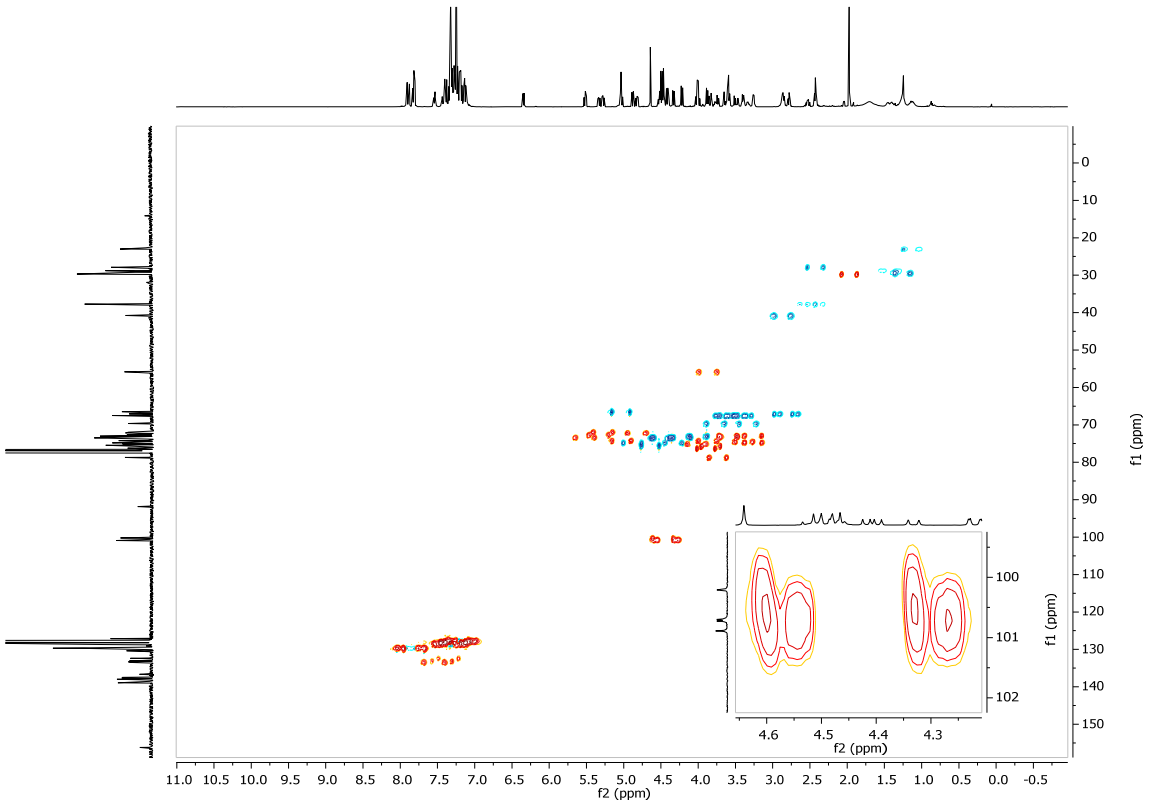

^{1}H NMR: **2.42**

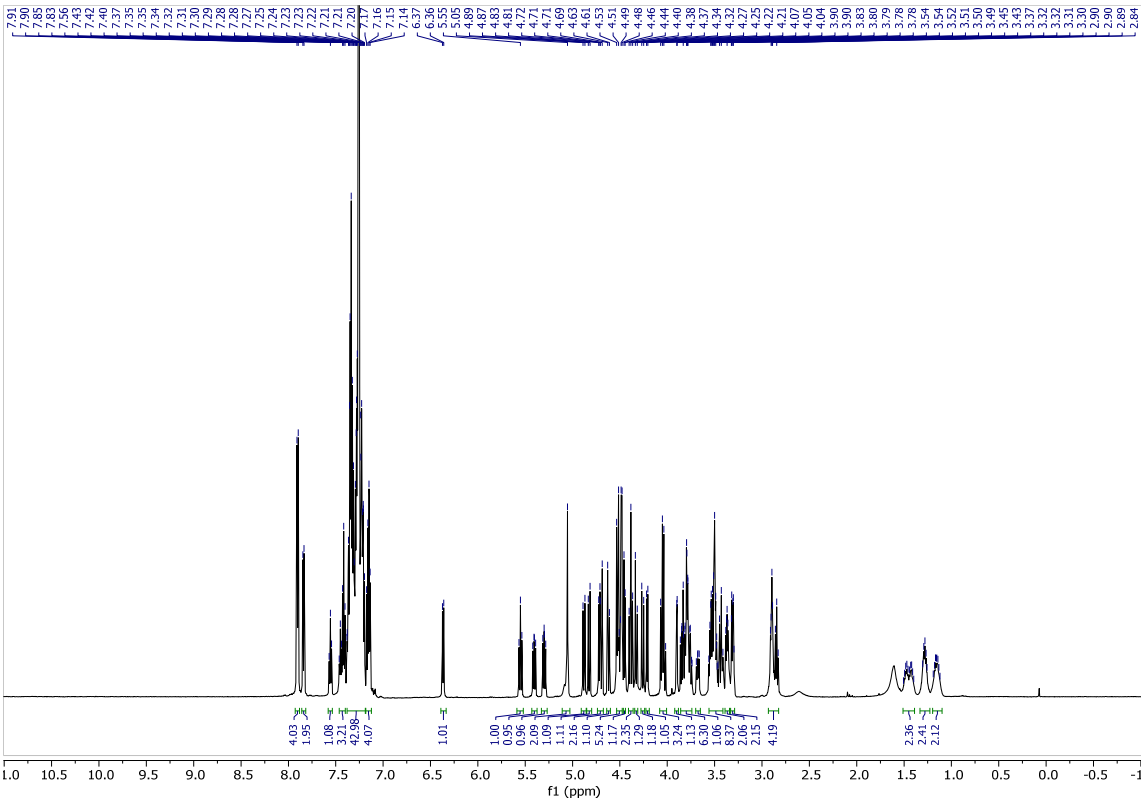

^{13}C NMR: **2.42**

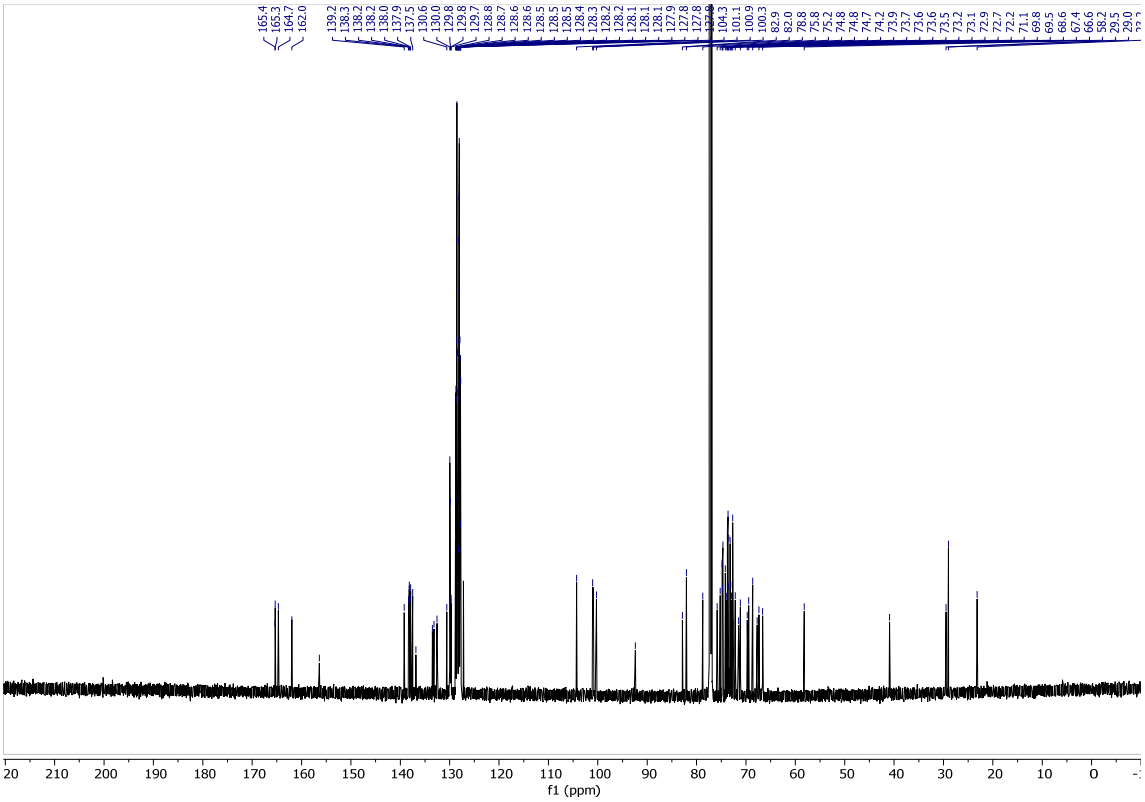

COSY: **2.42**

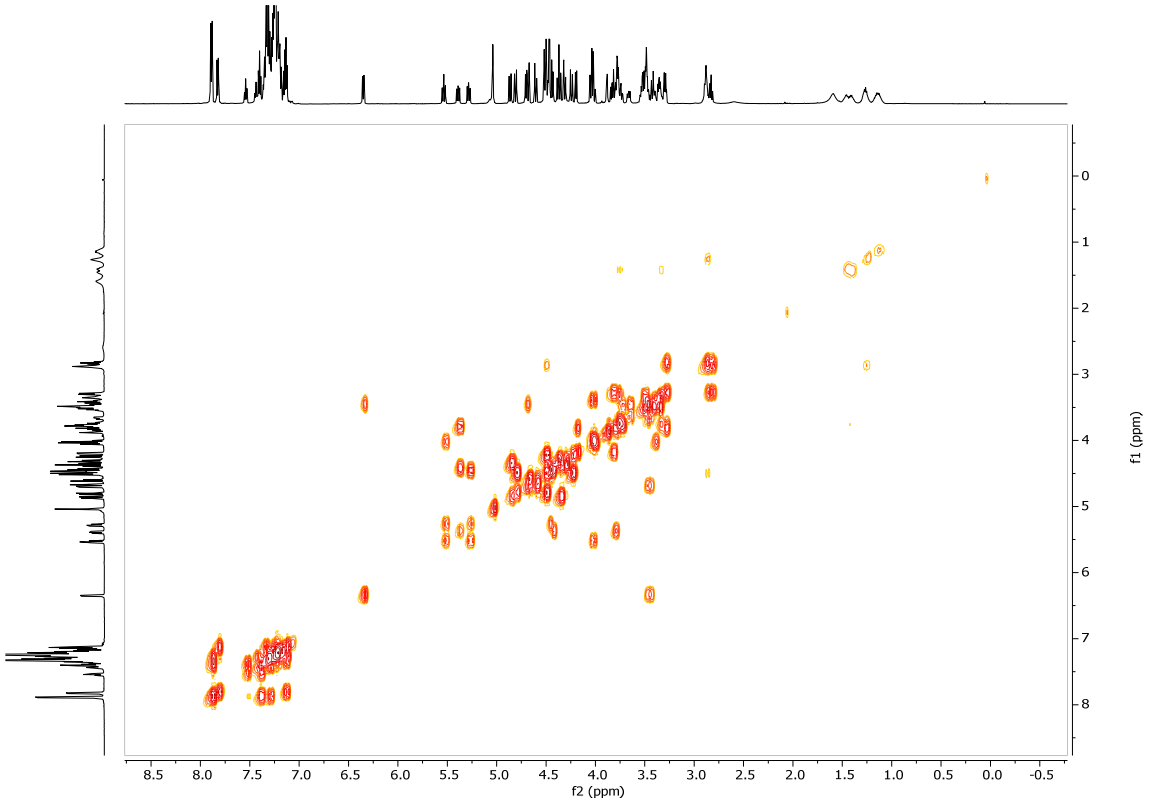

HSQC: **2.42**

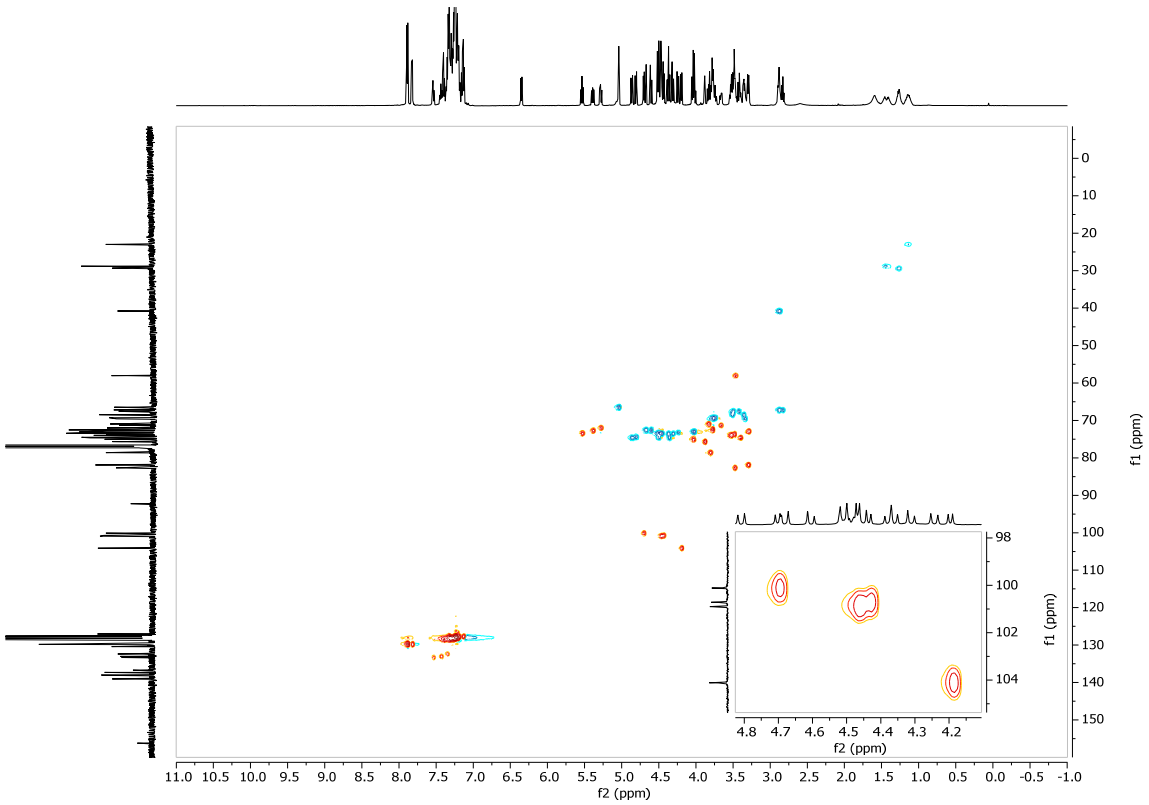

Coupled HSQC: **2.42**

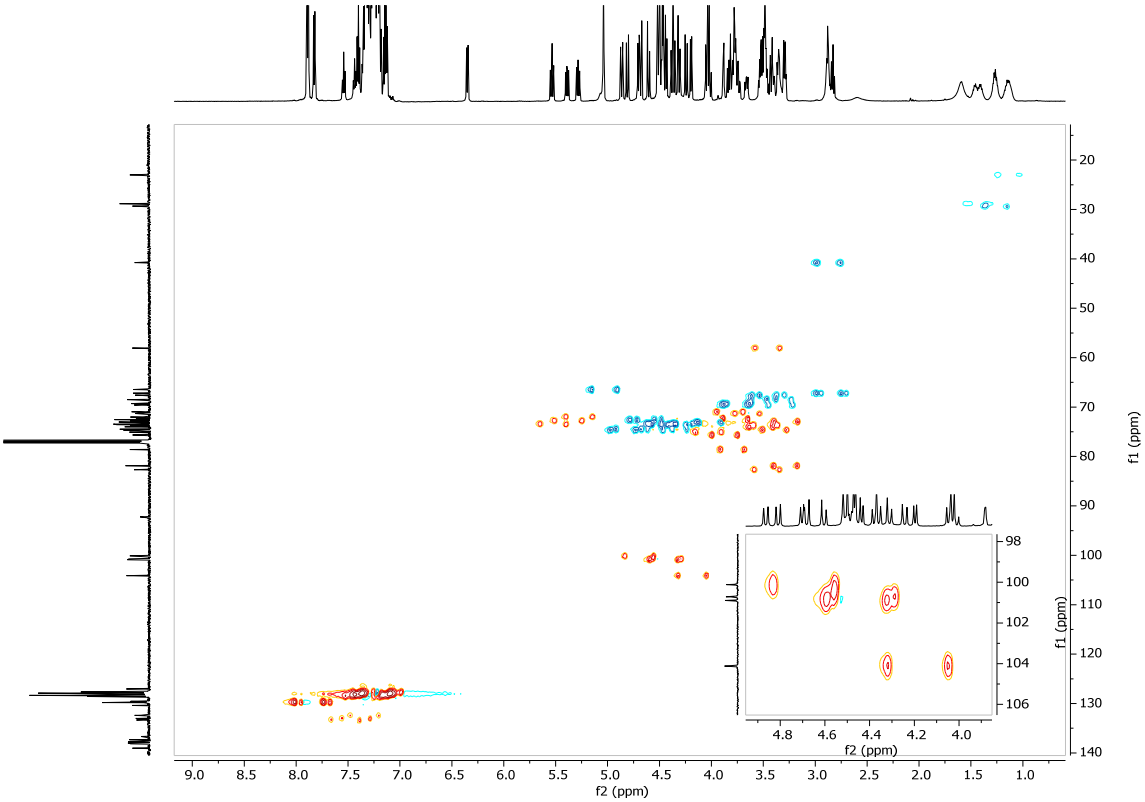

^{1}H NMR: **2.43**

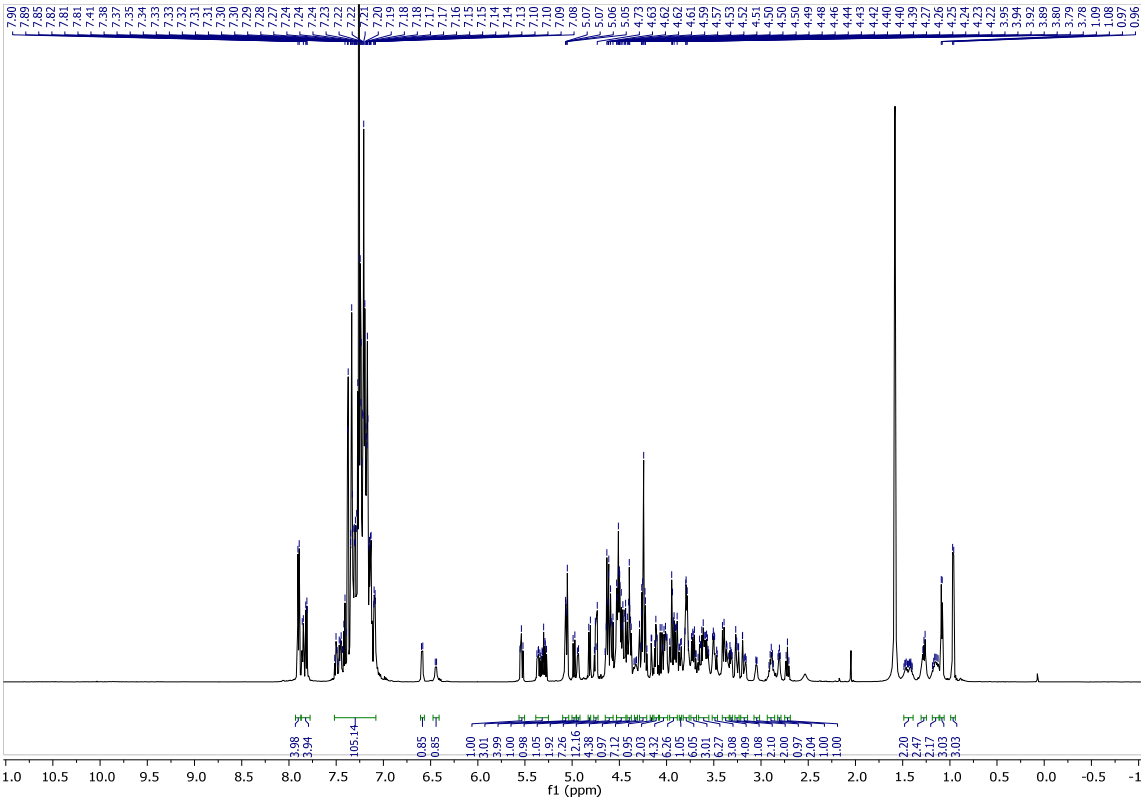

^{13}C NMR: HSQC: **2.43**

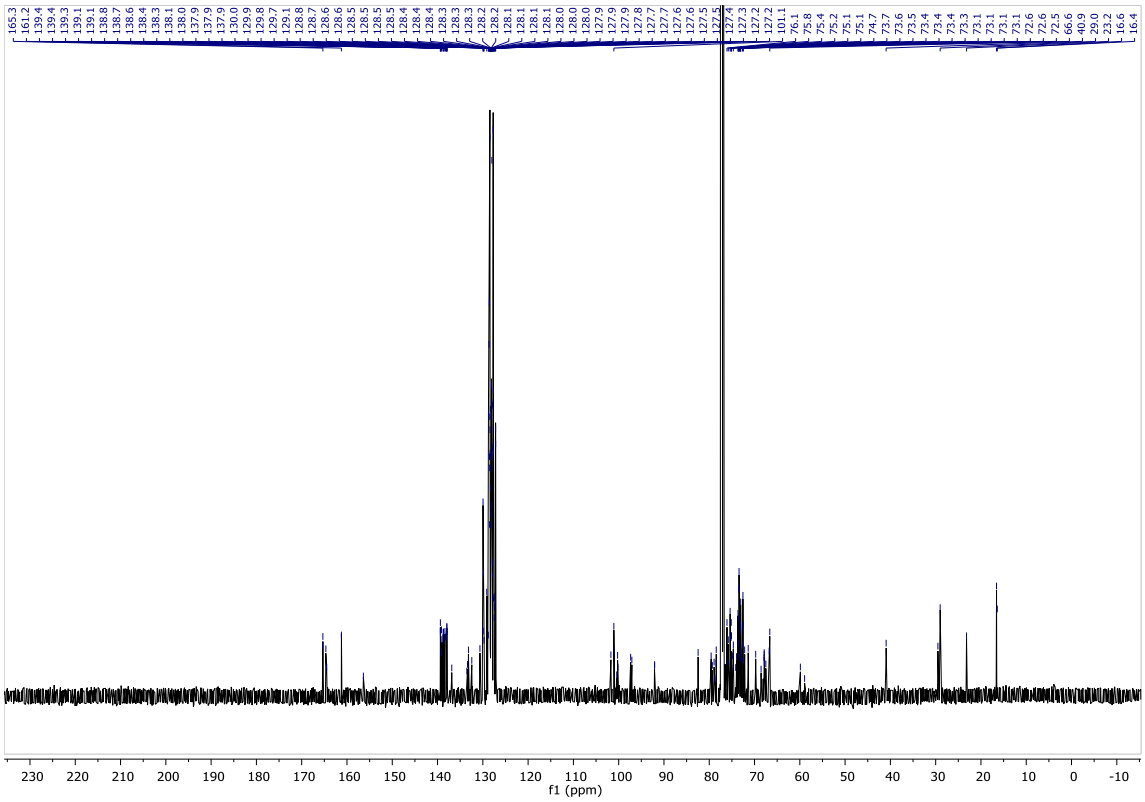

COSY: **2.43**

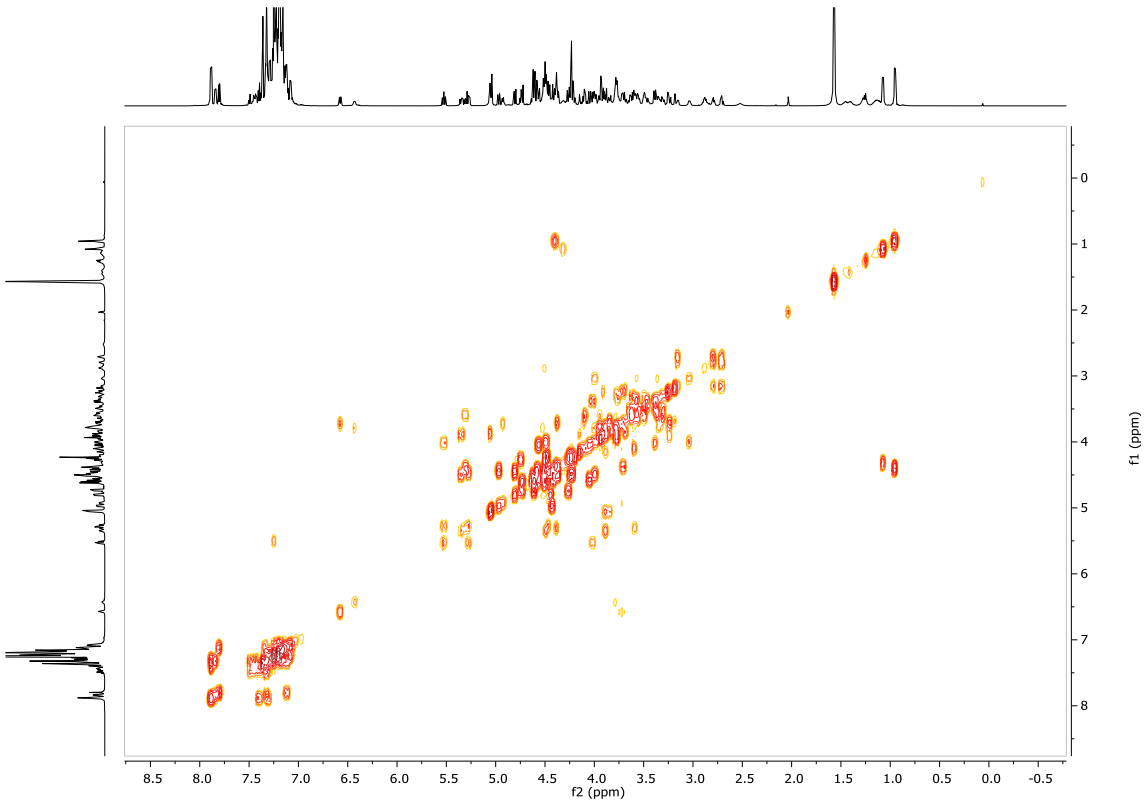

HSQC: **2.43**

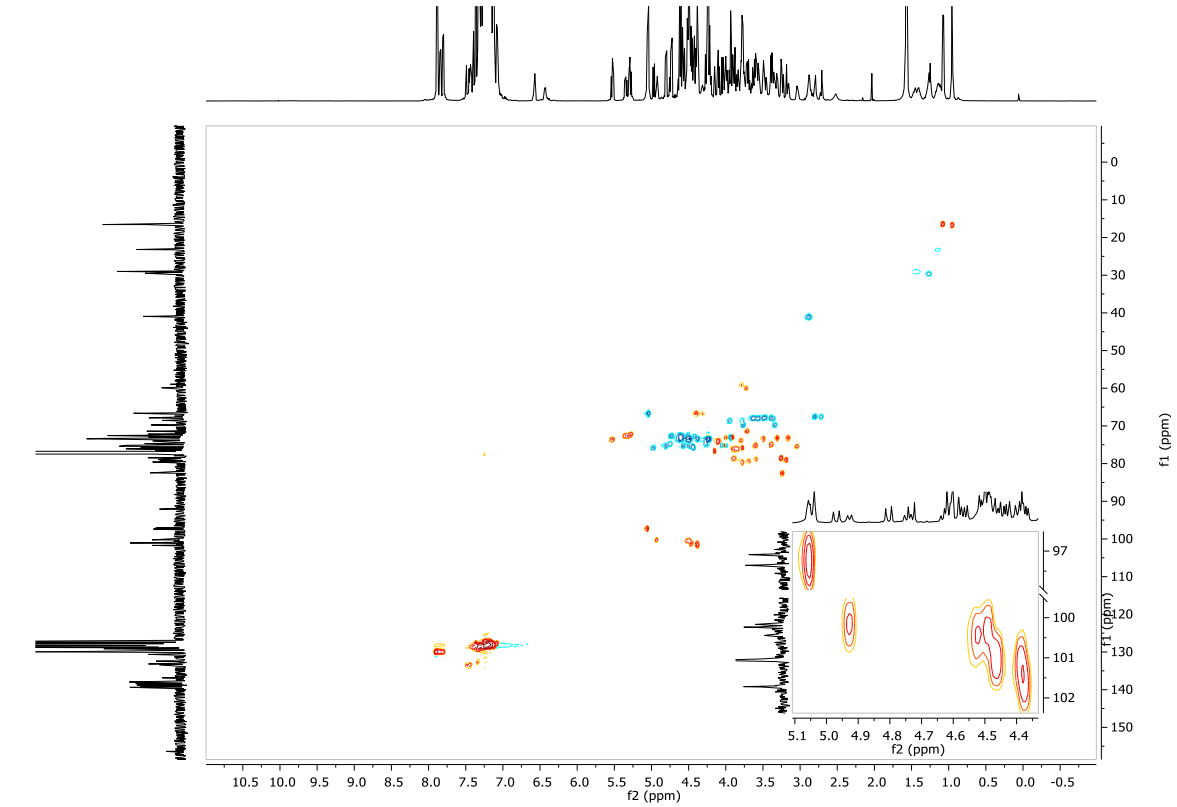

Coupled HSQC: **2.43**

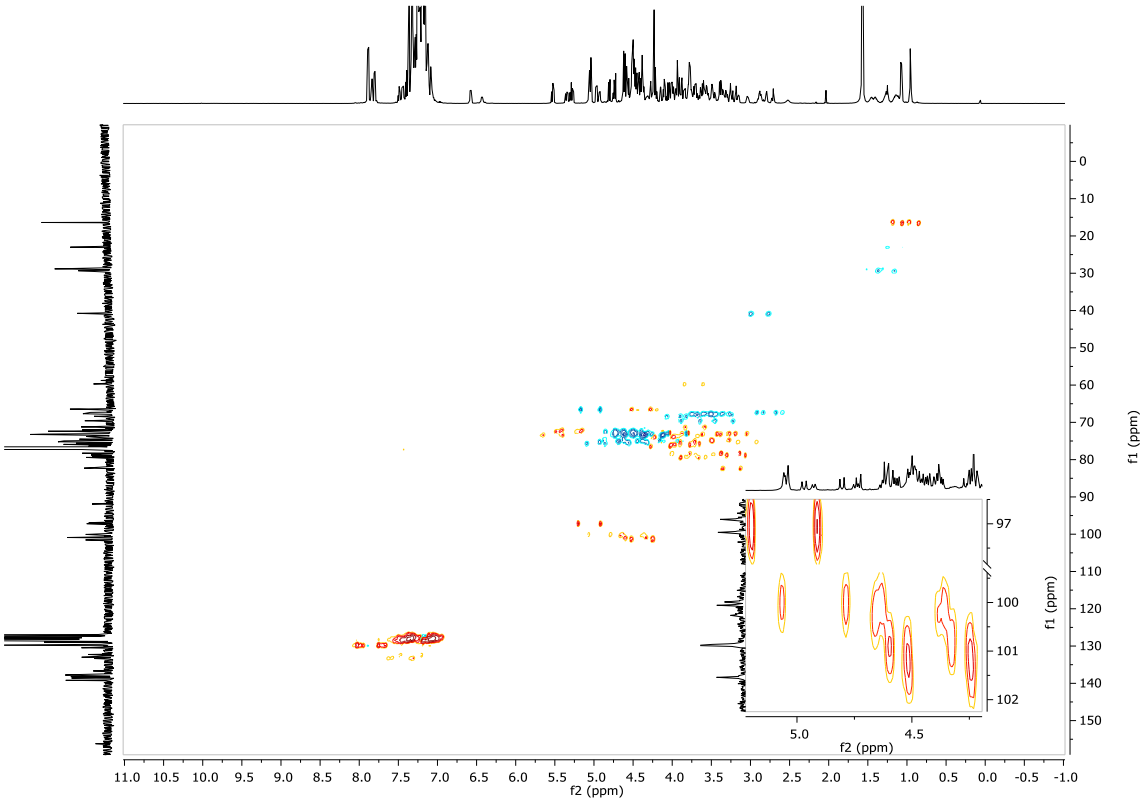

^{1}H NMR: **2.44**

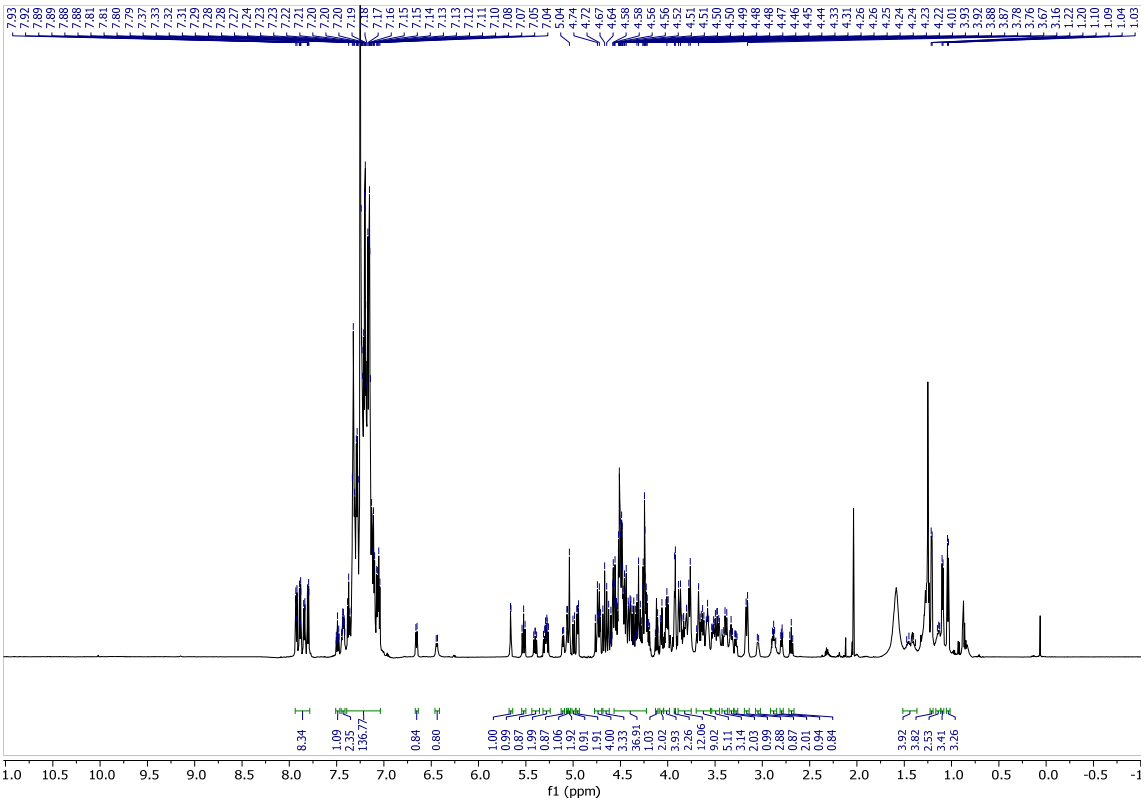

^{13}C NMR: **2.44**

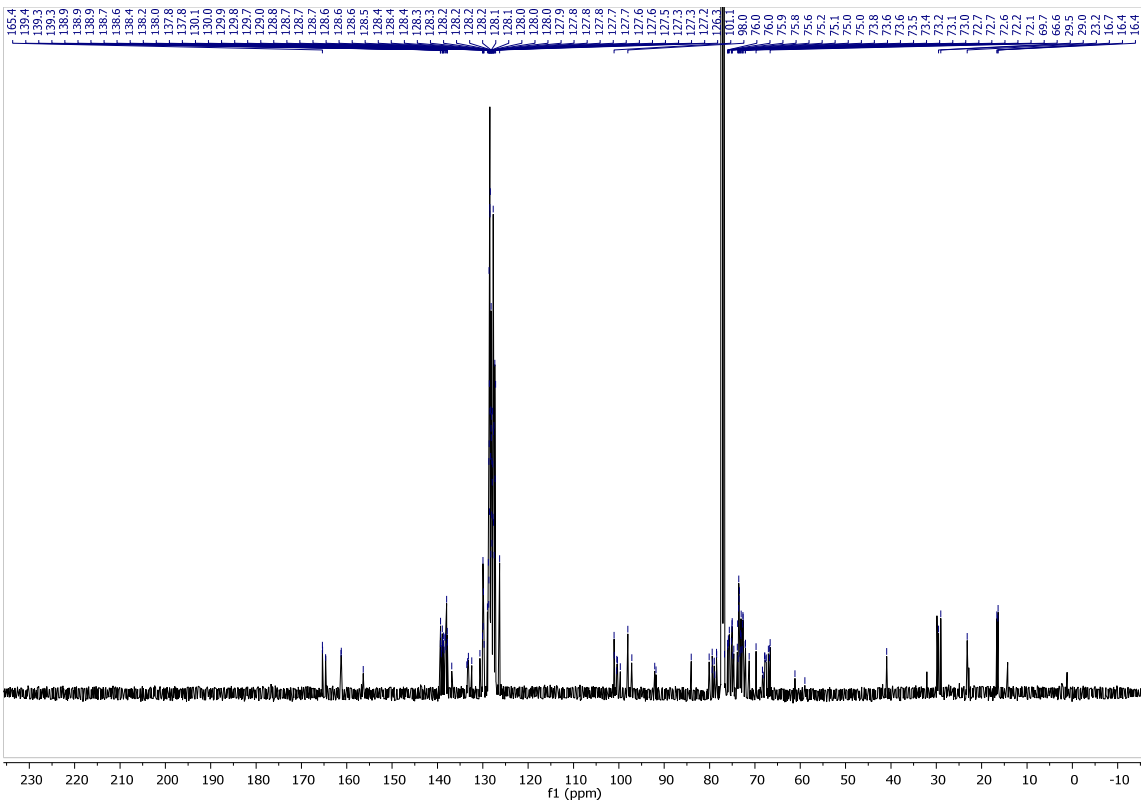

COSY: **2.44**

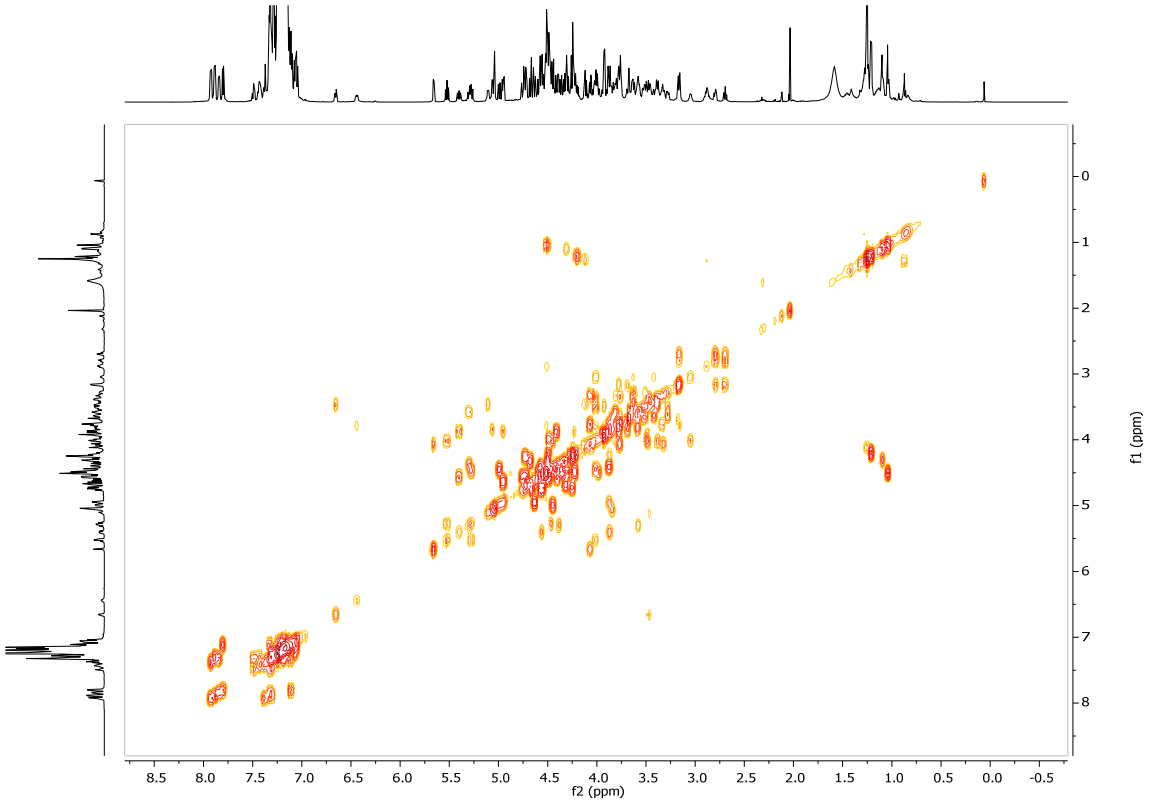

HSQC: **2.44**

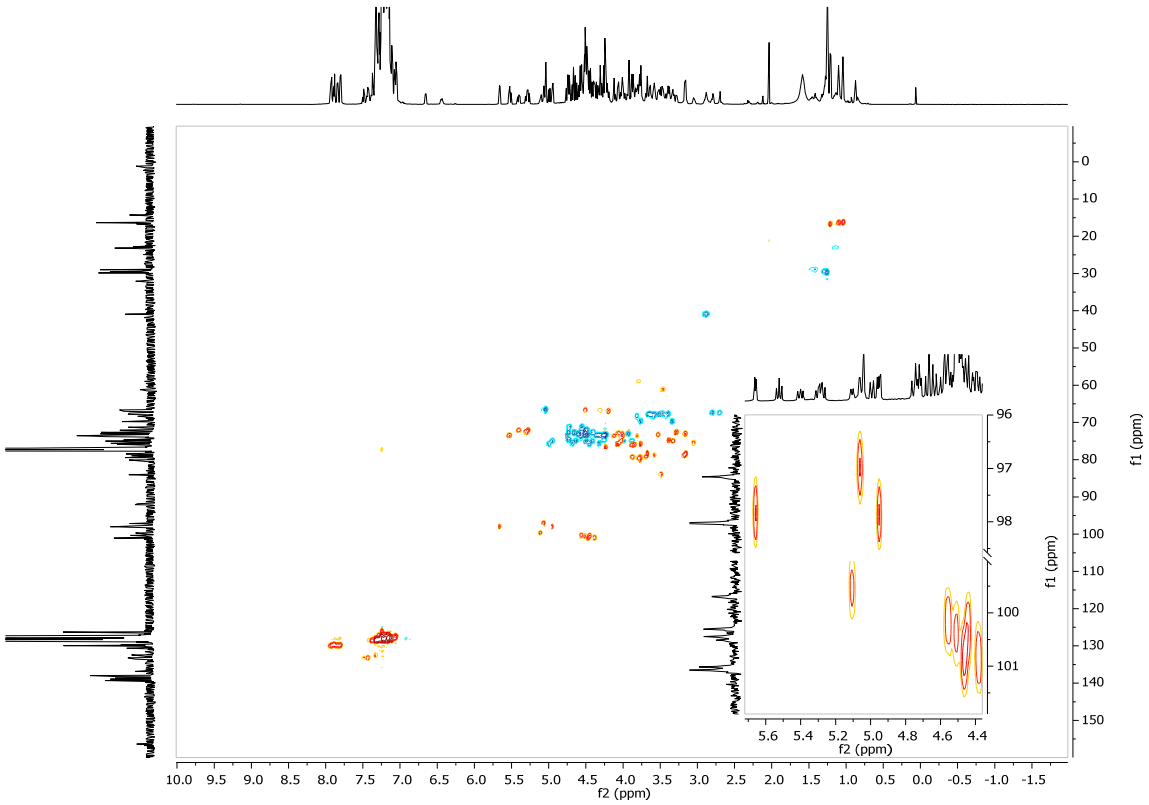

Coupled HSQC: **2.44**

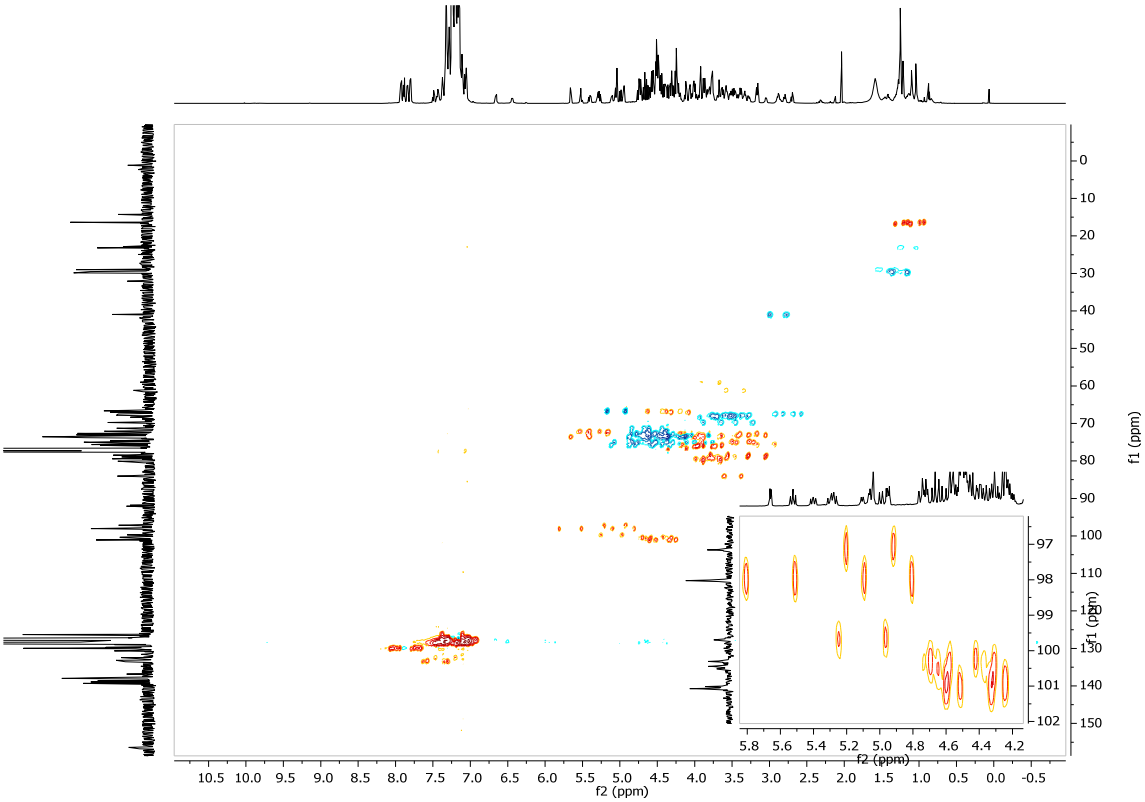

^{1}H NMR: **2.46**

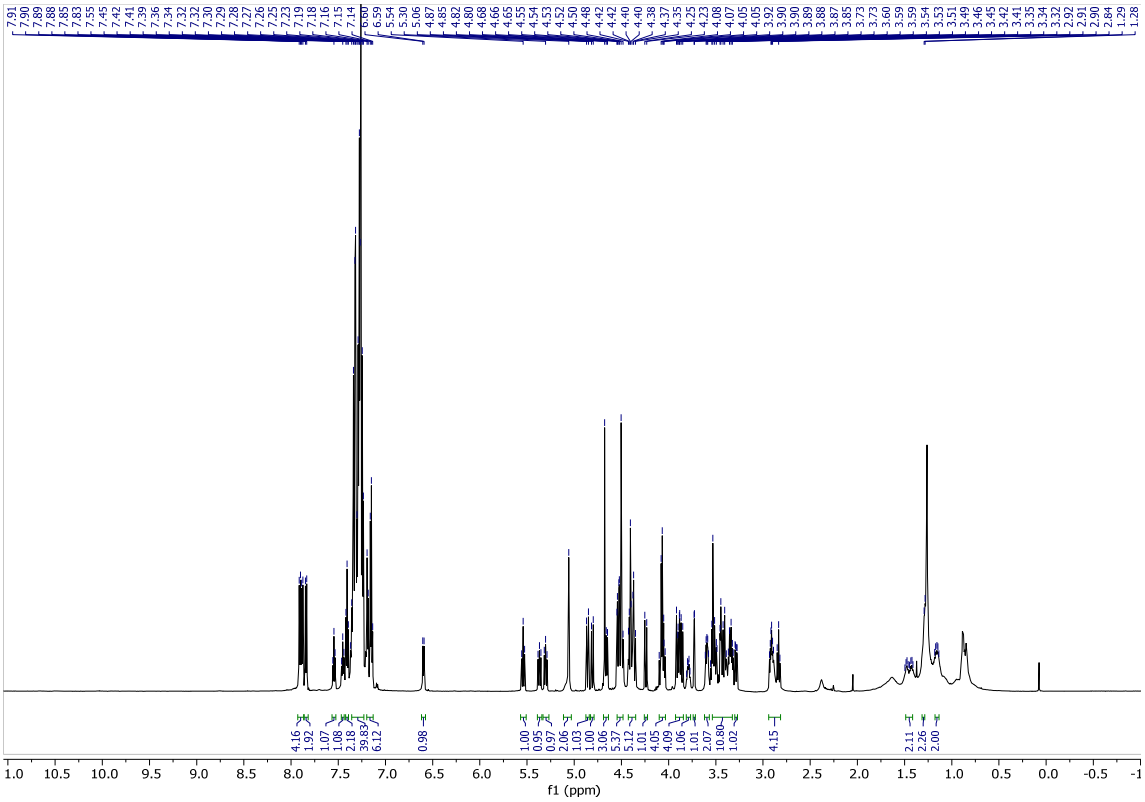

^{13}C NMR: **2.46**

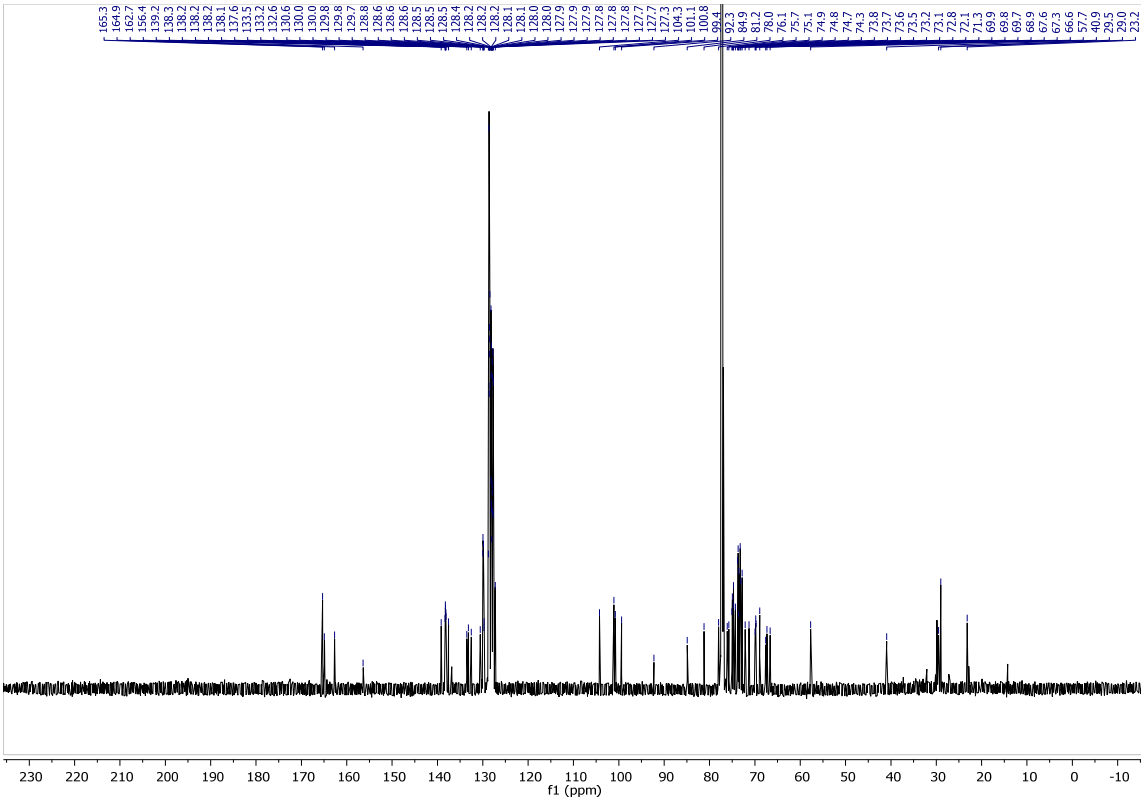

COSY: **2.46**

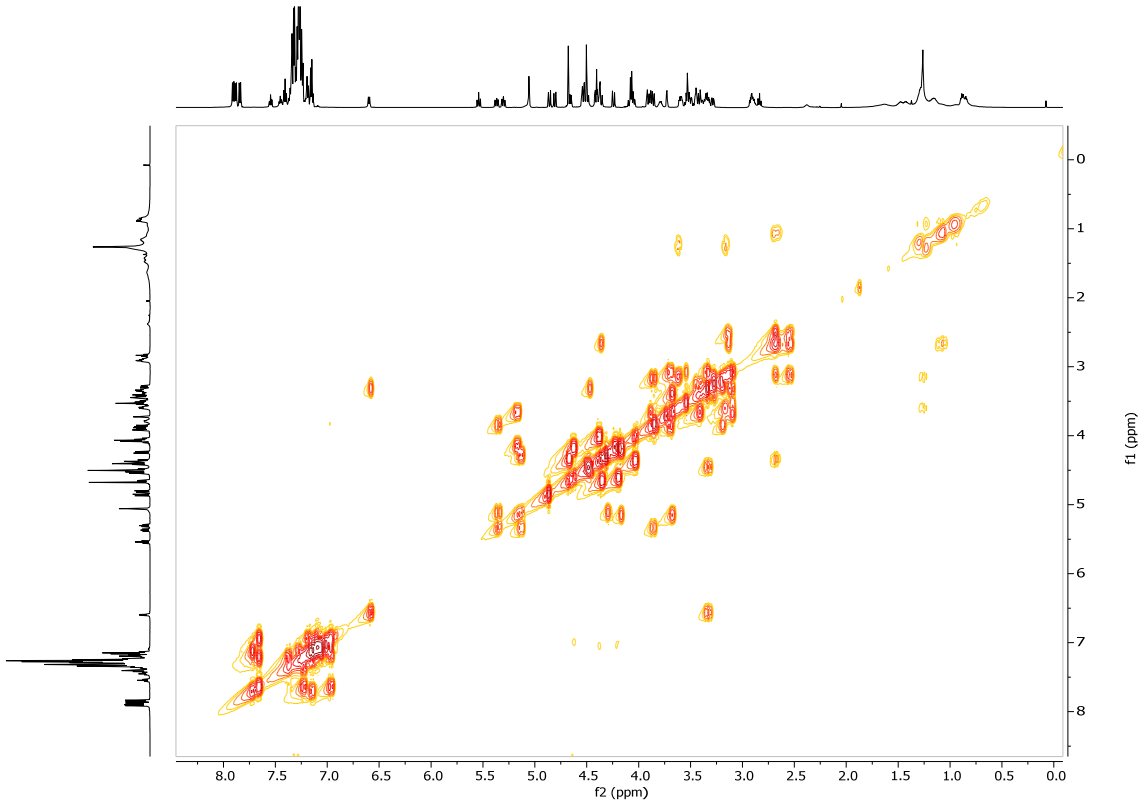

HSQC: **2.46**

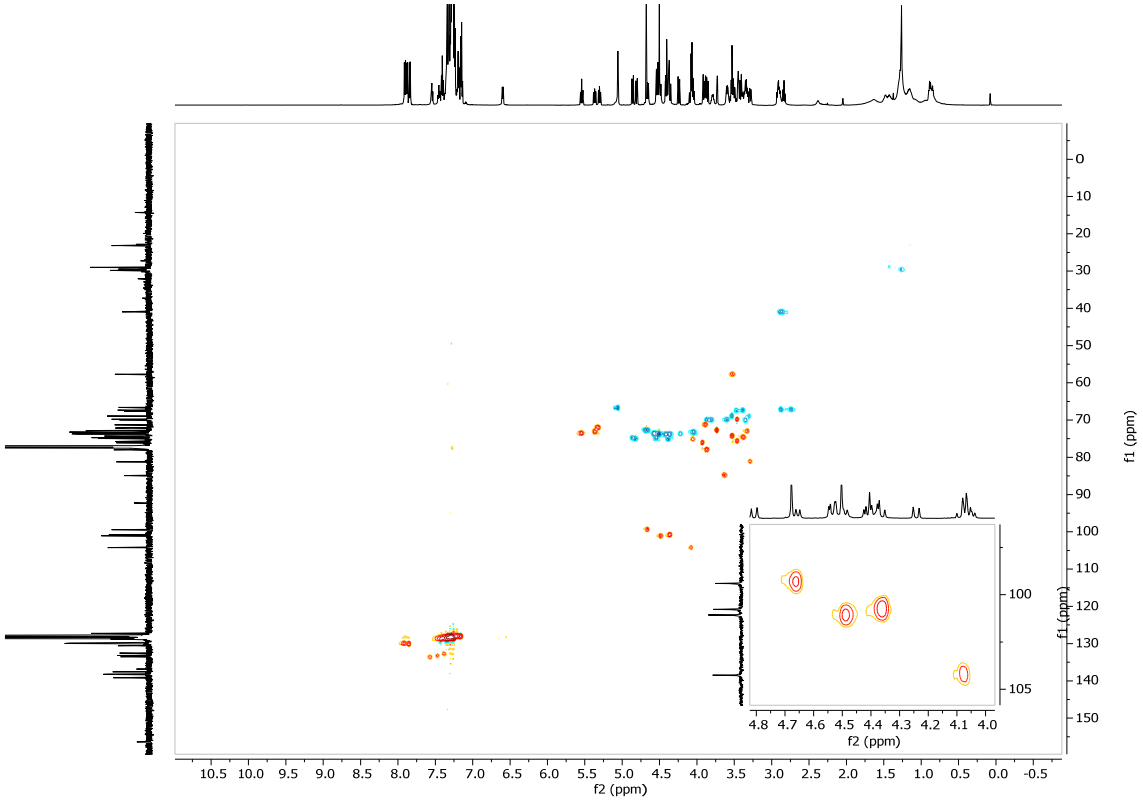

Coupled HSQC: **2.46**

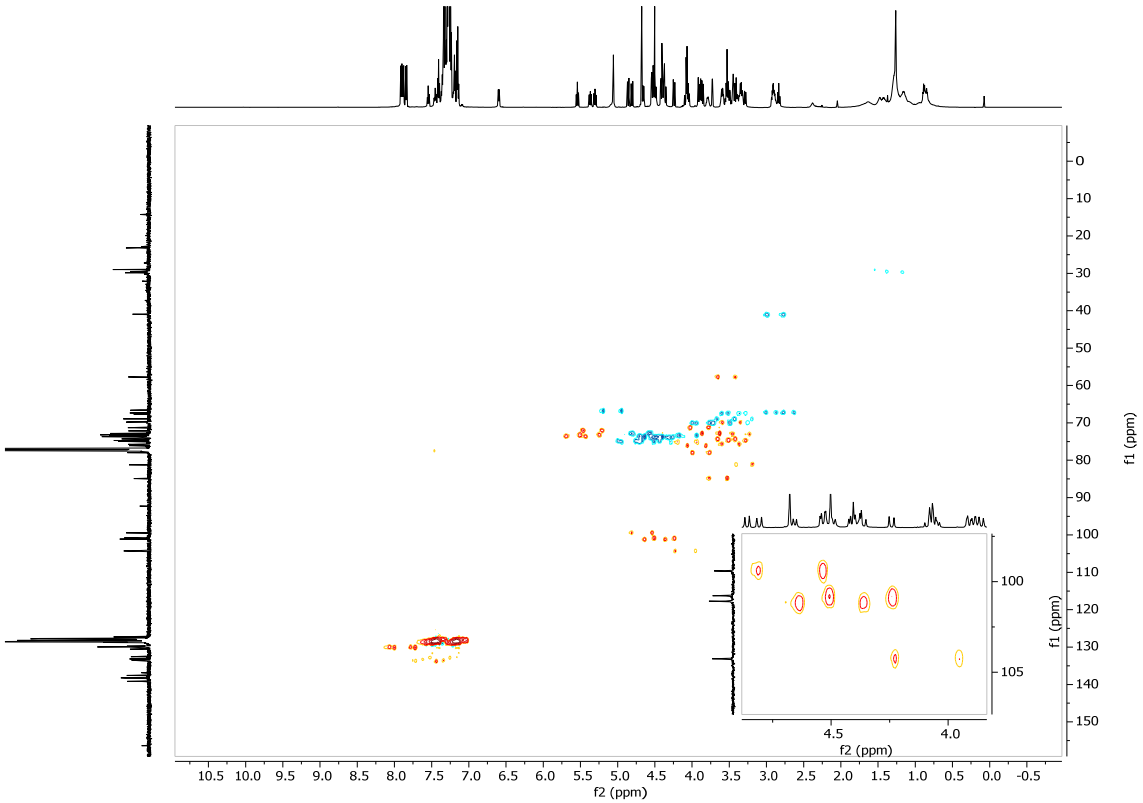

^{1}H NMR: **2.47**

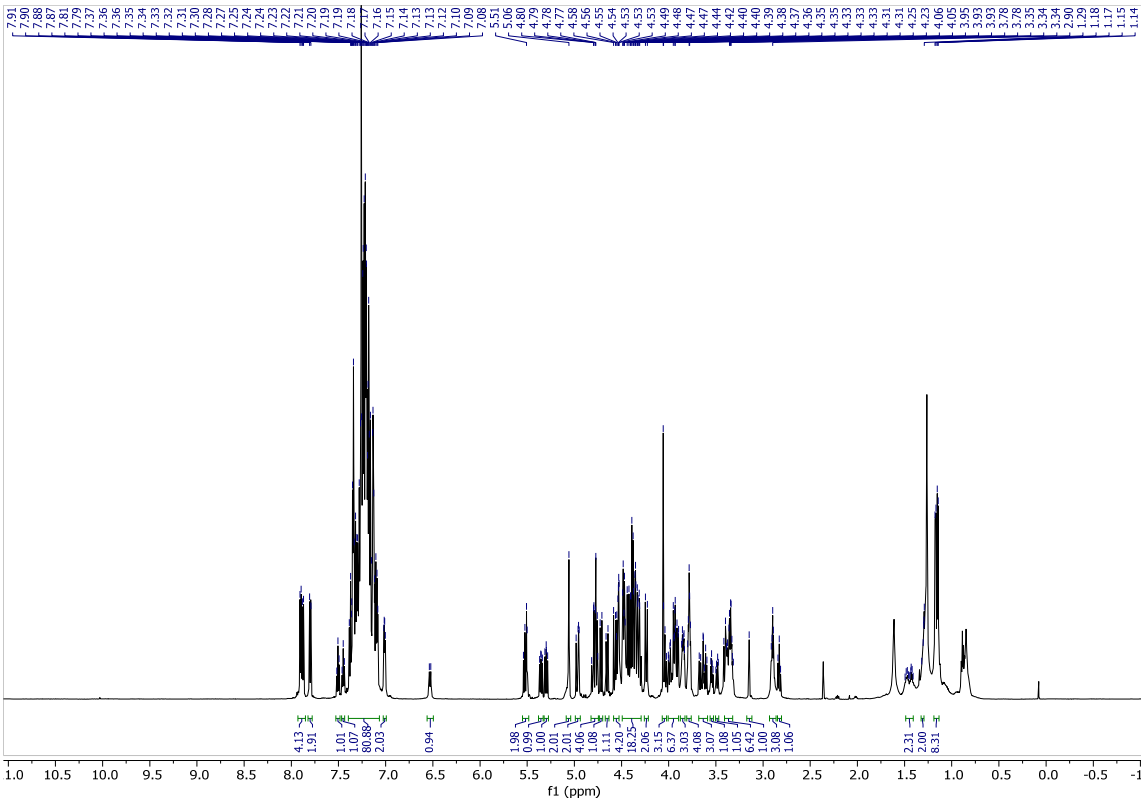

^{13}C NMR: **2.47**

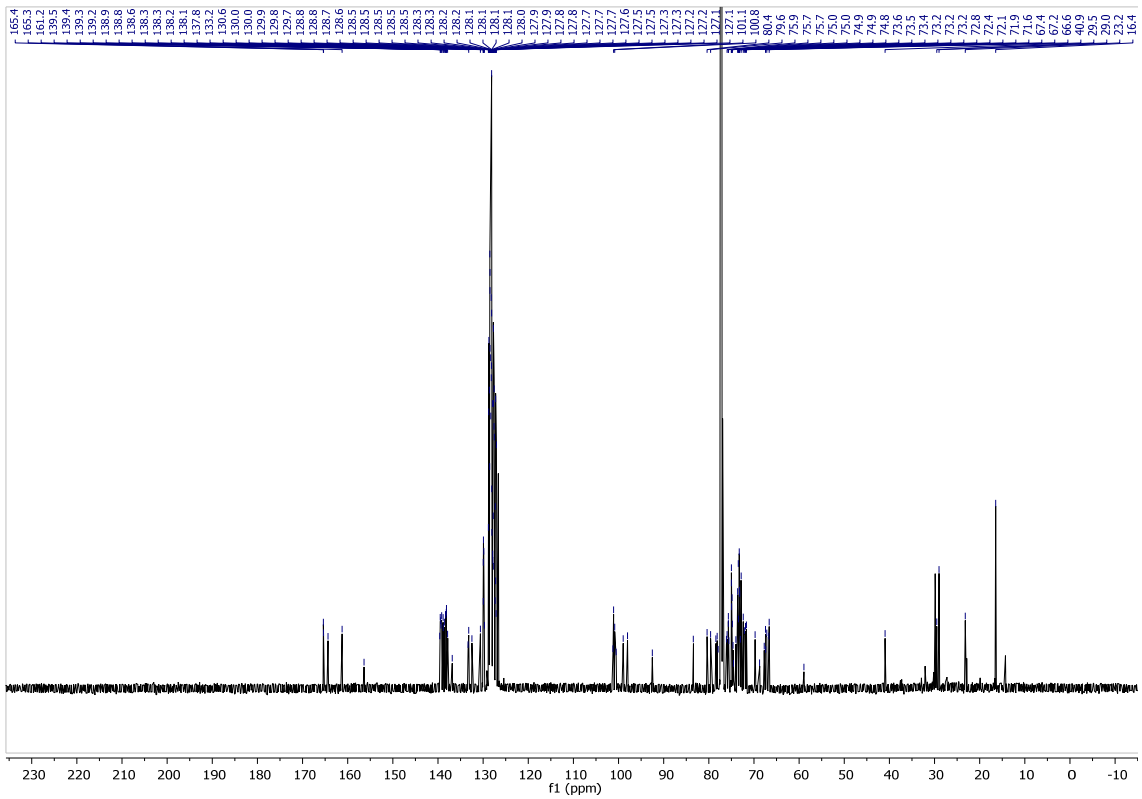

COSY: **2.47**

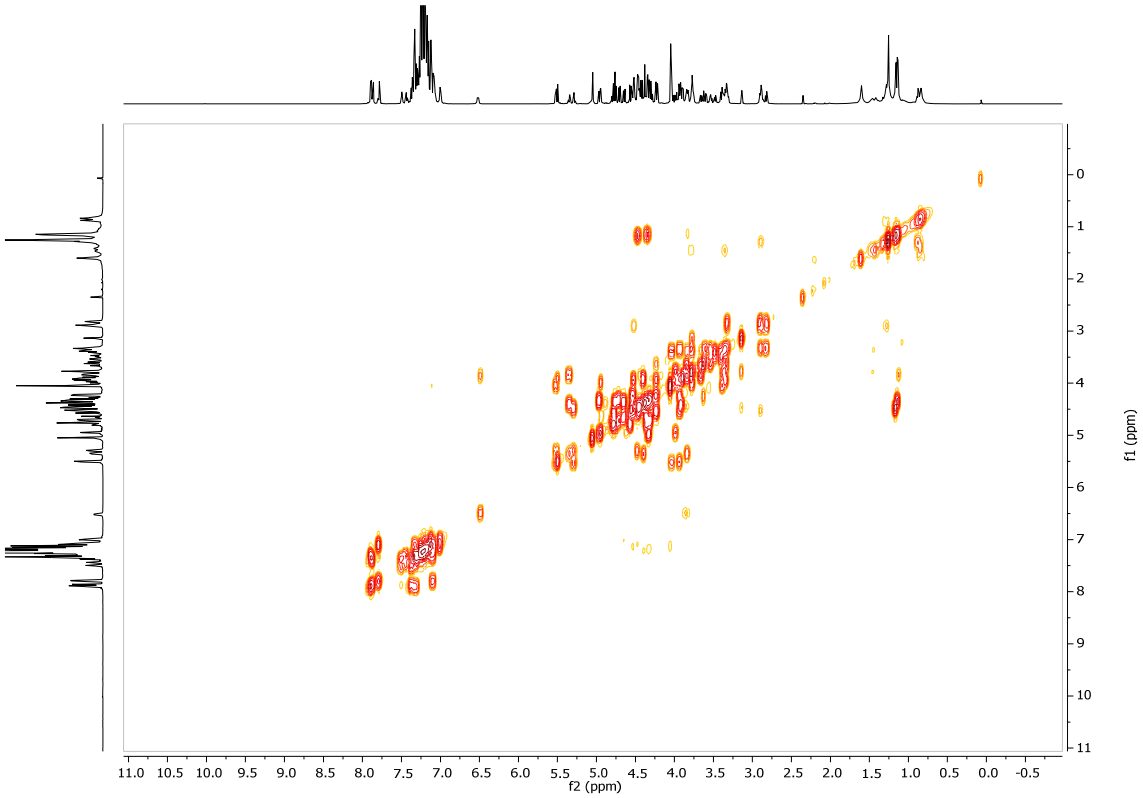

HSQC: **2.47**

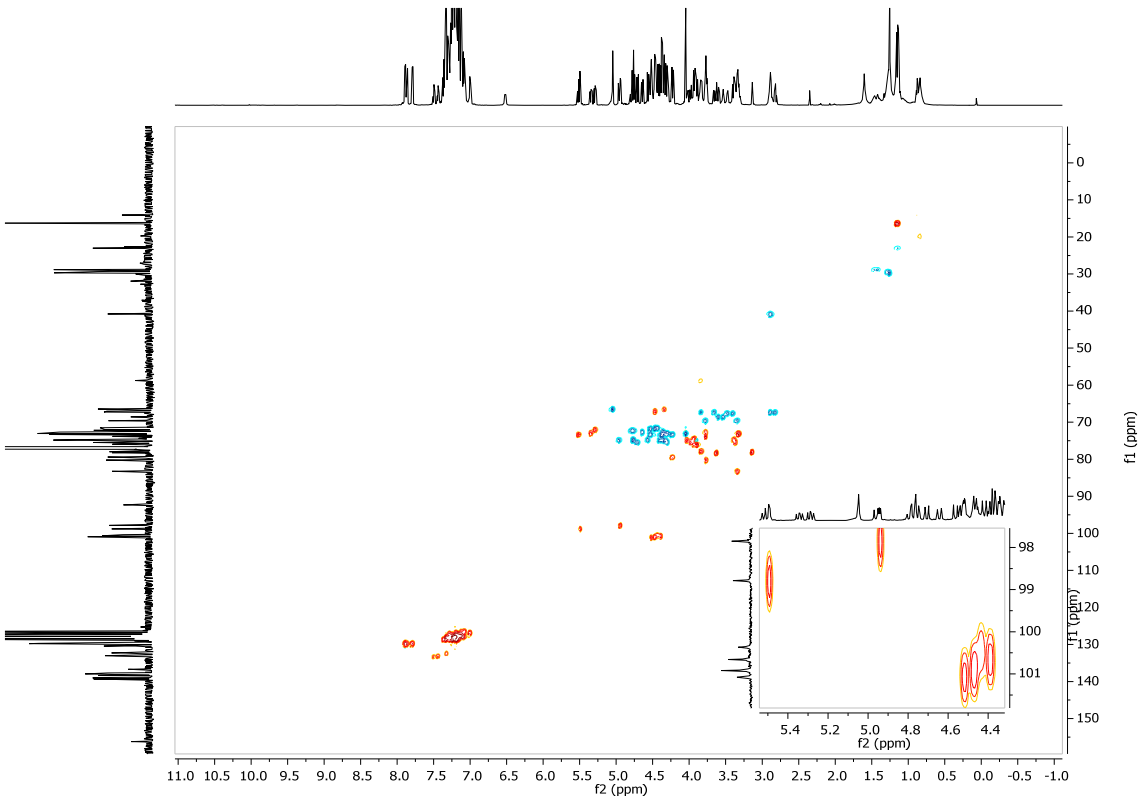

Coupled HSQC: **2.47**

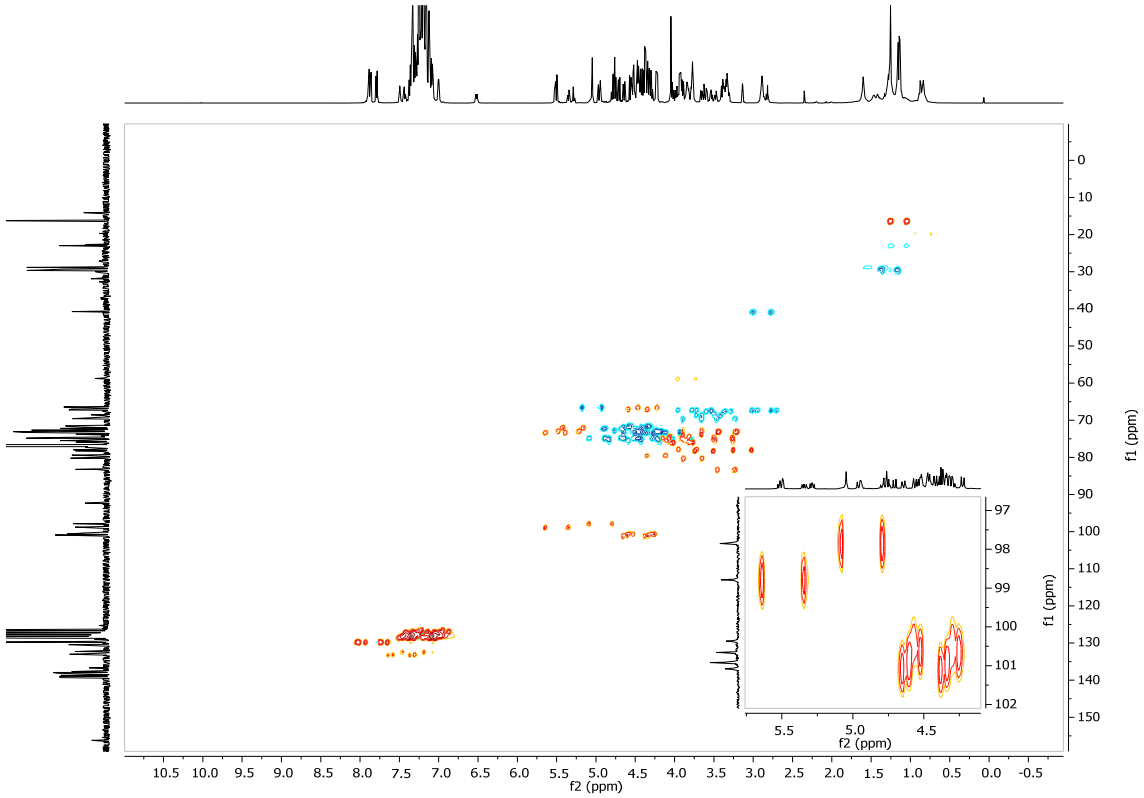

^{1}H NMR: **2.48**

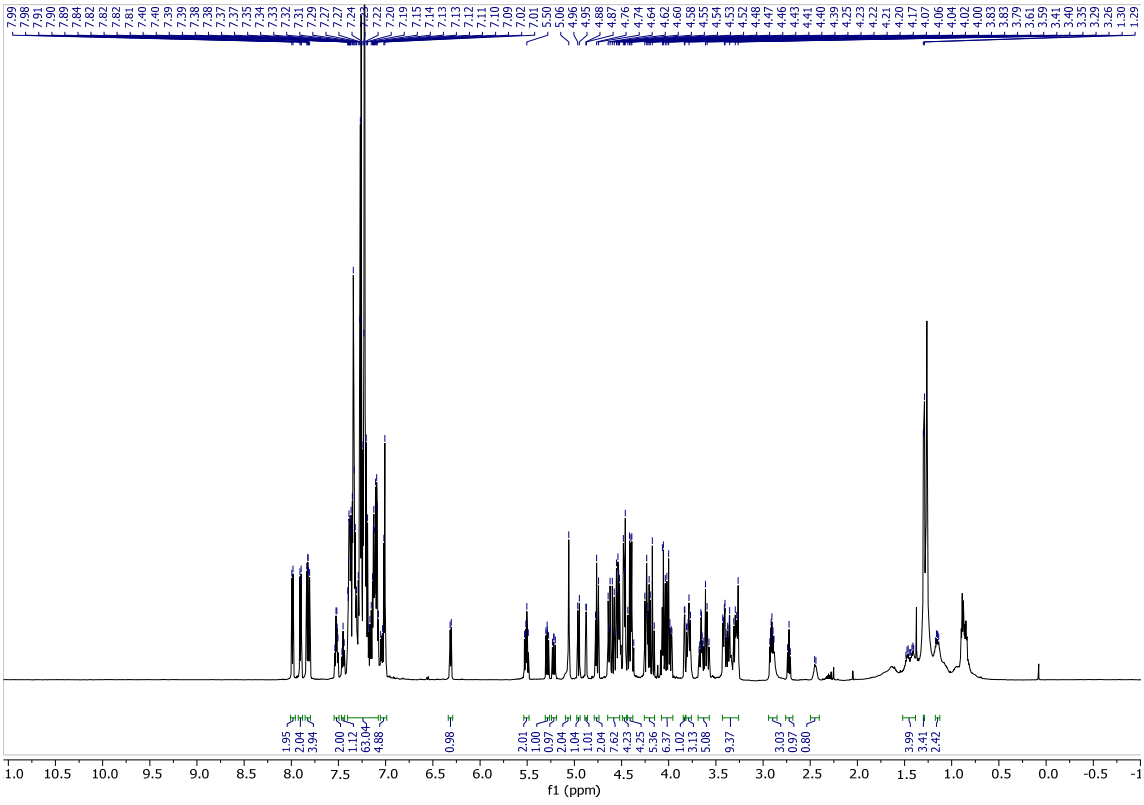

^{13}C NMR: **2.48**

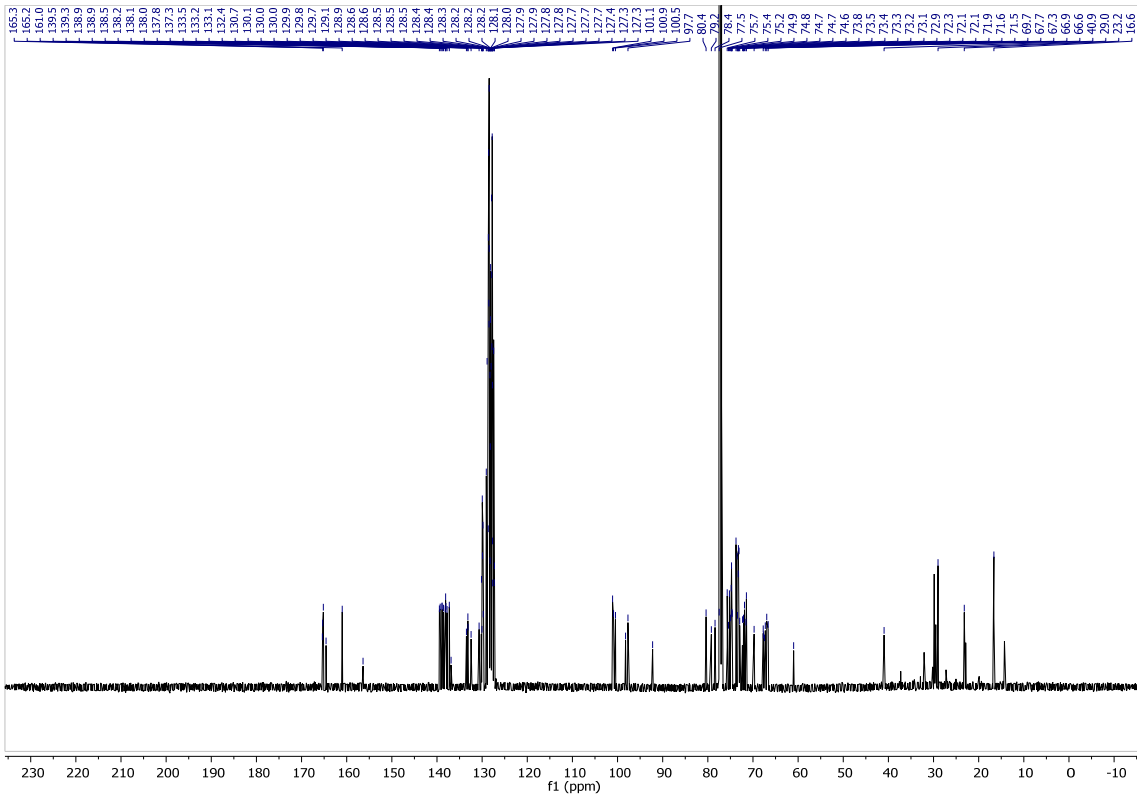

COSY: **2.48**

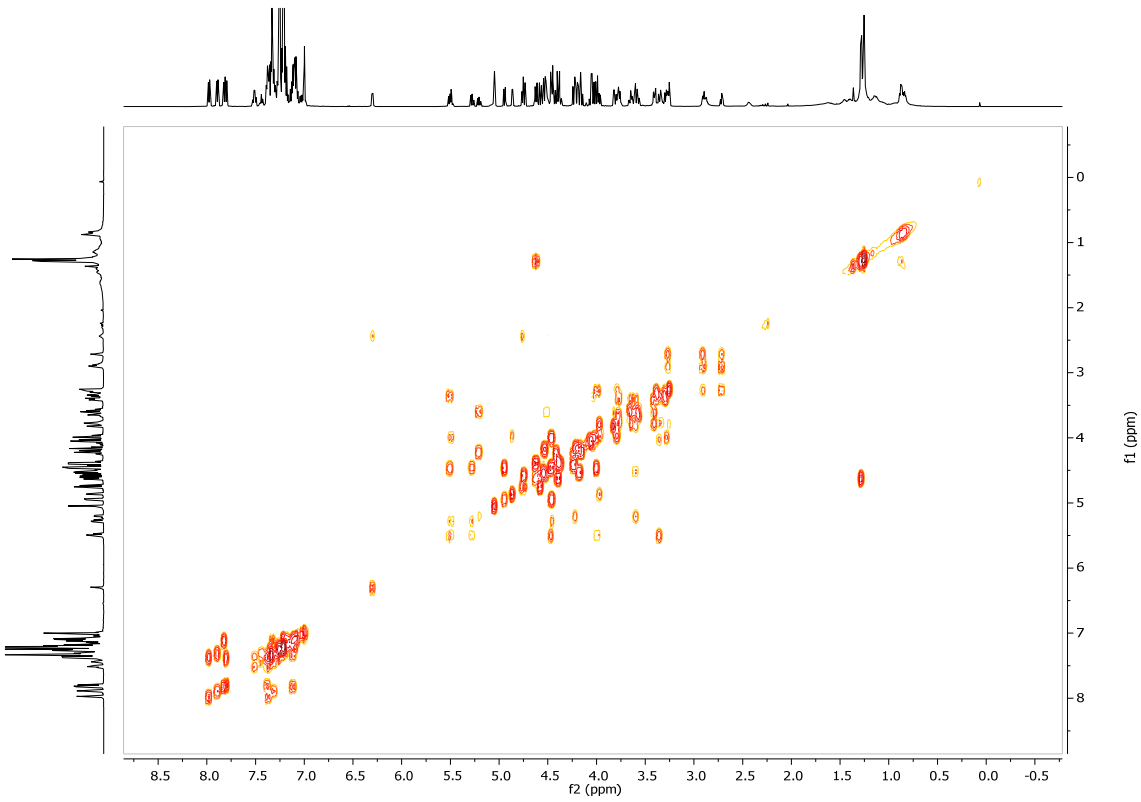

HSQC: **2.48**

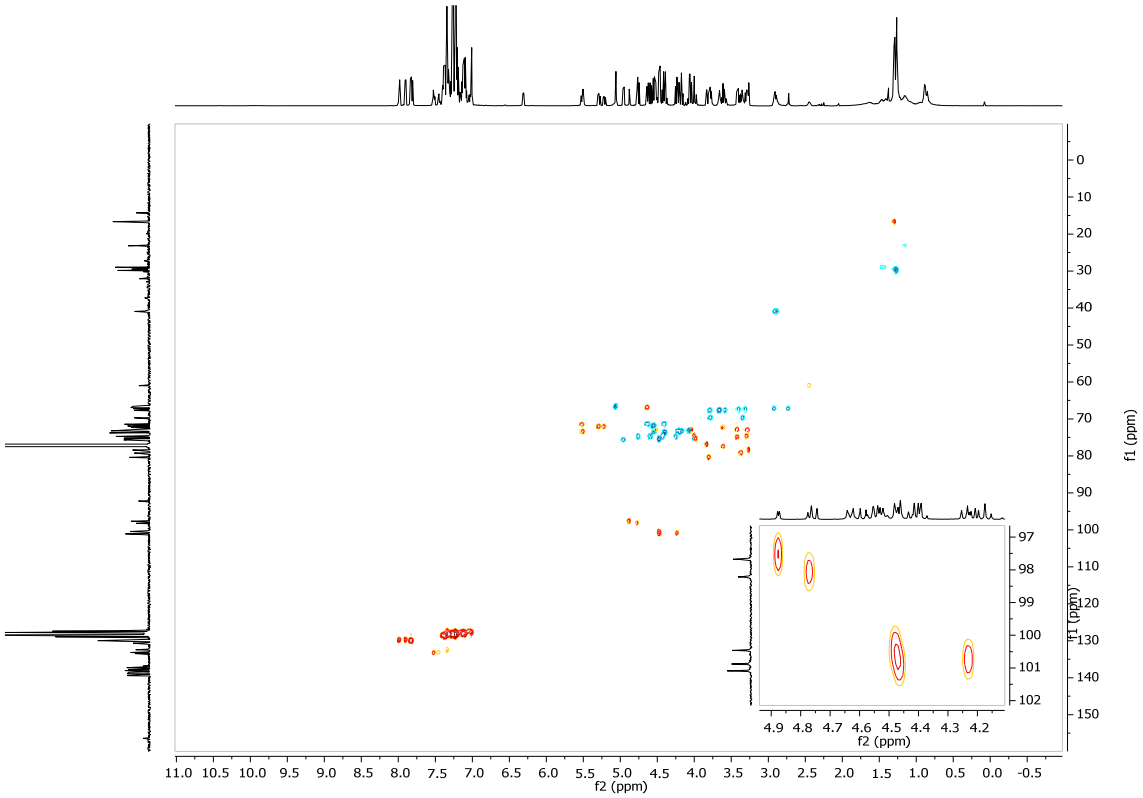

Coupled HSQC: **2.48**

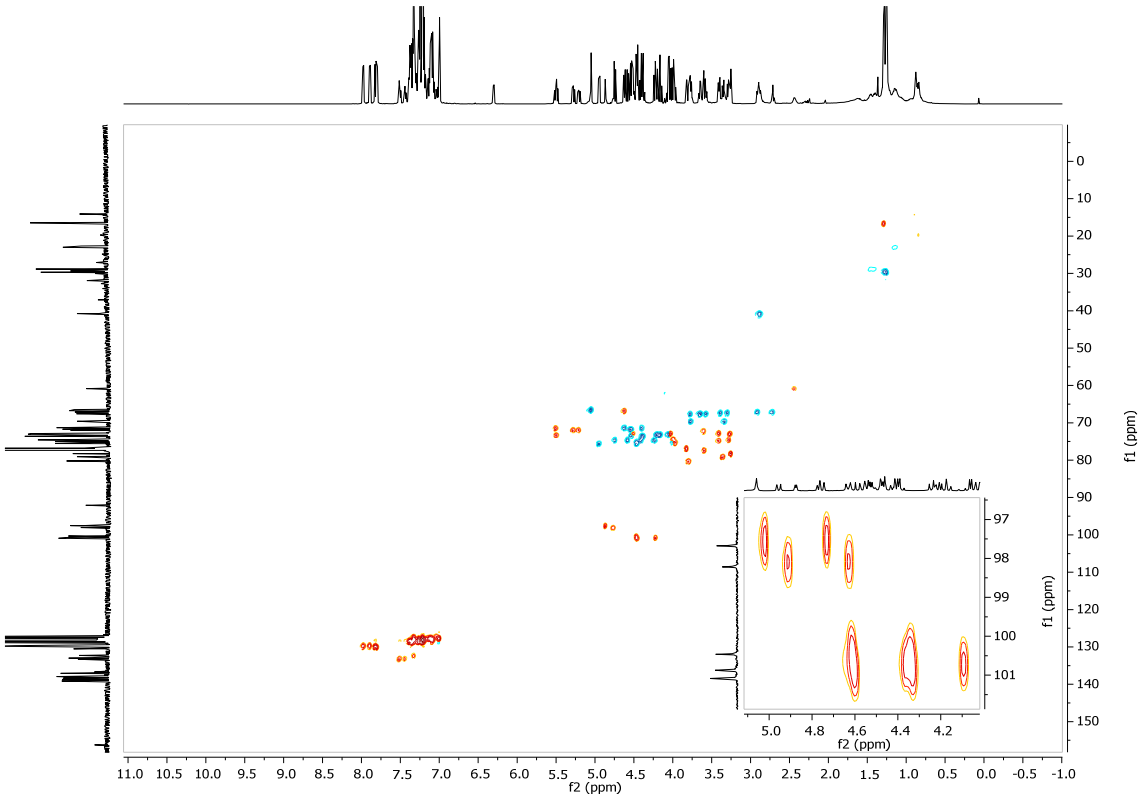

^{1}H NMR: **2.50**

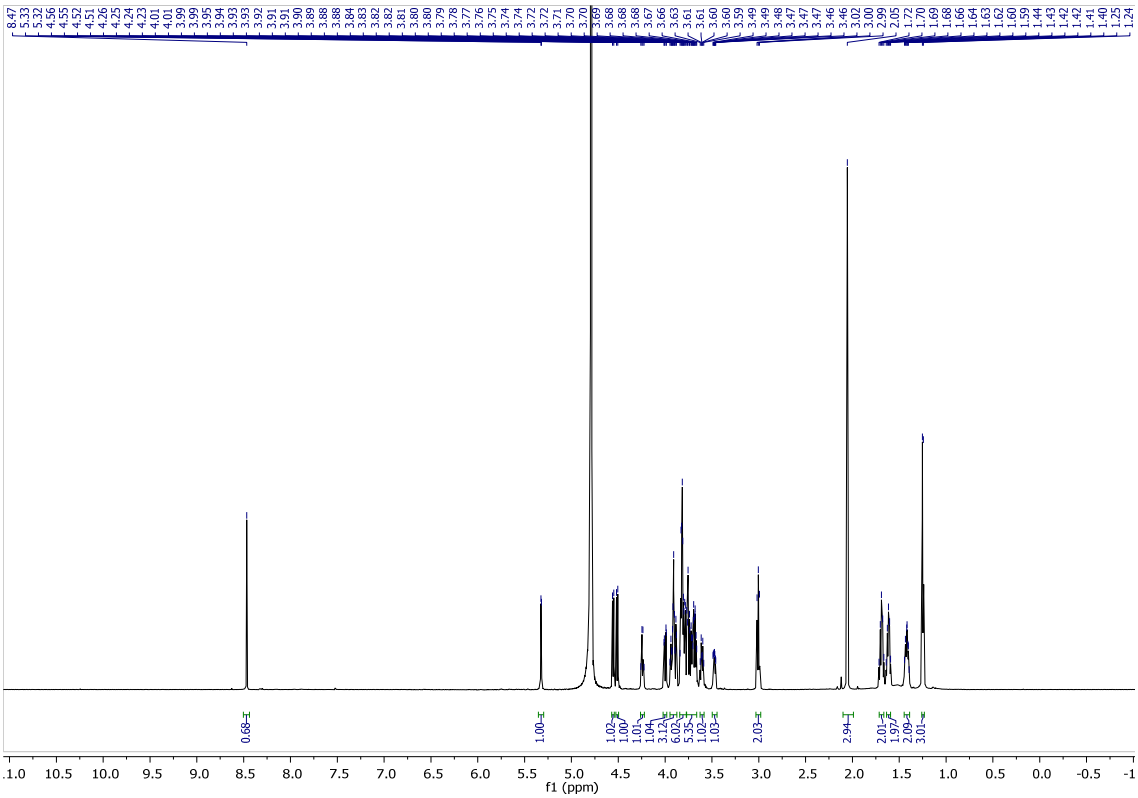

^{13}C NMR: **2.50**

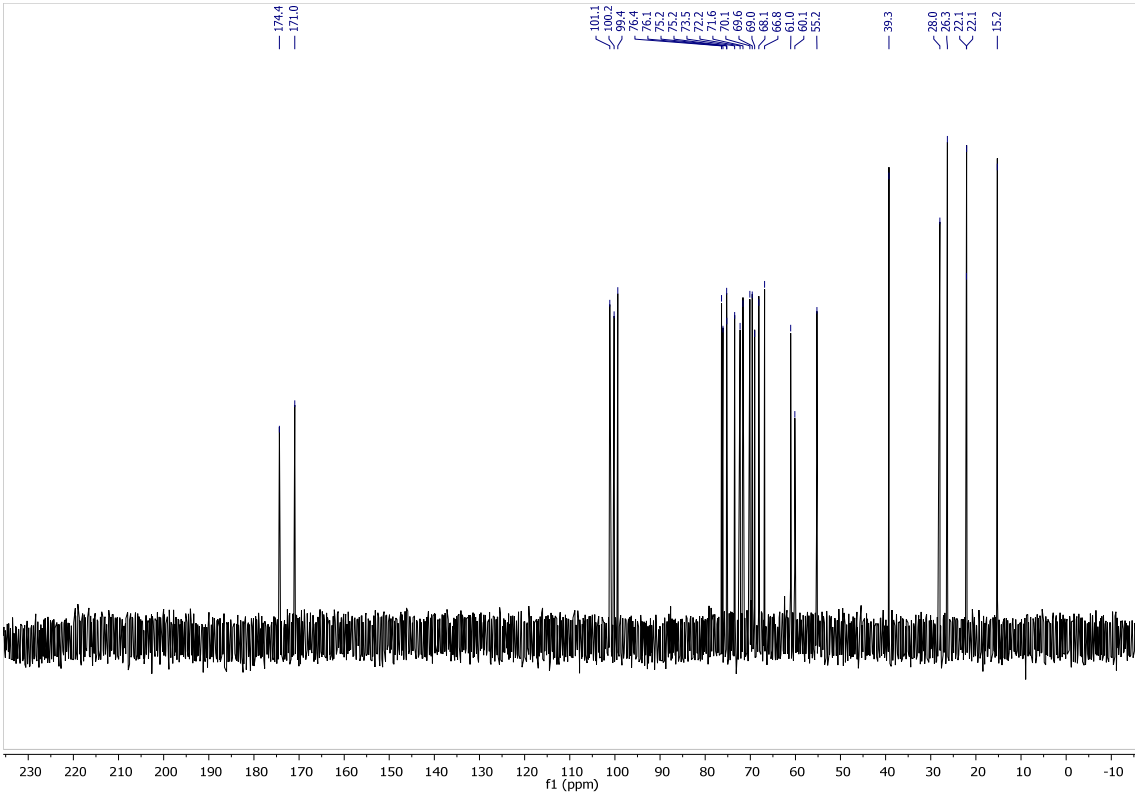

COSY: **2.50**

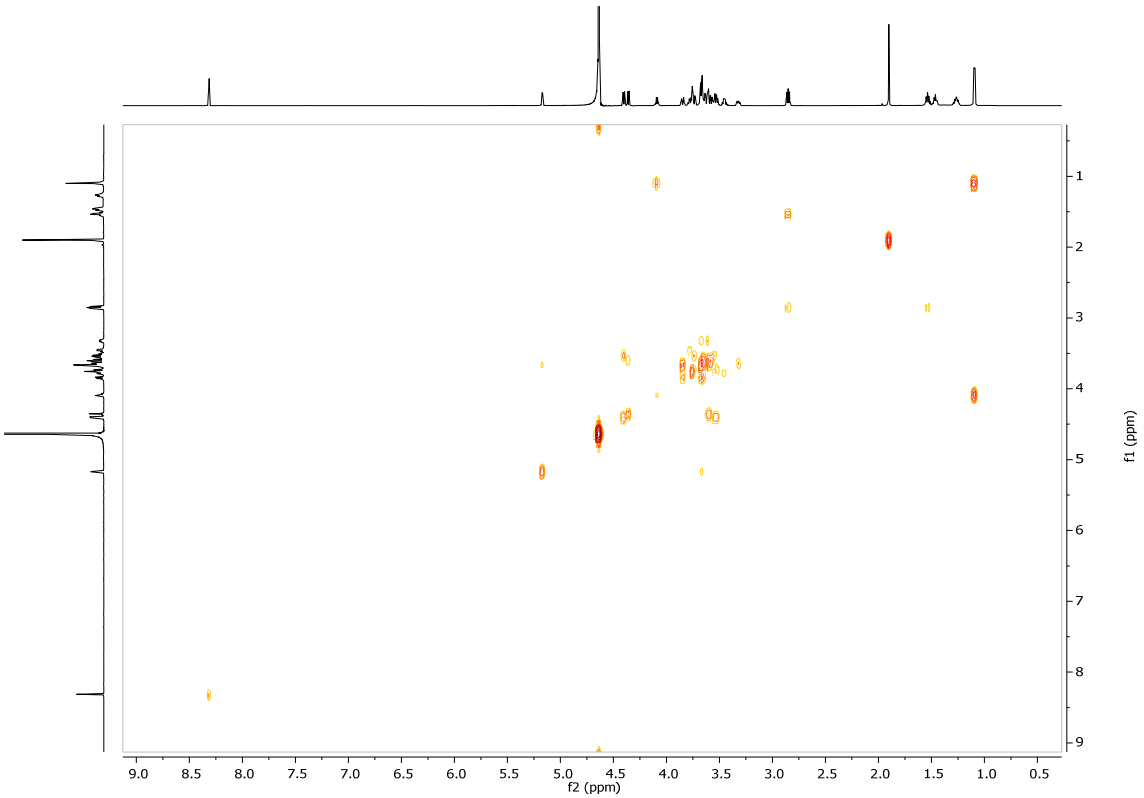

HSQC: **2.50**

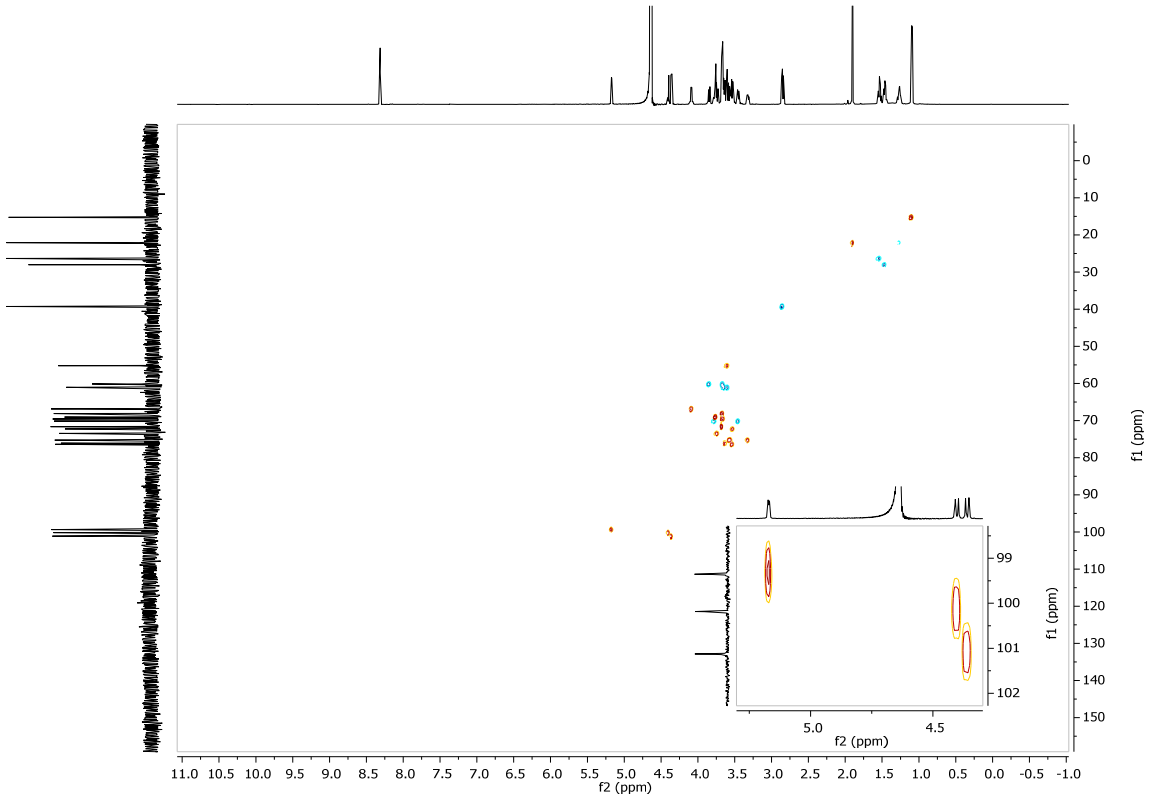

Coupled HSQC: **2.50**

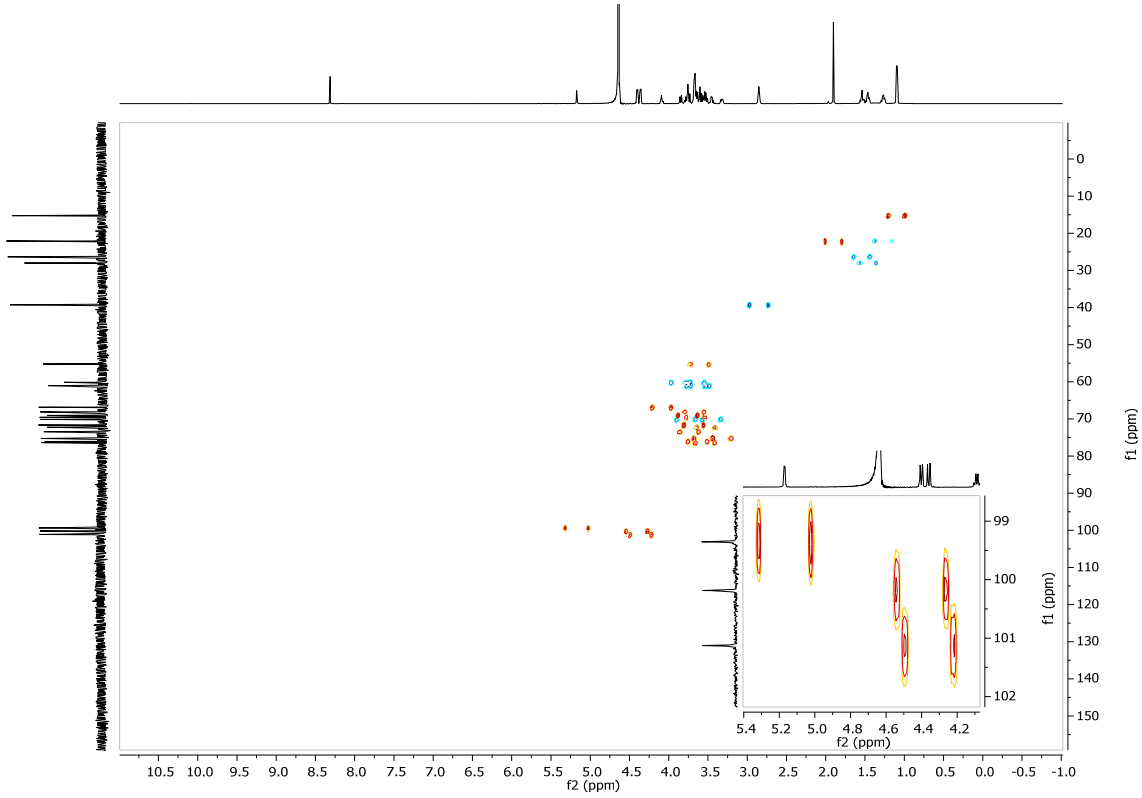

^{1}H NMR: **2.51**

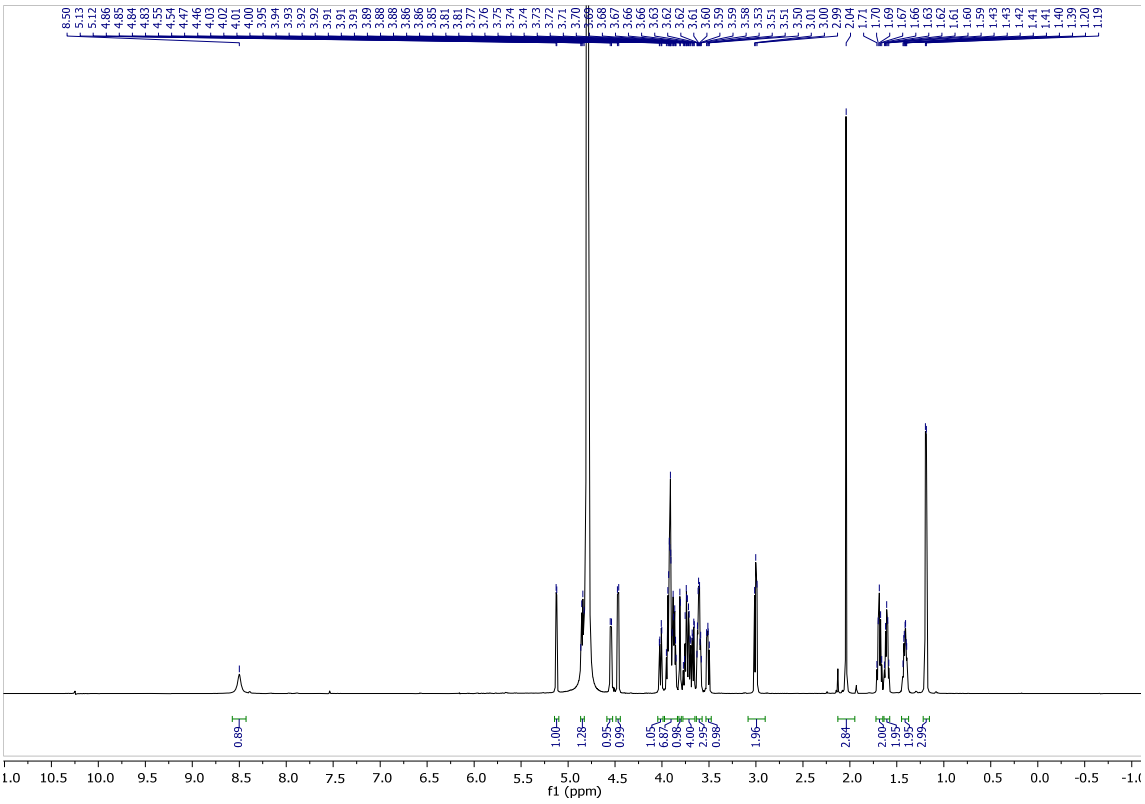

^{13}C NMR: **2.51**

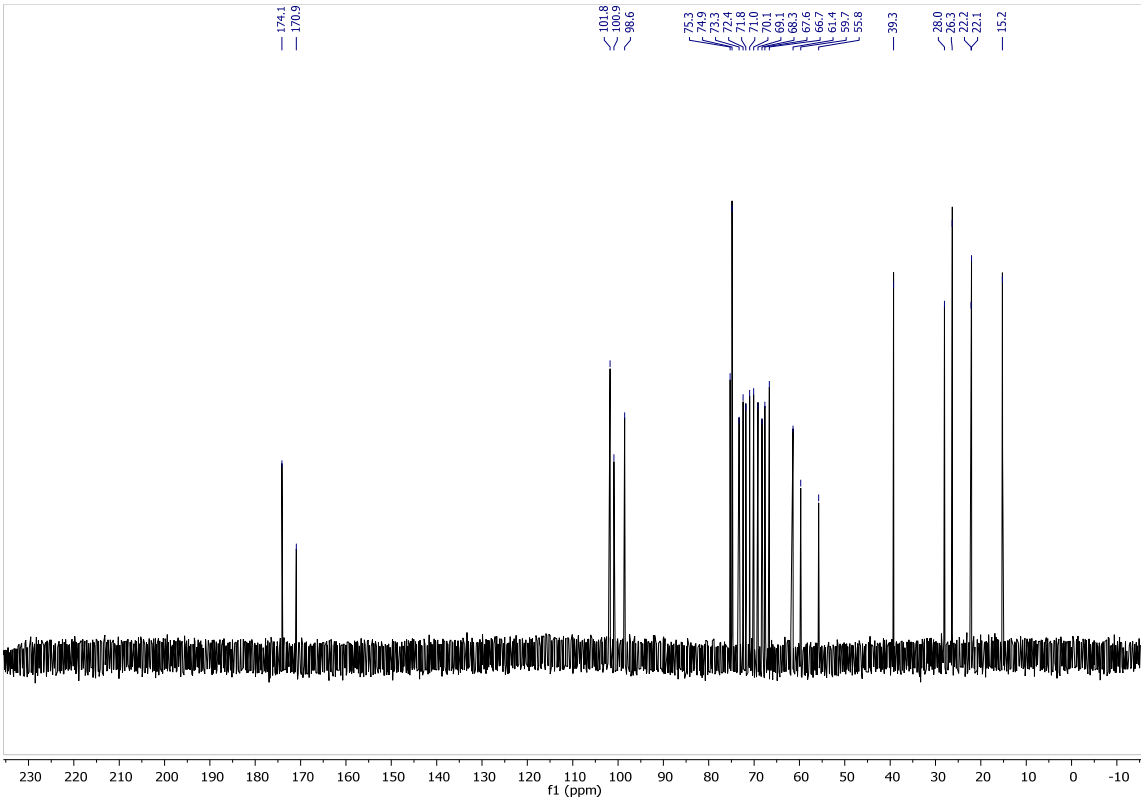

COSY: **2.51**

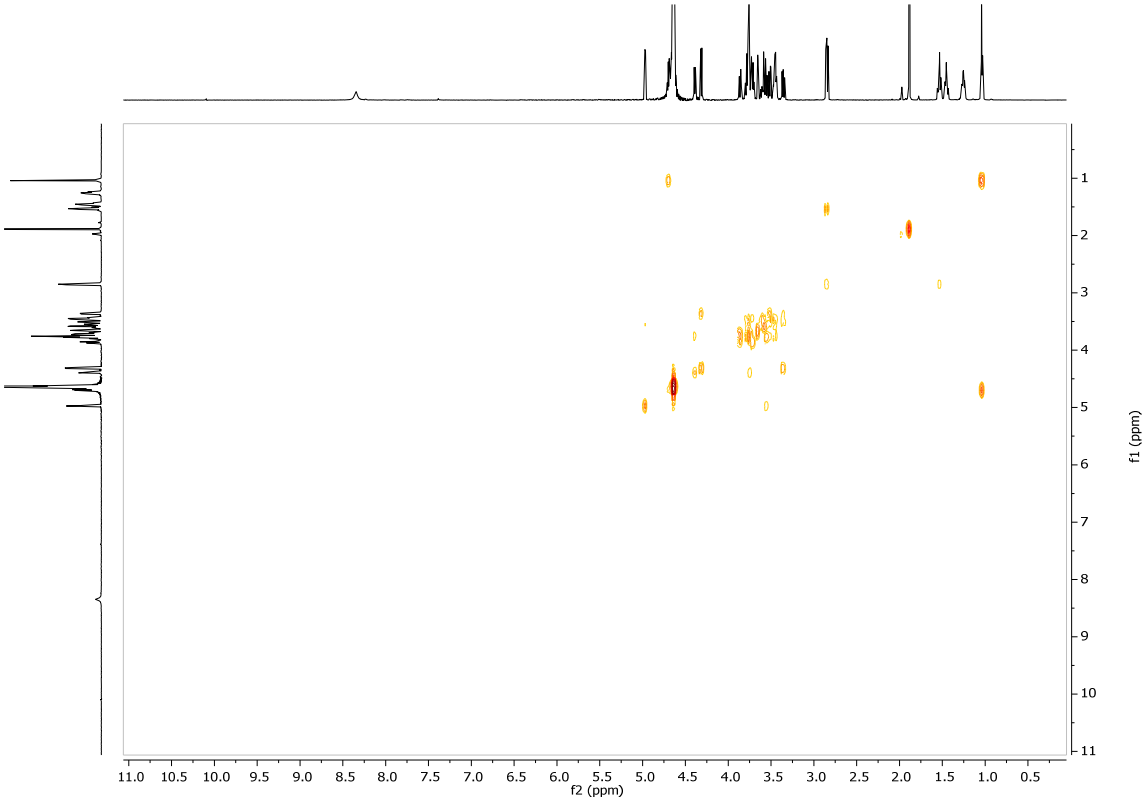

HSQC: **2.51**

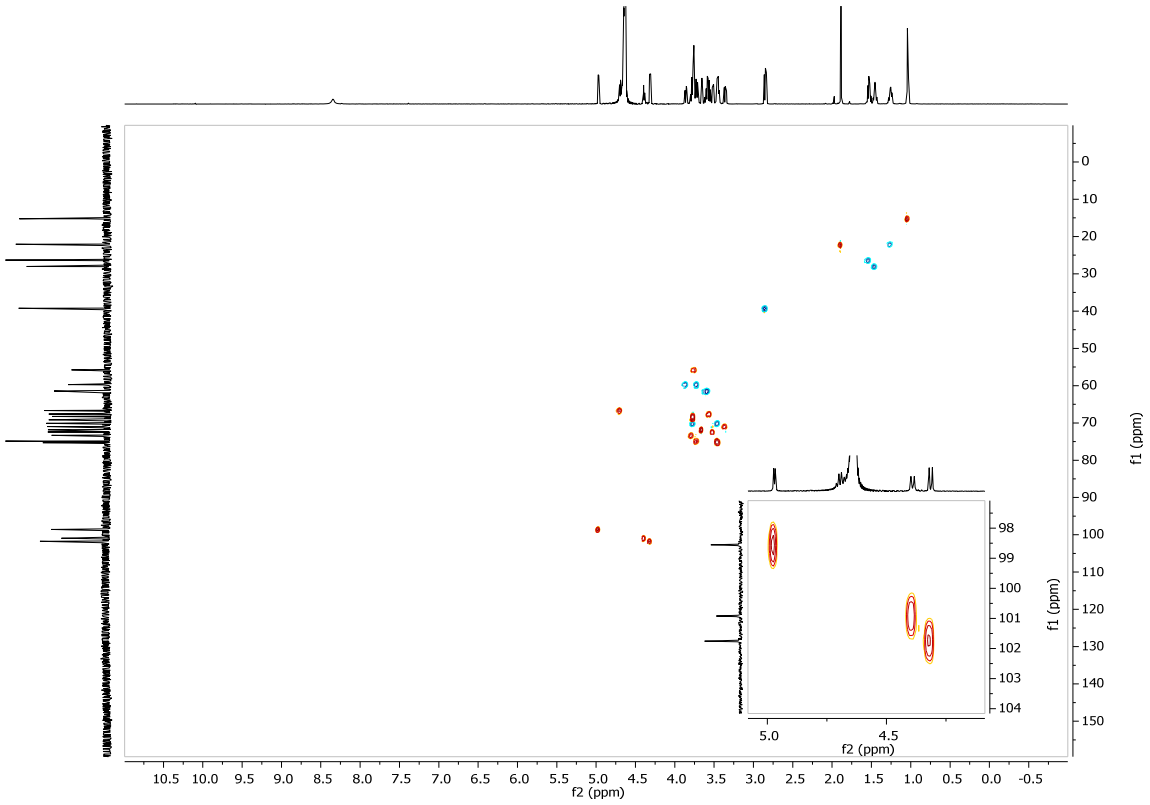

Coupled HSQC: **2.51**

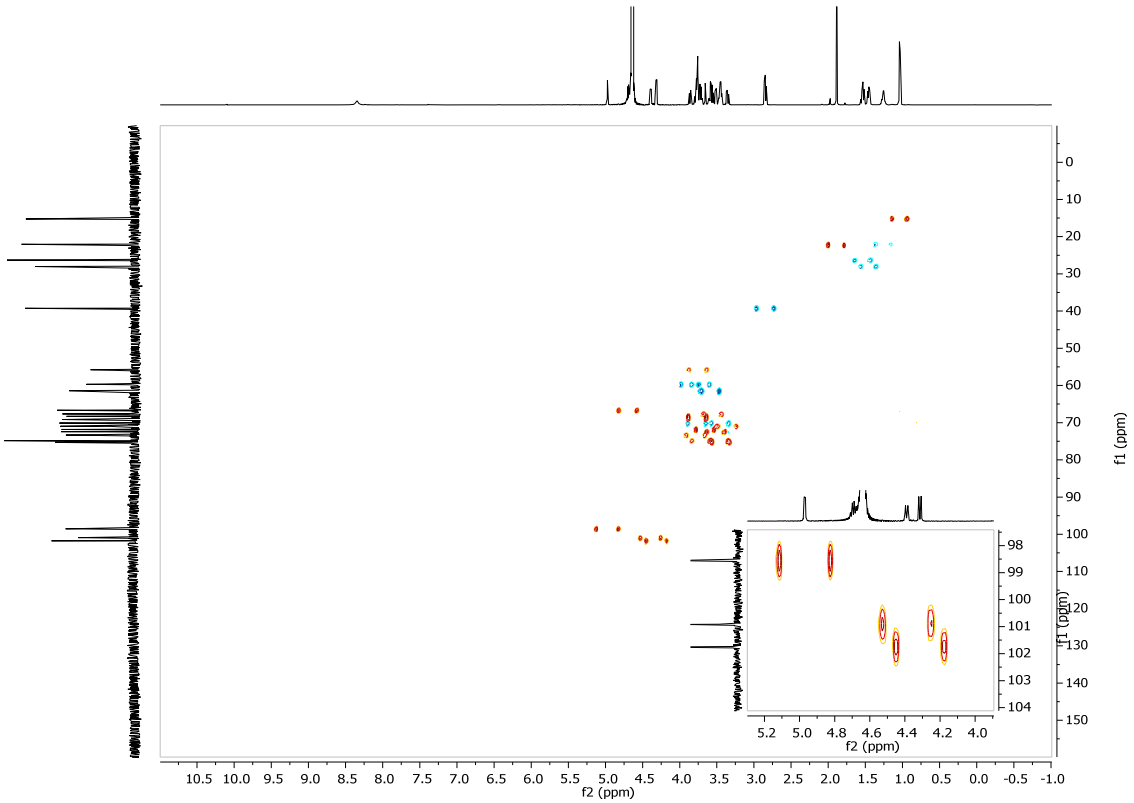

^{1}H NMR: **2.52**

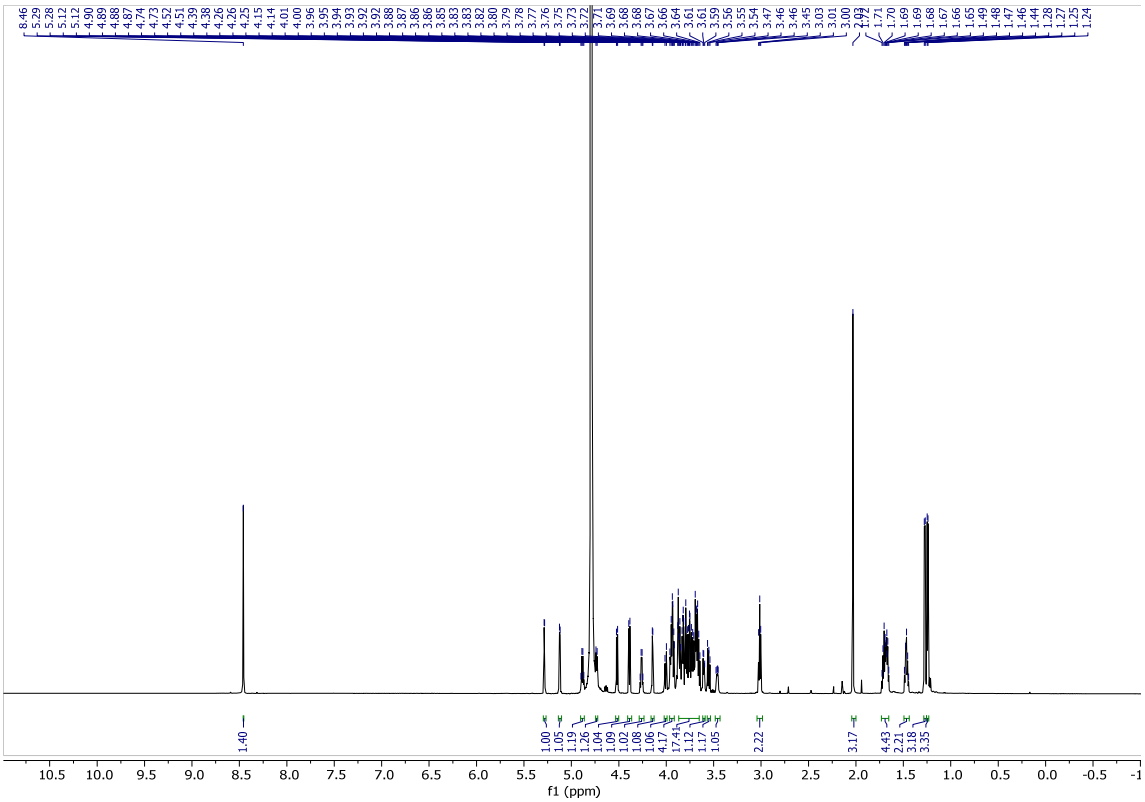

^{13}C NMR: **2.52**

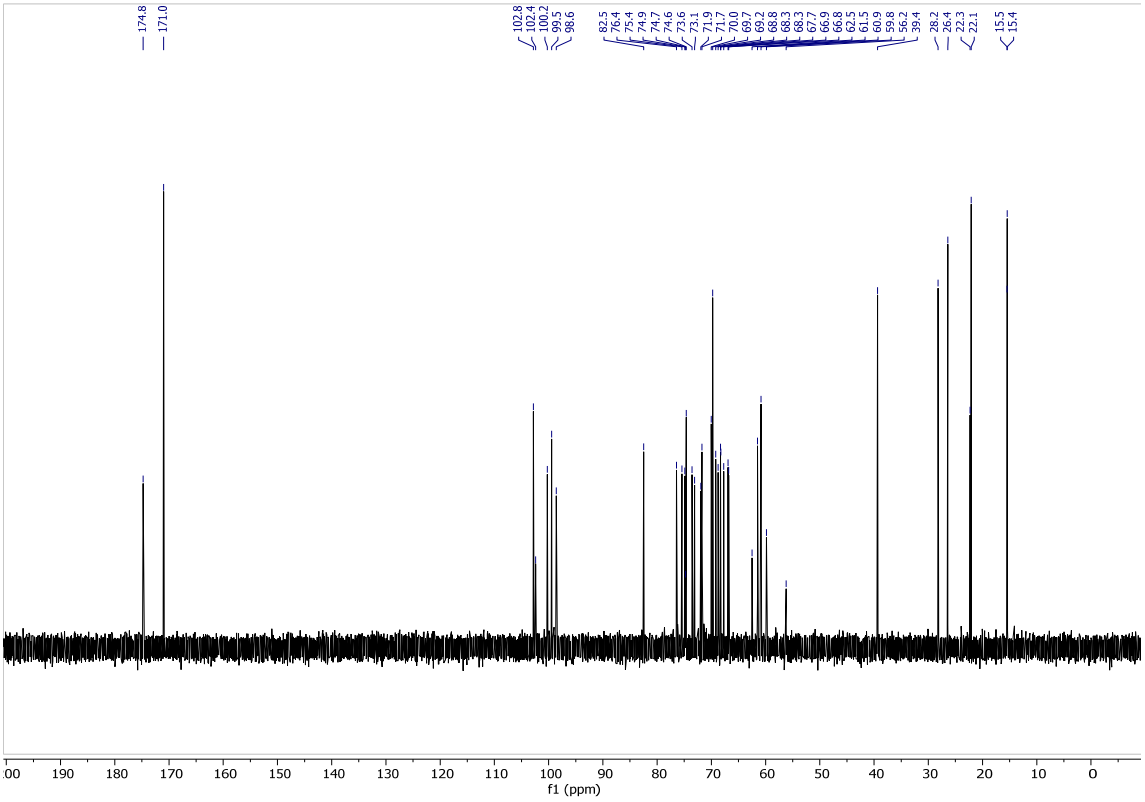

COSY: **2.52**

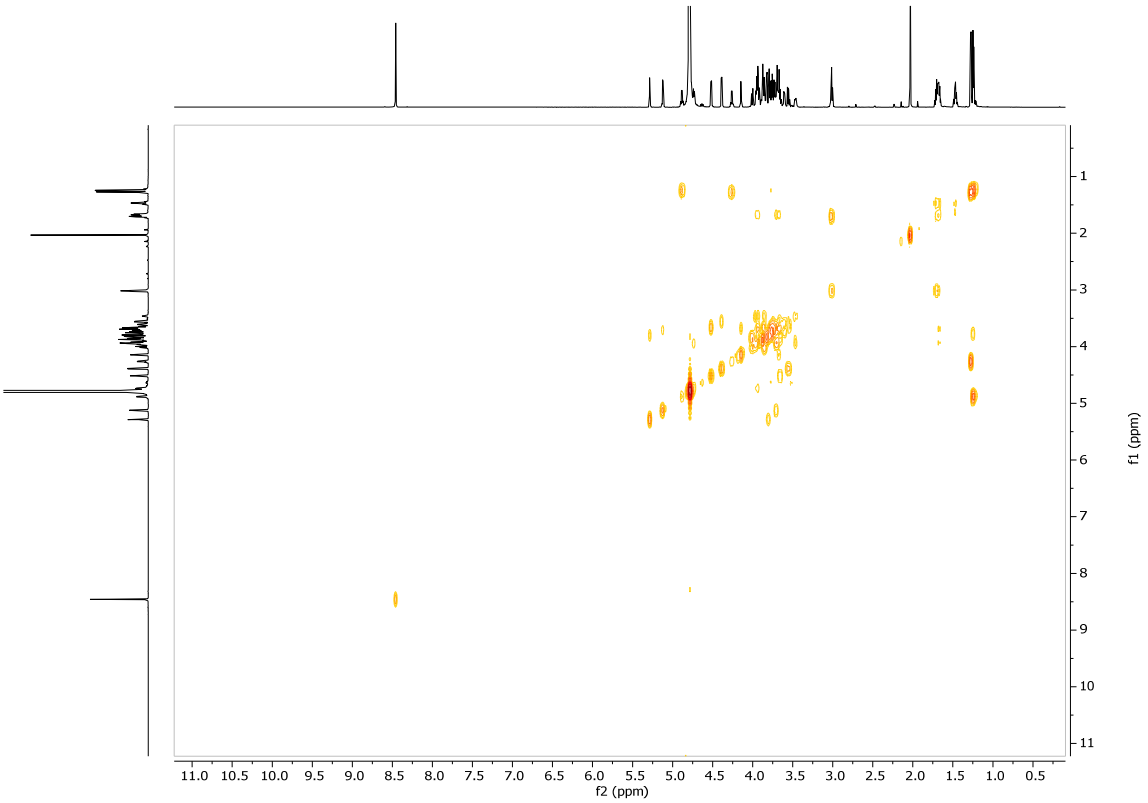

HSQC: **2.52**

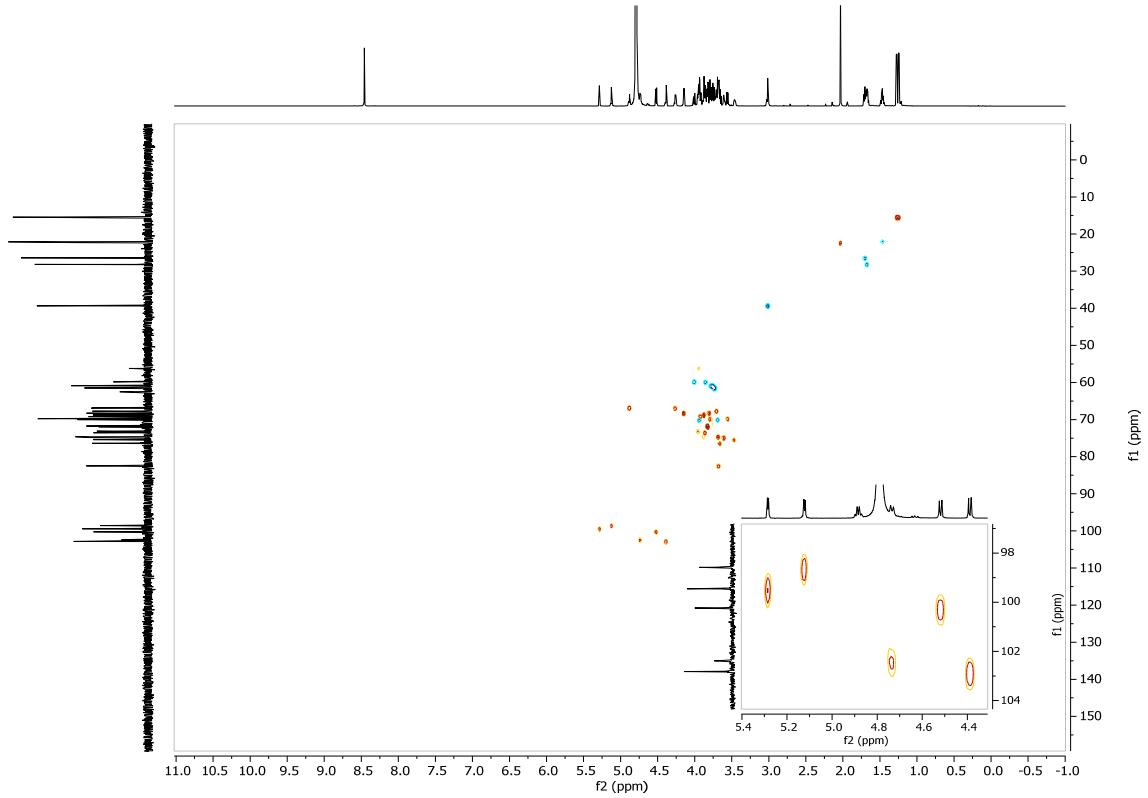

Coupled HSQC: **2.52**

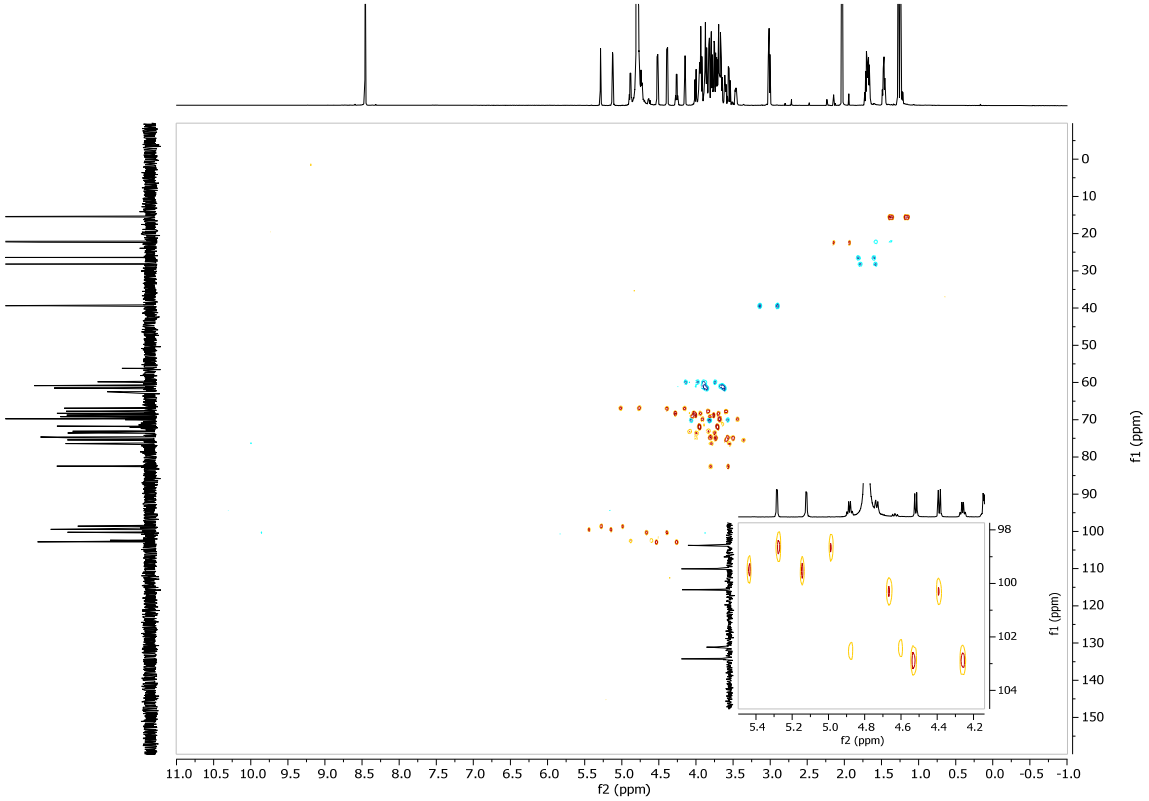

^{1}H NMR: **2.54**

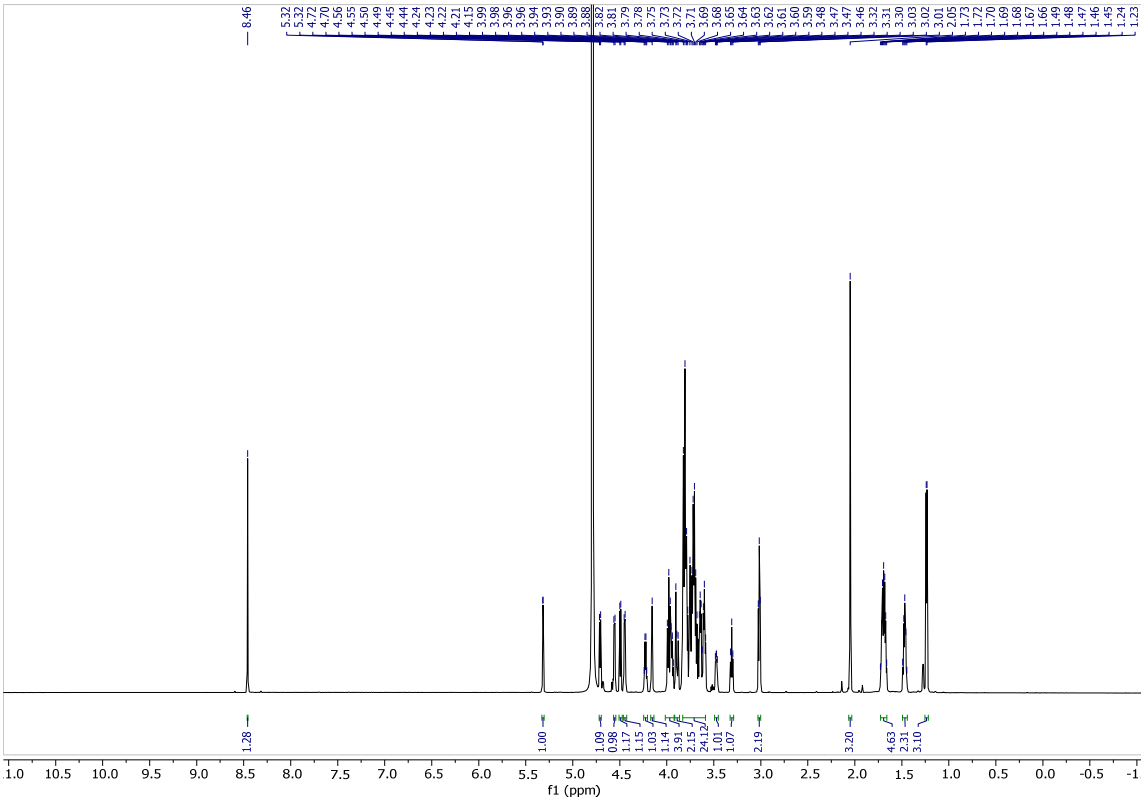

^{13}C NMR: **2.54**

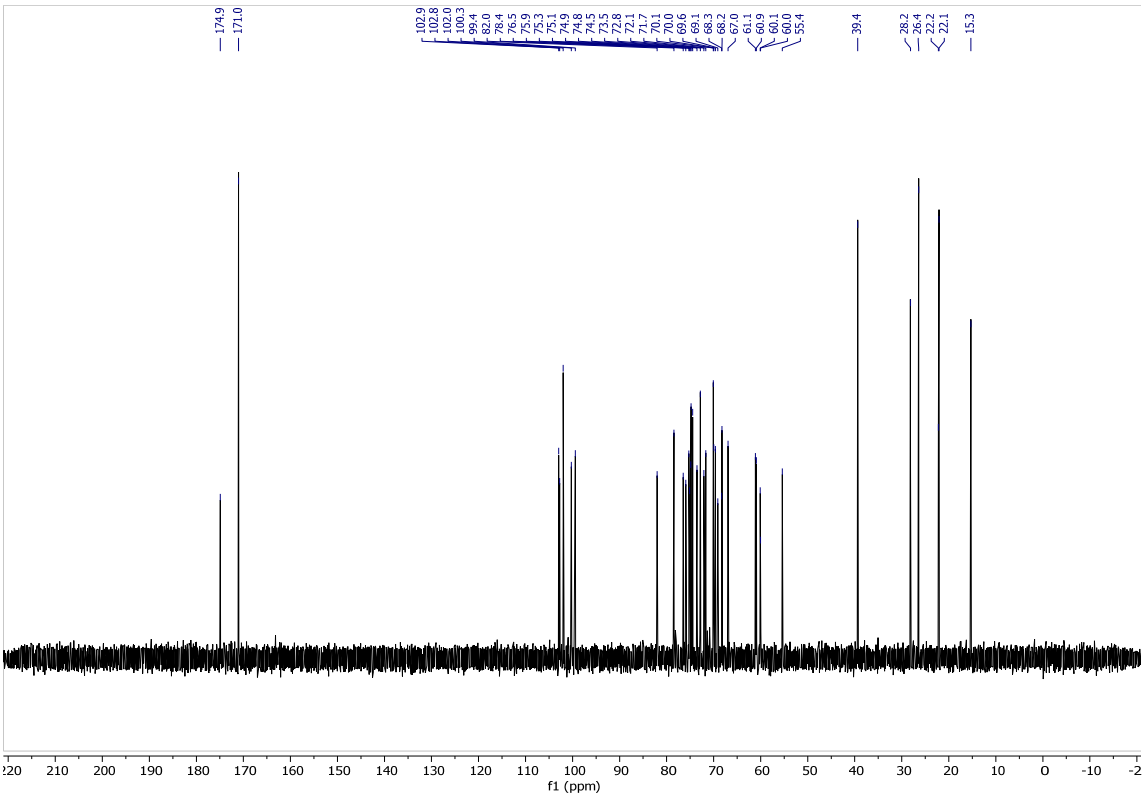

COSY: **2.54**

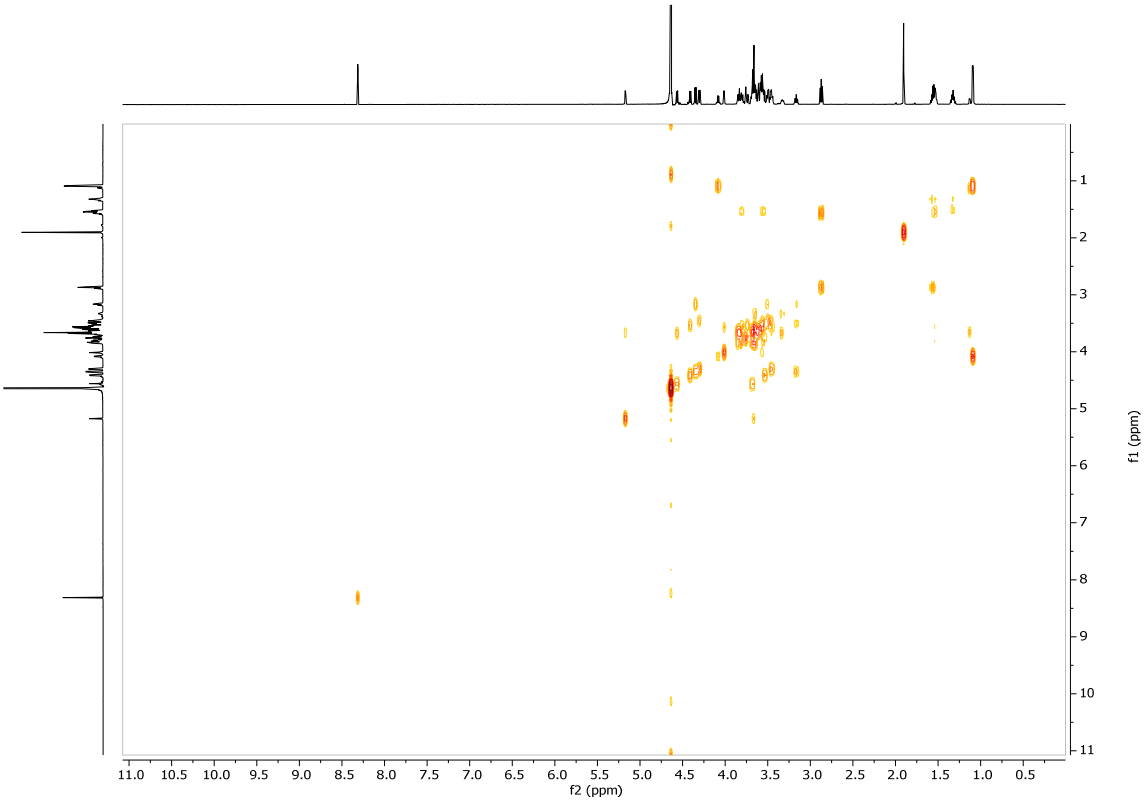

HSQC: **2.54**

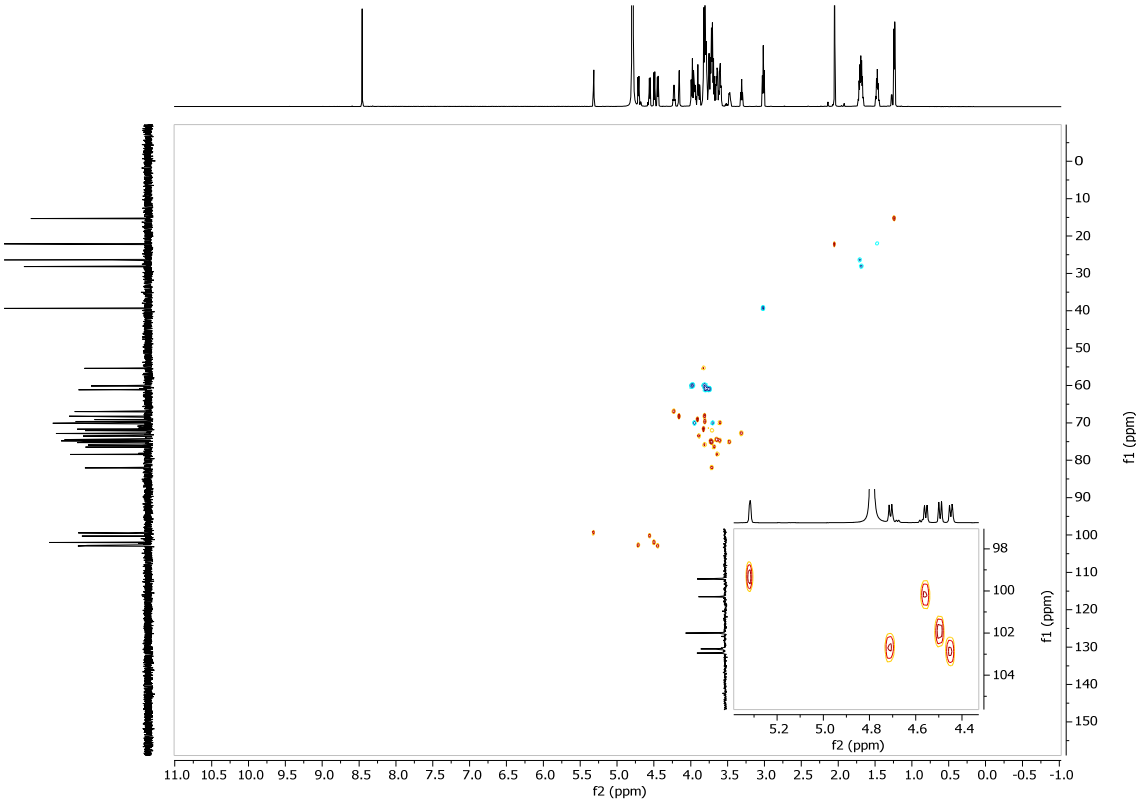

Coupled HSQC: **2.54**

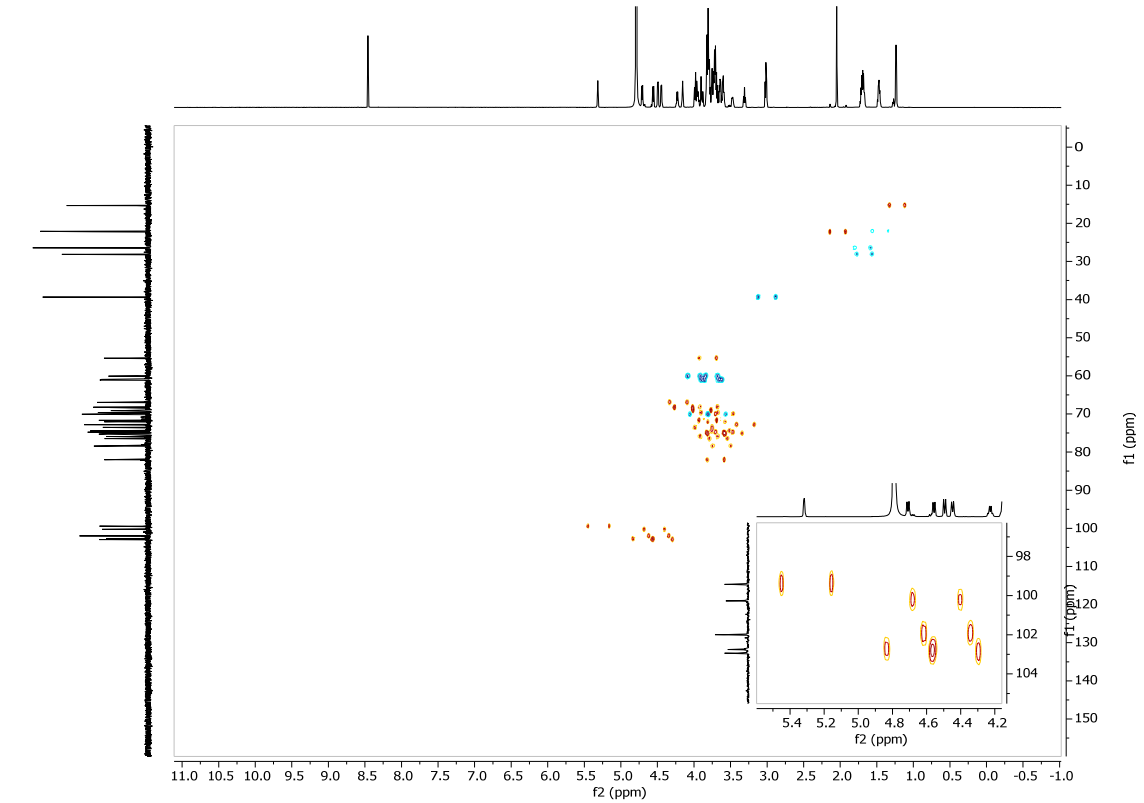

^{1}H NMR: **2.55**

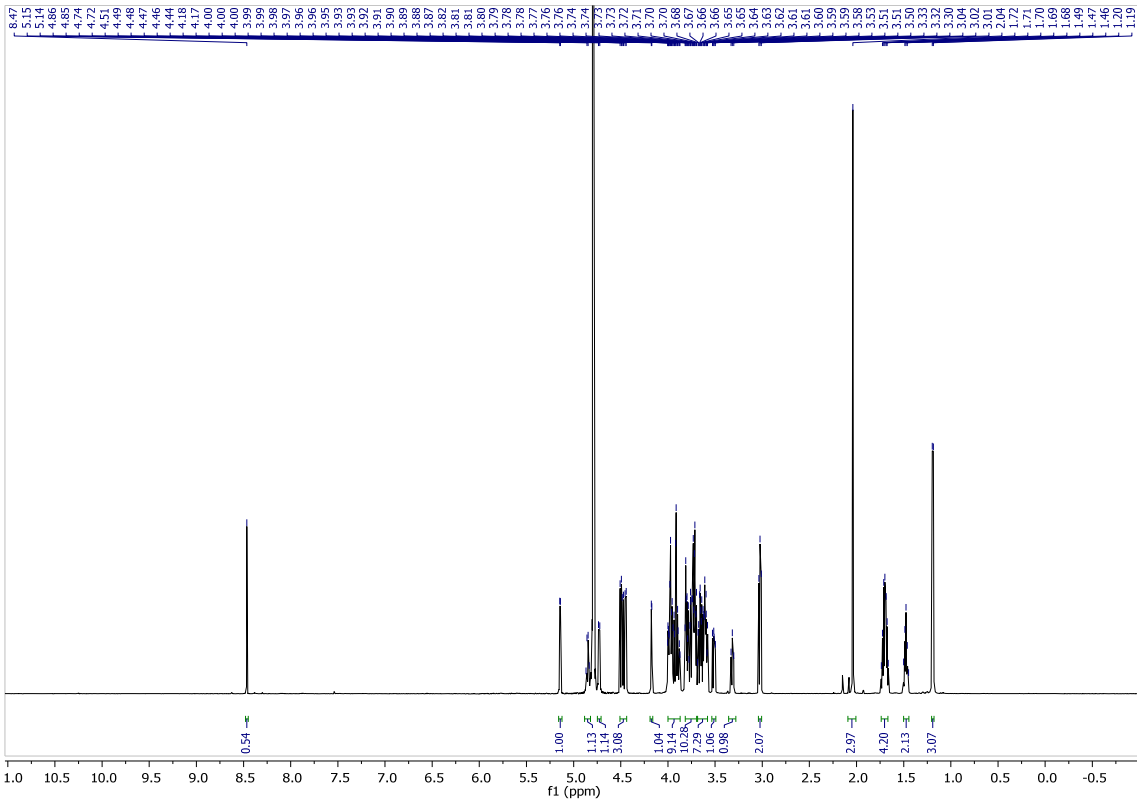

^{13}C NMR: **2.55**

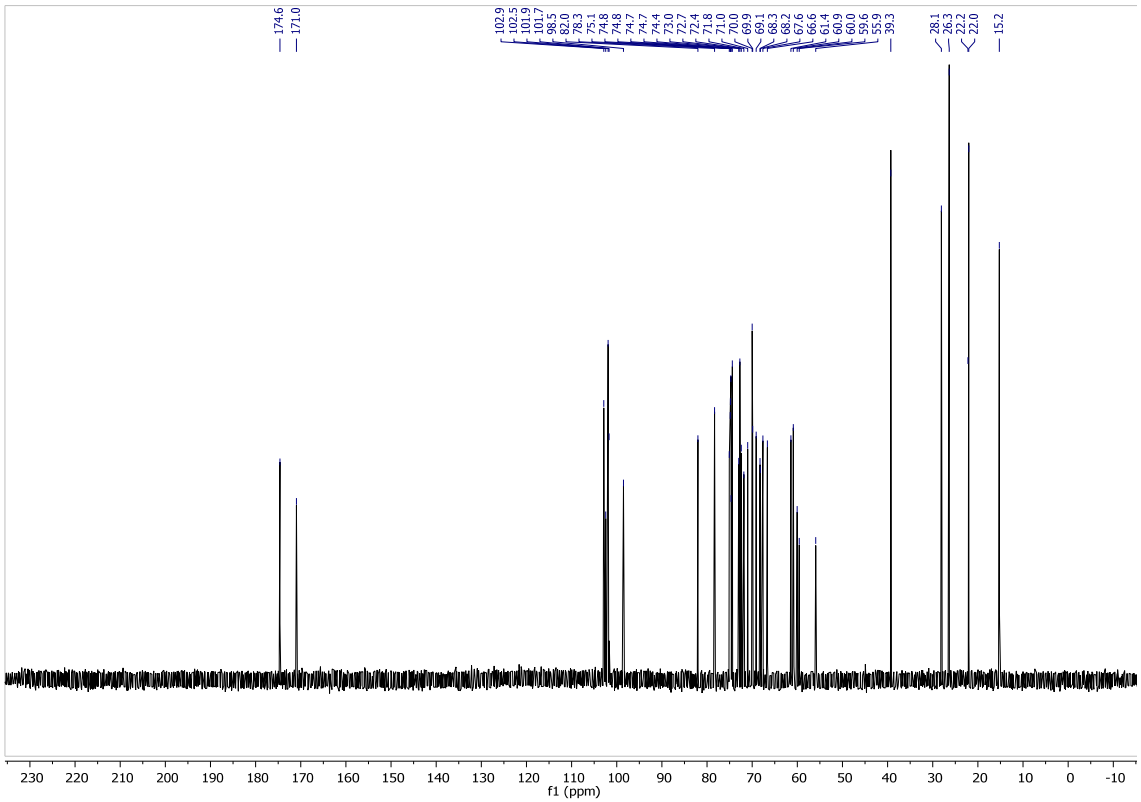

COSY: **2.55**

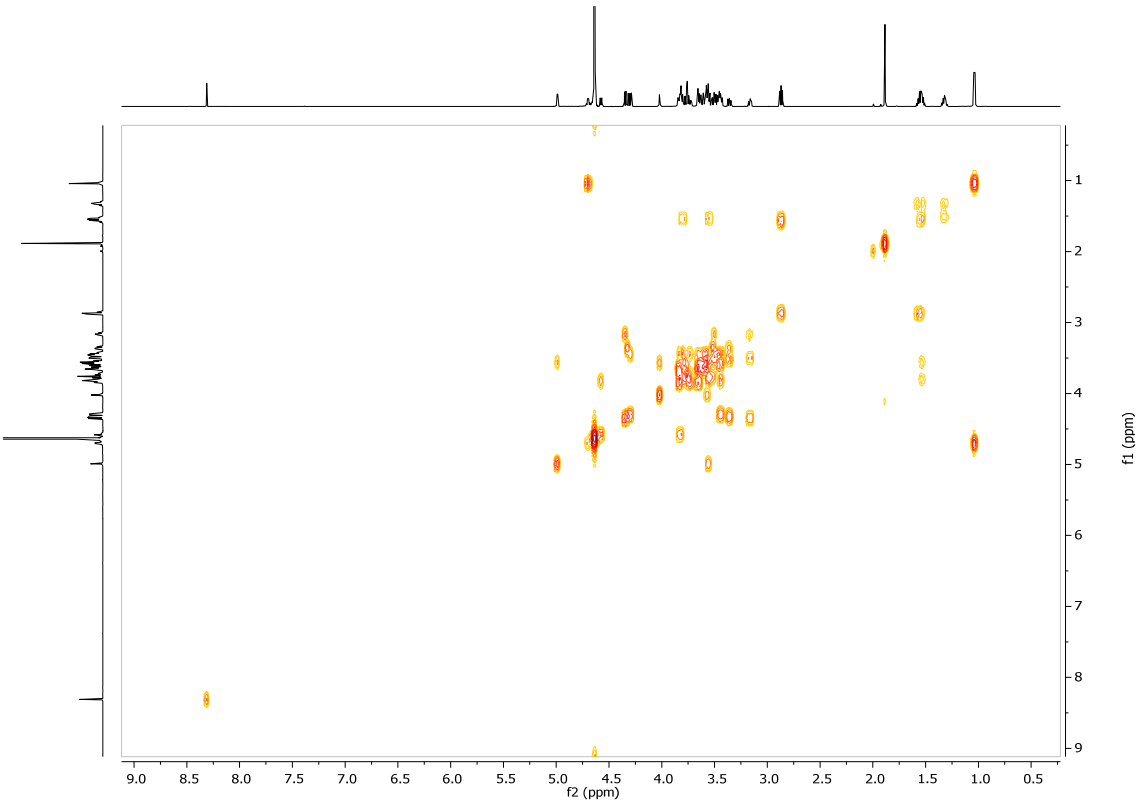

HSQC: **2.55**

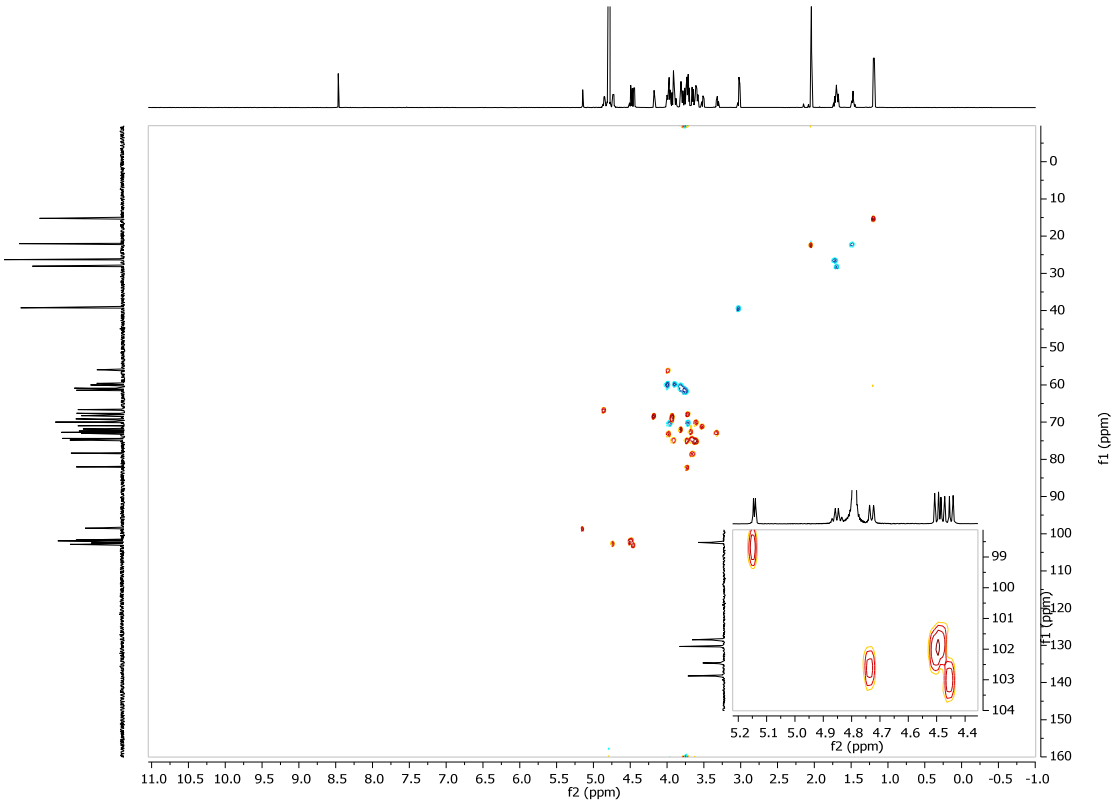

Coupled HSQC: **2.55**

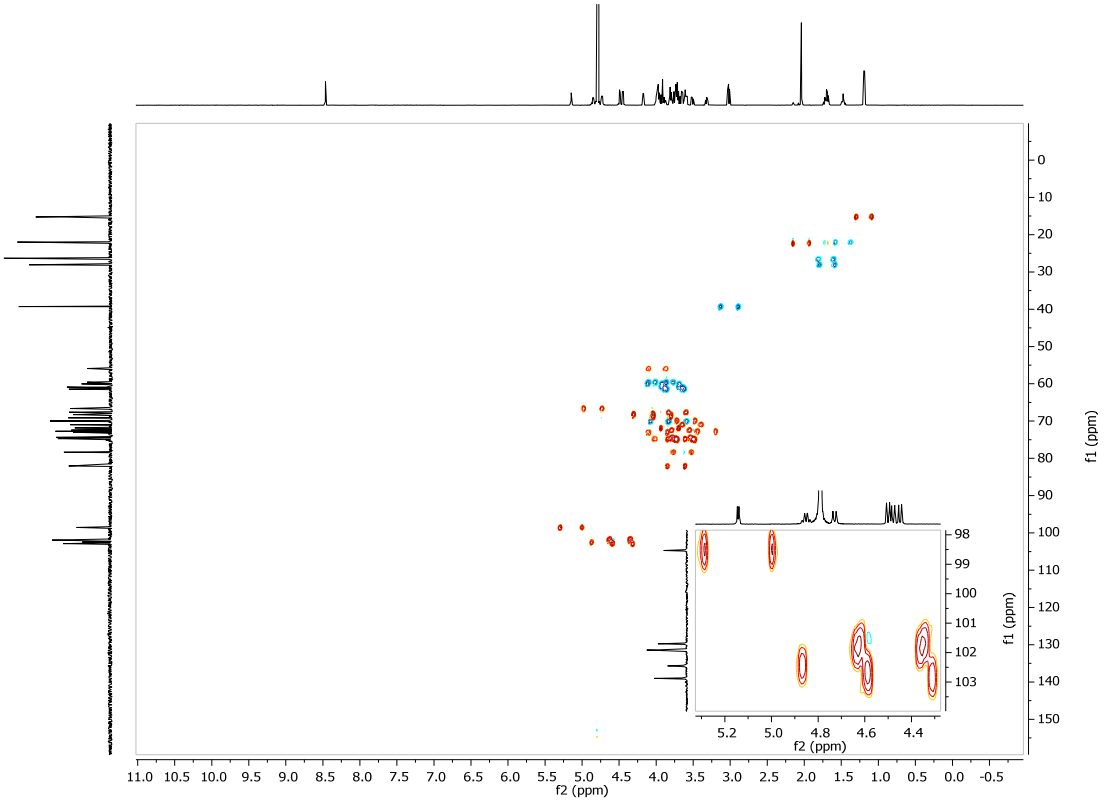

^{1}H NMR: **2.56**

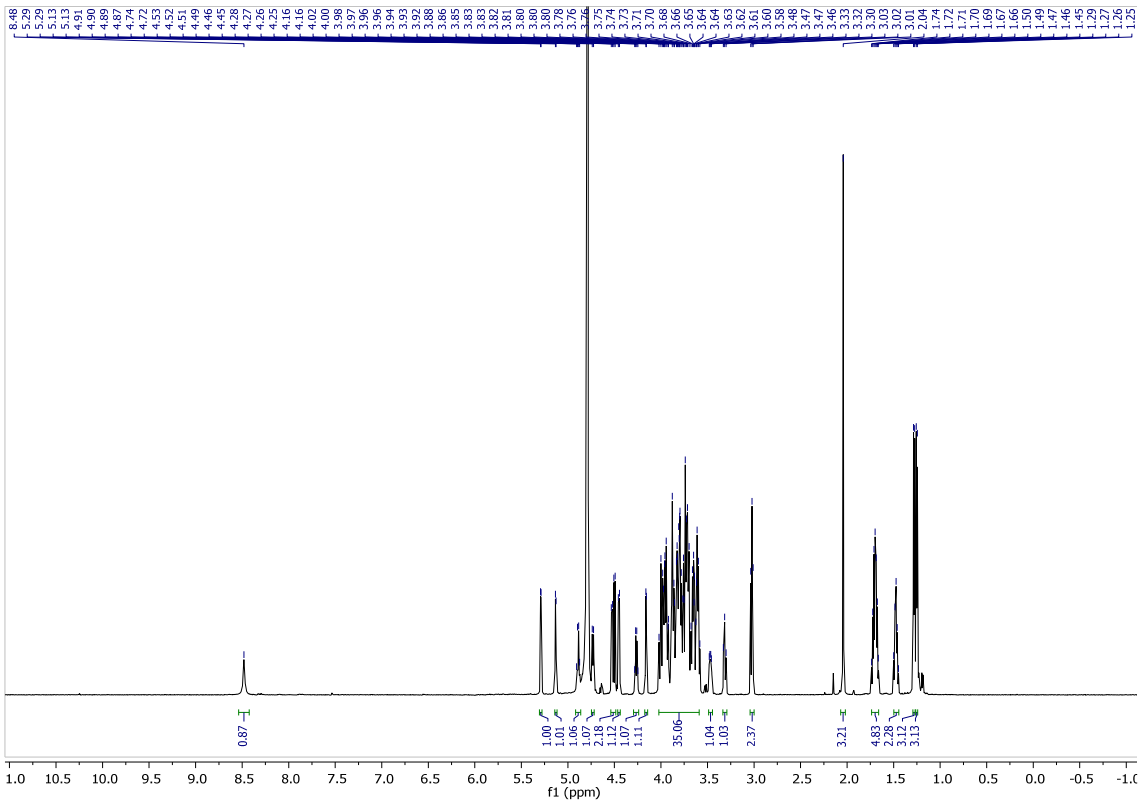

^{13}C NMR: **2.56**

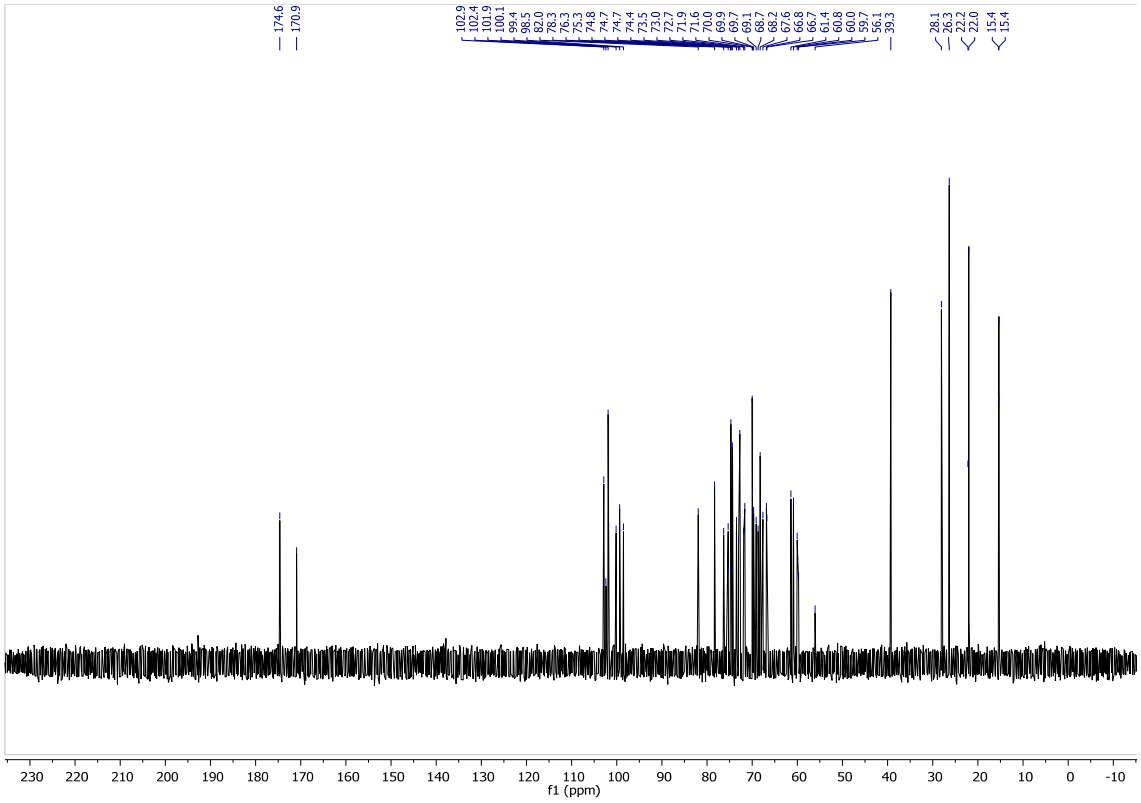

COSY: **2.56**

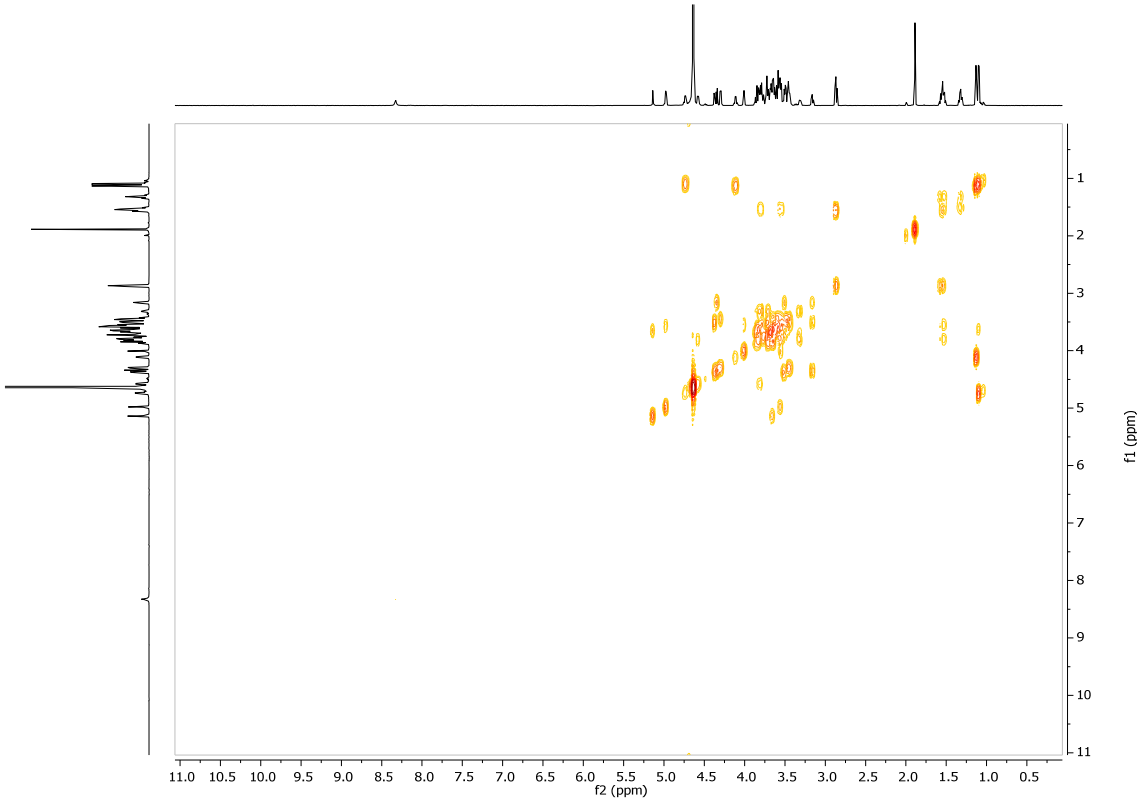

HSQC: **2.56**

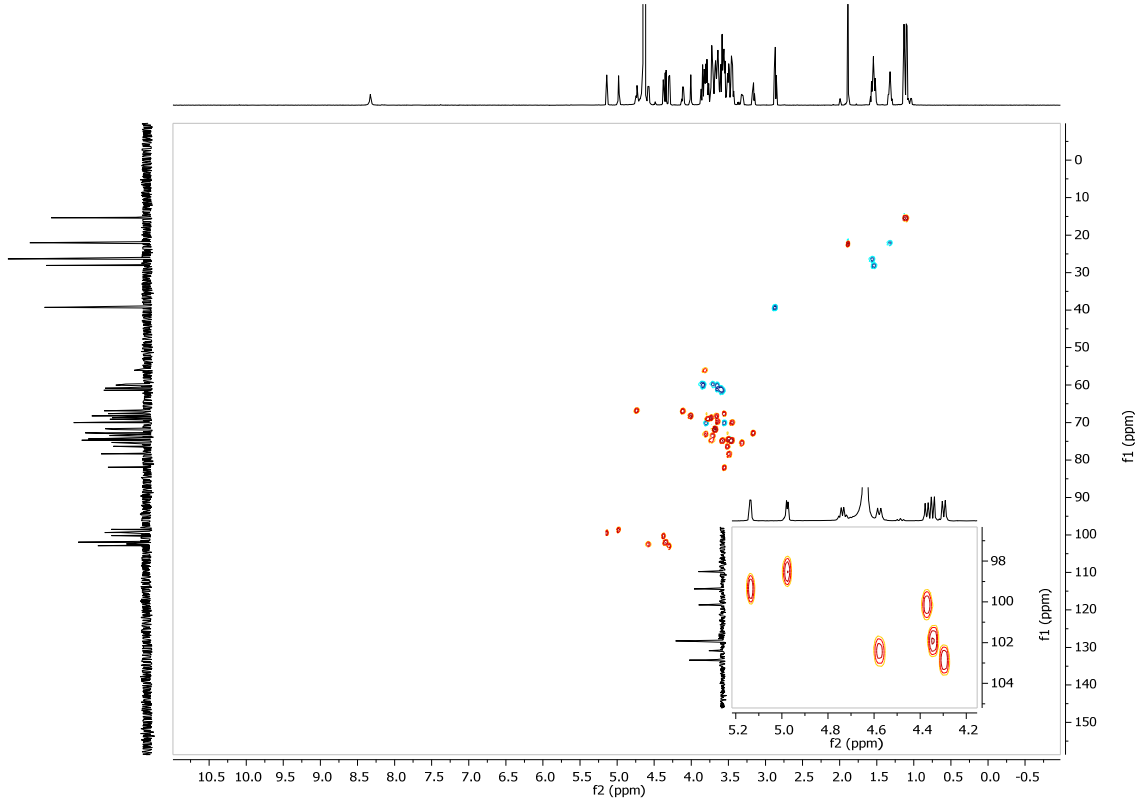

Coupled HSQC: **2.56**

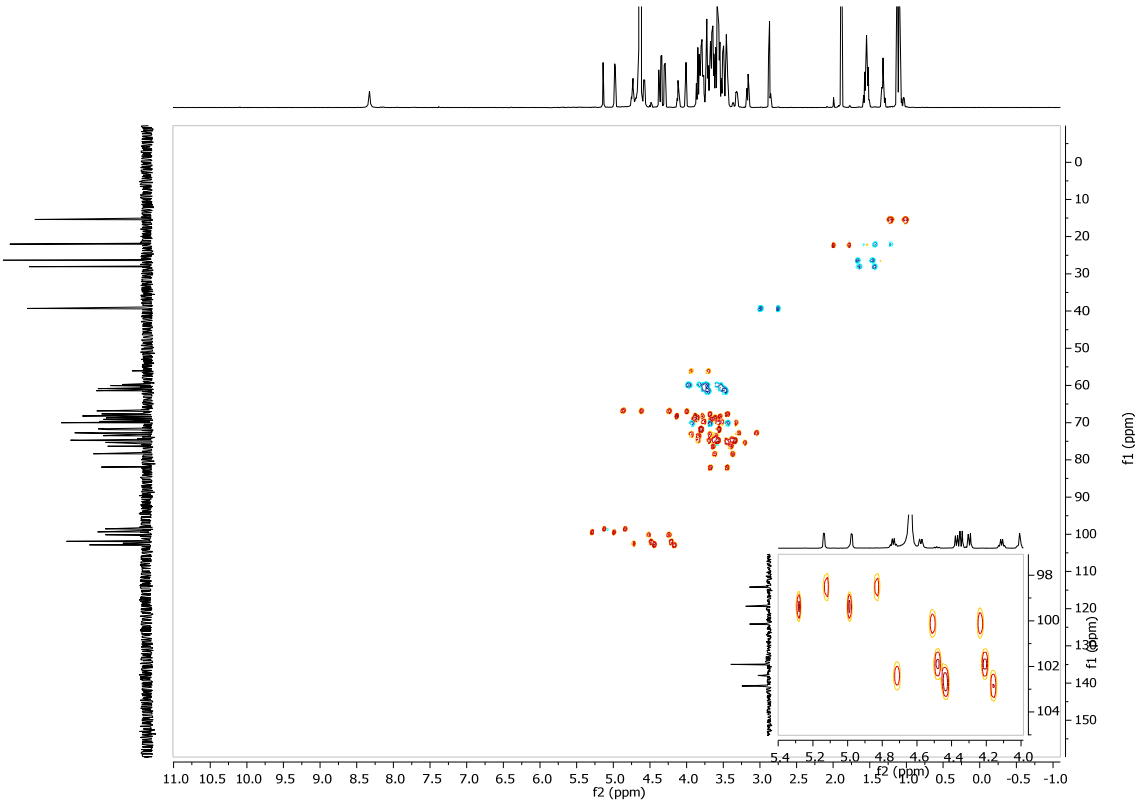

^{1}H NMR: **2.57**

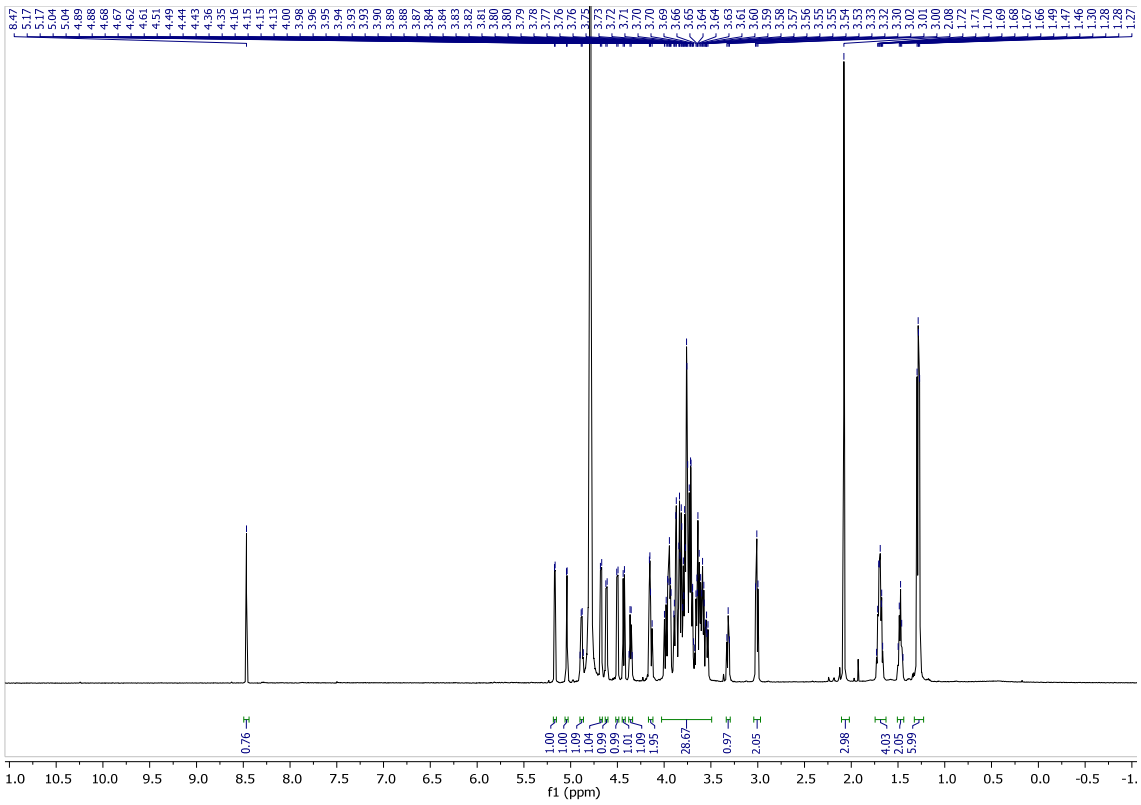

^{13}C NMR: **2.57**

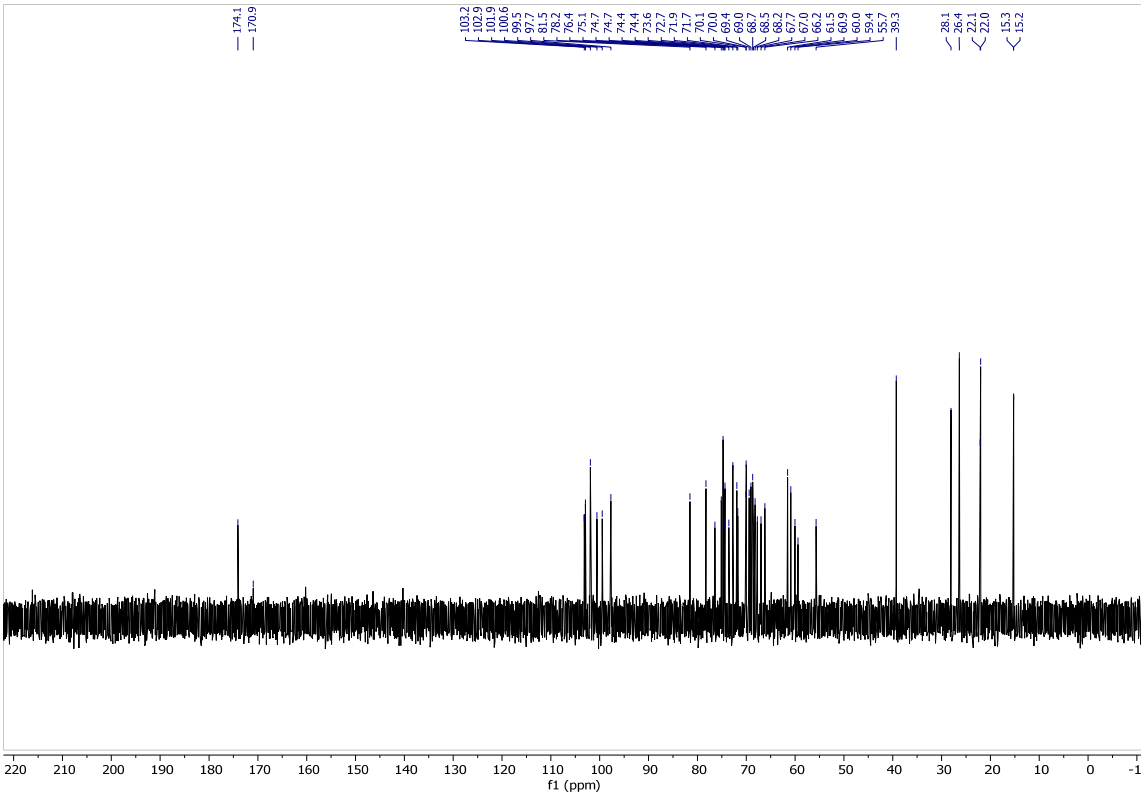

COSY: **2.57**

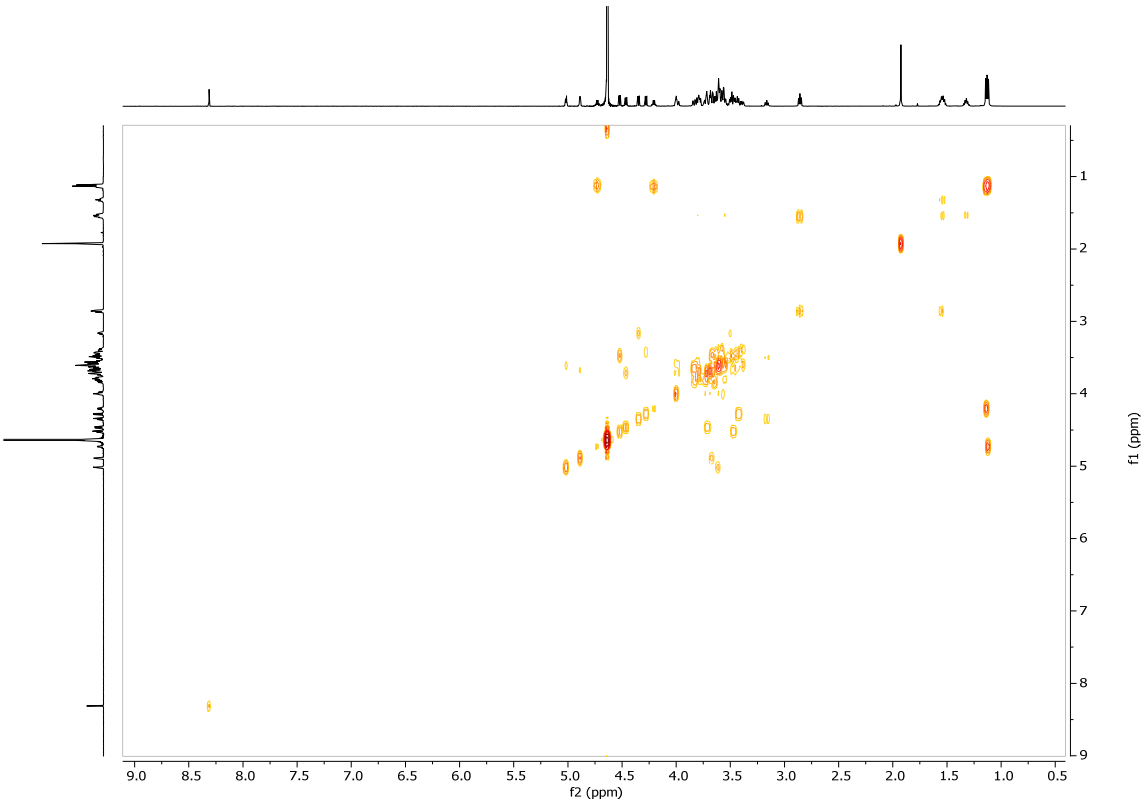

HSQC: **2.57**

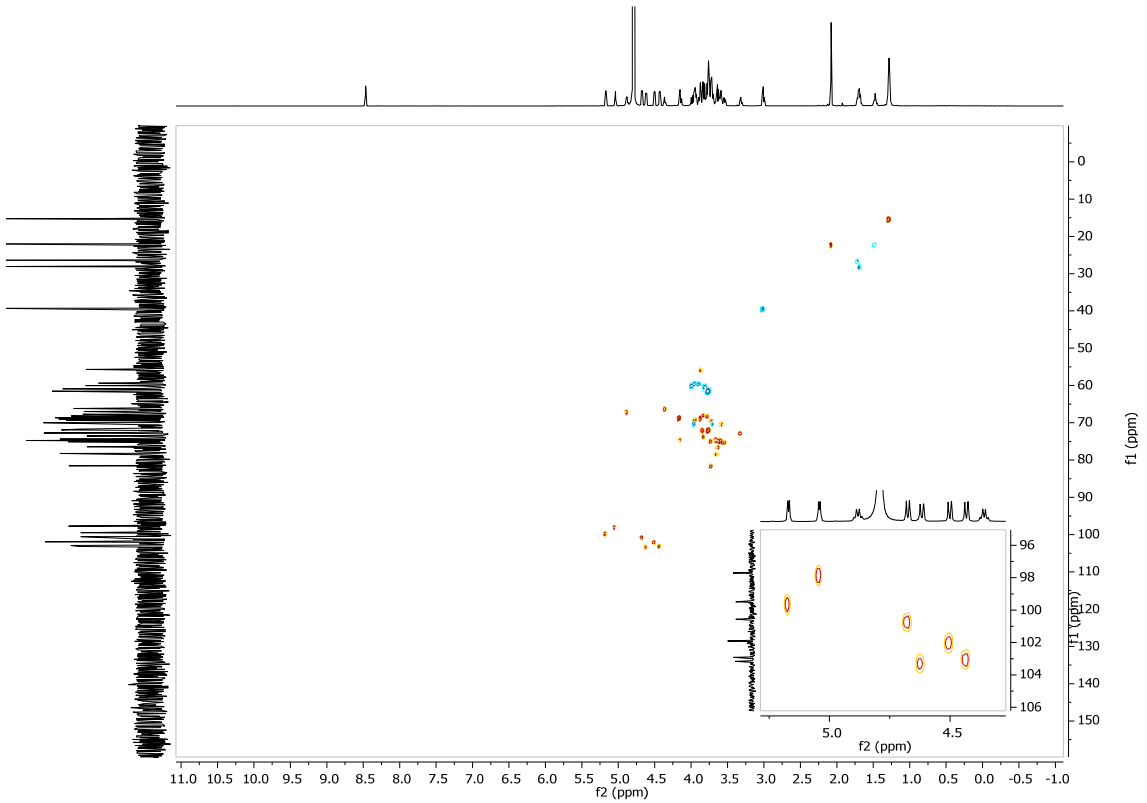

Coupled HSQC: **2.57**

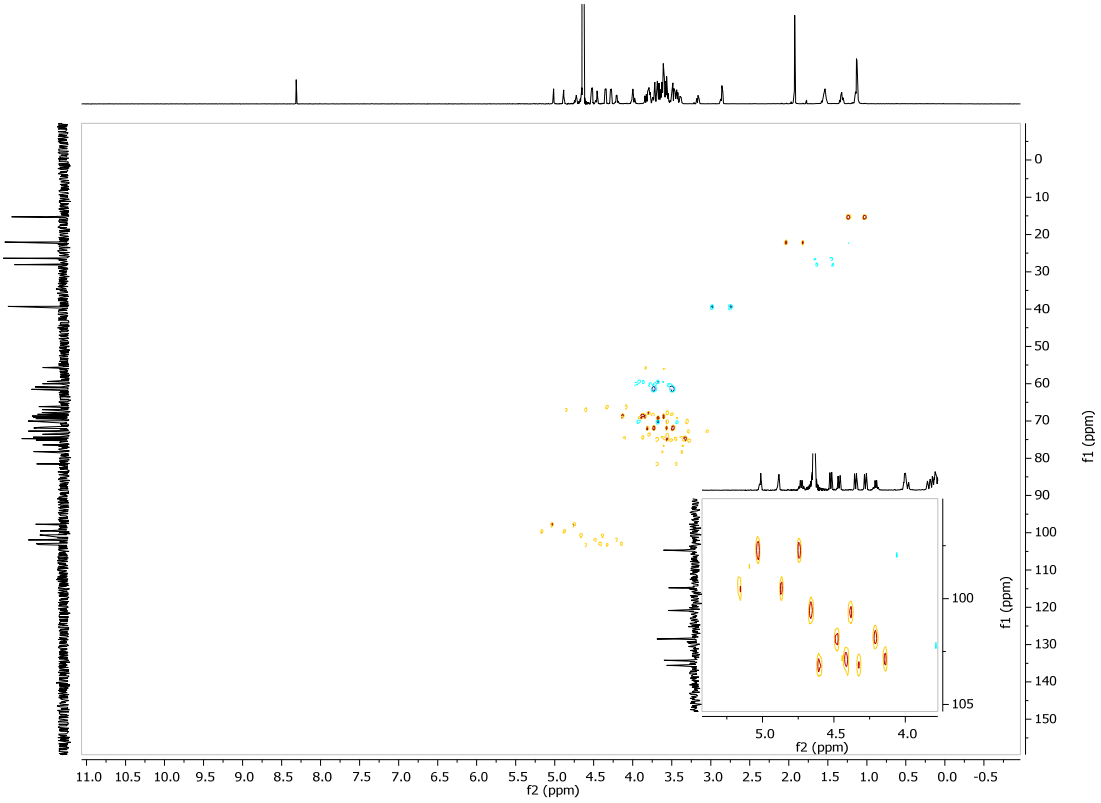

^{1}H NMR: **2.58**

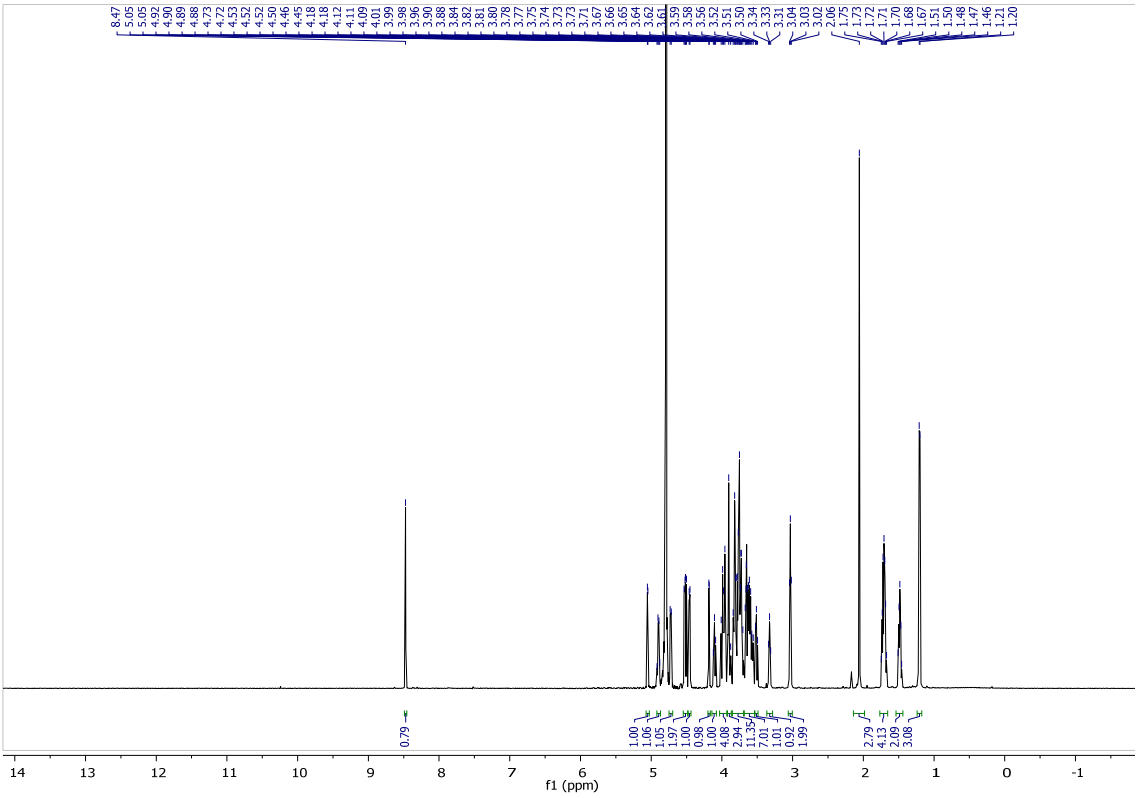

^{13}C NMR: **2.58**

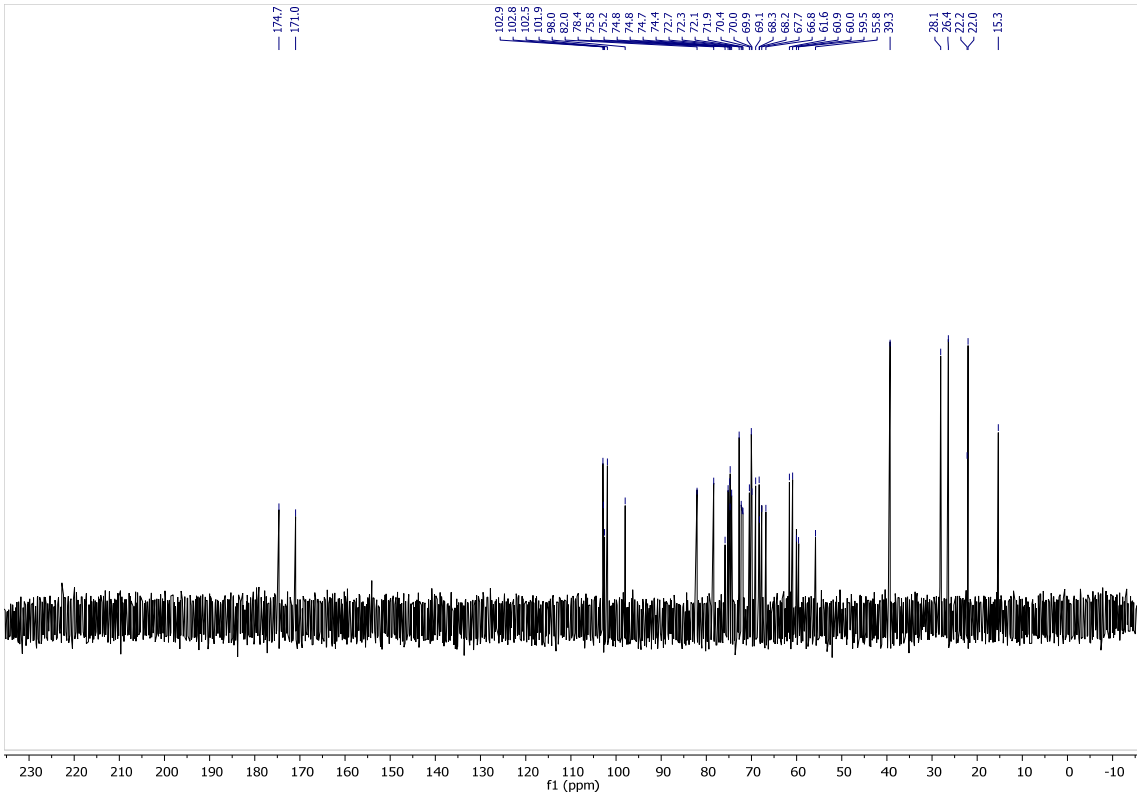

COSY: **2.58**

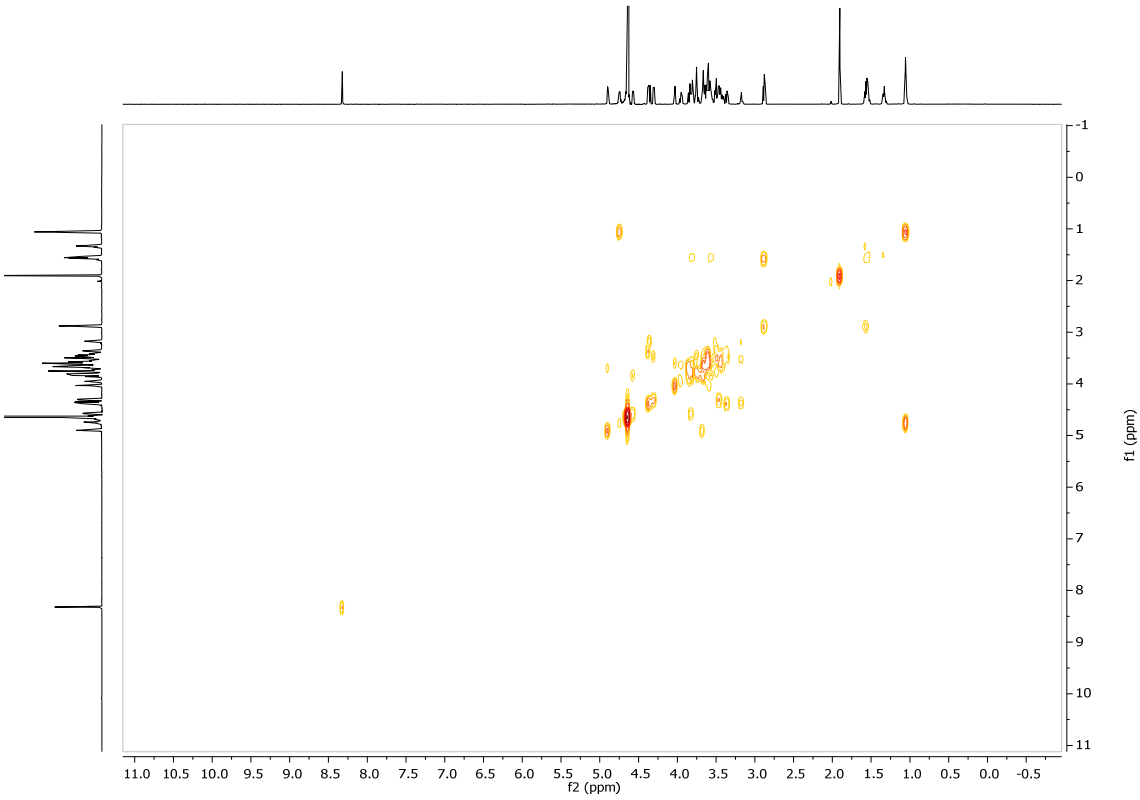

HSQC: **2.58**

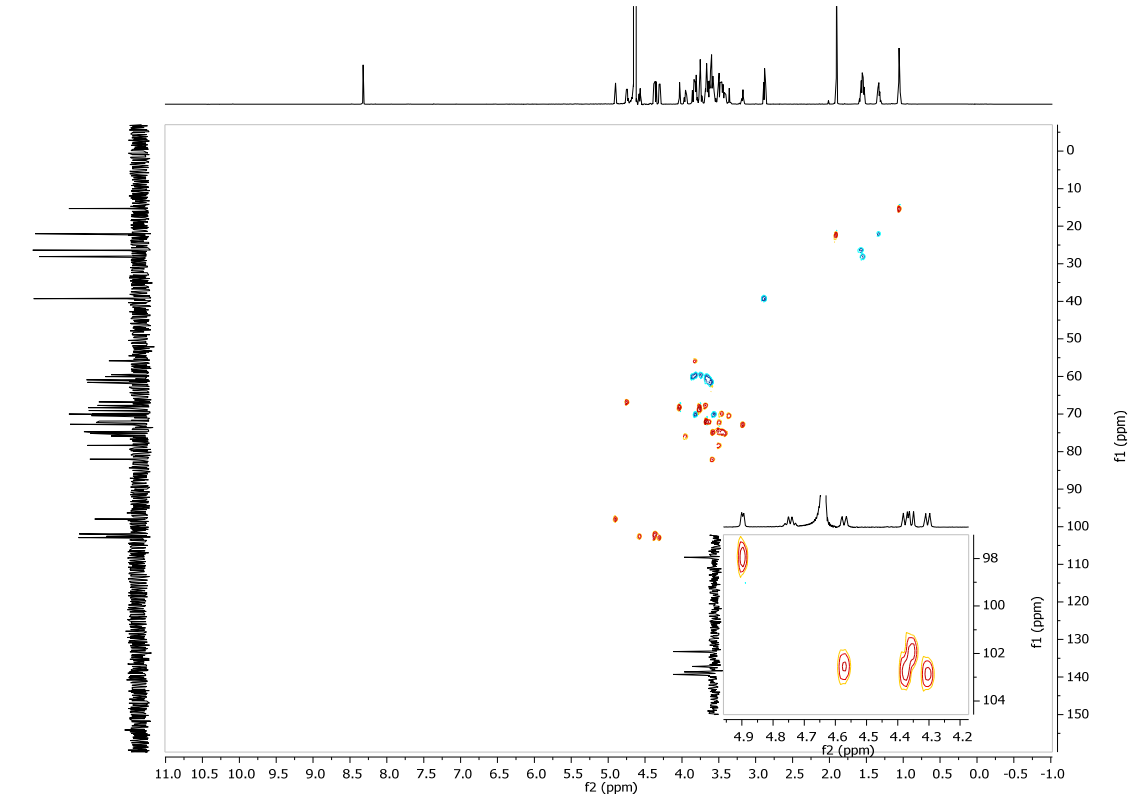

Coupled HSQC: **2.58**

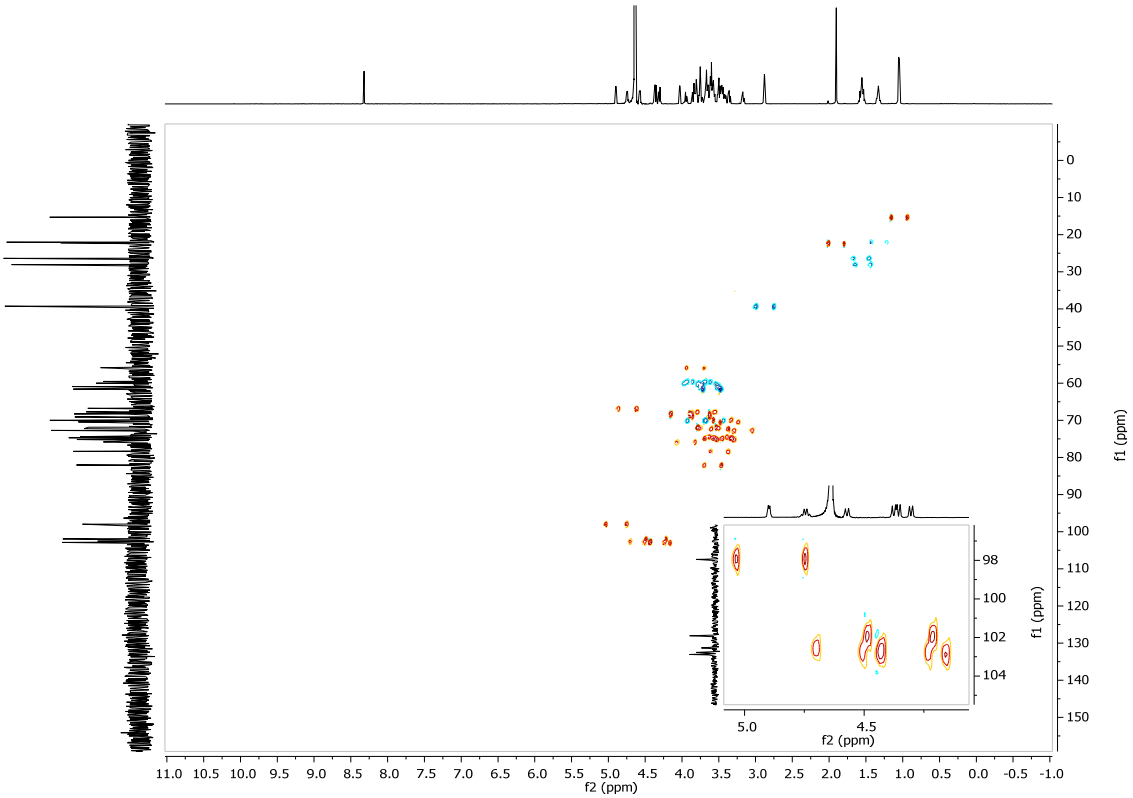

^{1}H NMR: **2.60**

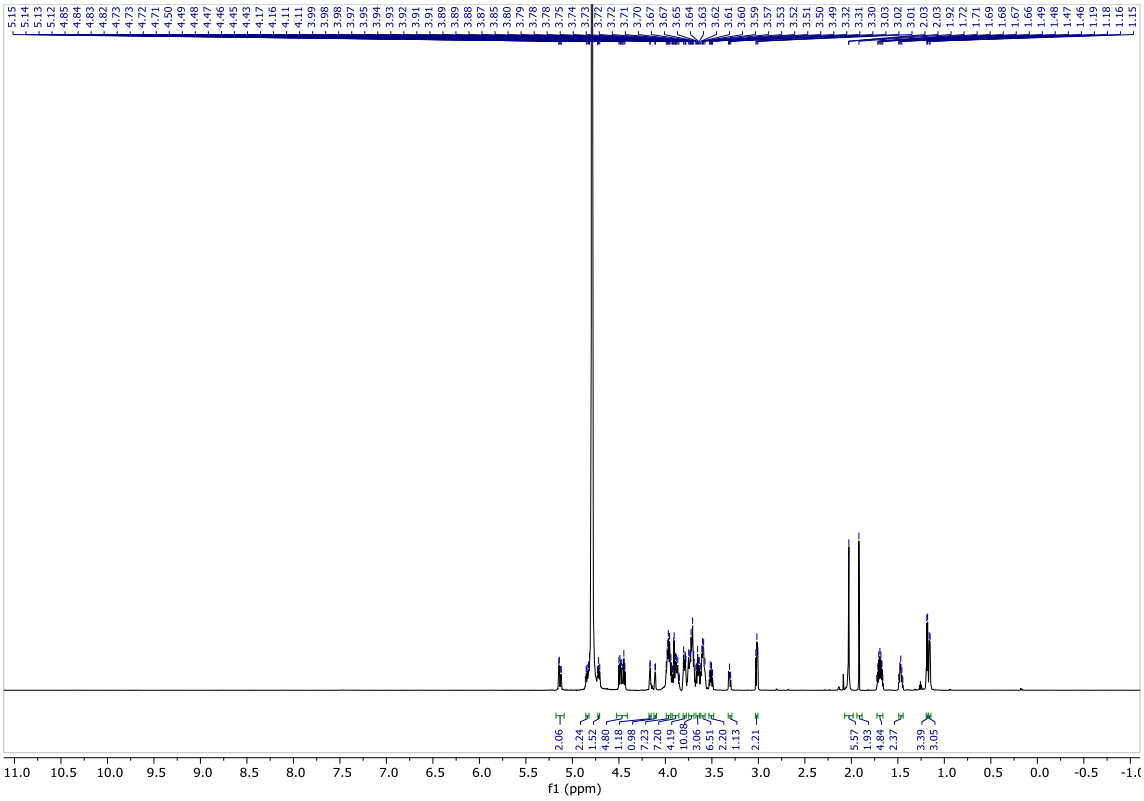

^{13}C NMR: **2.60**

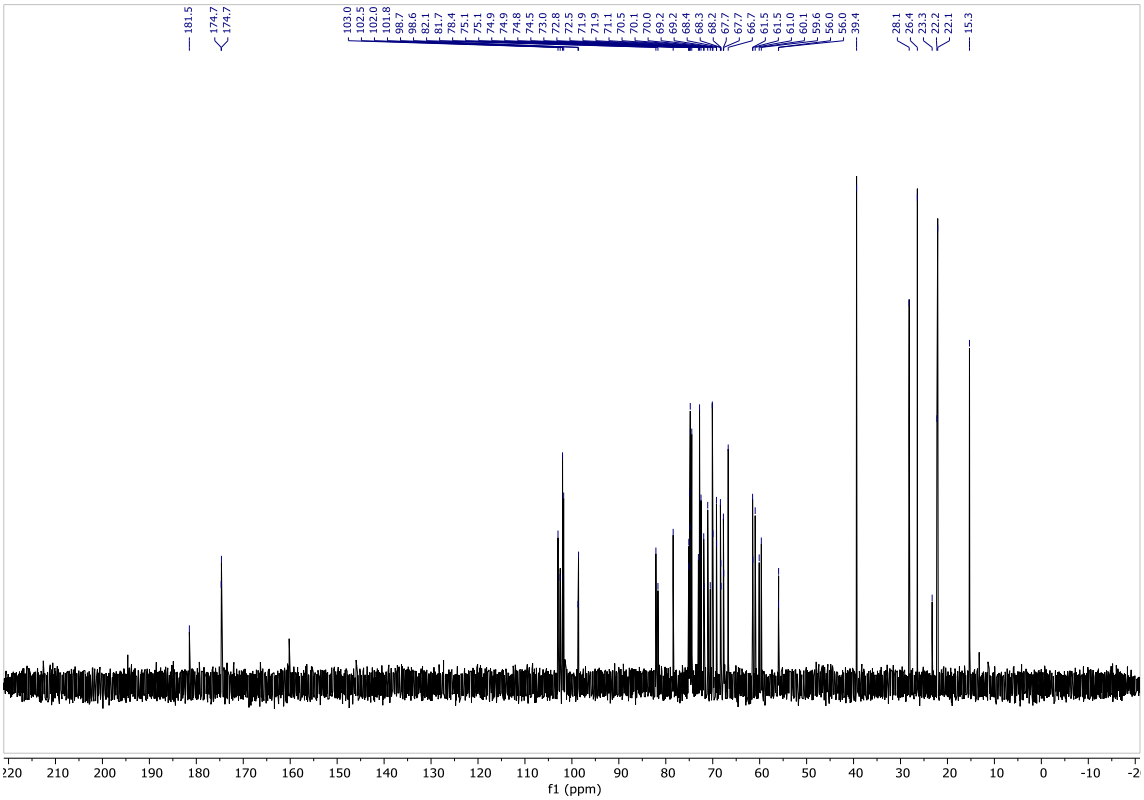

COSY: **2.60**

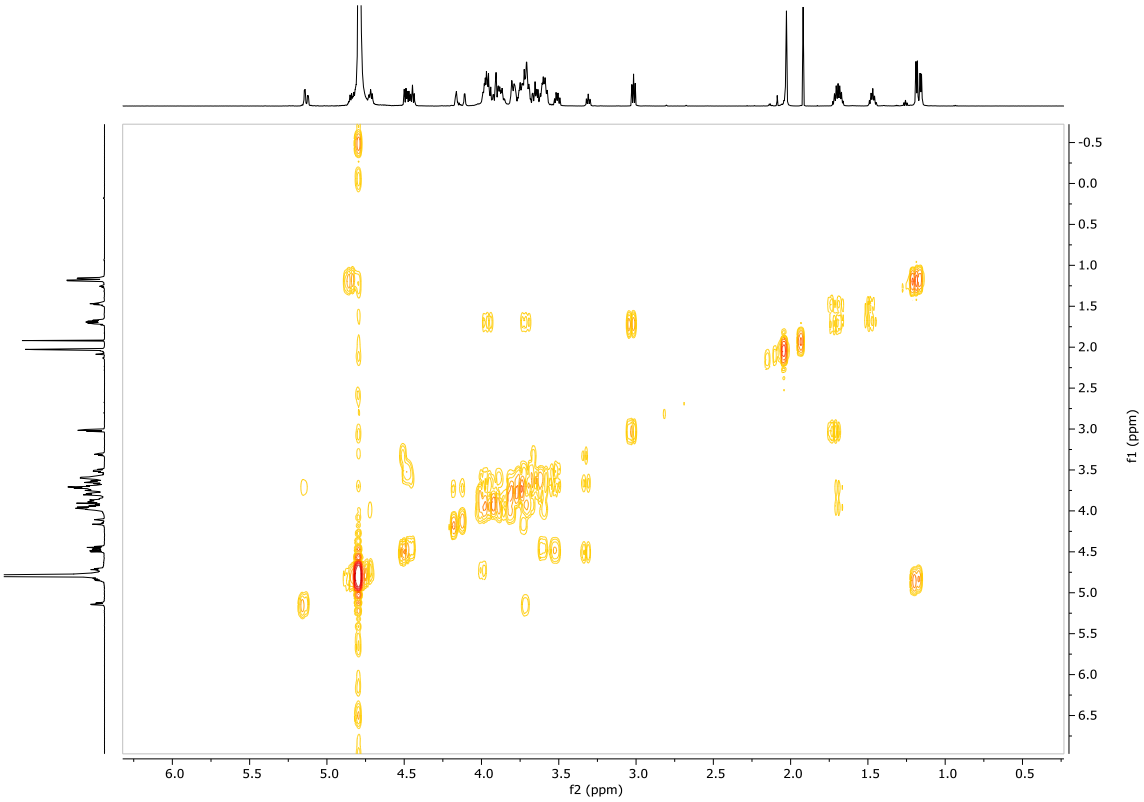

HSQC: **2.60**

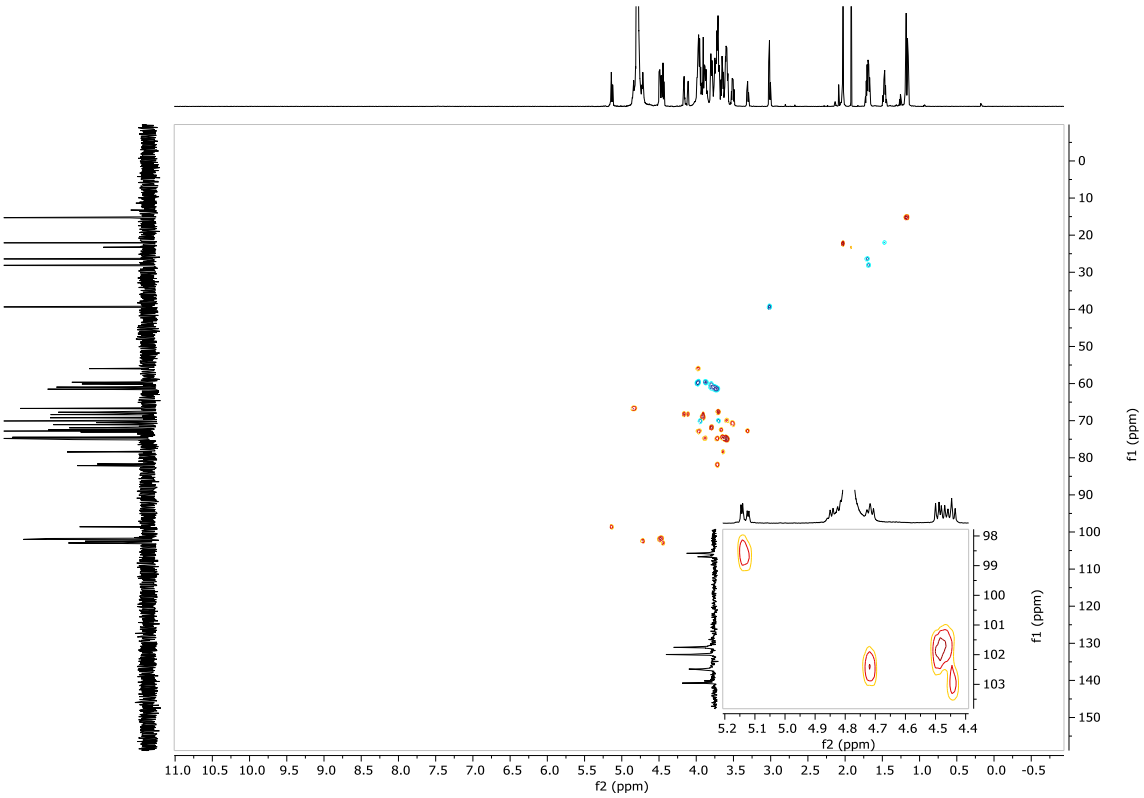

Coupled HSQC: **2.60**

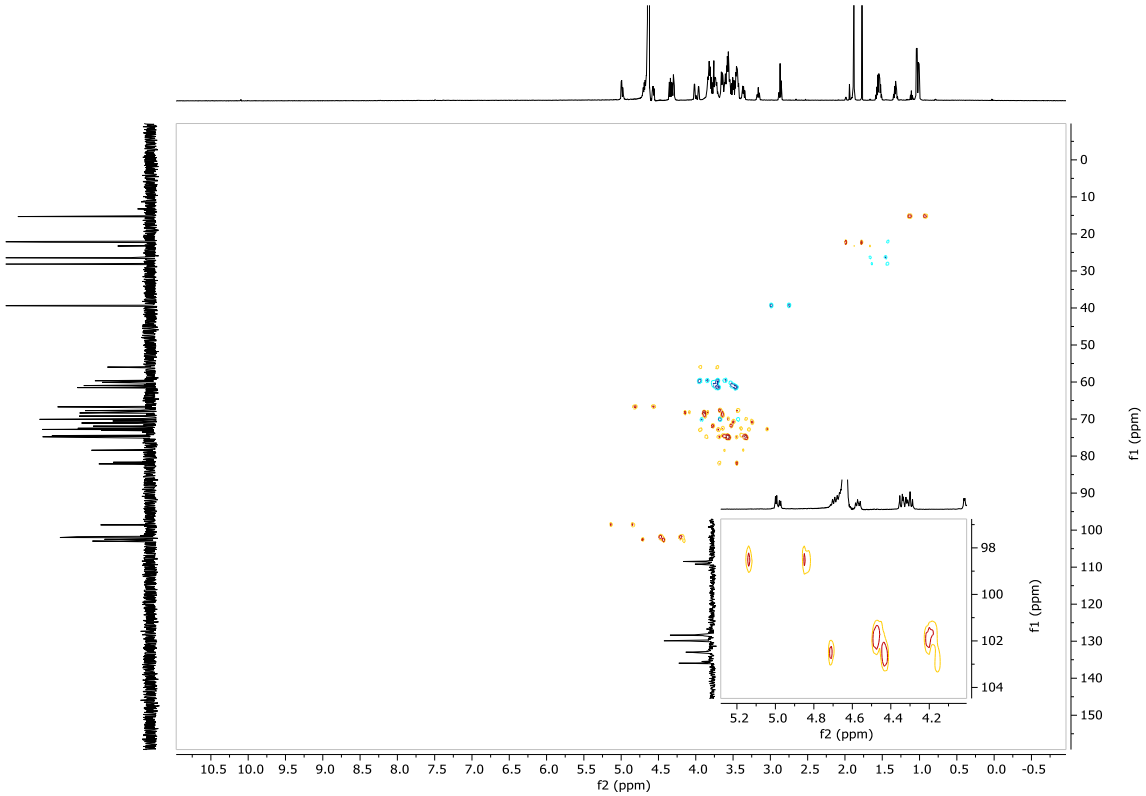

^{1}H NMR: **2.11**

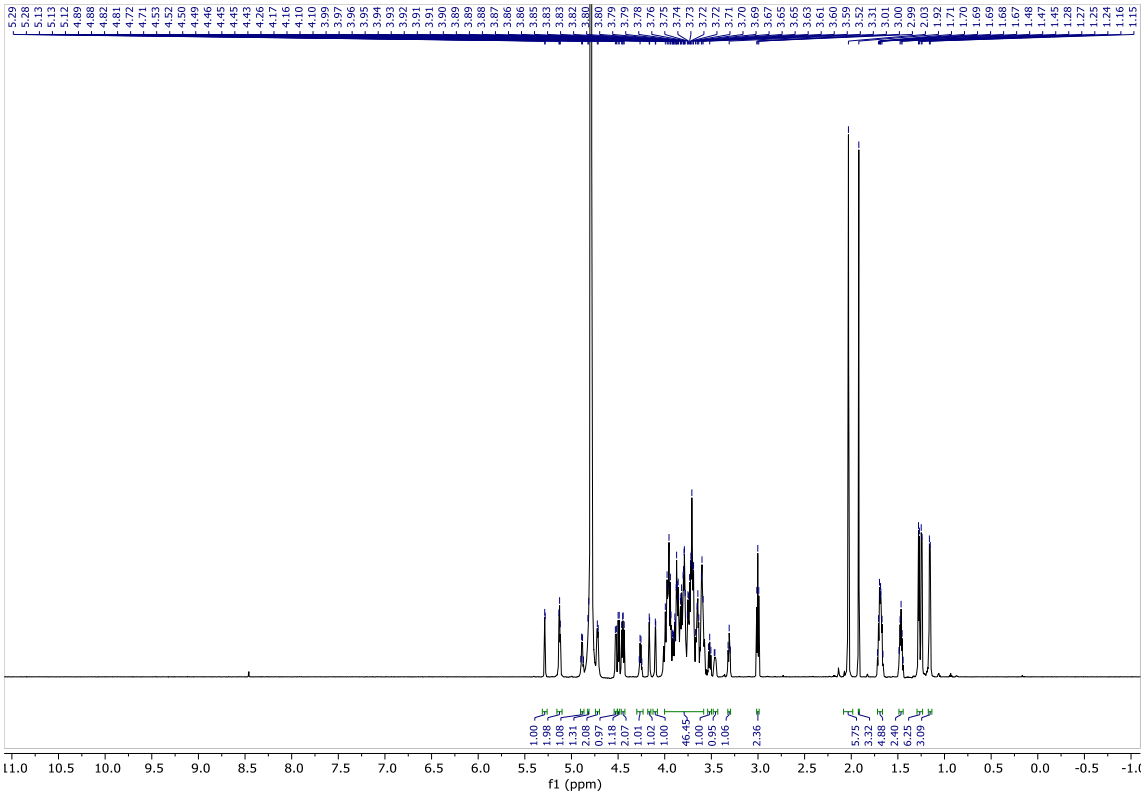

^{13}C NMR: **2.11**

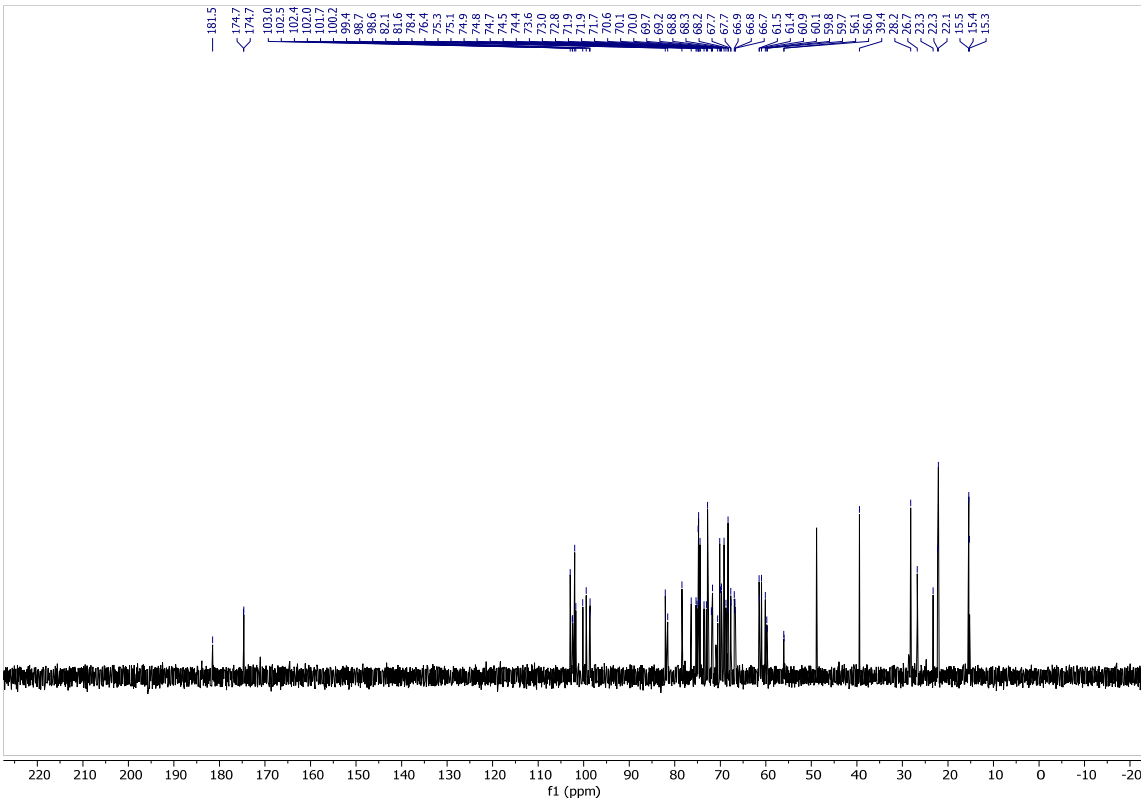

COSY: **2.11**

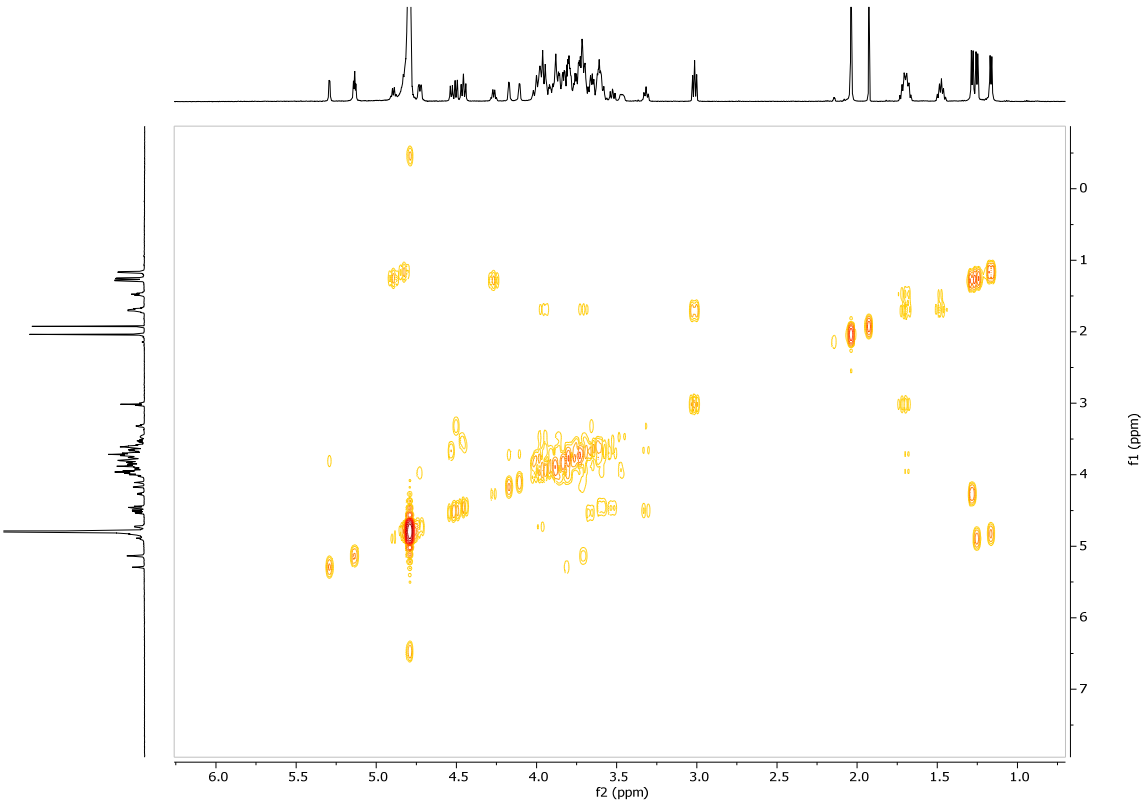

HSQC: **2.11**

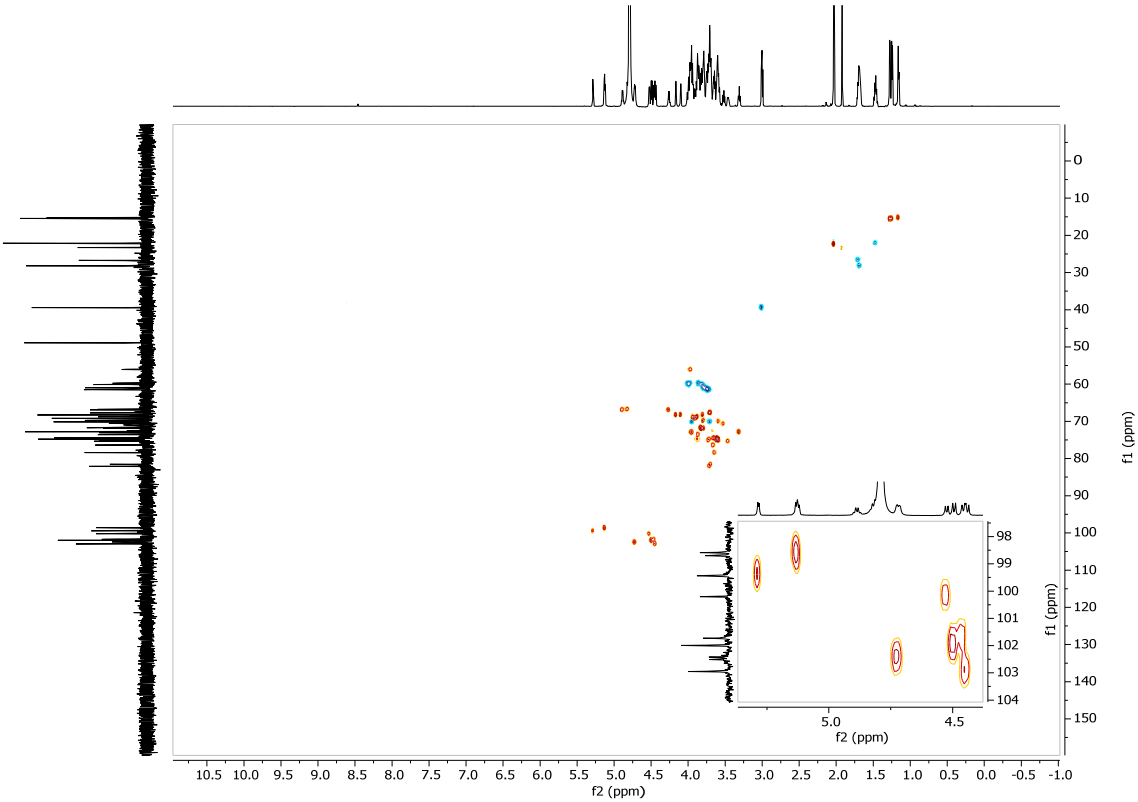

Coupled HSQC: **2.11**

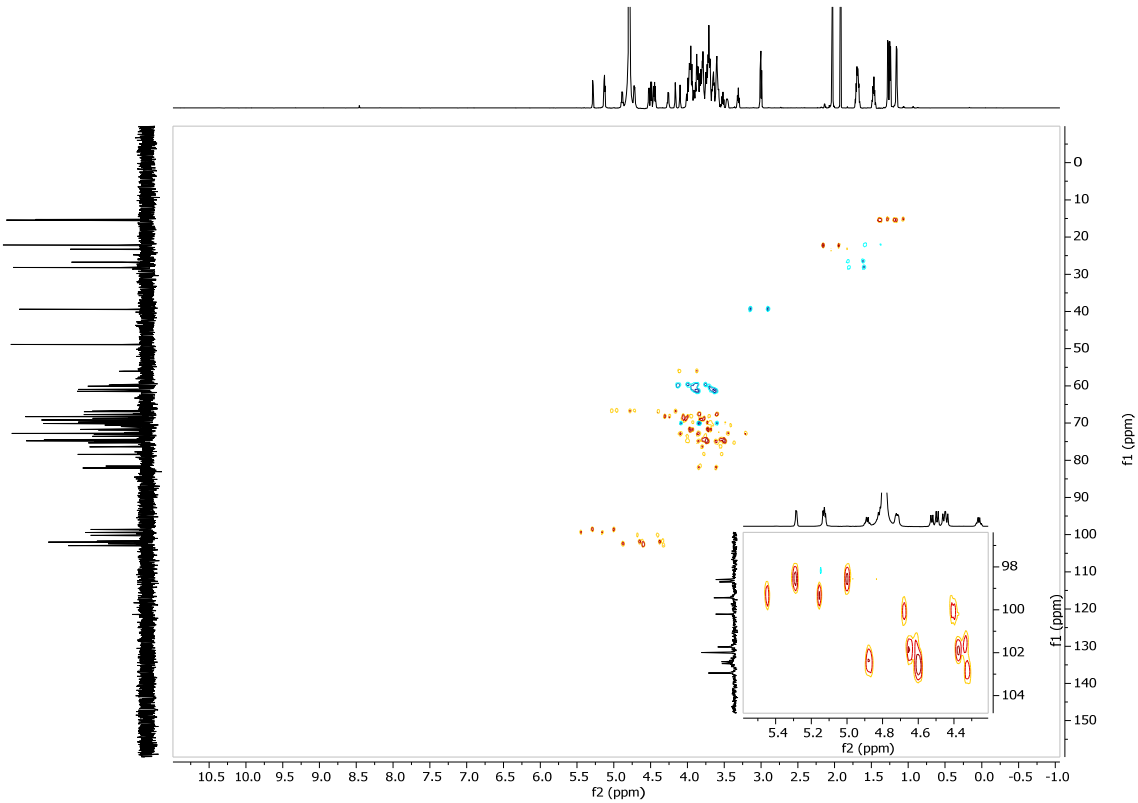

^{1}H-NMR: **3.2***

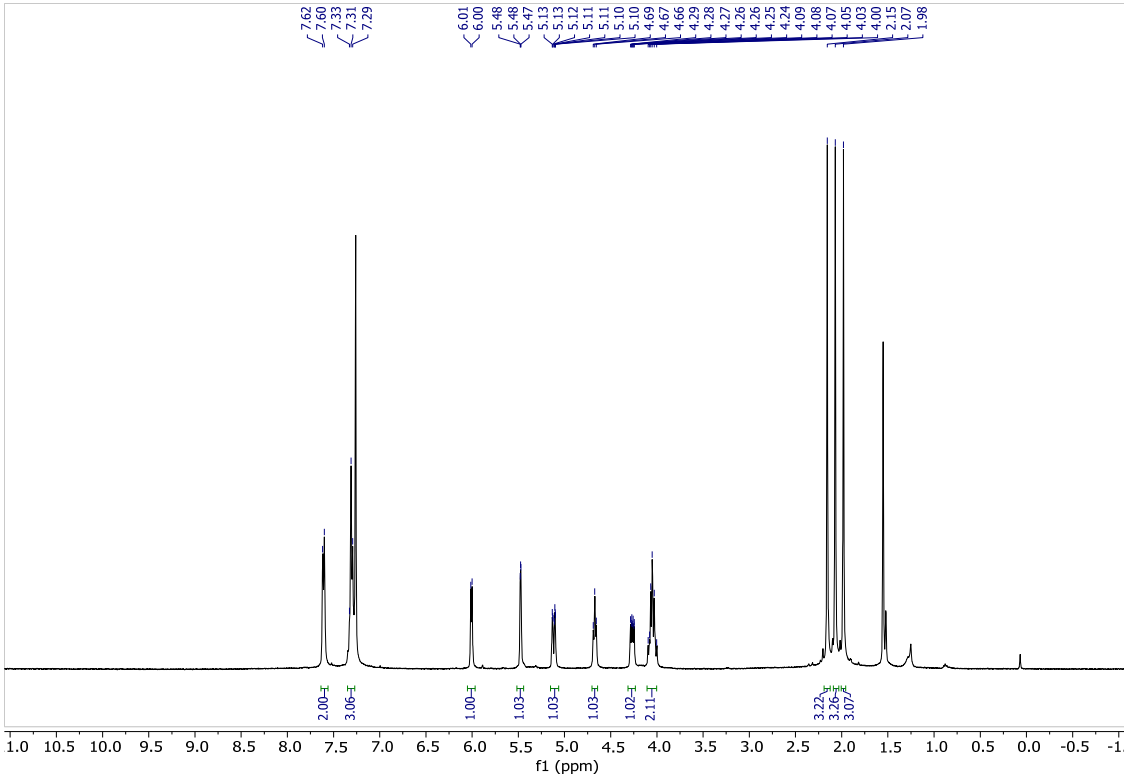

^{13}C NMR: **3.2**

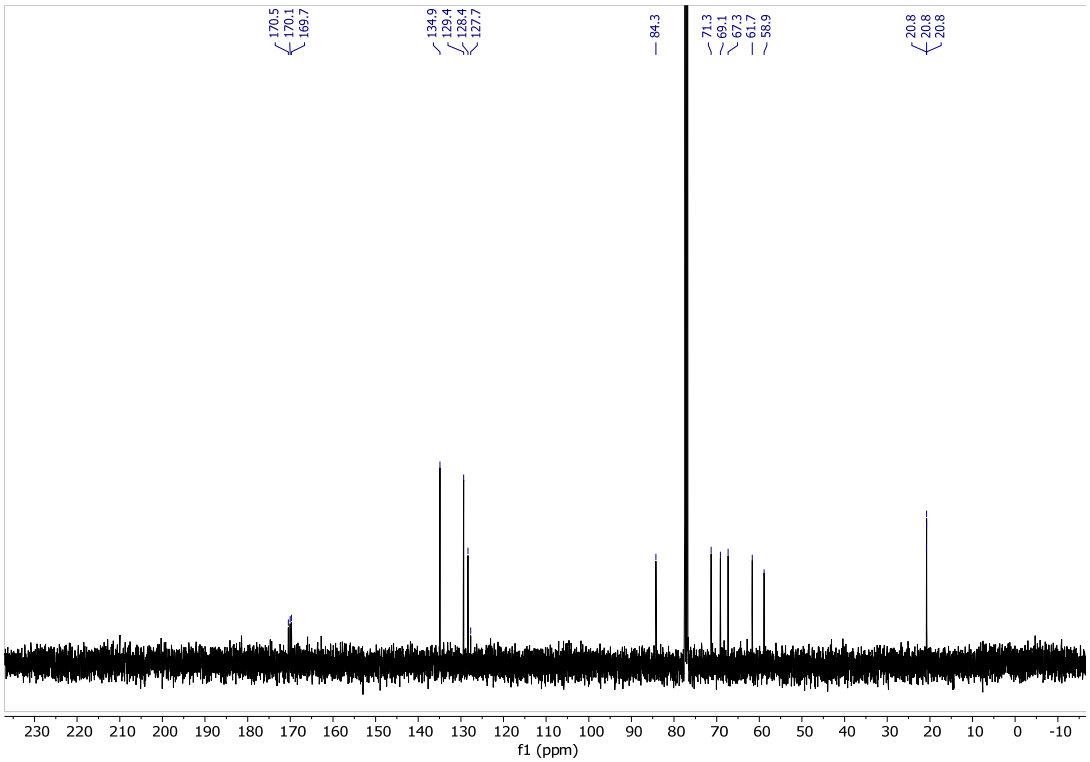

* ^{1}H, ^{13}C, COSY and HSQC NMR of known monosaccharide **3.2**[158] are provided, as signal assignment was necessary for the work in this thesis.

COSY: **3.2**

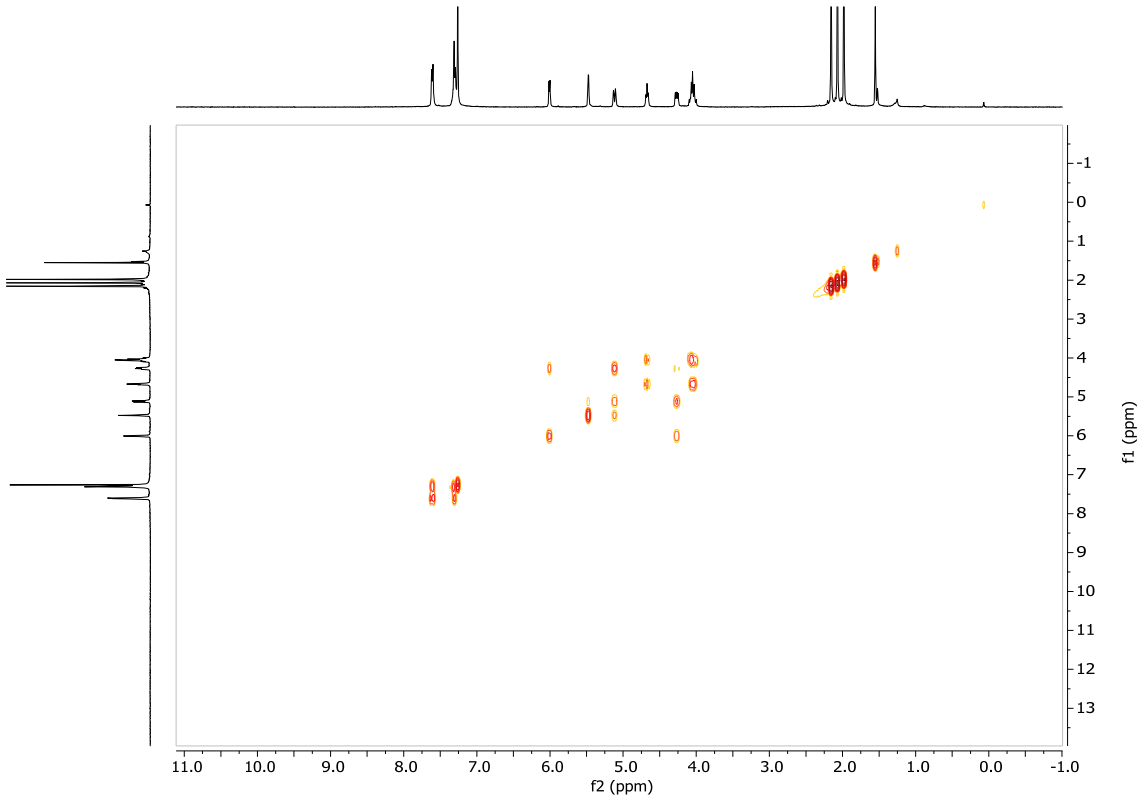

HSQC: **3.2**

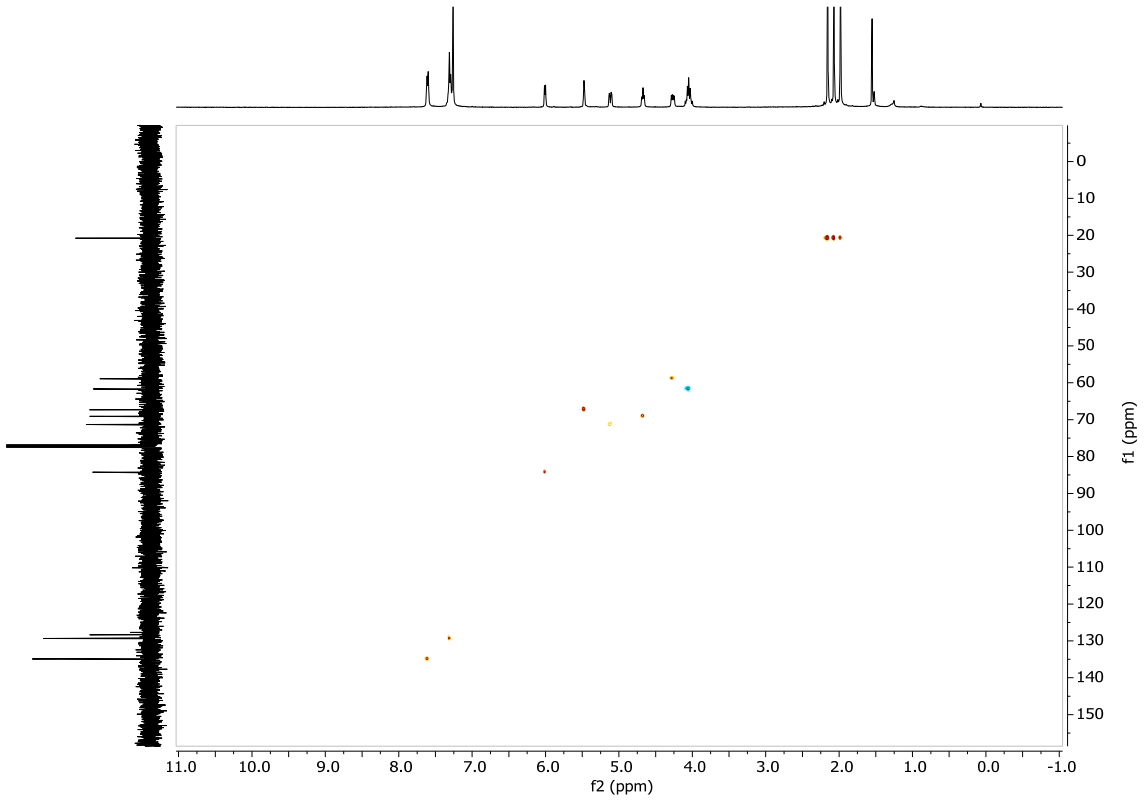

^{1}H-NMR: **3.3**

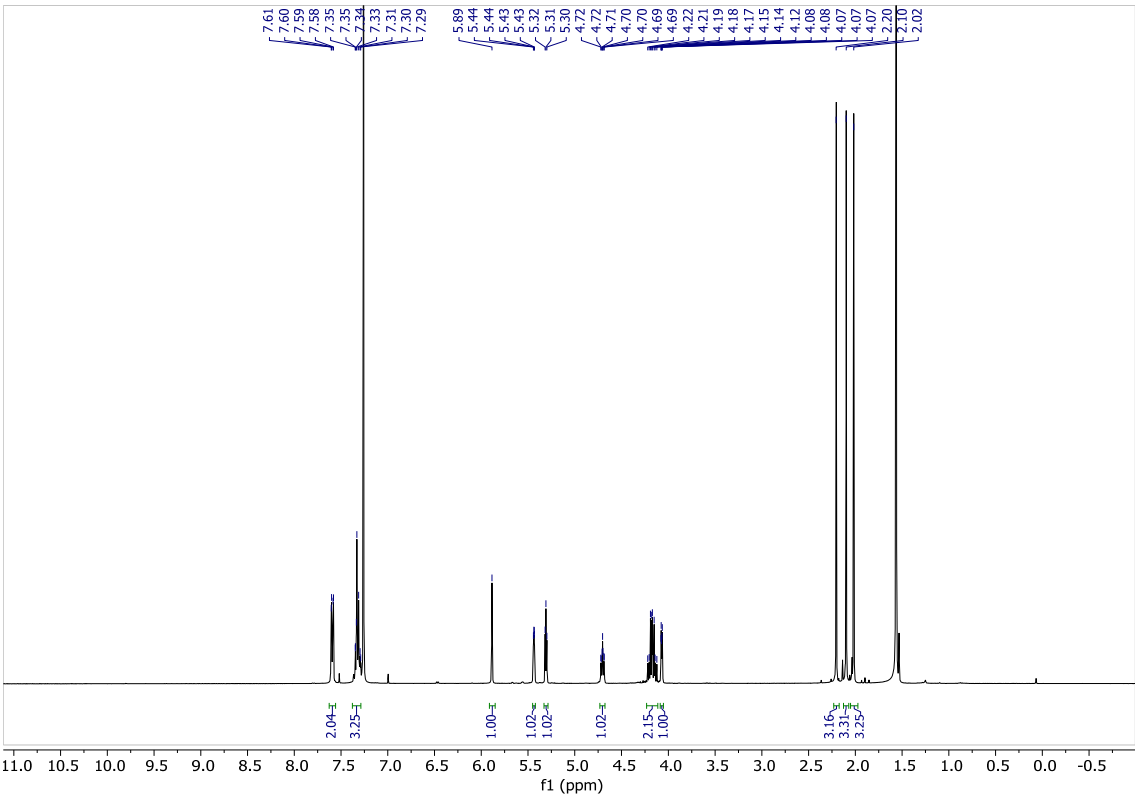

^{13}C NMR: **3.3**

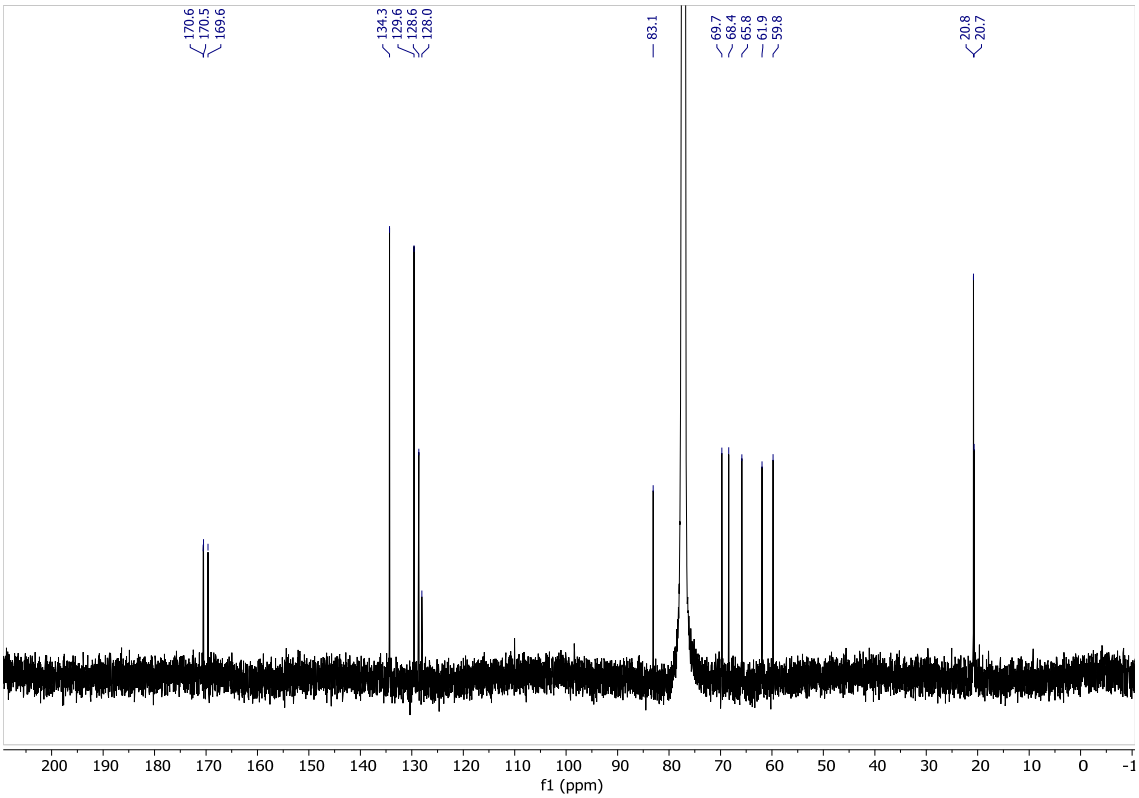

COSY: **3.3**

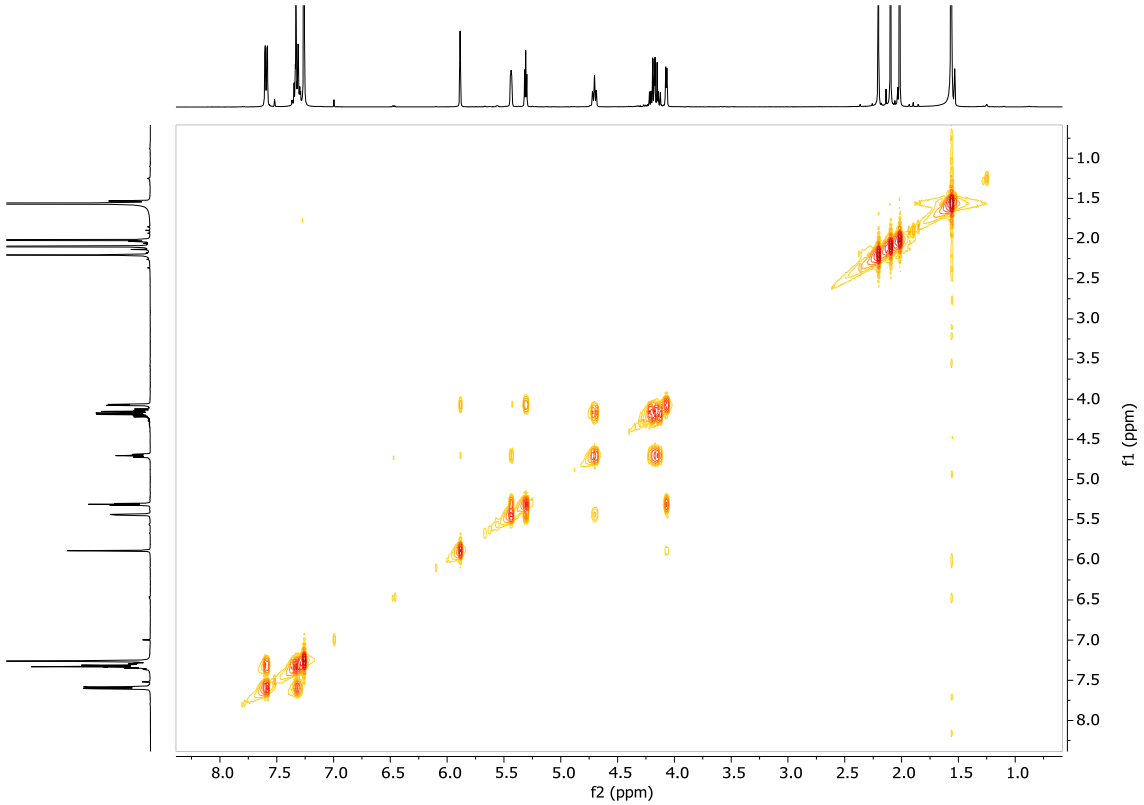

HSQC: **3.3**

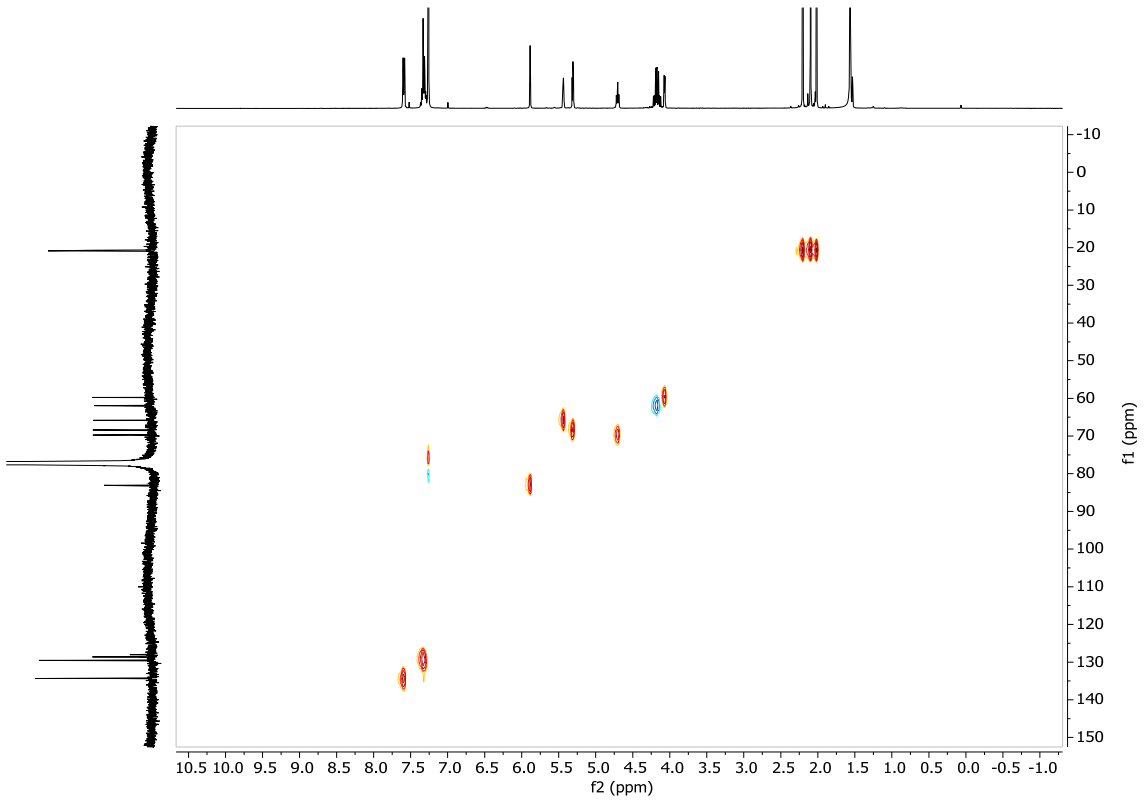

Coupled HSQC: **3.3**

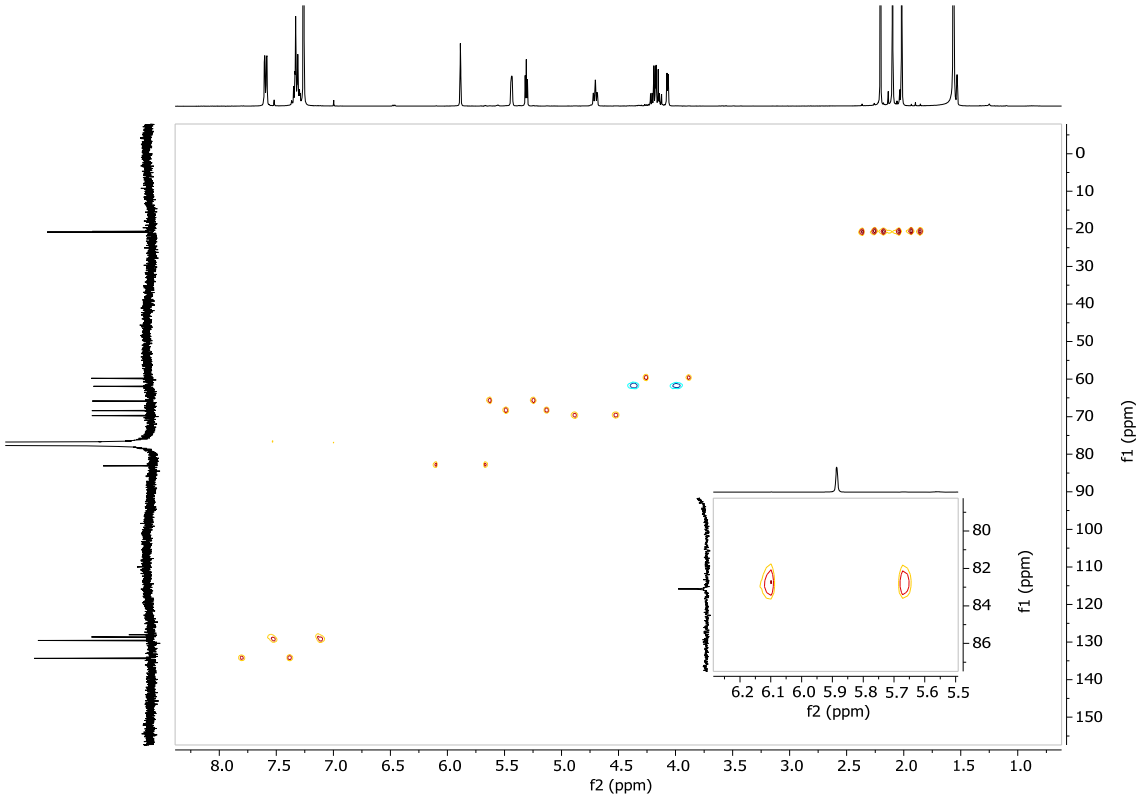

^{1}H-NMR: **3.4**, **3.5**

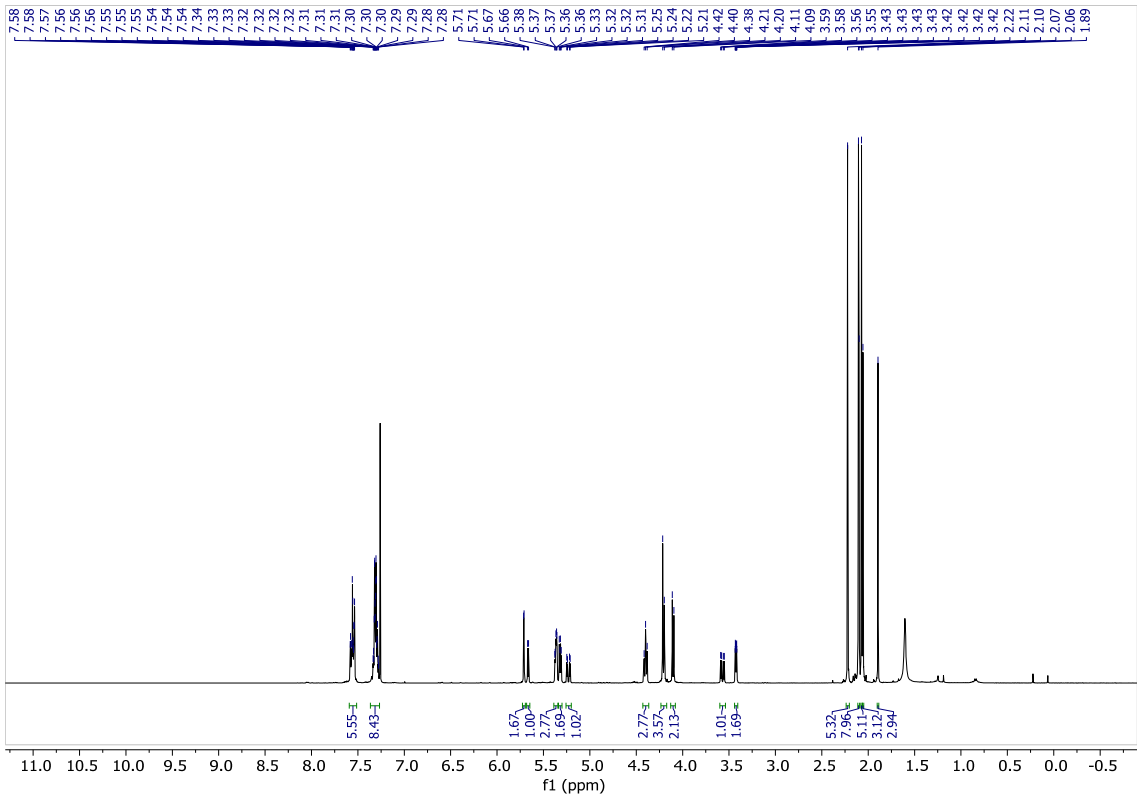

^{13}C NMR: **3.4**, **3.5**

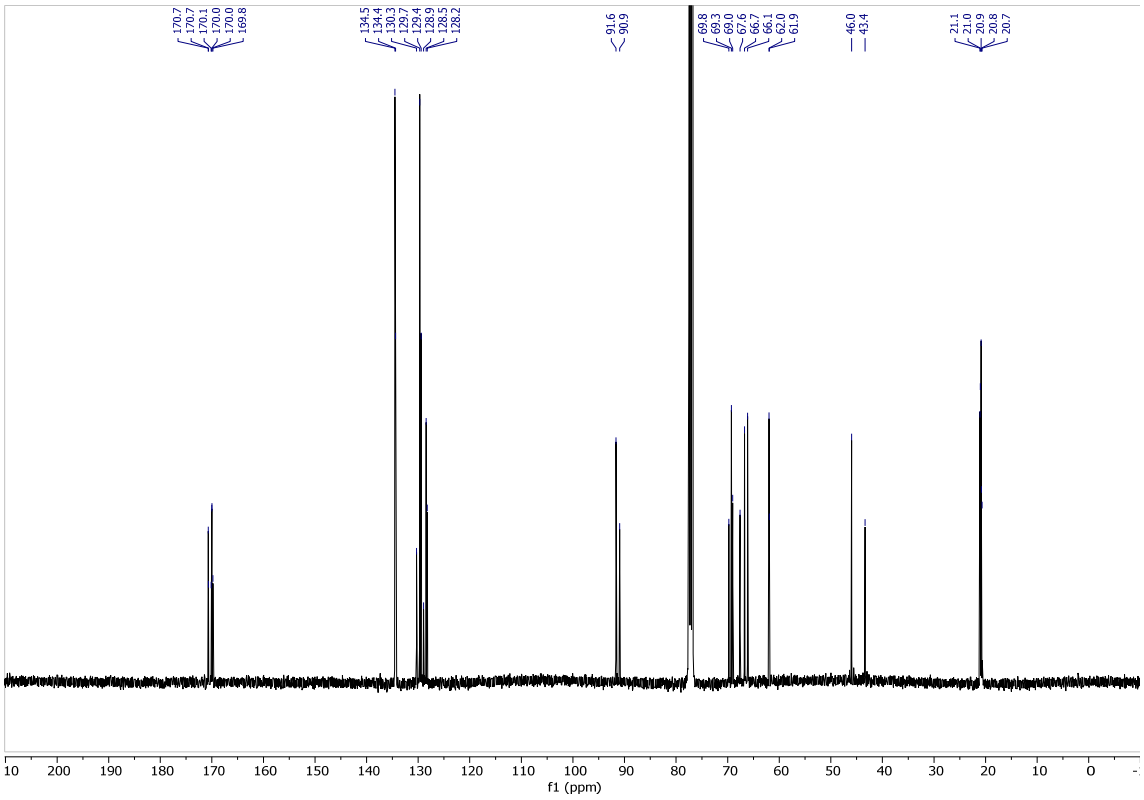

COSY: **3.4**, **3.5**

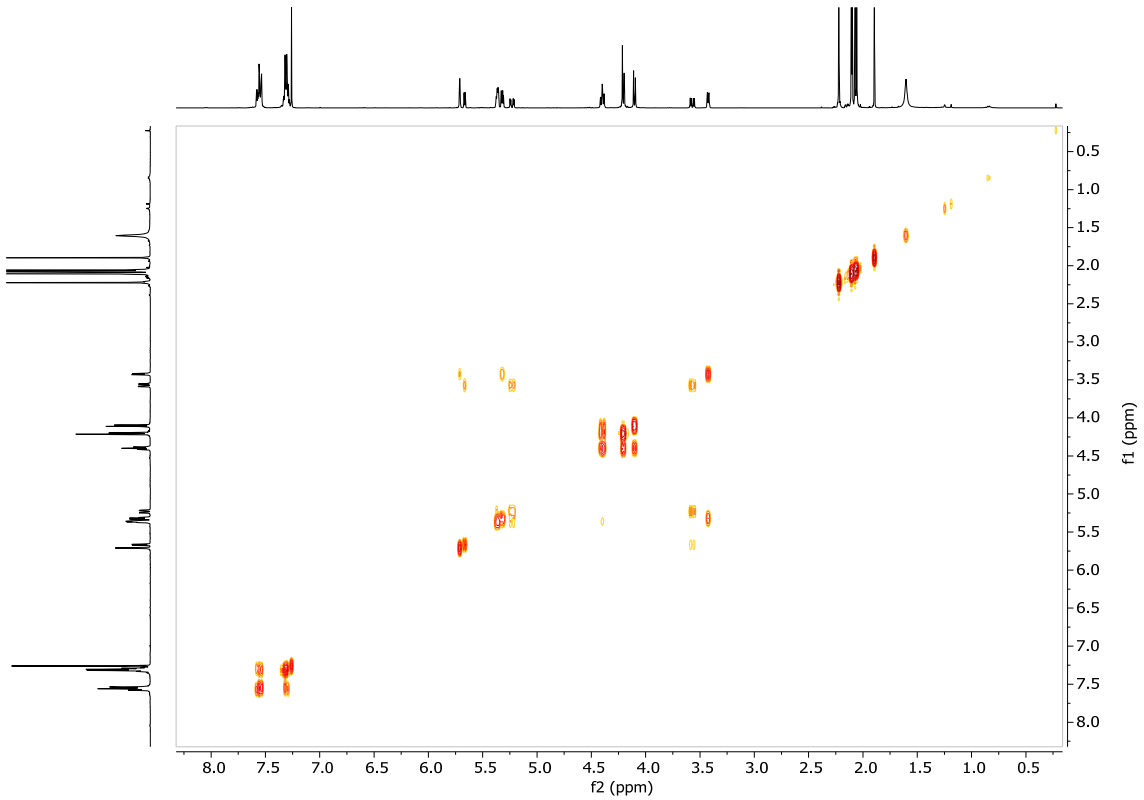

HSQC: **3.4**, **3.5**

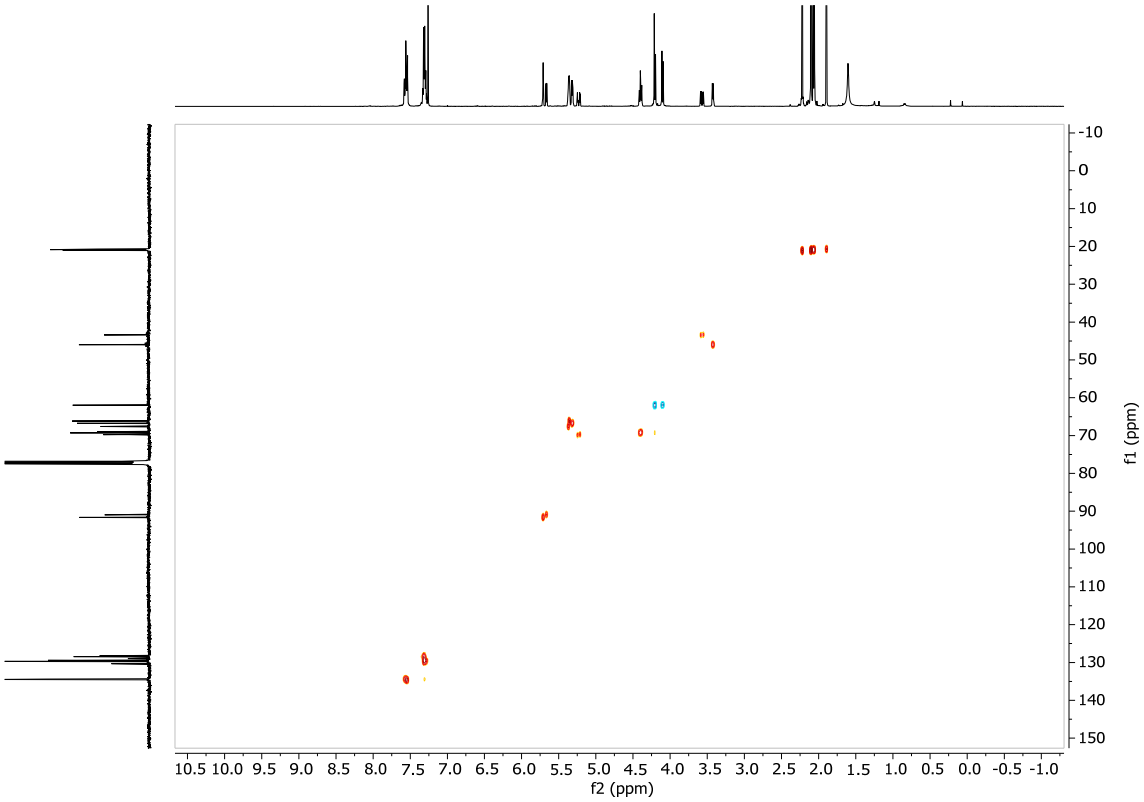

Coupled HSQC: **3.4**, **3.5**

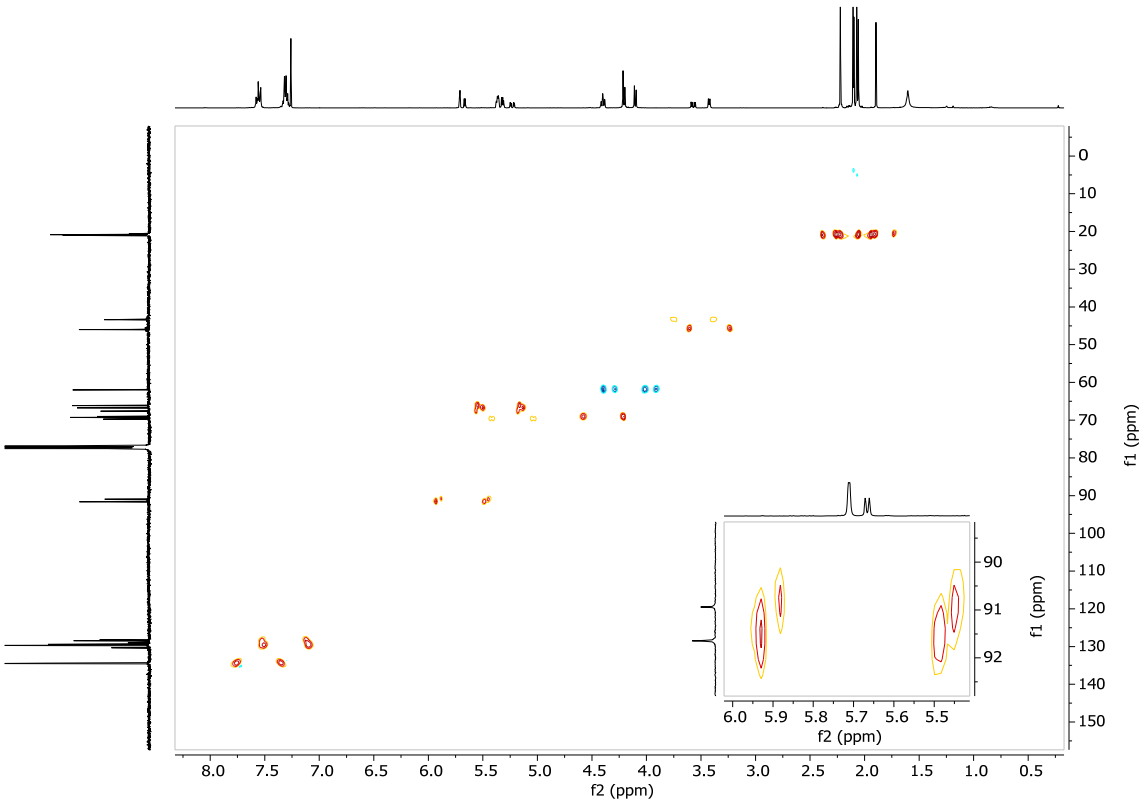

^{1}H-NMR: **3.6**, **3.7**[†]

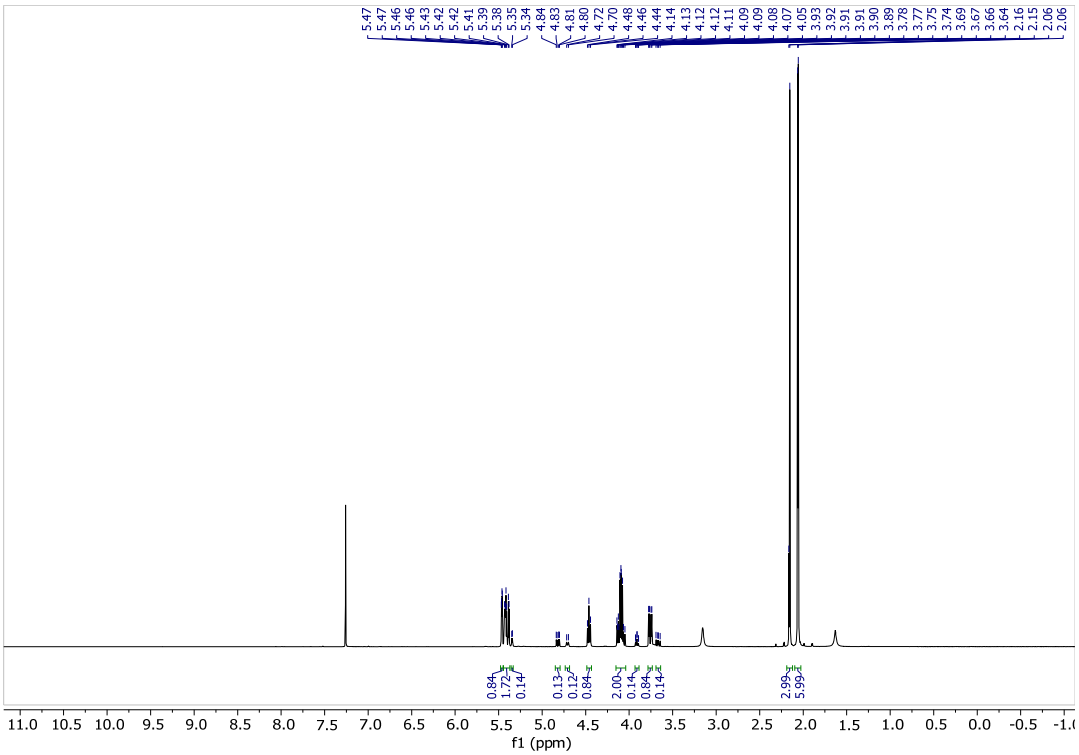

^{13}C NMR: **3.6**, **3.7**

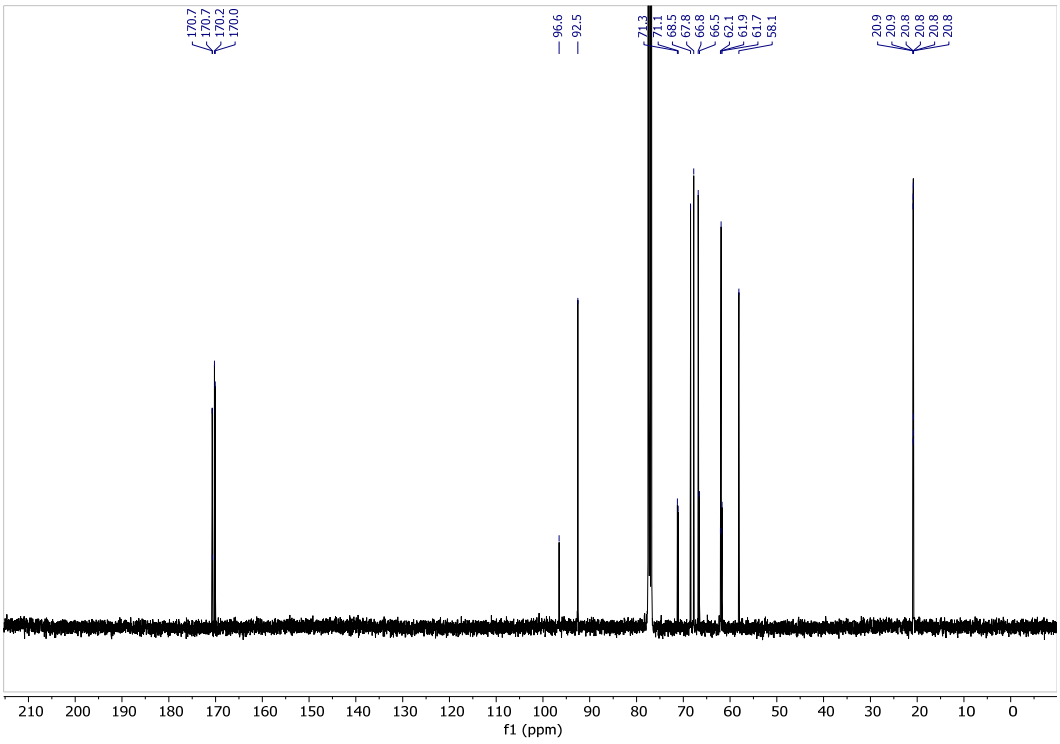

[†] ^{1}H, ^{13}C, COSY and HSQC NMR of known monosaccharides **3.4** and **3.5**[179] are provided as signal assignment was necessary for the work in this thesis.

COSY: **3.6**, **3.7**

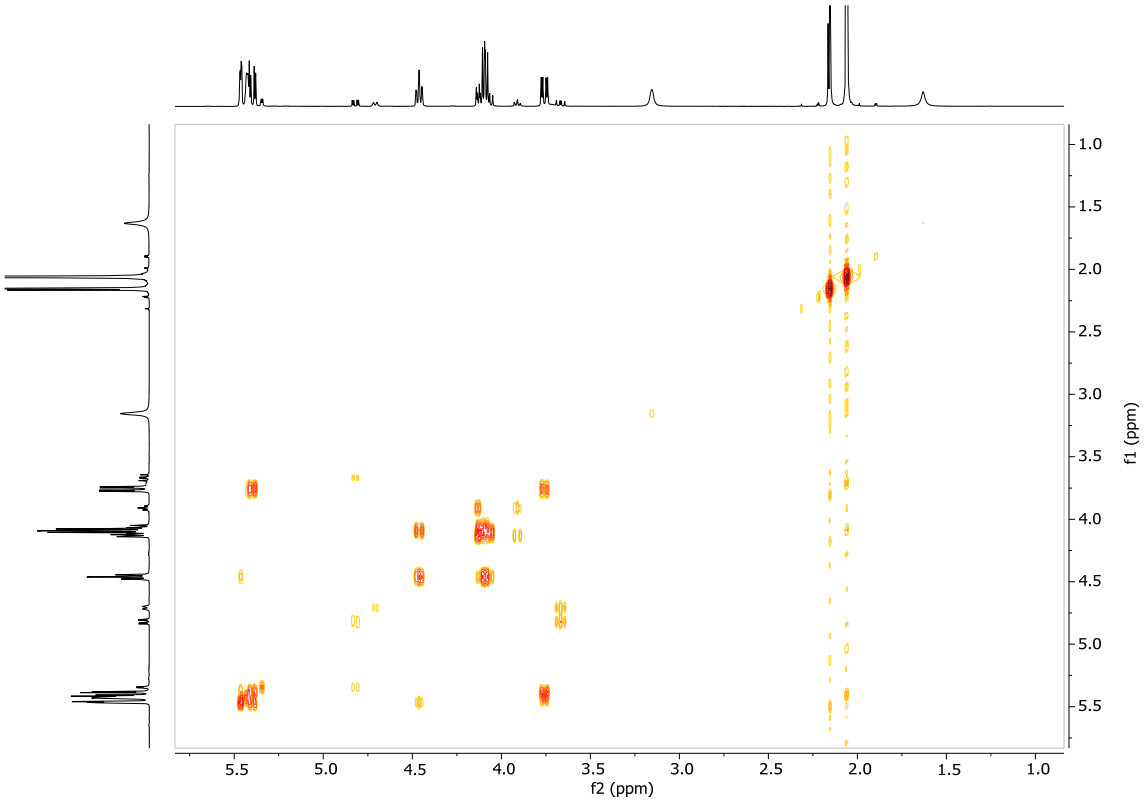

HSQC: **3.6**, **3.7**

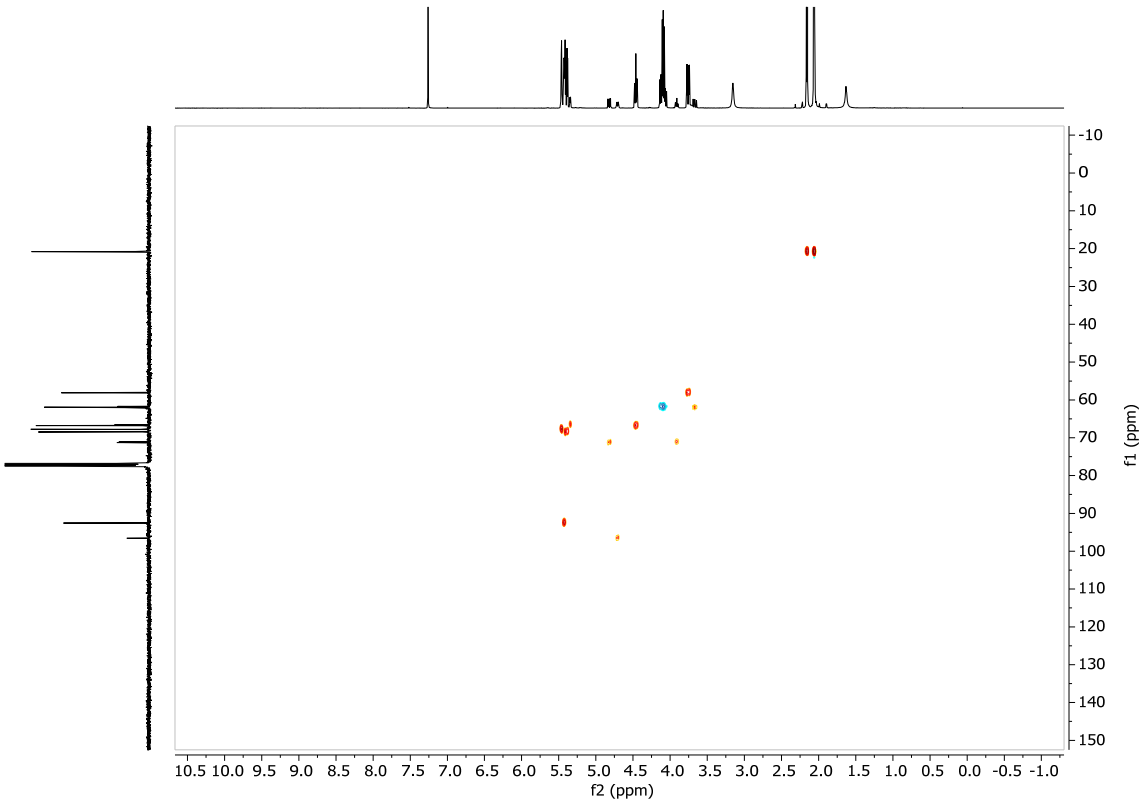

Coupled HSQC: **3.6**, **3.7**

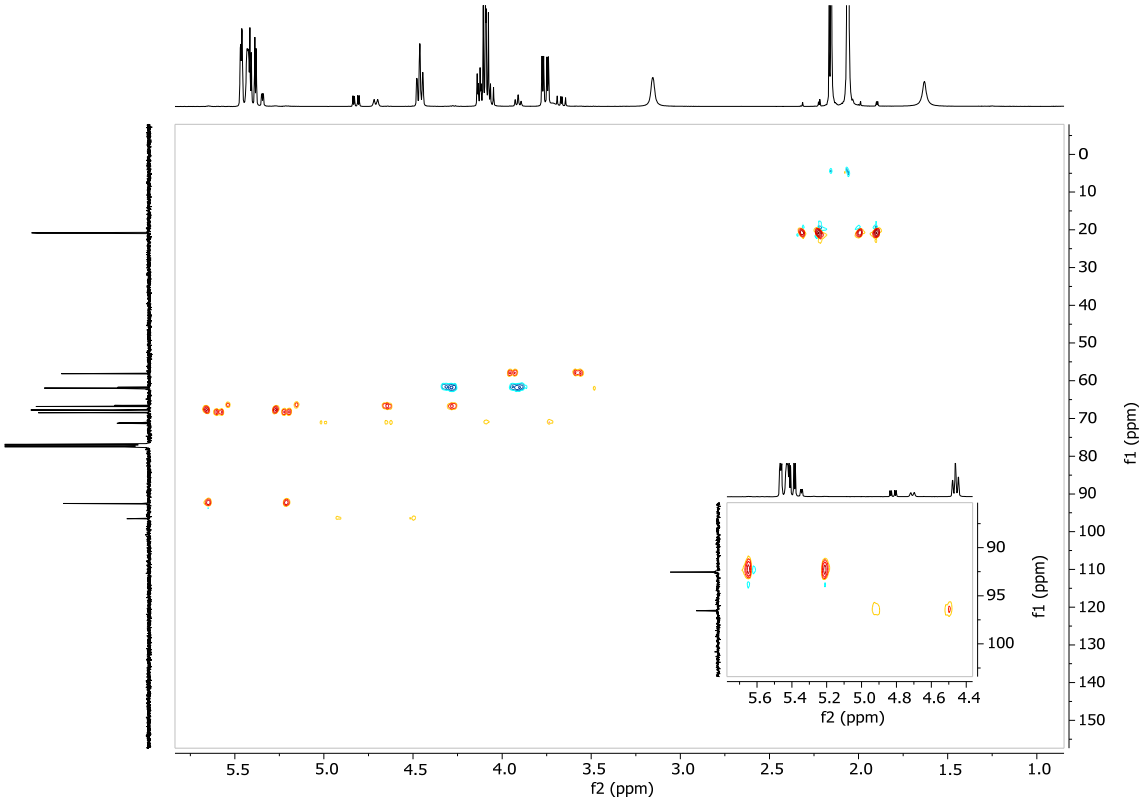

^{1}H-NMR: **3.8**

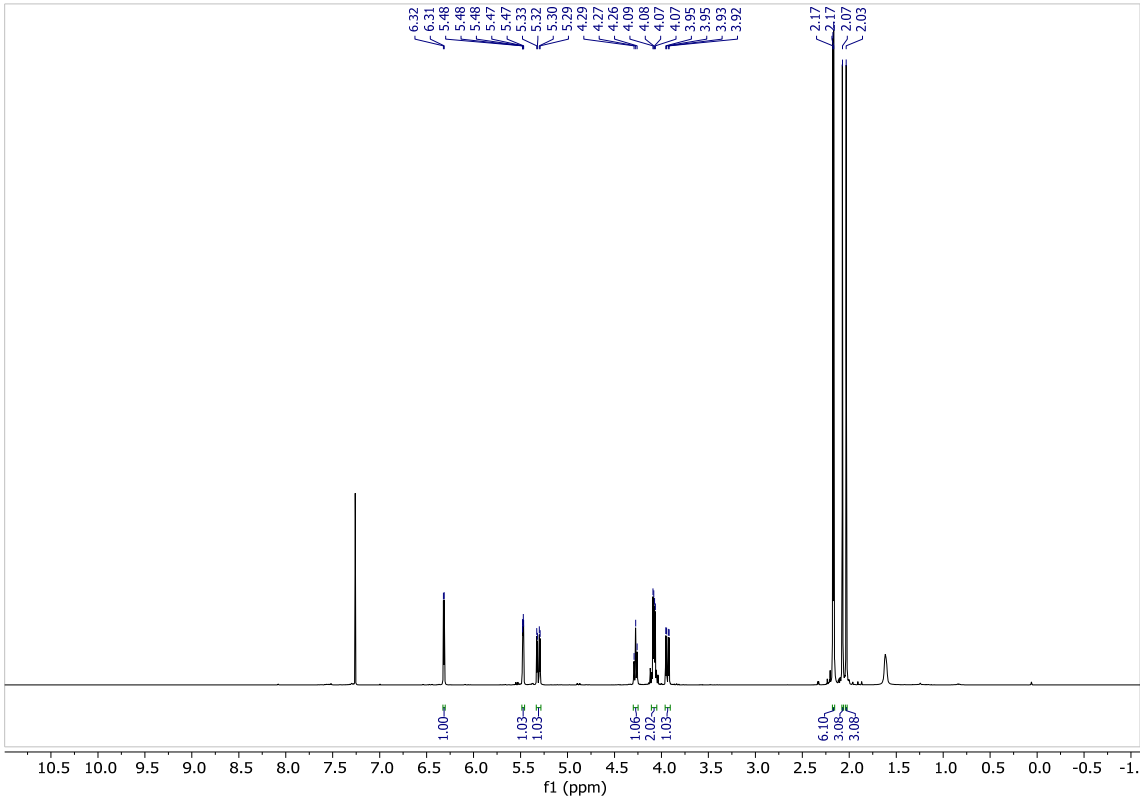

^{13}C NMR: **3.8**

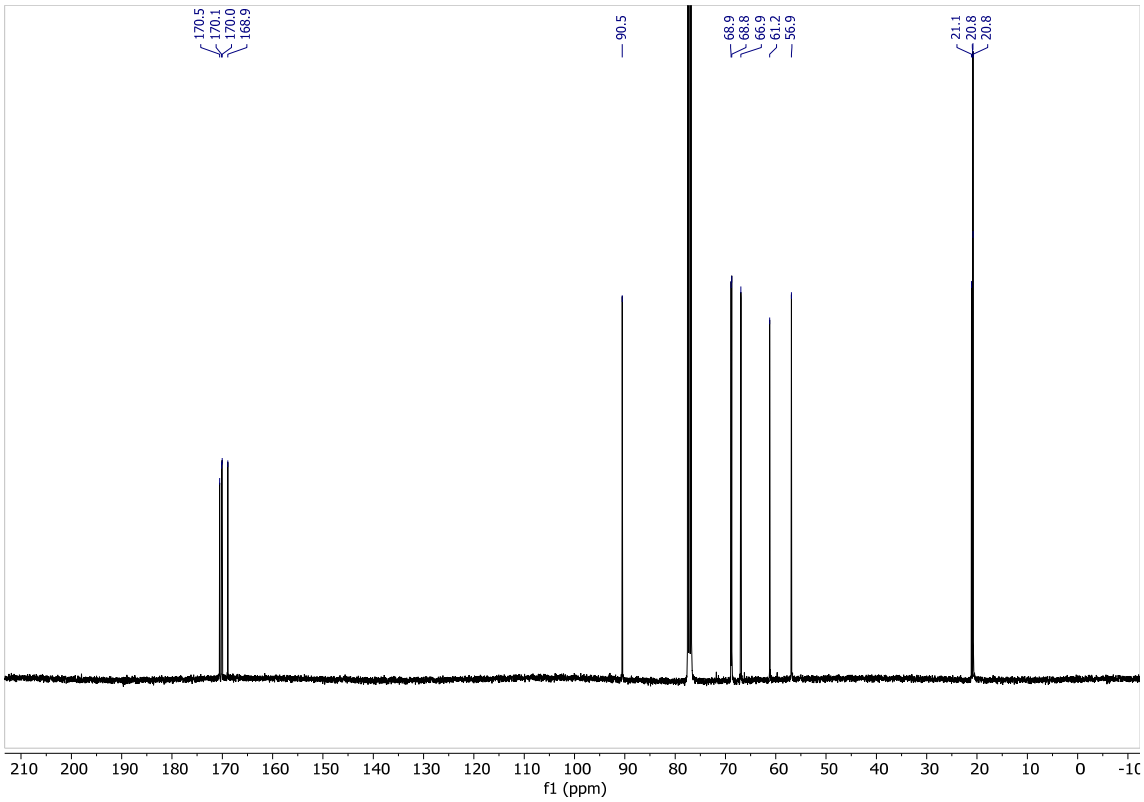

COSY: **3.8**

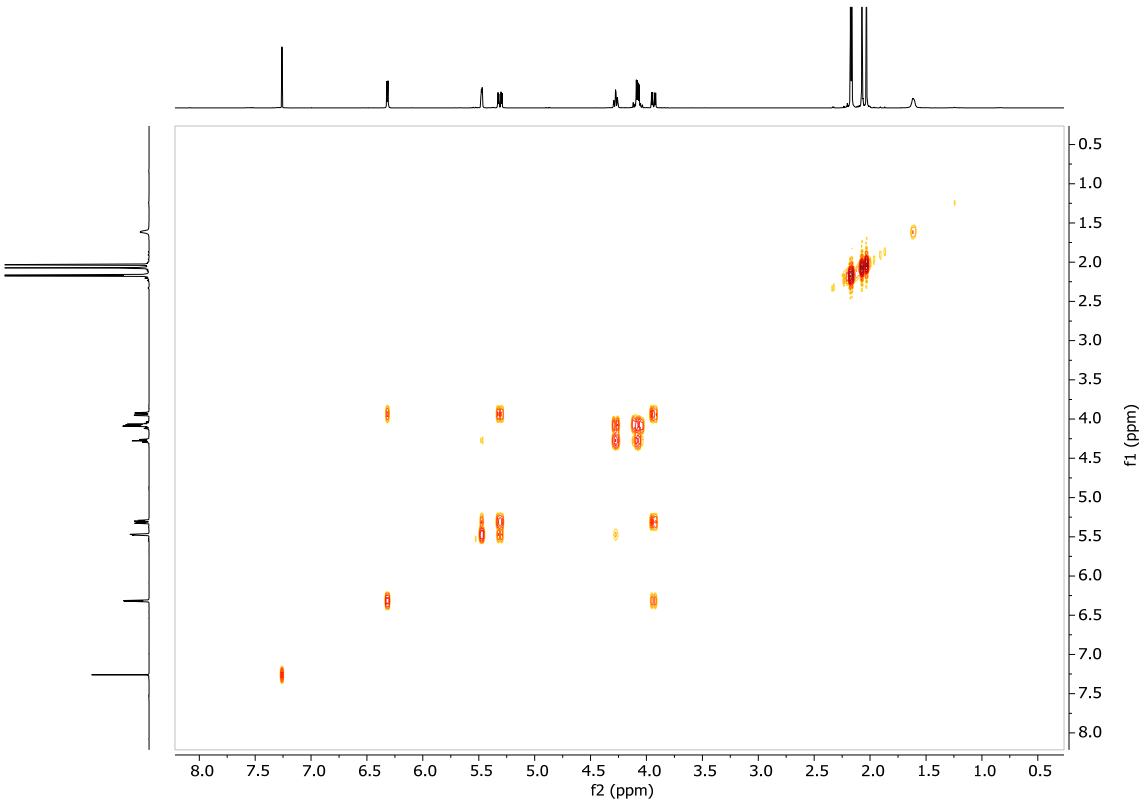

HSQC: **3.8**

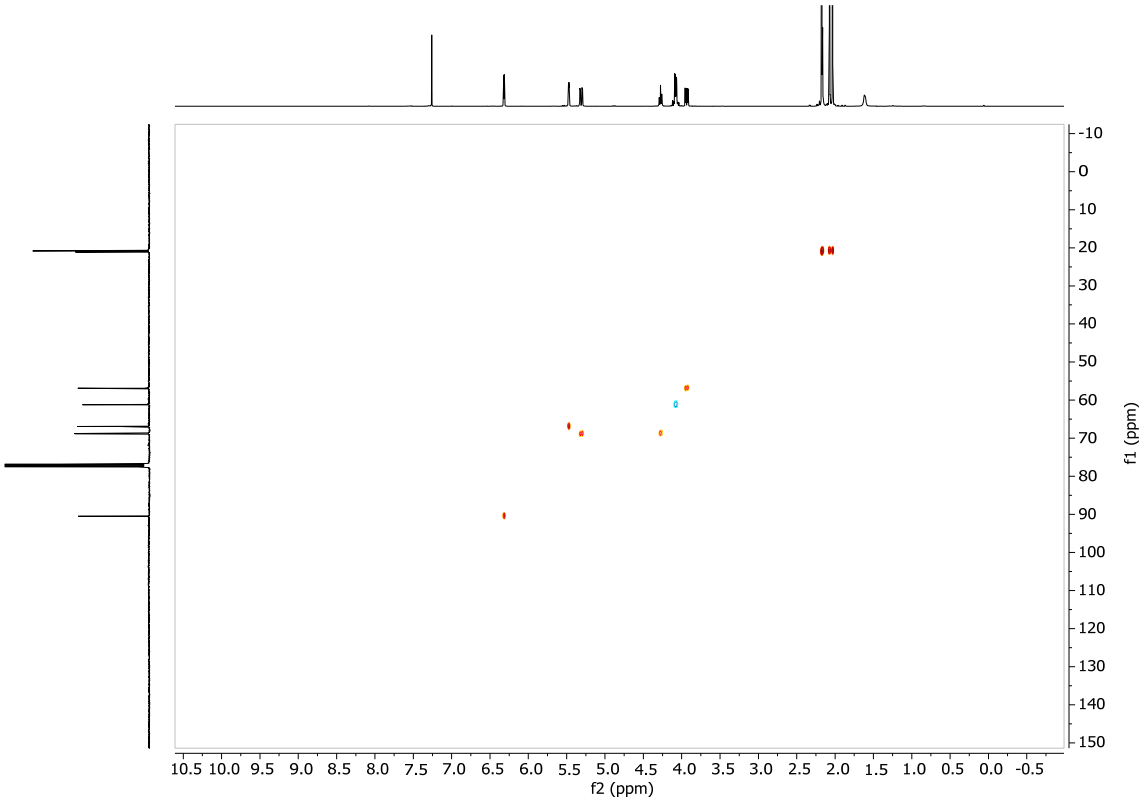

Coupled HSQC: **3.8**